

ACTA RADIOLOGICA

FOUNDED IN 1921 BY GÖSTA FORSSELL

PUBLISHED BY THE SOCIETIES OF MEDICAL RADIOLOGY IN DENMARK FINLAND NORWAY SWEDEN

DIAGNOSIS

MEDICAL IMAGING AND PHYSIOLOGIC RADIOLOGY

EDITOR
ERIK LINDGREN

EDITORIAL BOARD

Denmark G Thomsen S Kjaer
Finland P Virtama L R Holsjö

ASSOCIATE EDITORS
ULF RUDHE ULF BERGVALI

Norway T Aakhus E Poppe
Sweden L-G Larsson G F Saltzman

Editorial

Angiographic determination of splanchnic blood flow

Angiography in uterine and adnexal tumors

Angiography in angiomatous lesions of the gastrointestinal tract

Anatomy of the pancreatic veins—A post mortem and clinical phlebographic investigation

Compensatory hyperplasia of the human kidney evaluated by angiography and a dye dilution technique

Balloon catheters—In vitro experiments on pressure in fluence and risk of rupture

Idiopathic hypertrophic subaortic stenosis—I—Inter ventricular septum during the systolic contraction

Radiography of the small intestine with large amounts of cold contrast medium

Radiographic appearances in Crohn's disease—III—Colonic lesions following surgery

Radiography in primary tumors of the small bowel

Cisternal abnormalities produced by clinical tumours of the posterior cranial fossa—I—Cerebellar tumours

Radiographic healing and remodelling of cortical and cancellous bone grafts after rigid plate fixation—Experiments in the rabbit

Radiologic evaluation of the progression of rheumatoid arthritis

Arthrographic diagnosis of ruptured calcaneofibular ligament—I—A new projection tested on experimental injury post mortem

1

3 LANTZ B M T LINK D P FOERSTER J M and HOLCROFT J W

11 KARLSSON S and PERSSON P H

21 NYMAN U BOUSEN E LINDSTRÖM C and PERSSON J E

33 REICHARDT W and CAMERON R

43 GÖTHLIN J

47 JEKELL K PETERSSON N E and SANDQVIST S

53 KJAM G

65 BRUN B and HEGEDUS V

71 HILDELL J LINDSTRÖM C and WENCKERT A

79 EBERG O and EAHOLM S

85 LINDQVIST M

107 WARIS P KARAHARIU E SLATIS P and PAAVOLA LAINEN P

115 DE CARVALHO A GRAUDAL H and JORGENSEN B

123 VUUST M

INSTRUCTIONS TO AUTHORS

ACTA RADIOLOGICA consists of two series: **Diagnosis** (red) including all medical imaging techniques and physiologic radiography and **Oncology** (blue) including radiation therapy, chemotherapy, nuclear therapy, radiation physics and radiation biology. Only original manuscripts will be considered for publication, implying that the material has not already been published nor is intended for publication elsewhere. Extensive articles may be published as **Supplements** for which special conditions apply. Decisions on publication are based on the opinions of at least two reviewers (whose names are not revealed to the authors). The manuscripts are subject to editorial revision. The right is reserved to introduce such changes as may be necessary to make contributions conform to the editorial standards. The revised manuscript is submitted to the authors before typesetting. The journal does not hold itself responsible for opinions or statements expressed by the authors. The copyright resides with **Acta Radiologica**.

Manuscripts Only manuscripts written in English are accepted. They should be typed on one side of the paper only, with double spacing (at least 1 cm between the lines) and margins of at least 4 cm on the left side and at the top. The manuscript should be submitted in duplicate and two complete sets of figures supplied. The name and address of the institution or hospital at which the work was carried out should be given on the title page. A summary normally not exceeding 100 words should be included. The author should also add an address to which correspondence can be directed, and retain a copy of the manuscript for reference. A request for reprints should include full name, address and post code.

Abbreviations should be spelled out when first used in the text. Uncommon abbreviations and clinical jargon should be avoided. Footnotes are not accepted. Tables should be numbered in Arabic numerals and given on separate sheets, each with a short descriptive title. Legends for illustrations should be given on a separate sheet.

Contributions should be brief and concise, carefully revised before submission to exclude unessential matter. Alterations in the proofs are expensive, and with the exception of typographic errors will be charged to the author.

Units and Mathematics The International System of Units (SI) WHO 1975 should be used. A zero should always precede a decimal fraction (i.e. 0.123). Mathematical expressions should be set out clearly. Make a circled notation in the margin to explain possibly ambiguous characters such as 1 (numeral 1 and letter l), 0 (zero and letter O), \times (multiplication sign or letter x). In handwritten equations, mark clearly e and c, u and v, and letters in which capitals and lower case are nearly indistinguishable when handwritten, also primes and apostrophes. Use the solidus (/) for fractions and exp () when the exponent is complicated. In displayed formulae, the horizontal fraction line is preferable. Composite numbers should be expressed as $n \times m$

and not as $n m$. Equations should be numbered sequentially in Arabic numerals in parentheses on the right side of the page.

Illustrations Glossy prints, unretouched and unmounted, should be submitted. If the prints are not of a satisfactory standard, the author will be requested to submit the original film. Prints to be placed together should be of the same scale and of the same height to facilitate reproduction. The prints should have the same tonal relations as the original (for example, conventional angiographic films: white vessels on dark background; the reverse for subtraction films) with the patient's right to the reader's left. This is also valid for CT scans and other transverse images. Lettering and arrows are preferably marked lightly in pencil on the back, or removable from the prints.

Diagrams and graphs should be clearly drawn in black (Indian) ink on a white background and submitted as glossy prints or the original art work. Lettering must be large enough to be legible after photographic reduction. Computer print-outs are usually not satisfactory.

Colour drawings or photographs are accepted if the costs are defrayed by the author(s).

Each illustration must be provided with a suitable short legend, typewritten on a separate sheet and comprehensible without reference to the text. It must include explanations of all abbreviations and arrows used.

The figure number and the name of the first author must be marked lightly in pencil and the top indicated on the back of each illustration.

References The references should be arranged in alphabetical order with name(s) of author(s) followed by initials, full title of the article, and name of the journal as abbreviated in *Index Medicus*. The volume number, year of publication in parentheses and number of the first page of the article should follow. All authors of the article must be given in the reference list. Reference to books and journals should include the author, the title and edition of the book, the name of the publisher, and the place and year of publication.

Exhibits ACC No 238042
Dale 31104
Björk 3106
Björk and Zetterstrom: Selective angiography of bronchial and intercostal arteries. Acta radiol. Diagnosis 3 (1963) 313
KEITH A. Human embryology and morphology 6th edition p 533 Arnold & Co London 1948

Reference in the running text to an article by one author (BOUSEN 1975) by two authors (BOUSEN & LIND 1975) by three or more authors. First author's name followed by et coll (= co-workers) and not et al (= and others) (BOUSEN et coll 1975). The accuracy of reference data is the responsibility of the author.

One hundred reprints of each article are supplied free of charge; additional reprints may be purchased at cost price provided the order is placed when the proofs are returned.

Please submit all manuscripts to

ACTA RADIOLOGICA

P O Box 7449, S-103 91 Stockholm, Sweden

ACTA RADIOLOGICA

FOUNDED IN 1921 BY GÖSTA FORSSMÅLL

PUBLISHED BY THE SOCIETIES OF MEDICAL RADIOLOGY IN DENMARK, FINLAND, NORWAY AND SWEDEN

DIAGNOSIS

MEDICAL IMAGING AND PHYSIOLOGIC RADIOLOGY

EDITOR
ERIK LINDGREN

ASSOCIATE EDITORS
ULF RUDHE ULF ERIKSSON

EDITORIAL BOARD

Denmark G Thomsen S Kaas
Finland P Virtama L R Holsti

Norway T Aabø E Fjerp
Sweden L-G Larsson G-F Sjöström

General Radiology

- Cisternal abnormalities produced by clinical tumours in the posterior cranial fossa—II—Fourth ventricle tumours 129 LINDQVIST M
- Arachnoidal diverticula and cystlike dilatations of the nerve root sheaths in lumbar myelography 141 LARSEN J L SMITH D and FOSSAN G
- Angiographic determination of cerebral blood flow 147 LANTZ B M T FOERSTER J M LINK D P and HOLCROFT J W
- Videodensitometry for measuring blood vessel diameter 155 HOORNSTRA K HANSELMAN J M H HOLLAND W P J DEWEY PETERS G W and ZWABONGA A W
- Idiopathic hypertrophic subaortic stenosis—II—The shallow left ventricular cavity 165 KRAM G
- Angiography and ultrasound examination in the evaluation of pancreatic lesions 169 KARP W LUNDERQUIST A TYLÉN U and IHSE I
- Selective vein catheterization for hormone assay in endocrine tumours of the pancreas 177 REICHARDT W and INGEMANSSON S
- Angiography in cystadenoma and cystadenocarcinoma of the pancreas 189 UFLACKER R AMARAL N M LIMA S AAKHUST PEREIRA E and KURODA K
- Noninvasive measurement of fetal and neonatal blood flow 197 REID M H MACKAY R S and LANTZ B M T
- Effect of interposed skin at Doppler flow estimation at 8 and 10 MHz—With a description of a calibration device 203 FORSBERG L and OLIN T
- Diagnosis of abdominal aortic aneurysms by aortography computer tomography and ultrasound 209 ERIKSSON J HEMMINGSSON A and

Transcatheter embolization of the renal artery with butyrylate in renal carcinoma	215	SAJENVALD A KLEYMARK B and STENWIG J T
Radiographic appearances in Crohn's disease—IV— The new distal ileum after surgery	221	HILDEH J LINDSTRÖM C and WENCKERT A
Arthrographic diagnosis of ruptured calcaneofibular ligament—II—Clinical evaluation of a new method	231	VUUST M and NIEDERMANN B
Numerical assessment of asymmetry at scintigraphy of normal joint pairs with $^{99}\text{Tc}^m$ polyphosphate	235	NORDBERG M HEFRFORDT J DISSING I JENSEN M MÖLLER J and SNEFFEN O
Contrast media for computer tomography of the liver	239	WEGENER O H MUTZEL W and SOUCHON R
Prevention of experimental venous thrombosis in duced by contrast medium in the rat	249	MAFFEI F H A ROLLO H A and FABRIS V E
Modification of grey scale in computer tomographic images	253	HEMMINGSSON A and JUNG B

ACTA RADIOLOGICA

FOUNDED IN 1911 BY GÖSTA FORSSELL

PUBLISHED BY THE SOCIETIES OF MEDICAL RADIOLOGY IN DENMARK, FINLAND, NORWAY AND SWEDEN

DIAGNOSIS MEDICAL IMAGING AND PHYSIOLOGIC RADIOLOGY

EDITOR
ERIK LINDGREN

ASSOCIATE EDITORS
ULF RUDHE ULF BERGVALL

EDITORIAL BOARD

Denmark G. Thomsen S. Kaas
Finland P. Virtama L. R. Holsti

Norway T. Aakhus F. Pöppe
Sweden L.-G. Larsson G. F. Saltzman

Pediatric Radiology

- Complications of angiography in children and means of prevention 257 JACOBSSON B. CURTIN H. RUBENSON A. and SÖRENSEN S. E
- Metrizamide and metrizoate for cardioangiography in infants—Comparison of heart rate and arrhythmia 263 HELLSTRÖM M. JACOBSSON B. SÖRENSEN S. E. and ERIKSSON B. O
- Variations in vesicoureteral reflux—Influence on diagnostic validity 269 LAURIN S. and MORTENSSON W
- Size of the unaffected kidney in children with Unilateral hydronephrosis 275 MILLER M. and MORTENSSON W
- Arthrography of the hip in children—Technique, normal anatomy and findings in unstable hip joints 279 LÖNNERHOLM T
- Avulsion fracture of the proximal tibial metaphysis—Report of a case 293 DANIELSSON L. and THEANDER G
- Effects of percutaneous femoral artery catheterization on leg growth in infants and children 297 MORTENSSON W
- Voluntary habitual dislocation of the hip in children 303 PETTERSSON H. THEANDER G. and DANIELSSON L
- Congenital deformities of skull caused by fetal limbs 309 THEANDER G. and THUNANDER J
- Accuracy of echoventriculography as compared with computer tomography in children 315 ERASMIE U. HANSON J. and RINGERTZ H

INSTRUCTIONS TO AUTHORS

ACTA RADIOLOGICA consists of two series: *Diagnosis* (red) including all medical imaging techniques and physiologic radiography and *Oncology* (blue) including radiation therapy, chemotherapy, nuclear therapy, radiation physics and radiation biology. Only original manuscripts will be considered for publication, implying that the material has not already been published nor is intended for publication elsewhere. Extensive articles may be published as Supplements for which special conditions apply. Decisions on publication are based on the opinions of at least two reviewers (whose names are not revealed to the authors). The manuscripts are subject to editorial revision. The right is reserved to introduce such changes as may be necessary to make contributions conform to the editorial standards. The revised manuscript is submitted to the authors before typesetting. The journal does not hold itself responsible for opinions or statements expressed by the authors. The copyright resides with Acta Radiologica.

Manuscripts. Only manuscripts written in English are accepted. They should be typed on one side of the paper only, with double spacing (at least 1 cm between the lines) and margins of at least 4 cm on the left side and at the top. The manuscript should be submitted in duplicate and two complete sets of figures supplied. The name and address of the institution or hospital at which the work was carried out should be given on the title page. A summary normally not exceeding 100 words should be included. The author should also add an address to which correspondence can be directed and retain a copy of the manuscript for reference. A request for reprints should include full name, address and post code.

Abbreviations should be spelled out when first used in the text. Uncommon abbreviations and clinical jargon should be avoided. Footnotes are not accepted. Tables should be numbered in Arabic numerals and given on separate sheets, each with a short descriptive title. Legends for illustrations should be given on a separate sheet.

Contributions should be brief and concise, carefully revised before submission to exclude unessential matter. Alterations in the proofs are expensive, and with the exception of typographic errors will be charged to the author.

Units and Mathematics. The International System of Units (SI) WHO 1975 should be used. A zero should always precede a decimal fraction (i.e. 0.123). Mathematical expressions should be set out clearly. Make a circled notation in the margin to explain possibly ambiguous characters such as 1 (numeral 1 and letter l), 0 (zero and letter O), \times (multiplication sign or letter x). In handwritten equations, mark clearly e and c , u and v , and letters in which capitals and lower case are nearly indistinguishable when handwritten, also primes and apostrophes. Use the solidus (/) for fractions and $\exp()$ when the exponent is complicated. In displayed formulae, the horizontal fraction line is preferable. Composite numbers should be expressed as $n \times m$

and not as $m \times n$. Equations should be numbered sequentially in Arabic numerals in parentheses on the right side of the page.

Illustrations. Glossy prints, unretouched and unmounted, should be submitted. If the prints are not of a satisfactory standard, the author will be requested to submit the original film. Prints to be placed together should be of the same scale and of the same height to facilitate reproduction. The prints should have the same tonal relations as the original (for example, convert all angiographic films, white vessels on dark background, to the reverse for subtraction films) with the patient's right to the reader's left; this is also valid for CT scans and other transverse images. Lettering and arrows are preferably marked lightly in pencil on the back or removable from the prints.

Diagrams and graphs should be clearly drawn in black (Indian) ink on a white background and submitted as glossy prints or the original art work. Lettering must be large enough to be legible after photographic reduction. Computer print-outs are usually not satisfactory.

Colour drawings or photographs are accepted if the costs are defrayed by the author(s).

Each illustration must be provided with a suitable short legend, typewritten on a separate sheet and comprehensible without reference to the text. It must include explanations of all abbreviations and arrows used.

The figure number and the name of the first author must be marked lightly in pencil and the top indicated on the back of each illustration.

References. The references should be arranged in alphabetical order with name(s) of author(s) followed by initials, full title of the article and name of the journal as abbreviated in Index Medicus. The volume number, year of publication in parentheses and number of the first page of the article should follow. All authors of the article must be given in the reference list. Reference to books and monographs should indicate the author, the title and edition of the book, the name of the publishers and the place and year of publication.

Examples

BOUSEN E and ZSIGMOND M. Selective angiography of bronchial and intercostal arteries. *Acta radiol. Diagnosis* 3 (1965) 515.

KEITH A. Human embryology and morphology. 6th edition. P. 513. Arnold & Co. London 1948.

Reference in the running text to an article by one author (BOUSEN 1975), by two authors (BOUSEN & LIND 1975), by three or more authors. First author's name followed by et coll. (= co-workers) and not et al. (= and others) (BOUSEN et coll. 1977). The accuracy of reference data is the responsibility of the author.

One hundred reprints of each article are supplied free of charge. Additional reprints may be purchased at cost price provided the order is placed when the proofs are returned.

Please submit all manuscripts to

ACTA RADIOLOGICA

P O Box 7449, S-103 91 Stockholm, Sweden

ACTA RADIOLOGICA

FOUNDED IN 1921 BY GÖSTA FORSSELL

PUBLISHED BY THE SOCIETIES OF MEDICAL RADIOLOGY IN DENMARK, FINLAND, NORWAY AND SWEDEN

DIAGNOSIS

MEDICAL IMAGING AND PHYSIOLOGIC RADIOLOGY

EDITOR
ERIK LINDGREN

ASSOCIATE EDITORS
ULF RUDHE ULF BERGVALL

EDITORIAL BOARD

Denmark G Thomsen S Kaae
Finland P Virtama L R Holsti

Norway T Aakhus E Poppe
Sweden L-G Larsson G F Saltzman

-
- | | | |
|---|-----|---|
| Computer tomography in superior sagittal sinus thrombosis | 321 | BRISMAN J |
| Computer tomography in the evaluation of sub-arachnoid hemorrhage | 327 | ILIEQUIST B and LINDQVIST M |
| Epidurography with metrizamide in Rhesus monkeys | 333 | KIDO D K BAKER R A SAUBERMAN V A SALEM J SCHOENE W C and FOURNIER P |
| Cisternal abnormalities produced by clinical tumours in the posterior cranial fossa—III—Tumours of the brain stem and pontine angle | 339 | LINDQVIST M |
| Idiopathic hypertrophic subaortic stenosis—III—Analysis of the myocardial fibre shortening of the free left ventricular wall by means of geometric models | 357 | KVAM G |
| Ultrasound examination of lesions in the thorax | 375 | FORSBERG L and TILÉN U |
| Angiography in laryngeal carcinoma | 379 | SÖKJER H and OLOFSSON J |
| Adrenergic and cholinergic responses in the uteroplacental vascular bed of the guinea pig | 387 | EGUND N and CARTER A M |
| Proteinuria following nephroangiography—V—Influence of calcium and magnesium ions in non ionic contrast media | 397 | HOLTÅS S ALMÉN T GOLMAN K and TEJLER L |
| Proteinuria after selective nephroangiography in man—Comparison of three contrast media | 401 | KRÅKENES J ELSAYED S GÖTHLIN J and FARSTAD M |
| Contrast enhancement pharmacokinetics in experimental pancreatitis diabetes and subcutaneous granuloma | 407 | DEAN P B KIVISAARI L and KORMANO M |

RECEIVED
11-3-81
JIPUR

Radiologic evaluation of chondromalacia patellae
 Sacroiliac joint involvement in classical or definite
 rheumatoid arthritis
 External bony auditory canal and the tympanic
 bone—Morphologic properties and influences on the
 tomographic reproduction

413 LUND F and NILSSON B E
 417 DE CARVALHO A and GRAUDAL H
 425 ECKERDAL O and AHLQVIST J

SUBSCRIPTIONS

Acta Radiologica		in Scandinavia	outside Scandinavia
Diagnosis (red)	} both vols	Sw Kr 310 —	Sw Kr 375 —
Oncology Radiation Physics Biology (blue)			
Diagnosis	one vol	Sw Kr 200 —	Sw Kr 210 —
Oncology Radiation Physics Biology	one vol	Sw Kr 170 —	Sw Kr 180 —
All rates include regular mailing costs (surface mail)			

*All communications regarding advertising, subscription
 change of address etc should be sent to
 Acta Radiologica, P O Box 7449, S-103 91 Stockholm, Sweden*

EDITORIAL

With this issue Acta Radiologica begins publication in a new form after having had the same appearance and been produced by the same processes ever since it was founded in 1921 by Gosta Forssell. The design of the cover for the individual numbers has however been changed the table of contents being moved in 1951 to the front page in order to make it easier for readers to obtain information on the articles in the issue without having to open it. And in 1963 the journal was divided into two series one on diagnosis and one on radiation therapy physics and biology.

It is of great importance that the illustrations in a periodical presenting radiologic material should be of the highest quality. If a reader is able by examining the illustrations to satisfy himself that the author has interpreted the images correctly he will also find it easier to evaluate the conclusions drawn. In other words form a better opinion regarding the value of the article. Even with blocks of high quality it has sometimes been necessary because of the size of the journal to present illustrations which in some cases have been too small with the result that some of the details could not be readily distinguished. With increasing refinement of the imaging techniques and as ever smaller details have proved to have diagnostic significance a sense of dissatisfaction with the format of the journal has gradually developed. A change over to a larger size has in fact been under consideration for several years but has been deferred until a change to a more modern method of production could be effectuated at the same time.

As from the present issue the journal will be produced by means of modern computer generated phototypesetting and offset printing. Other periodicals have earlier adopted the offset technique but in the opinion of the editors of this journal images produced with this process have only recently attained a quality that can be considered acceptable

for use in radiologic publications. Thus the change to offset was not made until comparative trials had brought conviction that the new method for image reproduction has reached a stage giving results comparable to those obtained with the old block making system.

Apart from the change in appearance and the new method of production the principles of the journal will remain unchanged. This means that the two series will continue to be published also in the future. The diagnosis series will as before be a journal of general radiology with sidelines on some special fields such as neuroradiology and pediatric radiology. In the future as in the past considerable attention will be paid to the layout in order to ensure that the articles are presented in a clear and esthetically attractive form.

One of the reasons why Acta Radiologica was instituted was the desire to have a forum where experiences and results of research in radiology and allied fields in the Nordic countries could be published so that readily available information could be obtained regarding developments trends and future prospects in these countries. As the speech communities covered by these countries are small the articles had to be published in one of the major languages of the world if they were to be available to readers in other areas. In the beginning papers in English German and French were accepted. However English has gradually become the dominant international language in the medical world holding a position almost comparable to that of Latin in the world of science during the Middle Ages and the centuries immediately following that period and the journal therefore subsequently adopted the policy of publishing articles only in English. Summaries in German and French were retained but from this issue onwards they will be abandoned since it may be considered hardly possible these days to follow developments in any branch of medicine without a

knowledge of English *Acta Radiologica* will therefore from now on be published exclusively in English

Although the journal was originally intended to be a forum mainly for the Nordic nations its pages have always been open to authors from other countries as well. Many important articles by non Nordic writers have also been gratefully accepted for publication. It is hoped that these contributions will not only continue but also increase in number. Problems will thereby receive more all round treatment and comparisons with other points of view facilitated which should be to the mutual advantage of both *Acta Radiologica* and its readers.

In recent years new diagnostic methods based on imaging techniques have been introduced ultrasound scintigraphy computer tomography and possibly still others such as magnetic resonance will appear in the future. Opinions differ it is true regarding the appropriate speciality to which these methods should belong. *Acta Radiologica* holds most emphatically that all imaging techniques should be concentrated to the radiologic departments where the basic skills are centered. Furthermore the methods are as a rule such that the solution of a diagnostic problem is seldom gained by

one method alone the methods are supplied to each other as well as to conventional. Thus the most suitable way to achieve this is to assemble them all at one institution. In accordance with this opinion *Acta Radiologica* has published and will continue to publish articles on all imaging procedures. In order to emphasize more clearly this previously the fact that the diagnosis section of the series is a journal of medical imaging information to this effect has been added to the first page of the cover. It further appears that the journal will also accept reports on physiologic sequences analysed by radiologic methods in the widest sense.

Like other clinical specialties oncology needs the methods offered by diagnostic radiology but otherwise they have little in common. They should accordingly be practised by different specialists. As a consequence of this *Acta Radiologica* as the only radiologic periodical has run and will continue to run two series one diagnosis and one oncology the latter comprising not only radiation therapy but also chemotherapy and radiation physics and biology.

With this declaration of its programme *Acta Radiologica* is presented to the readers in its new form.

ANGIOGRAPHIC DETERMINATION OF SPLANCHNIC BLOOD FLOW

II M T LANTZ D P LINK J M FOERSTER and J W HOLCROFT

Treatment of bowel ischemia requires surgery. Unfortunately the results are poor. Embolization of the superior mesenteric artery leads to a mortality rate of 30 per cent. Ischemia due to atheromatous obstruction may result in a 60 per cent mortality (JACKSON 1963 PURDUE & SMITH 1970). A major impediment to successful therapy is the lack of diagnostic techniques which can identify reduced blood flow causing bowel ischemia. Recently it has been reported that 70 per cent of bowel infarction is due to non-occlusive disease with venous occlusion accounting for a further 10 per cent (BERGAN 1964 WILLIAMS et coll 1967). A high incidence of splanchnic atheromatous disease further complicates the picture because it may not necessarily cause ischemia. DERRICK & LOGAN (1958) reported a narrowed coeliac axis in 44 per cent of their autopsy series. Unfortunately the surgeon at laparotomy may be no more successful than the radiologist at determining the presence of reduced vascular perfusion (MARSTON et coll 1966 WILLIAMS et coll). The considerations mentioned suggest that a diagnostic measure of splanchnic blood flow is needed. With the application of videodensitometry during standard visceral angiography it appears that such a measure is now available.

The splanchnic circulation can be defined as the blood supply to the liver, spleen, gall bladder, pancreas and the gastrointestinal tract (stomach, small and large bowel). The arterial supply to the splanchnic region originates from the coeliac, superior and inferior mesenteric arteries. The entire blood flow returns to the general circulation through the inferior vena cava via the liver and the hepatic veins. In this respect the total splanchnic blood flow can be regarded as a single hypothetical organ. However,

two different sources of blood for the liver exist: the venous return from the gastrointestinal tract, pancreas and spleen which is collected in the portal vein provides the liver with 70 to 75 per cent of its total blood flow (ROWELL 1975) and the remaining 25 to 30 per cent is supplied by the hepatic artery, a branch of the coeliac artery.

The splanchnic blood flow receives about 20 to 25 per cent of the resting cardiac output (BRADLEY et coll 1953 GRAYSON & MENDEL 1965). The blood volume contained in this region serves as a reservoir for maintenance of the cardiac output during stress for regulation of the systemic blood pressure. Large blood volumes can be mobilized by constriction of the veins which have a large network of sympathetic innervation (MELLANDER & JOHANSSON 1968 ROSS 1971). Vasodilatation may be induced during elevation of the systemic blood pressure and during digestion. Thus splanchnic vascular resistance seems to be an important regulator and effector of the circulatory dynamics triggered by a variety of physiologic receptors (KORNER et coll 1967 BROOKSBY & DONALD 1971).

The total splanchnic blood flow can be estimated using the Fick principle, i.e. the constant infusion technique originally described by BRADLEY et coll (1945). Clearance rates and hepatic extraction of indicator injected as a single bolus can also be used for estimation of the hepatic or the splanchnic blood flow (ROWELL 1974). Utilizing drug infusions or embolization of selective branches of the mesenteric arteries it is possible to decrease or block part of the splanchnic circulation in patients with gastrointestinal bleeding. However, to date there are no clinical

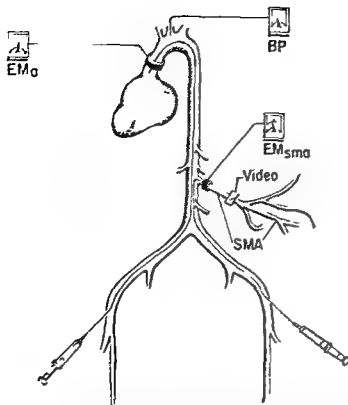


Fig. 1 Diagram of the canine model. Flow in the ascending aorta (EM_1) and in the superior mesenteric artery (EM_{sma}) was measured using electromagnetic probes. Angiographic catheters were positioned in the ascending aorta and in the superior mesenteric artery (SMA). The videodensitometric recordings and measurements were performed over a branch of the superior mesenteric artery (Video). Blood pressure (BP) was recorded via a carotid cannula and pressure transducer.

ly useful methods for measuring regional blood flow in the splanchnic region.

The objective of the present investigation is to validate a new method of determining blood flow in single splanchnic arteries as a per cent of cardiac output utilizing densitometry. The technique has been compared to electromagnetic flow readings in a canine model and it is intended to be used as a simple clinical method during routine abdominal angiography.

Principles of videodensitometry. The videodensitometric method of estimating relative blood flow has previously been described by LANTZ (1974, 1975) and has proven to be highly accurate in a hydrodynamic model. Application of the method has recently been tested in animal experiments regarding the renal circulation (LANTZ et coll. 1979) and in humans with arteriovenous fistula (LANTZ et coll. 1979). The densitometer records density changes in the television image caused by injected intravascular contrast medium. In this respect it is a circulatory indicator dilution technique (WOOD et coll. 1964).

The videodensitometric system is characterized by high sensitivity and a rapid dynamic response. Unlike conventional dilution techniques, no sampling catheters are needed. After injecting iodine contrast medium into the circulatory system and recording the angiography on videotape cassette in continuous fluoroscopy with fixed kV and mA, dilution curves can be obtained by placing a videodensitometric cursor of appropriate size over any artery displayed on the monitor.

The concept of relative flow has previously been described in depth by LANTZ (1974). It is based upon the principle of comparing flow at two sites of circulation where contrast medium has been injected. The integrated areas of the two dilution curves are inversely proportional to the flow at the sites of injection. If, for example, the flow in the superior mesenteric artery is to be estimated as a fraction of the cardiac output, two contrast injections should be made: one in the ascending aorta where total cardiac output passes and one in the proximal part of the superior mesenteric artery. By recording both dilution curves downstream at the same site of the mesenteric artery, the relative flow can be estimated according to (LANTZ 1975).

$$\frac{Q_1}{Q_2} = \frac{M_1}{M_2} \frac{A_2}{A_1}$$

where Q_1 and Q_2 are the flows at the sites of injection, M_1 and M_2 are the amounts of contrast medium injected at the two sites, and A_1 and A_2 are the integrated densitometric areas measured from the densitometric dilution curves at the same site downstream in the peripheral vessel.

Material and Methods

The blood flow in the superior mesenteric artery, the hepatic artery and the splenic artery was estimated as a fraction of the cardiac output in an *in vivo* canine model (Fig. 1). Estimates obtained by the videodensitometric method were compared to the corresponding electromagnetic flow readings in 4 mongrel dogs weighing between 22 and 27 kg. The dogs were anesthetized with 30 mg/kg of sodium pentobarbital and were ventilated with a Harvard pump on room air.

Electromagnetic flow. The cardiac output was continuously recorded by a circumferential elec-

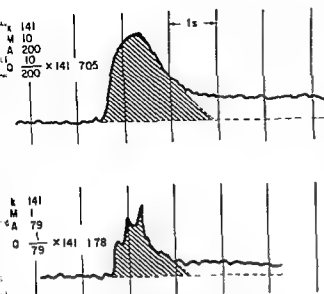


Fig. 2 Videodensitometric flow calculation in superior mesenteric artery as a fraction of the cardiac output. Top curve represents the recording obtained over the artery after injection of contrast medium into the ascending aorta. Bottom curve represents the recording at the same site after selective injection into the artery. The flow Q is calculated from M (amount of contrast medium injected), A (integrated densitometric area, shaded) and k (calibration factor for radiation intensity) according to $Q = M/A \times k$. The flow in the superior mesenteric artery as a fraction of the cardiac output is $1.78/7.05 = 25.2$ per cent.

tromagnetic flow probe around the ascending aorta 2 to 4 cm above the aortic valve. Similar flow probes were attached to the proximal part of the superior mesenteric artery, the splenic artery and the hepatic artery. All probes were connected to electromagnetic flow meters (Statham SP 2200). The systemic blood pressure was simultaneously recorded from the left main carotid artery by an intra-arterial cannula attached to a Statham P23DB pressure transducer.

Videodensitometric flow. The blood flow in a splanchnic artery as a fraction of the cardiac output was calculated from the videodensitometric dilution curves derived from a bolus injection of sodium iohalamate (Conray 400) through a 7 French pigtail catheter with its tip in the ascending aorta, and from a second bolus injection through a 6 French selective catheter with its tip in a splanchnic artery. With respiration suspended and the dog in a fixed position 10 ml of contrast medium was injected into the ascending aorta followed by an injection of 1 ml contrast medium into the splanchnic artery. The selective injections were performed manually and the aortic injection by pressure injector (Cordis II). Eighteen series of injections were performed each

containing one aortic injection followed by one or more selective injections at different time intervals. During injections in the aortic arch and selectively into the splanchnic artery the video image was recorded on video cassette with the image intensifier in a fixed position over the splanchnic vessel examined. Before each recording performed in constant fluoroscopy with fixed kV (65–80) and mA (3–5) a 10 mm aluminium filter was used for calibration of the radiation intensity. The left posterior oblique position of the dog was used to separate a major part of the main branch of the splanchnic arteries from interfering smaller branches. The videodensitometric dilution curves were displayed at a later time by replaying the cassette. A videodensitometer with an output voltage proportional to the logarithm of the incident radiation was used (T Strand Siemens Elema Sweden). Integration of the videodensitometric mass time curves was performed by planimetry.

Recording equipment. The video image was recorded on a Sony Umatic video cassette recorder. The data from the electromagnetic probes along with the arterial pressure was recorded on an Electromedics DR 8 photographic recorder and synchronized with the videotape recording of the contrast medium passage during fluoroscopy.

Röntgen equipment. A constant potential generator (CGR 1215 1200 mA) was used. The fluoroscopic equipment included a cesium iodide image intensifier with a plumbicon television camera (Coronax C arm CGR triple field image intensifier). The four inch (10 cm) intensifier input was used in all experiments.

Results

Eighteen series of measurements totaling 34 paired ratios of splanchnic flow to cardiac output were obtained by the videodensitometric and electromagnetic methods. The densitometric recordings from a typical data pair is illustrated in Fig. 2. Extrapolation of the densitometric curves from the aortic injection (Fig. 2a) and the selective injection into the superior mesenteric artery (Fig. 2b) was required because of remaining contrast medium in the tissues which prevents the curve from returning to baseline. This is an accepted technique in other dilution methods.

Superior mesenteric artery flow. Twenty-two paired data comparing the flow in the superior

Table 1

Twenty two measurements of the superior mesenteric artery flow as a fraction of the cardiac output were recorded by electromagnetic and videodensitometric methods. Each of the 12 series represents one injection of contrast medium into the ascending aorta followed by one or more subsequent selective injections into the superior mesenteric artery at different intervals. The difference in percentage between the two methods is displayed in column E.

Series	n	Time (min)	Electromagnetic flow (ml/min)		Electro-magnetic ratio (per cent sup mes artery flow) (C)	Videodensitometric ratio (per cent sup mes artery flow) (D)	Difference D-C (E)
			Cardiac output (A)	Sup mes artery flow (B)			
1		0	2 400				
	1	1		250	10.4	11.8	1.4
2		0	2 370				
	2	2		306	12.9	14.3	1.4
	3	3		298	12.6	12.2	-0.4
	4	5		242	10.2	13.4	3.2
3		0	2 290				
	5	2		250	10.9	11.9	1.0
	6	4		282	12.3	11.0	-1.3
4		0	1 897				
	7	1		508	26.8	26.1	-0.7
	8	3		500	26.4	26.8	0.4
5		0	1 744				
	9	1		524	30.0	28.6	-1.4
6		0	1 786				
	10	1		524	29.3	25.8	-3.5
	11	2		508	28.4	26.5	-1.9
7		0	1 720				
	12	2		442	25.6	24.4	-1.2
	13	3		426	24.8	25.1	0.3
8		0	1 770				
	14	2		519	29.3	28.4	-0.9
	15	4		473	26.7	29.2	2.5
9		0	1 927				
	16	3		473	24.5	24.7	0.2
10		0	460				
	17	1		197	42.8	39.0	-3.8
	18	2		176	38.1	40.2	2.1
11		0	751				
	19	1		228	30.4	28.0	-2.4
	20	2		210	28.0	29.2	1.2
12		0	865				
	21	1		251	29.0	29.1	0.1
	22	3		243	28.8	32.7	3.9

$\bar{x} = -0.22$
SD = 2.00

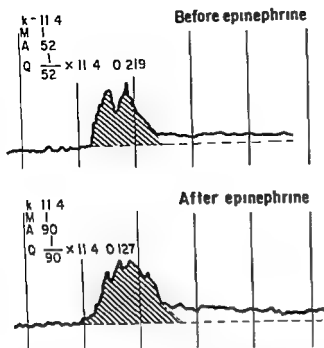


Fig 3 Effect of epinephrine. One ml Conray 400 was injected into the superior mesenteric artery (top curve) giving a calculated videodensitometric flow of 0.219. The absolute flow recorded by the electromagnetic method was 279 ml/min. Through the catheter 4 ml epinephrine (10 µg/ml) was injected. Fourteen min later another 1 ml Conray 400 was injected into the artery. The calculated flow using videodensitometry (bottom curve) was then 0.127. The corresponding electromagnetic flow was 163 ml/min. The decrease of flow caused by epinephrine was 41.6 per cent by the electromagnetic method and 42.0 per cent by the videodensitometric method.

mesenteric artery and the cardiac output were obtained (Table 1). The mean difference between the electromagnetic ratio and the videodensitometric ratio was -0.22 per cent (SD=2.00). This confirms the high accuracy of the videodensitometric method compared to the electromagnetic technique in the individual case. The superior mesenteric artery/cardiac output ratio varied within the range of 10 to 40 per cent. Higher ratios were found in experiments where the cardiac output was extremely low indicating inverse proportionality: the larger the cardiac output the smaller the superior mesenteric artery flow. However, in the individual experiments the videodensitometric ratio did not differ from the electromagnetic one by more than 2 per cent. This is illustrated in the change of flow induced by epinephrine infusion in the superior mesenteric artery causing a decrease in the flow of 41.6 per cent by the electromagnetic method compared to 42.0 per cent by the videodensitometric method (Fig. 3).

Hepatic artery flow. The hepatic artery flow in 7

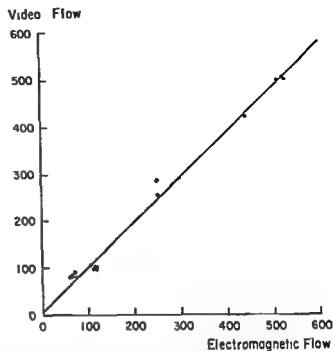


Fig 4 Correlation between blood flow simultaneously determined by the videodensitometric and electromagnetic methods in 34 measurements in splanchnic arteries ($r=0.985$). The solid line is a least squares regression line.

experiments was calculated as 10.2 per cent by the electromagnetic method and 8.66 per cent by the videodensitometric method (Table 2). The mean difference was -1.54 per cent (SD=1.08).

Splenic artery flow. Five paired data of the splenic artery flow ratio were calculated comparing the two methods. The mean splenic ratio was 7.02 per cent with the electromagnetic method and 8.0 per cent with the videodensitometric method. Thus the mean difference between the two techniques was 1.58 per cent (SD=0.58) (Table 3).

Comparison between the electromagnetic and videodensitometric methods. The splanchnic blood flow in absolute units (ml/min) was calculated in each of the 34 experiments from the videodensitometric ratio and the electromagnetic readings of the cardiac output according to

$$\frac{Q_s}{Q_A} \times (\text{cardiac output}) = \text{splanchnic blood flow in ml/min}$$

where

$\frac{Q_s}{Q_A}$ is the videodensitometric splanchnic flow ratio

The splanchnic flow in absolute units recorded by the two methods (Fig. 4) correlated well ($r=0.985$).

Table 2

The hepatic artery flow as a fraction of the cardiac output obtained from 7 measurements in 3 series was estimated by the electromagnetic and the videodensitometric methods. Difference in percentage of cardiac output between the methods is displayed in column E.

Series	n	Time (min)	Electromagnetic flow (ml/min)		Electromagnetic ratio (per cent hepatic artery flow) (C)	Videodensitometric ratio (per cent hepatic artery flow) (D)	Difference D-C (E)
			Cardiac output (A)	Hepatic artery flow (B)			
13		0	1 000				
	23	2		119	11.9	9.5	-2.4
	24	4		109	10.9	7.6	-3.3
14		0	1 057				
	25	2		119	11.3	9.5	-1.8
	26	3		134	12.7	11.3	-1.4
15		0	1 346				
	27	1		114	8.5	7.6	-0.9
	28	6		111	8.2	7.2	-1.0
	29	7		106	7.9	7.9	0.0
					$\bar{x}=10.2$ SD=1.95	$\bar{x}=8.6$ SD=1.49	$\bar{x}=-1.54$ SD=1.08

Table 3

The splenic artery flow was measured as a fraction of the cardiac output by electromagnetic and videodensitometric methods. Three series containing 5 paired determinations in percentage of cardiac output are displayed with the difference between the two methods in column E.

Series	n	Time (min)	Electromagnetic flow (ml/min)		Electromagnetic ratio (per cent splenic artery flow) (C)	Videodensitometric ratio (per cent splenic artery flow) (D)	Difference D-C (E)
			Cardiac output (A)	Splenic artery flow (B)			
16		0	980				
	30	1		65	6.6	8.6	2.0
	31	3		70	7.1	9.1	2.0
17		0	1 057				
	32	1		64	6.1	7.6	1.5
	33	4		60	5.7	7.5	1.8
18		0	769				
	34	3		74	9.6	10.2	0.6
					$\bar{x}=7.02$ SD=1.54	$\bar{x}=8.6$ SD=1.11	$\bar{x}=1.58$ SD=0.88

Discussion

Several factors should be seriously considered when using the videodensitometric technique for accurate flow measurement in selective arteries. In the clinical setting one catheter alone might be used or contrast medium injections in the aortic arch and in a selected splanchnic vessel. The catheter should contain at least 3 or 4 side holes close to the tip of the catheter to obtain a high injection rate in the ascending aorta. It is then advisable to wait at least five minutes to avoid flow changes in the splanchnic region caused by the contrast medium. Then the catheter will be withdrawn from the aorta and placed with its tip in the proximal part of the artery to be examined. It is important that the side holes do not spill contrast medium directly into the abdominal aorta during the injection of contrast medium. If this happens the densitometric area recorded from the selective injection will be spuriously low due to the spillover of contrast medium.

During the injection into the ascending aorta the contrast medium will be well mixed with the blood flow at the site of injection. However the selective injection in the splanchnic vessel should be performed manually over at least two seconds. Previously (LINK *et coll.*) it was found that an important error in the videodensitometric method is introduced when the injection rate approaches the blood flow at the site of injection. Thus when the injection flow rate was greater than one half the arterial flow rate there was an obvious discrepancy between the videodensitometric and electromagnetic methods. It has also been shown that perfect mixing of the contrast medium with the flow does not seem to be of great importance during selective injection into the artery since the videodensitometric window measures the total amount of contrast medium over an arterial cross section rather than local concentrations of medium within the vessel. The effects of contrast medium after selective injection into the splanchnic vessels can be neglected as they occur after the densitometric curve has been obtained over a main branch of the arterial tree. If a repeated injection into the splanchnic vessel is conducted it is again advisable to wait several minutes to obtain baseline flow.

The objective of this investigation was to compare the accuracy of the videodensitometric method with a known standard the electromagnetic method. The individual experiments showed an extremely good correlation ($r=0.985$). The technique can easily be

used to compare the effects of different drugs in the superior mesenteric artery (Fig. 3). The relationship among the flows in the splanchnic arteries can be compared by making a reference injection in the aorta above the origin of the coeliac axis not necessarily in the ascending aorta. The video camera would be positioned in a field covering the superior mesenteric, hepatic and splenic arteries. Then the same reference injection would be compared with each selective injection into these arteries. In the present investigation the hepatic artery flow was estimated to about 10 per cent of the cardiac output and the corresponding figure for the splenic artery flow was 7 per cent. On the other hand the flow in the superior mesenteric artery varied over a wide range (10–40% of the cardiac output). This could be due to a block of the compensatory mechanisms in that region caused by the extensive surgery required to attach the electromagnetic probes. Dissection of the superior mesenteric artery in its proximal part involves the ligation of multiple splanchnic nerves and this may destroy regulation of the blood flow.

The videodensitometric method seems to have several advantages over the previously described spillover technique (OLIN & REDMAN 1966, GIAN TURCO *et coll.* 1970). With this technique the blood flow in the superior mesenteric artery is estimated at angiography by increasing the rate of injection into this artery until spillover of contrast medium appears on the films. Multiple injections of higher and higher dose can be time consuming and may subject the patient to more risk from the injections of contrast medium than the benefits gained from the flow measurements. Other methods using dye dilution techniques involve catheterization of the superior mesenteric vein as well as arterial catheterization. Venous catheterization can be performed through transhepatic techniques or by catheterization of the umbilical vein. Both procedures carry some adherent risk and are time consuming.

The present investigation proposes the videodensitometric method as a simple clinical tool for estimating flows in splanchnic arteries as a fraction of the cardiac output. The simplicity of the method makes it well adapted to flow measurements during routine abdominal angiography and will give important functional data of the splanchnic flow not readily available by other means. With the aid of a densitometer and a videotape or cassette recorder the measurements can be performed by the radiologist during routine angiographic procedures.

SUMMARY

A new videodensitometric method of measuring blood flow in the splanchnic arteries as a fraction of the cardiac output was compared to electromagnetic flow readings in dogs. A previous investigation regarding the accuracy of the method in vitro was extended to prove that the videodensitometric technique was highly accurate also in vivo. The simplicity of the technique suggests that the videodensitometric method could be used to estimate blood flow in splanchnic arteries during routine angiography.

ACKNOWLEDGEMENTS

The authors wish to express their sincere thanks to C G R Medical Corporation for their support of a constant potential generator to Mallinckrodt Inc for supplying contrast media and to Steve Wilkins and Jane Kendrick for generous technical assistance. The investigation was partly funded by the Medical School University of California Davis.

Request for reprints: Dr B M T Lantz, Diagnostic Radiology, FOLB 2 F3 4301 X Street, Sacramento, California 95817, USA.

REFERENCES

- BERGAN J J. Recognition and treatment of intestinal ischaemia. *Surg Clin N Amer* 44 (1964) 71.
- BRADLEY S E, INGELFINGER F J, BRADLEY G P and CURRY J J. The estimation of hepatic blood flow in man. *J clin Invest* 24 (1945) 890.
- MARKS P A, REYNELL P C and MELTZER J. The circulating splanchnic blood flow volume in dog and man. *Trans Am Soc Physiol* 66 (1953) 294.
- BROOKSBY G A and DONALD D E. Dynamic changes in splanchnic blood flow and blood volume in dogs during activation of sympathetic nerves. *Circulat Res* 29 (1971) 227.
- DERRICK J K and LOGAN W D. Mesenteric arterial insufficiency. *Surgery* 44 (1958) 832.
- GIANTURCO C, SHIMIZU T, STEFFERDA F R and TAYLOR R P. Measurement of blood flow by angiography with increasing rate of injection. *Experimental Invest Radiol* 5 (1970) 361.
- GRAYSON J and MENDEL D. Physiology of the splanchnic circulation. Williams and Wilkins, Baltimore 1965.
- JACKSON H H. Occlusion of the superior mesenteric artery. Monograph in American Lectures in St. Charles C Thomas Springfield Illinois 1963.
- KORNER P I, CHALMERS J P and WHITE S W. Mechanisms of reflex control of the circulation by the sympatho-adrenal system. *Circulat Res* 20 (1966) 157.
- LANTZ B M T. A methodologic investigation of roentgen videodensitometric measurement of renal blood flow. University of California Press, Davis 1974.
- Relative flow measured by roentgen videodensitometry in hydrodynamic model. *Acta radiol Diagnost* (1975) 503.
- HOLCROFT J W, FOERSTER J M, LINK D P and REID M H. Determination of blood flow through arteriovenous fistulae and shunts. *Acta radiol Diagnost* 20 (1979) 727.
- LINK D P, LANTZ B M T, FOERSTER J M, HOLCROFT J W and REID M H. New videodensitometric method for measuring renal artery blood flow during routine arteriography. Validation in the canine model. *Invest Radiol* (1979) in press.
- MARSTON A, PHEILS M T, THOMAS M L and MORSE B C. Ischaemic colitis. *Gut* 7 (1966) 1.
- MELLANDER S and JOHANSSON B. Control of resistance, exchange and capacitance functions in the peripheral circulation. *Pharmacol Rev* 20 (1968) 117.
- OLIN T and REDMAN H. Spillover flowmeter. A preliminary report. *Acta radiol Diagnost* 4 (1966) 217.
- PURDUE G D and SMITH K B. Intestinal ischemia due to mesenteric arterial disease. *Amer J Surg* 36 (1948) 152.
- ROSS G. The regional circulation. *Ann Rev Physiol* (1971) 445.
- ROWELL L H. Dye techniques for estimating hepatic splanchnic blood flow in man. In: *Dye curves: The theory and practice of non diffusible indicator dilution*. Edited by D A Bloomfield. University Park Press, Baltimore 1974.
- The splanchnic circulation. In: *The peripheral circulation*. p 163. Edited by R Zelis. Grune and Stratton, New York 1975.
- WILLIAMS L F, ANASTASI L F, HASIOTIS C A, BARNIAK M A and BYRNE J J. Nonocclusive mesenteric infarction. *Amer J Surg* 114 (1967) 376.
- WOOD E H, STURM R E and SANDERS J J. Data processing in cardiovascular physiology with particular reference to roentgen videodensitometry. *May Clin Proc* 39 (1964) 849.

ANGIOGRAPHY IN UTERINE AND ADNEXAL TUMORS

B KARLSSON and P H PERSSON

Angiographic evaluation of gynecologic and obstetric lesions was introduced in 1952 by BORELL et coll followed by several later publications (BORELL & FERNSTROM 1953 1954 BORELL et coll 1955) The appearance of the uterine artery and its branches in cases of pelvic masses was described by FERNSTROM (1955) At that time the common angiographic technique was aortography and the diagnostic accuracy was poor Later the angiographic technique improved and the value of bilateral selective internal iliac angiography was pointed out by ALTEMUS (1968 1969) Selective angiography of the ovarian artery was introduced by KAHN & FRATES (1968) and FRATES (1969)

However angiography is seldom performed in the preoperative evaluation of adnexal tumors Although LANG (1967) stated The single most important advice toward an accurate preoperative diagnosis in the assessment of pelvic tumors can be attributed to the introduction of pelvic angiography to the diagnostic examinations of this area

Since then ultrasound has come into extensive use and later to some extent also computer tomography They are both easy and non invasive procedures but they fall short in differentiating between malignant and benign tumors

The angiographic appearance and the usefulness of angiography in patients with a pelvic mass were investigated in a prospective series and the results are now reported

Material and Methods

The material consisted of 106 females with a palpable pelvic tumor 63 of these being non

symptomatic and without previous history of gynecologic tumors These 63 have been presented previously (KARLSSON & PERSSON 1979) In all patients ultrasound examination confirmed the palpated mass before pelvic angiography All of the patients were operated upon and microscopic diagnosis of the tumors obtained The age of the patients varied from 27 to 80 years mean 55

The angiographic technique was the same as described previously (KARLSSON & PERSSON) Lumbar aortography and selective bilateral internal iliac angiography were performed in all 106 patients selective catheterization of the ovarian artery was performed in 8 The diameter of the arteries of interest was measured with a scale lupe with 10 times magnification

Results

Anatomic considerations One great difficulty in angiography of the uterus and the adnexa is that they receive their blood supply from four sources i.e. both ovarian arteries and both uterine arteries (Figs 1 2)

At aortography the ovarian artery was demonstrated on one side or both in 66 of the 106 patients (62%) the origins of the ovarian arteries could be determined in 85 (Table 1) When bilaterally demonstrated (29 patients) the origins were not separated in height by more than 1 cm except in one case in which the origin of the left artery was at the level of the upper border of L2 and the right at the upper border of L3 i.e. a difference of about 3 cm

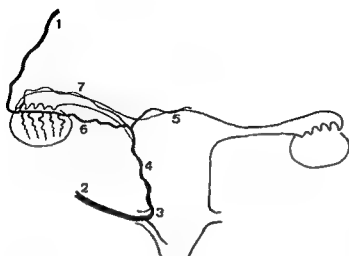


Fig. 1 Drawing of normal uterus and adnexa. 1 Ovarian artery. 2 Uterine artery in its parametrial course. 3 Junction of parametrial and marginal parts. 4 Uterine artery in its marginal course. 5 Fundal branch. 6 7 Tubo-ovarian branches.



Fig. 2 Branches from the normal iliac artery. 1 Superior artery. 2 Inferior gluteal artery. 3 Uterine artery. 4 Obturator artery. 5 Internal pudendal artery. 6 Vesical artery. 7 Haemorrhoidal artery.

The origin of the following main branches of the internal iliac artery could be determined: the superior and the inferior gluteal artery and the internal pudendal artery; the three groups suggested by NILSSON (1967) could be distinguished. The origin of the uterine artery, the vesico vaginal arteries and the middle haemorrhoidal artery could not be determined but these arteries could be identified by their typical course in the pelvis. The obturator artery had its origin from the external iliac artery in 33 cases (30%) in 16 cases bilaterally in 11 from the right and in 6 from the left side. In 2 cases an accessory pudendal artery was demonstrated.

Fibromyomas were found in 34 patients, aged 31 to 78 years, mean 56. The vascularity of the tumors is given in Table 2. In 28 of these 34 cases irregular tortuous vessels combined with arched capsular vessels typical for myomas (FERNSTRÖM 1955) appeared. The remaining 6 cases had no intrinsic ves-

sels at all but in 5 of them loss of tortuosity of marginal segment of the uterine artery and lateral displacement of the parametrial-marginal junction indicated enlargement of the uterus (ALTE 1969). In one patient the uterine arteries were demonstrated depending on severe atheromatosis. Intramural and subserous myomas occurred in 11 patients, pedunculated myomas in 4 and one patient had an intraligamentary myoma (Fig. 3). The angiographic appearances of all these myomas were the same except in one of the patients with a pedunculated myoma in whom a typical pedicle was demonstrated.

The width of the uterine arteries could be measured in all patients but one (Table 3). The sum of width of the two uterine arteries increased with size of the myomatous uterus. The two arteries sometimes differed markedly in diameter on the sides; the wider artery supplying the major part

Table 1

Level of origin of the ovarian artery observed at aortography

First lumbar vertebra	3
Second lumbar vertebra	60
Third lumbar vertebra	18
Right renal artery	2
Left renal artery	2
Total	85

Table 2

Degree of vascularity of the myomas related to size

Size (cm) of uterus/myoma	Intrinsic vessels		
	Many	Few	None
<4.9	3	1	1
5.0-9.9	6	2	2
10.0	13	3	3



a



b

Fig 3 Bilateral internal iliac angiography in a patient aged 59 with an intraligamentary myoma. a) Early and b) late arterial phase. Vessels of the normal uterus (→) left uterine artery stretched in

its parametrial course (↔) The myoma is outlined by arrows in (b)

the myoma. In 7 of the cases the ovarian arteries were demonstrated at aortography. In 3 of them bilaterally. The diameter of the ovarian artery varied from 1.0 mm to 3.0 mm. In 5 of the patients a small ovarian cyst on one side was also revealed at operation. One case with a 22 cm myomatous uterus had bilateral small endometrial cysts which were not demonstrated at angiography. A stalked myoma was erroneously considered as an ovarian carcinoma. One patient had besides the myoma pathologic vessels at the site of the left ovary. Operation proved this to be an old inflammatory lesion.

Benign ovarian tumors were found in 32 patients aged 27 to 80 years, mean 56 (Table 4). 3 of them had bilateral tumors. At aortography the ovarian artery

was demonstrated in 19 patients. In 17 of these on the same side as the tumor and in 11 cases bilaterally. The artery on the tumor side was at least 0.5 mm wider than the contralateral one in all but one case. In 17 cases with an ovarian artery supplying the tumor a tubo-ovarian branch from the uterine artery on the same side was observed. In 15 at selective iliac angiography. In 24 patients a tubo-ovarian branch from the uterine artery supplying the tumor was demonstrated. Often as a single non tortuous branch stretched and arched along the surface of the tumor (Fig 4). In 10 of these 24 cases the branch supplying the tumor had a diameter of less than 1 mm. In the remaining cases 1 mm or more. In 6 patients with unilateral tumor bilateral tubo-ovarian

Table 3

Size of the myomas related to the sum of the diameters of both uterine arteries

Size (cm) of uterus/myomas	Width (mm) of the uterine arteries						
	1	3	4	5	6	7	8
<4.9	1	1	1	1			
5.0-9.9		1	1	2	3	3	
10.0-		1	2	6	6	2	1

Table 4

Benign ovarian tumors

Diagnosis	No of cases	Size (cm)	Contrast accumulation in tumor
Cystadenoma			
Simple and serous papillary III	4	4-12	3
Mucinous	7	5-20	2
Teratoma	4	4-13	0
Endometrioid cyst	4	5-12	2
Fibroma	3	7-15	0



a

Fig 4 Simple cyst 6 cm in diameter in the left ovary of a 42 year-old woman. Internal iliac angiography. a) Early and b) late arterial phase. Uterine arteries (→) of normal width; the left



b

stretched. The left ovarian branch (↔) is supplying the cyst which is not outlined.



a

Fig 5 Woman aged 40 with a 5 cm endometrioid cyst of the left ovary not demonstrated at iliac angiography. a) Early and b) late



b

arterial phase. The normal uterus is slightly displaced to the right; a single and tortuous ovarian branch (→) on the left side.

branches were demonstrated: the one on the side of the tumor being wider in all but one case. No appreciable relationship was found between the width of the branches and the size or nature of the tumor, nor was further branching of the main stem of any significance. The appearance of the branch was the

same in solid and cystic tumors (Fig 5). In 6 patients, 2 with simple cysts, 2 with mucinous cysts, and 2 with fibromas, no branches supplying the tumors were demonstrated. Four of these patients had a severe atheromatosis while 2 had normal pelvic arteries.



Fig 6 Iliac angiography in a 57-year-old woman with a left-sided benign cyst. In the late arterial phase the shape and size of the cyst (→) is observed because of accumulation of contrast medium in its wall.



Fig 7 Inoperable bilateral ovarian carcinoma in a 58-year-old woman. The left uterine artery (++) is infiltrated the right is occluded by the carcinoma. Abnormal vessels originating from the ovarian branch (→).

Tumors larger than 6 to 7 cm in diameter as a rule caused elongation and stretching of the parametrial course of the uterine artery on the same side. Ovarian tumors larger than 6 cm always displaced the uterus over to the contralateral side. In 2 cases a change of caliber of the vessels and irregularities of the type usually associated with malignancy were observed. One of these patients had a localized fatty necrosis close to the left ovary and the other had a small benign endometrioid cyst.

Accumulation of contrast medium within the tumor occurred in 7 patients. In the capillary phase a faint rim of contrast medium in part of the tumor capsule was demonstrated (Fig 6). The tumor was well circumscribed in 2 cases with the rim clearly circumscribing the whole ovarian tumor. The drain-

ing veins were demonstrated in 8 cases in 6 bilaterally with the same contrasting effect on both sides. No difference was noted between cases of solid and cystic tumors.

Malignant ovarian tumors were found in 28 patients bilaterally in 8. The age of the patients varied from 29 to 77 years, mean 58. Type, size and vascularity of the tumors appear in Table 5.

In all cases but 2 an ovarian artery was demonstrated on the side of the tumor at aortography. Bilateral ovarian arteries were found in 12 cases, 4 of which had bilateral tumors. When bilaterally demonstrated the ovarian artery on the tumor side was always wider than the one on the contralateral side. In 2 cases with bilateral carcinomas the larger carcinoma measured 6 and 9 cm in diameter respectively while the contralateral malignant ovary was of normal size. In these 2 cases only the ovarian artery on the side of the larger tumor was demonstrated. Pathologic vessels were filled from both the ovarian artery and from the tubo-ovarian branch; no pathologic vessels were found in the two malignant ovaries of normal size. Four of the bilateral carcinomas were large, measuring 20 to 25 cm, and 3 of these had no pathologic vessels from either the ovarian arteries or tubo-ovarian branches. The fourth of these large bilateral carcinomas obtained

Table 5

Malignant ovarian tumors

Diagnosis	Size (cm)	Pathologic vascularity			
		Rich	Medium	Sparse	None
Adenocarcinoma	4-30	4	11	10	5
Struma ovarii	7-17		2		
Teratoma cystic	70	1			

pathologic vessels from the tubo ovarian branch (Fig 7)

Of the 20 cases with unilateral carcinoma tubo ovarian branches were demonstrated bilaterally in 4 cases in 2 of these it was wider on the tumor side and in one case wider on the side of the normal ovary In one case the tubo ovarian branch had the same width on both sides In 3 cases further branching of the main stem of the tubo ovarian branch was demonstrated all in tumors smaller than 10 cm one of them cystic Two cases had pathologic vessels from a wide ovarian artery (Fig 8) the other 16 from the tubo ovarian branch

Pathologic vessels were sparse in 10 cases and absent in 5 (Table 5) Four cases had a rich vascularity which was not related to degree of malignancy size or nature (solid-cystic) of the tumor (Fig 9) In 3 cases with extensive tumor growth pathologic vessels from the inferior mesenteric artery or the middle haemorrhoidal artery were demonstrated In no case was infiltration of the bladder arteries observed

The diameter of the ovarian artery varied from less than 1 mm to 3.5 mm The diameter of the tubo-ovarian branch as measured at the uterine cornu also varied from less than 1 mm up to 3.5 mm No relationship could be found between the width of the ovarian artery or the tubo ovarian branch and the size of the tumor or degree of malignancy

In 7 patients the draining veins were well observed in 6 bilaterally and with the same contrasting effect Another 3 cases had a faint venous phase No obvious early filling of the veins was demonstrated

Tumors of uncertain malignancy Whether the tumor was malignant or benign could not be established with certainty in 8 patients The age of these patients varied from 50 to 73 years The tumors were 3 serous cystadenofibromas 1 cystadenoma and 2 mucinous cystomas At fine needle aspiration biopsy preoperatively in 2 of these cases malignant cells had been found Both cases had serous cystadenofibromas and the ovarian tumours were bilateral in both cases Angiography showed pathologic vessels from the tubo-ovarian branch on only one side in both these cases The other 4 cases had no pathologic vessels 3 of them had a tubo ovarian branch supplying the tumor but it was not infiltrated One patient had a severe atheromatosis not permitting any diagnosis

Inflammatory lesions and miscellaneous Two pa-



Fig 8 Large malignant cystic teratoma in a 55 year old woman. Solid excrecences with abnormal vascularization in part III tumor

tients had old hematomas One measured 5 cm and was encapsulated after bilateral salpingo oophorectomy 3 years previously The other one was a descended rectus sheath hematoma and at palpation considered to be an ovarian tumor The angiography was normal in both

Two patients had unilateral sactosalpinx measuring 5 and 11 cm respectively In both cases the ovarian artery was wide on the same side 1.5 and 2 mm respectively Both these lesions were richly vascularized with a marked accumulation of contrast medium in the caudal part of the sacs The vessels had the same appearance as in a malignant lesion but the vascularity was more extensive than in ovarian carcinoma In these cases an early arterio venous shunting to the ovarian vein was demonstrated

Two patients had leiomyosarcoma originating from the small intestine both at palpation consid-



9 Large carcinoma in the left ovary of a 54-year-old woman. Internal iliac angiography. Tumor vessels filled. b) Selective



ovarian angiography. More extensive filling of the vessels. ovarian artery markedly widened.

er to be ovarian carcinoma. Both tumors had a rich vascularity with pathologic vessels from the inferior mesenteric artery. One case had a normal internal iliac angiography and gynecologic origin could thus be excluded (Fig. 10). The other patient had pathologic vessels from the lateral sacral arteries as well as from branches of the gluteal arteries. The origin of the tumor in this latter case could not be determined as uterus and the right adnex were involved in the large tumor mass.

Discussion

The ovarian arteries generally take their origin from the antero-lateral part of the aorta but may originate from one or both renal arteries most commonly the right. In autopsy materials this is reported to occur in 6 to 12 per cent by GERARD (1913), HASELHORST (1926) and JOACHIMOVITS (1931) but by ELISKA (1961) in 22 per cent. In 2 to 11 per cent two or more ovarian arteries originate from the aorta on one or both sides (GERARD, JOACHIMOVITS). In the present material only 4 of 85

ovarian arteries originated from a renal artery. No case of double ovarian arteries was observed. The difference between findings at autopsy and at angiography may be explained by the fact that the ovarian artery is small and usually insufficiently filled partly due to layering of the contrast medium partly to low flow in the narrow artery.

In the present material an ovarian artery was demonstrated in 62 per cent of the cases as compared to BORELL & FERNSTROM (1954) who reported only 20 per cent. Technical factors may account for this difference. Possibly aortography performed in prone position of the patient might improve the information.

Fibromyomas. The results (Table 3) confirm those of FERNSTROM (1955). In cases of large myomas he found an arched and non-tortuous course of the uterine artery in the parametrial and marginal part. ALTEMUS (1969) pointed out that the junction of the parametrial and marginal portions of the uterine artery becomes laterally displaced in cases of uterine enlargement and that this abnormality was pathognomonic. These findings were confirmed in



Fig. 10 Leiomyosarcoma of the small bowel in a 63 year old woman. Aortography. Large amount of pathologic vessels originating from the mesenteric arteries (→)

the present material. In cases of very large myomatous uteri the part of the main trunk running along the lateral pelvic wall looked shortened and the artery then took a direct course in latero cranial direction without the general horizontal course in the parametries. The uterine artery is often wide and divides directly into few and non tortuous arched vessels. In none of the 5 cases with very large 20 cm or more myomatous uteri was the vascularity rich in the intrinsic vessels were few in 2 cases and absent in 3.

As FAULKNER (1944) noted and FERNSTRÖM confirmed the two uterine arteries often differed in width the wider artery supplying the major part of the myomas. According to ALTEMUS (1969) extra uterine pedunculated myomas characteristically have a unilateral dilatation of the parametrial and marginal portion of the uterine artery unaccompanied by enlargement of the uterus. Two of the 4 cases with pedunculated myomas in the present material had this appearance while the other 2 had uterine arteries of the same width. The peduncu-

lated myoma falsely considered to be an ovarian carcinoma had an angiographic appearance indicating myoma at re examination of the films.

A rich vascularity occurred in 22 myomas of 1 (65%) but with increasing size, a tendency to less vascularity was found. In such cases the diagnosis may be established by a lateral displacement of the parametrial-marginal junction only or, if demonstrated, a lateral displacement of the marginal part.

Ovarian tumors. Detailed demonstration of ovarian and adnexal lesions requires demonstration of the tubo ovarian branches of either the ovarian artery or the uterine artery. This is not adequately obtained in aortography (DE DOMINICIS et coll. 1964, MARANTA et coll. 1964, LANG 1967, SMITH 1971). FERNSTRÖM described tubo ovarian branches in 42 of 71 cases with adnexal tumor, the demonstration not being related to size or type of tumor. He could relate the presence of a non tortuous and arched branch to the size of the tumor and the width of the branch to the nature of the tumor, solid tumors having wider branches than cystic ones. Further branching of the main stem of the tubo ovarian branch was present more often in cases of solid tumors. In this material no correlation between the width or the appearance of the tubo ovarian branch and the size or nature of the tumor was found. However, branching of the tubo ovarian main stem is more often present in cases of solid benign tumors and in cases of malignant ovarian tumors.

With pelvic angiography the size and shape of a benign ovarian tumor is only rarely demonstrated. FERNSTRÖM obtained good demonstration of the whole adnexal tumor in only one case, a richly vascularized ovarian fibroma. In the present material 1 benign ovarian tumor was entirely demonstrated, both were simple cysts and had a rim of contrast medium in the wall in the capillary phase. A satisfactory estimation of the size of the tumor but not the shape was given when the tubo ovarian branch encircled the tumor to at least half the circumference which occurred in about one fourth of the benign cases.

An ultrasound examination is mandatory to show the existence of an ovarian tumor and to determine its size, shape and nature. These last three qualities were impossible to evaluate angiographically in 30 of the 32 patients with benign ovarian tumors in the present material.

In patients with malignant tumors the ovarian

Table 6
Reliability myomas

Size (cm)	No. of patients	Correct diagnosis	False negative
< 5	5	4	1
6-15	10	9	1
16-	19	19	~
Total	34	32	2

Table 7
Reliability benign ovarian tumors

Size (cm)	No. of patients	Correct diagnosis	False negative
< 5	9	8	1
6-15	18	17	1
16-	5	5	-
Total	32	30	2

Table 8
Reliability ovarian carcinomas

Size (cm)	No. of patients	Correct diagnosis	False negative
< 5	3	2	1
6-15	17	16	1
16-	8	5	3
Total	28	23	5

tery on the tumor side was more frequently demonstrated than in patients with benign lesions. However, neither the diameter of the ovarian artery nor the diameter of the tubo-ovarian branch is of any significance in the differentiation between malignant and benign ovarian tumors. ALTFMUS (1969) noted a marked dilatation of the vessels comprising the ovarian arcade in 4 cases of ovarian malignant tumors, all solid and extremely vascular. He noted irregular distribution of contrast medium within a tumor in one case, a malignant ovarian teratoma.

The only criterion of malignancy is the presence of pathologic vessels, whereas other angiographic parameters typical of malignancy, such as accumulation of contrast medium, early arterio-venous shunting, irregular distribution of contrast medium within a tumor etc., are of much less importance.

Atheromatotic abnormalities in the pelvic vessels occur first in the uterine artery, probably due to postmenopausal uterine involution. Such a lesion in the uterine artery must not be considered as malignant infiltration, both conditions having the same angiographic appearance.

In this material 3 of 4 cases with bilateral ovarian carcinoma and large tumor masses had no pathologic vessels and this was probably due to tumor necrosis. In 2 cases of unilateral tumor, one being a 9 cm cystadenocarcinoma and the other a 5 cm adenocarcinoma, no pathologic vessels were demonstrated, but both these patients had advanced atheromatosis. Irregular distribution of contrast medium within the tumor was observed in one of the malignant tumors (Fig. 9); any obvious early arterio-venous shunting was not observed.

Thus 5 patients had malignant tumors which were considered benign, 2 having advanced atheromatosis and 3 a large and necrotic tumor. In 6 patients with large benign cystic tumors, no tumor vascularity was demonstrated, 4 due to advanced atheromatosis. These two factors, atheromatosis and tumor necrosis, appear to be the main reasons for erroneous diagnosis at angiography in gynecologic tumors. Also the size of the tumor is of importance. In 2 cases carcinoma was found in an ovary of normal size and shape and without pathologic vessels. The smallest angiographically diagnosed carcinoma in the present material measured about 4 cm in diameter and had a sparse vascularity.

Inflammatory lesions may simulate malignant tumors. Two patients with sacrosalpinx had rich vascularized tumors. The vascular appearance could not be distinguished from that in cases of malignancy.

The reliability of the angiographic diagnoses appears in Tables 6 to 8.

Thus taken together of 68 patients with ovarian lesions, 38 benign and 30 malignant, 5 false negative and 4 false positive diagnoses regarding malignancy were encountered; the angiographic accuracy being 87 per cent. Of the 34 myomas, a correct diagnosis could not be reached in 2 (6%).

In 21 of the 106 patients (20%) the vascular appearance did not allow a definitive diagnosis whether the tumor was ovarian or not. However, 5 of these had widening of the parametrial-marginal junction and a uterine enlargement suggesting myoma.

These figures show that angiography is a valuable examination and a good supplement to ultrasound examination for differentiating malignant and benign lesions and to discriminate between uterine and ovarian tumors.

SUMMARY

A series of 106 patients with uterine or adnexal lesions is presented. Bilateral selective internal iliac angiography proved to be valuable in the preoperative diagnosis of gynecologic tumors regarding their origin and in the differential diagnosis between malignant and benign tumors.

REFERENCES

- ALTEMUS H. Selective catheterization of the hypogastric arteries: advantages and discussion of technique. *Radiology* 91 (1968) 484.
- Differentiating uterine and extrauterine masses by bilateral selective hypogastric arteriography. *Radiology* 92 (1969) 1020.
- BORELL U. and FERNSTRÖM I. The adnexal branches of the uterine artery. An arteriographic study in human subjects. *Acta radiol* 40 (1953) 561.
- The ovarian artery. *Acta radiol* 42 (1954) 253.
- LINDBLÖM K. and WESTMAN A. The diagnostic value of arteriography of the iliac artery in gynecology and obstetrics. *Acta radiol* 38 (1952) 247.
- and WESTMAN A. The value of pelvic arteriography in the diagnosis of mole and chorionepithelioma. *Acta radiol* 44 (1955) 378.
- DE DOMINICIS R., PELU G., GIANNARDI G. F., GASPARRI F., BUFALINI G. N. and GERLI P. L'indagine radiologica nello studio dei tumori dei genitali femminili con particolare riguardo alle ricerche angiografiche. (*Italian*) *Radiol med* 50 (1964) 705.
- ELISKÁ O. Venae et arteriae spermaticae a Jeyich v tabulce (In Czech). *Čs Morfol* 9 (1961) 200.
- FAULKNER R. L. The blood vessels of the myometrium, uterus. *Amer J Obstet Gynec* 47 (1944) 185.
- FERNSTRÖM I. Arteriography of the uterine artery. *Acta radiol* (1955) Suppl. No. 122.
- FRATES R. Selective angiography of the ovarian artery. *Radiology* 92 (1969) 1014.
- GERARD G. Sur les variations d'origine et de nombre des artères génitales, spermaticques ou ovariennes, chez l'homme. *C R Soc Biol* 74 (1913) 778.
- HASELHORST G. und SCHILLING W. Die Bedeutung der Arteriae ovaricae für Postpartumblutungen insgesamt bei der Aortenkompression. *Arch Gynäk* 129 (1926) 300.
- JOACHIMOVITS R. Varietäten der Anastomosen zwischen Arteria ovarica und Arteria uterina. *Arch Gynäk* 16 (1931) 697.
- KAHN P. and FRATES R. The value of angiography of the small branches of the abdominal aorta. *Amer J Roentgenol* 102 (1968) 407.
- KARLSSON S. and PERSSON P. H. Angiography, ultrasound and fine needle aspiration biopsy in the evaluation of gynecologic tumors. *Acta radiol Diagn* 20 (1979) 779.
- LANG E. Arteriography in gynecology. *Radiol Clin* 1 (1967) 133.
- MARANTA E., CAMPONOVO F. und DEL BUONO M. S. Die Beckenangiographie. *Fortschr Röntgenstr* 10 (1964) 229.
- NILSSON J. Angiography in tumours of the urinary bladder. *Acta radiol* (1967) Suppl. No. 263.
- SMITH R. S. Pelvic arteriography in the differential diagnosis of pelvic mass. *Amer J Obstet Gynec* 111 (1971) 952.

FROM THE DEPARTMENTS OF DIAGNOSTIC RADIOLOGY (DIRECTOR PROF T OLIN) AND PATHOLOGY (DIRECTOR PROF S FALKMER) MALMÖ ALLMANNA SJUKHUS S 21401 MALMÖ AND THE DEPARTMENT OF DIAGNOSTIC RADIOLOGY (DIRECTOR PROF E BOJSEN) UNIVERSITY HOSPITAL S 22185 LUND SWEDEN

ANGIOGRAPHY IN ANGIOMATOUS LESIONS OF THE GASTROINTESTINAL TRACT

U NYMAN E BOJSEN C LINDSTRÖM and J E ROSENGREN

Angiomatous lesions of the gastrointestinal tract have rarely been encountered in the past. GENTRY et coll (1949) reviewed 1400 000 case charts at the Mayo Clinic and found 106 cases of gastrointestinal angiomatous lesions. A review of the literature covering the last century by DWYER & STEINLAUF (1964) revealed 200 cases. During the past 15 years an increasing number of vascular abnormalities have been diagnosed with angiography (BAER & RYAN 1976 MOORE et coll 1976 BOLEY et coll 1977 b). The stated incidence in the previous reports obviously reflects a lack of recognition rather than the true incidence, since many of these vascular lesions are too small to be diagnosed by traditional methods and may easily escape detection at surgery and autopsy.

The term angiomatous lesion is used to encompass terms like angioma, hemangioma, hamartoma, angiodysplasia, phlebectasia, and telangiectasia, which are frequently used indiscriminately and interchangeably in the literature.

These lesions may cause mechanical obstruction of the bowel, intussusception, perforation of the bowel, and consumptive coagulopathy (Kasabach-Merritt syndrome), but hemorrhage, sometimes massive, is the major complication which may occur in 25 to 50 per cent of the cases (GENTRY et coll CALEM & JIMENEZ 1963).

This report presents the experiences of gastrointestinal angiomatous lesions at these hospitals, draws attention to some conditions in which such lesions affect the bowel, and emphasizes the value and limitations of visceral angiography as a diagnostic tool.

Material and Methods

Angiography was performed in 20 patients with gastrointestinal angiomatous lesions: 11 females and 9 males ranging in age from 3 months to 28 years. Their data are summarized in the Table. Two patients were referred for angiography to evaluate the extension of angiomatous lesions already diagnosed. The remaining 18 were referred because of unexplained gastrointestinal hemorrhage: 16 because of chronic intermittent low grade blood loss, and 2 because of brisk rectal bleeding. In the group of chronic bleeders the duration of symptoms ranged from 5 months to 12 years (median 1 year). Repeated barium examinations and endoscopy had failed to reveal the bleeding source in these cases. No unrewarding explorative laparotomy had been performed in any patient before the angiography.

Results

Angiomatous lesions were found at angiography in all patients, but 3 in whom lesions were subsequently found at surgery (cases 2, 4) and autopsy (case 1). In most patients the lesion was one cm or less in diameter.

Surgery following angiography (14 patients). Excision of the lesion was performed in 5 patients and segmental bowel resections in 8. The angiomatous lesions were visible on the serosal surface of the bowel in 4 patients, on the mucosal surface in 4 when the bowel had been opened according to the

Table
Data on 20 patients with gastrointestinal angiomatous lesions

Case No	Sex/age*	Duration of symptoms	Type of angiography	Site of lesion		Extra gastrointestinal manifestation	Surgery
				Angiography	Other methods**		
1	F/82	3 yrs	Cc Ms	-	Esophagus stomach jejunum ileum and right colon	Tongue lungs liver and bone marrow	-
2	M/61	6 mos	Cc Ms	-	Jejunum	-	Segmental resection of jejunum
3	F/3 mos	1 mo	Ao	Jejunum and ileum	Jejunum and ileum	Skin	Diagnostic laparotomy
4	F/56	3 yrs	Cc Ao	-	Jejunum and ileum	Skin	Segmental resection of jejunum and ileum
5	F/62	6 mos	Cc Ms	Right colon	Jejunum and sigmoid colon	Tongue	Segmental resection of jejunum and sigmoid colon
6	M/47	1 yr	Cc Ms	Ileum	-	Skin liver pancreas and spleen	-
7	F/57	5 days	Cc Ms	Ileum	Ileum	-	Ileo-cecal resection
8	F/24	2 yrs	Cc Ms Ao	Ileum and right colon	Ileum	-	Segmental resection of ileum
9	M/47	2 days	Cc Ms Mi	Cecum	Cecum	-	Excision of lesion
10	M/55	6 mos	Cc Ms	Cecum	Cecum	-	Excision of lesion
11	M/61	6 yrs	Cc Ms	Cecum	Cecum	-	Excision of lesion
12	M/70	9 mos	Cc Ms Mi	Cecum	Cecum	-	Right hemicolectomy
13	M/73	2 yrs	Cc Ms	Cecum	Cecum	-	Excision of lesion
14	F/74	1 yr	Cc Ms	Cecum	Appendix	-	Right hemicolectomy
15	M/77	2 yrs	Cc Ms Mi	Cecum	Cecum	-	Excision of lesion
16	F/81	5 mos	Cc Ms Mi	Cecum	Cecum	-	Ileo-cecal resection
17	F/76	6 mos	Cc Ms Ao	Cecum and transverse colon	Cecum and transverse colon	Tongue	Right hemicolectomy and later colectomy
18	F/67	6 mos	Cc Ms Mi	Transverse colon	-	-	Ligation of branch from middle colic artery
19	M/58	-	Cc Ms Mi	Rectum and sigmoid colon	Rectum and sigmoid colon	Skin and right leg	Resection of sigmoid colon
20	F/58	12 yrs	Ms Mi Ao	Rectum	Rectum	-	-

At the time of the first angiography

Barium examination endoscopy surgery or microscopy

No further hemorrhage Cc = Celiac angiography Ms = Superior mesenteric angiography Mi = Inferior mesenteric angiography Ao = Aortic angiography

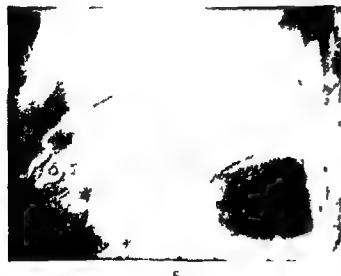


Fig 1 Case 8 Patient with thrombocytosis, intestinal hemorrhages and attacks of abdominal pain. a) Superior mesenteric angiography: enlarged ileal artery and filling of dilated veins during arterial phase (→). b) Microphotograph of ischemic stricture: mesenteric vessel occluded by organized thrombus (→); increased vasculation in the vicinity (++) Weigert's elastin (*) c) Superior mesenteric angiography (magnification view) 4 years later: Angiomatous lesion in the right colon, not present at previous angiography: slow filling of dilated veins beginning in late arterial phase

years later, recurrence of the disorder in the rectum and distal part of the colon was found at a routine rectoscopy followed by a double contrast colon examination (Fig 3a). No symptoms were present. At angiography, poor contrast filling of the vascular lesion occurred; slow circulation in the affected part of the bowel and several phleboliths were visible along the bowel wall (Fig 3b). This patient also had

angiomatous lesions of the right leg with varices since childhood, including soft tissue and bone hypertrophy, changes consistent with the Klippel-Trenaunay syndrome.

In a third patient (case 1), the angiography was without evident abnormality, but at autopsy 5 years later, numerous angiomatous lesions were found in the gastrointestinal tract.



a



b

Fig 2 Case 3 Infant with diffuse angiomatous lesion of the small intestine. Angiography a) Arterial phase enlarged superior mesenteric artery (→) same width as the lumbar aorta b) Capil-

lary phase Contrast accumulation within vascular spaces in jejunum and ileum and early filling of superior mesenteric vein (→) and portal vein (↔)

In a fourth patient (case 5) resection had been carried out of the jejunum and sigmoid colon because of angiomatous lesions. When the bleeding episodes continued postoperatively angiography was performed but no bleeding source was observed. Two years later angiography was repeated demonstrating early contrast filling of dilated veins lining the right colon but the bleeding was not severe enough to require surgical intervention. A fifth patient (case 6) previously reported by NYMAN (1977) had a small angiomatous lesion in the ileum. The low grade gastrointestinal hemorrhage could also have emanated from angiographically observed multiple angiomatous lesions in the liver and pancreas.

A sixth patient (case 20) had a rectal lesion found at endoscopy and angiography but it was not considered to represent the bleeding source.

Among all 20 patients a solitary angiomatous lesion in the gastrointestinal tract was found in 13 and only one of these had similar vascular abnormalities in other organs. Multiple lesions or a diffuse involvement were present in the remaining 7 patients

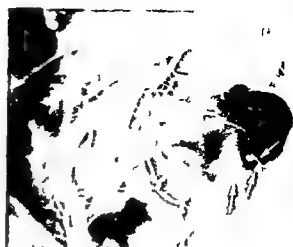
and all but one had similar abnormalities in other organs.

Discussion

Angiomatous lesions of the gastrointestinal tract are solitary or multiple. They may vary in size from a few mm to pedunculated or polypoid masses projecting into the bowel lumen or diffusely infiltrate large segments of the bowel wall adjacent soft tissue or organs (WOOD 1967). The bowel lesion may be only one manifestation of a widespread vascular disorder with multiple organs involved such as in hereditary hemorrhagic telangiectasia (Rendu), Osler-Weber disease (SMITH et coll 1963), HALPERN et coll 1968), blue rubber bleb nevus syndrome (BAKER et coll 1971), HAGOOD & GATHRIGHT (1975), Maffucci's syndrome (LEWIS & KETCHAM 1973), Kaposi's sarcoma (HAYLOCK 1963), KANTER et coll 1968, PALMER 1972, MANN 1974), Klippel-Trenaunay syndrome (GHAHREMANI et coll 1976) and diffuse neonatal hemangiomatosis (HOLDEN & ALEXANDER 1970). Cutaneous angiomatous lesions



a



b



c

Fig 3 Case 19 Klippel Trenaunay syndrome. a) Double contrast examination of rectum and distal colon with narrow-necked ampulla recti and flat indentations of the anterior aspect of bowel wall representing angiomatous lesions b) Inferior venteric angiography. Filling of widened vascular space and phleboliths along the bowel wall (++) c) Microphotograph of resected specimen 20 years previously. groups of cavernous vessels (→) in the submucosa with calcified thrombi. Hemala-eosin $\times 17$

are not seldom found concomitant with visceral ones. In the collective review of RISSIER (1959) this occurred in 30 per cent of the patients with intestinal lesions and in a pediatric age group the corresponding figures were 49 per cent (ABRAHAMSON & SHANDLING 1973).

Various classifications of angiomatous lesions in the gastrointestinal tract have been attempted based on macro- and microscopic appearances angio-

graphic characteristics and clinical behaviour of combination of these (KAUSER 1936 GENTRY 1936 coll WOOD MOORE et coll.) RISSIER pointed out that any classification is of limited value because of the great overlap between various types. Furthermore the etiologic and pathologic factors are probably multiple. Various theories have been proposed angiomatous lesions may represent restricted disorders congenital defects neoplastic



a

b

Fig 4 Case 10 Angiodysplasia of right colon a) Vascular tuft (b) filling of a dilated submucosal vein during arterial phase

proliferation vascular proliferation in inflammatory states or be the result of a degenerative process of ongoing mucosal ischemia functional shunting or an angiogenesis factor (HANSEN 1948 SHEPHERD 1953 ROBINS 1968 WARNER & O LOUGHLIN 1975 BAER & RYAN BAUM et coll 1977 BOLEY et coll 1977b)

The most common type observed at angiography is the angiodysplasia in the right colon (GENANT & RANNIGER 1972 SHEEDY et coll 1975 BAER & RYAN BAUM et coll BOLEY et coll 1977b ATHANASOULIS et coll 1978) They have the following features in common (1) they occur predominantly in patients over the age of 55 (2) are not associated with vascular lesions of the skin or internal organs (3) may produce chronic low grade or intermittent brisk rectal bleeding (4) are small usually 5 mm or less and can generally not be identified at surgery or at examination of the resected specimen unless special injection techniques are used and (5) cannot be detected by barium examinations and are only rarely identified with colonoscopy Angiography is therefore the primary method for their detection

In agreement with the literature the most common location of angiomatous lesions in the present series was in the right colon (12 patients) In 8 of these no vascular lesions were found outside the right colon and all 8 exhibited angiographic findings of angiodysplasia (Figs 4 5) i.e. a slowly emptying dilated and tortuous intramural vein a capillary accumulation of contrast medium or vascular tuft or early contrast filling of a dilated vein (BOLEY et coll 1977a) Though in one patient (case 14) the vascular abnormality proved to be confined to a short retrocecal appendix adherent to the colon at the pathologic examination thereby simulating a cecal angiodysplasia at angiography A similar case was reported by FOSTER et coll (1971)

In the remaining 4 patients the right colon lesions were associated with vascular lesions in other parts of the bowel and in other organs and they probably represent angiomatous entities different from right colon angiodysplasia Three of these 4 patients had hereditary hemorrhagic telangiectasia They belonged to the same age group as those in whom angiodysplasia of the right colon occurs The angiographic features of the right colon lesions in 2



Fig 5 Case 12 Angiodysplasia of the right colon a) Late arterial phase filling of a dilated submucosal vein b) Magnification view demonstrating the vascular tuft not seen in (a)

of the patients were the same as those described for angiodysplasia. This emphasizes the importance of detailed coeliac superior and inferior mesenteric angiography even though a typical right colon angiodysplasia has been found. In addition BAUM *et coll* reported that angiographic abnormalities considered to be angiodysplasia were presumably caused by cecal carcinoma in 2 patients and segmental right colitis in one. Similar difficulties occurred in one patient with a cecal carcinoma not included in the present series.

When bleeding is sufficiently severe and all examinations are normal except for an angiographic diagnosis of angiodysplasia of the right colon surgery is recommended. If no other lesions are found to account for the hemorrhage at laparotomy a right hemicolectomy is the mode of therapy since angiodysplasia can be multiple within the right colon (BOLEY *et coll* 1977 b).

A diagnosis of hereditary hemorrhagic telangiectasia was made in 4 patients. This disorder is probably due to congenital defects within the walls of small vessels resulting in angiomatous lesions with arteriovenous communications. Any organ in the body may be affected and hemorrhage from gastrointestinal telangiectasia occurs in approximately

15 per cent of the patients with Osler's disease (SMITH *et coll*). No family history could be obtained in 3 of the present patients with this disease. However this does not exclude the diagnosis which is based on the macro and microscopic appearance of the angiomatous lesions and the multiple or focal involvement. At visceral angiography these lesions appear as single multiple or diffusely scattered vascular tufts of various sizes and with arteriovenous shunting (HALPERN *et coll* LANDE *et coll* 1976 NYMAN). Early contrast filling of dilated vessels may be the only angiographic finding indicating telangiectatic lesions as in one of the present cases. Previous bowel resections because of telangiectatic lesions in previous normal angiography and a normal double contrast colon examination in this patient support the concept that the early filling vessels draining the right colon were due to diffusely scattered telangiectases which per se were too small to be demonstrated at angiography. Arteriovenous fistulas and arterial aneurysms are other features of the disease.

The presence of two angiomatous lesions and renal artery aneurysm in one case would suggest a diagnosis of Osler's disease. On the other hand the patient used oral contraceptives thromboxane

is present and the examination of the resected al specimen demonstrated an ischemic stricture with fibrosis and organized thrombi. Thus thrombosis with infarction of the bowel wall and inflammatory reactions could have caused abnormalities at angiographically had an angiomatous character (fig. 1).

Angiomatous lesions of the bowel in patients with Klippel Trenaunay syndrome have rarely been documented (GHAHREMANI et coll.). The predominant form of the vascular abnormality in these cases seems to be a so-called diffuse cavernous hemangioma of the colon. The vascular abnormality is confined to the venous side with sluggish circulation through the pathologic vessels where thrombi may develop and calcify appearing as phleboliths along the bowel wall (BEAN 1967). In one of the cases described by GHAHREMANI et coll. a 9 year-old child selective inferior mesenteric angiography showed slow circulation and marked retention of contrast medium within the vascular spaces. The extent of the lesions was well demonstrated. Slow circulation was also noted in the present case as well as phleboliths but only a few vascular spaces were outlined at angiography. The bowel lesion had similar angiographic features as those of the right leg femoral angiography. WESTERHOLM (1967) described a patient with a diffuse cavernous hemangioma of almost the entire colon where angiography was without evident abnormality while cavography resulted in retrograde contrast filling of the vascular abnormality.

Patients with bleeding from angiomatous lesions of the gastrointestinal tract have often been subjected to unrewarding abdominal explorations and blind bowel resections with a poor result since more traditional diagnostic methods have failed to demonstrate the lesions and they could not be identified at surgery (KLEIN et coll. 1971, BRUUSGAARD & JUHL 1974, SHEEDY et coll.). When there is reason to anticipate that an angiomatous lesion may represent the bleeding source, angiography should be carried out if bleeding is of such severity that surgery is contemplated. This is indicated in patients with known angiomatous lesions of external or internal organs or with a family history of such abnormalities even though other lesions have been found to account for the hemorrhage and in patients with chronic or intermittent brisk blood loss when meticulous barium examinations and endoscopy have failed to reveal the bleeding source. SHEEDY et

coll. in their series of 88 patients with chronic gastrointestinal bleeding of obscure origin found 22 patients with angiomatous lesions at angiography. With angiography it is possible to determine not only the site of the lesion but also its extension and the presence of multiple lesions which influences the therapeutic approach. It is usually not possible to demonstrate bleeding in terms of extravasation of contrast medium from angiomatous lesions since the hemorrhage generally is sparse.

Though angiography is the primary method to detect angiomatous lesions of the gastrointestinal tract it is not possible to observe the vascular abnormality or its full extension in certain cases. This may occur with diffuse cavernous hemangioma of the colon. The difference noted between the cases with this disorder may be due to a more advanced thrombus formation in the lesions with increasing age. In such cases endoscopy and barium examinations may better demonstrate the extension of the vascular abnormality.

In the present series no evident abnormality was found in 3 angiographic examinations. In one case angiography was performed 5 years before the detection of numerous telangiectatic lesions in the gastrointestinal tract at necropsy. Since bleedings had been present for 8 years it was considered likely that the vascular lesions were present at the time of the angiography but were too small to be diagnosed. In 2 patients angiomatous lesions with a diameter of approximately 1 cm were found at laparotomy following the angiography. In one of these no abnormalities could be identified on the films even in retrospect in spite of the high quality of the examination. In the other patient a lumbar aortography had been performed since catheterization of the superior mesenteric artery failed.

If coeliac superior and inferior mesenteric angiography reveal no abnormalities special techniques at the examination of the superior mesenteric artery are recommended. The use of 50 to 60 ml of contrast medium (60% meglumine salt) injected at a rate of 5 ml/s with films exposed over a time of 25 to 30 s magnification or coned down views especially of the right colon or any other area that was not well demonstrated on initial films may improve the information.

In 3 patients of the present series vascular abnormalities enlarged or developed between two angiographic examinations over a period of one, 2 and 4 years. In addition recurrence of the vascular disorder

der occurred after previous resection at the same site in one patient. This sometimes progressive character of angiomatous disorders emphasizes the value of repeated angiographic examinations if no bleeding source is found at the first one or if bleeding recurs after resection of such lesions.

SUMMARY

Twenty patients with various angiomatous lesions of the gastrointestinal tract such as right colon angiodysplasia and manifestations of Rendu Osler Weber disease and Klippel Trenaunay syndrome are reported. During the past 15 years an increasing number of such lesions have been reported, diagnosed mainly by angiography. The major complication from these vascular lesions is bleeding. Angiography is the primary method for their detection because of their often small size and is a prerequisite before surgery when reason exists for anticipating an angiomatous lesion as the source of bleeding. However, in certain cases angiography will fail to demonstrate the vascular abnormality or its full extent.

REFERENCES

- ABRAHAMSON J and SHANDLING B. Intestinal hemangioma in childhood and a syndrome for diagnosis. A collective review. *J Pediatr Surg* 8 (1973) 487.
- ATHANASOULIS C A, GALDABINI J J, WALTMAN A C, NOVELLINE R A, GREENFIELD A J and EZELETA M L. Angiodysplasia of the colon: A cause of rectal bleeding. *Cardiovasc Radiol* 1 (1978) 3.
- BAER J W and RYAN S. Analysis of cecal vasculature in the search for vascular malformations. *Amer J Roentgenol* 126 (1976) 394.
- BAKER A L, KAHN P C, BINDER S C and PATTERSON J F. Gastrointestinal bleeding due to blue rubber bleb nevus syndrome. A case diagnosed by angiography. *Gastroenterology* 61 (1971) 530.
- BAUM S, ATHANASOULIS C A, WALTMAN A C, GALDABINI J, SCHAPIRO R H, WARSHAW A L and OTTINGER L W. Angiodysplasia of the right colon: A cause of gastrointestinal bleeding. *Amer J Roentgenol* 129 (1977) 789.
- BEAN W B. Rare diseases and lesions. p. 14. Charles C. Thomas, Springfield, Illinois, 1967.
- BOLEY S J, SPRAYREGEN S, SAMMARTANO R, ADAMS A and KLEINHAUS S (a). The pathophysiologic basis for the angiographic signs of vascular ectasias of the colon. *Radiology* 125 (1977) 615.
- SAMMARTANO R, ADAMS A, DiBIASE A, KLEINHAUS S and SPRAYREGEN S (b). On the nature and etiology of vascular ectasias of the colon. *Gastroenterology* 72 (1977) 650.
- BRUUSGAARD A and JUHL E. Hereditary hemorrhagic telangiectasia with intestinal involvement successfully treated by surgery. *Gastroenterology* 67 (1974) 1001.
- CALEM W S and JIMENEZ F A. Vascular malformations of the intestine. Their role as a source of hemorrhage. *Arch Surg* 86 (1963) 75.
- DWYER W and STEINLAUF P. Surgical implications of intestinal hemangiomas. *Postgrad Med* 36 (1973) 330.
- FOSTER J H, MORGAN C V, THERIAKELL J B and H Y. Vascular malformation of the appendix: A rare cause of massive hemorrhage. *J Am Med Ass* 215 (1971) 636.
- GENANT H K and RANNIGER K. Vascular dysplasia of the ascending colon. Report of two cases and review of the literature. *Amer J Roentgenol* 115 (1977) 349.
- GENTRY R W, DOCKERTY M B and CLAGETT O. Collective review. Vascular malformations and vascular tumors of the gastrointestinal tract. *Internat J Surg* 1 (1949) 281.
- GHAHREMANI G G, KANGARLOO H, VOLBERG P and MEYERS M A. Diffuse cavernous hemangioma of the colon in the Klippel Trenaunay syndrome. *Radiol* 118 (1976) 673.
- HAGOOD M F and GATHRIGHT J B. Hemangiomas of the skin and gastrointestinal tract. Report of a case. *Dis Col Rect* 18 (1975) 141.
- HALPERN M, TURNER A F and CITRON B P. Hereditary hemorrhagic telangiectasia. An angiographic study of abdominal visceral angiodysplasias associated with gastrointestinal hemorrhage. *Radiology* 90 (1973) 1143.
- — — Angiodysplasias of the abdominal viscera associated with hereditary hemorrhagic telangiectasia. *Amer J Roentgenol* 102 (1968) 783.
- HANSEN P S. Hemangioma of the small intestine: A special reference to intussusception. Review of literature and report of three new cases. *Amer J Clin Path* 18 (1948) 14.
- HAYLOCK A. Angiography in Kaposi's Sarcoma. *Arch Surg* 14 (1963) 304.
- HOLDEN K M and ALEXANDER F. Diffuse neonatal hemangiomas. *Pediatrics* 46 (1970) 411.
- KAUSER H. Über Hemangioma des Tractus gastrintestinalis. *Arch klin Chir* 187 (1936) 351.
- KANTER I E, SCHWARTZ A J and FLEMING R J. Localization of bleeding point in chronic and acute gastrointestinal hemorrhage by means of selective arterial arteriography. *Amer J Roentgenol* 103 (1968) 386.
- KLEIN H J, ALFIDIRI J, MEANEY T F and POIRIER J C. Angiography in the diagnosis of chronic gastrointestinal bleeding. *Radiology* 98 (1971) 83.
- LANDE A, BEDFORD A and SCHECHTER L S. The spectrum of arteriographic findings in Osler Weber Rendu disease. *Angiology* 27 (1976) 223.
- LEWIS R J and KETCHAM A S. Maffucci's syndrome. Functional and neoplastic significance. Case report and review of the literature. *J Bone Jt Surg* 55A (1973) 1465.
- MANN H G. Kaposi's sarcoma. Experience with 20 cases. *Amer J Roentgenol* 121 (1974) 793.
- MOORE J D, THOMPSON N W, APPELMAN H D and FOLEY D. Arteriovenous malformations of the gastrointestinal tract. *Arch Surg* 111 (1976) 381.

- MAN U Angiography in hereditary hemorrhagic telangiectasia Acta radiol Diagnosis 18 (1977) 581
- MER P E S Haemangiosarcoma of Kaposi Acta radiol (1972) Suppl No 316
- SIEH H L Hemangiomatosis of the intestine Discussion review of the literature and report of two new cases Gastroenterologia 93 (1959) 357
- BINS L Pathology Third edition p 608 W B Saunders Philadelphia 1968
- EEDY P F FULTON R and ATWELL D T Angiographic evaluation of patients with chronic gastrointestinal bleeding Amer J Roentgenol 123 (1975) 338
- EPHERD J A Angiomatous conditions of the gastrointestinal tract Brit J Surg 40 (1953) 409
- SMITH C R BARTHOLOMEW L G and CAIN J C Hereditary hemorrhagic telangiectasia and gastrointestinal hemorrhage Gastroenterology 44 (1963) 1
- WARNER T F C and O LOUGHLIN Kaposi's sarcoma A byproduct of tumor rejection Lancet II (1975) 687
- WESTERHOLM P A case of diffuse hemangiomatosis of the colon and rectum Acta. chir scand 133 (1967) 173
- WOOD D A Tumors of the intestines Atlas of tumor pathology Section VI Fascicle 22 p 44 Armed Forces Institute of Pathology Washington D C 1967

ANATOMY OF THE PANCREATIC VEINS

A post mortem and clinical phlebographic investigation

W REICHARDT and R CAMERON

Selective catheterization of the pancreatic veins for clinical application can be performed using the cutaneous transhepatic or the transumbilical approach to the portal vein (GOTHLIN et coll 1974). Pancreatic phlebography is important in connection with blood sampling for hormone assay in endocrine tumours of the pancreas (INGEMANSSON 1977, LUNDERQUIST et coll 1978) and is also of importance in the morphologic examination of inflammatory pancreatic disease and exocrine tumours (REICHARDT et coll 1978). The description of the venous anatomy of the pancreas in textbooks is schematic and brief and often contradictory. PERREN (1929) gave a more detailed description of the pancreaticoduodenal venous anatomy but mainly the pyloric and duodenal drainage. With the increasing frequency of pancreatic surgery in the early fifteenth century reports on the anatomy of the blood vessels of this region appeared (DOUGLASS et coll 1950, FALCONER & GRIFFITHS 1950, DOEHNER et coll 1955). FALCONER & GRIFFITHS described the anatomy of the entire pancreas in 50 specimens, mainly from a surgical point of view.

The aim of the present report is to describe the venous anatomy of the pancreas and its variations to provide a guide for selective catheterization for blood sampling and to outline the normal selective phlebography of pancreatic veins.

Post mortem phlebography

Material and Methods

The material comprised 22 human adult cadavers without signs or history of pancreatic disease.

Injection technique At autopsy a polyethylene catheter with a diameter of 3 to 4 mm was inserted in

a peripheral tributary of the superior mesenteric vein. Preferably the ileocolic vein was used as this vessel is easily dissected without injury of other portal vein tributaries. The tip of the catheter was advanced to the estimated position of the confluence of the superior mesenteric and splenic veins and the catheter was tied with a ligature. Injury of other portal vein tributaries was carefully avoided.

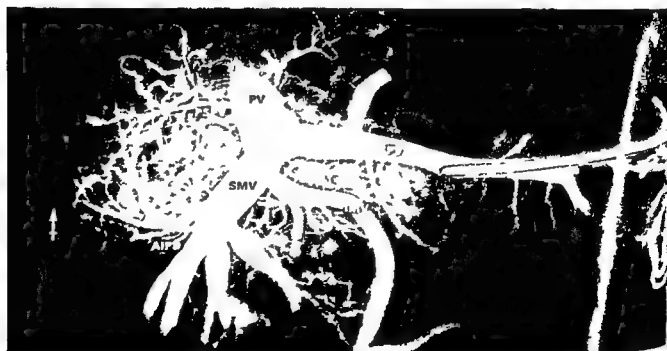
A modified Schlesinger buffered iodinated gelatin injection agent (HALES & CARRINGTON 1971) was prepared. Barium sulphate was used as pigment and the solidification time was adjusted to about 30 min. As rapidly as possible 150 to 200 ml of the agent was injected by hand since the consistency increased after only a few minutes. Filling of smaller gastric veins and superficial veins of the liver and spleen indicated as a rule also filling of the pancreatic veins. The agent was allowed to solidify for 45 min. The abdominal and retroperitoneal organs were then removed en bloc. The portal vein was cut off at the hilum of the liver. The main tributaries of the portal vein were identified and subsequently step by step the pancreas and its draining veins were dissected.

In some early cases the abdominal and retroperitoneal organs were removed en bloc before the catheter was inserted into the portal vein in the hilum of the liver or into the splenic vein in the hilum of the spleen. The periphery of the superior and inferior mesenteric veins was ligated. In these instances it was difficult to avoid leakage of contrast agent. Injection of the contrast agent before removal of the organs was later found to be preferable.

Radiographic technique In some instances survey films were exposed immediately after injection



a



b

Fig 1 Radiography of pancreaticoduodenal specimens PV = portal vein SPV = splenic vein SMV = superior mesenteric vein IMV = inferior mesenteric vein ASPD = anterior superior pancreaticoduodenal vein PSD = posterior superior pancreaticoduodenal vein PIPD = posterior inferior pancreaticoduodenal vein AIPD = anterior inferior pancreaticoduodenal vein CV = coronary vein a) In this specimen veins of

the body of the pancreas drain to the coronary vein b) of the tail of the pancreas drain to the splenic vein c) in this specimen a vein (→) drains a ventrocranial part of the head of the pancreas and the cranial part of the duodenum to the portal vein Inflow of the vein not filled with contrast medium (→) dotted lines demonstrate its course as found by dissection A pullary shape of the periphery of duodenal veins (++)



a

Fig 2 a) Dorsal aspect of dissected specimen. Small posterior superior pancreaticoduodenal vein (++) dominating dorsal pancreatic vein (++) An arcade runs in the pancreaticoduodenal



b

sulcus caudally ending in the first jejunal vein (→) b) Ventral aspect at the hepatoduodenal ligament CHV = choledochal veins PV = portal vein GB = gallbladder P = head of pancreas

the contrast agent. However, as the radiography equipment of the autopsy room did not allow adequate examination quality, films were later on exposed only after isolation of the pancreatic tissue with the specimen in contact with fine grain films.

In two instances only survey films with the pancreas in situ were obtained. As the specimens were dissected before complete solidification of the injection agent, filling of the pancreatic veins was incomplete in some cases after dissection. However, in these cases, the veins could be identified by dissection and documentation of the anatomy was made by drawings or photographs.

Results

Veins of the head of the pancreas The anterior aspect of the head of the pancreas was drained mainly by the anterior superior pancreaticoduodenal vein in 19 cases (Fig 1). This vein joined the gastroduodenal trunk, which ended in the right lateral wall of the superior mesenteric vein within 1 to 3.5 cm (average 2 cm) off the confluence of the splenic and superior mesenteric vein (in the following text named confluence).

In one case only tiny veins ran to the gastroduodenal trunk and the main ventral drainage was by the anterior inferior pancreaticoduodenal vein to the superior mesenteric vein. An ant inf vein was identified in 12 cases. The vein ended in the first jejunal vein in 7 instances, in the superior mesenteric vein

in 4, and was a tributary to the anterior superior vein in one case.

The dorsal aspect of the head was usually drained by the posterior superior pancreaticoduodenal vein running directly to the portal vein within 1.5 to 3 cm (average 1.8 cm) off the confluence. The post sup vein was identified in 21 cases. These veins draining the dorsal part of the head opened into the dorsal circumference of the portal vein. In 2 instances a ventral vein (Fig 1b) drained the cranioventral part of the head and ended in the ventral circumference of the portal vein 3.2 and 3.5 cm, respectively from the confluence. These veins drained even the cranial part of the duodenum and probably the pyloric region (the pylorus was already cut off before radiography). In 11 instances a dorsal pancreatic vein was observed draining the mediadorsal part of the head and ending in the dorsal wall of the confluence. In 3 cases the dorsal pancreatic vein was the dominant vein of the dorsal aspect of the head (Fig 2a).

In 2 instances the dorsal pancreatic vein formed an arcade together with the post inf pancreaticoduodenal vein running in the pancreaticoduodenal sulcus without changing its caliber (Fig 2a). In most cases only smaller collaterals between the post sup and the post inf pancreaticoduodenal veins were observed. The post inf pancreaticoduodenal vein could be identified in 9 cases. Insertion into the first jejunal vein was observed in 6 instances, into the superior mesenteric vein in one



Fig 3



Fig 4

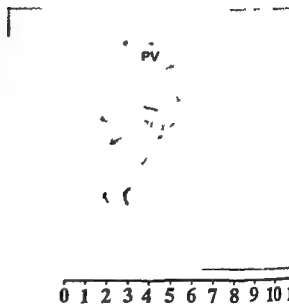


Fig 5

Fig 3 Dorsal aspect of dissected specimen. Body of the pancreas removed. Small post sup pancreaticoduodenal vein (\rightarrow) dominating post inf pancreaticoduodenal vein (\leftrightarrow) draining to the first jejunal vein

Fig 4 Dorsal aspect of dissected specimen. Duplicated post sup pancreaticoduodenal vein (\rightarrow) Transverse pancreatic vein (\leftrightarrow) draining to the sup mesenteric vein (SMV) near the confluence

Fig 5 Anterior aspect of dissected specimen. Pancreatic tissue anterior to the confluence is removed. PV = portal vein. GCT = gastrocolic trunk. Coronary vein (\rightarrow) transverse pancreatic vein (\leftrightarrow) Veins of the body draining to the coronary vein (\rightarrow)

case into the second jejunal vein in one and the post inf pancreaticoduodenal vein was a tributary to the dorsal pancreatic in one. The post inf pancreaticoduodenal vein was the dominant vein of the dorsal aspect of the head in one case (Fig 3).

Veins of the body of the pancreas The tiny veins of the pancreatic body were collected in main branches with considerably varying termination. The transverse pancreatic vein running along the inferior border of the body of the pancreas could be identified in 16 specimens. Its termination was the inferior mesenteric vein in 5 cases, the superior mesenteric vein in 3 (Fig 4), the confluence in 3 and the splenic vein in 5.

Veins of the body running to the post sup pancreaticoduodenal vein were found in 3 instances, the ant sup vein in one.

Collaterals to the coronary vein were situated in 8 specimens (Figs 1 & 5).

In 2 cases where the pancreatic body was located cranio-ventrally to the confluence, several small veins drained into the cranial wall of the region of the confluence.

Veins of the tail of the pancreas drained as a rule directly to the splenic vein, entering into its ventrocaudal circumference. As the tail of the pancreas was usually in close connection with the ventrocaudal wall of the splenic vein, these



6 Normal phlebography of the head of the pancreas a) Injection into the ant. sup. pancreaticoduodenal vein. Via collateral filling of the dorsal pancreatic vein (→) the dominant vein in the dorsal aspect the ant. inf. (++) and the post. inf. pancreatic vein (++) Filling of veins in the hepatoduodenal



b) Injection into dorsal pancreatic vein almost identical appearance Ant. sup. (→) ant. inf. (++) and post. inf. (++) pancreaticoduodenal veins and veins in the hepatoduodenal ligament (++)

veins were very short and embedded in pancreatic tissue

The number of tail veins draining to the splenic vein which could be identified varied from 3 to 9 (average 6). In cases with a large transverse pancreatic vein which also collected veins of the tail the number of veins draining to the splenic vein were less. In one specimen the transverse pancreatic vein was also the main vein of the tail collecting 5 tributaries. Two tail veins draining to the lower polar vein of the spleen were demonstrated in 2 cases (Fig. 1b).

The inferior mesenteric vein was identified in all but one case. It terminated in the splenic vein at the most 3.5 cm (average 1.8 cm) from the confluence in 15 cases. In one specimen the confluence was the point of inflow and in 5 it ended in the superior mesenteric vein at the most 1.5 cm (average 0.9 cm) from the confluence.

The coronary vein could be demonstrated in 21 of 22 specimens. In 9 cases this vein drained to the cranial circumference of the confluence, in 6 cases to the splenic vein within a distance of 2.5 cm (average 1.1 cm) from the confluence and in 4 cases to the portal vein within 2.5 cm (average 1.7 cm) from the confluence. In 2 specimens the coronary vein drained directly to intrahepatic portal vein branches of the left lobe.

Further observations. All main veins of the head and body of the pancreas were observed on the surface of the organ or only partly covered by a very thin layer of pancreatic tissue. The veins embedded in the tissue and connecting superficial dorsal and ventral veins were tiny. Only the veins of the tail had no or only a short extrapancreatic course.

No special interest was paid to the veins of the common bile duct which were often visible at clinical phlebography of the veins of the pancreatic head.



Fig 7a



Fig 7b

Fig 7 Phlebography of the body of the pancreas a) Injection into a vein draining to the splenic vein. Filling of another vein ending in splenic vein (→) and filling of transverse pancreatic vein (↔) b) Injection into transverse pancreatic vein. Filling of the same veins as in (a) and of two veins of the tail (↔)

Fig 8 Injection into a vein draining to the splenic vein. Collaterals in coronary vein (→) and to post sup pancreaticoduodenal vein (↔)



Fig 8

However in one instance the choledochal veins were dissected. Several collaterals existed to ventral veins of the head and to an arcade running along the dorsal pancreaticoduodenal border. The veins and their tributaries could be traced to the hilum of the liver (Fig 2b). Collaterals or inflow to intrahepatic portal veins were not observed.

Clinical phlebography

Material and Methods

During 1972 to 1978 selective pancreatic phlebography was performed in 140 patients at this Department of Diagnostic Radiology. During 1972 to 1974 41 patients were examined using the transumbilical approach to the portal vein. Later only percutaneous transhepatic puncture of the portal vein was used.

In 61 patients the indication for portography was portal hypertension, suggestion of metastatic lesion of the liver or malignancy of the gastrointestinal tract and pancreatic phlebography was performed en passant.

In 32 patients the examination was performed for blood sampling and hormone assay. In these cases as many veins as possible were catheterized. The success rate increased during the period. In general at least 4 veins of the pancreas were catheterized in this group.

A possible tumour in the region of the pancreas was the indication in 55 patients and selective catheterization was limited to the area of interest, usually the head of the pancreas.

The technique of percutaneous transhepatic portography is described in detail elsewhere (GOTHIN et coll 1974, HOEVELS et coll 1978, REICHARDT &



Fig. 9 Normal phlebography of the tail. a) Injection into a vein of the body. Filling of veins of the tail. Various points of inflow of

veins of the tail into the splenic vein (→) b) Injection of a vein of the tail near the hilum of the spleen

BERGMANSSON 1980) therefore only a short description is given here. The puncture was performed with a 25 cm needle coated with a polyethylene catheter (D 1.6 mm ID 1.0 mm Surgimed Denmark). With the catheter in the portal vein a 0.9 mm guide wire was introduced for further catheterization of the pancreatic veins. The tip of the guide wire was introduced according to the anatomy and introduced into a pancreatic vein. The catheter was then pushed over the guide wire into the vein.

Phlebography was carried out by manual injection of 2 to 10 ml of Isopaque Coronar 370 mg I/ml (Nyegaard Norway). The volume was adjusted to the size and flow of the injected veins. Eight films were exposed at a rate of 2/s.

The catheter should not be allowed to advance into sub branches in order to obtain a proper filling of the pancreatic and duodenal veins. Injection into peripheral tributaries results in incomplete filling and the appearance of the films may mimic an expanding lesion. Injection of too large volumes of contrast medium resulted in extravasation in 11 cases.

Phlebographic findings

Selective injection of contrast medium into the post sup pancreaticoduodenal vein usually caused filling of the majority of the duodenal branches. The ant sup vein was also filled via collaterals in the parenchyma of the pancreas and vice versa (Fig. 6). If several veins draining to the portal vein or conflu-

ence were present these were also filled by injection into one of them. Collaterals to the body of the pancreas were infrequently demonstrated. In these instances usually a branch to the main stem of the post sup vein was present. Flow of contrast medium from the post sup or ant sup vein to the transverse pancreatic vein was not observed. Demonstration of the ant inf or post inf vein by injections into the ant sup or post sup vein was a frequent but inconstant finding, probably depending mainly on the size of the inferior veins. Veins in the hepatoduodenal ligament with approximately the same diameter as the main veins of the head were not constantly filled. In one case an ant inf vein draining to the superior mesenteric vein was catheterized selectively.

The right coronary vein was filled by injection into the post sup vein in 4 cases. In these instances the right coronary vein had a smaller diameter than the post sup one, increasing in size in its course along the minor curvature of the stomach.

The shape of the peripheral branches of the duodenal and proximal jejunal veins was usually ampullary.

Veins of the body of the pancreas Selective examination of the veins of the body was often difficult to perform as the majority of these veins were tributaries to veins draining other organs (coronary vein, inferior mesenteric vein) or to veins of the head of the pancreas. The transverse pancreatic vein was easy to catheterize when draining directly to the splenic vein, to the superior mesenteric vein

or to the inferior mesenteric vein near its inflow to the superior mesenteric vein or confluence (Fig. 7)

Injection into the transverse pancreatic vein usually resulted in filling of the veins of the body positioned to the left of the superior mesenteric vein demonstrating the inflow into the splenic vein and—if present—into the coronary vein (Fig. 8). Collaterals to the post sup pancreaticoduodenal vein were filled in a few cases.

Selective phlebography of veins draining to the coronary vein was not performed and appears to be difficult due to their position and direction of inflow.

Veins of the tail of the pancreas Injection into a vein of the tail usually resulted in the filling of some minor branches and via collaterals the inflow of one or two adjacent veins was demonstrated (Fig. 9). Collaterals to the transverse pancreatic vein were observed.

The great number of separate veins of the tail draining into the splenic vein was the reason why a complete demonstration of all these veins became a difficult and time consuming procedure. In only a few of the present patients appeared the veins of the body and the tail to be demonstrated completely.

Discussion

The literature on venous anatomy of the pancreas is limited. A detailed description of the venous anatomy of the pancreatic head was given by PETRÉN and of the entire pancreas by FALCONER & GRIFFITHS. In the present specimens the main venous drainage of the head of the pancreas was found to correspond closely to these descriptions and their nomenclature was followed essentially. The drainage of the posterior aspect of the head by one or several posterior superior veins and drainage of the anterior aspect by the anterior superior vein was an almost constant finding. In only one case was the main drainage of the anterior aspect by the ant inf vein and also in one case only was the post inf the dominating draining vein of the dorsal aspect. PETRÉN described one case with two post sup veins ending in intrahepatic portal veins. Also in the present series the post sup vein could be duplicated and even 3 pancreatic veins terminating in the portal vein were observed. Usually the post sup vein ended in the dorsocaudal circumference of the portal vein. Veins inserting ventrally were observed twice but these veins drained a minor ventral aspect of the

head and may represent collaterals to pyloric veins. Veins draining to the confluence were called the pancreatic veins in analogy to the arterial nomenclature. Because of lack of experience previously erroneous conclusion had been arrived at namely that this vein drained the body into the anterior aspect of the confluence (LUNDERQUIST & TYL 1975, REICHARDT et coll.). In all the present specimens where a vein draining into the confluence was found it ended dorsally. Furthermore all the veins drained the dorsal aspect of the head and should be regarded as a duplication or variation of the post sup pancreaticoduodenal vein. This corresponds to the findings of FALCONER & GRIFFITHS who emphasized the fact that despite the close relationship of the neck of the pancreas to the portal vein in no case did a pancreatic tributary enter the portal vein on its anterior aspect. This was also in the present series regarding the region of the confluence.

In analogy to the arterial nomenclature the inferior to the pancreatic body (inferior pancreatic vein, FALCONER & GRIFFITHS) was here called transverse pancreatic vein.

Veins of the body of the pancreas may drain any main tributary of the portal vein terminating in that region. This fact must be considered when catheterization is performed for blood sampling, endocrine tumours. Veins draining to the coronary vein were relatively common in the present series.

The fact that the main veins of the head of the pancreas run on its surface limits the diagnostic value of selective pancreatic phlebography in expanding lesions of the pancreas.

The size of exocrine tumours demonstrated in pancreatic phlebography were more than 3 cm in diameter (REICHARDT et coll.). This relatively large size may be surprising but it may be difficult to observe occluded veins inside the gland because of superimposition by normal vessels on the surface of the organ.

SUMMARY

The venous anatomy of 22 autopsy specimens of human pancreas was examined by dissection and radiography after injection of gelatin agent. The most constant findings were the posterior superior pancreaticoduodenal vein draining to the portal vein and the anterior superior pancreaticoduodenal vein draining to the gastroduodenal and superior mesenteric vein. Both veins were identified in 21 and 20 of 22 cases respectively. All other pancreatic

ms varied considerably in their course. The normal findings in clinical selective pancreatic phlebography based on 148 examinations are described.

REFERENCES

- DEHNER G A, RUZICKA F F, HOFFMAN G and ROUSSELOT L M. The portal venous system. Its roentgen anatomy. *Radiology* 64 (1955) 675.
- DOUGLASS B E, BAGGENSTOSS A H and HOLLINSHEAD W H. Anatomy of the portal vein and its tributaries. *Surg Gynec Obstet* 91 (1950) 562.
- ALCOVER A and GRIFFITHS E. The anatomy of the blood vessels in the region of the pancreas. *Brit J Surg* 37 (1950) 334.
- JÖTHLIN J, LUNDERQUIST A and TYLÉN U. Selective phlebography of the pancreas. *Acta radiol Diagnosis* 15 (1974) 474.
- MALES M R and CARRINGTON C B. A pigmented gelatin mass for vascular injection. *Yale J Biol Med* 43 (1971) 257.
- ENTSCHEL M. Pankreas Anatomie. *Langenbecks Arch Klin Chir* 313 (1965) 233.
- HOEVELS J, LUNDERQUIST A and TYLÉN U. Percutaneous transhepatic portography. *Acta radiol Diagnosis* 19 (1978) 643.
- INGEMANSSON S. Pancreatic and intestinal vein catheterization with hormone assay. Bull No 13 of the Department of Surgery. University Hospital of Lund Sweden 1977.
- LUNDERQUIST A and TYLÉN U. Phlebography of the pancreatic veins. *Radiologe* 15 (1975) 198.
- ERIKSSON M, INGEMANSSON S, LARSSON L I and REICHARDT W. Selective pancreatic vein catheterization for hormone assay in endocrine tumors of the pancreas. *Cardiovasc Radiol* 1 (1978) 117.
- PETRÉN T. Die Arterien und Venen des Duodenums und des Pankreaskopfes beim Menschen. *Z Anat Entwickl Gesch* 90 (1929) 234.
- REICHARDT W and INGEMANSSON S. Selective vein catheterization for hormone assay in endocrine tumors of the pancreas. Technique and results. To be published in *Acta radiol Diagnosis* 21 (1980).
- LUNDERQUIST A and TYLÉN U. Selective phlebography in carcinoma of the pancreas. *Acta radiol Diagnosis* 18 (1978) 305.

)

COMPENSATORY HYPERPLASIA OF THE HUMAN KIDNEY EVALUATED
BY ANGIOGRAPHY AND A DYE DILUTION TECHNIQUE

J. GÖTHLIN

Compensatory renal hyperplasia (also called compensatory renal hypertrophy) is common after unilateral kidney disease or due to hypo- or aplasia of the contralateral kidney. It is known to occur early in life (LAUFER & GRISCOM 1971) and in old age (EKELOUND & GÖTHLIN 1976). CAVINA *et al.* (1971) performed experiments in dogs which indicated that the arteries of the hyperplastic kidneys increase in length and width and that the angiographic circulation time is reduced. An investigation in man is now reported.

Material and Methods

In 13 patients with aplasia, hypoplasia or disease of one kidney (occluded renal artery, pyelonephritis, multiple scars, staghorn calculus), measurements of the renal blood flow and related variables in the contralateral kidney were made in conjunction with bilateral selective serial nephroangiography. The area of the kidney of interest in a p.p. projection was always at least 50 per cent larger than that of the contralateral one. Catheters (ID/OD 1.4/2.2 mm) were placed in the renal artery and vein, respectively. A bolus of 0.3 to 1.0 ml of indocyanine green (Cardiogreen, Hynson Westcott & Dunning, USA) was injected into the renal artery while blood was continuously sucked from the renal vein through a spectrophotometer. Its deflections were recorded on a straight linear potentiometer writer. The analysis of the curves was made by copying them on stiff paper, cutting them out and weighing them, comparing their weight with that of 100 standard units of the paper. The blood flow was calculated according to a modified Stewart-Hamilton formula. For details of

the technique and mode of analysis of the curves see GÖTHLIN & OLIN (1973).

The projected kidney area, thickness of the cortex and width of the arteries were measured with compensation for the magnification. The blood pressure was measured sphygmomanometrically at the beginning of, during and after the blood flow measurements.

Results

The results by the dye dilution method and some of those obtained at angiography (thickness of cortex and possible lesions of the contralateral kidney) are summarized in the Table.

All kidneys with the diagnosis compensatory hyperplasia had an area that was at least 50 per cent larger than that of the contralateral kidney. In 7 kidneys also exceeding the upper normal limit of 91 cm² given by MOELL (1961). In the following, normal values according to GÖTHLIN & OLIN will be given within parentheses.

The mean diameter of the renal artery (RAD) was 7.1 mm (range 5.3–9.0) (GÖTHLIN & OLIN 5.5 (range 4.5–6.8)). The mean cross sectional area (RCA) calculated from the diameter of the artery on the films with compensation for magnification) of the renal artery was 39.5 mm² (range 22.1–63.6) (GÖTHLIN & OLIN 23.8 (range 16–36)).

The mean kidney area (KA) was 89 cm² (range 61–123) (in normal patients according to MOELL 70–83, SD 7.3–8.3 depending on whether the kidney was right or left sided, male or female). The 5 values above 100 cm² were encountered in 3 patients.

Table
Variables of hyperplastic kidney

No	Sex	Age	Side	RAD	RCA	KA	RBF	RBF/m ²	VV	VR	MTT	AT	Cortex	Contralateral kidney
1	M	29	L	8.3	54.0	123	840	465	115	9	8.3	3.9	13	Aplasia
2	F	27	R	6.7	35.1	107	740	455	125	8	9.9	4.0	10	Pyelonephritis
3	M	56	L	7.5	44.1	104	620	350	90	13	8.9	4.7	11	Occluded renal artery
4	F	35	L	7.2	40.7	103	445	260	65	14	8.7	4.3	13	Aplasia
5	M	33	R	7.8	47.8	101	700	440	100	11	8.5	4.0	12	Aplasia
6	F	30	R	7.1	39.6	97	630	355	105	■	10.3	4.6	11	Aplasia
7	F	34	L	6.9	37.4	94	605	340	100	■	10.0	4.1	11	Hypoplasia
8	M	58	R	9.0	63.6	83	495	280	75	12	8.9	4.1	9	Occluded renal artery
9	M	48	L	5.8	26.4	73	530	320	75	16	8.7	4.2	10	Occluded renal artery
10	M	64	R	6.8	36.3	72	580	325	70	19	7.0	4.3	10	Multiple scarring
11	M	55	R	5.6	24.6	88	510	300	80	22	9.3	4.5	10	Carcinoma
12	F	54	L	5.3	22.1	61	585	375	80	20	8.1	4.2	11	Staghorn calculus
n				13	13	13	13	13	13	13	13	13	13	
x				7.1	39.5	89	600	350	89	13	8.9	4.2	11	
SD				1.2	16.4	19	108	68	18	4.6	0.9	0.2	1.2	
SE				0.3	4.6	5.4	29	19	5	1.3	0.2	0.1	0.3	
t				22.1	8.7	17	20	19	18	10.4	3.6	6.2	33	

RAD=diameter of renal artery RCA=cross sectional area KA=kidney area RBF=renal blood flow VV=vascular volume VR=vascular resistance MTT=mean transit time AT=appearance time

with aplasia one with pyelonephritis and one with a renal artery occlusion 4 of these patients were below 40 years of age

The mean renal blood flow (RBF) was 600 ml/min range 445–840 (GÖTHLIN & OLIN 465 range 405–525 females around 30 ml/min lower than males) The mean RBF per square meter of body surface (calculated according to the formula of Du Bois) was 350 ml/min range 260–464 (GÖTHLIN & OLIN 265 range 220–365) with no difference between the two small groups of males and females

The vascular volume (VV) was calculated according to the formula $VV \text{ in ml} = RBF \text{ in ml/min} \times MTT \text{ in seconds}$ The mean VV was 89 range 65–125 (GÖTHLIN & OLIN 70 range 45–95)

The mean transit time (MTT) was calculated as the time from the start of the injection of dye to the baseline projection of the center of gravity in the cut-out curve (with compensation for the delay in the analysing sampling recording system) The mean MTT was 8.9 s range 7.0–10.3 (GÖTHLIN & OLIN 8.9 range 6.8–11.6) In the present series the deviation from the mean value was smaller than in normal kidneys

The appearance time (AT) of dye in the renal vein was measured as the time in seconds from the start of injection of dye to the point of the first deflection

of the potentiometer writer (with subtraction of delay in the analysing sampling recording system) The mean AT was 4.2 s (GÖTHLIN & OLIN 4 range 3.7–4.9)

The vascular resistance (VR) was calculated peripheral resistance units as mean arterial blood pressure in mmHg divided by the renal blood flow ml/s The mean value was 13 range 8–22 (GÖTHLIN & OLIN 19 range 11–25)

The mean cortical thickness measured in the thinnest section was 11 mm range 9–13 Reliable normal values are not available in the literature measurement of 20 normal kidneys yielded a mean cortical thickness of 9 mm range 7–11

The linear correlation between the following variables was positive

RAD – VR	r	0.627	t	2.676
KA – RBF	r	0.629	t	2.707
KA – MTT	r	0.658	t	2.917
KA – VV	r	0.601	t	2.628

The r factors are above 0.6 and the t values above 2.0 implying that the correlation is statistically significant though not highly so

At angiography in addition to increased width of the main renal artery increased kidney area and cortical thickness which have already been seen

oned the width and length of the intrarenal arteries including the subcortical and cortical vessels as also increased. No obvious abnormality was observed in the nephrographic phase. The intrarenal arteries when demonstrated were wider than normal.

Discussion

Compensatory renal hyperplasia (or hypertrophy) according to LALLI (1965) the most common cause of unilateral renal enlargement hydronephrosis being the second. Compensatory hypertrophy occurs in unilateral disease regardless of age (BONER et al 1972 EKLUND & GÖTHLIN). In dogs after nephrectomy increased volume of the remaining kidney increased arterial width and decreased circulation time at angiography has been demonstrated (AVINA et coll). In the present series increased size of the kidney and increased arterial diameters were accordant findings however the circulation time as evaluated by the appearance time of dye in the renal vein and the mean transit time of the dye as normal. The explanation for this discrepancy is obviously that due to the larger amount of contrast medium transported through the unilateral dog kidney per unit time CAVINA et coll were able to detect it at an earlier stage than in normal kidneys. The increased RBF in the present series should mainly be attributed to an increase in flow volume as the AT and MTT were within normal limits. This line of reasoning is supported by the fact that the increase in width of the renal arteries was proportionally greater than the lengthening.

A slightly positive correlation exists between the VV in ml and the kidney area in cm^2 and thus to the increase in kidney volume (inferring that the increase in kidney area to some extent reflects the increased vascular volume). Some degree of correlation between the vascular volume and the cross sectional area of the renal artery is to be expected as in normal kidneys (GÖTHLIN et coll 1973). The reason why the correlation in the present series is only slight may be that the material is small or that the enlarged kidneys in several of the patients to some extent also were diseased despite absent angiographic evidence of disease. In diseased kidneys no correlation between RCA and VV has been demonstrated (GÖTHLIN et coll).

No positive linear correlation was found between the diameter or cross sectional area of the renal artery and the area of the hyperplastic kidney. WOI-

TOWICZ (1967) reported some degree of correlation to exist between these variables in renal hypertrophy however not of a positive linear type. The mean total renal blood flow in the present series was definitely higher than normal 350 ml/m^2 as compared with a normal mean of 265 ml/m^2 . Glomerular filtration and tubular secretion are more or less dependent upon renal blood flow. The RBF thus to some extent reflects the increased function of the hypertrophied kidney which is known to occur (KROHN et coll 1966 LARSSON et coll 1975).

Bearing in mind that the groups are small it is interesting to note that the distribution of RBF/m values is similar in males and females. This may be merely coincidental however RBF/m is likely to offer a better means of interindividual comparison than does total RBF because of the wide variation in body size.

The cortical thickness is difficult to measure. In the present series the thickness was increased over that of normal control kidneys. With a special angiographic technique (HEGEDUS 1972) it is possible to quantitate the volume of the cortex. In most cases it corresponds to an increase in the thickness of the cortex. A correlation has been reported between the cross sectional area of the renal artery and the cortex volume and vascular volume (GÖTHLIN et coll) and between an increased cortex volume with the ensuing longer and wider vessels and the function of the cortex (KROHN et coll LARSSON et coll). All these variables reflect the increased function of the cortex in the kidney with compensatory hyperplasia.

The linear correlation between RBF and VR implies a lower peripheral resistance in cortical vessels probably widened. The arteries demonstrated at angiography are comparatively large and do not to a great extent influence the resistance thus a change in VR is plausibly elicited distally to the angiographically demonstrated arteries. Short circuits as the cause of a decrease in peripheral resistance are not compatible with the normal appearance time and mean transit time.

In conclusion compensatory hypertrophy of the kidney is characterized by (1) increase in renal blood flow kidney area (inferring also increased volume of the kidney including the cortex) renal artery diameter and vascular volume all reflecting an increased function of the kidney (2) decrease in the vascular resistance and (3) normal circulation time of the blood through the kidney increased flow volume and probably also increased flow velocity.

SUMMARY

The renal blood flow and related variables were assessed with a dye dilution technique in conjunction with angiography of the enlarged kidney in 13 patients with unilateral disease: hypoplasia or aplasia of one kidney. The total renal blood flow, the width of the arteries, the kidney area, the vascular volume and the thickness of the cortex were all increased. The vascular resistance was decreased. The circulation time through the kidney was normal but the flow volume and most likely also the intra-renal flow velocity were increased.

REFERENCES

- BONER G, SHERRY J and RIESELBACK R E. Hypertrophy of the normal human kidney following contralateral nephrectomy. *Nephron* 9 (1972) 364.
- CAVINA C, SOMIGLI M, TURINI D and PAMPANINI A. Arteriographic changes in compensatory renal hypertrophy. An experimental study in dogs. *Amer J Roentgenol* 113 (1971) 468.
- EKELUND L and GÖTHLIN J. Compensatory renal enlargement in older patients. *Amer J Roentgenol* 127 (1976) 713.
- GÖTHLIN J and OLIN T. Dye dilution technique with nephroangiography for the determination of renal blood flow and related parameters. *Acta radiol Diagn* 14 (1973) 113.
- HEGEDUS V and OLIN T. Relations between flow, arterial cross sectional area and total and cortical volumes of the kidney. *Acta radiol Diagn* (1973) 196.
- HEGEDUS V. Three dimensional estimation of renal size and volume at angiography. *Acta radiol Diagn* (1972) 481.
- KROHN A G, OGDEN D A and HOLMES J H R. Renal function in 29 healthy adults before and after nephrectomy. *J Amer med Ass* 196 (1966) 322.
- LALLI A F. Renal enlargement. *Radiology* 84 (1964) 101.
- LARSSON J, LINDSTEDT E, OHLIN P, STRAND S E and WHITE T. A scintillation camera technique for quantitative estimation of separate kidney function: use before nephrectomy. *Scand J Clin Lab Invest* 35 (1975) 517.
- LAUFER I and GRISCOM N T. Compensatory renal hypertrophy. Absence in utero and development in early life. *Amer J Roentgenol* 113 (1971) 464.
- MOELL H. Kidney size and its deviation from normal in acute renal failure. A roentgendagnostic study. *Acta radiol* (1961) Suppl. No. 206.
- WOJTCWICZ J. Relationship of the surface parameters of the kidney to the size of the renal artery. *Acta Radiol* 2 (1967) 23.

BALLOON CATHETERS

In vitro experiments on pressure influence and risk of rupture

K. JEKELL, N. E. PETTERSSON and S. SANDQVIST

Balloon catheters have been used in angiography for more than three decades. NORDENSTRÖM (1962, 1966) elucidated the clinical applications of balloon catheters. JENSEN & OLIN (1972) in animal experiments demonstrated that with the use of balloon catheters angiographic results can be achieved which are impossible to obtain with ordinary catheters. However, balloon catheters have not been used extensively probably due to technical difficulties and risks. JENSEN & OLIN (1979) reported that in animals balloon catheters may damage arteries and STRAUBE (1968) also in animal experiments found balloon rupture within a blood vessel. When balloon catheters are used in order to control haemorrhage or to diminish the blood flow in highly vascularized tumours injury to blood vessels caused by the catheter can be accepted if this treatment is of vital importance. When used for diagnostic purposes higher demands as to safety must be required. The risk with the balloon catheter technique appears to be considerable, a fact not sufficiently emphasized previously. The aim of the present in vitro experiments was to evaluate the risk in two respects: (1) the forces exerted on the walls of a tube in which the catheter is inflated and (2) under what conditions rupture of the balloon occurs.

Material and Methods

The experiments were made with single lumen balloon catheters. The catheter lumen was directly connected with the balloon ■ through side holes

in the catheter. The balloons were inflated with water either placed inside plastic tubes or free in the air. The volumes of the balloons were measured at the time of occlusion of the tube and at rupture. In connection with the dilatation of balloons inside the plastic tubes the pressure in the balloons (the intraluminal pressure) was measured and also the pressure exerted by the balloon on the tube wall (the lateral pressure).

The catheters were made of polyethylene and the external diameter was 2.8 mm. The balloon material was latex rubber; its elastic properties are given in Fig. 1. The balloons (manufactured by Nordiska Latex AB, Torekov, Sweden) were made of latex cylinders with an inner diameter of 3.0 mm and a length of 8 mm. The wall thicknesses of the balloons were 0.1, 0.3 or 0.5 mm. Some experiments were made with fusiform latex tubes with a wall thickness of 0.1 mm and a length of 20 mm. The balloons were inflated at a rate of 20 ml per minute.

The plastic tubes were made of transparent acrylate with inner diameters of 9, 15 and 23 mm.

The pressure was recorded with a Mingograf with two amplifiers EMT 311. Two Statham pressure transducers model P 23 DB were used measuring pressures up to 160 and 173 kPa (1 kPa = 7.5 mm Hg). The intraluminal pressure was measured inside the catheter and the lateral pressure as illustrated in Fig. 2. The volume or pressure figures presented are mean values of at least 3 measurements.

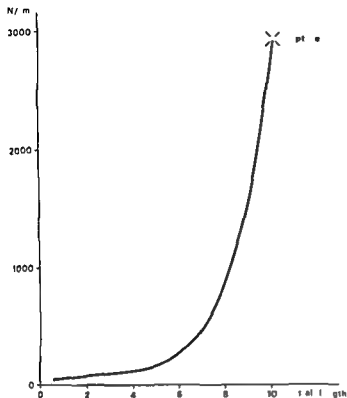


Fig 1 Elastic properties of latex balloons used in the experiments

Results

When a balloon catheter is inflated inside a tube two stages are of importance (1) when the tube is occluded i.e. when the shape of the balloon is transformed from a sphere to a cylinder and (2) when the balloon is at the point of rupture. The balloon volume at (1) is called ideal and at (2) maximum volume (Table 1).

The maximum volume of a balloon is smaller inside a tube than free in air and is reduced considerably in a narrow tube. The volume difference between ideal and maximum balloon volumes decreases when the diameter of the tube is diminished.

Table 1

Expansion capacity of balloons free in air and inside plastic tubes. a = ideal and b = maximum volume (ml)

Wall thickness of balloon (mm)	Volume (ml) of balloon in air	Tube diameter					
		9 mm		15 mm		23 mm	
		a	b	a	b	a	b
0.1	30	10	15	30	60	75	130
0.3	37	10	20	30	70	75	-

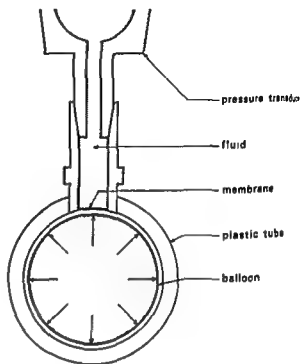


Fig 2 Apparatus for measuring lateral pressure

The friction properties of the tube wall play an important part when the inside of the tubes is treated with silicone lubricant the maximum volume of the balloon was increased by approximately 10 per cent. The length of cylindrical latex tubes was critical. When tubes of great length were inflated only a short segment of the balloon was inflated. First the dilated segment rolled over the rest of the balloon thereby hindering further inflation by compression of the undilated part of the balloon. When the balloon was made of a fusiform latex tube it was also possible to dilate long balloons.

Table 2

Lateral pressures (kPa) of balloons inside plastic tubes. c = lateral pressure at ideal volume and d = lateral pressure at maximum volume

Wall thickness of balloon (mm)	Tube diameter					
	9 mm		15 mm		23 mm	
	c	d	c	d	c	d
0.1			12	51	20	110
0.3			77	139	13	110
			40	173	-	-

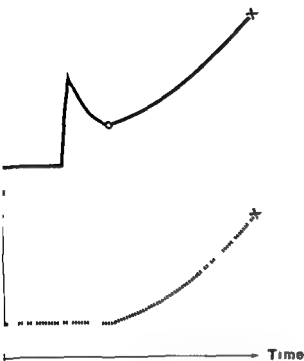


Fig 3 Intraluminal pressure (—) and lateral pressure (---) measured simultaneously during inflation of balloon within a tube. O balloon reaches tube wall x balloon rupture

The lateral pressures at ideal and maximum balloon volume appear in Table 2. Typical curves of intraluminal pressure and lateral pressure are illustrated in Fig 3. The highest lateral pressure over 13 kPa was obtained immediately before rupture of a balloon with a 0.5 mm membrane thickness in the 5 mm tube. With a balloon of a membrane thickness of 0.1 mm in the same tube a highest lateral pressure of 51 kPa was obtained.

The relationship between the intraluminal pressure and the lateral pressure is given in Table 3.

Table 3

Simultaneous measurement of intraluminal and lateral pressure (kPa) on inflation of balloons inside plastic tubes. e=intraluminal pressure and \equiv =lateral pressure at ideal volume

Wall thickness of balloon (mm)	Tube diameter					
	9 mm		15 mm		23 mm	
	e	\equiv	e	\equiv	e	c
0.1	37	79	16	17	16	≥ 0
0.3	91	71	39	77	37	13
0.5	—	—	91	40	—	—

only one measurement

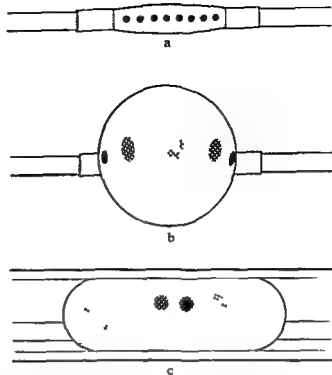


Fig 4 Inflation of balloon marked with equidistant dots of the same size. a) Uninflated balloon b) inflated balloon free in air c) inflated balloon inside tube

The mode of stretching of the balloon wall by inflation inside a tube can be demonstrated by marking the balloon with equidistant dots of the same size (Fig 4). When the balloon is inflated free in air the greatest expansion and thereby the greatest increase of size of the dots occurs in the mid section of the balloon. If the same balloon is inflated inside a tube the dots increase in size only as long as the balloon does not touch the tube wall. Since the mid section of the balloon reaches the tube wall first the dots increase in size in this part of the balloon less than at the ends where the distension is not hindered.

Discussion

The maximum volume of the balloons is smaller in narrow than in wide tubes. This is due to immobilization of part of the balloon wall that occurs when the balloon is inflated and reaches the tube wall. In a narrow tube a great part of the latex mass of the balloon is immobilized already when a small volume is injected. As a consequence the intraluminal pressure will increase quickly and the tension at the free ends of the balloon will soon reach the rupture limit of the material. The high pressure values in tubes with small diameters can be explained by

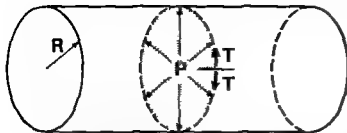


Fig. 5 Relation between tension (T), pressure (P) and radius (R) in cylindrical balloon (law of Laplace) $T = P \times R$

the law of Laplace (Fig. 5). As the tension in the part of the balloon wall immobilized against the tube cannot increase during further inflation, the increasing intraluminal pressure is transmitted to the tube wall i.e. the lateral pressure. The difference between the intraluminal pressure and the lateral pressure at a point at random in the contact surface between balloon and tube is therefore equal to the intraluminal pressure in the balloon when it reaches this point.

The discussion raises the questions whether (1) the intraluminal pressure indicates the lateral pressure, (2) the intraluminal pressure indicates a risk of rupture of the balloon, (3) a suitable size of the balloon in relation to the diameter of the tube minimizes the risk of high lateral pressure and simultaneously reduces the risk of balloon rupture, and (4) the risk of high lateral pressure and balloon rupture is minimized by giving the balloon a valve function.

Ad (1) The lateral pressure can be determined by measuring the intraluminal pressure at the moment the balloon reaches the tube wall. When this pressure is known, the difference between the intraluminal and the lateral pressure is also known and the lateral pressure can be calculated. It is difficult to determine when the balloon reaches the tube wall if the procedure is controlled by the eye; the determination of the pressure is then uncertain.

When the balloon reaches the tube wall and its spherical shape is transformed to a cylindrical one, a change of slope on the pressure curve occurs. This change of slope is observed only when the inflation of the balloon occurs inside the narrowest tube diameter 9 mm. On pressure curves from balloon inflations in 15 or 23 mm tubes a change of slope does not appear. Thus intraluminal pressure curves can be used for measurement of the lateral pressure only in certain cases.

Another method for determining the intraluminal pressure at the moment the balloon reaches the tube wall would be its calculation from the properties of the balloon material, the dimensions of the balloon and the diameter of the tube. Several mathematical models concerning inflation of balloons have been described (TAYLOR & GERRARD 1977), all being valid only when the relative change of the radius of the balloon is very small. This is not valid for balloon catheters; the radius of the uninflated balloon normally being increased several times at the occlusion.

Ad (2) If the radius of the tube is known, the tension in the balloon wall can be calculated by the law of Laplace. The maximum tension of the balloon material is supposed to be known. It is then possible to determine the intraluminal pressure that should not be exceeded without risk of rupture. The highest permitted intraluminal pressure (P_{max}) can be calculated with the same degree of certainty as the by which the radius of the tube is estimated, thus underestimation of the radius by 30 per cent causes an overestimation of P_{max} of 30 per cent.

Ad (3) The risk of high lateral pressure is small when a balloon is inflated in a wide tube (Table 1). The difference between ideal and maximum balloon volume in such a case may be small, resulting in rupture already at low intraluminal pressure.

The resistance to rupture is greatest when the balloon is inflated in a narrow tube. When the tube restricts increase of the balloon diameter, the tension in the free ends of the balloon first reaches critical values at high intraluminal pressure. At the same time a high lateral pressure is reached.

Thus there is a reverse relation between the demand of protection against high lateral pressure and that of avoiding rupture of the balloon. The choice of balloon size must be a compromise where the two factors are weighed against each other.

Ad (4) Balloon catheters with single lumen and end hole have a valve function. The use of catheters of this type involves great difficulties of balloon inflation. The inflation of the balloon must begin with a high initial injection pressure to dilate the balloon; the pressure must be decreased in order to keep the inflation constant. If the inflation is made by hand and under eye control, the injection pressure can be varied as desired. On the other hand, if the infla-

made with an injector with constant injection pressure the balloon may be overinflated with risk of high lateral pressure and rupture. Injections with constant high injection pressure were successful only when the tube had a diameter of 9 mm as the balloon is then very resistant to rupture. However this could only be achieved at the price of a high lateral pressure. In wider tubes it was possible to obtain the necessary variation of the injection pressure by using two injectors. With the first injector a small volume was injected with a pressure high enough to inflate the balloon. The inflation was then continued by the second injector at a lower pressure which was adjusted so that the balloon volume was constant.

The difficulty of balance can be avoided by the use of a single lumen catheter with a balloon of such size that the amount of contrast medium necessary for diagnostic purposes is small in comparison with the balloon volume. The inflation consequently can be made at high pressure and continued inflation of the balloon is tolerated during the short time the diagnostic injection is given (STRAUBE & DOTTER 1963). This method reduces the risk of rupture but may result in a high lateral pressure.

Balloon catheters with single lumen with pressure related valve function can be made by giving the balloon calibrated exit holes. This type of catheter worked excellently in certain cases while in others rupture occurred even at low injection pressure. CERBER (1976) described injections in patients with single lumen catheters with a reinforced hole in the balloon. He points out that the risk of balloon rupture exists if the injection pressure is too high. A functionally acceptable technique for injection with balloon catheters with valve function has not been found in the present experiments.

Clinical applications Balloon catheters are used clinically to occlude blood vessels from the size of the aorta to that of small arteries in the brain (SERBINENKO 1974). The dimensions of the plastic tubes used in the experiments corresponded to dimensions of main arteries. BURTON (1951) gave an account of the tension in the wall of blood vessels of different dimensions at normal blood pressure. Thus in an artery with a diameter of 10 mm the tension in the vessel wall is 60 N/m. In the plastic tube with approximately the same diameter (9 mm) a lateral pressure of 29 kPa was caused by the 11 mm balloon at ideal volume. This pressure corresponds to a tension in the tube wall which is about 2.5 times as

high as that in the wall of the artery. When the balloon was inflated to maximum volume a lateral pressure of 165 kPa was reached. This pressure corresponds to a tension in the tube wall which is more than 13 times as high as that in the artery at normal blood pressure.

The lateral pressures measured during the present experiments cannot be directly applied to physiologic conditions. In blood vessels movement may occur between the balloon and the glossy intima of the vessel. Thereby the lateral pressure is reduced as when the plastic tubes were treated with a lubricant. In addition the vessel walls are elastic and unlike the plastic tubes distend on increasing the balloon pressure causing a decrease of the lateral pressure. The elastic properties of the blood vessels vary. The diameter of the vessel and the age of the patient also play an important role. Veins have great elasticity and can be distended considerably. Atherosclerotic arteries have very little elasticity and even a small dilatation may cause irreversible damage to the vessel.

Even if the lateral pressures in vivo are lower than during the experiments it must be considered that balloon catheters may cause dangerously high lateral pressures. JENSEN & OLIN (1979) showed in animal experiments that arteries with a diameter of ≥ 4 mm cannot be dilated more than 20 per cent without injury to the walls.

Balloon rupture should not only be considered as a technical complication during angiography but also as a medical risk. When a balloon ruptured during the experiments fragments of latex were of ten torn off. An intravascular rupture of a latex balloon may thus cause rubber emboli.

Conclusion

A continuous recording of the intraluminal pressure makes it possible to estimate the highest conceivable lateral pressure since this is always lower than the intraluminal pressure. If the intraluminal pressure is not allowed to exceed an acceptable level for the lateral pressure harmful lateral pressures can be avoided.

The risk of balloon rupture can be reduced by determination of the pressure at which rupture occurs preferably with the balloon free in air. This procedure means extra safety because the balloon will rupture at lower pressures than when contained in a vessel.

In order to avoid high lateral pressure and balloon rupture the following factors must be known (1) the ideal volumes of balloon catheters in vessels with different diameters so that a suitable balloon size and inflation volume can be chosen (2) the highest permissible lateral pressure in the vessel to be injected (3) the intraluminal pressure at the time of rupture of the chosen balloon free in air. The intraluminal pressure must not exceed the pressure levels given under (2) and (3).

Balloon catheter technique is a valuable tool in angiography but the risks involved must be considered significant and difficult to handle. Those who use balloon catheters must be aware of the specific mechanical problems connected with catheters of this type.

SUMMARY

Balloon catheters with latex balloons were inflated in plastic tubes of different diameters. The volume at rupture of the balloons was measured. The pressure inside the balloon and that caused by the balloon against the tube walls were recorded. Measures to avoid high pressure on the vessel wall and balloon rupture are discussed.

REFERENCES

- BURTON A C: On the physical equilibrium of small vessels. *Med Phys* 164 (1951) 319
- JENSEN R and OLIN T: Balloon catheters in angiography. *Acta radiol. Diagnosis* 12 (1972) 721
- : Complications at balloon catheter angiography. Experiments in rabbits and dogs. *Acta radiol. Diagnosis* 20 (1979) 593
- KERBER C: Balloon catheter with a calibrated balloon. *Radiology* 120 (1976) 547
- NORDENSTROM M: Balloon catheters for percutaneous insertion into the vascular system. *Acta radiol.* 57 (1976) 411
- : Percutaneous balloon occlusion of the aorta. *Acta radiol. Diagnosis* 4 (1966) 356
- NERBINENKO F A: Balloon catheterization and occlusion of major cerebral vessels. *J Neurosurg* 41 (1974) 1
- STRAUBE K R: Self placing balloon streamer for aortic occlusion. *Angiology* 19 (1968) 534
- and DOTTER C T: Single lumen balloon catheter for percutaneous insertion. *Amer J Roentgenol* 117 (1963) 650
- TAYLOR L A and GERRARD J H: Pressure-radius relationship for elastic tubes and their application to catheters. *Med Biol Eng Comput* 15 (1977) 11

IDIOPATHIC HYPERTROPHIC SUBAORTIC STENOSIS

I Interventricular septum during the systolic contraction

G KVAM

A The shortening of the muscular interventricular septum

Idiopathic hypertrophic subaortic stenosis (IHSS) also referred to as asymmetric septal hypertrophy (ASH) hypertrophic cardiomyopathy with or without obstruction hypertrophic obstructive cardiomyopathy muscular subaortic stenosis and symmetric ventricular hypertrophy (GLICK & RAUNWALD 1977)

Disproportionate hypertrophy of the interventricular septum is the diagnostic feature of the disease (HENRY et coll 1973) although not absolutely specific (WIGLE & SILVER 1978). The septal dimension can be measured on echography (SHAH 1977). However disproportionate septal hypertrophy is not pathognomonic as it may also occur in patients with concentric hypertrophy and in some normal subjects.

IHSS is a genetically transmitted disease affecting both sexes. It may be asymptomatic. Patients with symptoms may or may not have subaortic obstruction. CLARK et coll (1973) observed at echography that septal hypertrophy was present in 48 per cent of parents in 55 per cent of siblings but in only 30 per cent of children of the patients and concluded that the disease is inherited as an autosomal dominant trait with a high degree of penetrance. The reason for the discrepancy between the observed rates in children and among the other relatives is probably that in patients genetically destined to have the disease septal hypertrophy is not always present in childhood but develops gradually and is detected at echography only in later years. However they do

not exclude that the reason might be technical difficulties when examining the children.

The disproportionate septal hypertrophy of IHSS is combined with normal sized or small ventricular cavities. If the thickness of the septum/free wall ratio exceeds 1.3 the most likely diagnosis is idiopathic hypertrophic subaortic stenosis but ABASSI et coll (1973) have required a septum/free wall ratio of 1.5 for the diagnosis of IHSS. The normal average value is 0.95 and in hearts with hypertrophy due to other causes the ratio is about 0.98 on the average.

ROBERTS (EPSTEIN et coll 1974) found in 40 hearts from patients with IHSS that in all cases the ventricular septum was thicker than the part of the left ventricular wall located directly behind the posterior mitral leaflet.

The free left ventricular wall in IHSS is generally also hypertrophic. In patients with subaortic obstruction at rest or after provocation the left ventricular wall directly behind the posterior mitral valve is hypertrophic as the rest of the free wall. In the nonobstructive form of the disease on the other hand the myocardium is unevenly thickened. Thus the portion of the left ventricular free wall directly behind the posterior mitral leaflet is always of normal thickness even when major portions of the left ventricular wall may be greatly thickened (EPSTEIN et coll).

The myocardial microarchitecture of the hypertrophic septum is bizarre with fibre disarray and

cardiac muscle cells coursing in various directions giving a swirling appearance. The myocardium has a similar appearance also in other cardiac diseases with probable isometric contraction (BULKLEY et coll 1977 a). Foci of such disarray may also occur in normal hearts (BULKLEY et coll 1977 b).

Also in patients without obstruction myocardial fibre disarray is observed in the free left ventricular wall while in contrast in patients with obstruction the myocardium forming the free wall is more normal (MARON et coll 1974).

HUTCHINS & BULKLEY (1978) describe the left ventricular septal surface as catenoid like: convex in the longitudinal and concave in the transverse direction. They seem to be of the opinion that the septal abnormalities in IHSS are caused by isometric contraction secondary to the tension distribution across the septal surface because of its specific shape.

The IHSS left ventricular cavity is distorted by the hypertrophic myocardial masses. Generally it has a flattened S shape with reduced depth downwards from the hypertrophic septum to the free wall (EPSTEIN et coll).

When intraventricular obstruction occurs the stenosis is regularly located between the dorsally bulging septum and an anteriorly moving anterior mitral leaflet in the left ventricular outflow tract (ROSS et coll 1966, HENRY et coll 1973). The reason for the systolic anterior movement is probably the shallow cavity outflow tract and malaligned papillary muscles secondary to cavity distortion allowing anterior suction or forward pushing of the anterior leaflet by the blood stream during systole (HENRY et coll 1975) or both in combination.

MARON et coll (1978 a) report outflow obstruction due to systolic anterior mitral valve movement in 5 patients with concentric hypertrophy. 3 of these without signs of IHSS indicating that this kind of obstruction is not absolutely pathognomonic.

Sometimes the intraventricular obstruction may be midventricular between the protruding muscular masses which occurs when the hypertrophic process predominates at the midventricular level (FALICOV & RESNEKOV 1977).

The most common symptoms are dyspnoea, anginal pains, syncope and left ventricular failure. Sudden death may be the first definitive manifestation of cardiac disease (MARON et coll 1978 b). Generally the natural history of IHSS varies with some patients improving, some deteriorating and some remaining stable (GLICK & BRAUNWALD).

The intraventricular obstruction in IHSS may present differently between examinations or from beat to beat reflecting the dynamic obstructive mechanism. This obstruction being related to contraction is subaortic and evolves progressively during the course of each cardiac systole. The obstruction exists initially but the early sharp aortic pressure upstroke falls rapidly as the obstruction develops. An increased resistance to ventricular filling from the left atrium is reflected in an elevated ventricular and diastolic pressure. A reduced ventricular compliance leads generally to a jugular venous pulse with a prominent a wave (ROSS 1977).

The cardioangiographic appearance has been described by BRAUNWALD et coll (1964), COHEN et coll (1964), BOURDARIAS et coll (1968) and SHAPIRO (1968). The shallow left ventricular cavity in diastole is recognized in the 30° right anterior oblique projection. The hypertrophic septal bulge is also identified by a concave right heart border and regularly also a small concavity cranially on the left heart border in this projection. The shallow diastolic left ventricular cavity is not so easily recognized in the 60° right posterior oblique position. The dorsally protruding upper part of the septum in diastole appearing inverted cone together with the anterior mitral leaflet during the streaming in of non contrast containing blood may however be recognized.

In systole the dorsally bulging septum and the anteriorly moving anterior mitral leaflet are recognized. A concomitant mitral regurgitation usually moderate has been reported in slightly more than half of the patients.

What appears to be a very forceful contraction with a high systolic ejection fraction is regularly observed in both views. GOTSCHALK & LEWIS (1977) report an average ejection fraction of 0.87 (SD 0.08) among their patients with IHSS. Nevertheless, in several reports based on echographic measurements conclude that the interventricular septum in IHSS has a clearly reduced systolic thickening and therefore is hypo- or non contractile (ROSS et coll 1974, COHEN et coll 1975, CATE et coll 1977). On the other hand they regularly measure an increased maximum rate of the systolic thickening of the posterior wall (COHEN et coll (1975) and CATE et coll) also found increased absolute values for the thickening. The increased ejection fraction and the early emptying of a large fraction of the stroke volume in IHSS (HERNANDEZ et coll 1964) is consequently considered to be effected by extra

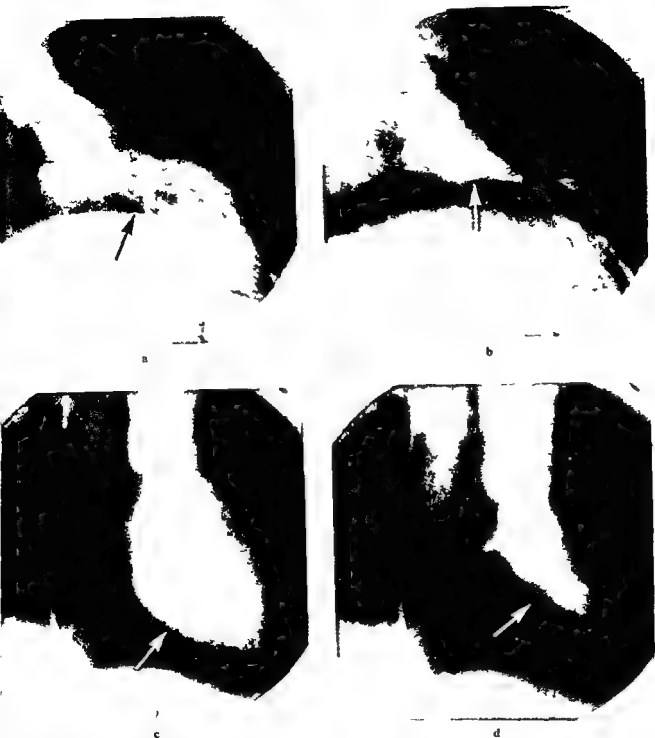


Fig 1 Papillary point identification 30° right anterior oblique left cineangiography in a patient with IHSS a) in diastole and b) systole and a control patient c) in diastole and d) systole

Arrows indicate the upper part of the attachment of the posterior papillary muscle

ous contractions of the free wall (COHEN et coll 1975 CATE et coll)
 Starting an exploration of the systolic contraction process in IHSS a cardioangiographic analysis of the degree of shortening of the interventricular septum is now reported

Materials Methods and Results

Left ventricular cineangiographies in the 30° right anterior oblique projection at 75 frames per second from 4 IHSS and 15 control patients were analysed

The 4 IHSS patients all males and aged 24 to 64 years had a subaortic chamber with gradients regis

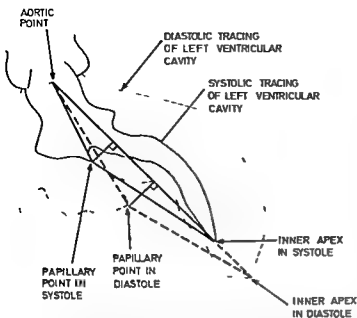


Fig 2 Composite drawing of the outline of the ventricular cavity of a patient with IHSS in diastole (dashed line) and in systole (solid line). It demonstrates how the diastolic and systolic triangles were drawn (thick dashed and thick solid lines respectively)

tered at rest from 35 to 130 mmHg. All had elevated left ventricular end diastolic pressure. 3 of the negligible mitral regurgitation.

The control patients were 7 males and 8 females, aged 23 to 64 years, examined because of angina pectoris but with normal coronary angiography and no elevation of the left ventricular end diastolic pressure.

The cardioangiographic appearance in the IH group was characteristic. In the control group, the left ventricle appeared normal in all the patients without abnormal contractions.

In every patient a heart beat not preceded by an extrasystole was analysed. An end diastolic and subsequent end systolic frame were identified. The end diastolic frame chosen had the largest observed area of the left ventricular cavity before any contraction could be observed. Correspondingly, the systolic frame was identified as the one with the smallest observed area of the left ventricular cavity.

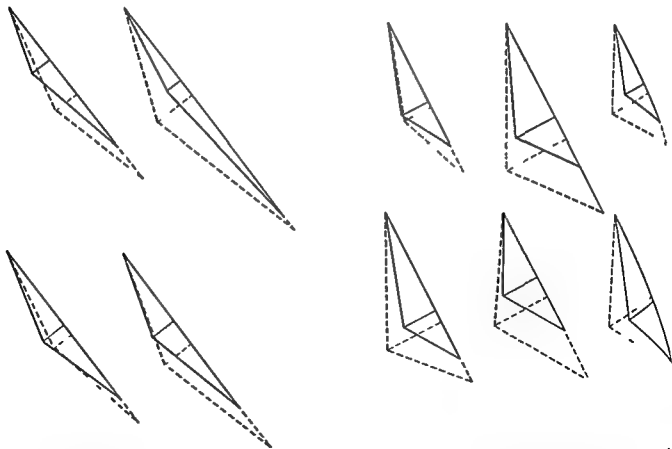


Fig 3 The composite diastolic/systolic triangles drawn a) from the 4 patients with IHSS and b) from 11 controls. The diastolic

and systolic heights are also drawn. The orientation of the triangles relative to the ventricular cavities are as shown in Fig 2.

Table

Analysis of the composite diastolic/systolic triangles from patients with IHSS and from the controls
Significance is at the 0.1 per cent level

	IHSS group	Control group	Significant difference
Apico papillary distance	0.058	0.757	Yes
Systolic shortening	Range 0.047-0.155 SD 0.096	Range 0.083-0.429 SD 0.084	
Papillo-aortic distance	0.235	0.185	No
Systolic shortening	Range 0.081-0.390 SD 0.127	Range 0.032-0.274 SD 0.0729	
Apico-aortic distance	0.137	0.188	No
Systolic shortening	Range 0.048-0.203 SD 0.068	Range 0.087-0.250 SD 0.061	
Height	0.190	0.318	No
Systolic shortening	Range 0.186-0.609 SD 0.068	Range 0.018-0.565 SD 0.128	
Diastolic height	0.102	0.255	Yes
As fraction of diastolic apico-aortic distance	Range 0.012-0.156 SD 0.064	Range 0.170-0.330 SD 0.050	
Systolic height	0.089	0.212	Yes
As fraction of systolic apico-aortic distance	Range 0.013-0.140 SD 0.067	Range 0.156-0.279 SD 0.046	
Lengthwise papillary point movement	0.109	0.102	No
Distance between heights divided by diastolic apico-aortic distance	Range 0.053-0.207 SD 0.068	Range 0.036-0.191 SD 0.050	
Lengthwise papillary point movement	0.130	0.127	No
Distance between heights divided by systolic apico-aortic distance	Range 0.060-0.245 SD 0.086	Range 0.032-0.217 SD 0.063	

fore any ventricular dilatation could be observed the upper part of the attachment of the posterior papillary muscle (papillary point) was identified both in diastole and in systole (Fig. 1). The inner apex of the middle of the aortic ring were also identified both in diastole and in systole. Diastolic and systolic triangles were measured (Fig. 2). The systolic triangles were drawn on top of the diastolic with the centres of the aortic ring exactly on top of each other with the systolic and the diastolic apico-aortic line running in the same direction. Normals were drawn from the systolic and the diastolic papillary points to the common apico-aortic line (Fig. 3). These normals were called the systolic and diastolic heights of the ventricular cavity. These heights as well as the distance between them were measured.

The systolic shortening of the sides of the triangles and of the cavity height was calculated by dividing the difference between the diastolic and systolic measured value by the diastolic one thus: Systolic

shortening = $(l_d - l_s)/l_d$ where l_d = diastolic measured value and l_s = systolic measured value.

The diastolic height was calculated as a fraction of the diastolic apico-aortic length. The corresponding systolic height to apico-aortic length fraction was also calculated.

The distance between the diastolic and systolic heights which reflects the movement of the papillary point in a direction along the apico-aortic axis was calculated as fraction both of the diastolic and of the systolic apico-aortic lengths. These values expressed as mean values, range of values and standard deviation for the two groups of patients are given in the Table. An obvious difference exists between the registered apico-papillary shortening in the two groups. The probability that the apico-papillary shortening in the 4 IHSS patients come from the same population as the control apico-papillary values is less than 0.1 per cent assuming normal distribution.

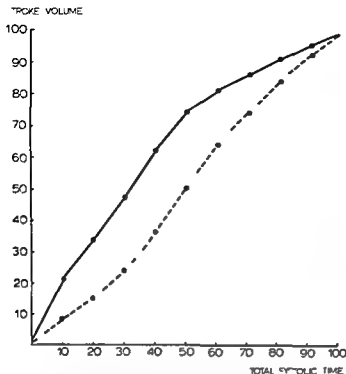


Fig 4 Percentage of total stroke volume ejected during the systolic time span expressed as percentage of total systolic time elapsed. Interpolated average values — IHSS group Control group

A difference between the heights of the ventricular cavity also exists expressed as a fraction of the apico aortic distance both in diastole and in systole as significant as the other difference mentioned.

No clear difference between the other measured parameters was found (cf the Table).

In each patient the relative ventricular volume was measured according to the area length method (KASSER & KENNEDY 1969) from the end diastolic and the end systolic frames. The systolic ejection fraction was calculated $EF = (V_d - V_s)/V_d$ where V_d = relative diastolic volume and V_s = the corresponding systolic ventricular volume. In the IHSS group EF averaged 0.85 (range 0.82–0.88) while in the control group EF averaged 0.69 (range 0.63–0.79). Three of the IHSS patients had only a very slight mitral insufficiency. Thus no significant calculation error is made by equating left ventricular volume reduction to the amount of blood passing through the aortic valve.

The ventricular relative volume was also measured for every third frame between the end diastolic and end systolic frames. From these relative volumes and from the number of systolic frames the fraction of the stroke volume passing through the aortic valve by every 10 per cent of systolic time was calculated by interpolation. Mean values at every

systolic time interval were calculated and the mean values are presented as systolic ejection curves for the IHSS patients and the control group respectively (Fig. 4).

At all systolic time intervals between the start and the end of systole a larger mean fraction of stroke volume had been ejected in the IHSS group. When half the systolic time had passed the IHSS patients had ejected an average of 74 per cent of stroke volume (range 67–81%). The corresponding mean value among the controls was 50 per cent (range 42.5–57%).

Discussion

The difference between the height of the cavity is merely a reflection of the well known septal indentation of the left ventricle in IHSS (BRAUNHART & COLL 1961).

The posterior papillary muscle arises from the posterior ventricular wall close to the groove between the muscular septum and the posterior wall. The hypertrophic septum of IHSS impinges this region of the posterior wall as can be seen from the indentation deformity. Non or hardly the contractility of the muscular septum will restrict movement of this region of the posterior wall during systole. The degree of systolic shortening of the apico papillary distance is most probably an unreliable assessment of lengthwise septal shortening during systole. The individual values for systolic shortening were -0.042 , -0.005 , $+0.01$ and $+0.155$ in the IHSS group. The reason for the negative values probably is that the walls of the left ventricle encroach upon each other in late systole resulting in a twisting of the ventricular geometry when the contractile posterior wall drags the anterior wall upwards using the bulging septum as a fulcrum. Because of the patient position in relation to the longest axis of the heart the effect of this will differ from patient to patient. In some it will result in overestimation of the systolic shortening, in others the effect will be the opposite that a lengthening of the apico-papillary distance during systole occurs is unlikely. On this basis the degree of systolic shortening of the apico papillary distance in the IHSS group supposedly lies somewhere between the observed value but the individual data give an overestimation of the deviation from this value. There seems to be no reason for a systematic error of observation in the control group. These considerations do not invalidate the statistical

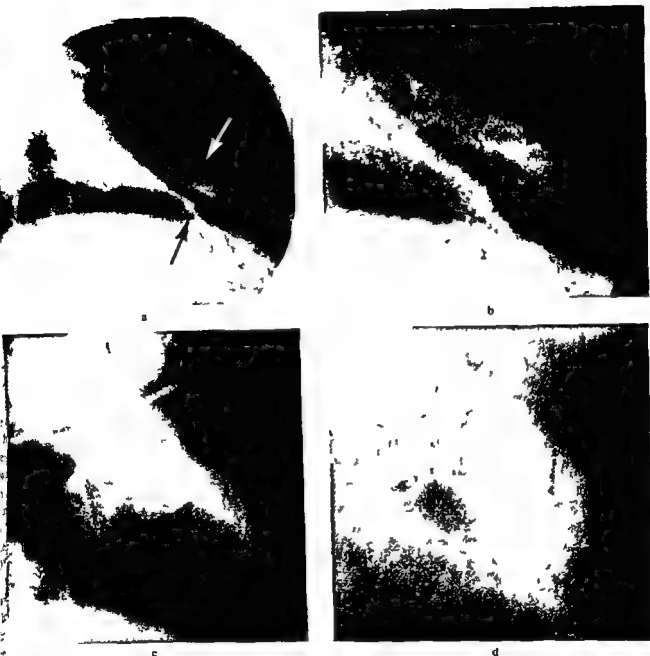


Fig. 5 Late systolic lateral tapering of left ventricular cavity in IHSS 30° right anterior oblique view from 7 patients. The arrows indicate the outer limits of visible contrast medium a) Streaked

lateral tapering between the muscle bundles b) Magnification c) Lateral tapering with a more homogeneous appearance d) Magnification

evaluation given concerning the difference between the groups because in the relevant calculation the number of patients and the arithmetic mean value of the IHSS group were used and the arithmetic mean should be approximately correct

It was shown that the IHSS septum shortens 6 per cent on the average in the longitudinal direction which must be compensated for by an increase of 6 per cent in thickness if the septal volumes is to remain constant

An average systolic increase in septal thickness

from 9.3 to 22.5 per cent in IHSS has been reported (ROSSEN et coll COHEN et coll 1975 CATE et coll) If the order of magnitude of these observations is correct the septum cannot shorten much transversely

This can be observed as a lateral tapering of the ventricular cavity towards the end of systole. As the relatively non mobile septum does not bend away from the ventricular cavity it acts as a suspender the free wall encroaching upon it during the systolic contraction (Fig 5)

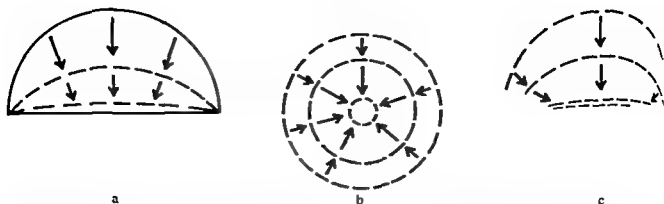


Fig 6 a) Transverse section of a hypothetical left ventricle with semicircular outline, flat stiff septum (the diameter) and zero wall thickness. When the semicircular free wall contracts from the diastolic phase, it changes into a segmental arc. The volume (represented by the area) is reduced rather fast; the cavity being obliterated when the length of the wall outline is reduced to the same length as the diameter. b) Transverse section of a hypothetical left ventricle with circular outline and a concentric contraction. The volume is reduced slower relative to the reduction in

length of the contractile wall. The wall outline must be before the cavity is obliterated. c) Transverse section of a hypothetical left ventricle with a semicircular outline and with zero wall thickness. The septum, represented as the diameter, and during contraction by the arc, is depicted curved, but it does not contract. Even a reduction of the contractile wall length to zero, a residual cavity persists.

Consequently, it may be concluded that the shortening of the septum is markedly reduced also in the transverse direction.

The high systolic ejection fraction and the early systolic expulsion of a large part of the stroke volume coincides well with the observations made by HERNANDEZ *et al.* and GOTSMAN & LEWIS. The 4 analysed IHSS patients are representative in these respects.

Conclusion The analysis presented supports the views of ROSSEN *et al.* and others that the muscular interventricular septum in IHSS is non or hypocontractile in the sense that septal shortening is markedly reduced in either direction during systolic contraction.

B. Analysis of the protruding non bending muscular interventricular septum

HUTCHINS & BULKLEY describe the transverse outline of the IHSS interventricular septum as concave towards the left ventricular cavity. Towards the end of systole, however, a lateral tapering of the cavity occurs, only the axial part remaining somewhat more open (Part A). This is most probably due to the fact that contraction of the myocardium around the septal circumference reduces the thickness of the lateral parts of the septum, i.e. by reducing the thickness of the septal attachment. This is compensated for by some increase in thickness of the more axial parts of the septum, the septal volume remaining constant. Thus the left ventricular

septal surface loses more and more of its transverse concavity during the contraction, thereby contributing to the lateral tapering of the ventricular cavity.

As a simplification, the diastolic transverse section of the IHSS left ventricular cavity may be regarded as a half circle, the diameter representing the septum, which the free wall encroaches during systolic contraction. This simplification may be allowed as transverse sections of the left ventricular cavity in specimens from cases with IHSS resemble half circles, the diameter being the septal surface. The transverse concavity of the septal surface is quite modest relative to that of the free wall (RUBIN & BROWN 1977, HUTCHINS & BULKLEY).

In IHSS, a large fraction of the left ventricular stroke volume is ejected during the first half of systole, and the ejection fraction is high. The interventricular septum shortens very little. Therefore, it has been reasonable to suppose that the fast stroke volume ejection and the high ejection fraction are effected by extra vigorous contraction of the left ventricular wall. Echography has shown that the increase in thickness of the posterior wall of the septum occurs faster than normally, some authors also report that the increase is greater as well (ROSSEN *et al.*, COHEN *et al.* 1975, CATE *et al.*).

These different aspects represent a geometrical enigma. If the free wall is attached to the edges of the septum, which in principle may be regarded as flat and immobile, and the transverse section of the cavity is about half circular, calculations show that the percentage of volume per unit myocardial shortening is $\frac{1}{2}$ if the contraction is

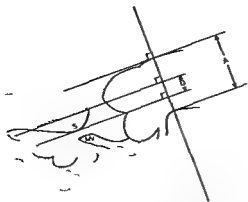


Fig 7 Patient with IHSS Composite drawing from which dorsal aortic movement was measured. The aortic width (A) was measured along a line drawn from above the posterior sinus of Valsalva at right angles to the opposite aortic wall. The distance (D) between perpendiculars to this line and tangential to the dorsally protruding septum in diastole (broken line) and in systole (solid line) was also measured. The fraction D/A was used as estimate of dorsal septal movement during systole. Prolapsing mitral valve (M) and dorsally protruding septum in systole (S).

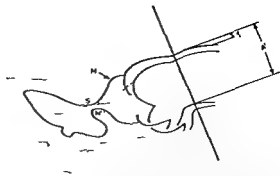


Fig 8 Patient with IHSS Composite drawing from which ventral aortic movement was measured. The diastolic and systolic figures were drawn on top of each other as they actually were observed while viewing the cine film. The systolic aortic width (A) was measured along a line drawn between two points located just above the diastolic posterior and anterior sinuses of Valsalva. Along the same line the forward movement (D) of the anterior contrast delineated aortic contour during systole was measured. The fraction D/A was used as estimate of anterior aortic movement. Systolic prolapse of mitral valve (M) membranous interventricular septum in systole (M).

centric. This principle is illustrated for the simple theoretic case of zero wall thickness in Fig 6b. If the septum curved towards the right ventricle during systolic contraction, a practically non shortening septum combined with vigorous contraction of the free wall would be easier to understand. On the other hand, a high systolic ejection fraction would then be rather difficult to account for: blood could collect in a pocket between the contracting free wall and the septum bending towards the right ventricle, with a reduction to zero of the transverse dimension of the free wall (Fig 6c).

An analysis has been performed to find out whether the interventricular septum bends towards the right during the systolic contraction and the results are now presented.

Materials, Methods and Results

Cine films obtained at left ventricular cineangiography in the 60° right posterior oblique projection from the male patients with obstructive IHSS and from 10 of the control patients described in Part I were analysed, as cine films had been proposed in the 60° right posterior oblique position only in 10 (5 men and 5 women aged 23 to 60 years) of the 15 controls. The 60° right posterior oblique cine films at 75 frames per second were obtained simultaneously with the 30° right anterior oblique cine films analysed in Part A.

The end diastolic and systolic frames were identified as the ones with the largest and smallest area respectively. Tracings of the inner surface of the left ventricle in systole and in diastole were made as well as of that of the ascending aorta above the sinuses of Valsalva.

The tracings were redrawn on top of each other, care being taken to draw the diastolic inner anterior aortic border exactly on top of the systolic. On this composite drawing a normal was drawn from the inner wall of the aorta just above the dorsal sinus of Valsalva to the opposite wall. Perpendiculars to this normal were drawn tangential to the muscular septum in diastole and in systole where it bulged backwards (Fig 7). The distance between these two perpendiculars expressed as a fraction of the diameter of the aorta along the normal drawn first was used as an estimate of the dorsal septal movement.

In late systole the aortic root has a slight ventral movement. A new composite diastolic/systolic drawing was made where the aortic root movement was not compensated for. Thus, on this drawing the diastolic and the systolic tracings do not correspond exactly. A line was drawn immediately cranial to the anterior and posterior diastolic sinus of Valsalva and along this line the diameter of the systolic aorta was measured. Along the same line the distance between the anterior inner margin of the aorta in diastole and in systole was measured (Fig 8). The latter distance was calculated as a fraction of the systolic aortic diameter and used as an estimate of the anterior aortic movement during systole.



Fig 9 60 right posterior oblique cine frame from a patient with IHSS a) in diastole and b) in systole Anteriorly bulging membranous septum (→) with its continuation below in the upper



muscular septum The convexity is more prominent than in diastole because of the dorsally moving septal prolapsing mitral valve in systole (↔)

Dorsal systolic movement of the septum in the IHSS group averaged 0.324 (range 0.234–0.453). In the control group the dorsal systolic movement averaged 0.097 (range 0.044–0.177) with SD 0.038.

Systolic ventral movement of the ascending aorta averaged 0.081 in the IHSS group (range 0.054–0.104). In the controls the corresponding value was 0.189 (range 0.145–0.250) with SD 0.035.

For both parameters the probability that the four IHSS patients came from the same population as the controls was less than 0.1 per cent assuming normal distribution.

Discussion

The increased backward/downward movement into the left ventricular outflow tract of the bulging upper muscular interventricular septum is a well known mechanism of the subaortic stenosis in IHSS. This systolic movement is quantitated by the method used.

The anterior movement of the aortic root during systole is less marked in the IHSS patients than in the controls. This is probably related to the dorsally moving and bulging interventricular septum. In all 4 IHSS patients in agreement with images and tracings of images previously published by BRAUNWALD et al. and COHEN et al. (1964) the upper anterior

margin of the left ventricular outflow anterior bulge in the steep right posterior projection (Fig 9). However this anterior protrusion is an illusion. When the anterior diastole is put exactly on top of the anterior diastole the systolic upper bulge does not in front of the corresponding diastolic structure upper muscular septum is drawn backwards contracting walls of the left ventricle and the muscular septum in turn dragging the membranous septum with it. The membranous septum with its attachments in turn keeps a dorsal pull on the aortic root its anterior movement thereby being restricted. The anterior bulge is formed by the dorsally moving muscular septum above the most dorsally protruding muscular ridge and its continuation into the membranous septum which is pulled anteriorly by the aortic root. The restricted aortic root movement indirectly implies that the septum does not move anteriorly to any significant degree. An anteriorly bending muscular septum would not pull the membranous septum dorsally.

The shortening of the muscular interventricular septum is markedly reduced in IHSS during systole (Part A) and it does not bend during systolic contraction. HUTCHINS & BULKLEY have shown that the septal surface is convex longitudinally and concave transversely in IHSS. They are probably re-

Supposing that the shape of the septum causes an isometric contraction. Their argument however rests upon assumptions which can hardly be supported. They use a model composed of infinitely thin walled structures (soap bubbles) and with ideal isometric surfaces and they seem to believe the pressure distribution across the septal surface to be the cause of the isometric contraction. However it is more likely that a surface with zero net tension on one side is the consequence of the forces at work and not the cause of such forces.

Therefore an alternative explanation is brought forward. The contracting longitudinal septal muscle fibres tend to straighten out the longitudinal convexity work against the contracting transverse muscle fibres which tend to move the septal surface towards the cavity centre. These two contractile components of the septum then have the net effect of the contracting IHSS septum is locked in opposition to isometric contraction. They necessarily balance each other because shortening in one direction stretches the myocardial fibres in the opposite direction thereby increasing the opposing force according to the Starling principle until an equilibrium is reached and vice versa.

The basic defect of the disorder thus most probably is an anomalous shape of the muscular interventricular septum as assumed by HUTCHINS & BULKLEY leading to isometric contraction and secondary hypertrophy of the septum. The septal myocardial abnormalities are thereby accounted for (WIGLE & SILVER).

Conclusion: The analysis supports the idea that the IHSS hypertrophic muscular septum is relatively rigid and non bending during systole.

The abnormality of the septum is most probably of an anomalous form leading to isometric contraction of a stiff septum with markedly reduced systolic shortening and with an active myocardial wall attached around it acts as a suspender. An ordinary degree of myocardial fibre shortening by the free left ventricular wall will expel the stroke volume faster and also give a higher ejection fraction than in an ordinary heart which has a more concentric contraction. Whether this explanation is sufficient or whether it is necessary to suppose a more vigorous contraction of the IHSS free left ventricular wall in addition in order to explain the high ejection fraction and the fast stroke volume ejection of the disease is open to discussion.

Echographic observations certainly seem to sup-

port the idea that hypercontractility of the free wall is also involved even though this is not the only explanation. In a later communication this problem will be analysed by using cardioangiographically determined parameters as input in geometric models in order to determine the actual fibre shortening of the free wall of the IHSS left ventricle.

SUMMARY

Biplane left ventricular cineangiographies in 4 patients with typical obstructive idiopathic hypertrophic subaortic stenosis (IHSS) and in control patients with normal left ventricles were analysed. In the protruding hypertrophic muscular interventricular septum of IHSS a markedly reduced shortening occurs in either direction during the systolic contraction. It does not bend towards the right ventricle. It is suggested that the septum of IHSS acts as a suspender during the systolic contraction thereby accounting for the fast stroke volume ejection and the high ejection fraction of IHSS.

ACKNOWLEDGEMENTS

My thanks are due to Professor Jan Gothlin who made stimulating suggestions during the work and criticized the manuscript. Dr Richard Eastgate gave valuable assistance with the statistical evaluations and with the language of the manuscript. The cardiologists of the Department of Clinical Physiology Haukeland Sykehus supplied the patients and the photographic department and Mrs G S Johansen kindly placed their technical skill at my disposal.

REFERENCES

- ABASSIA S, MACALPINE R N, EBER L M and PEARLE M L. Left ventricular hypertrophy diagnosed by echocardiography. *New Engl J Med* 289 (1973) 118.
- BOURDIAS J P, OUBAK P, FERRAS J, SOZUTEN Y, SCEBAT L and LENEGRÉ J. Obstructive cardiomyopathy. Cineangiographic study of 50 cases. *Am J Roentgenol* 102 (1968) 853.
- BRAUNWALD E, LAUREN S, ROCKOFF H, ROSS J and MORROW A G. Idiopathic hypertrophic subaortic stenosis. *Circulation* 30 (1964) Suppl No 4 p 3.
- BULKLEY B H, WEISFELDT M L and HUTCHINS G M. (a) Isometric cardiac contraction. A possible cause of the disorganized myocardial pattern of idiopathic hypertrophic subaortic stenosis. *New Engl J Med* 296 (1977) 135.
- — — (b) Asymmetric septal hypertrophy and myocardial fibre disarray features of normal developing and malformed hearts. *Circulation* 56 (1977) 292.
- CATE T F, J HUGENHOLTZ P G and ROELANDT J. Ultrasound study of dynamic behaviour of left ventricle in genetic asymmetric septal hypertrophy. *Brit Heart J* 39 (1977) 627.

- CLARK C E HENRY W L and EPSTEIN S E Familial prevalence and genetic transmission of idiopathic hypertrophic subaortic stenosis *New Engl J Med* 289 (1973) 709
- COHEN J EFFATH H GOODWIN J F OAKLEY C M and STEINER R E Hypertrophic obstructive cardiomyopathy *Brit Heart J* 26 (1964) 16
- COOPERMAN L B and ROSENBLUM R Regional myocardial function in idiopathic hypertrophic subaortic stenosis. An echoradiographic study *Circulation* 52 (1975) 842
- EPSTEIN S E HENRY W L CLARK C E ROBERTS W C MARON B J FERRANS V J REDWOOD D R and MORROW A G Asymmetric septal hypertrophy NIH Conference Ann intern Med 81 (1974) 650
- FALICOV R E and RESNEKOV L Mid ventricular obstruction in hypertrophic obstructive cardiomyopathy. New diagnostic and therapeutic challenge *Brit Heart J* 39 (1977) 701
- FARRER BROWN G Primary cardiomyopathies. In A colour atlas of cardiac pathology p 91 Wolfe Medical Publications London 1977
- GLICK G and BRAUNWALD E Idiopathic hypertrophic subaortic stenosis (IHSS) In Harrison's principles of internal medicine p 1292 Edited by G W Thorn R D Adams E Braunwald K J Isselbacher and R S Peterdorf McGraw Hill Book Company New York 1977
- GOTSMAN M S and LEWIS B S Left ventricular volumes and compliance in hypertrophic cardiomyopathy *Chest* 66 (1974) 498
- HENRY W L CLARK C E and EPSTEIN S E Asymmetric septal hypertrophy (ASH) the unifying link in the IHSS disease spectrum. Observations regarding its pathogenesis pathophysiology and course *Circulation* 47 (1973) 827
- GRIFFITH J and EPSTEIN S E Mechanism of left ventricular outflow obstruction in patients with obstructive asymmetric septal hypertrophy (idiopathic hypertrophic subaortic stenosis) *Amer J Cardiol* 35 (1975) 337
- HERNANDEZ R R GREENFIELD JR J C and MCCALL B W Pressure flow studies in hypertrophic subaortic stenosis *J clin Invest* 43 (1964) 401
- HUTCHINS G M and BLICKLEY B H Catenoid shape of the interventricular septum possible cause of idiopathic hypertrophic subaortic stenosis *Circ* 58 (1978) 392
- KASSER I S and KENNEDY J W Measurement of ventricular volumes in man by single plane angiocardiology *Invest Radiol* 4 (1969) 83
- MARON B J FERRANS V J HENRY W L CLARK C E REDWOOD D R ROBERTS W C MORROW and EPSTEIN S E Difference in distribution of cardiac abnormalities in patients with obstructive non obstructive asymmetric septal hypertrophy (ASH) Light and electron microscopic findings *Circulation* 50 (1974) 436
- GOTTDIENER J S ROBERTS W C HENRY W C SAVAGE D D and EPSTEIN S E (a) Left ventricular outflow tract obstruction due to systolic closure of the anterior mitral leaflet in patients with asymmetric left ventricular hypertrophy *Circulation* 58 (1978) 527
- ROBERTS W C EDWARDS J E MCALLISTER R FOLEY D D and EPSTEIN S E (b) Sudden death in patients with hypertrophic cardiomyopathy. Quantization of 26 patients without functional impairment *Amer J Cardiol* 41 (1978) 803
- ROSS JR J Idiopathic hypertrophic subaortic stenosis. Textbook of medicine p 973 Edited by P B Braun and W McDermott W B Saunders Company Philadelphia London Toronto 1975
- BRAUNWALD E GAULT J H MASON D T and ROW A G The mechanism of the intraventricular pressure gradient in idiopathic hypertrophic subaortic stenosis *Circulation* 34 (1966) 558
- ROSSEN R M GOODMAN D J INGHAM R E and R L Ventricular systolic septal thickening and dilation in idiopathic hypertrophic subaortic stenosis *Engl J Med* 291 (1974) 1317
- SHAH P M Echocardiography in the diagnosis of hypertrophic obstructive cardiomyopathy *Amer J Med* 58 (1977) 830
- SIMON A L Angiographic diagnosis of idiopathic hypertrophic subaortic stenosis *Radiol Clin N Am* 16 (1968) 423
- WIGLE E D and SILVER M D Myocardial fibre disorganization and ventricular septal hypertrophy in asymmetric hypertrophy of the heart *Circulation* 58 (1978) 1317

RADIOGRAPHY OF THE SMALL INTESTINE WITH LARGE AMOUNTS OF COLD CONTRAST MEDIUM

BIRGITTE BRUN and VIKTOR HEGEDUS

Although numerous methods for radiologic examination of the small bowel have been described during the last half century (PANSORF 1937 WEIN AUB & WILLIAMS 1949 GOLDEN 1959 MATTSSON coll 1960 SELLINK 1974 1976 MARSHAK & JEDNER 1976) no method has been accepted as a standard procedure and many departments are still in need of a simple and rapid method for daily routine. The examination of the small bowel is often performed as a continuation of a gastric series with a relatively small amount of barium contrast medium. This method gives only segmental demonstration of the small intestine and the contrast medium tends to pool after a couple of hours in ileal loops in the lower part of the abdomen (Fig. 1a). The diagnostic value of the examination is doubtful and the transit time is long. Little information on the anatomy of the small bowel is obtained and the appearance of the mucosa is seldom demonstrated. In addition the protracted examination is tiring to the patient often uninspiring to the radiologist and disturbs other fluoroscopic work.

Forty years ago it was pointed out that the use of large amounts of contrast medium improves the quality of the examination and reduces the transit time (WELTZ 1937). At nearly the same time it was reported that cold fluid leaves the stomach sooner and passes more rapidly through the intestine than meals at room temperature (GERSHON COHEN et coll 1940).

Thus a combination of these methods, i.e. the use of a large amount of cooled contrast medium should give rapid demonstration of the small intestine and

films of high quality. However this method does not seem to be universally used (PIERCE personal communication).

Material and Method

During 1976 and 1977 203 examinations of the small bowel with a large amount of cold contrast medium were performed in 170 adults and 33 children. Indication for the examination findings transit time and total examination time were recorded. Furthermore in 25 patients two examinations were performed with an interval of 1 to 6 years the first one being a follow through after gastric examination at the second one 500 ml cold contrast medium was used. The difference in transit time between the two examinations was recorded.

Technique Adult patients were given 500 ml Mixobar (Astra Denmark) 1 g/ml in a 30% dilution children somewhat less. The contrast medium was mixed with tap water cooled to approximately 5°C. After the barium meal the patient was placed in the right lateral position. Fluoroscopy was performed at short intervals especially at the beginning of the examination. Films surveys and spot films were taken when the various parts of the intestine were well filled. The examination was concluded when all segments of the small intestine had been satisfactorily demonstrated. The exposures were made at 120 kV.



a

Fig 1 13 year-old girl with ulcerative colitis. a) Small bowel examination with a small amount of contrast medium pooling in ileal loops in lower part of the abdomen. This film has no diagnostic value. b) Almost the entire length of the small bowel



b

demonstrated on one film with a large amount of cold contrast medium. The filling is uniform and the appearance of the mucosa is visible.

Results

The indications for the examination are given in Table 1 and the findings in Table 2. A diagnosis was reached in 189 patients. Well defined lesions were found in 71 cases, no abnormalities in 118. The group named 'others' represents a broad spectrum of conditions such as jejunal diverticulosis

Table 1

Indications for small bowel examination

	No of patients
Malabsorption and diarrhoea	64
Crohn's disease	48
Pain and dyspepsia	38
Gastrointestinal haemorrhage	8
Sib-ileus	22
Abdominal tumour	14
Others	9

Meckel's diverticulum, sequelae to intestinal intussusception, internal hernia (Fig 2). In 14 patients the examination was incomplete or inconclusive.

Six of the 203 examinations were excluded from the series, either because the transit time in the small intestine was not recorded or because the examination was concluded before the contrast medium had reached the caecum. In the remaining 197 cases the transit time to the caecum was less than one hour in 56, between 1 and 2 h in 71, between 2 and 3 h in 87 per cent.

The examination was completed in less than 3 hours in 89 per cent of the 203 cases, in 31 per cent in less than one hour. In 118 cases no abnormalities were found. In this group the transit time to the caecum was less than 3 hours in 95 per cent, the examination was completed in less than 3 hours in 93 per cent. A comparison of the transit time in 25 patients examined by both the conventional and the small bowel follow-through examination and the one with a large amount of cold contrast medium showed that the mean transit time was reduced from 267 to 137



a

2. 43 year-old man with intermittent intestinal obstructions followed by spontaneous relief since childhood. Examination shows a large amount of cold contrast medium during an attack called a paraduodenal hernia. a) A p view. Mesenteric mal



b

rotation. Air filled small bowel loops in left side of abdomen. b) Lateral view. Contrast filled ileal loops dorsal in the hernial sac. the neck →

Discussion

The aim of a radiologic examination of the small bowel should be the demonstration of the entire length of the jejunum and ileum. Contrast filling should be uniform and make it possible to evaluate details in the mucosa. Since SELINK (1974, 1976) introduced double contrast examination of the small intestine, it has been increasingly realized that this part of the gastrointestinal tract requires just as careful an examination as the stomach and colon. SELINK used a duodenal tube through which large amounts of barium plus water or air were injected. This method demonstrates the entire small bowel mucosa excellently and rapidly. However, a method more comfortable to the patient, giving adequate clinical information without duodenal intubation is preferable. The large amount of diluted and cooled contrast medium was well accepted by the patients, both adults and children.

As early as 1937 it was pointed out by WELTZ that the quality of small bowel examination depends upon the degree of filling. In recent years MARSHAK & LINDNER, in particular, have emphasized the

importance of large quantities of contrast medium which stimulates gastric emptying and reduces the transit time (CALDWELL & FLOCH 1963, KIM 1968, MARSHAK & LINDNER). The large volume gives uniform filling of the intestinal loops and protects the barium meal from the disintegrating influence of the gastric and intestinal contents. The effect of water absorption from the ileum is reduced when the volume of the contrast medium is large and the transit accelerated.

Table 2

Radiologic abnormalities

	No of patients
Malabsorption	17
Crohn's disease	11
Adhesions	22
Ascites	2
Space filling lesions	6
Malrotation	11
Others	23



Fig 3 Two cases of biopsy proven celiac disease a) Flocculation of small amount of barium at follow through examination Evaluation of the mucosa not possible b) The appearance of the



mucosa demonstrated with the use of a large amount of contrast medium

Superimposition of small bowel loops may constitute difficulties when a large amount of contrast medium is used. By diluting the contrast medium and by the use of high kilovoltage and compression films these difficulties can usually be overcome.

GERSHON COHEN et coll found that an ice cold meal leaves the stomach much faster and passes more rapidly through the small intestine than meals at room temperature or heated meals. WEINTRAUB in 1941 observed (WEINTRAUB & WILLIAMS 1949) that iced drinks after a meal increased the motility of the contents in the gastrointestinal tract and resulted in diarrhoea. After several experiments these authors presented a rapid method for examination of the small bowel. They used isotonic saline at room temperature and afterwards ice cold physiologic saline. They reported good film quality and a short transit time with this method but drinking this fluid cannot have been pleasant for the patients.

In the present series Mixobar was diluted with cold tap water and the patients were given 500 ml of this suspension. The contrast medium was easily

accepted in this form. Mixobar has proved a suitable contrast medium which does not flocculate even during long lasting examinations or in cases of malabsorption. The transit time was considerably reduced by changing the barium meal from 250 ml at room temperature to 500 ml cooled contrast. In 89 per cent of the patients the examination was completed in less than 4 hours. However many of the patients had pathologic conditions in the small intestine which per se may increase the transit time. Therefore a group of examinations without abnormalities was considered separately. In these the total examination time was less than 3 hours in 93 per cent. The comparison of the two diagnostic methods in 25 patients revealed that the use of a large amount of cold contrast medium reduced the transit time by about one half.

From a diagnostic point of view the method presented has also proved an advantage. If the amount of contrast medium is too small the barium has a tendency to accumulate in intestinal loops which is impossible to identify and thus gives little diagnostic



Fig. 4 17 year-old girl with Crohn's disease in terminal ileum and ascending colon. Displacement of intestinal loops indicates extra intestinal extent of the disease.

information (Fig. 1a). The use of a large amount of cold contrast medium affords uniform filling of the intestinal loops and often makes it possible to demonstrate the entire small intestine on one film (Fig. 1b). Changing the patient's position and the use of compression can disclose even minor abnormalities of the mucosa.

In patients with malabsorption the advantage of the method is obvious (Fig. 3). When a large amount of cold contrast medium is used flocculation and segmentation of the contrast medium rarely occur. The intestinal mucosa is well coated with barium and the appearance of the mucosa well demonstrated. Furthermore, in patients with localized swelling of the intestinal wall indentations in the surrounding loops indicate the extent of the lesion (Fig. 4).

SUMMARY

A rapid method using a large amount of cold Mixobar for radiography of the small bowel without duodenal intubation is presented. The diagnostic value of the method

and the transit time were analysed in 203 patients. The quality of the examinations was good. The transit time was reduced compared with conventional methods.

ACKNOWLEDGEMENTS

Supported by a grant from Statens Videnskabelige Forskningsfond, Denmark.

REFERENCES

- CALDWELL W. L. and FLOCH M. H. Evaluation of the small bowel barium motor meal. *Radiology* 80 (1963) 383.
- GERSHON COHEN J., SHAY H. and FELSS S. The relation of meal temperature to gastric motility and secretion. *Amer. J. Roentgenol.* 43 (1940) 237.
- GOLDEN H. Technical factors in the roentgen examination of the small intestine. *Amer. J. Roentgenol.* 82 (1959) 965.
- KIMS E. Small intestine transit time in the normal small bowel study. *Amer. J. Roentgenol.* 104 (1968) 522.

- MARSHAK R H and LINDNER A E Radiology of the small intestine Second edition Saunders Philadelphia 1976
- MATTSSON O PERMAN G and LAGERLÖF H The small intestine transit time with a physiologic contrast medium *Acta radiol* 45 (1960) 334
- PANSDORF H Fraktionierte Dunndarmfüllung und ihre klinische Bedeutung *Fortschr Röntgenstr* 56 (1937) 627
- PIERCE J W Personal communication
- SELLINK J L Radiological examination of the small intestine by duodenal intubation *Acta radiol* *Enn* 15 (1974) 318
- Radiological atlas of common diseases of the small bowel H E Stenfort Kroese B V Leiden 1976
- WELTZ G A Der kranke Dunndarm im Röntgen *Fortschr Röntgenstr* 55 (1937) 20
- WEINTRAUB S and WILLIAMS R G A rapid method of roentgenologic examination of the small intestine *Amer J Roentgenol* 61 (1949) 45

RADIOGRAPHIC APPEARANCES IN CROHN'S DISEASE

III Colonic lesions following surgery

J. HILDELL, C. LINDSTRÖM and A. WENCKERT

Considerable interest has been given to analysis of the problem of recurrences following operation for Crohn's disease (VAN PATTER et coll 1954, COLICK & VANSANT 1960, STAHLGREN & FERGUSON 1961, BARBER et coll 1962, ATWELL et coll 1965, JILL et coll 1969, DE DOMBAL et coll 1971a, b, FLIGHER et coll 1971, WALLENSTEN 1971, WENCKERT 1971, NUGENT et coll 1973). However, attempts have been made to analyse the existence and localization of the recurrences in relation to both the preoperative distribution of the lesions and the operative methods employed. Neither have the recurrence in the small intestine and recurrence in the colon been considered separately.

In previous reports radiographic features of unoperated patients with Crohn's disease were considered, with special reference to minor lesions (Part I, HILDELL et coll 1979). The purpose of the present communication is to describe the postoperative radiographic appearance of the colon. The findings are also correlated with the preoperative distribution of the lesions, the operative procedures employed and the appearance of the new distal ileum.

Material and Methods

The same material as in Parts I and II was used (HILDELL et coll 1979). The postoperative films of all patients in whom the disease preoperatively was located in the distal ileum, the distal ileum and the colon or the colon alone and in whom the entire or large parts of the colon were left behind at re-

sectional procedures were reviewed. The series consisted of 317 small and 247 large intestine examinations performed in 114 patients. The postoperative appearance of the colon and the small intestine was recorded and correlated with the preoperative distribution of the lesions and the operative procedures employed (Fig. 1).

Results

Postoperative appearance of the colon

In 86 of 114 patients no abnormality was found. In the remaining 28 patients various types of lesions were recorded.

Postoperative submucosal edema (12 patients). The patients had no clinical evidence of recurrent colonic disease (Fig. 2).

Postoperative colitis (16 patients). a) Superficial fluctuating colitis. The patients had no definite clinical evidence of recurrent disease in the colon (7 patients, Fig. 3). b) Colitis with clinical evidence of recurrent disease in the colon (9 patients, Fig. 4).

Comparison between pre- and postoperative appearances

Colonic lesions were left behind in 14 patients (D-F, Fig. 1). The occurrence of postoperative colitis was strongly related to the existence of preoperative lesions in segments left behind at operation (Fig. 5). Of 16 patients with postoperative colitis, 13 had preoperative lesions, while in 3 patients no relationship with preoperative lesions was





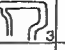


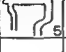





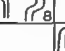


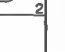
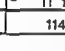
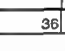
Extent at time of op Op. methods	No recurrent disease	Abnormalities characteristic of recurrence		
		Distal ileum	Distal ileum and colon	Colon
A	 5	 5		
B	 83	 54	 26	 3
C	 11	 6	 5	
D	 2		 2	
E	 10	 1	 8	 1
F	 2			 2
G	 1	 1		
	114	62	36	13
				3

Fig. 1 Correlation between the extent of disease at the time of operation, the operative procedures employed and the postoperative appearance of the colon and the new distal ileum

found. More detailed information is given in Fig. 6. The different types of postoperative colonic lesions are correlated with the preoperative distribution of the lesions and the operative procedures employed.

In the patients with postoperative submucosal edema no correlation with preoperative lesions was found. In 3 of the 16 patients with postoperative colitis no correlation with any preoperative lesion was found. No preoperative examination of the colon was performed in one of these 3; the second was examined only once. The quality of the films was unsatisfactory and possible existence of minor lesions could not be evaluated. In the third patient a resection of a kissing lesion in the sigmoid colon was performed in addition to an ileotransverse colostomy. In the remaining 13 patients lesions were recorded both pre- and postoperatively.

Thus in 13 of 14 patients (93%) a relationship existed between postoperative colitis and preopera-

Postoperative lesions in the small intestine

Different types of lesions were observed in the small intestine (more detailed information is available in a forthcoming report).

(a) Edema. Broadened and irregular mucosal folds but no ulcers and no local progression. Patients had no clinical evidence of recurrence.

(b) Radiographic recurrence. Abnormalities characteristic of recurrence in asymptomatic patients.

(c) Recurrence. Radiographic and clinical evidence of recurrence.

The two latter groups are referred to as postoperative ileitis.

The relationship between postoperative colonic lesions and the postoperative appearance of the distal ileum appears in the table.

Of 16 patients with postoperative colitis 11 had no postoperative ileitis. Two of these were operated upon with segmental resection of the ileum (Fig. 1 VI in Fig. 6) and both ileal and colonic lesions persisted postoperatively. Another 2 patients (F in Fig. 1 VIII in Fig. 6) were operated upon with resection of the rectum and the aboral colon; neither pre- nor postoperatively had any ileal lesions. In the remaining 12 patients a presumed normal ileal segment was operatively connected with a colonic segment that was postoperatively (and in the majority of the patients also preoperatively) involved by colitis. In 11 of these 12 patients (92%) recurrence had developed in the new distal ileum in addition to postoperative colitis.

In 31 patients no postoperative ileitis was found in the ileal segment (Fig. 1 B, C) that was anastomosed to a preoperatively normal segment of the colon (3 patients accounted for above being included II in Fig. 1 III and V in Fig. 6). In 28 of these 31 patients was any postoperative colitis found.

Thus it appears that linear extension of lesions across an ileocolic anastomosis was significantly more frequent in oral (92%) than in aboral (0%) direction ($p < 0.001$).

Also in 12 patients with postoperative submucosal edema in the colon a high rate of additional ileal lesions existed: 7 patients had postoperative ileitis and 3 had edema (I + II in Fig. 6).



Fig. 2 a) Postoperative submucosal edema in the transverse colon in a patient with an ileocolic anastomosis b) Detail of the transverse colon

Management of postoperative colitis

Of the 16 patients with *postoperative colitis* 13 were reoperated upon 8 of 9 patients with clinical evidence of recurrent colitis and 5 of 7 with superficial colitis. In 7 of the 8 patients colectomy and ileostomy was performed. None of these patients

had another recurrence. In the remaining patient the distal ileum was anastomosed with a slightly diseased rectum. This patient soon had another recurrence.

Of the 7 patients with superficial colitis 5 were operated upon with resection of the new distal ileum and a new ileocolic anastomosis was performed.

Table

Relationship between postoperative colonic lesions and the postoperative appearance of the new distal ileum

Colonic lesions	No. of patients	Postoperative appearance of the new distal ileum			
		Normal	Edema	Postoperative ileitis	
				Radiographic recurrence	Recurrence
Submucosal edema	12	2	3	3	4
Postoperative colitis					
Superficial	7	1			6
Recurrent	9	2			7
Total	28	5	3	3	17



Fig 3 a) Postoperative superficial colitis in a patient with ileocolic anastomosis. Multiple superficial ulcers in the remaining

colon and extensive lesions in the distal ileum. b) Detrusor colon. Multiple punched out and aphthoid ulcers

The indications were recurrent disease in the distal ileum and the colon was normal to inspection and palpation at operation. Microscopy of the resected colonic segments revealed inflammatory lesions. All patients had a second recurrence in the distal ileum and the colonic lesions persisted.

Two patients of 13 with *postoperative submucosal edema* in the colon were operated upon because of recurrent disease in the new distal ileum. In both patients microscopic examination of the resected colonic segments confirmed the radiographic diagnosis of edema.

Discussion

In the literature recurrence of Crohn's disease is accounted for in different ways in regard to both frequency and localization. In most reports recurrence of the disease is principally correlated with the operative methods employed and the localization of

recurrent disease is not further specified (BA coll ATWELL et coll BRILL et coll DE DON coll 1971 b). Some authors however have such a specification but have not correlated localization of recurrent disease with the preoperative distribution of the lesion of the operative dures employed (DE DOMBAL et coll 1971 a J & VIGNAL 1976).

Still others provide information concerning recurrence rates correlated with the postoperative distribution of the lesions but further particulars concerning operative procedures and localization of current diseases are absent (SCHOFIELD 1965 LENSTEN).

In the radiologic literature little has been reported on recurrence of Crohn's disease in the colon. Some authors mention parenthetically that spread of disease to the colon is more common after surgical intervention than before (BRAHME & WENCKERT 1970 MARSHAK & LINDNER 1970 BRAHME & LINDNER 1970).



Fig 4 a) Radiographic and clinical recurrent colitis 3 months after the primary operation. Multiple punched-out ulcers in the descending colon. Air filled and featureless distal ileum. b) Detail of framed area in the descending colon in (a). Multiple punched out ulcers.

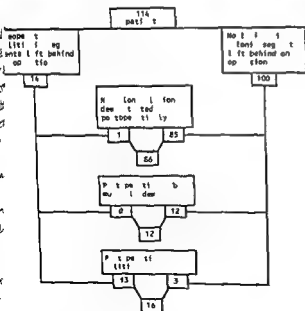


Fig 5 Correlation between postoperative colitis and the preoperative appearance of colonic segments left behind on operation.

1975 SIMPKINS 1976) but no attempts have been made at a closer analysis. The present results may be summarized as follows:

Postoperative findings	No of cases	Preoperative appearance and management
Recurrent colitis	9	Colonic lesions left behind (8) Resection of a kissing lesion (1)
Superficial colitis	7	Colonic lesions left behind (5) No examination of colon (1) Unassessable examination (1)
Submucosal edema	12	Normal preoperative colon (12)

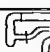

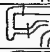
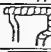










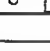
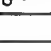



Group and No of cases	Extent at time of op Op. methods	Postop colonic lesions	Postoperative lesions in the small bowel			
			Normal	Edema	Radiogr recur	Recur
I 9			1	3	1	4
II 3			1		2	
III 2						2
IV 5			1			4
V 1						1
VI 2						2
VII 4						4
VIII 2			2			
28			5	3	3	17

Fig 6 Correlation between postoperative colonic lesions, the postoperative appearance of the new distal ileum, the extent of disease at the time of operation and the operative procedures employed.  Severe lesions  Superficial lesions  Submucosal edema

Thus in 8 patients of 9 with clinical and radiographic recurrence the colonic lesions existed already preoperatively. Therefore the recurrence must be considered to be due to an exacerbation of the disease in segments left behind at operation. The ninth patient had recurrence after surgical removal of a kissing lesion in the sigmoid colon. The cause of the recurrence in this patient is not clear. In the literature only a few authors have touched upon the problems concerning the surgical approach to kissing lesions. CHÉRIGIÉ *et coll* (1973) reported the same experience in 2 patients after resection as was encountered in one patient in the present series. SCHOFIELD had in 5 patients 2 recurrences and one operative death. This does not prove that there is a causal relationship between resection of a kissing lesion and recurrence of the disease in the colon but the possibility must be considered.

A superficial fluctuating colitis was recorded in 5 patients postoperatively. In 5 of these the lesions existed preoperatively and were left behind at operation. In one of the remaining 2 patients no testine examination was performed preoperatively and in the other only one which was not extensive with regard to minor lesions. In this particular of the disease the mucosal lesions have a tendency to appear intermittently and therefore it is probable that the colon in these 2 patients was involved also preoperatively.

Hence if colonic lesions were left behind at operation a significantly high risk of postoperative recurrence of the disease in the colon exists. On the other hand if no lesions were left behind at operation the risk was low no matter whether postoperative lesions were found in the new distal ileum or not. This is probably supported by reports on postoperative spread of disease to the colon (BRAHME & WENCKERT 1974, SHAK & LINDNER 1974, BRAHME & FORK 1974). This may be explained by the fact that colonic lesions were overlooked at the preoperative examination and during operation.

Submucosal edema is not specific for Crohn's disease but appears in any type of colitis. Its presence in 12 patients in this series is difficult to evaluate. It may be representative of the basic disorder. On the other hand the lesions did not progress which indicates that the edema might be a nonspecific reaction to for example diarrhea caused by contralateral ileal lesions or malabsorption.

It is hard to explain the high rate of recurrence in the new distal ileum that was recorded in addition to postoperative colitis (13 of 16 patients).

One explanation may be that ileal lesions were left behind at operation and hence that the postoperative ileal lesions represented an exacerbation of the disease. However considering the results of effective treatment for recurrent disease this theory seems less plausible. After reoperation patients operated upon with colectomy obviously differed from patients with a new ileocolic anastomosis. In the former patients no further recurrence developed while in the latter (11 patients with superficial colitis) another recurrence occurred in the new distal ileum in addition to persistent colonic disease.

More plausible is that recurrence in the new distal ileum was caused by spread of the disease from the colon, a spread that was made possible by the effectively accomplished anastomosis. This theory is supported by the results of operation for recurrence.

It should also be mentioned that recurrence developed in the distal ileum of several patients (not included in this series) after an operative connection of the ileum to a slightly diseased rectum. However, if this theory is true, there is no reason why the disease should not spread in the opposite direction from a diseased distal ileum to a nondiseased colon. As is obvious from the results, this did not happen. An explanation for this phenomenon might be afforded on the basis of the theory of lymphatic drainage that was postulated previously (Part II). A diseased ileum and a diseased transverse colon may have their lymphatic drainage through the inferior mesenteric system of lymphatics and the ileum has no alternative way of drainage. On the contrary, if a diseased ileum is connected to a nondiseased transverse colon, this has an alternative way of drainage through the inferior mesenteric system of lymphatics. Whatever theory is correct, patients in whom colonic lesions are left behind at operation run a high risk of developing recurrent disease in the colon and new distal ileum. This is also true in patients in whom the mucosal lesions have regressed or the disease manifests itself only in the form of superficial mucosal ulcers. The capricious and fluctuating nature of colonic Crohn's disease should always be kept in mind and temporary healing of mucosal lesions should not be regarded as permanent healing. A patient once has been proved to have lesions in the entire colon, he should always be regarded as having pancolitis. The postoperative prognosis is probably the same whether mucosal lesions are found at the time of operation or not.

It is obvious that a careful preoperative evaluation of the extent of disease is of the utmost importance for the diagnosis of minor mucosal lesions in the colon cannot be made at the operation as only limited possibilities for making a true diagnosis of the lesions exist at operation. Consequently, the diagnosis of minor mucosal lesions should be made at the radiographic examination and the diagnostic radiographic methods by which these lesions are demonstrable must be used (Part I).

SUMMARY

Postoperative films of 114 patients subjected to a primary operation for Crohn's disease were reviewed with special regard to postoperative lesions in the colon. Re-

currence in the colon was in 13 patients of 16 due to an exacerbation of the disease in segments left behind at operation. Recurrence in the new distal ileum in addition to persistent colonic disease occurred in 11 patients of 12. This was probably due to the operative connection of the ileum to a diseased colon.

REFERENCES

- ATWELL J D, DUTHIE H L and GOLIGHER J C. The outcome of Crohn's disease. *Brit J Surg* 52 (1965) 966.
- BARBER JR K, W WAUGH J M, BEAHR O W and SAUER W G. Indications for and the results of surgical treatment of regional enteritis. *Ann Surg* 156 (1962) 472.
- BRADME F and FORK T. Dynamic aspects of colonic Crohn's disease. *Radiologe* 15 (1975) 463.
- and WENCKERT A. Spread of lesions in Crohn's disease of the colon. *Gut* 11 (1970) 576.
- BRILL C H, KLEIN S F and KARK A E. Regional enteritis and enterocolitis. A study of 74 patients over 15 years. *Ann Surg* 170 (1969) 766.
- CHERIGIE E, MONNIER J P and DONELLI G. Les aspects radiologiques des recidives de l'ileo-colite granulomateuse. *Ann Radiol* 16 (1973) 433.
- COLCOCK B P and VANSANT J H. Surgical treatment of regional enteritis. *New Engl J Med* 262 (1960) 435.
- DE DOMBAL F T, BURTON I and GOLIGHER J C (a). Recurrence of Crohn's disease after primary excisional surgery. *Gut* 12 (1971) 519.
- — — (b). The early and late results of surgical treatment for Crohn's disease. *Brit J Surg* 58 (1971) 805.
- GOLIGHER J C, DE DOMBAL F T and BURTON I. Surgical treatment and its results. In: Regional enteritis (Crohn's disease). Skandia International Symposia 11, 166. Edited by A. Engel and T. Larsson. Nordiska Bokhandeln, Forlag, Stockholm 1971.
- HILDELL J, LINDSTROM C and WENCKERT A. Radiographic appearances in Crohn's disease. I. Accuracy of radiographic methods. *Acta radiol. Diagnosis* 20 (1979) 609.
- — — Radiographic appearances in Crohn's disease. II. The course as reflected at repeat radiography. *Acta radiol. Diagnosis* 20 (1979) 933.
- JULIEN M and VIGNAL J. La maladie de Crohn recto-colique. *J. Chir. (Paris)* 112 (1976) 51.
- MARSHAK R H. Granulomatous disease of the gastrointestinal tract (Crohn's disease). *Radiology* 114 (1975) 3.
- and LINDNER A E. Granulomatous colitis and ileocolitis with emphasis on the radiological features. *Progr Gastroenterol* 1 (1970) 357.
- NUGENT F W, VEIDENHEIMER M C, MEISSNER W A and HAGGIT R C. Prognosis after colonic resection for Crohn's disease of the colon. *Gastroenterology* 65 (1973) 398.
- SCHOFIELD P F. The natural history and treatment of Crohn's disease. *Ann Roy Coll Surg Engl* 36 (1965) 258.

- SIMPKINS K C The barium enema in Crohn's colitis *In* The management of Crohn's disease p 62 Edited by I T Weterman A S Pena and C C Booth Excerpta Medica Amsterdam 1976
- STAHLGREN L H and FERGUSON L K The results of surgical treatment of chronic regional enteritis *J Amer med Ass* 175 (1961) 986
- VAN PATTEN W N BARGEN J A DOCKERTY M II
FELDMAN W H MAYO C W and WAUGH J M
Regional enteritis *Gastroenterology* 26 (1954) 347
- WALLENSTEN S Results of surgical treatment in *In* Regional enteritis (Crohn's disease) International Symposia p 177 Edited by A Engel and T Larsson Nordiska Bokhandelns Forlag Stockholm 1971
- WENCKERT A In discussion with Goligher Ober and Wallensten *In* Regional enteritis Crohn's disease Skandia International Symposia p 208 Edited by A Engel and T Larsson Nordiska Bokhandelns Forlag Stockholm 1971

RADIOGRAPHY IN PRIMARY TUMORS OF THE SMALL BOWEL

OLLE EABERG and SVEN EKHOLM

The preoperative diagnosis of tumors in the small bowel is still not satisfactory. The symptoms of the tumors are vague and unspecific and therefore often overlooked by the clinician. Consequently the patient will not have any proper radiologic examination (SILBERMAN et coll 1974). These tumors have low frequency and a correct radiologic diagnosis is thought to be rare even on those occasions when tumors are observed on the films (VUORI & VUORI 1971). The present investigation was performed to find out the frequency of primary tumors of the small bowel and to what extent radiology was resorted to in these hospitals which are referring patients to Southern Sweden. A retrospective evaluation was also performed to assess how often correct radiologic diagnosis could be made and the importance of different radiographic methods.

Material and Methods

The files of these two hospitals and of other hospitals in the region were reviewed for patients who had undergone operation or autopsy were found to have tumors of the small bowel during a period of 7 years (1971-1977). Only tumors of the jejunum and ileum were included. The duodenum was omitted because the examination of this region was felt to be less controversial, being routinely included in barium examination of the stomach. It is also possible to explore this region via endoscopy. Primary lymphomas of the small bowel have been excluded from the material because of the difficulties in separating them from secondary lymphomas even on autopsy. Examinations of interest were abdominal survey films

barium contrast examinations of the small bowel and angiography.

Results

The mean annual number of inhabitants in the area was 1 424 282. A total of 133 confirmed primary small bowel tumors were found which corresponds to a mean annual incidence of 1.33 per 100 000. Of these 133 tumors 118 were available for further clinical and radiologic evaluation. Radiography was carried out in 63 patients (53%) and of these 30 (47%) were correctly diagnosed as small bowel tumors (Tables 1-2). Of the tumors 28 were benign and 90 malignant with a preponderance of carcinoid tumors, leiomyomatous tumors and adenocarcinomas (Table 1).

Patients examined radiologically. In no case did abdominal survey films give reason to suggest a tumor; however one of the carcinoids contained calcific deposits. Obstruction of the small bowel by ileus was present in 19 patients.

Acute conventional follow through examinations during episodes of obstruction were carried out in 21 patients and the tumors were then diagnosed in 7 of these (33%). In 2 patients this examination was regarded as normal. In the remaining 12 patients the examination indicated the presence of mechanical obstruction but no abnormalities indicating tumor were present.

Small bowel examinations performed on 36 patients by oral administration of the barium in periods

Table 1

The material classified according to type of tumor

Type of tumor	Radiography	No radiography	No of patients
Angiomatous lesion	3	5	8
Unspec. granuloma	-	1	1
Polyp	2	-	2
Fibroma	-	2	2
Fibrolipoma	1	-	1
Lipoma	-	3	3
Peutz-Jeghers disease	2	-	2
Leiomyoma	3	6	9
Leiomyosarcoma	12	7	19
Adenocarcinoma	9	9	18
Carcinoid	29	21	50
Neurofibrosarcoma	2	-	2
Malignant mesenchymal tumor	-	1	1
Total	63	55	118



Fig. 1 Characteristic desmoplastic reaction with retract mesentery (→) in a patient with small carcinoid tumor distal part of the ileum

with no clinical or radiographic indication of ileus disclosed 18 tumors (50%). These tumors had a mean diameter of 4 cm and the overlooked ones 2 cm but in some cases larger tumors were overlooked. In these cases the examinations were hampered by inadequate separation of the bowel loops or poor quality of the films. Nor could the tumors be observed at a review of the films. In 2 cases of large leiomyosarcomas the intraluminal part of the tumor was less than 2 cm in diameter.

Six of the small bowel examinations were performed via duodenal intubation and in 5 of these the tumors were disclosed. The overlooked case was a carcinoid tumor with a diameter of 3 cm without desmoplastic reaction. The films were of high quality but the tumor could not be identified even at review.

Angiography was performed in 32 patients. Most of them had leiomyomatous tumors (9 cases) and carcinoids (15 cases) (Table 2). All leiomyomas were observed. In 4 cases with carcinoids angiography did not disclose the small bowel tumor but in 3 of these cases metastases were demonstrated which led to a correct diagnosis.

Patients not examined radiologically. Of these 55 cases 16 were available for further clinical evaluation to find out why no radiologic examination had been performed. Acute laparotomy was carried out in 7 patients due to life threatening bleeding or

peritonitis. Three tumors were incidentally found at gynecologic operations when a palpated abdominal mass was thought to be of genital origin. During 6 patients had symptoms for up to 5 years but during this period no patient had received medical care. These tumors were incidental findings at operation (4 cases) or autopsy (2 cases).

Leiomyomatous tumors (15 cases) were found both in the jejunum and in the ileum but with increasing frequency in aboral direction. The examination demonstrated the tumor in 11 cases. In the case of benign leiomyoma examined and in 10 cases of leiomyosarcomas and angiography in all 9 patients examined.

Adenocarcinomas (9 cases) were found with increasing frequency in aboral direction in the jejunum and in only one case in the ileum. The small bowel barium examination was diagnostic in 6 cases (67%) in which the examination was of adequate quality. Angiography demonstrated the tumor in 3 cases examined; vessels were displaced and contracted but no tumor vessels were found.

Carcinoids existed only in the ileum and with increasing frequency in aboral direction. Most carcinoids were found in the distal part of the ileum. Of 29 small bowel barium examinations 10 disclosed filling defects in the contrast medium with or without a characteristic desmoplastic reaction (Fig. 1) while 11 of 15 angiographies were diagnostic (73%). The desmoplastic reaction with traction of the mesentery seen at the barium examination

Table 2

Diagnostic outcome of different examinations in primary tumors of the small bowel

Type of tumor	Abdominal survey		Acute follow through			Barium examination		Angiography		No of patients
	Ileus	No abn	Tumor	Ileus	No abn	Tumor	No abn	Tumor	No abn	
Hamman-Rich lesion						2		2		3
Polyp		1		1						1
Adenoma	1					1		1		1
Jejunoileal disease		1	2			1				1
Myoma	1					1	1	1		3
Myosarcoma	4		1	3		5		8		12
Carcinoma	6		2	2		4		2	1	9
Carcinoid	7	1	2	6	2	8	11	11	4	19
Neurofibrosarcoma		1					2	2		1
	19	4	7	12	2	18	11	24	8	63

ions was well correlated with the stellate formation of the vessels on the angiograms. One patient had small carcinoid tumors in the distal part of the ileum. There was submucosal edema and cobblestoning of the mucosa together with a marked deformity of the lumen. This led to the radiologic diagnosis of Crohn's disease (Fig. 2). On operation the carcinoid tumors were found together with a marked desmotic reaction with fibrosis in the mesentery and serosal wall. The tumor had spread locally to the ileum. When the tumor was situated in the most distal part of the ileum the ileocecal valve was patent (3 cases).

Two neurofibrosarcomas in patients with known Crohn's disease were included in the series. In both the barium examinations were normal while angiography disclosed the tumor. Two patients with known Peutz-Jeghers disease (hereditary intestinal polyposis and melanin pigmentation of the skin) had multiple polyps at barium examinations.

One patient had symptoms and signs of obstruction by ileus. At operation adhesions were found either with a smooth polyp with a diameter of 1 cm. The polyp had not caused the obstruction. One patient had intermittent melena and severe anemia. Barium examinations of the stomach, small bowel and colon were considered normal as was angiography of the superior mesenteric artery. At exploration a tumor with a diameter of 3.5 cm x 5.5 cm was found 40 cm distal to the ligament of Treitz. The tumor had a small intraluminal part. At microscopic examination the tumor was found to be a leiomyoma.

Discussion

Carcinoma of the small bowel is rare. It accounts for only 3 to 6 per cent of all gastrointestinal neoplasms and less than 1 per cent of all malignant tumors (EBERT & ZUIDEMA 1965). In this region of Southern Sweden all pathologic examinations are performed at a few hospitals. In spite of this fact a few tumors may have been missed and thereby the figure of a mean annual incidence of 1.33 per 100,000 inhabitants may be low.

The diagnosis is difficult to make preoperatively because the condition is uncommon in clinical practice, the possible existence of such a tumor thus not being taken into account and because the symptoms are vague and often unspecific (SILBERMAN et coll.). Although tumors of the small bowel are rare, 60 per cent of all gastrointestinal sarcomas are located in the small bowel (SKANDALAKIS et coll. 1962).

In a series of 659 cases from the Mayo Clinic equal numbers of benign and malignant tumors were found: leiomyomas (including leiomyosarcomas) and carcinoid tumors made up 23 per cent each, adenocarcinomas 13 per cent (GOOD 1963). In the present series carcinoids preponderated (43% of all the tumors). The number of malignant tumors was also higher than expected from other series when compared with the benign tumors.

The frequency with which the small bowel tumors can be correctly diagnosed before operation or autopsy varies. In a review of the literature SANDERS & AXTELL (1964) found 828 carcinoid cases and concluded that these tumors could only exceptionally be diagnosed preoperatively and that the



Fig 2 Infiltration of the distal part of the ileum (→) and marked edema in proximal parts of the ileum (←) with cobblestone formation. Marked edema and deformity of the cecum. The lesion was

initially diagnosed as Crohn's disease. At operation was disclosed and a marked desmoplastic reaction was

majority was found on autopsy or incidentally at operation. In other series the preoperative diagnosis varied in frequency between 21 and 63 per cent (PAGTALUNAN *et coll.* 1964, STRAUCH 1964, OSTER MILLER *et coll.* 1966, VUORI & VUORI).

MOERTLER *et coll.* (1961) in their survey of 209 carcinoid tumors had only 15 preoperatively performed radiologic examinations of the small intestine; of these only 6 revealed some kind of occlusive tumour. In comparison with their series the present one contains a significantly higher proportion of radiologic examinations and also a higher proportion of correct preoperative diagnoses. The poor results reported by MOERTLER *et coll.* led them to conclude that radiologic examinations yield only negative or misleading results—a statement that is not valid according to the result in the present series.

Radiologic examinations with barium have been proved to reveal a distinct appearance of abnormalities in neoplasms of the small bowel (GOOD MAR SHAH & LINDNER 1976). According to DARLING & WELCH (1959) these appearances are so character-

istic that a diagnosis could be made in 84 per cent of the small bowel tumors. This is in contrast to the present series where only the adenocarcinomas and carcinoids exhibited a characteristic appearance while other types of tumors could not be differentiated with any degree of certainty.

It appears that selective visceral angiography is mandatory in order to achieve a diagnostic accuracy of the level of DARLING & WELCH.

A correct preoperative radiologic diagnosis of small bowel tumors was achieved in 10 of 66 patients reported by SILBERMAN *et coll.* The material consisted of 32 malignant and 34 benign tumors. They found a higher preoperative diagnostic rate among malignant tumors. This was ascribed to the fact that these more often caused symptoms leading to an examination of the small bowel. In their series 16 were found incidentally at autopsy. Also in the present series a higher proportion of correct preoperative diagnoses existed in the group with malignant tumors compared to the benign group.

closed often have a considerable size (RAMER et coll 1971 KAUDE et coll 1972) The angiographic appearance of the leiomyomatous neoplasms are their constant and can be demonstrated by selective visceral angiography (BOUSEN & OLIN 1964 RAMER et coll KAUDE et coll) The discrepancy between barium examinations of the small intestine and angiography in leiomyomas has been pointed out by RAMER et coll who reported 4 cases with gastrointestinal hemorrhage The barium examinations failed in spite of the fact that they were repeated while angiography revealed the tumors their site and localization Their poor result with barium examinations is in contrast to that of KAUDE et coll who recognized small bowel leiomyomas in 9 of 11 cases examined with barium In all reported 13 cases angiography revealed the tumors These latter results are in accordance with those in the present series

Carcinoid tumors are often small when diagnosed leiomyomas have a characteristic angiographic appearance (BOUSEN et coll 1974) In the desmoplastic tissue initiated by the carcinoid tumor calcium deposits may appear (BOUSEN et coll BALTHAZAR 1978) but are not pathognomonic as they occur also in leiomyosarcomas (KAUDE et coll) In this series one carcinoid tumor contained calcific deposits The great variety of the appearances of carcinoid tumors found at barium examinations has been pointed out by several authors (SKANDALAKIS et coll BANCKS et coll 1975 SCHLANGEN 1976) The carcinoid tumors which were diagnosed preoperatively in the present series had a strong desmoplastic reaction

The adenocarcinomas arise from the mucosa and produce like their counterpart in the left colon a localized stricture Therefore unlike leiomyomas and carcinoids they cause early obstruction while bleeding is a late sign

It is apparent that small bowel tumors are more easily detected in the jejunum Adenocarcinoma is also relatively easy to diagnose This can be due to their ability to cause obstruction in contrast to leiomyosarcomas which often have an extraluminal mode of growth However the leiomyosarcoma usually bleeds which favors early clinical detection

Angiography is the examination of choice for demonstration of the exact tumor size and it is also accurate in predicting the specific type of the tumor Angiography should be used in all patients with unexplained hemorrhage from the gastrointestinal tract

(SHEEDY et coll 1975) Chronic complaints of abdominal pain even if these are unspecific also constitute an indication for angiography (KINKHABWALA & BALTHAZAR 1978)

The present series indicates that the clinical and radiologic diagnosis of small bowel tumors is not as discouraging as was presumed

SUMMARY

The value of radiography in patients with tumors of the small bowel was assessed retrospectively in 63 patients who had been subjected to radiography in a series of 118 patients treated for such tumors Thirteen of 17 jejunal tumors (76%) and 19 of 46 ileal tumors (41%) were diagnosed preoperatively Elective barium examination of the small bowel was performed in 36 patients in whom the tumors were diagnosed in 18 When the small bowel examination was performed during obstruction 7 of 21 tumors were diagnosed With the barium examination adenocarcinomas and carcinoid tumors were often diagnosed correctly In 32 patients angiography was carried out and the nature of the tumor was disclosed in 24 (75%)

REFERENCES

- BALTHAZAR E S Carcinoid tumors of the alimentary tract I Radiographic diagnosis *Gastrointest Radiol* 3 (1978) 47
- BANCKS N H GOLDSTEIN M H and DODD G D The roentgenologic spectrum of small intestinal carcinoid tumors *Amer J Roentgenol* 123 (1975) 274
- BOUSEN E and OLIN T: Zoliakographie und Angiographie der Arteria mesenterica superior In *Ergebnisse der medizinischen Strahlenforschung* p 122 Herausgegeben von H R Schütz R Glenner und A Ruttmann G Thieme Verlag Stuttgart 1964
- KAUDE J and TYLÉN U Radiologic diagnosis of ileal carcinoid tumors *Acta radiol* Diagnosis 15 (1974) 65
- DARLING R C and WELCH C E Tumors of the small intestine *New Engl J Med* 260 (1959) 397
- EBERT P A and ZUIDEMA G D Primary tumors of the small intestine *Arch Surg* 91 (1965) 452
- GOOD C A Tumors of the small intestine *Amer J Roentgenol* 89 (1963) 685
- KAUDE J SILSETH C and TYLÉN U Angiography in myomas of the gastrointestinal tract *Acta radiol* Diagnosis 12 (1972) 691
- KINKHABWALA M and BALTHAZAR E J Carcinoid tumor of the alimentary tract II Angiographic diagnosis of small intestinal and colonic lesions *Gastrointest Radiol* 3 (1978) 57
- MARSHAK R H and LINDNER A E *Radiology of the small intestine* 2nd Ed W B Saunders Philadelphia 1976
- MOERTLER C G SAUER W G DOCKERTY M B and BAGGENSTOSS A H Life history of the carcinoid tumor of the small intestine *Cancer* 14 (1961)

- OSTERMILLER W, JOERGENSEN E G and WEIBEL L A
clinical review of tumors of the small bowel. *Amer J Surg* 111 (1966) 403
- PAGTALUNAN R J G, MAYO C W and DOCKERTY M B
Primary malignant tumors of the small intestine. *Amer J Surg* 108 (1964) 13
- RAUER M, MITTY H A and BARON M G
Angiography in leiomyomatous neoplasms of the small bowel. *Amer J Roentgenol* 113 (1971) 263
- SANDERS R J and AXTELL H K
Carcinoids of the gastrointestinal tract. *Surg Gynec Obstet* 119 (1964) 369
- SCHLANGEN J T
Radiology of carcinoid tumors of the small intestine. *Radiol clin* 45 (1976) 105
- SHEEDY P F, FULTON R E and ATWELL D T
Angiographic evaluation of patients with chronic intestinal bleeding. *Amer J Roentgenol* 123 (1975) 338
- SILBERMAN H, CRICHLAW R W and CAPLAN P
Neoplasms of the small bowel. *Ann Surg* 180 (1974) 157
- SKANDALAKIS J E, GREY S, SHEPHERD D and BROWN F
Smooth muscle tumors of the alimentary tract. Charles C Thomas Publisher, Springfield, Ill 1970
- STRAUCH G O
Small bowel neoplasms. Elusive cause of abdominal symptoms. *Surgery* 55 (1964) 71
- VUORI J V A and VUORI M K
Radiological findings in primary malignant tumors of the small intestine. *Ann clin Res* 3 (1971) 16

CISTERNAL ABNORMALITIES PRODUCED BY CLINICAL TUMOURS IN THE POSTERIOR CRANIAL FOSSA

I Cerebellar tumours

M LINDQVIST

Few methods for radiographic examination of the arachnoid cisterns have been introduced during the last few years e.g. computer tomography (JUNSFELD 1973), computer cisternography (JEITZ & HINDMARSH 1974, GREPE & GREITZ 1977), conventional radiography of the cisterns using water soluble contrast medium (GREPE 1975, BERSON *et al.* 1976). These methods have realized the need for a systematic detailed analysis of the cisternal abnormalities in different tumour locations in the posterior cranial fossa.

Since the introduction of lumbar encephalography (OBERTSON 1941, 1957, LINDGREN 1949), the distortion of subarachnoid cisterns has been used in the diagnosis of posterior fossa tumours, mainly in order to define extraaxial tumours and to distinguish these from intraaxial tumours (LINDGREN 1950, CASTELANO & RUGGIERO 1953, FALK 1953, RUGGIERO 1956, LILIEQUIST 1959b).

However, for the diagnosis of intraaxial tumours, cisternal abnormalities have been of less importance even after the presentation of the normal radiographic anatomy of the cisterns (LILIEQUIST 1959a) and after improvement of the pneumographic technique by means of rotation chairs and the easy application of tomography, which made it possible to outline details of the subarachnoid cisterns as a matter of routine.

Already in 1935 DYKE & DAVIDOFF reported tonsillar herniation and compression of the cisterna pontis and the cisterna magna in cases with expanding lesions of the posterior fossa. LINDGREN & DI

CHIRO (1953) described the deformity of the aqueduct and the quadrigeminal cistern in patients with tumours located in the posterior fossa. RUGGIERO (1957) reported on some cisternal abnormalities in a clinical material of posterior fossa tumours examined by means of encephalography. LILIEQUIST (1963) reported briefly on cisternal abnormalities associated with tumours in the pons and cerebellum and he described for instance changes in the shape of the quadrigeminal cistern for different tumour locations. NEWTON (1968) reported cisternal distortion in several tumour locations in the posterior fossa, mainly tumours growing within the cisterns or otherwise directly affecting them. Some cisternal abnormalities associated with intra- and paraventricular tumours of the posterior fossa, especially in the pontonsillar spaces, were reported by MÖLLER (1974).

A total comprehensive and detailed description of the cisternal changes resulting from tumours in different locations has however not been given. Therefore a general survey and analysis of the appearances of the cisterns in cerebellar tumours has been performed and the results are now reported with a suggestion how the distortion of the cisterns can be used for localizing the tumours.

Definitions. For the orientation of the structures of the posterior fossa the principles introduced by CORRALES & GREITZ (1972) have been used, i.e. anteriorly-posteriorly perpendicular to the clivus.

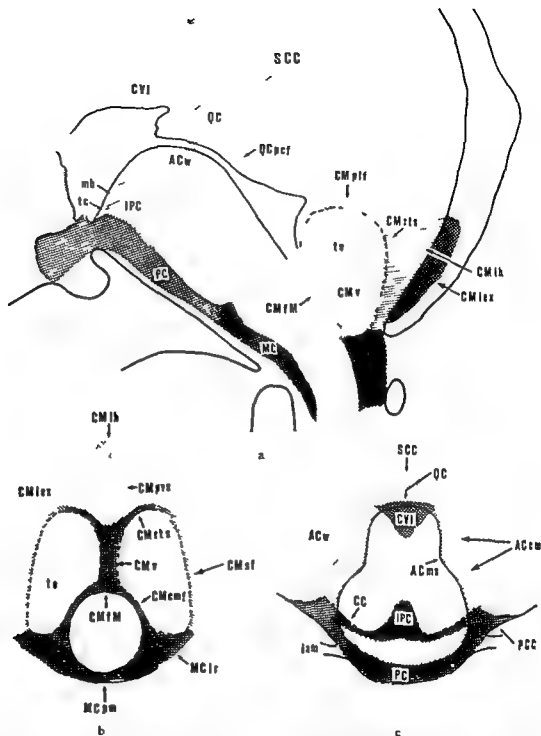


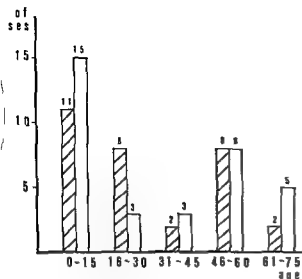
Fig 1 Drawings of the subarachnoid cisterns. a) Lateral view b) Axial view of the cisterns inferior to the fourth ventricle c) Axial view of the cisterns adjacent to the tentorial notch (From Lindqvist 1978) Labelled structures AC=ambient cistern (cm=circum-mesencephalic part ms=mesencephalic sulcus w=wing) CC=crural cistern CM=cisterna magna (cmf=cerebellomedullary fissure IM=foramen of Magendie th=interhemispheric part lex=lateral extension plf=postero-lateral

fissure pvs=paravermian sulcus rts=retrotonsillar secondary fissure v=vallecula) CVI=cisterna vel v lam=internal auditory meatus IPC=interpeduncular mb=mamillary body MC=medullary cistern (lr=lateral pm=premedullary part) PC=pontine cistern PCC=peduncular cistern QC=quadrigeminal cistern (plf=paravermian fissure) SCC=superior cerebellar cistern tc=tuber

superiorly and inferiorly at right angles to this perpendicular. This means, among other things, that a beam direction parallel to the clivus is termed the axial projection. Nomenclature and a schematic survey of the normal anatomy of the cisterns are

presented in Fig 1. Patients aged 0 to 15 years are termed children, patients aged 16 years or more are termed adults.

The ventricular system is classified as follows: (a) in adults if the index as d f



2 Sex and age distribution of 65 cases of cerebellar tumours
 males \square females

INDGREN in more than 0.33 or in cases where the frontal horn index cannot be evaluated the width of the third ventricle is more than 12 mm (LINDGREN 1966) (b) in children if the frontal horn index is more than 0.30 or the width of the third ventricle more than 8 mm (LODIN 1968)

Material and Methods

The material consisted of the cerebellar tumours of a series of patients with posterior fossa tumours examined by encephalography at the departments of neuroradiology at the hospital of Umeå and Karolinska Sjukhuset Stockholm during the period 1969-1975. Patients previously operated upon in the posterior cranial fossa were not included.

The examination technique was the same at both departments and during the whole period. The pneumographic examination started with a lumbar encephalography in accordance with the technique described by LINDGREN (1949) and later modified by GREITZ & GREPE (1967). In cases with increased intracranial pressure a prophylactic burr hole was made and sometimes a ventricular catheter was inserted. The examinations were carried out using a Mimer stand with rotation chair and tomography. In addition to standard films with varying magnification factors, tomography of the posterior fossa with a constant magnification factor of 1.4 was carried out in the axial and lateral projection in almost all cases. In the majority of cases with insufficient passage of gas to the ventricular system

Table 1

Cerebellar tumours in children and adults

Type of tumour	Children (0-15 years)	Adults (16 years or more)	Total	
			No of cases	Per cent
Juvenile astrocytoma	17	8	25	38.5
Hemangioblastoma (Lindau)	1	9	10	15.4
Metastasis	0	8	8	12.3
Ependymoma	3	4	7	10.8
Medulloblastoma	5	2	7	10.8
Meningioma	0	5	5	7.8
Astrocytoma poly- morphous	0	2	2	3.1
Angioma	0	1	1	1.5
Total	26	39	65	

supplementary ventriculography was also performed usually on the same day.

The total number of patients was 76 and of these only those cases have been included in which the type and position of the tumour was confirmed at surgery or autopsy. For benign tumours a time interval of 6 months between encephalography and operation was accepted for malignant tumours a maximum of 2 months. A total of 11 cases were excluded: 4 cases in which surgery was not performed because of old age or complicating disease; 5 cases with multiple tumours, multicentric tumour growth or for other reasons not definitely determined location; one case with too long an interval between encephalography and surgery; one case in which encephalography failed completely for technical reasons.

The remaining 65 cases form the basis for the present evaluation. The sex and age distribution of the material appears in Fig. 2 and the types of tumours in Table 1.

The size and position of the tumours were finally established by two experienced neuroradiologists who had access to all neuroradiologic examinations, surgical and autopsy reports.

Of the 65 cases 44 have been classified as cerebellar tumours according to the definitions used by CORRALES & GREITZ. 15 cases as paraventricular tumours according to the definitions of MÖLLER and 11 as extraaxial cerebellar tumours. Pontine angle tumours were not included.

Many of the paraventricular tumour positions are

Table 2

Cerebellar tumours divided into 8 groups according to their positions

Tumour position		No of cases
Midline tumours or tumours of the vermis	A I (A 1 Ia)	11
	A II (A 2 IIa A 2 ex)	5
	A III (A 3 IIIa 1	9
	IIIa 2 A 3 ex)	
Total		25
Lateral tumours or tumours of the hemisphere	B I (B 1 B 1 + B 2)	7
	B II (B 2 B 2 ex)	7
	B III (B 3 Va 2)	12
	B IV (B 4 VIa)	9
	C (C C ex)	5
Total		40

by definition identical or almost so with the corresponding cerebellar positions and have therefore been grouped together. The positions of the extra-axial cerebellar tumours have a close relation to those of the corresponding intra-axial tumours and have therefore been treated in common.

After these regroupings the following tumour positions were obtained: 3 groups of midline tumours called A I, A II, A III, roughly corresponding to tumours in the superior, posterior and inferior vermis respectively; 5 groups of lateral tumours termed B I, B II, B III, B IV and C, C corresponding to the lateral part and B to the medial part of the cerebellar hemispheres with positions B I adjacent to the tentorial notch, B II adjacent to the inferior surface of the tentorium, B III adjacent to the occipital bone and B IV adjacent to the pontine angle. In Table 2 the number of cases in each position is recorded and the original positions according to CORRALES & GREITZ and MÖLLER are given in parentheses.

The films were reviewed with regard to filling and distortion of different cisternal structures and also filling and size of the ventricular system. Distortion of the cisterns was graded as none, minimum, moderate or marked. The recorded changes in cisternal size and shape were related to the different tumour positions by computer analysis. For technical reasons all lateral tumours in this connection were treated as if situated on the right side and in all cases of midline tumours with a tendency to lateraliza-

tion the predominance was treated as if on the right side.

Results and Discussion

In Tables 3, 4 and 5 the frequency of the average distortion of the most important cisternal structures are given for tumours in the cerebellar hemispheres. In Table 6 some internal abnormalities for tumours with different positions in the vermis and the cerebellar hemispheres are summarized. Only cisternal structures filled in at least 20 per cent of the cases and regarded as formative as regards the localization of the tumour have been included in the tables.

Cisterna magna

Distortions of this cistern are summarized in Table 3.

Tonsillar herniation below the foramen magnum was present in the majority of cases and the distortion was as a rule more marked with slowly growing tumours e.g. juvenile astrocytomas than with rapidly growing tumours such as medulloblastomas and metastases. The shape of the herniated tonsils seemed to be of less importance in different types of lesions.

With tumours of the vermis tonsillar herniation was present in 90 per cent of the cases; the exceptions consisted of cases of intra- and extracerebellar tumours in position A III in which the tonsils were separated by the tumour so that they could herniate through the foramen magnum.

With tumours of the cerebellar hemispheres tonsillar herniation was present in 87 per cent of the cases; the exceptions consisted of a few cases of tumours in position B III in which the tumour displaced the cerebellum with the tonsils superiorly.

Tonsillar herniation caused by tumours in the posterior cranial fossa was described by DIXON & DAVIDOFF and has ever since been regarded as indicative of expanding lesion in the posterior cranial fossa. RUGGIERO (1957) for instance found tonsillar herniation in all of his 25 cases of cerebellar tumours. LILIEQUIST (1960) and WICKBOM & HANSSON (1963) pointed out that the herniation as a rule was more marked in slowly growing tumours.

The cervical medulla was in the majority of cases displaced anteriorly below the foramen magnum but in a few cases posteriorly instead (Fig. 7). The reason for this posterior displacement was

Table 3

Filling and distortion of the cisterna magna in cerebellar tumours. All hemispheric tumours treated as if situated on the right side. Symbols and abbreviations: a=anterior p=posterior s=superior i=inferior R=right L=left 0=no change (+)=minimal change or increase ++=marked change or increase (-)=minimal decrease --=moderate decrease ---=marked decrease open space=structure not possible to evaluate

Tumour position	Cerebellum			
	Vermis		Hemisphere	
	Filling (%)	Distortion	Filling (%)	Distortion
Cisterna magna				
1 Extracranial part lat proj tonsillar herniation	100		100	
a p displacement of cervical medulla		++		++
2 Interhemispheric part lat proj s i diameter	92	a(+)	97	a(+)
3 Foramen of Magendie lat proj	40	--	20	--
■ p displacement		a++		a+
4 Vallecule axial proj width	52	(-)	70	-
lateral displacement		0		L++
5 Retrotonsillar spaces lat proj	12		12	
■ displacement				
s i displacement				
6 Cerebellomedullary fissures				
a right side axial proj	24		17	
a p displacement		0		a++
lateral displacement		R(+)		L++
b left side axial proj	74		20	
a p displacement		0		0
lateral displacement		L(+)		L++
7 Paravermian sulci axial proj	24		24	
width of inferior vermis		++		0
lateral displacement of inferior vermis		0		L++

ident— it may as was pointed out by JIROUT (1959) be the consequence of a downward hernia on of the brain stem in the foramen magnum

The interhemispheric part of the cisterna magna as in the lateral projection usually compressed against the occipital crest. However in a few cases of tumour in position B III the cistern was widened (Fig. 4) due to an upward displacement of the inferior vermis by a very large tumour

The compression of the cisterna magna against the occipital crest in the case of cerebellar tumours was pointed out by DYKE & DAVIDOFF and KRAUSOVA & JIROUT (1963) but the paradoxical widening in some B III tumours has not been described previously

The foramen of Magendie was displaced anterior

ly in all tumours of the vermis. With tumours in the cerebellar hemispheres the foramen of Magendie was seldom identified. When visible it was markedly displaced anteriorly with tumours in the B II position and slightly so in the B I and B III positions and usually not displaced at all in the B IV and C positions (Table 6)

The vallecule could not be identified in the axial projection in more than half of the cases. Axial views with slightly varying beam direction and axial tomography were often necessary for definite identification of the vallecule and for distinguishing it from superimposition of the interpeduncular cistern or the anterior part of the interhemispheric fissure. Poor filling of the vallecule was most common in cases with tumours in the posterior and inferior



Fig 3

Fig 3 Large tumour in the BIV position. Posterior displacement of the cervical medulla (\rightarrow) below the foramen magnum



Fig 4a

Fig 4 Large tumour in the BIII position with marked superior displacement of the inferior vermis (\rightarrow) a) Axial projection b) Lateral projection. Marked lateral displacement of the inferior vermis (\rightarrow) (X=soft tissue tumour of unknown origin not explained by the examination or in the surgical report.)



Fig 4b

parts of the vermis (positions AII and AIII). Widening of the vallecula was unusual and was only observed in some of the cases with a tumour in the inferior vermis (position AIII) and in a few cases of paraventricular tumours in position BIII with infiltration of the brain stem. In all other cases the width of the vallecula was reduced or normal.

A definite lateral displacement of the vallecula towards the contralateral side regularly occurred in hemispheric tumours (Fig 5). In tumours of the vermis situated in the midline the vallecula was not laterally displaced. On the other hand, with asymmetric tumours of the vermis some lateral displacement of the vallecula was observed, but in such cases the degree of displacement was as a rule less than in cases of hemispheric tumours.

Both RUGGIERO (1957) and LILJEQUIST (1963) have pointed out that lateral displacement of the

vallecula is an important indication of lateral tumour in the posterior fossa. However, in RUGGIERO's series of 25 cases the vallecula could be identified in the axial projection in only 2 cases. MÖLLER has reported widening of the vallecula in cases of intra- and paraventricular tumours in the inferior part of the posterior fossa.

The cerebellomedullary fissures were often separated in cases of tumours of the vermis, especially tumours of the inferior vermis. In hemispheric tumours the cerebellomedullary fissure on both sides was displaced towards the contralateral side on the tumour side also in the anterior direction.

The paravermian sulci indicate the width of the inferior vermis. A definite widening of the inferior vermis was present in most cases of vermis tumours without any definite difference between tumours of the superior and the inferior vermis. In hemispheric



Fig. 5 Tumour of the right cerebellar hemisphere position III a b) Encephalography Compression and lateral displacement to the left of the vallicula (→) and the interhemispheric part of the cisterna magna (++) Tonsillar herniation (++) and

in tumours the vermis was slightly widened with tumours in the positions B I and II In the remaining positions the width of the vermis was normal or reduced In many cases of hemispheric tumours also a definite lateral displacement of the vermis was encountered (Fig. 4 a)

Widening of the inferior vermis in cases of intra

marked compression of the pontine and medullary cisterns (→) c d) Ventriculography No filling of the fourth ventricle Only the supratentorial part of the aqueduct is outlined by gas (++)

and paraventricular tumours of the fourth ventricle was described by MÖLLER

The retrotonsillar spaces posterolateral fissures and secondary fissures were so poorly filled in most cases of cerebellar tumours that they could not be analysed in detail

The lateral extension of the intracranial part of

Table 4

Filling and distortion of the medullary cistern, pontine cistern and the pontocerebellar cisterns in cerebellar tumours. Tumour position symbols and abbreviations as in Table 3. Additional abbreviations: Ra=right side rotated anteriorly, Rp=right side rotated posteriorly.

Tumour position	Cerebellum			
	Vermis		Hemisphere	
	Filling (%)	Distortion	Filling (%)	Distortion
Medullary cistern				
1 Premedullary part lat. proj.	56		42	
a p diameter		--		--
2 Lateral recesses				
a right side axial proj.	46		55	
a p diameter		-		--
lateral extension		-		
b left side axial proj.	46		52	
a p diameter		-		-
lateral extension		-		--
3 Diameter of medulla oblongata				
a p diameter lat. proj.		-		-
transverse diam. axial proj.		+		+
4 Lateral displacement of medulla oblongata axial proj.		0		L +
5 Rotation of medulla oblongata around axis parallel to clivus		0		Ra +
Pontine cistern lat. proj.				
a p diameter	80		87	
tendency of superior part of pons to recede from clivus		0		(+)
Pontocerebellar cisterns				
1 Right side axial proj.	33		31	
width of lateral part		-		--
width of medial part		-		--
2 Left side axial proj.	58		59	
width of lateral part		-		-
width of medial part		-		-

the cisterna magna was defined in the axial projection on one or both sides in 15 per cent of the cases. If unilateral filling sometimes occurred on the tumour side sometimes on the contralateral side. These structures therefore have no value for the localization, as was also pointed out by RUGGIERO (1957).

Medullary cistern

Distortions of this cistern are summarized in Table 4.

Compression of the premedullary part of the

medullary cistern was a very constant feature in all tumour positions. In most cases of tumours of the vermis the medulla oblongata in the axial projection was moderately widened without lateral displacement or rotation. In the case of hemispheric tumours a slight widening of the medulla oblongata occurred in some cases of B I and B II tumours, also in paraventricular B III tumours with infiltration of the medulla oblongata. In practically all cases of hemispheric tumours in which the medullary cistern could be evaluated in the axial projection a lateral displacement of the medulla oblongata was evident. Anterior rotation of the medulla oblongata on



Fig 6

Fig 6 Tumour of the right cerebellar hemisphere position BII axial tomography through the vallicula and medulla oblongata lateral displacement of the vallicula (\rightarrow) reduced a p. diameter the right lateral recess (\leftrightarrow) and of the premedullary part (\leftrightarrow) the medullary cistern Medulla oblongata displaced to the left and rotated anteriorly on the tumour side

Fig 7 a) Tumour of the inferior vermis position AIII Superior part (\rightarrow) of posterior part of superior surface of the pons b) Hemispheric tumour position BIII The superior part of the pons recedes from the clivus (\leftrightarrow)

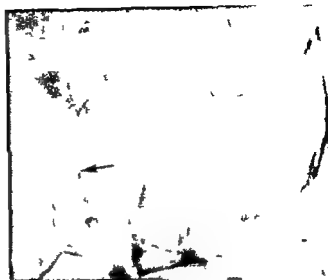


Fig 7a



Fig 7b

On the tumour side occurred in most cases of tumour in the AII and BII position (Fig 6) but not with other tumour positions (Table 6)

Compression of the medullary cistern is an important indication of an expanding lesion in the posterior fossa and has been pointed out by RUGGIERO (1957) KRAUSOVA & JIROUT and LILJEQUIST (1963) but the other distortions of the medullary cistern in cerebellar tumours have not been reported in detail previously

Pontine cistern

Distortions of this cistern are summarized in Table 4

Compression of the pontine cistern against the clivus was a constant finding for all tumour posi-

tions. The superior and the inferior part were compressed to the same degree in all cases of midline tumours and in most cases of hemispheric tumours.

A tendency of the superior part of the pons to recede from the clivus occurred in some cases of hemispheric tumours (Fig 7b) but not in vermis tumours.

Also compression of the pontine cistern is a well known sign of an expanding lesion in the posterior fossa (DYKE & DAVIDOFF RUGGIERO 1957 KRAUSOVA & JIROUT LILJEQUIST 1963)

Pontocerebellar cisterns

Distortions of these cisterns are summarized in Table 4

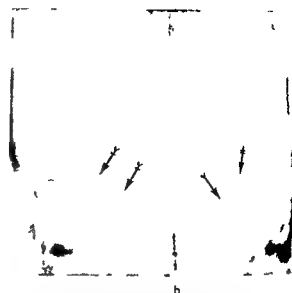
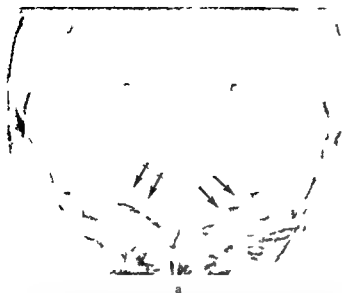


Fig 8 a) Paraventricular tumour on the left side position B III Marked compression (\rightarrow) of the ipsilateral pontocerebellar cistern. The contralateral cistern (\leftrightarrow) is not distorted b) Tentorial meningioma on the left side position C Widening (\leftrightarrow)

of the lateral part of the pontocerebellar cistern on the left side. Marked compression of the medial part of the cistern and of the whole contralateral pontocerebellar cistern (\rightarrow)

The pontocerebellar cistern was filled almost twice as often on the contralateral side as on the tumour side both in cases of hemispheric tumours and in cases of asymmetric tumours of the vermis. When they were filled bilaterally the cistern on the tumour side was usually more compressed than on the contralateral side and the compression was in most cases the same in the lateral as in the medial part of the cistern (Fig 8a). Widening of the lateral part of the pontocerebellar cistern with compression of the medial part occurred in one case of extra-axial meningioma in the C position (Fig 8b).

Poor filling or marked compression of the pontocerebellar cistern on the tumour side has previously been reported by LILIEQUIST (1963) and PRIBRAM (1966). RUGGIERO (1957) found that the pontocerebellar cisterns were often compressed or poorly filled in cases with cerebellar tumours and that in cases with unilateral filling it was sometimes filled only on the side of the tumour, sometimes only on the contralateral side. On the other hand KRAUSOVÁ & JIROUT claimed that the pontocerebellar cistern was usually wider on the tumour side than on the contralateral side but they did not clearly distinguish between intra- and extra-axial tumours.

Interpeduncular cistern

Distortions of this cistern are summarized in Table 5.

The inferior limit of the interpeduncular cistern

is made up of the superior surface of the pons. The position of the pons can be used as a measure of the degree of upward displacement in the tentorial notch. This displacement, which depends on the size and position of the expanding lesion in the posterior fossa, can be counteracted by a widening of the supratentorial part of the ventricular system even to such an extent that an expected upward displacement is paradoxically replaced by a downward displacement (Fig 9).

The degree of supero-inferior compression of the interpeduncular cistern depends not only on the upward displacement of the pons but also on the extent on the width of the third ventricle. In connection with widening of the anterior part of the third ventricle the tuber cinereum may cause a marked compression of the interpeduncular cistern (Fig 10). In some cases, especially in children, this compression was sometimes total or nearly total and the cistern then often took on a rabbit's ears appearance (Fig 11). The filling defect between the two parts probably comprising the oculomotor nerves.

The degree of supero-inferior compression of the interpeduncular cistern was approximately the same for both hemispheric and vermis tumours. The diameter of the cistern was reduced in most tumours as a rule more in medial than in lateral tumours. With medial tumours the upward compression was more marked in tumours in the superior vermis (A I) than in the inferior vermis (A III, Table 6).

Table 5

Filling and distortion of the interpeduncular cistern, ambient cistern and quadrigeminal cistern in cerebellar tumours. Tumour position symbols and abbreviations as in Tables 3 and 4. Additional abbreviations: fr=frontally, sag=sagittally, ia=inferior end rotated anteriorly, ip=inferior end rotated posteriorly.

Tumour position	Cerebellum			
	Vermis		Hemisphere	
	Filling (%)	Distortion	Filling (%)	Distortion
Interpeduncular cistern				
Lat. proj.	80		88	
a p. diameter		—		(—)
s i. diameter		—		—
s i. displacement of pons		s +		s +
s i. inclination of the posterior part of the superior surface of the pons		s +		s (+)
Ambient cistern				
Circum mesencephalic part axial proj.				
a. width of posterior part				
right side	42	0	57	II
left side	50	0	47	0
b. width of anterior infratentorial part				
right side	12		12	
left side	21		15	
c. width of anterior supratentorial part				
right side	29	0	42	II
left side	33	0	41	0
d. rotation around sagittal axis perpendicular to clivus				
right side		fr (+)		fr (+)
left side		fr (+)		sag (+)
Quadrigeminal cistern				
1. Body of cistern lat. proj.	72		87	
a p. displacement		II		0
kinking of quadrigeminal plate		++		++
rotation of inferior end of quadrigeminal plate		ia +		ia +
2. Precentral fissure lat. proj.	44		49	
a p. displacement		a +		a +

lateral tumours the a p. compression was moderate in positions II I and B II, slight in the C position and absent in positions II III and B IV (Table 6).

Upward displacement of the pons was observed both in the case of hemispheric and vermian tumours but the degree of displacement varied greatly and was not obviously correlated with the tumour position.

The superior tilt of the posterior part of the superior surface of the pons was as a rule more evident

with vermian (Fig. 7a) than with hemispheric tumours.

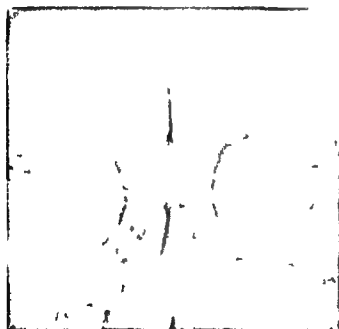
A widening of the third ventricle as the cause of compression of the interpeduncular cistern was reported at autopsy by SPATZ & STROESCU (1934) and was demonstrated radiographically by EPSTEIN (1951). RUGGIERO (1957) found an upward displacement of the pons in most cases of cerebellar tumours and in many cases also a compression of the interpeduncular cistern. However, he did not dis-



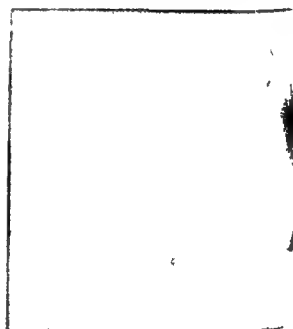
a



b



c



d

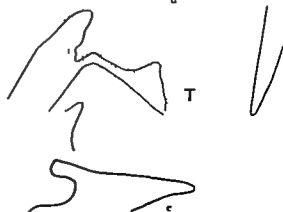


Fig 9 Astrocytoma of the inferior vermis position AIII a b) First examination Lateral ventricles of ordinary size c d) Second examination 9 months later Ventricular dilatation in spite of increasing size of the tumour slight inferior herniation in the tentorial notch of both the pons and the third ventricle e) Combined drawing of b) (dotted lines) and d) (continuous lines) T=tumour



Fig 10a



Fig 10b



Fig 11

Fig 10 Tumour of the left cerebellar hemisphere position B III a) Encephalography in the sitting position lateral view b) Ventriculography in supine position lateral view The interpeduncular cistern compressed by the dilated third ventricle (→) In the sitting position the cistern of the lamina terminalis (↔) and the pericallosal cistern (↔) are also filled

Fig 11 Lateral view sitting position 3-year-old patient with a huge tumour in the right cerebellar hemisphere position B III The interpeduncular cistern almost totally compressed and resembling a pair of rabbit's ears because of a filling defect probably caused by the oculomotor nerves (→)

ass the significance of the widening of the third ventricle RUGGIERO & CASTELLANO (1953) described a measuring method for determining an upward displacement of the posterior part of the third ventricle in cases with tumours of the posterior fossa. However, also with this method the results were influenced by the width of the anterior part of the third ventricle.

Ambient cistern

Distortions of this cistern are summarized in Table 5.

The *circum mesencephalic parts* were seldom filled infratentorially, especially on the tumour side. The supratentorial parts were filled approximately equally often on both sides, but as a rule without appreciable changes in width. In vermis tumours, sometimes a tendency to frontal rotation of the ambient cistern on both sides was noted, while in hemispheric tumours a frontal rotation on the tumour side and a sagittal rotation on the contralateral side were sometimes observed (Fig 12 regarding this complex rotation cf. also LINDQVIST 1978). However, cases also existed with sym-

Table 6

Cisternal abnormalities that can be used to distinguish between cerebellar tumours of different locations. Symbols and abbreviations as in Tables 3 to 5

	Tumour position				
	AI	AII	AIII		
Tumours of the vermis					
Cisterna magna					
Extracranial part lateral projection tonsillar herniation	++	++	+		
Interpeduncular cistern					
lateral projection a p diameter	--	-	(-)		
	Tumour position				
	BI	BII	BIII	BIV	C
Tumours of the hemispheres					
Cisterna magna					
1 Interhemispheric part lateral projection	--	-	(-)	-	--
2 Foramen of Magendie lateral projection a p displacement	a+	a++	a+	0	0
Medullary cistern axial projection a p rotation of the medulla oblongata on the tumour side					
	a+	a(+)	0	0	0
Interpeduncular cistern					
lateral projection a p diameter	-	-	0	0	(-)

metric ambient cisterns in spite of lateral tumour positions

RUGGIERO (1957) stated that unilateral filling of the circum mesencephalic part of the ambient cistern was of no use for localizing posterior fossa tumours. LILIEQUIST (1963) reported that the infratentorial part of the cistern on the tumour side was usually more compressed, often not filled at all, but that this change was subtle and not reliable for purposes of localization.

Quadrigeminal cistern

Distortions of this cistern are summarized in Table 5.

Displacement of the quadrigeminal cistern and the quadrigeminal plate was seldom observed; appreciable distortions appeared instead as a kink in the

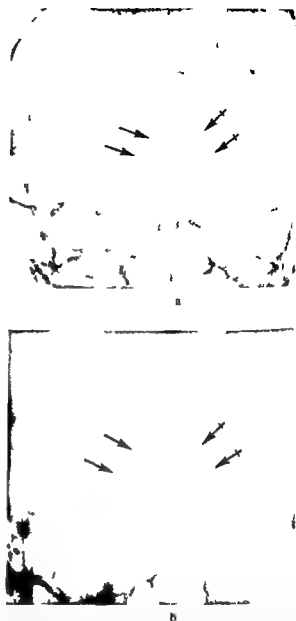


Fig. 17. Metastasis in the right cerebellar hemisphere. Axial view: a) without and b) with tomography. Tendency of frontal rotation (→) of the circum mesencephalic part of the ambient cistern on the tumour side and to sagittal rotation on the contralateral side.

quadrigeminal plate, often combined with a rotation anteriorly or posteriorly of the inferior part of the quadrigeminal plate. The width of the fourth ventricle and the aqueduct greatly influenced the appearance of the quadrigeminal cistern. Cases with approximately the same tumour positions can exhibit quite different deformities of the quadrigeminal cistern depending on whether the fourth ventricle and aqueduct were widened or compressed (Fig. 13). Widening of the fourth ventricle and aqueduct is present in most cases of intraventricular tumours in the fourth ventricle due to obstruction of



13 Two cases of tumour of the inferior vermis a) Fourth ventricle and aqueduct compressed. Abrupt reduction of the width of the aqueduct (→) where it passes through the tentorial notch. b) The inferior part of the aqueduct and the quadrigeminal



plate are rotated anteriorly b) Widening of the fourth ventricle and the aqueduct. The inferior end of the quadrigeminal plate is somewhat rotated posteriorly

cerebrospinal fluid flow from the ventricle caused by the tumour

A similar widening of the aqueduct and the fourth ventricle also occurred in several cases of paraventricular tumours in the inferior part of the posterior fossa mainly in the A III position but also in some cases with positions B III and B IV (Fig 14c, d). The deformity of the quadrigeminal cistern in these cases was similar to that usually caused by tumours of the fourth ventricle, i.e. the quadrigeminal plate was more or less kinked and its inferior part was somewhat rotated posteriorly if rotated at all. The precentral fissure was in these cases usually displaced superiorly but not anteriorly.

With all other cerebellar tumour positions both the aqueduct and the fourth ventricle were compressed. Sometimes with an abrupt reduction of the width of the aqueduct at the tentorial notch (Fig 14b). These cases also exhibited the well known and characteristic kinking of the quadrigeminal plate with anterior and superior displacement of the precentral fissure (Fig 14a). The displacement of the lateral parts of the precentral fissure was sometimes greater than the displacement of the aqueduct.

The kinking of the quadrigeminal plate was well correlated to the presence of ventricular dilatation. In 28 cases with ventricular dilatation in which the quadrigeminal cistern could be evaluated the quadrigeminal plate was definitely kinked in 22 cases, slightly in 4 cases and without kinking in 2 cases. Of the 4 cases without ventricular dilata-

tion in which the quadrigeminal cistern could be evaluated no kinking of the quadrigeminal plate occurred in 3 cases and slight kinking in one case.

The deformity of the aqueduct and the quadrigeminal cistern was reported in detail by LINDGREN & DI CHIRO for different types of posterior fossa tumours, as also the posterior rotation of the inferior part of the quadrigeminal plate in cases with a widening of the aqueduct and the fourth ventricle. For instance in cases with tumours of the inferior vermis LILIEQUIST (1963) and PRIBRAM also described this appearance of the quadrigeminal cistern in cases of tumours in the inferior vermis and in the fourth ventricle.

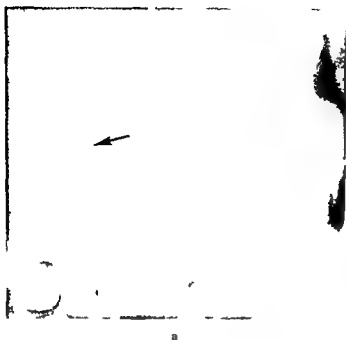
Remaining cisterns

The crural cisterns were filled on one or both sides in 40 per cent of the cases, approximately as often on the side of the tumour as on the contralateral side, and the appearance of these cisterns did not seem to be correlated with the tumour positions.

The chiasmatic cistern was filled in approximately 90 per cent of the cases. It was moderately compressed by the anterior part of the third ventricle in most cases of ventricular dilatation but was otherwise without specific distortion.

The cistern of the lamina terminalis was filled in 15 per cent of the cases, also without diagnostic appearance.

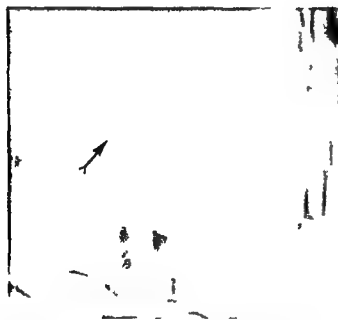
The superior cerebellar cistern was identified in the lateral view in 40 per cent of the cases. It was



a



b



c



d

Fig 14 a) Encephalography and b) ventriculography of a tumour in the BIV position. Compression of the fourth ventricle. Typical kink and anterior displacement of the inferior part of the quadrigeminal plate (\rightarrow) and the aqueduct (\leftrightarrow). c) Encephalography

and d) ventriculography of another tumour in the BIV position. Dilatation of the fourth ventricle. Inferior part of the quadrigeminal plate is not rotated anteriorly (\rightarrow) because of widening of the fourth ventricle and the aqueduct.

often difficult to distinguish from superimposed supratentorial structures such as the calcarine and the posterior parietal fissures. The shape of the superior vermis could be evaluated in 20 cases, 17 of which exhibited a bulging of the superior vermis as in tumours of the posterior compartment. In 3 cases the appearance of the superior vermis was normal.

In the axial view the superior cerebellar cistern

could be evaluated in approximately 20 per cent of the cases. With lateral tumours it was somewhat more often filled on the contralateral side than on the tumour side. In a few cases extraaxial tumours were surrounded by gas in the superior cerebellar cistern (Fig 15).

Bulging of the superior cerebellar cistern was described by RUGGIERO (1957) in 4 of 25 cases of cerebellar tumours.

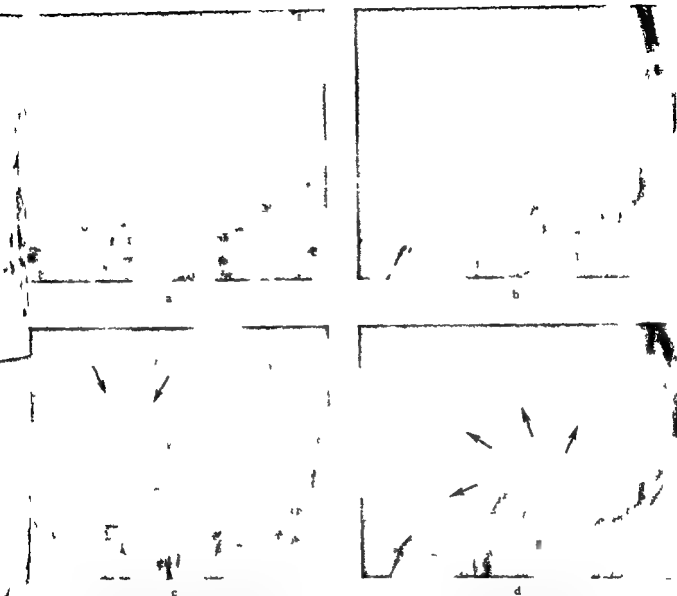


Fig. 15 Tentorial meningioma on the right side. a) b) Tomography before air filling of the cisterns. The aqueduct and the fourth ventricle are deformed as with large tumour of the pontine

angle. c) d) Tomography after air filling of the cisterns. The tumour (→) almost completely surrounded by air

The pericallosal cisterns were filled on one or both sides in 40 per cent of the cases. In the axial projection the wings of the ambient cisterns were observed in approximately 50 per cent of the cases and the cisterna veli interpositi in approximately 70 per cent of the cases. All these cisternal structures were often markedly dilated in cases with ventricular dilatation but of normal size or only slightly dilated in cases without hydrocephalus. Unilateral filling did not correlate with the tumour side. In no case was any rotation or lateral displacement of the cisterna veli interpositi observed.

Widening of the pericallosal cisterns, the cisterna

veli interpositi and the wings of the ambient cistern are well known indirect signs of expanding lesions of the posterior fossa described by SASSAROLI (1955) and by SCHECHTER et coll (1958). PRIBRAM pointed out that unilateral abnormalities are not correlated to the side of the tumour and he also reported that the same cisternal appearances could be present in cases of ventricular dilatation from other causes than expanding lesions of the posterior fossa. ROTH et coll (1972) claimed that the mechanism behind these cisternal distortions is to be found in mechanical changes of the cerebrospinal fluid circulation.

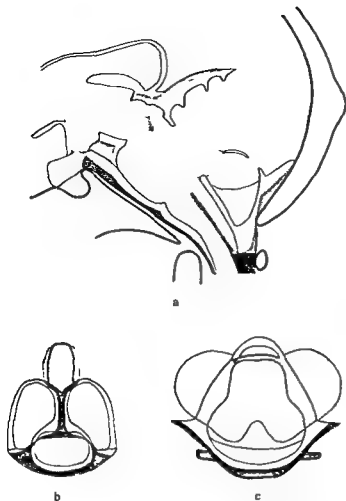


Fig 16 Drawings of some important cisternal deformities in tumours of the vermis a) Lateral view b) Axial view of the cistern inferior to the fourth ventricle c) Axial view of the cisterns adjacent to the tentorial notch The normal appearance of the cisterns is indicated by continuous lines cisternal structures possible to evaluate in tumour cases by shaded areas (cf Fig 1)

Comparison with cisternal distortions caused by experimental tumours

Total agreement does not exist between the cisternal abnormalities in clinical cases and those produced by experimental tumours (LINDQVIST) and is not to be expected. Cisternal distortions caused by ventricular dilatation and not by the tumour itself could not be imitated experimentally for instance widening of the pericallosal cisterns the ambient wings and the cisterna veli interpositi compression of the chiasmatic cistern and interpenduncular cistern. One of the most striking differences was that the evident contralateral displacement and rotation of the cisterna veli interpositi present in almost all cases of lateral experimental tumours was not observed at all in the clinical material. This might be due to the fact that in the experimental series there

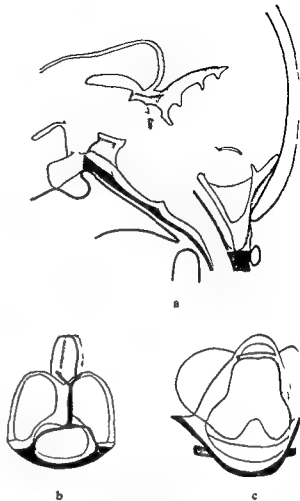


Fig 17 Drawings of some important cisternal deformities in tumours of the right cerebellar hemisphere a) Lateral view b) Axial view of the cistern inferior to the fourth ventricle c) Axial view of the cisterns adjacent to the tentorial notch (cf Fig 1)

was no supratentorial intracranial pressure. Also displacement of the brain stem inferiorly thus resulted in a passive displacement of the supratentorial part of the brain stem towards the contralateral side and thereby also a displacement of the cisterna veli interpositi. Other differences are easily explained by the fact that the experimental tumour developed instantaneously without the slow remodelling of the surrounding brain structures that occurs in clinical cases.

However in many respects a good agreement is found between the clinical and the experimental situation. This is true of many of the abnormalities of the cisterna magna the medullary cistern and the pontine cistern. For instance the changes in the shape and position of the medulla oblongata are of great importance for determining the tumour pro-

Typical cisternal distortions caused by tumours in the vermis and in the cerebellar hemispheres

Lateral projection

These abnormalities are similar for tumours in the vermis and in the hemispheres. In most cases the following cisternal distortions are present:

Tumour of the vermis	Tumour of the hemispheres
Tonsillar herniation Exception: Intra- and extra-axial tumour in the inferior part of the posterior fossa with marked separation of the tonsils	Tonsillar herniation Exception: Some cases of tumour in the inferior part of the posterior fossa with marked superior displacement of the cerebellum
Compression of the interhemispheric part of the cisterna magna against the occipital crest	Compression of the interhemispheric part of the cisterna magna against the occipital crest Exception: Some cases of tumour in the inferior part of the posterior fossa with marked superior displacement of the cerebellum
Anterior displacement of the Magendie	Anterior displacement of the foramen of Magendie Exception: Lateral hemispheric tumour and tumour close to the pontine angle
Compression of the premedullary part of the medullary cistern	Compression of the premedullary part of the medullary cistern
Compression of the pontine cistern	Compression of the pontine cistern
Moderate superior-inferior compression of the interpeduncular cistern especially in cases with hydrocephalus. Moderate anterior compression of the cistern	Moderate superior-inferior compression of the interpeduncular cistern especially in cases with hydrocephalus
Bulging of the quadrigeminal plate	Bulging of the quadrigeminal plate
Anterior rotation of the inferior part of the quadrigeminal plate Exception: Tumour with widening of the fourth ventricle	Anterior rotation of the inferior part of the quadrigeminal plate Exception: Tumour with widening of the fourth ventricle
Compression of the superior cerebellar cistern with bulging of the superior vermis	Compression of the superior cerebellar cistern with bulging of the superior vermis

Axial projection

Important differences exist between the abnormalities resulting from tumours of the vermis and those resulting from hemispheric tumours. In most cases the following cisternal distortions are present:

Tumour of the vermis	Tumour of the hemispheres
Widening of the inferior vermis	Compression and contralateral displacement of the inferior vermis
Slight compression and no lateral displacement of the vallicula Exception: Tumour in the inferior part of the posterior fossa may cause a widening of the vallicula. In asymmetric tumour some lateral displacement of the vallicula may occur	Compression and contralateral displacement of the vallicula
Anterior compression and some widening of the medulla oblongata. Symmetric compression of the lateral recesses of the medullary cistern Exception: Some asymmetry may occur in cases of asymmetric tumour	Contralateral displacement of the medulla oblongata with compression of the lateral recess of the medullary cistern on the contralateral side In cases with tumour of the posterior part of the hemisphere sometimes an anterior rotation of the medulla oblongata occurs on the tumour side
Symmetric and uniform compression of the pontocerebellar cisterns Exception: Some asymmetry may occur in cases of asymmetric tumour	Asymmetric compression of the pontocerebellar cisterns with more marked compression on the tumour side than on the contralateral side. The cisterns are usually compressed to the same extent in their medial and lateral parts Exception: Extraaxial tumour may cause a widening of the pontocerebellar cistern on the tumour side
Slight symmetric rotation frontally of the circum-mesencephalic part of the ambient cistern	Slight frontal rotation of the circum-mesencephalic part of the ambient cistern on the tumour side and slight sagittal rotation on the contralateral side

tions. The complex rotation movements of the circum mesencephalic parts of the ambient cistern were also to some extent present in the clinical material.

Typical cisternal abnormalities in cerebellar tumours of the vermis and the right hemisphere respectively are listed on page 103 and illustrated in Figs 16 and 17.

The cisternal abnormalities associated with other tumour locations in the posterior fossa will be reported separately with a discussion of the possibilities of differential diagnosis.

SUMMARY

A detailed analysis of the deformities of the subarachnoid cisterns was carried out in a clinical material of 65 cases with cerebellar tumours examined by encephalography. The distortion of the cisterns was related to 8 different tumour positions and the results compared with those from a previous experimental investigation. Typical cisternal distortions for cerebellar tumours are listed constituting a basis for a general analysis of the cisternal abnormalities demonstrated by whatever means of neuro-radiologic procedure employed: pneumography, computer tomography or cisternography with positive contrast medium.

ACKNOWLEDGEMENTS

This investigation was supported by grants from the Swedish Cancer Society and the Medical Faculty University of Umeå.

REFERENCES

- CASTELLANO F and RUGGIERO G. Meningiomas of the posterior fossa. *Acta radiol* (1953) Suppl No 104.
- CORRALES M and GREITZ T. Fourth ventricle II. Tumours of the cerebellum. *Acta radiol Diagnosis* 12 (1972) 241.
- DYKE C G and DAVIDOFF L M. The significance of abnormally shaped subarachnoid cisterns as seen in the encephalogram. Correlation with clinical cases. *Amer J Roentgenol* 32 (1935) 743.
- EMSTEN B. Shortening of the posterior wall of the sella turcica caused by dilatation of the third ventricle or certain suprasellar tumors. *Amer J Roentgenol* 65 (1951) 49.
- FALK B. Encephalography in cases of intracranial tumour. *Acta radiol* 40 (1953) 220.
- GREITZ T and GREFF A. Mimer II and rotating chair. Application in neuroradiology. Elema Schönander Stockholm 1967.
- and HINDMARSH T. Computer assisted tomography of intracranial CSF circulation using a water soluble contrast medium. *Acta radiol Diagnosis* 15 (1974) 497.
- GREFF A. Cisternography with the non ionic water soluble contrast medium metrizamide. A preliminary report. *Acta radiol Diagnosis* 16 (1975) 146.
- and GREITZ T. C A T investigation of the subarachnoid space. In: The first European seminar on computerised axial tomography in clinical practice by G H du Boulay and I F Moseley. Springer-Verlag Berlin Heidelberg 1977.
- HOUNSFIELD G N. Computerized transverse axial scanning (tomography). Part I. Description of the system. *Brit J Radiol* 46 (1973) 1016.
- JIROUT J. Myelographic syndrome of caudal displacement of the brain stem. Changes in the position and form of the upper cervical spinal cord in case of intracranial expanding lesions. *Brit J Radiol* (1959) 188.
- KRAUSOVÁ L and JIROUT J. Das pneumographische der subtentorialen Arachnoidalräume im normalen Zustand und bei raumfordernden Prozessen. *Fortschr Röntgenstr* 98 (1963) 733.
- LILJEQUIST B. (a) The subarachnoid cisterns. Anatomic and roentgenologic study. *Acta radiol* (1959) Suppl No 185.
- (b) Pontine angle tumour. Encephalographic appearances. *Acta radiol* (1959) Suppl No 186.
- Encephalographic changes in the axial pressure syndrome. *Acta radiol* 54 (1960) 369.
- Lumbar encephalography in pontine and intracerebellar tumours. *Acta radiol Diagnosis* 1 (1963) 1.
- LINDGREN E. Some aspects on the technique of encephalography. *Acta radiol* 31 (1949) 161.
- Encephalographic examination of tumours in the posterior fossa. *Acta radiol* 34 (1950) 331.
- Encephalography in cerebral atrophy. *Acta radiol* (1951) 277.
- and DI CHIRO G. The roentgenologic appearance of the aqueduct of Sylvius. *Acta radiol* 39 (1953) 11.
- LINDQVIST M. Cisternal changes produced by experimental balloon tumours in the posterior cranial fossa. A post mortem investigation. *Acta radiol Diagnosis* 19 (1978) 561.
- LODIN H. Size and development of the cerebellar trigonular system in childhood. *Acta radiol Diagnosis* (1968) 385.
- LÖNNUN A. The clinical significance of central cerebellar ventricular enlargement. Universitetsforlaget 1966.
- MÖLLER A. Pneumography in paraventricular and intraventricular tumours of the posterior fossa. *Acta radiol* (1974) Suppl No 342.
- NEWTON T H. Cisterns of posterior fossa. *Clin Neurosurg* 15 (1968) 190.
- PRIEBRAM H F W. The differentiation of extrinsic from intrinsic intracranial tumors with particular reference to posterior fossa tumours. *Amer J Roentgenol* (1966) 452.
- ROBERSON G H, BRISMAN J, DAVIS K R, TAYLOR J M and WEISS A. Metrizamide cisternography with hypocyclusal tomography. Preliminary results. *Amer J Roentgenol* 127 (1976) 965.
- ROBERTSON F G. Encephalography. Macmillan and Co. London 1941.

- Pneumoencephalography Blackwell Scientific Publications Oxford 1957
- WIRTH M, KORBICKA J and TOMAN I Cisternal dilatation in infratentorial tumours. Experimental reproduction of the probable pathogenetic mechanism in the human cadaver Acta radiol Diagnosis 13 (1972) 467
- GIUGGIO G Diagnostic value of encephalographic examination of the subarachnoid space Acta radiol Diagnosis 46 (1956) 99
- LE ENCEPHALOGRAPHIE fractionnee Masson et Cie Paris 1957
- and CASTELLANO F Upward displacement of the posterior part of the third ventricle Acta radiol Diagnosis 13 (1953) 377
- SASSAROLI S Sul comportamento dei solchi della faccia mediale degli emisferi nella pneumoencefalografia (In Italian) Radiol med 41 (1955) 358
- SCHUCHTER M M, BULL J W D and CAREY P Two new encephalographic signs of pressure hydrocephalus Brit J Radiol 31 (1958) 318
- SPATZ H and STROESCU G J Zur Anatomie und Pathologie der äusseren Liquorraume des Gehirns (Die Zisternenverquellung beim Hirntumor) Nervenarzt 7 (1934) 481
- WICKBOM I and HANAFEE W Soft tissue masses immediately below the foramen magnum Acta radiol Diagnosis 1 (1963) 647

FROM THE INSTITUTE OF OCCUPATIONAL HEALTH (DIRECTOR J. RANTANEN) AND THE DIVISION OF ORTHOPEDIC SURGERY AND TRAUMATOLOGY (DIRECTOR P. SLATIS) UNIVERSITY CENTRAL HOSPITAL SF-00130 HELSINKI FINLAND

RADIOGRAPHIC HEALING AND REMODELLING OF CORTICAL AND CANCELLOUS BONE GRAFTS AFTER RIGID PLATE FIXATION

Experiments in the rabbit

P. WARIS, E. KARAHARJU, P. SLATIS and P. PAAVOLAINEN

The healing of bone grafts after plate osteosynthesis has not been widely investigated radiographically. OLERUD & DANCKWARDT LILLIESTRÖM (1971) and HURZSCHENREUTER (1972) showed that cortical interposition grafts mend by primary bone healing without evident periosteal reaction.

The osteoinductive capacity of cancellous bone exceeds that of cortical bone (ABBOT et coll. 1947; CHWEIBERER 1971). Ever since NICOLI (1956) presented his method of cancellous interposition grafting, it has been widely used in connection with plate osteosynthesis. The cancellous graft provokes abundant bone formation (SIFPERT 1955) in connection with rigid osteosynthesis; cancellous interposition grafts also seem to mend by primary bone healing (DOAJR et coll. 1975).

The incorporation of a bone graft is accomplished by so-called creeping substitution (STRINGA & MIGNANI 1967; ALBREKTSSON 1971; ENNEKING et coll. 1975) which is characterized by the simultaneous resorption of necrotic old bone and the formation of new bone on the lattice work of old bone trabeculae. This repair is vivid and usually complete in cancellous grafts (BOYNE 1970; SIFPERT 1955) but in cortical grafts it is retarded for years and can remain incomplete (ALBREKTSSON, ENNEKING et coll.).

No comparison of cortical and cancellous interposition grafts after rigid plate fixation appears to have been made. Therefore using radiography the healing of cortical and of cancellous grafts were compared concomitant changes in the plated host

bone analysed and the remodeling of the grafts followed for one year.

Material and Methods

Operative technique. The material consisted of 130 rabbits weighing from 2450 to 5100 g. The animals were anaesthetized with mebumal sodium and ether. The right tibiofibular bone was exposed through a straight incision. A 6 mm long segment of the tibia was cut with a double blade circular saw during continuous cooling with saline. The proximal osteotomy was performed just below the tibiofibular junction.

In 70 of the rabbits the cortical bone transplant was turned 180° and replaced in the defect (A in Fig. 1). In the other 60 rabbits the defect was filled with a 6 mm long cancellous graft from the anterior iliac crest (B in Fig. 1). Osteosynthesis was made with a 6-hole DCP/ASIF plate attached to the bone with 5 screws in the cortical graft series and 6 in the cancellous graft series. All the screws were tightened with a calibrated torque wrench which exerted an axial force of 5 to 10 kPa. In the cancellous graft this procedure resulted in a moderate squeezing of the trabeculae and loss of axial compression force in the cortical graft. Compression was exerted on the tubular graft.

After the operation the animals wore no external splints and were allowed to move freely in separate

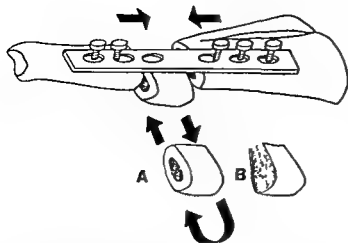


Fig. 1 Operative technique. A—Cortical transplant turned 180 and replaced. B—Defect filled with cancellous graft.

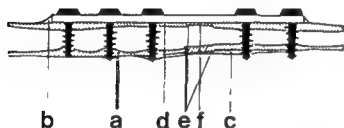


Fig. 2 Diagram of the cortical bone transplant 12 weeks after rigid plate fixation (cf. Fig. 3c). Sites at which the radiographic abnormalities were semi-quantitatively recorded: a) New bone formation around the screw; b) new bone formation around the plate; c) periosteal reaction opposite the plate; d) resorption in cortical host bone under the plate; e) incorporation of the graft; f) resorption of the graft.

cages. Animals were killed 1, 3, 6, 12, 24, 36 and 52 weeks after the operation; the tibiofibular bones removed and the soft tissues stripped off, leaving the periosteum and all callus tissue intact.

In the cortical bone graft series, 20 of the 70 rabbits were excluded because of fracture or loosening of the implant; for another 10, no films were obtained because of technical errors. In the cancellous graft series, 5 of the 60 rabbits were excluded because of fracture, and no films were obtained in 10. Thus, for further analysis, 40 animals with cortical grafts and 45 animals with cancellous grafts remained.

Radiography of the plated bone was performed immediately after the operation and before and after the removal of the plate after the animal had been killed. Agfa-Gevaert Structurix D7 mammography

film was used and exposed with a Machlett 80 tube at 70 kV, 10 mA for 3–5 s at a focus-object distance of 1 m.

Transverse specimens of the proximal and host bone of the graft and of the contralateral control bone were embedded in methylmethacrylate and sawn into sections of 80 μ m. Films were exposed with a Machlett AEG 50 tube at 10 kV for 1 s at a focus-object distance of 20 cm.

The radiographic bone appearances were graded as follows (cf. PAAVOLAINEN et al. 1978):

- a) New bone formation around the screws
 - None
 - +
 - ++
 - +++
- b) New bone formation around the plate
 - None
 - +
 - ++
 - +++
- c) Periosteal reaction opposite the plate
 - None
 - +
 - ++
 - +++
- d) Resorption in cortical host bone under the plate
 - None
 - +
 - ++
 - +++
- e) Incorporation of the graft
 - None
 - +
 - ++
 - +++

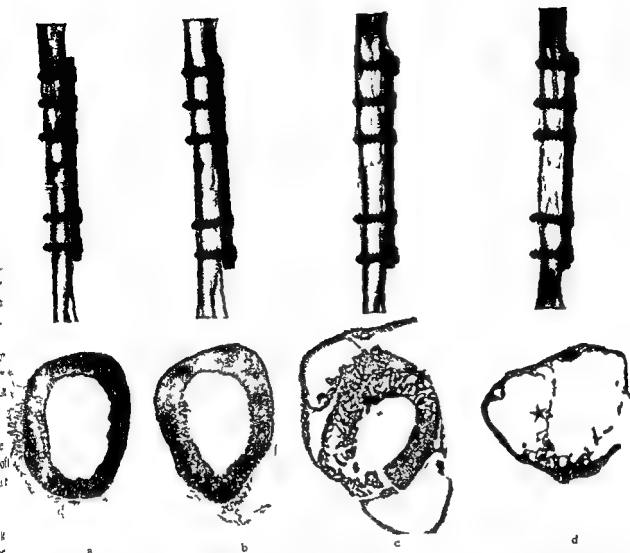


Fig. 3 Cortical bone transplant after rigid plate fixation and corresponding cross-sections of the graft (The plate is situated to the right of the graft) a) After 3 weeks. Periosteal new bone formation around the graft in the cross section beginning enlargement of the haversian canals in the opposite cortex and newly formed subperiosteal bone b) After 6 weeks. Primary bone healing in the cross section enlargement of the haversian canals

c) After 12 weeks. Porotic transformation of the host bone and the proximal graft in the cross section marked double layer d) After 36 weeks. Marked porosity of the cortical host and graft bone underlying the implant in cross section almost total resorption of the old cortex (marked with an asterisk) new subperiosteal bone cuff enlarging the medullary canal

b) Resorption of the graft

- None
- + Slight porosity of the graft
- ++ Porosity and thinning of the cortex of the graft less than half the thickness of normal cortex
- +++ Marked porosity and thinning of the cortex of the graft more than half the thickness of normal cortex

Results

The healing and remodelling of the cortical and cancellous grafts are exemplified in Figs 3 and 4

The radiologic features assessed according to the criteria mentioned are summarized in the Table

New bone formation around the screws A slight endosteal reaction to the screws appeared already after one week in both graft series. The periosteal reaction around the screws increased up to 12 weeks with a tendency to be more prominent in the cancellous graft specimens. Towards the end of the experiment the newly formed bone condensed into a dense juxtacortical bone collar which united with the periosteal reaction opposite the plate.

New bone formation around the plate Three weeks after the operation new bone had formed around the implant in half of the cortical and in

Table

Summary of radiographic changes in bone grafts after rigid plate fixation

Time after operation (weeks)	New bone formation around the screws		New bone formation around the plate		Periosteal reaction opposite the plate		Resorption in cortical bone under the plate		Incorporation of the graft		Resorption of the graft	
	Cortical	Cancellous	Cortical	Cancellous	Cortical	Cancellous	Cortical	Cancellous	Cortical	Cancellous	Cortical	Cancellous
1	2- 5+	7+	7-	7-	7-	4- 3+	7-	7-	6- 1+	7-	7-	7-
3	5+ 3++	1+ 4++	4- 4+	1- 2+ 7++	1- 6+ 2++	1- 1+ 3++	4- 4+	5- 6+	2- 3+ 3++	1- 4+	8-	5
6	5++	6++ 1+++	3+ 2++	4+ 2++ 1+++	3+ 2++	3+ 4++	5++	6+ 1++	5++	4+ 3++	3+	1
12	5++ 2+++	6++ 3+++	4++ 1+++	6+ 2++ 1+++	2+ 3++ 2+++	5+ 3++ 1+++	6++ 1+++	1+ 8++	6++ 1+++	1+ 7++ 1+++	4+ 3++	4
24	6++	7++	5+ 1+++	4+ 3++	2+ 4++	1+ 6++	1+ 4++ 2+++	1+ 6++	6+++	2++ 5+++	5++ 1+++	5
36	5++	7++	5+ 7+	3+ 7+	7++ 7++	7++ 7++	2++ 3+++	2++ 5+++	5+++	1++ 6+++	2++ 3+++	4
52	2++	4++ 1+++	1+ 1++	3++ 7+++	1+ 1++	4++ 1+++	1++ 1+++	4++ 1+++	2+++	1++ 4+++	1++ 1+++	3

almost all cancellous graft specimens. In the cancellous bone graft series the reaction around the plate was greatest at 6 weeks and in the cortical bone graft series at 12 weeks. Later the periosteal reaction subsided.

Periosteal reaction opposite the plate. A slight periosteal reaction in the host bone occurred in the cancellous bone graft series already at one week in 3 of 7 specimens. In the cortical bone graft series the periosteal new bone reaction was visible at 3 weeks. These periosteal reactions were greatest in both groups at 12 weeks when a double cortical layer was observed in the cross sections of 5 of 7 specimens from the cortical bone graft series and in 4 of 9 samples from the cancellous bone graft series. Towards the end of the experiment the periosteal bone condensed without increasing in thickness.

Resorption in cortical host bone under the plate. In the cortical bone graft series the first resorptive changes appeared at 3 weeks when the cortex of the host bone had slightly thinned in half of the speci-

mens. In the cancellous graft series the resorption of the host bone did not start until 6 weeks after the operation. In both series the resorption first occurred in the proximal part of the host bone. It exceeded that of the distal part in all group cross section specimens. The resorption began endosteally and progressed outwards in the cortex. At 36 and 52 weeks the cortex was almost completely resorbed under the plate in half of animals in both series.

Incorporation of the graft. Three weeks after operation incorporation of the graft was visible in 6 of 8 cortical bone graft specimens and in 4 of 6 cancellous bone graft samples. At this time the osteotomies healed predominantly through periosteal bone formation. In 12 weeks all the osteotomies had healed but remnants were still visible in 6 of 7 cortical bone grafts and in 8 of 9 cancellous bone grafts. In all cases the distal host-graft interface remained visible longest. From 24 to 52 weeks both types of grafts were completely incorporated.

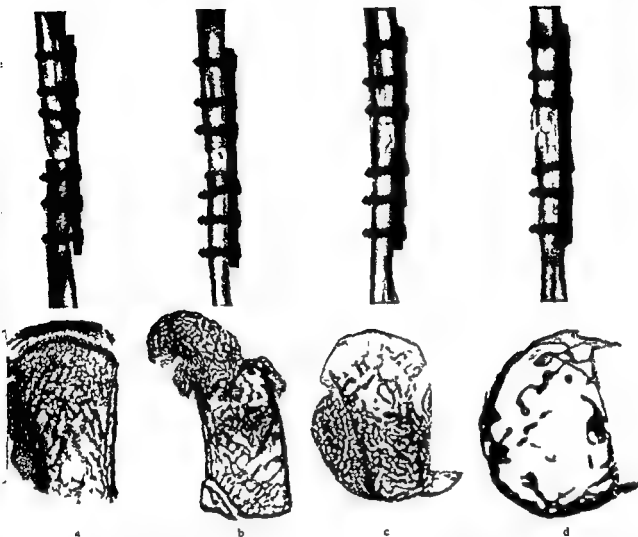


Fig. 4 Cancellous bone transplant after rigid plate fixation and corresponding cross-section of the graft. a) After 3 weeks. Subperiosteal new bone around the screws in the cross section. b) After 6 weeks. Primary bone healing. c) After 12 weeks. Thinning of the

cortical host bone. Porosis of the host bone and the proximal graft condensed subperiosteal new bone which in the cross section is remodelling to a new tubular bone. d) After 36 weeks. Marked porosity of the host bone and the graft similar to the cortical graft series in the cross-section a new thin walled tubular bone.

Resorption of the graft The resorption of the cortical graft first appeared after 6 weeks as a mild thinning and porosity in the cortex of the graft while that of the cancellous graft was not observed until 12 weeks after the operation. This resorption always began in the proximal part of the graft and had a patchy porotic appearance with marked thinning of the subendosteal cortex. In specimens examined later the resorption was more marked in the graft than in the surrounding host bone.

Discussion

The results show that with rigid plating both cortical and cancellous interposition grafts mend by

primary bone healing that incorporation of both grafts is followed by progressive remodelling of the graft and the host bone and that this remodelling causes cancellous transformation and thinning of the cortex both in the graft and in the host bone.

The amount of periosteal callus is influenced by the stability of the osteosynthesis (WIESER 1964, ANDERSSON 1965, HUIZSCHE-REUTER *et al.* 1969, RÜDI & ALLGÖWER 1974) and the degree of periosteal (KÜNTSCHER 1967, OLERUD & DANCAWARDT LILLIESTRÖM, TRUEYA 1974) or medullary (RICHANY *et al.* 1965, DANCAWARDT LILLIESTRÖM 1970) trauma. In the present series the periosteal reaction around the screws and the plate occurred slightly earlier in the cancellous graft than in the

cortical graft series which suggests that greater osteoinductive activity occurs in cancellous grafts

The radiographic healing of both graft types was basically the same. The incorporation of the graft started at 3 weeks by periosteal new bone formation around the graft. The healing was completed by bone bridges traversing the host-graft interface 6 to 12 weeks after both types of grafting. In all cases the distal host-graft interface healed last. This sequential mode of healing was also noted by ZUCMAN *et coll* (1968) in triple level fractures of rabbit tibiae stabilised with a medullary rod.

The remodelling of the cortical host bone which gradually occurred after graft incorporation can mainly be attributed to the reactions provoked by rigid plate (PAAVOLAINEN *et coll*). Thus the resorption of the cortical host bone was similar to that reported in plated intact rabbit tibiofibular bone by SLATIS *et coll* (1978) and in plated osteotomies of rabbit tibiofibular bone by GÖRDES *et coll* (1975). A phenomenon not occurring in simple osteotomies but found in the present series was bone resorption later in both the distal part of the graft and the host bone (Figs 2c and 3c). This occurrence as well as the delayed healing of the distal host-graft interface is obviously due to a less abundant blood supply to this area (GÖTHMAN 1960; TRUETA).

The remodelling of both graft types was accomplished by the simultaneous subperiosteal condensation of new bone and the progressive resorption of the old bone matrix. This mode of remodelling has previously been observed in bone grafts both with (ALBREKTSSON) and without (ENNEKING *et coll*) internal fixation. Similar haserian remodelling also occurs after intramedullary reaming (DANCKWARDT LILLIESTRÖM) and in connection with rigid plate fixation (SLATIS *et coll*) and it is obviously a common feature in cortical bone undergoing repair.

The tibiofibular bone including the graft had an increased over all diameter, a widened medullary canal and a thinned porotic cortical wall 36 to 52 weeks after the grafting procedure. The radiographically visible resorption was more marked in the bone grafts than in the host bone. Thus the uneventful healing of the grafts after rigid plate fixation seems to be counterbalanced by untoward structural changes in the cortical bone underlying the rigid metallic implant.

Recent observations (P WARIS in progress) show that the torque strength of the grafted bone increases during the healing of the graft but then diminishes.

This phenomenon suggests that after graft procedures combined with rigid plate fixation the implants should remain in place until healing is completed but should be removed before the deleterious effects of the implant have caused weakening of the bone. However further experiences are needed before the optimum time for implant removal is determined.

SUMMARY

Cortical and cancellous interposition grafts with rigid plate fixation in the tibiofibular bones of 120 rabbits followed radiographically for one year. The cancellous grafts healed earlier but by 12 weeks both graft types had been incorporated. The distal host-graft interface healed last to heal. Progressive cancellous transformation occurred in the graft and host bone led to an increased overall diameter, a widened medullary canal and a thinned cortical wall.

REFERENCES

- ABBOT L C, SCHOTTSTAEDT E R, SAUNDERS J B, BOST C F. The evaluation of cortical and cancellous bone as grafting material. *J Bone Jt Surg* 59A: 381.
- ALBREKTSSON B. Repair of diaphyseal defects. *Acta Orthop Gothburg* 1971.
- ANDERSSON L D. Compression plate fixation: the effect of different types of internal fixation on fracture healing. *J Bone Jt Surg* 47A (1965) 191.
- BOYNE P J. Autogenous cancellous bone and cancellous transplants. *Clin Orthop* 73 (1970) 199.
- DANCKWARDT LILLIESTRÖM G. Reaming of the medullary cavity and its effect on diaphyseal fracture healing. *Orthop scand* (1970) Suppl No 1-8.
- DLER J, HARLE F and NIEDERDELMANN H B. Transplantat im Unterkiefer unter Belastung. *Verhältnisse im Tierversiment Fortschritt Med* 19 (1975) 21.
- ENNEKING W F, BURCHARDT M S, PUGH J J, PIOTROWSKI G. Physical and biological aspects of repair in dog cortical bone transplants. *J Bone Jt Surg* 57A (1975) 237.
- GÖRDES W, KOSSYK W und HOLLANDER H. Histologische und histomorphometrische Veränderungen bei Plattenosteosynthesen nach Osteotomie an Tibia des Kaninchens. *Arch Orthop Unfall-Chir* (1975) 123.
- GÖTHMAN L. The normal arterial pattern of the rabbit tibia. A microangiographic study. *Acta chir scand* 120 (1960) 201.
- HILTZSCHENREITER P. Beschleunigte Einheilung von allogenen Knochentransplantaten durch Präverlebung des Empfängers und stabile Osteosynthese. *Langenbecks Arch Chir* 331 (1977) 31.
- PERREN S M, STEINMANN S, GERTZ J.

- KLEBL M Some effects of rigidity of internal fixation on the healing pattern of osteotomies *Injury* 1 (1969) 77
- NTSCHER G Experimental and clinical solution of the callus problem *Symp Biol Hung* 7 (1967) 153
- OLL E A The treatment of gaps in long bones by cancellous insert grafts *J Bone Jt Surg* 38B (1956) 70
- ERUD S and DANCKWARDT LILLIESTROM G Fracture healing in compression osteosynthesis *Acta orthop scand* (1971) Suppl No 137
- VOLAINEN P KARAHARJU E and SLATIS P Radiographic abnormalities in tubular bone after rigid plate fixation in rabbits *Acta radiol Diagnosis* 19 (1978) 119
- CHANY S F SPRINZ H KRANER K ASHBY J and MERRILL T G The role of the diaphyseal medulla in the repair and regeneration of the femoral shaft in the adult cat *J Bone Jt Surg* 47A (1965) 1565
- EDI T und ALLGÖWER M Die Frakturheilung nach Osteosynthese im Röntgenbild *Helv chir Acta* 41 (1974) 213
- SCHWEIBERER L Der heutige Stand der Knochentransplantation *Chirurg* 6 (1971) 252
- SIFFERT R S Experimental bone transplants *J Bone Jt Surg* 37A (1955) 742
- SLATIS P KARAHARJU E HOLMSTRÖM T, AHONEN J and PAAVOLAINEN P Structural changes in tubular bone after rigid plate fixation *J Bone Jt Surg* 60A (1978) 516
- STRINGA G and MIGNANI G Microradiographic investigation of bone grafts in man *Acta orthop scand* (1967) Suppl No 99
- TRUETA J Blood supply and the rate of healing of tibial fractures *Clin Orthop* 105 (1974) 11
- WARIS P Torsional strength of long bones after cortical and cancellous bone grafting with rigid plate fixation Unpublished data 1979
- WIESER C Die primäre Knochenheilung und ihre Störung im Röntgenbild *Langenbecks Arch Chir* 308 (1964) 434
- ZUCMAN J MAURER P and BERBESSON C The effect of autografts of bone and periosteum in recent diaphyseal fractures *J Bone Jt Surg* 50B (1968) 409

RADIOLOGIC EVALUATION OF THE PROGRESSION OF RHEUMATOID ARTHRITIS

A. DE CARVALHO · H. GRAUDAL and B. JØRGENSEN

The purpose of this report is to survey the degree of rheumatoid joint involvement based on radiography of all limb joints and to describe the relationship between the joint involvement and the duration of the disease. Previous reports have been based on radiography of selected joints. It seems that no investigations have been carried out which show by uniform criteria to which extent a particular joint of a group of patients is affected by the rheumatoid process.

Material and Methods

The series consisted of 149 females and 39 males with classical or definite rheumatoid arthritis (ROPES et coll. 1958) of the adult type. The mean age of the females at the onset of the disease was 38.1 years (range 14–74) that of the males 42 years (range 17–62). The patients had been hospitalized in a specialized rheumatology unit and afterwards followed for periods of 3 to 12 years.

At least two radiographic examinations had been performed on each patient at an interval of at least 3 years. On average each patient was examined 3.5 times (range 2–7) and with few exceptions radiography of all the limb joints was performed on at least 2 occasions. A total of 661 skeletal examinations were performed of these were 429 complete. Affections of the cervical spine and the sacroiliac joints will be reported separately because they present special problems. All films were evaluated by the same author (A. C.) without knowledge of

clinical findings. The joint involvement was classified by grades 0 to 5 by comparison with the standard films of LARSEN et coll. (1977) and according to the following definitions:

- Grade 0 normal findings
- Grade 1 slight abnormality including periarticular soft tissue swelling, juxta articular halos, teresis possibly with slight narrowing of the joint space
- Grade 2 early but definite abnormality consisting of bone erosion and distinct narrowing of the joint space. Erosion is obligatory except in the weight bearing joints
- Grade 3 medium destructive abnormality with marked narrowing of the joint space and bone erosion also in weight bearing joints
- Grade 4 severe destructive abnormality. Only minor parts of the articular surfaces remain
- Grade 5 mutilating lesions

An example of staging of the same joint at different times appears in Fig. 1. Although the standard films of LARSEN et coll. illustrate regions e.g. radiocarpal and carpal joints in the present series each joint was evaluated separately with the exception that the carpal joints, the tarsal joints (subtalar, calcaneo-cuboideal and talo-navicular) and the mid tarsal joints (including the tarso-metatarsal joints)

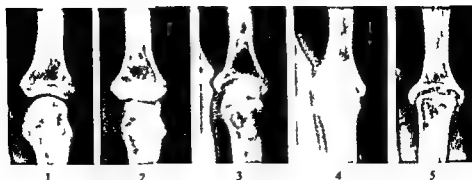


Fig. 1. Staging of the same joint at different dates.

Table 1

Example of mapping the condition of one joint (right wrist) by means of absolute counts and relative frequencies of joint involvement by grades 0 to 5 at a given time after the onset of disease

Years from onset	Grade						Total
	0	1	2	3	4	5	
1	5	18	14	0	0	11	37
	13.5	48.6	37.8	0	0	0	6.2
2	0	8	13	3	0	0	24
	0	33.3	54.2	12.5	0	0	4.0
3	3	12	16	4	2	0	37
	8.1	32.4	43.2	10.8	5.4	0	6.2
4	4	11	20	11	1	1	45
	8.9	24.4	44.4	17.8	2.2	2.2	7.5
5-6	1	12	36	25	3	2	79
	1.3	15.2	45.6	31.6	3.8	2.5	13.2
7-8	2	7	32	20	10	3	74
	2.7	9.5	43.2	27.0	13.5	4.1	12.3
9-10	1	10	21	17	16	5	70
	1.4	14.3	30.0	24.3	22.9	7.1	11.7
11-12	0	4	16	15	11	5	51
	0	7.8	31.4	29.4	21.6	9.8	8.5
13-14	0	5	9	12	15	3	44
	0	11.4	20.5	27.3	34.1	6.8	7.3
15-16	0	2	10	7	15	5	39
	0	5.1	25.6	17.9	38.5	12.8	6.5
17-18	0	0	7	2	18	4	31
	0	0	22.6	6.5	58.1	12.9	5.2
19-22	0	0	3	8	12	7	30
	0	0	10.0	26.7	40.0	23.3	5.0
23<	0	0	2	10	12	15	39
	0	0	5.1	25.6	30.8	38.5	6.5
Total	16	89	199	131	115	50	600
	2.7	14.8	33.2	21.8	19.2	8.3	100.0

Table 2

Joints that may be grouped without significant loss of information in the description of the progression of the disease. The right and left sides have been grouped together in all cases

Arms and hands	Legs and feet
Shoulder and acromioclavicular	Hip
Elbow	Knee
Wrist and carpus	Ankle
Carpometacarpal joint 1	Tarsus
Carpometacarpal joints 2-5	Metatarsal joints
Metacarpophalangeal joint 1	Metatarsophalangeal joint 1
Metacarpophalangeal joints 2-5	Metatarsophalangeal joints 2-5
Proximal interphalangeal joints 2-5	Proximal interphalangeal joints
Distal interphalangeal joints 2-5	Distal interphalangeal joints
Interphalangeal joint of the thumb	Interphalangeal joint of great toe

were regarded as units. Satisfactory control of the information has been effected by random sampling; the result has been subjected to electronic data processing.

Results

The results have been recorded in a table for each of the 86 joints examined. An example is given in table 1. It shows the percentage of joints which was involved by grades 0 to 5 at a given time after the onset of the disease.

An analysis of the involvement of individual joints showed that some joints could be grouped together without any essential loss of information due to a uniform progression (Table 2). The groups also include the corresponding joints of the right and left side.

In Figs 2 and 3 the distribution of the lesions is related to the duration of the disease. The figures summarize the classifications of 40872 joints or joint units. The curves indicate the limits between the different grades for each group of joints so that the areas between the curves express the relative frequency of each grade. The frequency of joint involvement of grade 2 or higher after one, 4, 7-8 and 11-12 years appears in Table 3. The frequency of, for example, grade 4+5 is not necessarily increasing because different patients appear at different times. In several groups of joints the progression of the disease never ceased.

Some special features appearing within some of the groups of joints should be mentioned. The in-

volvement of the second and third carpometacarpal joints, right and left, was more severe than that of the first, fourth and fifth joints. The second and third metacarpophalangeal joints were more often affected than the fourth and fifth joints and the involvement of the first metacarpophalangeal joint was still smaller. The involvement of the right second and third metacarpophalangeal joints was more marked than that of the left joints.

Regarding the proximal interphalangeal joints of the left hand, the degree of involvement increased from the fifth to the second joint and the second joint was more involved than the corresponding joint of the right hand. On the right hand the third proximal interphalangeal joint showed the highest degree of involvement and the third to fifth joints of the right hand were more involved than the corresponding joints on the left hand.

By contrast the lateral metatarsophalangeal joints, especially the fifth, were more severely involved than the medial joints.

Discussion

The grading system of LARSEN *et al.* has been found to provide satisfactory distinction between slight, definite, moderate, severe and mutilating rheumatoid joint involvement. Thus, it is useful as a tool for evaluating the progression of the disease, especially during longer periods, whereas a detailed description is necessary for diagnostic purposes and for evaluating the progression during the early period of the disease.

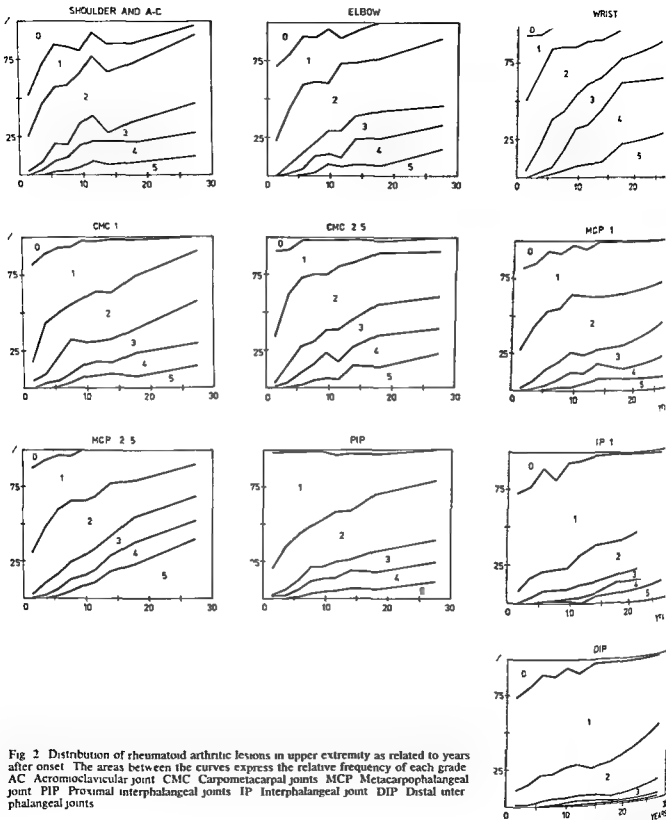


Fig. 2 Distribution of rheumatoid arthritic lesions in upper extremity as related to years after onset. The areas between the curves express the relative frequency of each grade. AC Acromioclavicular joint, CMC Carpometacarpal joints, MCP Metacarpophalangeal joint, PIP Proximal interphalangeal joints, IP Interphalangeal joint, DIP Distal interphalangeal joints.

The patients in the present series are not representative of rheumatoid disease in the population but probably the series is fairly representative of rheumatoid patients referred to Danish hospitals. This implies that the findings regarding single joints

and joint groups may be used as a general prognostic estimate as far as hospitalized patients are concerned. For example, as regards any proximal interphalangeal joint of the fingers, after 7 to 8 years of the disease the probability of grade 2 involvement

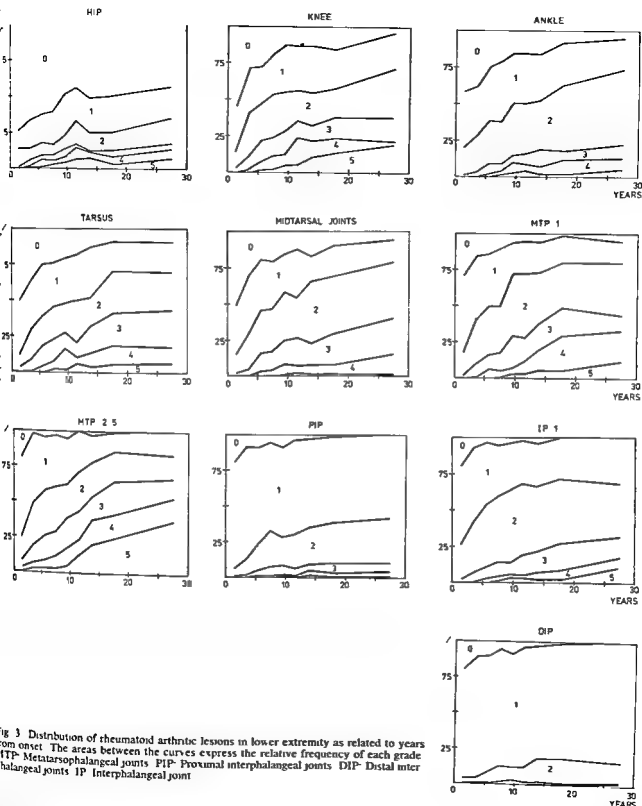


Fig 3 Distribution of rheumatoid arthritic lesions in lower extremity as related to years from onset. The areas between the curves express the relative frequency of each grade. MTP—Metatarsophalangeal joints PIP—Proximal interphalangeal joints DIP—Distal interphalangeal joints IP—Interphalangeal joint

would be 27 per cent of grade 3 it would be 10 per cent and of grade 4 to 5 it would be 11 per cent. It may be estimated whether the course in a single patient is more or less serious than usual. This applies both to single joints and to the total progress

of the disease. Since in the majority of the cases all the joints of a patient have been examined at the same time it is justifiable to compare the amount of involvement of different joints or groups of joints after the same duration of the disease. It seems that

Table 3

Percentage of joints with lesions of grade 2 or higher

		No classified joints	Years from onset											
			1			4			7-8			11-12		
		Grade	2	3	4+5	2	3	4+5	2	3	4+5	2	3	4+5
Upper extremity														
Shoulder/A C joint	2 251		23	2	0	37	6	3	39	8	11	39	17	??
Elbow	1 079		23	0	0	37	6	2	40	8	13	44	17	12
Wrist/carpus	2 415		47	4	0	47	16	4	42	25	18	78	27	34
CMC 1	1 228		17	5	0	34	6	4	23	22	10	33	13	18
CMC 2-5	4 924		31	2	0	47	12	3	45	15	15	47	22	17
MCP 1	1 710		26	2	0	36	5	1	36	17	7	39	13	17
MCP 2-5	4 908		29	2	0	38	8	2	41	12	12	35	14	10
PIP 2-5	4 905		18	1	1	29	4	2	27	10	11	34	11	14
DIP 2-5	4 906		10	1	0	14	1	0	14	4	1	21	4	4
IP	1 274		8	0	0	13	4	0	14	7	2	20	8	4
Lower extremity														
Hip	1 112		13	1	0	8	4	2	7	4	6	16	2	15
Knee	1 169		11	3	0	29	9	2	30	13	11	21	11	24
Ankle	1 071		18	1	0	25	3	0	29	5	4	34	7	9
Tarsus	1 071		9	3	0	21	8	1	23	15	8	29	11	11
Metatarsal joints	1 198		13	2	0	25	4	0	29	13	4	27	20	7
MTP 1	1 111		16	2	0	31	9	1	32	13	5	44	16	17
MTP 2-5	4 553		17	5	3	30	12	7	32	17	12	28	20	23
PIP 2-5	4 708		5	1	0	11	1	0	25	7	1	24	5	1
DIP 2-5	4 681		3	0	0	3	1	0	11	1	0	10	1	0
IP	1 198		24	2	0	35	7	1	45	10	5	49	14	5

A C Acromioclavicular joint CMC Carpometacarpal joints MCP Metacarpophalangeal joints PIP Proximal interphalangeal joints DIP Distal interphalangeal joints IP Interphalangeal joint MTP Metatarsophalangeal joints

an estimate of progressive involvement of one joint should preferably be viewed in the light of the state of other joints. When the prognosis of single joints is analysed the finding may vary according to a casual composition of the patient group especially if the group is not large.

It is not extraordinary that the general trend of the present findings concord with the opinion generally held. Regarding some joints the findings have been in accordance with those reported in other series: proximal interphalangeal joints of the hand (JACOBY et coll 1973, FLEMING et coll 1976, VAN DAM 1964), knees (JACOBY et coll 1958, SOILANEN 1964), talocrural joints (FORESTIER 1964), tarsal and metatarsal joints (FORESTIER, ANSELL 1964), metatarsophalangeal joints of the feet (BROOK & CORBETT 1977, SOILA, FLETCHER & ROWLEY 1952, MARTEL 1968). As regards some other joints other authors have found a lower or higher degree of involvement: acromioclavicular joints (MEIJERS 1964),

humeroscapular joints (DE SÈZE et coll 1964), elbows (FLEMING et coll.), proximal interphalangeal joints of the hands (BROOK & CORBETT 1977, FLETCHER & ROWLEY 1952), hips (JONSSON 1961, KELLGREN 1964), talocrural joints (FLEMING et coll 1976, SOILA, LINDSTRÖM & KAINEN et coll 1977). The discrepancies may be explained by the variability of the disease.

It is not known why some joints are more often more severely affected by rheumatoid arthritis than others. At present it is not possible to formulate a hypothesis for the localization and progression of this disease based on joint anatomy, vascular supply, chemistry, function or temperature. Local factors are possibly not the only ones. However, a further exact knowledge of the appearances of the dynamic changes in rheumatoid joint involvement seems to be important for an understanding of some of the factors which determine a predisposition to rheumatoid involvement and progression.

The purpose of radiographic examination

umatology is not only to be diagnostic but also form a basis for the therapeutic strategy and for evaluation of therapeutic results and the prognosis. Radiography reflects biologic processes which do not always conform to the social consequences of the disease.

SUMMARY

The severity of rheumatoid arthritis in 20 groups of limb joints was evaluated by means of 661 skeletal radiologic examinations on 188 patients. The severity of the disease is classified by grades II to V in accordance with LARSEN's grading system and was related to the duration of the condition. The result differs at several points from results in other surveys.

ACKNOWLEDGEMENTS

The authors wish to express their gratitude towards Anders Holst Andersen, advisory statistician for invaluable assistance. This investigation has been supported by the Danish Medical Research Council.

REFERENCES

- ELL B M. The ankle joint. In: Proceedings of the International Symposium on the radiological aspects of rheumatoid arthritis. p. 103. Excerpta Medica, Amsterdam 1964.
- OK A and CORBETT M. Radiographic changes in early rheumatoid arthritis. Ann rheum Dis 36 (1977) 71.
- JEZE S, DEBEYRE N and MANUHL R. The shoulder. In: Proceedings of the International Symposium on the radiological aspects of rheumatoid arthritis. p. 147. Excerpta Medica, Amsterdam 1964.
- MINGA CROWN J M and CORBETT M. Incidence of joint involvement in early rheumatoid arthritis. Rheumatol Rehabil 15 (1976) 92.
- FLETCHER D E and ROWLEY K A. The radiological features of rheumatoid arthritis. Brit J Radiol 25 (1952) 282.
- FORESTIER J. Ankles. In: Proceedings of the International Symposium on the radiological aspects of rheumatoid arthritis. p. 105. Excerpta Medica, Amsterdam 1964.
- JACOBY R K, JAYSON M I V and COSH J A. Onset, early stages and prognosis of rheumatoid arthritis. A clinical study of 100 patients with 11 year follow up. Brit med J 2 (1973) 96.
- JONSSON E. On the prognosis of rheumatoid arthritis. Acta orthop scand 30 (1961) 115.
- KELGREN J H. The hip joint. In: Proceedings of the International Symposium on the radiological aspects of rheumatoid arthritis. p. 301. Excerpta Medica, Amsterdam 1964.
- LARSEN A, DALE K, FEAM. Radiographic evaluation of rheumatoid arthritis and related conditions by standard reference films. Acta radiol. Diagnosis 18 (1977) 481.
- LUUKKAINEN R, ISOMAKI H and KAJANDER A. Effects of gold treatment on the progression of erosions in RA patients. Scand J Rheumatol 6 (1977) 123.
- MARTEL W. Radiologic manifestations of rheumatoid arthritis with particular reference to the hand, wrist and foot. Med Clin N Amer 52 (1968) 653.
- MEIJERS K A A. Shoulder joint. In: Proceedings of the International Symposium on the radiological aspects of rheumatoid arthritis. p. 137. Excerpta Medica, Amsterdam 1964.
- ROPES M W, BENNET G A, COBB S, JACOB R and JESSAR R A. 1958 revision of diagnostic criteria for rheumatoid arthritis. Bull rheum Dis 9 (1958) 175.
- SOHLA P. Roentgen manifestations of adult rheumatoid arthritis. Acta rheum scand (1958) Suppl No 1.
- SOSMAN J L. Radiological aspects of the knee in rheumatoid arthritis. In: Proceedings of the International Symposium on the radiological aspects of rheumatoid arthritis. p. 167. Excerpta Medica, Amsterdam 1964.
- VAN DAM G. The hand. In: Proceedings of the International Symposium on the radiological aspects of rheumatoid arthritis. p. 63. Excerpta Medica, Amsterdam 1964.

ARTHROGRAPHIC DIAGNOSIS OF RUPTURED CALCANEOFIBULAR LIGAMENT

I A new projection tested on experimental injury post mortem

M VUUST

Arthrography of the ankle in cases of acute distortions was introduced by WOLFF (1940) and has been of particular value for the diagnosis of rupture of the lateral ligaments of the talocrural joint (GLASTRUP 1965 BROSTRÖM *et coll* 1965 PERCY *et coll* 1969 APLES 1975 SPIEGEL *et coll* 1975 LINDHOLMER *et coll* 1978 PRINS 1979). Most frequent are isolated rupture of the anterior talofibular ligament and combined rupture of this ligament and the calcaneofibular ligament. Rupture of the posterior talofibular ligament is infrequent (BROSTRÖM 1965). Isolated rupture of the calcaneofibular ligament has been reported by PRINS but was not found by BROSTRÖM or LINDHOLMER *et coll* in their series.

The usefulness of arthrography for the diagnosis of acute ruptured anterior talofibular ligament was established by BROSTRÖM *et coll* and LINDHOLMER *et coll* found that 97 per cent of the pathologic arthrograms demonstrated rupture of this ligament. However, it is difficult to determine whether rupture of the calcaneofibular ligament has also occurred. Several attempts to find valid criteria for this diagnosis have been made.

BROSTRÖM *et coll* found that contrast filling of the peroneal sheath was a reliable indication of rupture of the calcaneofibular ligament as did FONDYCE & HORN (1972) and PERCY *et coll*. On the other hand SPIEGEL *et coll*, STAPLES, LINDHOLMER *et coll*, PRINS considered such a finding less reliable. In all cases of calcaneofibular ligament rupture operated upon, filling of the peroneal sheath occurred in only 31 (LINDHOLMER *et coll*).

PERCY *et coll* based their criteria on the size and

location of the contrast leakage at the lateral malleolus. They suggested that a leakage anterior to the malleolus indicated rupture of the anterior talofibular ligament alone, whereas enlargement of the leakage and extension laterally indicated rupture of both lateral ligaments. In the 61 cases of calcaneofibular ligament rupture reported by LINDHOLMER *et coll*, the diagnosis was made in only 37 using the criteria of PERCY *et coll*.

Other indications of rupture of both lateral ligaments have been suggested: poor contrast filling of the recesses of the talocrural joint, size of the leakage measured using an index (LINDHOLMER *et coll*) and recording of low pressure at the injection of the contrast medium (PERCY *et coll*, SPIEGEL *et coll*) but none of these have gained a wider use.

A new projection for the diagnosis of rupture of the calcaneofibular ligament is described in the present report. It has been tested in arthrography of experimental post mortem lesions.

Previously projections at right angles to the lower leg have been used in arthrography of the ankle joint. These include antero-posterior and lateral projections and antero-posterior projections with 20 to 30° lateral and medial rotation of the foot. On such views it may be difficult to observe the exact position of the leakage at the lateral malleolus because of superimposition of bones and intra-articular contrast medium.

Therefore it was aimed at finding a projection which demonstrated the ligament without such a



Fig. 1 Position of the foot for the oblique axial projection

superimposition of bone intraarticular contrast medium or of anterior leakage through a rupture of the anterior talofibular ligament. This projection is now described.

Material and Methods

The investigation was performed on 14 ankle joints from 9 fresh cadavers (average age 51 years range 34 to 74) without lesions of the extremities. The normal trauma mechanism was imitated by manual forced supination of the foot. In case of

fracture caused by the experimental trauma ankle was excluded from the series.

Arthrography was performed by injection of meglumine iothalamate (Conray meglumine 78%) lateromedially into the talocrural joint. Giemsa stain was added to the contrast medium in order to compare the leakage visible on the dissected specimen with that on the arthrographic film. Two projections were used: an antero-posterior, a lateral and a new one, an oblique axial projection.

The patient is in supine position with the maximum bent. The hip is rotated 40° laterally, the foot 25° laterally with the plantar surface of the foot kept in horizontal position. The central ray is directed 50° from the vertical plane cranially, centered in the malleolar fossa (Fig. 1).

A drawing of the oblique axial projection is presented in Fig. 2a. Exposures with metal markers at both ends of the calcaneofibular ligament are shown to indicate the position of the ligament in this projection. It extends from the anterior part of the lateral malleolus through the malleolar fossa to the calcaneus and inserts on a prominence always visible in this projection.

Evaluation of the films. The antero-posterior and lateral views were evaluated using the criteria described by PERCY et al. Three types were distinguished.

Type I. Anterior rupture of the capsule with no injury to the lateral ligaments. Contrast medium is located anterior to the tibia.

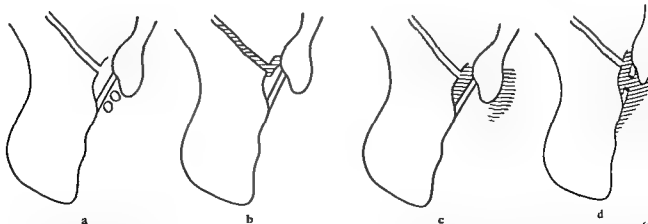


Fig. 2 Oblique axial projection: a) The malleolar fossa is located between the calcaneus and fibula. The calcaneofibular ligament traverses the fossa with the sheath of the peroneus tendon situated just behind it. b) Normal arthrography. Contrast medium in the posterior calcaneotalar joint. No injury to the lateral ligaments. c) Maximum leakage from a rupture of the anterior

talofibular ligament. No contrast medium in the malleolar fossa. d) Leakage from a rupture of the calcaneofibular ligament. Contrast medium lateral to the malleolus may be absent.



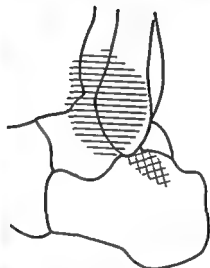
a



b



c



d

Fig. 3 Total rupture of both lateral ligaments a) A p b) lateral view assessed to have the contrast leakage mainly anterior to the lateral malleolus c) Oblique axial view Contrast medium lateral to the malleolus (→) Separated from this medium close to the calcaneus (↔) its posterior part situated behind the calcaneo-

fibular ligament (between ↔) d) Drawing of the dissected ankle (same projection as in b) Two separated regions of contrast leakage The lined area is the leakage from the ruptured talofibular ligament and the crossed area is located around the ruptured calcaneofibular ligament

Type II Rupture of the capsule and the anterior talofibular ligament Contrast medium is situated anterior to the lateral malleolus

Type III Both lateral ligaments ruptured Contrast medium is situated laterally and anterior to the lateral malleolus occasionally spreading upwards along the fibula and often situated around the tip of the fibula

The oblique axial view was evaluated according to the criteria defined in Fig. 2 b-d

All films were evaluated before the dissection

Dissection was performed in order to assess the types and extension of the lesions and the leakage of the contrast medium The tendons and the peroneal sheath were removed and the capsule and ligaments on the lateral aspect of the ankle joint were exposed

Results

At the dissection rupture of the anterior talofibular ligament was found in 7 cases and of both lateral



Fig. 4 Rupture of both lateral ligaments. a) A-P. b) lateral view. Slight leakage mainly anterior to the lateral malleolus.

considered Percy type II. c) Oblique axial view. Leakage extends behind the calcaneofibular ligament (++)

ligaments also in 7 cases. Using the criteria of PERCY et coll., rupture of the anterior talofibular ligament was diagnosed correctly in all cases with this lesion but of the cases with rupture of both lateral ligaments only the anterior one was considered ruptured in 5 cases; the other 2 cases were diagnosed correctly. On the oblique axial film using the criteria defined in Fig. 3, 2 b-d, all cases with rupture of anterior talofibular ligament and all cases with rupture of both lateral ligaments were diagnosed correctly.

All seven ruptures of the calcaneofibular ligament were total. Five of these were Z ruptures, i.e. a lesion where some of the fibers of the ligament are broken anteriorly and the rest posteriorly. At first sight the lesions were thought to be partial ruptures. The fibers were held so close together by the peritendinous connective tissue that the ligament resisted even rather severe strain.

In one case of rupture of the anterior talofibular ligament a few fibers had remained intact.

The peroneal sheath was filled in all cases of rupture of both lateral ligaments. No contrast filling occurred if only the anterior talofibular ligament was ruptured. The appearance of total rupture of the lateral ligaments is illustrated in Fig. 3. On the post mortem films the leakage had a more well defined outline and less of the characteristic flame shape than on films exposed *in vivo*.

Discussion

The extension and position of the leakage of contrast medium assessed on the antero-posterior and lateral films are dependent not only upon rupture of the calcaneofibular ligament. This may explain the results of LINDHOLMER et coll. applying the criteria of PERCY et coll. found 8 false positive and 24 false negative arthrograms in the 61 cases with ruptures of calcaneofibular ligament operated upon.

The anterior talofibular ligament is strongly related to the capsule of the talocrural joint. Therefore rupture of the ligament is always followed by a rupture of the capsule. Consequently a leakage anterior to the lateral malleolus nearly always indicates rupture of the anterior talofibular ligament (BROSTRÖM et coll., LINDHOLMER et coll.). It is difficult to distinguish this lesion from the pure rupture of the capsule, but since such a rupture is infrequent the problem is of little practical importance.

The calcaneofibular ligament is a cord like and much thinner ligament and in contrast to the anterior talofibular ligament not closely related to the capsule. A varying portion of the capsule between the ligaments may rupture together with the anterior talofibular ligament without simultaneous rupture of the calcaneofibular ligament. Consequently the contrast leakage may vary both in extension and position in the isolated rupture of the anterior

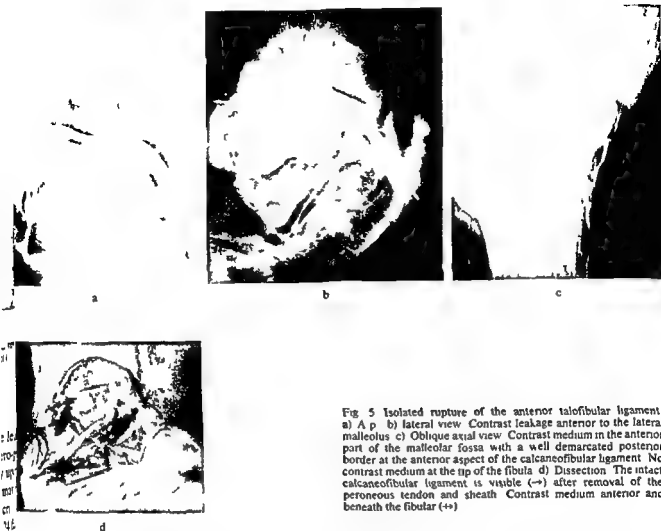


Fig 5 Isolated rupture of the anterior talofibular ligament a) A p b) lateral view Contrast leakage anterior to the lateral malleolus c) Oblique axial view Contrast medium in the anterior part of the malleolar fossa with a well demarcated posterior border at the anterior aspect of the calcaneofibular ligament No contrast medium at the tip of the fibula d) Dissection The intact calcaneofibular ligament is visible (\rightarrow) after removal of the peroneous tendon and sheath Contrast medium anterior and beneath the fibula (\leftrightarrow)

talofibular ligament. The volume of the talocrural joint the lesion of the surrounding soft tissue and the habitual condition of the tissues may also influence the extension of the contrast medium. There is no indication of the rupture of the calcaneofibular ligament. Extensive leakage may occur in cases of rupture of the anterior talofibular ligament alone and small leakage in rupture of both lateral ligaments (Fig 4). On this figure it is difficult to decide from the antero-posterior and lateral films the posterior extension of the contrast medium. Thus an isolated rupture of the anterior talofibular ligament may be suggested. The correct diagnosis was obtained when viewing the position of the contrast medium in relation to the calcaneofibular ligament on the oblique axial film.

The position of the leakage as determined from the antero-posterior and lateral films is not a reliable indicator of calcaneofibular ligament rupture

either. Most often the contrast medium spreads upwards along the fibula because distally the skin is more firmly attached to the bone. It seldom spreads more than one cm distally beyond the tip of the fibula. If the calcaneofibular ligament is ruptured the contrast medium can spread backwards from the ruptured capsule and beneath and medially to the tip of the fibula. If the ligament is intact the medium stops at the ligament (Figs 5, 6). In such cases it may spread laterally and backwards around the lateral aspect of the fibula and the intact calcaneofibular ligament. It is not possible to distinguish these two types of leakage on the antero-posterior or lateral films. For this distinction the oblique axial film is necessary because only the contrast medium beneath the tip of the fibula in the malleolar fossa indicates a rupture of the calcaneofibular ligament.

This investigation has shown that the contrast medium in the malleolar fossa is easily observed on the oblique axial film. The results confirm that a



Fig. 6 Two oblique axial exposures from the same case with isolated rupture of the anterior talofibular ligament. a) Leakage in the malleolar fossa with a sharp posterior outline. b) Piece of lead indicates the position of the calcaneofibular ligament.

leakage in the fossa behind the position of the calcaneofibular ligament indicates a rupture of the ligament. However, this experimental investigation was performed post mortem and clinical evaluation of the validity of the criteria defined in Fig. 3 is needed. The results of such an evaluation will be given in a forthcoming report.

Contrast filling of the peroneal sheath was a reliable criterion on rupture of both lateral ligaments. This is at variance with the in vivo findings of several authors (LINDHOLMER et coll., STAPLES and SPIEGEL et coll.). The reason for this discrepancy is not clear.

It is interesting to note that 5 of 7 total calcaneofibular ligament ruptures were Z ruptures. Neither the report by BROSTRÖM nor by RUTH men-

tions this type of lesion. Maybe it is only found post mortem trauma. On the other hand, it cannot be excluded that it is an overlooked type of lesion. The latter possibility is supported by the fact that thorough dissection is needed to enable detection of the lesion. Partial ruptures may in fact have to be regarded and treated as if they were total ruptures.

SUMMARY

A new projection, oblique axial, is recommended for arthrography of the acute sprained ankle for the diagnosis of a ruptured calcaneofibular ligament. Its use is experimentally confirmed.

REFERENCES

- BROSTRÖM L. Sprained ankles. I. Anatomic lesions recent sprains. *Acta chir. scand.* 130 (1965) 560.
— LILJEDAHN S. O. and LINDVALL N. Sprained ankle. II. Arthrographic diagnosis of recent ligament rupture. *Acta chir. scand.* 129 (1965) 485.
FONDYCE A. J. W. and HORN C. V. Arthrography of recent injuries of the ligaments of the ankle. *J. Bone Surg.* 54 B (1972) 116.
GLASTRUP H. Arthrographies in acute ankle joint injury. *Radiographica* 12 (1965) 281.
LINDHOLMER E., FOGED N. and JENSEN J. Th. Arthrography of the ankle. Value in diagnosis of rupture of the lateral ligaments. *Acta radiol. Diagnosis* 19 (1978) 585.
PERCY E. C., HILL R. O. and CALLAGHAN J. E. Th. Sprained ankle. *J. Trauma* 9 (1969) 972.
PRINS J. G. Diagnosis and treatment of injury to the lateral ligament of the ankle. A comparative clinical study. *Acta chir. scand.* (1979) Suppl. No. 486.
SPIEGEL P. K. and STAPLES O. B. Arthrography of the ankle joint. Problems in diagnosis of acute lateral ligament injuries. *Radiology* 114 (1975) 587.
STAPLES O. S. Ruptures of the fibular collateral ligaments of the ankle. *J. Bone Jt. Surg.* 57 A (1975) 101.
WOLFF A. A. Artrografi av ankelled. (In Norwegian). *Nord. Med.* 8 (1940) 2449.

CISTERNAL ABNORMALITIES PRODUCED BY CLINICAL TUMOURS
IN THE POSTERIOR CRANIAL FOSSA

II Fourth ventricle tumours

M LINDQVIST

The pneumographic diagnosis of fourth ventricle tumours was originally based only on ventriculography (LYSHOLM 1935). LINDGREN & DI CHIRO (1953) discussed distortions of the aqueduct and the quadrigeminal cistern in cases with different tumour locations in the posterior cranial fossa describing among other things the posterior rotation of the inferior part of the quadrigeminal plate when a tumour is causing dilatation of the fourth ventricle. LILJEQUIST (1963) pointed out that when intraventricular tumours protrude through the foramen of Magendie the inferior pole of the tumour can be demonstrated with encephalography.

MÖLLER (1974) on the basis of the origin and mode of growth of the tumours divided tumours within and adjacent to the fourth ventricle into 15 different groups. For each group a detailed description was given of the pneumographic appearance of the fourth ventricle and the aqueduct as well as of some of the cisterns especially the pontonsillar spaces, the vallecula and the pontine interpeduncular and quadrigeminal cisterns.

In previous reports cisternal distortions produced by experimental tumours in the posterior cranial fossa (LINDQVIST & MÖLLER 1978, LINDQVIST 1978) and the pneumographic cisternal abnormalities in cerebellar tumours (LINDQVIST 1980a) were described. The purpose of the present report is to present in a similar way the cisternal characteristics associated with tumours in the fourth ventricle.

Definitions The orientation of the structures of the posterior fossa is that given by CORRALES & GREITZ (1972) and used previously (LINDQVIST & MÖLLER 1978, 1980a) implying that a

beam direction parallel to the clivus is termed the axial projection. For nomenclature and a schematic survey of the normal anatomy of the cisterns see LINDQVIST (1980a, Fig. 1).

Material and Methods

The material consisted of the intraventricular tumours from the same series of patients with posterior fossa tumours including the cerebellar tumours reported previously (LINDQVIST 1980a) examined by encephalography during the period 1969 to 1975. In all cases the position and type of tumour was confirmed at surgery or autopsy. Patients previously operated upon in the posterior cranial fossa were not included.

The pneumographic examination technique has been described previously (LINDQVIST 1980a). The initial lumbar encephalography in cases with unsatisfactory passage of gas to the ventricular system was usually supplemented by ventriculography.

The total number of patients was 34. From these 4 were excluded: 2 because the position of the tumour could not be definitely established, one because encephalography failed completely for technical reasons and in a fourth case the film material was lost. The remaining 30 cases form the basis for the present report. The sex and age distribution of the series appears in Fig. 1 and the tumour classification in Table 1.

From the Department of Neuroradiology (Director: H. Liljequist), University Hospital S-90185 Umeå and the Department of Neuroradiology (Director: T. Greitz), Karolinska Sjukhuset S-10401 Stockholm, Sweden. Submitted for publication 21 May 1979.

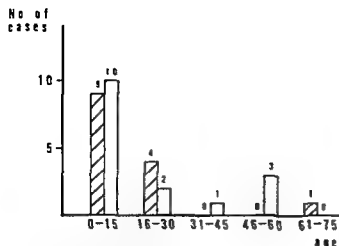


Fig 1 Sex and age distribution of 30 cases of intraventricular tumours of the fourth ventricle ■ males □ females

As in the previous analysis of cerebellar tumours the position of the tumours was established by two experienced neuroradiologists who had access to all neuroradiologic examinations surgical and autopsy reports. The tumours have been grouped in the positions given by MÖLLER. However the cisternal distortions indicate that the paraventricular tumours originating from the posterior surface of the medulla oblongata are more closely related to tumours originating from the floor of the fourth ventricle than to cerebellar tumours. They were therefore included in the present analysis while other paraventricular tumours were grouped together with the cerebellar tumours (LINDQVIST 1980a).

The tumours were divided into the following two main groups

(1) Tumours from the roof or walls of the fourth ventricle termed here *tumours from the roof* including the following tumour positions according to MÖLLER's classification Ib IIb IIIb and VIb

(2) Tumours from the floor of the fourth ventricle or from the posterior surface of the medulla oblongata inferior to the fourth ventricle termed here *tumours from the floor* including the following tumour positions according to MÖLLER's classification IV Vb 1 Vb 2 Vb 3 Vb 4

The distribution of the tumours in the two groups and also the distribution according to MÖLLER's classification is given in Table 2.

The films were reviewed with respect to filling and distortion of different cisternal structures and also to filling and size of the ventricular system. The findings were analysed in the same way as in the previous report on cerebellar tumours (LINDQVIST 1980a). Thus in order to facilitate data processing

Table 1

Classification of intraventricular tumours of the fourth ventricle in children and adults

Type of tumour	Children (0-15) years	Adults (16 years or more)	Total
	No of cases	No of cases	No of cases
Medulloblastoma	8	1	9
Juvenile astrocytoma	8	1	9
Ependymoma	3	4	7
Plexus papilloma	0	2	2
Exophytic glioma of the brain stem	0	2	2
Hemangioblastoma (Lan- dau)	0	1	1
Total	19	11	30

Table 2

Intraventricular tumours of the fourth ventricle grouped according to their positions

Tumour position	Tumour positions (MÖLLER's classification)	No of cases
Tumours from the roof	Ib	1
	IIb	3
	IIIb	3
	VIb	3
Total		10
Tumours from the floor	IV	4
	Vb 1	5
	Vb 2	1
	Vb 3	1
	Vb 4	9
Total		20

all asymmetric tumours were treated as if the pre-
dominance was right sided

The peritonsillar spaces were often better filled in patients with tumours in the fourth ventricle than in those with cerebellar tumours. Since a detailed analysis of these structures in tumours of the fourth ventricle was included in MÖLLER's report they have been given less attention in the present report.

Results and Discussion

The frequency of demonstrable filling and the characteristic distortion of the most important cys-

Table 3

shape and distortion of the cisterna magna in fourth ventricle
 notations: Symbols and abbreviations: a=anterior p=posterior
 s=superior i=inferior R=right L=left 0=no change (+)
 minimal change or increase ++=moderate change or increase
 +-marked change or increase (-)=minimal decrease
 -moderate decrease ---=marked decrease open space=
 structure not possible to evaluate

Tumour position	Fourth ventricle			
	Roof		Floor	
	Fill ing (%)	Distor tion	Fill ing (%)	Distor tion
Cisterna magna				
1 Extracranial part				
lat. proj.	100		95	
tonsillar herniation		+		(+)
a.p. displacement				
cervical medulla		a(+)		p+
2 Interhemispheric part				
lat. proj.	100		95	
s.i. diameter		--		()
Foramen of Magendie				
lat. proj.	70		30	
a.p. displacement		a+		p+
Vallecula axial proj.	90		47	
width		++		++
lateral displacement		0		0
Retrotonsillar spaces				
lat. proj.	70		35	
a.p. displacement		p++		p++
s.i. displacement		i++		i+
Cerebellomedullary fissures				
a. right side axial proj.			30	
a.p. displacement		0		p(+)
lateral displacement		R(+)		R(+)
b. left side axial proj.	80		30	
a.p. displacement		0		p(+)
lateral displacement		L(+)		L(+)
7 Paravermian sulci axial				
proj.	70		21	
width of inferior vermis		++		++
lateral displacement of inferior vermis		0		0

Internal structures associated with tumours originating from the roof and from the floor of the fourth ventricle are summarized in Tables 3, 4 and 5. Only structures filled in at least 20 per cent of the cases and considered of value for locating the tumour or for comparing the cisternal distortions with those occurring in tumours with other locations in the posterior fossa have been included.

Cisterna magna

Tonsillar herniation below the foramen magnum was present in 50 per cent of the cases with tumours from the roof but in less than 20 per cent of those with tumours from the floor (Table 3).

A tumour pole extending below the foramen magnum was present in 10 per cent of the tumours from the roof but in almost half of the tumours from the floor.

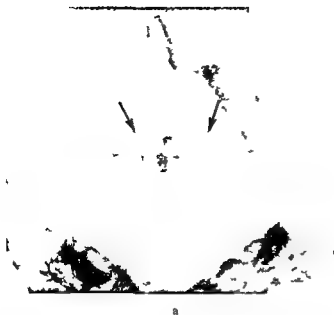
Tonsillar herniation was thus much less common in cases with intraventricular tumours of the fourth ventricle than in the case of cerebellar tumours. In some cases it was difficult to decide from the films whether a soft tissue structure below the foramen magnum was part of a tumour or a herniated tonsil. As pointed out by MÖLLER, in such cases it is important to identify the position of the upper pole of the tonsil, using as a guide the retrotonsillar spaces, the posterolateral fissures and postero superior recesses of the fourth ventricle. In addition the vallecula should be evaluated, as a rule it is widened if the tumour grows out from the fourth ventricle into the cisterna magna via the foramen of Magendie.

The cervical medulla was usually somewhat displaced anteriorly below the foramen magnum, but posterior displacement was also encountered. This was especially the case with tumours from the roof in the vicinity of the fastigium (position IIb according to MÖLLER's classification); the posterior displacement of the cervical medulla can then be assumed to be secondary to a marked anterior displacement of the medulla oblongata.

The interhemispheric part of the cisterna magna was usually compressed against the occipital crest. However, two important exceptions from this rule existed, namely cases where a tumour or part of it was situated in the cisterna magna (positions IV and Vb 3). In such cases the cisterna magna was usually markedly widened (Fig. 2) as has also been described by MÖLLER.

Filling of the foramen of Magendie was more often associated with tumours from the roof than with tumours from the floor. In the former situation an anterior displacement of the foramen of Magendie was usually present, indicating compression or anterior displacement of the medulla oblongata, while in the latter the foramen of Magendie was instead displaced posteriorly.

The vallecula was widened in all assessable cases with tumours from the floor as well as with the majority of the roof tumours (Fig. 3). In a few cases



a



b



c

Fig 2 Tumour from the posterior surface of the medulla oblongata (position IV) a b) Encephalography Only a small part of the tumour is visible (→) above the air fluid level in the markedly dilated cisterna magna c) Ventriculography lateral tomography The fourth ventricle is free from tumour except for a small indentation from below (→) The supero inferior diameter of the interpeduncular cistern is markedly reduced (→)

with tumours from the roof the width of the vallicula was normal or slightly decreased

When tumours were situated in the midline as a rule the vallicula was not displaced laterally In cases with asymmetric tumours both from the roof and from the floor a moderate lateral displacement of the vallicula towards the contralateral side was evident

The *retrotonsillar spaces* were often well demonstrated in both axial and lateral projections especially in the case of tumours from the roof In the lateral projection they were usually displaced posteriorly and inferiorly both in roof and in floor tumours the average inferior displacement being more marked in the former location

The *retrotonsillar spaces* are important indicators of the position of the superior posterior poles of the

tonsils Deformity and displacement of each of the tonsils can be evaluated by analysing these spaces as well as the secondary fissures in the axial projection as emphasized by MÖLLER this is of importance for a detailed analysis of the origin and mode of growth of the tumours

The *cerebellomedullary fissures* which indicate the border between the tonsils and the medulla oblongata were separated both in the roof and in the floor tumours with the latter tumour location they were also slightly displaced posteriorly

The *paravermian sulci* which indicate the width of the inferior vermis were more often demonstrated in cases with tumours from the roof than in floor tumours Widening of the vermis was evident in both groups of tumours in all cases assessable (Fig 3a) In some cases with asymmetric



Fig. 3. Tumour from the inferior part of the roof (position III b) cephalography. a) Axial tomography. The vallecula is widened. b) Lateral tomography. Separation of the paravermian sulci (+) indicates increased width of the inferior vermis. Tumour (++) in the foramen of Magendie. The interpeduncular cistern is compressed (---).

Tumours on slight lateral displacement of the inferior vermis was observed this being a more common feature among the roof tumours.

Medullary cistern

The premedullary part of the medullary cistern was markedly compressed in both groups of tumours (Table 4). In the axial projection the lateral recesses of the medullary cistern appeared bilaterally compressed both the a p and lateral extension these features which were present in a majority of cases in both groups of tumours are due to anterior displacement and increased width of the medulla oblongata. The increase in width was as a rule more marked in cases with tumours from the floor than in

Table 4

Filling and distortion of the medullary cistern, pontine cistern and the pontocerebellar cisterns in fourth ventricle tumours. Symbols and abbreviations as in Table 3. Additional abbreviations: Ra=right side rotated anteriorly, Rp=right side rotated posteriorly.

Tumour position	Fourth ventricle			
	Roof		Floor	
	Fill ing (%)	Distor tion	Fill ing (%)	Distor tion
Medullary cistern				
1 Premedullary part				
lat. proj.	70		50	
a p diameter		-		--
2 Lateral recesses				
a right side axial proj.	70		50	
a p diameter				--
lateral extension		-		-
b left side axial proj.	90		50	
a p diameter		-		--
lateral extension		-		-
3 Diameter of medulla oblongata				
a p diameter lat. proj.		-		
transverse diam. axial proj.		+		++
4 Lateral displacement of medulla oblongata axial proj.		0		0
5 Rotation of medulla oblongata around axis parallel to clivus				0
Pontine cistern				
lat. proj.	90		80	
a p diameter		-		-
tendency of superior part of pons to recede from clivus		(+)		+
Pontocerebellar cisterns				
1 Right side axial proj.	50		60	
width of lateral part		-		-
width of medial part		-		--
2 Left side axial proj.	40		80	
width of lateral part		-		-
width of medial part		-		--

those from the roof. With tumours from the roof the medulla oblongata was compressed from behind and the a p diameter reduced. With tumours from the floor the a p diameter of the medulla oblongata could seldom be evaluated.

An increase in the transverse width of the medulla

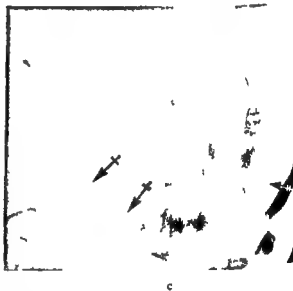


Fig. 4 a b) Intraventricular tumour from the floor (position V b 1) Encephalography lateral tomography in the sitting position a) Before and b) after filling of the cisterns. The superior part of the pons (\rightarrow) recedes markedly from the clivus c) Tumour from the posterior surface of the medulla oblongata (position IV) Encephalography lateral tomography in the sitting position. The pontine cistern is uniformly compressed and the anterior surface of the pons ($+$) is approximately parallel to the clivus. The tumour ($++$) visible in the cisterna magna.

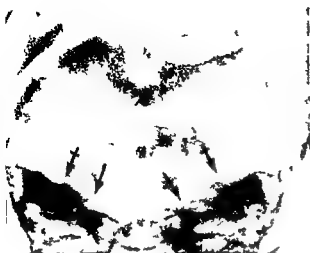
oblongata in the axial projection was not evident in some cases of lateral tumours from the roof especially in those with tumours originating from the lateral wall of the fourth ventricle (position VI b). In cases with an asymmetric tumour the medulla oblongata was also slightly displaced laterally. Asymmetric tumours originating from the roof in the vicinity of the fastigium (position II b) and the inferior part of the roof (position III b) could also cause an anterior rotation of the medulla oblongata on the tumour side.

A p compression and increased width of the medulla oblongata was observed by MÖLLER in some patients with fourth ventricle tumour both in roof and in floor tumours.

Pontine cistern

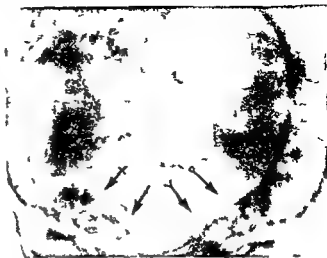
A moderate compression of the pontine cistern was encountered in both groups of tumours (Table 4). In approximately one third of the cases the inferior part of the brain stem was compressed against the clivus while the superior part was displaced posteriorly in other words the superior part of the pons receded from the clivus (Fig. 4 a b). In the remaining two thirds of the cases the anterior surface of the pons was parallel to the clivus (Fig. 4 c) but the two groups did not seem to differ in any other respect for instance in the size, type or position of the tumours or the degree of hydrocephalus.

Compression of the pontine cistern is a recognized and important indication of tumour of the posterior



a

Fig 5 a) Intraventricular tumour from the floor (position Vb 1).
neurophography, axial view. Symmetric compression of both
pontocerebellar cisterns. The medial parts (→) somewhat more
compressed than the lateral parts (←→) b) Asymmetric tumour



b

from the roof with right-sided predominance (position IIIb). The
right pontocerebellar cistern compressed both medially (→) and
laterally (←→) the width of the left cistern normal both medially
(→) and laterally (←→)

lossa (DYKE & DAVIDOFF 1935 RUGGIERO 1957
LILIEQUIST) Posterior displacement of the superior
part of the brain stem in some cases with fourth
ventricle tumours was reported by MOLLER

Pontocerebellar cisterns

In both groups of fourth ventricle tumours the
pontocerebellar cisterns were moderately com-
pressed on both sides. In cases with tumours from
the floor the medial part of the cistern was usually
more compressed than the lateral part (Fig 5a) due
to expansion of the brain stem. In cases with roof
tumours the degree of compression was usually the
same medially as laterally and in the case of lateral
or asymmetric tumours from the roof sometimes
only the cistern on the tumour side was compressed
(Fig 5b).

Interpeduncular cistern

The average a p diameter of the interpeduncular
cistern was not altered while the supero inferior
diameter was reduced in both groups of tumours,
more so in cases with tumours from the roof (Table
5). On the other hand the superior displacement of
the pons was somewhat more marked in cases with
tumours from the floor. The posterior part of the
superior surface of the pons was slightly tilted in an
upward direction in most cases in both groups.

Changes in the supero inferior diameter of the
interpeduncular cistern are due not only to the de-

gree of supero inferior displacement of the pons but
also largely to the width of the anterior part of the
third ventricle i.e. to the presence of a widened
supratentorial ventricular system (LINDQVIST
1980a). The a p diameter of the cistern depends
mainly on the degree of antero-posterior displace-
ment of the brain stem. The apparent discrepancy
between the supero inferior diameter of the cistern
and the degree of upward displacement of the pons
in cases with tumours from the floor and from the
roof (Table 5) can thus be explained by the fact that
supratentorial ventricular dilatation was more
marked in the latter group (Fig 6). Even though the
average a p diameter of the interpeduncular cistern
was normal, great variations existed in both groups
with cases of both increased and decreased a p dia-
meter. An increased a p diameter was noted partic-
ularly in the cases in which the superior part of the
pons receded from the clivus.

Ambient cistern

The circum mesencephalic parts were insuffi-
ciently filled in most of the cases, particularly the
infratentorial parts in cases with tumours from the
roof. The width of the supratentorial anterior part of
the cistern was possibly slightly reduced on both
sides in cases with tumours from the floor but
otherwise no distortion of the circum mesencephalic
parts of the ambient cistern was demonstrated (Table 5).

Table 5

Filling and distortion of the interpeduncular cistern, ambient cistern and quadrigeminal cistern in fourth ventricle tumours. Symbols and abbreviations as in Tables 3 and 4. Additional abbreviations: fr=frontally, sag=sagittally, i a=inferior end, rotated anteriorly, i p=inferior end rotated posteriorly.

Tumour position	Fourth ventricle			
	Roof		Floor	
	Fill ing (%)	Distor tion	Fill ing (%)	Distor tion
Interpeduncular cistern				
Lat. proj.	90		90	
a p diameter		0		0
s i diameter		—		—
s i displacement of pons		s(+)		s+
s i inclination of the posterior part of the superior surface of the pons		s(+)		s(+)
Ambient cistern				
Circum mesencephalic part				
axial proj.				
a width of posterior part				
right side	30	0	35	0
left side	30	0	35	0
b width of anterior infra tentorial part				
right side	10		25	0
left side	10		25	0
c width of anterior supra tentorial part				
right side	20	0	25	(-)
left side	20	0	40	(-)
d rotation around sagittal axis perpendicular to clivus				
right side		0		0
left side		0		0
Quadrigeminal cistern				
1 Body of cistern lat. proj.	50		75	
a p displacement		p++		p+
kinking of quadrigeminal plate		++		+
rotation of inferior end of quadrigeminal plate		ip++		ip+
2 Precentral fissure lat. proj.	30		50	
a p displacement		p++		p++

Quadrigeminal cistern

Posterior displacement of the quadrigeminal cistern occurred in both groups of tumours but was as a



Fig. 6 Tumour from the roof in the vicinity of the fourth ventricle (position IIb). Encephalography lateral tomography in a supine position. The anterior part of the third ventricle is markedly dilated with compression of the interpeduncular cistern (—). No definite superior displacement of the pons (—) in spite of the supero-inferior compression of the interpeduncular cistern. Also the chiasmatic cistern is compressed by the widened fourth ventricle.

rule more marked in the cases with tumours from the roof (Table 5). A kinking of the quadrigeminal plate was present in many cases in both groups and it also was more marked in the cases with tumours from the roof. Anterior rotation of the inferior part of the quadrigeminal plate was not observed in any of the cases whereas posterior rotation was common in both groups, being as a rule more marked in the cases with roof tumours.

The precentral fissure was usually markedly displaced in the posterior direction in both groups of tumours.

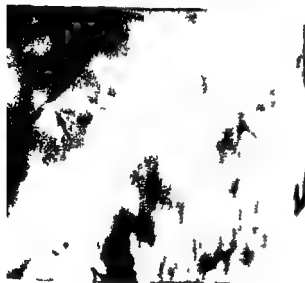
As has been pointed out previously (LINDGREN & DI CHIRO, LINDQVIST 1980a) the appearance of the quadrigeminal cistern is intimately related to that of the aqueduct and the fourth ventricle. Intraventricular tumours of the fourth ventricle cause dilatation of the ventricle (MÖLLER) and as a rule also of the aqueduct. This dilatation causes a posterior displacement of the quadrigeminal cistern and the precentral fissure and the inferior part of the quadrigeminal plate rotates posteriorly (Fig. 7a, b). In cases with marked dilatation of the aqueduct and the fourth ventricle an upward herniation of the anterior medullary velum below the quadrigeminal plate sometimes occurs (MÖLLER). In these cases the precentral fissure is either totally compressed (Fig. 7c, d) or displays extreme posterior displacement.



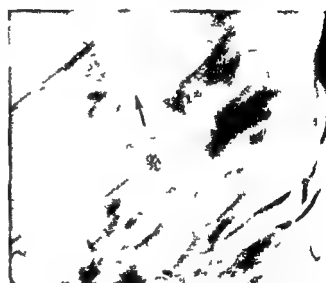
a



b



c



d

Fig. 7 a b) Intraventricular tumour from the floor (position b 1) a) Encephalography lateral tomography. The inferior part of the quadrigeminal plate is somewhat rotated posteriorly. The precentral fissure (++) is moderately displaced posteriorly. The superior cerebellar cistern (P--P) is compressed and the distance between the precentral fissure and the superior cerebellar cistern is decreased indicating a compression of the superior vermis. b) Ventriculography lateral tomography. Moderate widening of the fourth ventricle and a slight widening

of the aqueduct. c) Encephalography lateral tomography. Only slight filling of the quadrigeminal cistern or the precentral fissure in spite of good filling of the cisterna veli interpositi (t--t) and the pericallosal cistern (t--t). d) Ventriculography lateral tomography. Extreme widening of the aqueduct and the fourth ventricle. The anterior medullary velum (t--t) herniated upwards below the quadrigeminal plate.

Remaining cisterns

The *crural cisterns* were filled in approximately 40 per cent of the cases; no specific distortions were noted.

The *chiasmatic cistern* was filled in all cases with floor tumours and in 80 per cent in the other group. As in cerebellar tumours (LINDQVIST 1980a) the

chiasmatic cistern was compressed in cases with supratentorial ventricular dilatation (Fig. 6). The cistern was otherwise not significantly abnormal.

The *cistern of the lamina terminalis* was demonstrated in approximately 50 per cent of the cases without specific features.

The *superior cerebellar cistern* was demonstrated

*Typical cisternal distortions produced by tumours
from the roof and from the floor of the fourth
ventricle*

Lateral projection

Tumours from the roof	Tumours from the floor
<p>Tonsillar herniation Exception In a few cases the tumour extends out into the foramen of Magendie and the vallecula causing separation of the tonsils. In these cases the tumour pole instead of the tonsils may extend below the foramen magnum.</p> <p>Marked posterior and inferior displacement of the retrotonsililar spaces.</p> <p>Compression of the interhemispheric part of the cisterna magna against the occipital crest. Exception In cases with a tumour component in the cisterna magna this part of the cistern is widened instead.</p> <p>Anterior displacement of the foramen of Magendie.</p> <p>Compression of the premedullary part of the medullary cistern.</p> <p>Moderate compression of the pontine cistern sometimes more marked inferiorly than superiorly.</p> <p>Marked supero-inferior compression of the interpeduncular cistern and slight superior displacement of the pons.</p> <p>Kinking and posterior displacement of the quadrigeminal plate with posterior rotation of the inferior part of the plate.</p> <p>Marked posterior displacement of the precentral fissure.</p>	<p>Tumour extension via the foramen of Magendie to the cisterna magna below the foramen magnum. Exception In some cases the tumour does not grow out through the foramen of Magendie and in these cases tonsillar herniation may be present instead.</p> <p>Marked posterior displacement and moderate inferior displacement of the retrotonsililar spaces.</p> <p>Compression of the interhemispheric part of the cisterna magna against the occipital crest.</p> <p>Posterior displacement of the foramen of Magendie.</p> <p>Compression of the premedullary part of the medullary cistern.</p> <p>Moderate compression of the pontine cistern sometimes more marked inferiorly than superiorly.</p> <p>Marked supero-inferior compression of the interpeduncular cistern and moderate superior displacement of the pons.</p> <p>Slight kinking and posterior displacement of the quadrigeminal plate with slight posterior rotation of the inferior part of the plate.</p> <p>Marked posterior displacement of the precentral fissure.</p>

Axial projection

Tumours from the roof	Tumours from the floor
<p>Increased width of the inferior vermis.</p> <p>Widening of the vallecula without lateral displacement. Exception In cases without tumour extension to the foramen of Magendie the width of the vallecula may be normal or reduced. Lateral displacement may occur in cases with asymmetric tumours.</p> <p>Separation of the cerebellar medullary fissures.</p> <p>Anterior compression with increased transverse diameter of the medulla oblongata.</p> <p>Symmetric compression of the lateral recesses of the medullary cistern. Exception In cases of asymmetric tumour a slight lateral displacement as well as some anterior rotation of the medulla oblongata may occur on the tumour side.</p> <p>Symmetric compression of the pontocerebellar cisterns and the same degree of compression medially as laterally.</p> <p>Exception In cases of asymmetric tumour the compression may be more marked on the tumour side.</p>	<p>Increased width of the inferior vermis.</p> <p>Widening of the vallecula without lateral displacement. Exception Lateral displacement may occur in cases with asymmetric tumours.</p> <p>Separation of the cerebellar medullary fissures.</p> <p>Anterior compression with increased transverse diameter of the medulla oblongata.</p> <p>Symmetric compression of the lateral recesses of the medullary cistern.</p> <p>Symmetric compression of the pontocerebellar cistern usually more medially than laterally.</p>



Fig 8 Drawings of some important cisternal deformities in tumours from the roof of the fourth ventricle. a) Lateral view. b) Axial view of the cisterns inferior to the fourth ventricle. c) Axial view of the cisterns adjacent to the tentorial notch. The normal appearance of the cisterns is indicated by means of continuous lines. Cisternal structures possible to evaluate in tumour cases are indicated with shaded areas (cf. LINDQVIST 1980a Fig 1).



Fig 9 Drawings of some important cisternal deformities in tumours from the floor of the fourth ventricle. a) Lateral view. b) Axial view of the cisterns inferior to the fourth ventricle. c) Axial view of the cisterns adjacent to the tentorial notch (cf. Fig 8).

in the lateral projection in approximately 30 per cent of the cases. Its width varied. In most cases where the cistern could be evaluated, the superior vermis was compressed (Fig 7a) as with tumours of the anterior compartment of the posterior fossa.

The pericallosal cisterns were demonstrated in the axial projection on one or both sides in approximately 20 per cent of the cases with tumours from the roof and in approximately 40 per cent in the other group. The wings of the ambient cistern were filled in 20 per cent of the cases with roof tumours and in 75 per cent of those with floor tumours. The cisterna veli interpositi was filled in approximately 10 per cent of both groups. All these cisternal structures were often markedly dilated in cases with hydrocephalus, normal or insignificantly dilated in cases without hydrocephalus.

As in the case of the cerebellar tumours (LINDQVIST 1980a) no correlation was found in cases with unilateral filling between the side of the tumours and the filled side of these cisterns in the presence of a lateral tumour.

Typical cisternal distortions associated with intraventricular tumours from the roof and from the floor respectively are listed on page 10 and illustrated schematically in Figs 8 and 9.

The cisternal abnormalities in cases with tumours of the pontine angle and of the brain stem will be discussed in a forthcoming report (LINDQVIST 1980b) and the differences between cisternal abnormalities in various tumour sites will be discussed in that context.

SUMMARY

A detailed analysis of the distortion of the subarachnoid cisterns produced by intraventricular tumours of the fourth ventricle was carried out on a clinical material of 30 patients examined with pneumography. The cisternal distortions in cases with a tumour originating from the roof of the ventricle have been compared with those in tumours originating from the floor and the typical appearances for each group of tumours are recorded. The results should be applicable when analysing cisterns examined not only with pneumography but also with other radiologic methods such as computer tomography and cisternography with positive contrast media.

ACKNOWLEDGEMENTS

The investigation was supported by grants from the Swedish Cancer Society and the Medical Faculty University of Umeå.

REFERENCES

- CORRALES M. and GREITZ T. Fourth ventricle. II. Tumours of the cerebellum. *Acta radiol. Diagnosis* 12 (1972) 241.
- DYKE C. G. and DAVIDOFF L. M. The significance of abnormally shaped subarachnoid cisterns as seen in

- the encephalogram. *Amer. J. Roentgenol.* 37 (1977) 743.
- LINDBQVIST B. Lumbar encephalography in pontine intracerebellar tumours. *Acta radiol. Diagnosis* (1963) 593.
- LINDGREN E. and DI CHIRO G. The roentgenologic appearance of the aqueduct of Sylvius. *Acta radiol.* (1953) 117.
- LINDQVIST M. Cisternal changes produced by intracranial balloon tumours in the posterior cranial fossa: post mortem investigation. *Acta radiol. Diagnosis* (1978) 161.
- (a) Cisternal abnormalities produced by claustrum tumours in the posterior cranial fossa. I. Cerebellum. *Acta radiol. Diagnosis* 21 (1980) 85.
- (b) Cisternal abnormalities produced by claustrum tumours in the posterior cranial fossa. III. Tumours of the brain stem and pontine angle. To be published. *Acta radiol. Diagnosis* 21 (1980).
- and MÖLLER A. Postmortem radiography of the subarachnoid cisterns. *Acta radiol. Diagnosis* 19 (1978) 101.
- LINDBQVIST E. Das Ventrikulogramm. III. Teil. *Acta radiol.* (1935) Suppl. No. 26.
- MÖLLER A. Pneumography in paraventricular and intraventricular tumours of the posterior fossa. *Acta radiol.* (1974) Suppl. No. 342.
- RUGGIERO G. L'encephalographie fractionnée. Masson, Paris 1957.

ARACHNOIDAL DIVERTICULA AND CYSTLIKE DILATATIONS OF THE NERVE-ROOT SHEATHS IN LUMBAR MYELOGRAPHY

J. L. LARSEN, D. SMITH and G. FOSSAN

The anatomy and the radiologic appearance of lumbosacral nerve roots and their sheaths have been described by numerous authors (for review see CAPESIUS & BABIN 1978). It is well known that the width of the root sheaths varies considerably and that they sometimes may appear as cystlike pouches. They are not to be confused with epidural cysts nor with the perineurial cysts first described by TARLOV (1938). They must be regarded as unusually wide root pockets covering the emerging nerve root between the dural sac and the fusion of the arachnoid and the perineurium. Such dilated root sheaths were reported by CAPESIUS & BABIN in an incidence of 5 to 10 per cent. The present investigation was undertaken with the following intentions: to establish the incidence of root sheath diverticula in a series of patients examined by lumbar myelography; to estimate the possible significance with regard to clinical symptoms and signs; and to establish a possible relationship with a wide dural sac (mega-cauda or mega sac).

Material and Methods

Lumbar myelography with 6.75 g metrizamide (Ampaque Nyegaard Norway) at a concentration of 250 mg/ml was performed in 136 patients referred because of low back pain or sciatica. The usual projections were used: horizontal in right and left lateral positions, prone and oblique decubitus, a p in standing and lateral views in sitting position with flexion and extension of the spine were included. Due to differing sizes of the patients and difficulties in obtaining films in exactly reproducible

positions a system with proportionate measurements was chosen. Based on a preliminary analysis of normal roots and sheaths the normal limit was defined as the root occupying at least half of the combined diameter of the root and the root sheath, the measurement being performed at right angles to the direction of the root in the view demonstrating the largest diameter of the root sheath (Fig. 1). Roots obviously affected by prolapse or osteochondrotic lesions with deformity caused by compression or edema should not be included; however, no case with such lesions affecting widened sheaths was found, but as the filling of the root pockets was often scanty in the diseased roots, the possibility of such lesions cannot be excluded.

Results

Abnormally wide nerve root sheaths were found in 24 of the 136 patients. The total number of wide sheaths was 49. Twelve of the patients had only one in the lumbosacral region and the highest number in one patient was 7. The most commonly affected root was the first sacral (Table 1).

It has been assumed that wide root pockets are more common in advanced age. Grouping the present patients revealed no significant sex or age differences between patients with and without widened sheaths.

The distribution of dilated sheaths according to relative size at proportionate measurements appears in Table 2.

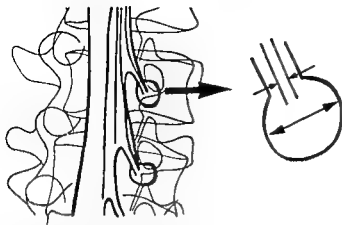


Fig. 1 Method of measurement. As the root has an even diameter along its distal course it is often conveniently measured a little proximal to a diverticulum.

Morphologically the widened sheaths or diverticula could be divided into three categories: tubular with a more or less even diameter along the course (Fig. 2a), saccular also known as drop like located at the distal end of the root sheath (Fig. 2b) and uneven in appearance often as a combination of 1 and 2 (Fig. 2c). Of the 49 dilated sheaths 12 belonged to the first category, 24 to the second and 12 to the third, one patient having a drop like widening at the proximal part of the root was not classified (Fig. 3).

It has been assumed that root sheath dilatations occur more often when the dural sac is large, so called mega cauda or properly mega sac. Two methods of classification in this condition have been described. In the first one described by KOMMINOTH *et coll.* (1968) the transversal diameter of the dural sac is related to the interpeduncular distance at L5, a ratio of one or close to one being taken as representing mega sac (Fig. 4). The other method was described by CHAQUAT *et coll.* (1974) who proposed sagittal measurements and considered an antero-posterior diameter of the sac of more than half that of the corresponding vertebral body to indicate mega sac (Fig. 4). In the present series both methods were employed at the level of L5 (in a few of the patients supplemented at the L4 level when in doubt). Only measurements on films in the erect or sitting position were used in order to ensure good filling and distension of the sac. One patient with paraplegia was therefore omitted and in two other patients only one of the methods could be used with reliability. The results were affirmative for mega sac

Table 1

Distribution of root sheath diverticula

Root affected	Right	Left
L1	1	2
L2	3	2
L3	3	1
L4	1	1
L5	1	1
S1	11	7
S2	6	5
S3	1	3
Total	27	22

by the method of CHAQUAT *et coll.* in 5 of 73 patients with wide root sheaths, in 3 of these 5 also by the method of KOMMINOTH *et coll.* with one questionable (index 37/42 mm) and one not measurable as the remainder.

There was a tendency for patients with wide lumbar root sheaths also to have wide sheaths in the thoracic region. The conus and lower thoracic region was often included but not as a strict routine. Thus the concordance cannot be numerically assessed. One female aged 69 in whom the spinal canal was filled by contrast medium from Th7 distally had diverticula on 14 of the 26 demonstrable root sheaths (Figs 2c, 5).

All patients had a complete neurologic examination by an experienced neurologist or neurosurgeon. In no case could symptoms or signs from the roots with wide sheaths or diverticula be demonstrated.

Discussion

Incidence of diverticula. A diverticulum is defined in the present series as a widening of the root sheath in which the subarachnoid space occupies more than

Table 2

Total transversal diameter of root and sheath

Ratio	$\frac{2}{1}$	$\frac{2-3}{1}$	$\frac{3}{1}$
No. of diverticula	22	11	16



Fig 2a

Fig 2b



Fig 2c

Fig 3

Fig 2 a) Tubular diverticulum on S1 root (→). The root sheath of S7 also appears wide although not classified as a diverticulum. b) Typical drop-like diverticulum (→) on right S1 root. c) Narrow connection between the diverticulum and the caudal sac. d) The left L5 and S1 roots (→) are encircled by a large uneven diverticulum. Small diverticulum on L2 root (Same patient as in Fig 5).

Fig 3 Proximal dilatation of the root sheath of S7 (→)

Fig 4 Assessment of possible mega sac using a p (KOMNINOTH et coll) and lateral (CHAOUAT et coll) projection

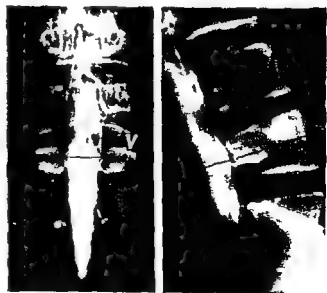


Fig 4

50 per cent of the total transversal diameter of root and sheath together. Using this definition 17.6 per cent of the 136 patients had diverticula in the lumbosacral region. This figure is higher than those given in most radiologic, anatomic or pathologic publications. One reason for this may be the limit

set towards normality. Perusal of the literature has not revealed any precise criteria, which is an obvious difficulty in comparing materials.

Of pathologic reports reference will be made to two. SMITH (1961) reported cystlike formations in 11 per cent of 100 consecutive autopsies. They were



Fig. 5 Same patient as in Fig. 2c. Several diverticula in the thoracic region (the patient with the largest number of diverticula)

found at thoracic, lumbar and sacral levels. No further details as to location or frequency were given. HOLT & YATES (1964) examining 120 specimens of the cervical spine from elderly patients found cystic changes in 37 (30.8%). However, some of these were stated to have been detected only at microscopy, the frequency not given. The number of widenings varied from 1 to 6. Totally 65 roots were affected, giving an average of 1.8 per patient. Considering the number of cervical roots in relation to that in the lumbosacral region, this result is in accordance with the incidence in the present series.

The lower figure of 5 to 10 per cent cystlike conditions and dilatations of the lumbosacral nerve root sleeves reported by CAPESIUS & BABIN, who did not state the usual cranial extension of contrast medium at myelography, can be explained by the fact that the upper lumbar roots were not demonstrated in all their patients. Both ARNELL (1948) and LINDBLOM (1948) stated that the root sheaths vary in length and width without further analysis. SCHÖBER (1963) in a material of 247 myelographies in different regions found 20 patients with cystic lesions, 16 lumbosacral and 4 cervically, but none in the thoracic region. From the illustrations it is evident that both oily and water soluble contrast media were employed. As the root sheaths are not adequately demonstrated with the oily media, a true incidence is not to be expected.

Clinical significance. In no case was any correlation found between dilated meningeal sheaths and clinical symptoms or signs. This is in accordance with previous experiences (SCHÖBER, CAPESIUS & BABIN, STEWART & RED 1971). A diverticulum must be large enough to produce pressure upon the roots for symptoms to occur. In case of a narrow

communication with the main subarachnoid space, the possibility exists that this may be closed and a true cyst be formed and possibly impinge upon the bony spinal canal, the medulla and the nerve root. Hypothetically, the same effect may be elicited by a valve mechanism at the entrance of the diverticulum, making possible entrance but not escape of spinal fluid.

Relation to mega sac. In 5 of 23 patients (22%) the dural sac was found to be unusually large in relation to the bony canal. KOMMINOTH *et al.* (1964) found an incidence of mega sac in 60 of 4941 selected lumbosacral myelographies, i.e. an incidence of 1.3 per cent. The positive correlation between mega sac and diverticula thus seems to be evident. It is known that the wall of the diverticulum in many cases is thin and atrophic (HOLT & YATES). Information as to whether the meningeal wall in mega sac is atrophic is not available, but such is the case, the pulsatile force of the cerebrospinal fluid could explain the concordance of mega sac and diverticula.

The hydrostatic pressure of the cerebrospinal fluid is assumed to play a role in the formation of the subarachnoid diverticula (STRULLY 1956, SMITH 1966). HOLT & YATES found a definite increase in diverticular size in caudal direction, but this referred only to the cervical region. SMITH too reported increasing diverticular size in caudal direction without any further details as to frequency of location. In the present series the S1 and S2 roots were most often affected, these two locations carrying approximately 60 per cent of the diverticula. For the rest, the diverticula were haphazardly distributed, with no definite predominance in caudal direction. This means that factors other than the hydrostatic pressure must

an important role these factors being predominantly present in the root sheaths of the first and second sacral nerve. If dilatation should occur on the basis of a large root sleeve a greater tendency for diverticula would be expected on the L5 roots. These together with the first sacral harbour the largest sleeves. Mechanical factors could also be involved as the lower lumbar and first sacral roots are subject to the relatively largest movements in relation to the intervertebral foramina in flexion of the spine (BREIG 1960). However the low incidence of diverticula of L5 is then difficult to explain. No significant difference in age existed between patients with and without diverticula in the present series. If hydrostatic pressure should be the major factor responsible for meningeal dilatation increased frequency in the older age groups is to be expected.

SUMMARY

Diverticulum like widening of one or several nerve root sheaths was found in 24 of 136 patients examined by lumbar myelography. No clinical significance of the diverticula was demonstrated. The roots most commonly affected were the S1 and S2 roots carrying approximately 10 per cent of the diverticula. A system of classification according to morphology and to size compared with the root involved is proposed. A relationship between mega- and arachnoidal diverticula is confirmed.

REFERENCES

- ARNEIL S. Myelography with water soluble contrast. *Acta radiol* (1948) Suppl. No 75.
- BREIG A. Biomechanics of the central nervous system. Almqvist & Wiksell, Stockholm 1960.
- CAPESEUS P. and BABIN E. Radioculosaccography with water soluble contrast media. Springer Verlag, Berlin 1978.
- CHAQUAT Y., KANOVITCH B., FAURES B., GIVET C., PIATECKI A. et VIGNAUD J. Lomboradiculalgies par canaux larges. *Rev. Rhum.* 41 (1974) 491.
- HOLT S. and YATES P. O. Cervical nerve root cysts. *Brain* 87 (1964) 481.
- KOMMINOTH W., WÖRINGER E. et PHILIPPI R. Mega cisternae de la racine. Étude clinique de 60 cas. *Neuro-chirurgie* 14 (1968) 607.
- LINDBLOM K. The subarachnoid spaces of the root sheaths in the lumbar region. *Acta radiol* 30 (1948) 419.
- SCHOBER R. Klinische und diagnostische Bedeutung zystischer Wurzelstaschen Erweiterungen. *Acta radiol* 1 (1963) 754.
- SMITH D. T. Cystic formation associated with human spinal nerve roots. *J. Neurosurg.* 18 (1961) 654.
- STEWART D. H. and RED D. E. Spinal arachnoid diverticula. *J. Neurosurg.* 35 (1971) 65.
- STRULLY K. J. Meningeal diverticula of sacral nerve roots (perineural cysts). *J. Amer. med. Ass.* 161 (1956) 1147.
- TARLOV I. M. Perineural cysts of the spinal nerve roots. *Arch. Neurol. Psychiat.* 40 (1938) 1067.

ANGIOGRAPHIC DETERMINATION OF CEREBRAL BLOOD FLOW

H. M. T. LANTZ, J. M. FOERSTER, D. P. LINK and J. W. HOLCROFT

Currently no ideal technique for measuring cerebral blood flow in humans is available. Such a technique would be non-invasive, instantaneous and repeatable (POSNER 1972). Furthermore, the method could measure regional as well as total blood flow to the brain, i.e. extracranial as well as intracranial flow. The ideal technique would not involve radioactivity and not require hospitalization (CARR & FISHKIN 1970). At present several different techniques are employed, each of which has its advantages and disadvantages, limiting its properties as an ideal method for measuring cerebral blood flow. Four major principles are utilized in this regard: Fick principle, Stewart-Hamilton principle (indicator dilution), bolus transit time by extracranial counting, and mechanical flow meters.

By the Fick principle (KETTY & SCHMIDT 1948) the arteriovenous difference of inhaled nitrous oxide is measured over a period of 10 min from several arterial and jugular venous blood samples. The method requires arterial as well as venous catheterization. By the same principle, isotope clearance methods require arterial as well as venous catheterization (1969) and ^{15}O (TER POGOSIAN *et al.* 1970). These isotope clearance methods have the advantage of measuring regional blood flow and can be repeated several times. However, self-absorption and scatter can lead to overlap of regions, and carotid puncture is required. The ^{15}O method has the advantage of simultaneously measuring regional cerebral flow and central nervous system metabolism, but the emission is difficult to collimate; the isotope has a short half-life and requires a cyclotron.

Conventional indicator dilution methods using non-diffusible isotopes have been used for a long time. The technique is however cumbersome and difficult to use. Bolus injection of hydrogen gas into each internal carotid artery has been described by MAYER & SHINOHARA (1970). By this method it has become possible to estimate hemispheric blood flow and to compare one hemisphere with the other, utilizing dissolved hydrogen as the indicator. The method requires bilateral catheterization of the carotid arteries and jugular veins.

The brain transit time of intravenously injected isotopes has been used to estimate the cerebral blood flow. The method is easy to perform, repeatable and atraumatic to the patient. However, it does not measure the cerebral blood flow but rather the transit time across the brain (OLDENDORF 1970).

Of the mechanical methods of measuring cerebral blood flow, thermal velocity and thermal dilution techniques have found little use in humans. The Doppler principle is non-invasive and instantaneous and will give continuous measurements of velocity. It provides only semiquantitative measurements of relative changes in blood velocity and is quite sensitive to the patient's movement and to the position of the probe. On the other hand, electromagnetic flow meters are quite accurate and give a continuous measure of the blood flow. This technique requires surgical exposure of the carotid arteries and thus is not fit for use in normal clinical examinations.

A new method of determining the cerebral blood flow is now presented which can easily be used in conjunction with routine cerebral angiography. A catheter is positioned in the carotid artery fluoroscopically. Injected contrast medium then is utilized as dilution indicator for estimating the flow in each artery as a fraction of the cardiac output. No sampling catheters are required. Besides the usefulness of the method as a basic physiologic and pathophysiologic tool, clinical situations appear where such measurements can be of great importance. JENNETT et al. (1966) demonstrated that a flow decrease of 25 per cent or more in the carotid flow would be extremely valuable in evaluating patients with intra-cerebral aneurysms requiring carotid artery ligation. Such a method might also be useful before carotid endarterectomy in the diagnosis of cerebral ischemia in determining the prognosis in a comatose patient and in treatment of stroke and brain injury (HARPER 1971).

The present method measures relative flow utilizing the videodensitometric technique described by LANTZ (1974, 1975). The method has recently been applied for measurements of renal blood flow (LINK et al. 1979) and splanchnic blood flow (LANTZ et al. 1980). The blood flow of each cerebral vessel can be measured as a fraction of the cardiac output.

Videodensitometric estimate of relative flow

The videodensitometer is an electronic instrument capable of measuring density changes in a selective region of the television image. It is characterized by high sensitivity and a rapid dynamic response. Density changes in the fluoroscopic television image caused by injected contrast medium can be quantified and recorded as a dilution curve. The integrated area under the densitometric curve reflects the blood flow at the site of injection upstream and not at the site of recording. The densitometric area A is directly proportional to the amount of injected contrast medium M and inversely proportional to the blood flow Q at the site of injection according to (LANTZ 1975)

$$A = \frac{M}{Q} k$$

thus

$$Q = \frac{M}{A} k$$

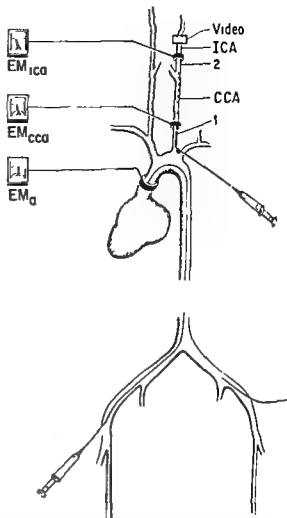


Fig. 1. Diagram of the canine model. Flow in the ascending (EM_{ica}) the common carotid artery (EM_{cca}) and the internal carotid artery (EM_{ia}) was continuously monitored utilizing magnetic flow probes. One angiographic catheter was permanently positioned in the ascending aorta and another one placed with the tip in the common carotid artery (position 1) and in the internal carotid artery (position 2). Alternately videodensitometric recordings were performed at the same site over a branch of the internal carotid artery (Video). Blood pressure (BP) was recorded via an iliac cannula and pressure transducer.

where k is a proportionality constant affected by radiation intensity and the gains of the television chain and recording equipment. By injecting contrast medium at two sites of the circulatory system and by recording the densitometric dilution curve downstream at a fixed site of the artery, it is possible to compare the flows at the sites of injection

$$\frac{Q_1}{Q_2} = \frac{M_1 A_2}{M_2 A_1}$$

where Q_1 and Q_2 are the flows at the sites of injection. M_1 and M_2 are the amounts of contrast medium

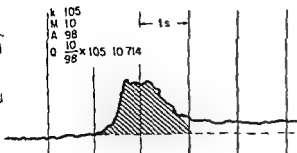


Fig. 1. Videodensitometric flow calculation in the common carotid artery as a fraction of the cardiac output. Top curve represents the recording obtained over the internal carotid artery after intrast medium injection in the ascending aorta. Bottom curve presents the videodensitometric recording at the same site after selective injection in the common carotid artery. The flow Q is calculated from M (amount of contrast medium injected), A (integrated densitometric area, shaded) and k (calibration factor or radiation intensity) according to $Q = \frac{M}{A} k$. The flow in common carotid artery as a fraction of the cardiac output is $\frac{0.7}{1.4} = 70$ per cent.

ected at the two sites and A_1 and A_2 are the integrated densitometric areas measured from the densitometric dilution curves. If for example the flow in the right common carotid artery is to be estimated as a fraction of the cardiac output, two contrast injections will be made: one in the ascending aorta where total cardiac output passes and one in the proximal part of the right common carotid artery. The two dilution curves recorded over the right internal carotid artery will then reflect the blood flow in these areas.

Materials and Methods

The blood flow in the common carotid artery and the internal carotid artery was determined as a fraction of the cardiac output in an *in vivo* canine model (Fig. 1). Estimates obtained by the videodensitometric method were compared to the corresponding electromagnetic flow readings in 2 mongrel dogs weighing 25 and 32 kg, respectively. The dogs

were anesthetized with 30 mg/kg of sodium pentobarbital and were ventilated with a Harvard pump on room air. The cardiac output was continuously recorded by a circumferential electromagnetic flow probe around the ascending aorta 2 to 4 cm above the aortic valve. A similar electromagnetic probe was attached to the proximal part of the left common carotid artery and another to the proximal part of the left internal carotid artery. The probes were connected to electromagnetic flow meters (Statham SP 2200). The systemic blood pressure was recorded via a cannula in the left common iliac artery attached to a Statham P23DB pressure transducer.

The videodensitometric flow in the left common carotid artery was calculated as a fraction of the cardiac output from two dilution curves derived from a bolus injection of sodium iohalamate (Conray 400) through a 7 French pigtail catheter with its tip in the ascending aorta and from a second bolus injection through a 6 French catheter with its tip in the proximal part of the left common carotid artery. With respiration suspended and the dog in a fixed position, 10 ml contrast medium was injected in the ascending aorta followed by a 1 ml injection into the common carotid artery. When the blood flow in the internal carotid artery was determined as a fraction of the cardiac output, the selective 6 French catheter was advanced to the internal carotid artery for a 1 ml contrast injection. The selective injections were performed manually and the aortic injections by a Cordis II pressure injector. Nine series of injections were performed, each consisting of one aortic injection followed by one or more selective injections. The video image was recorded on video cassette with the image intensifier in a fixed position covering a main branch of the left internal carotid artery. Before each recording, performed in constant fluoroscopy with fixed kV and mA = 10 mm aluminum filter was used for calibration of the radiation intensity. The videodensitometric dilution curves were displayed at a later time by replaying the cassette. A videodensitometer with an output voltage proportional to the logarithm of the incident radiation was used (T Strand Siemens Elema, Sweden). Integration of the videodensitometric mass time curves was performed by planimetry.

The video image was recorded on a Sony Umatic video cassette recorder. The data from the electromagnetic probes along with the arterial pressure were recorded on an Electronics for Medicine DR 8 photographic recorder and synchronized with the

Table I

Twenty nine measurements of the flow in the common carotid artery as a fraction of the cardiac output were recorded by the magnetic and videodensitometric methods. Each of the 7 series represents one contrast injection in the ascending aorta followed one or more subsequent selective injections in the common carotid artery at different time intervals. The difference in percentage between the videodensitometric and electromagnetic method is displayed in column E.

Series	n	Time (min)	A	B	C	D	E
			Electromagnetic output	flow (ml/min) Common carotid artery	Electromagnetic ratio (per cent common carotid flow)	Videodensitometric ratio (per cent common carotid flow)	Difference (per cent) D-C
1		0	4 090				
	1	9		261	6.4	6.3	-0.1
	2	11		261	6.4	5.6	-0.8
	3	15		279	6.8	5.4	-1.4
	4	16		264	6.5	5.3	-1.2
2	5	18		245	6.0	5.1	-0.9
		0	3 240				
	6	2		256	7.9	5.1	-2.8
	7	3		256	7.9	5.6	-2.3
	8	4		261	8.0	6.6	-1.4
3		0	3 350				
	9	4		279	8.3	8.9	0.6
	10	5		290	8.7	7.3	-1.4
4	11	6		297	8.7	6.7	-2.0
		0	4 100				
	12	14		299	7.3	5.2	-2.1
	13	18		299	7.3	5.6	-1.7
	14	20		377	8.0	7.6	-0.4
5	15	23		322	7.9	7.4	-0.5
	16	25		372	7.9	8.8	0.9
		0	4 150				
	17	2		346	8.3	7.5	-0.8
	18	5		307	7.4	8.7	0.8
6	19	7		299	7.2	6.8	-0.4
	20	9		315	7.6	6.8	-0.8
	21	11		315	7.6	7.6	0.0
		0	3 400				
	22	15		88	2.6	2.5	-0.1
7	23	18		109	3.2	3.5	0.3
	24	19		81	2.4	2.6	0.2
	25	20		85	2.5	2.3	-0.2
		0	3 400				
8	26	2		154	4.5	3.8	-0.7
	27	4		158	4.6	3.6	-1.0
	28	6		158	4.6	3.5	-1.1
	29	11		153	4.5	3.2	-1.3
					$\bar{x}=7.53^{**}$	$\bar{x}=6.64$	$\bar{x}=-0.78$
				S D = 0.76	S D = 1.21	S D = 0.97	

Partial obstruction (manual) of the common carotid artery
Series 6 and 7 excluded

Table 2

ven measurements of the internal carotid flow as a fraction of the cardiac output were recorded by electromagnetic and videodensitometric methods. Each of the 2 series represents one contrast injection in the ascending aorta followed by several subsequent selective injections in the internal carotid artery at different time intervals. The difference in percentage between the videodensitometric and electromagnetic method is displayed in column E.

Series	n	Time (min)	A	B	C	D	E
			Electromagnetic flow (ml/min)	Cardiac output	Electromagnetic ratio (per cent internal carotid flow)	Videodensitometric ratio (per cent internal carotid flow)	Difference (per cent) D-C
		0	3 250				
	30	3		216	6.7	5.9	-0.7
	31	5		216	6.6	5.8	0.8
	32	6		213	6.6	6.3	0.3
	33	7		221	6.8	6.0	0.8
	34	9		208	6.4	6.3	-0.1
	35	11		198	6.1	6.6	0.5
		0	2 750				
	36	10		183	6.7	5.5	-1.2
	37	13		216	7.9	5.5	-2.4
	38	14		193	7.0	4.1	-2.9
	39	15		188	6.8	5.1	-1.7
	40	16		188	6.8	4.5	-2.3
					$\bar{x}=6.75$ SD = 0.45	$\bar{x}=5.60$ SD = 0.77	$\bar{x}=-1.15$ SD = 1.06

ideo tape recording of the contrast medium injections. A constant potential generator (C G R 1215, 200 mA) was used. The fluoroscopic equipment included a cesium iodide image intensifier with a Lumibicon television camera (C arm C G R triple field image intensifier). A 10 cm (4") intensifier input was used in all experiments.

Results

Nine series of measurements were obtained with 40 paired ratios of cerebral blood flow and cardiac output by the videodensitometric and electromagnetic methods. The videodensitometric recordings from a typical data pair are illustrated in Fig. 2. Extrapolation of the videodensitometric curves was required because of background accumulation of contrast medium which prevented the curve from returning to baseline. This is a generally accepted technique in other dilution methods.

Common carotid artery flow. Twenty nine paired data comparing the common carotid flow and the cardiac output are displayed in Table 1. In series 6 and 7 partial obstruction of the common carotid artery was manually performed to decrease the flow.

The mean common carotid flow ratio (series 1-5) was 7.53 per cent (SD=0.76) calculated by the electromagnetic method and 6.64 per cent (SD=1.21) by the videodensitometric method respectively. The mean difference between the methods was -0.78 per cent (SD=0.92) for all 7 series.

Internal carotid artery flow. Two series containing 11 paired ratios of the internal carotid artery flow are displayed in Table 2. The mean flow as a fraction of the cardiac output was 6.75 per cent (SD=0.45) calculated by the electromagnetic method and 5.60 per cent (SD=0.77) by the videodensitometric method. Thus the mean difference was -1.15 per cent (SD=1.06).

Comparison of the electromagnetic and videodensitometric methods. The cerebral blood flow in absolute units (ml/min) was calculated in each of the 40 experiments from the videodensitometric ratio and the electromagnetic readings of the cardiac output according to

$$\frac{Q_C}{Q_A} \times (\text{electromagnetic cardiac output}) = \text{cerebral blood flow in ml/min}$$

where Q_C and Q_A are the videodensitometric flow in the cerebral artery and aorta respectively and

Video Flow

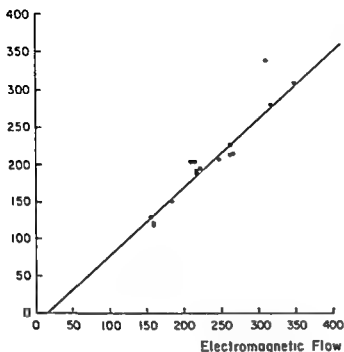


Fig 3 Correlation between simultaneously determined videodensitometric and electromagnetic blood flow (ml/min) for 40 measurements in cerebral arteries ($r=0.91$). The solid line is a least squares regression line

$\frac{Q_c}{Q_a}$ is the videodensitometric cerebral flow ratio

The cerebral flow in absolute units recorded by the videodensitometric and electromagnetic methods (Fig 3) displayed a good correlation ($r=0.91$)

Discussion

Present data indicate that about 17 per cent of the cardiac output in the resting state is devoted to the cerebral circulation (REINMUTH et coll 1965). In the present experiments the unilateral common carotid artery flow was estimated to be 6 per cent by the videodensitometric method. Taking into account both common carotid arteries and both vertebral arteries the figure seems to be within a reasonable range. However the aim was not to estimate the cerebral flow in a canine model but to compare the new videodensitometric method with a given standard the electromagnetic method. In the individual experiments the methods correlated well ($r=0.91$). Review of the data in Tables 1 and 2 shows that the videodensitometric values were significantly lower than the electromagnetic values. A similar difference between the methods was previously noticed regarding the renal blood flow (LINK et coll). The difference may reflect an error in extrapolation of

the dilution curve and the corresponding integrals of the videodensitometric areas. It could represent a consistent error in delivering the amount of contrast medium through the catheter. The accurate delivery of the desired amount of contrast medium depends on a completely filled catheter. Before each injection the catheter was flushed with contrast medium. A small washout at the tip of the catheter could occur between the time of catheter filling and the injection. A deficit from washout could represent a significant fraction of the 1 ml injection into the cerebral artery. Recirculation of contrast medium from veins and other brain vessels superimposed on the videodensitometric curve may be another cause of error. However if other vessels are included in the window the video image can be replayed and the window location changed to a more appropriate position. The effect of overlapping veins can also be avoided by a short arterial injection such that the arterial videodensitometric curve ends before venous recirculation begins.

Incomplete mixing of contrast medium and blood including layering might also be a source of error. The ascending aortic injection of contrast medium through the multi side hole pigtail catheter should give accurate mixing of blood and medium. With selective injection it is anticipated that incomplete mixing occurs. However it has been shown (LINK et coll) that perfect mixing does not seem to be of great importance as the videodensitometric method measures total contrast mass over an arterial cross section rather than local concentrations of contrast medium within the vessel. The injection rate should always be less than half of the arterial flow rate, preferably not more than a fourth of the flow in the ascending aorta and the cerebral artery. In the present experiments 1 ml of contrast medium was injected over a period of not less than two seconds (30 ml/min) in a flow which was usually 200 ml/min or greater.

In a clinical situation only one catheter with 4 side holes close to the tip will be used. After injection in the ascending aorta the catheter will be placed selectively into each main cerebral artery. After injection into the aorta it would be advisable to wait at least 5 to 10 min before the selective injection to avoid contrast effects upon the general circulation. Although no substantial change of the cerebral flow after ascending aortic injections was observed the issue has been disputed vigorously in the literature (TAVERAS & WOOD 1976). The effects

contrast medium after selective injection into the cerebral arteries can be neglected as they occur after the densitometric curves have been obtained over a main cerebral artery. However, when repeating the selective injections, the same rule of thumb should be applied, i.e. a time delay of at least 5 min. The effect of contrast medium on the cerebral circulation depends upon the chemical constituents of the compound. In the present experiments Conray 400 was used which is not approved for cerebral angiography in humans. Using a very low dose (1 ml) no complications occurred in the dogs despite the considerable accumulated dose over the entire experimental period.

It may thus be concluded that the videodensitometric method can be used as a simple clinical tool to evaluate the blood flow in the main cerebral arteries as a fraction of the cardiac output. It is especially convenient to perform in conjunction with routine clinical cerebral angiography as selective catheterization is a normal part of the radiologic procedure. The flow determination can be done in the interim between film series when the radiologist is waiting for the films to be processed. The measurements can be made in any angiographic suite with the aid of a densitometer and video cassette recorder.

ACKNOWLEDGEMENTS

The authors wish to express their sincere thanks to C.G.R. Medical Corporation for their support of a constant potential generator, to Mallinckrodt Inc. for supplying contrast medium, and to Steve Wilkins, M.S. and Jane Kendrick for generous technical assistance. The investigation was partly funded by the Medical School, University of California, Davis, U.S.A.

Request for reprints: Dr B. M. T. Lantz, Diagnostic Radiology, 4301 X Street, Sacramento, California 95817, U.S.A.

SUMMARY

Determination of blood flow in the cerebral arteries as a fraction of the cardiac output was performed by the videodensitometric method and compared to electromagnetic flow readings in dogs. The method proved to be highly accurate in vivo, confirming previous experiments in vitro. It is simple to perform during routine cerebral angiography and may produce significant physiologic data not readily available by other means.

REFERENCES

- CARR C J and FISHER K D. A study of new methods of measuring cerebral circulation. Life Sciences Research Office, Federation of American Societies for Experimental Biology, Bethesda, Maryland, 1970.
- HARPER A M. Measurement of cerebral blood flow by radioisotopes and its value in clinical practice. Practitioner 207 (1971) 291.
- JENNETT W H, HARPER A M and GILLESPIE F C. Measurement of regional cerebral blood flow during carotid ligation. Lancet II (1966) 1162.
- KETY S and SCHMIDT C F. The nitrous oxide method for the quantitative determination of cerebral blood flow in man: Theory, procedure and normal values. J. clin. Invest. 27 (1948) 476.
- LANTZ B M T. A methodologic investigation of roentgen videodensitometric measurement of relative flow. University of California Press, Davis, 1974.
- Relative flow measured by roentgen videodensitometry in hydrodynamic model. Acta radiol. Diagnosis 16 (1975) 503.
- LINK D P, FOERSTER J M and HOLCROFT J W. Angiographic determination of splanchnic blood flow. Acta radiol. Diagnosis 21 (1980) 3.
- LINK D P, LANTZ B M T, FOERSTER J M, HOLCROFT J W and REID M H. New videodensitometric method for measuring renal artery blood flow at routine arteriography. Validation in the canine model. Invest. Radiol. (1979) in press.
- MEYER J S and SHINOHARA Y. A method for measuring cerebral hemispheric blood flow and metabolism. Stroke 1 (1970) 419.
- OLDENDORF W H. Radioisotopic methods for cerebral blood flow determination. In: Radionuclide applications in neurology and neurosurgery, p. 27. Edited by Y. Wang and P. Paoletti. Charles C. Thomas, Springfield, Illinois, 1970.
- POSNER J B. Newer techniques of cerebral blood flow measurement. Stroke 3 (1972) 227.
- POTCHEN E J, DAVIS D O, WHARTON T, HILL R and TAVERAS J M. Regional cerebral blood flow in man. I. A study of the Xenon 133 washout method. Arch. Neurol. 20 (1969) 378.
- REINMUTH O M, SCHEINBERG P and BOURNE B. Total cerebral blood flow and metabolism. Arch. Neurol. 12 (1965) 49.
- TAVERAS J M and WOOD H H. Diagnostic neuro-radiology. Volume II. 3. cerebral angiography. Williams & Wilkins, Baltimore, 1976.
- TER POGOSIAN M M, EICHENJ G O, DAVIS D O and WELCH M J. The measure in vivo of regional cerebral oxygen utilization by means of oxyhemoglobin labeled with radioactive oxygen 15. J. Clin. Invest. 49 (1970) 381.

FROM THE DEPARTMENTS OF DIAGNOSTIC RADIOLOGY (DIRECTOR PROF. K. HOORNSTRA) AND THE CENTRAL RESEARCH LABORATORY (DIRECTOR H. A. BAK) ERASMUS UNIVERSITY, 3000 DR ROTTERDAM, THE NETHERLANDS

VIDEODENSITOMETRY FOR MEASURING BLOOD VESSEL DIAMETER

K. HOORNSTRA, J. M. H. HANSELMAN, W. P. J. HOLLAND
G. W. DE WEY, PETERS and A. W. ZWAMBORN

Determining the intensity of blood flow with the aid of videodensitometry by measuring the flow rate of a contrast medium introduced into the vessels is a well known method which is now made suitable for clinical application in this department. Knowledge of the cross sectional area of the blood vessel is needed for calculating the intensity of flow by this method. If the cross section of the vessel may be assumed to be round, the required area can be found by making a single measurement of the internal diameter. However, the accuracy with which the measurement is made has to meet high demands, since the square of the diameter value is involved in the flow calculation (LANTZ 1975).

Various intravascular sensors specially designed for determining the diameter of blood vessels have been described in the literature. One of them is based on the principle of electric impedance and measures the mean cross sectional area in the vessel (CONSTANTINESCO & MERLE 1977), while another operates on the electromagnetic induction principle (KOLIN & MACALPIN 1977).

The objection to these sensors is that they are invasive and as such expose the patient to extra stress. This objection is not so strong in the case of another category of methods for measuring diameter, with linear dimensions being measured on fluoroscopic images of blood vessels filled with contrast medium. These methods require only the routine insertion of a conventional catheter into the vessel for injecting a contrast medium. They are all the more attractive since they combine well with the determination of blood flow rates by videoden-

sitometry, after all a catheter is already located in the proper place.

Moreover, the fluoroscopic images made for measuring the blood flow rate can also be used for measuring the diameter, so that the quantity of contrast medium can be restricted. With the aid of simple instruments for measuring length, linear measurements on the fluoroscopic images can be performed directly on a TV monitor screen (RUTISHAUSER 1969), on a photograph of the image or on cinefluorographic films (HELLSTEN & PETTERSSON 1977). These methods do not, however, yield the degree of accuracy which is required.

A higher degree of accuracy can be obtained by TV fluoroscopy, with which dimensions can be measured electronically from the video signal (videometry). The diameter of the contrast filled blood vessels can then be determined videodensitometrically, employing a technique for measuring the pulse width in the horizontal TV lines.

On the basis of a single horizontal TV line, this method of measuring the video diameter was used by SILVERMAN (1971). GARDNER & WARNER (1967) described a system employing a special purpose diameter computer for measuring the pulse width in TV lines, an external general purpose digital computer being used for averaging the measured pulse width obtained from several lines.

The present report also describes a system for diameter measurement which is based on the application of videometry on fluoroscopic images.

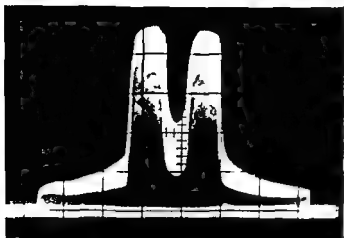


Fig 1 Photograph of a raw video signal. The densitometric pulse obtained from a single tube filled with contrast medium

produced after injection of contrast medium into a blood vessel. Use is made of a special video diameter computer instrumented with analog and digital elements. This computer has the following special features:

The densitometric pulse width in a TV line is measured on line with a half-depth width computing technique.

The mean measured pulse width is established from several TV lines as an internal operation and the optimum moment for diameter determination is found automatically.

In vitro experiments were carried out on a transparent plastic phantom fitted with cylindrical channels

and on plastic tubes of known diameter and set water flow to test the quality of this method of measuring diameter.

As a control of the practicability of the method, *vivo* trials were performed in the abdominal aorta of an experimental animal (dog). The values found were compared with the results obtained with an intra arterial diameter sensor (VAN DER SCHEE, BAKKER 1978).

Materials and Methods

The video diameter computer (VDC)

A series of figures are given to illustrate the operation of the computer. In Fig 1 an oscilloscopic image displaying the video signal ($5 \mu\text{s/div}$, 0.2 V/div) is illustrated.

All TV lines in an image are superimposed on the oscilloscopic image. The photograph was made at the moment contrast medium was present in a plastic tube. As the contrast medium passes, a momentary dip appears in the video signal (the artery of the tube is made darker by the contrast medium); the width at half the depth of the dip being a yardstick for the diameter.

The width at half the depth of the dip was chosen to ensure minimum disturbance from the noise contained in the video signal. A visible window in which the location and dimensions can be set is introduced into the video image with the window generator (Fig 2). The window is adjusted so that it encompasses

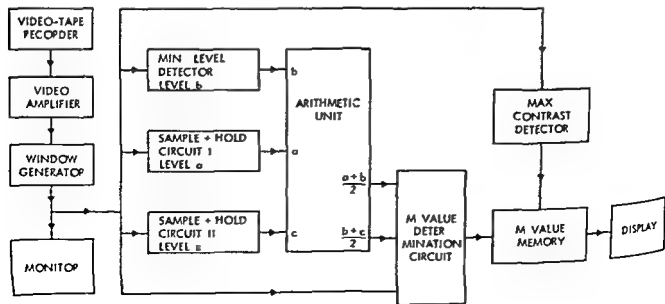


Fig 2 Block diagram of the video diameter computer (VDC)



Fig 3 Photograph of a TV monitor screen on which are displayed the image of a dog, a rectangular electronic window and the detected vessel wall during injection of contrast medium

measures the diameter of the artery or tube to be measured (Fig 3). The window generator allows only the video signal contained within the window to pass through to the measuring circuits.

Fig 4 is a diagram showing the video signal of one TV line within the window during the presence of contrast medium. The time axis is electronically divided into intervals of 30 ns. At the instant of the first window edge appearing, before the start of the dip in the video signal, sample and hold circuit I measures and holds the voltage of the video signal (value a in Fig 4). Next, the minimum voltage of the dip is detected and held by the minimum level detector (value b in Fig 4). Then, at the instant at which the last window edge appears, when the dip has gone from the video signal, sample and hold circuit II measures and holds the voltage of the video signal (value c in Fig 4). From these three values, the arithmetic unit (Fig 2) determines and holds the two threshold values $(a+b)/2$ and $(b+c)/2$. All these operations are completed before the next TV line begins.

When the next TV line appears, there is a pause until the video signal enclosed by the window has dropped below the stored threshold value $(a+b)/2$ (as determined in the preceding TV line). From that moment on, the number of 30 ns intervals is counted by an electronic counter in the M value determination circuit. Counting stops when the video signal enclosed by the window exceeds the threshold value $(b+c)/2$ stored in the preceding TV line.

When the value of the video signal drops below or rises above the threshold, this is indicated by a luminous spot in the video image, so that the detected blood vessel wall is visible in the window (Fig 3).

For each frame, all the lines lying within the set window are processed in this way. In the M value

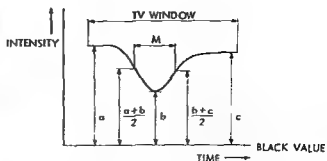


Fig 4 Diagram showing one TV line with the densitometric diameter pulse

determination circuit, the sum of the 30 ns intervals is found and divided by the number of lines, the width of which has been determined at the half depth of the dip. This results in a value M (the VDC value).

During the passage of the contrast medium, an appropriate detector determines the moment of maximum contrast, at which the value M is stored in a memory. The VDC value M may be read off from a three-digit display.

Measuring systems All the experiments were made with standard equipment (Pandoros Optimatic Roentgen generator, Siemens Bi 150/30/50 tube, Siemens Sirecon Duplex 25/17 HN image intensifier, Siemens TV chain with Plumbicon Koordinat Kombi diagnostic table, Siemens Elema).

The fluoroscopic images were recorded with a video tape recorder (IVC 801 psm). The contrast medium (Isopaque 440, Nyegaard & Co.) was injected with a flow-controlled angiographic injector (Medrad Mark III).

Photofluorography was performed with the aid of pulsed TV technique, using a constant tube potential of 68 kV and an average tube current of 5 mA. The focal spot was 0.6 mm. The electron-optic enlargement of the image intensifier was 170 mm. The focus-input screen distance was constant at 95 cm. The radiation beam was collimated down to a width of about 5 cm, measured in the object plane, to reduce scattered radiation. For each measurement, the tube current was adjusted to give a uniform level of luminescence on the output screen of the image intensifier for each experiment. The optimum white level in the video signal was adjusted with the aid of the iris diaphragm in the TV camera. Care was taken to ensure that the axes of the cylindrical channels of the phantom, the tubes and of the aorta were always projected perpendicularly to the lines in the TV image.



Fig. 5 Fluorographic image. Intra-arterial diameter sensor in situ in the aorta of a dog.

Static test A transparent plastic block (Perspex) was used (approx. 20 cm × 6 cm × 2 cm) into which eight cylindric channels (diameters 1.02, 2.03, 4.01, 6.03, 8.02, 10.03, 12.04 and 14.02 mm) had been drilled. The axes of the channels were arranged parallel in one plane. After the channels had been filled with contrast medium, the block was put into a tray filled with water and placed on the coordinate table. The columns of contrast medium were brought into the centre of the image one after the other by sliding the tabletop. One series of exposures of the columns of contrast medium was made with the block lying on the bottom of the tray and with 10 cm of water above it. The distance between the focal spot of the tube and the axis of a channel in the block was always 51 cm. A second series of exposures was made with the block raised by 10 cm, i.e. with 10 cm of water below it. Both series were repeated with a 50 per cent water-diluted solution of contrast medium in the channels.

Dynamic test In this test measurements were made with lengths of tubing of a flexible silicone plastic (Silastic, Dow Corning). The internal diameters were 1.39 ± 0.04 , 2.83 ± 0.06 , 4.80 ± 0.07 , 6.45 ± 0.05 , 7.9 ± 0.2 , 9.6 ± 0.1 and 15.4 ± 0.3 mm. The wide spread in some of these values is due to the fact that the tubing used was found to be not exactly round. One after the other the lengths of tubing were laid on the bottom of a water-filled tray which was placed on the coordinate table. Each turn was brought into a recirculation system and flushed through with a constant flow of water (adjustable and readable) from a thermostatically controlled (37°C) reservoir. The depth of water in the tray was 12 cm. The distance between the focal spot of the tube and the axis of each length of tubing was 51 cm. A straight 7 French multi-side hole closed-end catheter (Cook) was introduced into each length of tubing at the upstream end and pushed forward until its tip appeared in the image. Contrast medium was injected via this catheter.

Television images of the formation and movement of the resulting contrast boluses in the lengths of tubing were recorded on video tape. Injections were made into each length of tubing at three set values of the water flow velocity of $v = 10$, 20 and 40 cm/s. Per velocity contrast medium was injected in quantities of $q = 1$, 3 and 6 ml, the injection flow rate always being 17 ml/s. No injections of the maximum quantity of 6 ml were made into the four narrowest gauge tubes to avoid exceeding the 500 psi pressure limit set in the injector. The injections were repeated five times per setting.

In vivo experiment A dog weighing 20 kg was used for the in vivo experiments. The animal was kept without food for 12 hours before the examination given a general anaesthesia with Pentothal (thiopental) and then connected to a respiration unit. Next catheterization was performed in accordance with usual angiographic practice.

A 7 French pigtail catheter (Cook) was introduced into the right carotid artery and pushed through to the aorta until about 2 cm upstream of the bifurcation of the renal artery. The tip of the catheter and the abdominal part of the aorta located downstream of it (about 10 cm in length) were brought into the image. Upon injection of contrast medium, photofluorography of the resulting contrast boluses in movement was performed. Altogether 10 injections were made of 3 ml contrast medium each and at an injection flow rate of 17 ml/s. The interval between

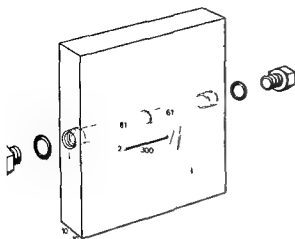


Fig 6

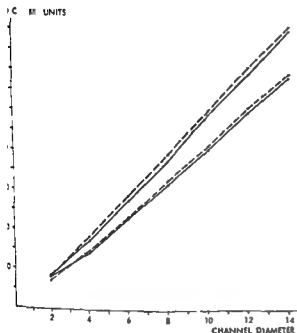


Fig 7

Fig 6 Transparent view of the calibration block (dimensions in cm)

Fig 7 Results of static tests. Relative diameters (in mm) determined by videodensitometry plotted against the internal diameters of cylindrical channels in a perspex block filled with contrast medium (100% — 50%) and for two distances from focal spot of tube to centre line of the channels (upper curves 51 cm lower curves 61 cm)

injections was at least 5 min. This had been found experimentally to be long enough for disturbing pharmacologic reactions of the injected contrast medium to subside before the following injection.

After the fifth injection the diameter measurements were controlled with the aid of the intra-arterial diameter sensor with resilient feelers (VAN DER SCHEE & DE BAKKER). Previously this sensor had been calibrated in the linear measuring range

from 6.5 to 8.5 mm with an accuracy of ± 0.5 per cent of the measured value.

The sensor was inserted into the femoral artery and pushed through to the visible section of the abdominal aorta (Fig 5). During these measurements the contrast medium catheter was temporarily slightly withdrawn to make room for the diameter sensor. Under fluoroscopic control the feelers were positioned in five locations in the aorta (corresponding to the positions of vertebrae L2/L3, L3/L4, L4/L5 and L5 respectively). At each location the diameter was measured with the sensor.

After completion of the last injection a calibration procedure was started in order to determine the absolute diameter values. First the scale of enlargement of the aorta was established. For this purpose the diameter sensor was removed and a special wire guide put in its place. One end of the wire guide was built up of sections of metal alternating with sections of polyethylene, each section was 20.0 mm long. Photosfluorography was performed on the end of the wire guide in the abdominal part of the aorta.

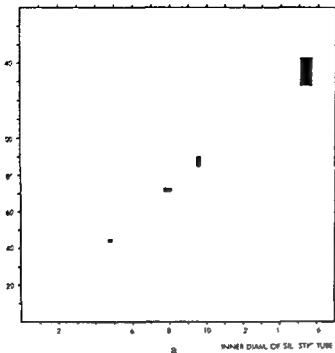
After the animal experiment was concluded the calibration procedure continued with the aid of a specially made transparent plastic calibration block (Fig 6). The block contained two calibration ducts of known diameter (61 mm and 81 mm respectively) filled with contrast medium as well as a piece of copper wire of known length (30.0 mm). After the block had been placed in a water-filled tray the latter was positioned on the coordinate table; the water level in the tray was 12 cm. The calibration ducts were positioned in the horizontal plane estimated to have been previously occupied by the abdominal aorta of the experimental animal.

Experiments were made of the block with the axes of the calibration ducts and the copper wire lying in the same horizontal plane. The ducts in the calibration block were filled with undiluted contrast medium corresponding to the state in the aorta of the experimental animal immediately after injection of the contrast medium.

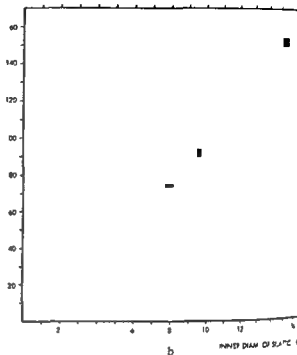
Results

The tapes of the video recordings were played back on the recorder connected to the video diameter computer. Before playback the window determining the diameter measurement site was projected onto a previously selected position in the TV image. The height of the window was set at 14 TV lines while the width was adjusted for each measurement.

D.C. M. UNITS



D.C. M. UNITS



D.C. M. UNITS

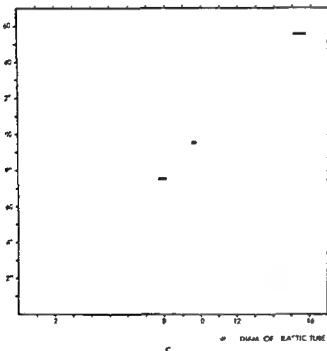


Fig. 8 Results of dynamic tests. Relative diameters determined by videodensitometry plotted against the internal diameter (mm) of silastic tubes for injections of a) 1, b) 3 or c) 6 ml contrast medium into water passing through the tubes in a steady flow (1 cm/s). The error is represented by a rectangle (the height is twice the standard deviation of the mean of repeated injections); the width is the uncertainty interval of the true diameter of a tube.

Static test. The window was positioned in the centre of the TV image on the image of the column of contrast medium. During playback (lasting about 4 min) 15 consecutive measurements of the column width were made with the VDC, thus producing a group of 15 VDC values per test. As a rule the maximum spread per group was \pm one VDC unit. The standard deviation in the group of the second narrowest column (diameter 2.03 mm) was greater

viz 4 units. As a result of insufficient contrast reliable measurements could be made from 11 images of the narrowest column (diameter 1.02 mm).

The results of the static test are plotted in Fig. 9. For the sake of clarity the mean values for each of the four series are joined by straight connecting line segments in the graph. The mean VDC values are a function of the concentration of the contrast medium in the channels, an inversely proportion-

Table 1

Results of dynamic tests. Mean and standard deviations ($n=5$) of the relative diameters of silastic tubes determined by videodensitometry with a steady flow of water through the tubes. Three ml of contrast medium were injected

Tube diameter (mm)	Mean water flow velocity					
	10 cm/s		20 cm/s		40 cm/s	
	M units	SD	M units	SD	M units	SD
8.3	75.6	0.5	25.4	1.1	25.6	0.5
6.3	45.4	0.5	45.4	0.5	45.6	0.5
4.5	61.6	0.5	62.2	0.5	61.4	0.7
3.9	73.7	0.5	74.1	0.5	72.9	0.5
3.6	90.0	0.9	97.3	1.9	97.7	0.5
3.4	151.0	3.0	151.0	2.0	151.0	4.0

rection of the focal spot distance and a linear function of the diameter of the channel—diameters over 3 mm

Dynamic test The window was moved into the centre of the TV-screen and placed over the image of the Silastic tube the true distance from the visible tip of the catheter was about 5 cm. During playback of the dynamic tests the instant of diameter measurement during passage of the bolus of contrast medium was automatically determined by the VDC value. The VDC value was obtained per test. The contrast of the images of the boluses in the narrowest tube (diameter 1.39 mm) was found to be insufficient for obtaining useful measuring results. VDC values based on five repeated experiments each (those carried out under identical circumstances) were combined and their mean values and standard deviations were determined.

The results of the dynamic tests are plotted in Fig 4 for the three quantities of contrast medium used ($q=1, 3$ and 6 ml) and one water flow velocity ($v=20$ cm/s). The graph shows the trend of the average of the measured VDC values declining and of the spread increasing as the amount of contrast medium employed decreases. This trend can be explained by the increasing chance of dilution of the contrast medium and incomplete formation of bolus under the circumstances referred to. The static test results indicate that dilution of contrast medium entails declining VDC values. Incomplete formation of bolus leads to inhomogeneous distribution of contrast medium over the cross section of the tube which in turn affects the proper functioning of the VDC.

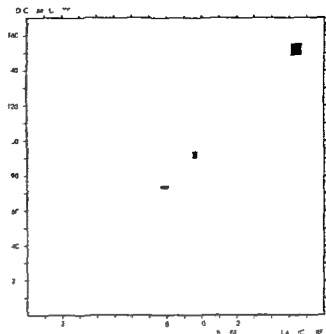


Fig 9 Results of dynamic tests. Relative diameters determined by videodensitometry plotted against the internal diameters (in mm) of silastic tubes after injection of 3 ml contrast medium into water passing through the tubes in a steady flow. Each point is the mean of 15 injections. 3 injections each at three values of water flow in the tubes (10, 20 and 40 cm/s). The error is represented by a rectangle: the height is twice the standard deviation, the width is the uncertainty interval of the true diameter of a tube.

Following the method described, an amount of 3 ml contrast medium per injection is adequate for measuring diameters up to a maximum of 8 mm in tubes through which water is flowing (Fig 8).

The results of diameter measurements for the three water flow velocities ($v=10, 20$ and 40 cm/s) and one quantity ($q=3$ ml) of injected contrast medium appear in Table 1. The table shows no correlation between the magnitude of the mean water velocity and the mean VDC value. Similar tables drawn up for $q=1$ and 6 ml (not included here) lead to the same conclusion.

The results of Table 1 are plotted in Fig 9 which is based on the mean values per group of 15 VDC values (relating to three settings of the water flow velocities and five repeated experiments per setting).

It is to be noted that the measured values in Fig 9 tally best with those in Fig 7 for a focal spot distance of 51 cm and a contrast medium concentration of 100 per cent. Thus the static and the dynamic tests produce essentially the same results. In practical terms the consequence of this agreement is that calibration procedures for *in vivo* experiments can be carried out with simple static test methods.

In vivo experiment The video tape with the 10 recordings of the 10 contrast medium injections into the aorta of the experimental animal was played back five times altogether. For each playback the window was shifted to another position along the image of the aorta on the monitor screen. The window positions chosen corresponded with the five lumbar vertebrae positions at which the check diameter measurements were made. Upon playback of each recording it was played back once again with the window position unchanged. Thus a group of 10×2 VDC values was obtained for each window position. These VDC values were calibrated with the aid of the experiments with the plastic calibration block and the wire guide. The VDC values M_{c1} and M_{c2} were measured on the images of the two contrast filled ducts in the calibration block with diameters D_{c1} and D_{c2} respectively. By linear interpolation a calibration relation was derived which relates the true diameter of the aorta D_a to the appearing VDC value M_a . It reads

$$D_a = (D_{c2} - D_{c1}) \frac{\delta M_a - M_{c1}}{M_{c2} - M_{c1}} + D_{c1}$$

in which $\delta = G_c/G_a$ is the ratio between the imaging scales G_c and G_a in the plane of the calibration block and the aorta respectively. The ratio δ was determined from the lengths of metal wire (length $L_m = 20.0$ mm) at the end of the wire guide in the aorta and of the length of copper wire (length $L_c = 30.0$ mm) in the calibration block.

N_a and N are the numbers of horizontal TV lines which intersect the images of one of the lengths of metal wire and of the length of copper wire respectively. Then $\delta = (N/L_c)/(N_a/L_a)$. Electronic counts on these images gave $N_a = 59$ and $N_c = 94$ from which it follows that $\delta = 1.062$.

Substitution of this value in the calibration relation and also of the known values $D_{c1} = 6.1$ mm and $D_{c2} = 8.1$ mm and of the measured VDC values $M_{c1} = 58$ and $M_{c2} = 79$ gives $D_a = 0.101 M_a + 0.576$. By means of this latter relation all VDC values (M) were converted into true diameter values in millimeters.

The aorta diameters obtained with the VDC (D_a) and with the intra arterial diameter sensor (D_i) on the five sites measured appear in Table 2.

Discussion

The results of diameter measurements in vivo in experiments with identical window position have a

Table 2

In vivo results Comparison of the diameters of the aorta measured with a calibrated videodensitometer (D_a) and with an intra arterial sensor (D_i). D is the standard deviation of the results in a repeated injections

Location	n	VDC (mm)		Diameter sensor (mm)	D (%)
		D	SD	D	
L7/L3	10	7.31	0.10	7.44 ± 0.10	0.14
L3/L4	20	7.19	0.23	7.24 ± 0.04	0.05
L4	20	6.85	0.18	7.19 ± 0.04	0.04
L4/L5	20	6.66	0.18	6.97 ± 0.04	0.04
L5	20	6.71	0.20	6.80 ± 0.04	0.05

standard deviation of approximately 0.2 mm irrespective of the selected window position (Table 2). This non reproducibility spread is the result of minor differences occurring in the course of contrast medium injection and the subsequent bolus formation and is also due to the mixing of quantum and electronic random noise in the image signal stemming from imaging system. Repetition of experiments will reduce the influence of the non reproducibility spread. If for example four experiments were to be repeated the standard deviation in the mean measured diameter value would be halved to 0.1 mm.

In addition systematic differences between the measured mean (VDC) diameter values D_a and the true (diameter control) diameter values D_c appear in Table 2. As the window position changes the amount of these differences fluctuates irregularly with an amplitude of 0.15 mm around an average of minus 0.2 mm. The explanation for the fluctuations about the average is a non homogeneous background in the form of organs and vertebrae which differs from one site to the other during exposure of the in vivo experiments. These background structures are superimposed on one another in the image; they influence the shape of the detected metric pulse of the image of the contrast filled blood vessel and thus cause errors in the result of the VDC diameter measurement.

Inaccurate calibration is the second source of systematic errors and is the result of employing a calibration relation lacking in precision. The latter in turn results from rounding off errors in the integrally measured values M , M_c , N , N_a (± 0.5 units) and from measuring errors in D_{c1} and D_{c2} (± 0.1 mm). The consequent error in the diameter determination can be calculated as maximum ± 0.20 mm.

an error propagation analysis applied to the dilution relation. The average difference of 0.20 mm referred to earlier can be explained (at least partially) by this inaccurate calibration. The aforementioned systematic errors due to the non homogeneous background (± 0.15 mm) and to inaccurate calibration (± 0.20 mm) add up to a total maximum systematic error to be expected in the diameter measurement of ± 0.35 mm (or approximately $\pm 5\%$ in the measured aorta diameter of 7 to 8 mm).

A method enabling a more accurate calibration to be made (not yet tested) consists of repeating the calibration procedure employed but with the calibration block or wire guide being shifted each time to a somewhat different distance between the tube and the image intensifier. By averaging all the calibration values obtained a kind of average calibration relation can then be produced which may be expected to result in a smaller calibration error.

The disturbing influence of the non homogeneous background will diminish when the volume of a certain section of a blood vessel is to be determined. For the purpose of determining the intensity of blood flow by videodensitometry. For the vessel volume determination several blood vessel diameters are measured at different points along the relevant section. The errors in the individual diameter values resulting from the non homogeneous background will then more or less average out so that the volume will be determined with a higher accuracy. This advantage directly benefits the videodensitometric dilution method in which a blood vessel volume (V) is needed to calculate the blood flow intensity (F) (from $F = V/\delta t$ where δt is a mean transit time).

Conclusion

The described videodensitometric method is suitable for measuring the internal diameters of contrast filled blood vessels in all those parts of the body where a catheter can be inserted. Additional conditions to be met for making absolute measurements are the following. It must be possible to replace the catheter temporarily by a special wire guide and the blood vessel must lie plane parallel with the image intensifier. Another condition is that the blood in the vessel at the measuring site is displaced by the injected contrast medium. For arteries of a diameter up to 8 mm the quantity required is 3 ml or less. As a rule four repeated injections (at intervals of about 5 min) are sufficient to achieve

satisfactory results. Taking the photofluorographic images as a basis and using the videodensitometric equipment in conjunction with the adjustable window diameters can be determined over a distance of at least 10 cm along the vessel as was found during measurements in the aorta of a dog (8 mm diameter). Thanks to the videorecording of the fluoroscopic images and the application of a special computer which operates both automatically and autonomously the diameter measurement is a rapid and simple procedure.

The range of measurement in which usable results were obtained (as established with *in vitro* tests) extends from 2 to 16 mm. The maximum systematic error that will occur under *in vivo* conditions is ± 0.35 mm, the standard deviation of the random error is 0.20 mm. These estimations of error are based on duplicate measurements made in the aorta of a dog (7 to 8 mm diameter) but they may also be applied to the extended measuring range from 4 to 8 mm. This is subject to the condition that the determinations are made under comparable circumstances such as the use of 3 ml contrast medium per injection of a window with 14 TV lines and of a calibration procedure as prescribed. The random error can be made arbitrarily small by repeating the experiments. It is anticipated that the maximum systematic error can be halved by adopting a suggested improved method of calibration. The error diminishes even further when the average diameter is determined over a certain length of a vessel (e.g. for calculating the volume of a vascular segment).

SUMMARY

A method employing a special computer for determining the internal diameters of blood vessels from photofluorographic images is described. *In vitro* and *in vivo* experiments are performed with the system. The amount of contrast medium injected is restricted to 4×3 ml and it is possible to determine the diameter (in the range from 2 to 16 mm) at any place where blood vessels can be catheterized. In the *in vivo* experiments the maximum systematic error is ± 5 per cent in the 7 to 8 mm range.

ACKNOWLEDGEMENTS

The authors wish to thank Mr and Mrs J. F. Fassotte for their valuable technical and radiologic advice and Mr H. van der Meulen and Mr B. C. Dirkzwager for their advice on technical aspects. They are also grateful to Mr E. J. van der Schee and Mr J. V. de Bakker for making the measurements and producing the results with the diameter sensor and to Mr T. Rysdijk for his photographic work.

REFERENCES

- CONSTANTINESCO A and MERLE M Continuous blood velocity and flow measurements by intravascular elutherm probe *Euro surg Res* 9 (1977) 12.
- GARDNER R. M. and WARNER H. R. Dynamic aortic diameter measurements *in vivo* *Comp Biomed Res* 1 (1967) 52.
- HELLSTEN S and PETTERSSON H Hydro- and hemodynamic effects of catheterization of vessels IV Catheterization in the dog. *Acta radiol Diagnost* 18 (1977) 17.
- KOLIN A and MACALPIN R. N. Induction angiometer *Blood vessels* 14 (1977) 1-1.
- LANTZ B Relative flow measured by radioactive densitometry in hydrodynamic model *Acta radiol Diagnost* 16 (1977) 503.
- REUTSCHAUER W *Kreislaufanalyse mittels Röntgenkymographie* Verlag Hans Huber Bern 1969.
- VAN DER SCHEE E J and DE BAKKER J A. In vivo measurement of the inner diameter of arteries *In Abstracts International Workshop on Biomed p 97* *Producers and Measurements Madrid 1978*.
- SILVERMAN N. R. Viduometry of blood vessels *Exlogn* 101 (1971) 597.

IDIOPATHIC HYPERTROPHIC SUBAORTIC STENOSIS

II The shallow left ventricular cavity

G KVAM

The left ventricular cavity in idiopathic hypertrophic subaortic stenosis (IHSS) is rather shallow (EPSTEIN et coll 1974). Previously (Part I B KVAM 1980) it was shown that the hypertrophic IHSS interventricular septum does not bend towards the right ventricle during the systolic contraction. As the septum does not shorten significantly neither lengthwise nor crosswise (Part I A) it was concluded that the septum acts as a suspender for the free ventricular wall during the systolic contraction. A larger percentage of the ventricular volume will thereby be ejected per per cent myocardial fibre shortening than ordinarily. This effect is more marked when the ventricular cavity is rather shallow in a direction at right angles to the septal plane. In the 60° right posterior oblique projection the direction of the radiation beam is approximately parallel to the average septal plane. If the ventricular cavity had a reduced depth it could be expected to appear shallow in this projection but this is not the case (Fig 1).

In the present report drawings of the ordinary diastolic 60° right posterior oblique outline and drawings made by a reduction method in the same projection as if the cavity was shallow are used in the biplane estimation of the end diastolic volume (EDV) according to the area length method. These two estimates of EDV are compared with a third method the EDV calculated from the systolic ejection fraction (EF) and the stroke volume (SV) measured by a dye dilution technique.

Materials and Methods

Biplane left ventricular cineangiographies at 75 frames per second from the same 4 IHSS and 15 control patients as in Part I were analysed.

The angiography was performed as follows: 40 to 45 ml Isopaque Coronar (370 mg I/ml Nyegaard Norway) were injected into the left ventricle using a pressure injector at 7 kg/cm² and a William Cook pigtail catheter French 8 with side holes within 2 to 3 seconds. In 2 of the patients with IHSS the injection time was slightly longer and in one who was given 30 ml 1.8 seconds.

The series were exposed in the 30° right anterior oblique (RAO) and 60° right posterior oblique (RPO) positions.

In 16 other patients biplane cineangiography was performed with an identical set up and with an identical catheter. In both projections a metal grid positioned at right angles to the central ray was then exposed with the same focus-object and object-film distance at the centre of the left ventricular cavity previously exposed. The catheter diameter on the film was measured in the aortic outflow tract when viewed under standard magnification. Some blurring particularly in the 60° PRO view made exact measuring difficult. However in both projections a linear correlation was found between the



Fig 1 The end diastolic frame in the 60° right posterior oblique projection from a patient with IHSS

catheter diameter and the enlargement factor of the grid when viewed with the same magnification. The linear correlation coefficient was 0.74 in the 30° RAO view and 0.54 in the 60° RPO view (with the tube lateral t value for the latter 2.37).

The frames from the IHSS and the control patients were viewed with the same standard magnification. The catheter was measured in the left ventricular outflow tract. From the relationship described, individual enlargement factors of the IHSS and the control films were calculated in both projections. Both in the IHSS and in the control group an end diastolic and a consecutive end systolic frame were identified as the one with the largest and smallest ventricular area respectively before contraction or dilatation could be seen. The ECG was not registered during the cardioangiography.

The end diastolic volume was determined according to the biplane area length method (DODGE 1971) although the ellipsoid formula was used directly without any correction.

In the IHSS group the 60° RPO area was also drawn according to a reduction method (dashed lines in Fig 2). The broken line was drawn across the valvar part of the cavity towards the dorsal part of the aortic root continuing the dorsal curvature of the apical part. When using this alternative area the volume was in all other respects calculated according to the same method as mentioned.

The ejection fraction was calculated according to

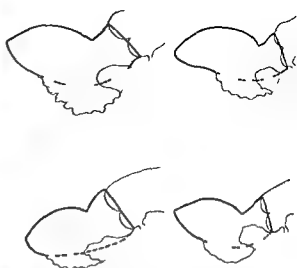


Fig 2 The 60° right posterior oblique outline of the left ventricular cavity from the 4 patients with IHSS drawn from the end diastolic cine frames. The heavy lines (dashed and solid) show the outline drawn for the 60° right posterior oblique area when the reduction method was applied.

the 30° RAO uniplane area length method using the midsagittal axes

$$EF = \frac{\frac{Ad}{Ld} - \frac{As}{Ls}}{\frac{Ad}{Ld}}$$

Ad , As , Ld and Ls are the diastolic and systolic areas and diastolic and systolic midsagittal lengths respectively directly as observed. The enlargement factor being eliminated in the formula.

The stroke volume was measured by a dye dilution technique (Stewart Hamilton) and the end diastolic volume of the left ventricle was then also calculated according to the SV/EF method.

Results

The different values for EDV are given in the Table. Individual values are given for the IHSS patients, the mean values, ranges of values and standard deviations for the control group.

In the IHSS group a paired t test shows that a significant methodologic difference exists between the ordinary biplane method and the SV/EF method for calculating EDV ($t=2.75$, $p<0.05$) but no difference between the reduction method and the SV/EF method for calculating EDV.

In the control group a paired t test shows that

Table

nd diastolic volume in the 4 patients with IHSS individual and mean values measured by an ordinary biplane method a biplane method according to the reduction method described and by a method implying dividing the stroke volume (estimated by a dye dilution technique) by the systolic ejection fraction. In the control group the volumes estimated by the first and the last of these methods are presented as mean values ranges of values and standard deviation

	End diastolic volume		
	Biplane method	Biplane reduction method	SV _e /EF method
IHSS group			
Individual values	170	130	110
	174	103	117
	139	114	115
	14	117	90
	144	116	109
Mean values			
control group			
Mean values	165		155
Ranges	13-177		87-277
Standard deviation	78		38

makes no difference whether EDV is measured according to the ordinary biplane method or according to the SV/EF method

Discussion

Among the present 4 IHSS patients an ordinary biplane volumetric calculation from the 30° RAO and the 60° RPO cine views overestimates EDV systematically

In the formula for the EDV calculation the area in the 30° RAO projection and the depth in the 60° RPO projection are used. The 60° RPO depth D is calculated according to the formula $D = 4A/\pi L$ where A is the area and L the greatest length in the 60° RPO projection. The depth is thus calculated from the formula of the ellipse. A significant indentation of a structure into the area not registered in the area measurement because of superimposition therefore causes a systematic overestimation of the overall depth and thus of the volume. The IHSS hypertrophic septum is such a structure.

CONN et coll (1966) reported an average EDV of 177 ml among 15 IHSS patients while their controls had an average EDV of 133 ml a difference between the means of about 8 per cent. They used a biplane angiographic method.

GOTSMAN & LEWIS (1974) reported an average EDV of 66 ml/m among 14 patients with IHSS and 70 ml/m among controls a difference between the means about 8 per cent. They used uniplane RAO for estimating the volume which presupposes a normal relationship between the 30° RAO width and the 60° RPO depth.

The present patients with IHSS had a mean EDV 11 to 12 per cent smaller than the controls when different ordinary area length methods were applied. When the reduction method was applied the difference was nearly 30 per cent.

Assuming that CONN et coll and GOTSMAN & LEWIS investigated patients with the same morphologic characteristics as the present patients they have overestimated the EDV in their IHSS groups.

Conclusion The IHSS left ventricular cavity is shallow even though it does not have this appearance in the 60° RPO projection. The EDV is overestimated in IHSS with ordinary angiographic volumetric methods because the influence of the hypertrophic bulging muscular interventricular septum is neglected.

SUMMARY

Using different volumetric methods for the estimation of the end diastolic volume in patients with idiopathic hypertrophic subaortic stenosis it is concluded that in this condition the left ventricular cavity is shallower than it appears in the 60° right posterior oblique projection and that ordinary cardioangiographic volumetric methods probably overestimate the end diastolic volume because of the septal bulge.

ACKNOWLEDGEMENTS

Professor Jan Gothlin kindly read and criticized the manuscript and Lars Mörkrid gave valuable assistance with the statistical evaluations.

REFERENCES

- CONN R D, BLACKMON J R, FIGLEY M M, PAULSON P S, KENNEDY J W. Quantitative left ventricular angiography in idiopathic hypertrophic subaortic stenosis. Clin Res 14 (1966) 123 (Abstract).
- DODGE H T. Determination of left ventricular volume and mass. Radiol Clin N Amer 9 (1971) 459.
- EPSTEIN S E, HENRY W L, CLARK C E, ROBERTS W C, MARON B J, FERRANS V J, REDWOOD D R and MORROW A G. Asymmetric septal hypertrophy. NIH Conference Ann intern Med 81 (1974) 650.

- GOTSMAN M. S. and LEWIS B. S. Left ventricular volumes and compliance in hypertrophic cardiomyopathy. *Chest* 66 (1974) 498.
- KVAM G. Idiopathic hypertrophic subaortic stenosis. I. Interventricular septum during the systolic contrac-

tion. A. The shortening of the muscular interventricular septum. B. Analysis of the protruding non-benign muscular interventricular septum. *Acta radiol* 21 (1980) 53.

ANGIOGRAPHY AND ULTRASOUND EXAMINATION IN THE EVALUATION OF PANCREATIC LESIONS

W KARP A LUNDERQUIST U TYLÉN and I IHSE

Until recently angiography of the pancreas was one of the first diagnostic procedures used when pancreatic abnormality was clinically suggested. However new methods such as ultrasound computer tomography and ERCP have been introduced and in order to find their proper place in the examination of pancreatic diseases these methods must be compared with those previously established. In this report ultrasound and angiography are compared in a group of patients examined with both methods.

Material and Methods

The experience is based on 380 examinations of the pancreas using gray scale ultrasound. Only patients in whom both ultrasound and angiography of the pancreas were performed within a period of one and a half year were included in the present series which consisted of 68 patients: 24 females and 44 males, 20 to 77 years of age. The clinical diagnosis was carcinoma in 23, chronic pancreatitis in 19, pseudocyst in 3 and insulinoma in one patient. The diagnosis of carcinoma and pseudocyst was confirmed by operation and microscopic examination. The insulinoma was also confirmed at operation. The diagnosis of chronic pancreatitis was based on clinical data supported by ERCP in 7 cases. In the remaining 22 patients examined in most cases because of abdominal pain, no clinical evidence of pancreatic disease was found on follow up of more than 6 months.

Ultrasound was usually performed before angiography. An ultrasound unit with gray scale and focused transducers of 13 and 19 mm diameter, 2.25 and 3.5 MHz was used. A standard technique of examination (SAMPLE et coll 1975, CARLSEN & FILLY 1976, DOUST & PEARCE 1976, WEILL et coll 1977) was employed including transversal longitudinal and oblique scans, sometimes with the transducer angled about 10° caudally or cranially in an effort to avoid bowel gas. Single pass technique was used. Examination of the tail of the pancreas through the left kidney was always made (GOLDSTEIN & KATRAGADA 1978).

The pancreatic area was located by anatomic landmarks, mainly the vascular structures. The results of the ultrasound examination were classified as normal when the pancreas was of normal size or when it could not be directly demonstrated despite optimum conditions. The pancreas was also considered normal if no mass could be demonstrated in this area (SAMPLE et coll, Di MAGNO et coll 1977). The examination was regarded as abnormal when the antero-posterior diameter of the gland was more than 3 cm and when echo abnormalities were observed. An attempt to make a specific diagnosis of carcinoma, pseudocyst or pancreatitis was also made. The criteria suggesting chronic pancreatitis were diffuse or local enlargement of the gland with



a

Fig 1 Male aged 67. Operation revealed chronic pancreatitis. a) Transverse b) longitudinal scan. Mass in head of pancreas (→)



b

with decreased echogenicity. Aorta (→) and A) Inferior vena cava (→)

scattering of the internal echoes which were usually of decreased intensity (Fig 1). Occasionally strong echoes associated with acoustic shadowing typical for calcification suggested the diagnosis of chronic pancreatitis. Pancreatic carcinoma was diagnosed in the presence of a solid mass which was indistinctly outlined and with few internal echoes (Fig 2). An echo free structure with more or less regular posterior wall was regarded as representing pancreatic pseudocyst (Fig 3).

Selective angiography was performed by simultaneous injection into the coeliac and superior mesenteric arteries including a series with vaso dilating agent in the superior mesenteric artery for better demonstration of the veins. Superselective examination was performed in 26 patients.

The results of the angiography were classified as normal or abnormal. A specific diagnosis of chronic pancreatitis, pseudocyst or carcinoma was at

tempted in all patients. The criteria for chronic pancreatitis were vascular alterations consisting of smooth regular arterial stenosis, irregularity and tortuosity of pancreatic arteries. The abnormalities in chronic pancreatitis were usually extensive while in carcinoma they were more localized. The vascular alterations suggesting pancreatic carcinoma consisted of encasement, irregularity of the arteries and presence of abnormal vessels. Involvement of the veins was regarded as specific neither for malignancy nor for chronic pancreatitis. The diagnosis of pseudocyst was based on displacement of the arteries due to an avascular expanding lesion.

Evaluation of the ultrasound and angiographic examinations was made independently by several experienced radiologists and the first conclusion was regarded as definitive. The results of both examinations were later correlated with the surgical findings or clinical follow up.

Table 1

Ultrasound in 62 patients (6 examinations unsatisfactory due to intestinal gas)

	No of cases	Correct diagnosis	Incorrect diagnosis	Accuracy (per cent)
Normal pancreas	11	18	—	100
Pancreatic carcinoma	27	15	7	68
Chronic pancreatitis	18	4	14	22
Pseudocyst	3	3	—	100
Insulinoma	1	—	1	—
Total	60	40	22	
		(66.5%)	(35.4%)	

One incorrectly considered as chronic pancreatitis

Two incorrectly considered as pancreatic carcinoma



a



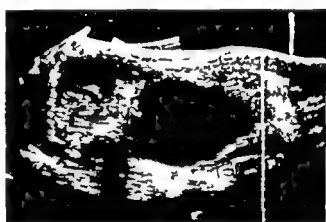
b

Fig. 2 Female aged 76 with carcinoma of the body of the pancreas. a) Transverse b) longitudinal scan. Mass in body of pan

creas (→) with alteration of the echoes (echo-intensity increased centrally in mass and decreased peripherally). Aorta (↔)



a



b

Fig. 3 Male aged 70 with pseudocyst in the head of the pancreas. a) Transverse b) longitudinal scan. Echo-free expansivity in head

and body of pancreas. Inferior vena cava is compressed (→) K=right kidney

Results

Six of the 68 ultrasound examinations were unsatisfactory because of the presence of too much intestinal gas. All of the angiographic examinations were satisfactory. The results of the ultrasound and angiographic examinations are summarized in Tables 1 and 2. Ultrasound had an overall diagnostic accuracy of 64.5 per cent and angiography 76.4 per cent.

In 15 of the 23 patients with pancreatic carcinoma the correct diagnosis was made by both methods (Fig. 4). In 2 patients the carcinoma was overlooked at both methods and in 5 cases the pancreas was reported normal on ultrasound but the tumour was correctly diagnosed on angiography. In one patient the ultrasound examination was unsatis-

factory due to bowel gas (pancreatic carcinoma found at angiography).

The size of the mass in the pancreas estimated at surgery ranged in cm from 2.5×2 to 7×4. Two carcinomas overlooked at ultrasound had diameters of about 7 cm, one of 4, one of 3, and two of about 2 cm. The one carcinoma incorrectly considered as chronic pancreatitis was 6 cm×4 cm. Two on angiography overlooked carcinomas had diameters of 3 cm and 2 cm respectively. In all patients but one the mass was located in the head or body and in one patient in body and tail.

The ultrasound and angiographic examinations were compared in 18 of the 19 patients with chronic pancreatitis. In one patient the ultrasound examination was unsatisfactory due to bowel gas. In 4 of the

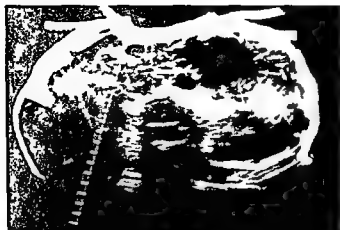


Fig 4a



Fig 5



Fig 4b

Fig 4 Female aged 76 with carcinoma of the body and tail of the pancreas. a) Transverse scan. Echo-free mass in the body and tail of pancreas (→). Aorta (↔). Inferior vena cava (≡). b) Selective simultaneous angiography of coeliac and superior mesenteric arteries. Slightly irregular lumen of hepatic and splenic arteries. Occlusion of middle part of splenic artery. Pathologic vessels adjacent to the occlusion. Collateral circulation in left gastric artery to the spleen.

Fig 5 Male aged 54 with chronic pancreatitis. Longitudinal scan. Echo-free mass in head of pancreas with strong echoes (++) and acoustic shadowing (→) due to calcifications. Punctate echo revealed cystic fluid collection.

patients correct diagnosis was made on ultrasound and in only one of these by both methods (Figs 5-6). In 3 of these 4 patients angiography failed to demonstrate any lesion. In 6 patients with correct angiographic diagnosis ultrasound failed to demonstrate any lesion in the pancreas. In 2 cases chronic pancreatitis erroneously was considered at both methods as pancreatic carcinoma. In 3 cases incorrectly diagnosed at angiography as pancreatic carcinoma ultrasound failed to demonstrate any lesion. In the remaining 3 patients pancreatic lesion was overlooked at both methods.

All 3 pseudocysts were correctly diagnosed on ultrasound and 2 on angiography. Angiography suggested chronic pancreatitis without pseudocyst formation in one instance.

Neither on ultrasound nor angiography was the insulinoma demonstrated.

All patients with a normal pancreas were diagnosed correctly with ultrasound as well as angiography. However cases erroneously considered as normal occurred with both methods. Thus the predictive value of a normal condition was at ultrasound 45 per cent and at angiography 57.9 per



Fig 6 Same case as in Fig 5 Selective simultaneous angiography of coeliac and superior mesenteric arteries a) A/P and b) oblique view Displacement of gastroduodenal artery and pan-

creatic arcs surrounding avascular expansivity Calcification in head of pancreas

ment The falsely normal findings were mainly due to false evaluation of chronic pancreatitis

Discussion

Previously it was generally agreed that a normal pancreas could not be demonstrated with ultrasound (FILLY & FREIMANIS 1970 BURGER & BLAUENSTEIN 1974 WALLS et coll 1975) However progress in ultrasound technology with the use of gray scale has made it possible to outline the pancreas

(DOUST & PEARCE HANCKE 1976 HABER et coll 1976 WEILL et coll)

The normal pancreas appears as an echo-producing structure with echoes similar to those of the liver These echoes can be slightly stronger than those of the liver depending on the kind of equipment used The pancreas is located in close anatomic relationship to the large abdominal vessels (LEOPOLD 1975 a b GHORASHI & RECTOR 1977) which are easily demonstrated by ultrasound (Fig 7) Nevertheless the normal pancreas is sometimes

Table 2
Angiography in 68 patients

	No of cases	Correct diagnosis	Incorrect diagnosis	Accuracy (per cent)
Normal pancreas	22	22	—	100
Pancreatic carcinoma	23	21	2	91
Chronic pancreatitis	19	7	12	36.8
Pseudocyst	3	2	1	66.6
Insulinoma	1	—	1	—
Total	68	5	16	
		(76.4%)	(23.5%)	

Five incorrectly considered as pancreatic carcinoma

One incorrectly considered as chronic pancreatitis without pseudocyst



Fig 7 Transverse scan through pancreatic area a) Male aged 78 b) male aged 43 L=liver Pancreas (→) Aorta (++) Superior mesenteric artery (++) Portal vein (→) Splenic vein (→)

difficult to demonstrate. The size and configuration of the left liver lobe are in this respect of great importance as the lobe can sometimes be used as sonic window (HANCKE). A great disadvantage is that ultrasound is greatly hampered by obesity and intestinal gas. Pharmacologic agents such as Simethicone have been tried to reduce the amount of gas (PEPPER & KEENE 1976 SOMMER et coll 1977). Filling of the stomach with water in an effort to displace the gas (KOBAYASHI 1971 CRADE et coll 1978) has been tried but all these attempts have been without great success. The best alternative seems to be to repeat the examination another day.

The echographic size of the normal pancreas is subject to discussion (HANCKE HABER et coll GARDFUR et coll 1976 WEILL et coll). Great individual variations exist with a tendency for the pancreas to be larger in young people (GHORASHI & RECTOR WEILL et coll). In this series the proposal was accepted that an antero-posterior diameter of more than 3 cm indicates abnormality (HANCKE WEILL et coll). WEILL (1978) has considered the mean thickness of the pancreatic head to be 17 mm (range 11 to 30 mm) body 10 mm (range 4 to 20 mm) and tail 17 mm (range 7 to 28 mm) on ultrasound. These findings are in accordance with results from dissection and computer tomography (HAERTEL & KRFFEL 1978). However it appears that measurements alone are of limited value because of great individual variations; other factors such as the appearance of the echoes and the outline of the organ are more important in the assessment of the findings.

Although 7 cases were missed the accuracy of ultrasound was higher in the diagnosis of carcinoma than of chronic pancreatitis. This also applies for

angiography (REUTER et coll 1969 TYLÉN & ARNESJÖ 1973 a). At angiography 91 per cent of carcinomas (106 of 116 patients) were identified and moreover gave information as to resectability (TYLÉN & ARNESJÖ 1973 b). With the exception of pseudocyst where ultrasound seems to be an ideal method angiography should therefore be the method of choice in the diagnosis of pancreatic disease. However demonstration of a normal pancreas with ultrasound is of great value. This fact makes the method suitable for the screening of patients with abdominal pain in whom pancreatic disease is less probable. Furthermore the method is non-invasive and without radiation risk.

Very small carcinomas may sometimes be defined at angiography through the demonstration of local encasement. Ultrasound mainly demonstrates lesions which deform the outline of the gland. Both carcinoma of the pancreas and chronic pancreatitis may enlarge the gland and if such enlargement is localized differentiation between the two diseases may be difficult (HANCKE LEVITT et coll 1978 MULLENS & SALEM 1978). In the present series both small and large carcinomas were missed the size per se seems therefore not to be important. Alterations of the echo appearances may also be of help (LLOPOLD HUSBAND et coll 1977 WOOD et coll 1976).

The echo appearance of the gland loses the normal homogeneity in carcinoma of the pancreas increase as well as decrease in echo intensity may occur in comparison with normal pancreatic echoes. However increase was rare in the present series. This observation agrees with that of JOHNSON & MACK (1978) who claim that an increase in echo-intensity supports the diagnosis of chronic pancreatitis.

in an atrophic gland. The presence of calcifications in pseudocysts which often accompany chronic pancreatitis can also be of value for establishing the correct diagnosis. Secondary abnormalities such as dilatation of the biliary ducts, hepatic metastases and ascites can be diagnosed with ultrasound and can also contribute to the differentiation.

A pseudocyst which often appears as an echo free structure may have scattered echoes inside due to pus. Such a pseudocyst may be overlooked if smaller than 2 cm. SOKOLOFF et coll (1974) have reported that it may be difficult to differentiate acute pancreatitis from a pseudocyst because the pancreas may appear as an echo free structure due to oedema. However generally the diagnosis of pseudocyst is easy and accurate. An 87.5 per cent accuracy in the diagnosis of uncomplicated pseudocyst was found by KRESSEL et coll (1978).

Similar differential diagnostic difficulties are well known in all other methods employed in the diagnosis of pancreatic disease. A specific diagnosis can only be suggested after demonstration of a pathologic condition in the pancreas. It should be confirmed by percutaneous fine needle biopsy guided by the ultrasound finding (ISAACSON et coll 1974, SMITH et coll 1975, HANCKE et coll 1975). The success rate of fine needle biopsy guided by ultrasound is 70 per cent according to HANCKE et coll and 61 per cent according to TRILLER et coll (1978). The success rate of biopsy guided by angiography varies from 60 to 75 per cent (OSCARSON et coll 1972, TYLEN et coll 1976, CLOUSE et coll 1977, EVANDER et coll 1978).

The reported accuracy of ultrasound in the diagnosis of pancreatic disease varies from 73 to 91 per cent (FILLY & FREIMANIS HAAGA et coll 1976, 1976, HANCKE et coll). The accuracy in the present series was 64.5 per cent if unsatisfactory examinations are eliminated. This is to be compared with an accuracy rate of 76.4 per cent with angiography. However recent developments in ultrasound imaging techniques have improved the diagnostic results. BRAGANZA et coll (1978) presented material with a low rate of erroneous normal and pathologic ultrasound results in examination of pancreatic lesions and concluded that this method is valuable in screening when pancreatic disease is suggested.

Ultrasound is a valuable and simple screening method to be used in pancreatic disease. Computer tomography if available is an important complementary method (HAAGA et coll 1977, GO &

SCHEEDY 1978, KRESSEL et coll). Angiography will be used mainly to predict prognosis and operability in selected cases (FRENNY & BALL 1978). The diagnosis of chronic pancreatitis is still difficult with these methods as well as with angiography. ERCP must therefore be regarded as an important additional method in patients with possible pancreatic disease (WOOD et coll 1976).

SUMMARY

Ultrasound and angiography of the pancreas were performed in 68 patients. Ultrasound reached an accuracy of 64.5 per cent and angiography 76.4 per cent. Both methods excluded disease of the gland in all patients without clinical evidence of disease at follow up. Both methods had higher accuracy in the diagnosis of carcinoma than of pancreatitis. Although angiography has higher accuracy ultrasound is recommended for screening of patients with abdominal pain. Because of the differential diagnostic difficulties percutaneous fine needle biopsy is recommended when a pancreatic lesion is demonstrated. Angiography is used mainly to predict operability and prognosis.

REFERENCES

- BRAGANZA J M, FAWCITT R A, FORBES W, ST C, ISHERWOOD I, RUSSEL J G B, PRESCOTT M, TESTA H J, TORRANCE H B and HOWAT H T. A clinical evaluation of isotope scanning, ultrasonography and computed tomography in pancreatic disease. *Clin Radiol* 29 (1978) 639.
- BURGER J and BLACENSTEIN U W. Current aspects of ultrasonic scanning of the pancreas. *Amer J Roentgenol* 122 (1974) 406.
- CARLSEN F N and FILLY R A. Newer ultrasonographic anatomy in the upper abdomen. I. The portal and hepatic venous anatomy. *J clin Ultrasound* 4 (1976) 85.
- CLOUSE M E, GREIG J A, McDONALD D G and LEGG M A. Percutaneous fine needle aspiration biopsy of the pancreatic carcinoma. *Gastrointest Radiol* 2 (1977) 67.
- GRADE M, TAYLOR K J W and ROSENFELD A T. Water distension of the gut in the evaluation of the pancreas by ultrasound. *Amer J Roentgenol* 131 (1978) 348.
- DI MAGNO E P, MALAGELADA J M, TAYLOR W F and GO V L W. A prospective comparison of current diagnostic tests for pancreatic cancer. *New Engl J Med* 297 (1977) 737.
- DOLST B D and PEARCE J D. Gray scale ultrasonic properties of the normal and inflamed pancreas. *Radiology* 120 (1976) 653.
- EVANDER A, ISE I, LUNDEQUIST A, TYLEN U and AKERMAN M. Percutaneous cytodiagnosis of carcinoma of the pancreas and bile duct. *Ann Surg* 188 (1978) 90.
- FILLY R A and FREIMANIS A K. Echographic diagnosis of pancreatic lesions. *Radiology* 96 (1970) 575.

- FREENY P C and BALL T J Evaluation of endoscopic retrograde cholangiopancreatography and angiography in the diagnosis of pancreatic carcinoma *Amer Roentgenol* 130 (1978) 683
- GARDEUR D LAVAL JEANTET P TABOURY J MONNIER J P et BIGOT J M Anatomie échographique du pancréas normal *J Radiol Electrol* 57 (1976) 149
- GHORASHI B and RECTOR W R Gray scale sonographic anatomy of the pancreas *J clin Ultrasound* 5 (1977) 25
- GO V L W and SCHEEDY P F Ultrasonography computed tomography endoscopic retrograde cholangiography and angiography in the diagnosis of pancreas cancer *Med Clin N Amer* 62 (1978) 129
- GOLDSTEIN H M and KATRAGADA C S Prone view ultrasonography for pancreatic tail neoplasms *Amer J Roentgenol* 131 (1978) 231
- HAAGA J E ALFIDRI R J ZELCH M G MEANEY T F BOLLER M GONZALES L and JELDEN G L Computer tomography of the pancreas *Radiology* 120 (1976) 589
- — HAVRILLAA T R TUBBS R GONZALES L MEANEY T F and CORSI M A Definitive role of CT scanning of pancreas *Radiology* 124 (1977) 723
- HABER K FREIMANIS A K and ASHER W M Demonstration with gray scale echography *Amer J Roentgenol* 126 (1976) 624
- HAERTEL M und KREEL L Das normale Pankreas im computersierten Tomogramm *Fortschr Röntgenstr* 129 (1978) 1
- HÄNCKE S Ultrasonic scanning of the pancreas *J clin Ultrasound* 4 (1976) 223
- HOLM H H and KOCH F Ultrasonically guided percutaneous fine needle biopsy of the pancreas *Surg Gynec Obstet* 140 (1975) 361
- HUSBAND J E MEIRE H B and KREEL L Comparison of ultrasound and computer assisted tomography in pancreatic diagnosis *Brit J Radiol* 5 (1977) 855
- ISAACSON R WEILAND L H and MCILRATH D C Biopsy of the pancreas *Arch Surg* 109 (1974) 227
- JOHNSON M L and MACK L A Ultrasonic evaluation of the pancreas *Gastrointest Radiol* 3 (1978) 257
- KOBAYASHI N Diagnosis of pancreatic diseases by ultrasound *Med Ultrasonics* 9 (1971) 1
- KRESSSEL H Y MARGULIS A R GOODING G W FILLY R A MOSS A A and KROBOKIN M CT scanning and ultrasound in the evaluation of pancreatic pseudocyst A preliminary report *Radiology* 126 (1978) 153
- LEOPOLD G (a) Echographic study of the pancreas *J Amer Med Ass* 232 (1975) 287
- (b) Gray scale ultrasonic angiography of the upper abdomen *Radiology* 117 (1975) 665
- LEVITT R G GEISSE G G SAGELS S STANLEY R J EVANS R B KOEHLER R E and JOST R G Complementary use of ultrasound and computed tomography in studies of the pancreas and kidney *Radiology* 126 (1978) 149
- MULLENS J E and SALEM S Diagnostic tools in the management of chronic pancreatitis *Canad J Surg* 1 (1978) 60
- OSCARSON J STORMBY N and SUNDGREN R Selective angiography in fine needle aspiration cytodiagnosis of gastric and pancreatic tumours *Acta radiol Diagnost* 12 (1972) 737
- PEPPER H W and KEENE J Use of Simethicone in abdominal echotomography *Ultrasound in Med* 1 (1976) 197
- REUTER S E REDMAN H C and JOSEPH R B Angiographic findings in pancreatitis *Amer J Roentgenol* 107 (1969) 56
- SAMPLE W F PO J B GRAY R K and CAHILL P J Gray scale ultrasonography *Appl Radiol* 4 (1976) 63
- SMITH E H BARTRUM R J CHANG Y C DORSI C J LOKICH J ABBRUZZESE A and DANTONO J Percutaneous aspiration biopsy of the pancreas under ultrasonic guidance *New Engl J Med* 297 (1977) 82
- SOKOLOFF S GOSINK H B LEOPOLD G R and FRY SYTHE J R Pitfalls in the echographic evaluation of pancreatic disease *J clin Ultrasound* 2 (1974) 371
- SOMMER G FILLY R A and LAING F C Use of Simethicone as a patient preparation for abdominal sonography *Radiology* 125 (1977) 219
- TRILLER J ZAUNBAUER W FUCHS W A und GRETTLER L A Die ultraschallgezielte perkutane Feinnadelaspirationsspunktion beim Pankreaskarzinom *Fortschr Röntgenstr* 129 (1978) 695
- TYLÉN U and ARNESJÖ B (a) Angiographic diagnosis of inflammatory disease of the pancreas *Acta radiol Diagnost* 14 (1973) 215
- (b) Resectability and prognosis of carcinoma of the pancreas evaluated by angiography *Scand J Gastroenterol* 8 (1973) 691
- LINDBERG L G and LUNDERQUIST A Percutaneous biopsy of carcinoma of the pancreas guided by angiography *Surg Gynec Obstet* 142 (1976) 737
- WALLS W J GONZALES G MARTIN N L and TEMPLETON A W B scan ultrasound evaluation of the pancreas *Radiology* 114 (1975) 127
- WEILL F S Ultrasonography of digestive disease C V Mosby St Louis 1978
- SCHRAUB A EISENSCHER A and BOURGOIN A Ultrasonography of the normal pancreas Success and criteria for normality *Radiology* 123 (1977) 417
- WOOD R A B MOOSSA A R BLACKSTONE M O BOWIE J COLLINS P and LU C T Comparison of the value of four methods of investigating the pancreas *Surgery* 80 (1976) 518

SELECTIVE VEIN CATHETERIZATION FOR HORMONE ASSAY IN ENDOCRINE TUMOURS OF THE PANCREAS

Technique and results

W REICHARDT and S INGEMANSSON

The morphology of the pancreas can be examined using different techniques such as scintigraphy ultrasound computer tomography angiography and cholecystography. Active endocrine tumours are often too small to be detected with most of these methods. Successful localization of insulinomas by computer tomography has been reported in a few cases (FRICKF *et coll* 1978). Best results of the imaging techniques are obtained with angiography. The reported accuracy varies widely between 20 and 100 per cent (BOOKSTEIN & OBERMAN 1966 BOJSEN & SAMUELSSON 1970 SKJOLDBORG & MADSEN 1971 FUJII *et coll* 1974). The majority of authors account for about 80 per cent positive angiographic diagnosis in patients with proved insulinomas. However GRAY *et coll* (1970) pointed out that the angiographic accuracy in series comparing positive and negative findings was 63 per cent.

Selective vein catheterization with hormone assay is since long used for diagnosis and localization of parathyroid and adrenal tumours. The percutaneous transhepatic approach to the portal vein (WIECHEL 1971) made an extensive selective catheterization of the pancreatic veins feasible (LUNDERQUIST & TY LÉN 1975). It has been demonstrated that localization of insulin glucagon gastrin and serotonin producing tumours of the pancreas by arteriovenous hormone gradients is possible (INGEMANSSON 1977). The method has proven to be sensible enough to locate microscopic lesions as islet cell hyperplasia (INGEMANSSON *et coll* 1977). The present report summarizes the pertinent anatomy of the pancreatic

veins describes the technique of selective catheterization and accounts for the results.

As the venous anatomy of the pancreas has been described in detail previously (REICHARDT & CAMERON 1980) only a short summary is given here (Fig 1).

The venous drainage of the pancreas is varying. Most constant is the venous anatomy of the head of the pancreas. The anterior superior pancreaticoduodenal vein is draining the ventral part of the head joining the gastroduodenal trunk which is ending in the superior mesenteric vein. The dorsum of the head is drained by the posterior superior pancreaticoduodenal vein which empties into the dorsolateral aspect of the portal vein. The post sup vein may be double or even triple. In these instances one of these veins may drain a ventrocranial part of the head of the pancreas. The veins of the uncinate process are ventrally connected in an anterior inferior pancreaticoduodenal vein and dorsally in a posterior inferior pancreaticoduodenal vein. Both end into the superior mesenteric or the first jejunal vein. Often a ventral and a dorsal arcade are running in the pancreaticoduodenal sulcus along the duodenal loop connecting the main veins of the head.

The body of the pancreas is often drained by a transverse pancreatic vein ending in the inferior mesenteric superior mesenteric or splenic vein. Furthermore small branches can join the coronary vein or end in the post sup vein. Veins of the body

may even drain directly into the splenic vein as the veins of the tail of the pancreas. Sometimes a vein of the distal part of the tail ends in a lower polar vein of the spleen.

Material

From January 1974 until November 1978 45 triple catheterizations of the pancreatic veins were performed in 32 patients: 17 females and 15 males, aged 23 to 70 years. Fourteen patients were examined in order to locate clinically and laboratory confirmed endocrine tumours of the pancreas (7 patients with hyperinsulinism, 4 patients with Zollinger-Ellison syndrome, 3 patients with glucagonoma syndrome). Thirteen examinations were performed postoperatively to confirm surgical radicality or to locate recurrences. In 11 patients catheterization was employed to diagnose and locate or to exclude endocrine tumours when clinical symptoms suggested this diagnosis but laboratory findings were non-conclusive.

Methods

Catheterization technique

Percutaneous transhepatic puncture of the portal vein was performed according to the technique introduced by WIECHEL and described in detail previously (GÖTHLIN et al 1974; HOEVELS et al 1978). Using a 25 cm long needle (Surgimed, Denmark) coated with a polyethylene catheter (OD 1.6 mm, ID 1.0 mm) the puncture was performed in the right midaxillary line towards the hilum of the liver. The needle was withdrawn and the catheter slowly pulled back until blood could be aspirated without resistance. After injection of a small amount of contrast medium during fluoroscopy to assure the correct position in a portal vein branch, a guide wire with soft tip was manipulated into the portal vein. The catheter was then pushed over the guide wire into the same position.

A cranially directed puncture was avoided as a sharp intrahepatic angle of the catheter would be the result and the further catheterization procedures would be difficult. A puncture directed in a right angle to the spine or slightly caudally was preferred. The latter was often practicable in elderly patients without risk to hurt the lung.

All catheterizations were performed using a 0.9 mm guide wire (Surgimed, Denmark) with a soft tip

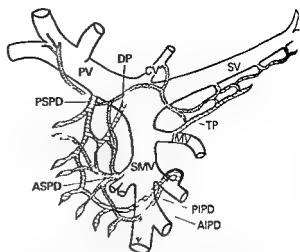


Fig. 1 Venous anatomy of the pancreas: schematic. PV = portal vein, SV = splenic vein, SMV = superior mesenteric vein, IMV = inferior mesenteric vein, PSPD = posterior superior pancreaticoduodenal vein, ASPD = anterior superior pancreaticoduodenal vein, PIPD = posterior inferior pancreaticoduodenal vein, AIPD = anterior inferior pancreaticoduodenal vein, TP = transverse pancreatic vein, DP = dorsal pancreatic vein, CV = coronary vein. The dotted veins are posterior to the pancreas, the striped veins anterior to the pancreas.

but stiff enough to be formed by hand according to the desired course of the catheter. This guide wire was also stiff enough to allow the catheter to be pushed over it without leaving its position in a portal vein tributary. Catheterization procedures with the catheter alone were strictly avoided as they could result in injury to the vessel wall and subsequent extravasation of contrast medium. For the same reason the catheter should not be allowed to advance beyond the tip of the guide wire.

A series of 16 films was exposed (5 films/4 s, 8 films/4 s, 3 films/6 s) after injection of 40 ml of Isopaque Coronar 370 mg I/ml (Nyegaard, Norway) at a rate of 8 ml/s into the superior mesenteric vein or splenic vein to document the position of the main tributaries of the portal vein and to examine the parenchyma of the liver.

Selective catheterization of the pancreatic veins was started with a main vein of the head, the posterior or the anterior superior pancreaticoduodenal vein.

A 2 cm long curve of the tip of the guide wire (Fig. 2a) was as a rule usable to enter the post-superior mesenteric vein which could be found in the dorsocaudal wall of the portal vein within 2.5 cm from the confluence of the superior mesenteric and splenic vein (in the following text called confluence). After successful manipulation of the guide wire into the post-superior mesenteric vein the catheter was pushed over it.



Various shapes of guide wires used for selective catheterization of a) post sup vein b) ant sup vein c) transverse pancreatic vein d) veins of the tail e) Shape of catheter tip for catheterization of veins of the tail side hole close to the

During fluoroscopy a small amount of contrast medium was injected to assure a correct position of the catheter. After having emptied the contrast medium out of the catheter a blood sample could be withdrawn.

A phlebography was performed to document the place of blood sampling and to chart the venous anatomy. Into a post sup pancreaticoduodenal vein of normal caliber about 6 to 8 ml of contrast medium was injected by hand. Eight films were exposed 2 films/s. In general several adjacent veins of the head of the pancreas and the inflow of the ant sup and infior veins into the main tributaries of the portal vein system were demonstrated on these films (Fig. 3). Knowing the topography of the veins an adequate shape of the guide wire could be formed and catheterization was facilitated. Catheterization of the ant sup vein demanded in general an almost circular shape of the tip of the guide wire with a diameter of about 3 to 4 cm (Fig. 2b).

The transverse pancreatic vein was searched for in the left lateral wall of the superior mesenteric vein near the confluence in the left lateral wall of the inferior mesenteric vein or caudally in the splenic vein near the confluence. An example of a usable shape of the guide wire for catheterization of this vein appears in Fig. 2c.

The main veins of the body were often demonstrated when contrast medium was injected into a pancreatic vein draining to the splenic vein. Thus knowing their course selective catheterization of these veins could usually be made (Fig. 4).

The veins of the tail of the pancreas usually can be entered in the ventrocaudal circumference of the splenic vein using a 1 to 1.5 cm long curve at the tip of the guide wire (Fig. 2d). Sometimes the guide wire slips out of the vein when the catheter is pushed over it. In these instances it can be helpful to preshape the catheter with an about 1 cm long curve (Fig. 2e). For catheterization of the veins of the tail the 25 cm long catheter as a rule had to be replaced by a 40 cm long one. In corpulent patients some times even catheterization of the ant sup pancreaticoduodenal vein demanded the longer catheter.

Blood sampling and injection of contrast medium in small pancreatic veins was facilitated by a side hole close to the tip (Fig. 2e).

The amount of contrast medium used for filling of the veins of the body and tail depended on the size of the vessels and varied between 2 and 8 ml. All injections were made by hand.

Blood sampling technique

After 10 to 12 hours of fasting catheterization of the coeliac artery, hepatic veins and portal vein was performed.

Samples were taken from all 3 catheters at the beginning and the end of the examination some times even once more during the catheterization procedure. In the portal vein system samples were withdrawn at 2 or 3 levels of the splenic superior mesenteric and portal veins.

Selective catheterization of the post and ant superior pancreaticoduodenal vein and the transverse pancreatic or corresponding vein of the body and one or two veins of the tail was always aimed at. At the beginning when the knowledge of pancreatic vein topography was limited the success rate of selective catheterization was about 2 veins per examination. Later examinations comprised 4 to 6 selectively catheterized pancreatic veins. In smaller



a



b



c



d

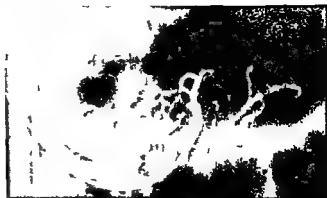
Fig 3 Stepwise selective catheterization in a patient with unusual anatomy a) Injection into post sup vein Via collaterals filling of ant sup vein which drains to the right branch of a double sup mesenteric vein Ant inf vein (→) Post inf vein (→) ending in the left branch of the double sup mesenteric vein (→) b) Injection into ant sup vein Via collaterals filling of post

sup vein and veins of hepatoduodenal ligament c) Injection into post sup vein the catheter more caudally directed Gastroduodenal vein (→) vein to the right colon (→) and ant inf vein (→) filled d) Injection into ant inf vein Filling of ant sup (→) post inf (→) veins



a

Fig 4 Same case as in Fig 3 a) Injection into a vein of the tail draining to splenic vein. Inflow of a vein of the body (→) b) Injection into this vein of the body results in filling of other veins



b

of the body which have an unusual location cranial to the confluence. Veins of the body are draining in the cranial circumference of the region of the confluence.

pancreatic veins blood samples could not be withdrawn but were obtained by dripping. From the portal vein system 8 to 30 blood samples were taken for hormone assay.

Angiography

In all cases an examination including simultaneous coeliac and superior mesenteric artery injection superselective injections of the gastroduodenal or common hepatic artery and splenic artery were aimed at but performed only in 14. In one of these even the dorsal pancreatic artery was examined. In 13 patients the coeliac, superior mesenteric and either gastroduodenal or splenic or inferior pancreaticoduodenal artery was injected. In 5 patients only coeliac and superior mesenteric angiography was obtained due to anatomic conditions or morphologic abnormalities such as coeliac artery stenosis which made more selective catheterization impossible.

Radioimmunologic techniques

Blood samples for radioimmunoassay of gastrin, vasoactive intestinal polypeptide and insulin were collected, centrifuged and sera were stored at -20°C until assayed. Blood samples for radioimmunoassay of glucagon and somatostatin were collected in tubes containing trasylol and heparin (for references see INGEMANSSON).

Surgery

At exploratory laparotomy the pancreas was palpated and inspected carefully. Dissection was performed in a way that the pancreatic veins could be identified and compared to the phlebographic findings. Resections of the pancreas were performed

according to angiographic findings, the venous and phlebographic anatomy as well as the arteriovenous hormone differences.

Tissue analysis. Tissue specimens obtained at surgery were processed for immunocytochemistry (for references see INGEMANSSON).

Results

Angiography

Two of 5 insulin producing tumours were correctly demonstrated at angiography. In one case a hypervascular lesion 1 cm in diameter in the body and furthermore a hypervascular lesion in the hilum of the spleen were found. The latter was correctly considered as an accessory spleen. In the other case a hypervascular lesion adjacent to an avascular expanding lesion with a diameter of 10 cm was found. The latter turned out to be a cyst. No angiographic abnormality was found in 3 patients with insulinomas and in 2 patients with B-cell hyperplasia.

In 3 patients with multiple gastrin producing tumours angiography revealed one tumour (1.5 cm \times 2.5 cm) in one patient, two 6 mm large tumours in the second patient and was suggestive of further two 3 mm large tumours. No abnormality was found in the third patient. In the fourth patient with Zollinger-Ellison syndrome a 1.5 cm hypervascular lesion was demonstrated in the body of the pancreas. The patient refused surgery and thus the tumour is not confirmed.

In 3 patients with glucagonoma syndrome the tumours were located by angiography in 2. The size of the tumours was 5 cm and 4 cm respectively in the

third patient a hypervascular lesion 6 mm in diameter in the head of the pancreas was found retrospectively (Fig 5)

In one patient with a 9 year history of diarrhoea a hypervascular tumour 6 cm in diameter was demonstrated in the head of the pancreas. This tumour contained and released somatostatin.

In one patient with heredity for multiple endocrine adenomatosis and previously operated upon for parathyroid adenoma a hypervascular tumour 2 cm in diameter was demonstrated. At surgery this tumour and an additional tumour 4 mm in diameter were found. These tumours could not be classified by immunocytochemistry but were classified as D₁ cell tumours by electron microscopy.

In 15 patients without confirmed tumours the angiography was normal.

Phlebography

Three tumours 4, 5 and 6 cm in diameter as well as the cyst 10 cm in diameter could be demonstrated as expanding lesions with displacement of the veins (Fig 6). The other tumours were less than 2 cm in diameter and were not observed at phlebography. In one patient previously operated upon a branch from the ant sup pancreaticoduodenal vein was obliterated, probably ligated.

At postoperative examinations in patients with enucleated islet cell tumours no morphologic abnormalities were demonstrated. In patients with hemipancreatectomy only ligation of the splenic vein was found and no abnormalities at selective phlebography of the remaining pancreatic tissue (Fig 7).

Hormone analyses

Detailed results of hormone analyses have been published previously (INGEMANSSON et coll 1975, 1977, 1978; REICHARDT et coll 1979) and are therefore only summarized here.

Insulin producing tumours and islet cell hyperplasias. Seven patients, 2 with B-cell hyperplasia and 5 with B-cell adenomas were examined. In 2 patients islet cell hyperplasia in the tail and in the body of the pancreas respectively was correctly located by arteriovenous insulin concentration gradients. In 3 of 5 patients with B cell adenomas the tumours were correctly located, 2 in the body and one in the tail of the pancreas.

In one patient with hyperinsulism operated upon twice with partial resection of the pancreas and

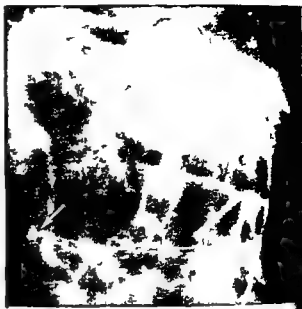


Fig 5 Glucagonoma of the head of the pancreas. Injection gastroduodenal artery, parenchymal phase. Small hypervascular lesion (→).

ligation of the splenic vein, high insulin concentration was found in an anastomosing vein between the hilum of the spleen and the superior mesenteric vein. At laparotomy an insulinoma was found in the remaining part of the tail. In one patient with an insulinoma in the dorsocranial part of the head of the pancreas the tumour could not be located by arteriovenous hormone differences though the sampling procedures were performed twice.

Gastrin producing tumours. Four patients with Zollinger-Ellison syndrome were examined. In 3 the gastrin concentration was increased in general in the portal vein system and the analyses could not locate the tumours. At operation performed within 6 weeks after sampling multiple tumours were found with and around the pancreas. In one patient 2 examinations were performed after total gastrectomy and enucleation of a gastrinoma; gastrin concentrations were normal. An examination 4.5 years after gastrectomy revealed increased gastrin concentrations in all veins in the region of the pancreas with a maximum in the post sup pancreaticoduodenal vein. At operation one tumour in the head 1 cm in diameter and multiple small tumours in the body and tail were found. In one patient all gastrin concentrations were increased with a maximum in the post sup vein. The patient refused surgery.

Glucagon producing tumours. Three patients with glucagonoma syndrome were examined. All glucagon producing tumours were correctly located.



Fig 6a



Fig 6b

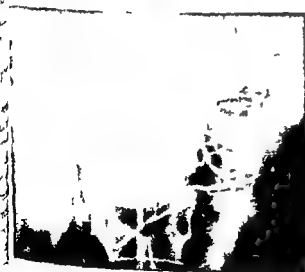


Fig 7

Fig 6 Tumour of the head of the pancreas 3 cm in diameter a) Injection into the common hepatic artery parenchymal phase b) Phlebography of the head Slight curved displacement of the veins (→)

Fig 7 Selective phlebography of the body of the pancreas in a patient in whom the tail has been resected No morphologic abnormality

by arteriovenous hormone gradients 2 in the head and one in the tail of the pancreas In one patient with a tumour in the head of the pancreas the tumour even contained insulin and serotonin and furthermore insulin concentrations were increased in the veins of the tail Resection of the tail was

performed No hyperplasia or adenoma was found at light microscopy Parts of the tissue were also examined by electron microscopy and immunochemistry even then without pathologic findings

Other tumours One tumour of the head of the pancreas could not be classified preoperatively

Table

Hormone concentrations in tumour draining veins compared with the portal vein tributaries outside the tumour draining veins

	Hormone concentration		Range of concentrations in the main portal vein tributaries
	In tumour draining vein	In main portal vein tributary at tumour level	
	$\mu\text{U/ml}$	$\mu\text{U/ml}$	$\mu\text{U/ml}$
Insulinomas			
1	—	865	93–260
2	600	300	13–58
3*	1 130	45	11–165
4*	745	14	11–68
5	1 200	179	14–78
6	974	95	95–230
	pg/ml	pg/ml	pg/ml
Glucagonomas			
1	74 000	2 900	1 370–2 400
2	10 000	800	600–1 750
3	10 650	?	856–2 213

* B-cell hyperplasia

Postoperative analyses proved that the tumour secreted somatostatin and localization of the tumour by arteriovenous somatostatin concentration differences was possible. One islet cell tumour could not be localized by the hormones analysed but could be classified as a D₁ cell tumour by electron microscopy.

Postoperative examinations Six patients in whom resection of the pancreas had been performed were catheterized postoperatively. 3 of them twice.

In 3 patients in whom adenomas had been enucleated postoperative triple catheterization was performed in one of them twice.

In one patient with Zollinger–Ellison syndrome recurrence was suggested which was confirmed operatively. A recurrence was suggested also in one patient operated upon for a glucagonoma but the patient refused further investigations and operation.

Value of selective catheterization Three insulin producing islet cell tumours could have been located by blood sampling in the main tributaries of the portal vein system (Table). The islet cell hyperplasia had not been located without selective catheterization of pancreatic veins. In one patient with glucagonoma the location of the tumour could only have been suggested and one had been missed without



Fig. 8. Insulinoma of the head of the pancreas. The hormone analyses could not locate the tumour. Injection into ant. sup. v. reveals a venous connection between the head of the pancreas and the left lobe of the liver (→).

selective examination. In one case no sample was withdrawn outside the tumour draining vein.

Complications

In one patient abdominal pain and fever followed necessary puncture of the gallbladder. The coagulation was normalized after 2 days. In one patient a 10 cm × 12 cm hematoma in the right lobe of the liver developed after percutaneous transhepatic portography. No specific treatment was needed.

Discussion

Angiography is regarded as the method of choice for localization of islet cell tumours of the pancreas. The reported accuracy in localization of insulinomas varies widely. In a review of 170 cases of the literature STEFANINI *et al.* (1974) found a success rate of 66 per cent. All islet cell tumours producing hormones known today have the same angiographic appearance. The accuracy of angiography in localizing



a

Fig. 9 Phlebographic anatomy can be identified during operation. a) Phlebography of the head. Injection into ant sup vein colon vein (↔) ant sup branches (→) b) Veins of the head of the



b

pancreas after dissection in situ. Colon vein (↔) ant sup branches (→)

ation of other tumours than insulin producing is not known as the number of reported cases is too small.

Gastrinomas are often multiple and in the present series it was not possible to demonstrate all the tumours in one patient by angiography. Neither was it possible to locate multiple gastrinomas by portography and hormone analyses. Generally elevated gastrin concentrations were certainly suggesting multiplicity of gastrin releasing tumours but could not locate these tumours. Total gastrectomy has been the accepted method of treatment in patients with Zollinger-Ellison syndrome. The recently introduced histamin H₂-receptor antagonists (STAGE et coll 1976, BOV-FILS et coll 1977) have raised new possibilities. If an accurate preoperative localization of gastrinomas can be obtained, extirpation of the tumours and resection of the antrum of the stomach and duodenum will be the therapy of choice. In patients with multiple gastrinomas, which cannot be located, treatment with H₂-antagonists should be tried.

All glucagon producing tumours could be demonstrated by angiography. In one patient with a glucagonoma of the head of the pancreas, which even released insulin and serotonin, high insulin concentrations were found in a vein of the tail. These concentrations were 7 to 10 times higher than the insulin

concentration of the main portal vein tributaries, strongly indicating that an adenoma or II cell hyperplasia was present in the tail even if it was not demonstrated by immunocytochemistry.

In one patient with an insulinoma of the head of the pancreas, neither angiography nor hormone analyses could locate the tumour. The failure of triple catheterization was due to an unusual anatomy of the veins of the head of the pancreas. Injection of the post superior pancreaticoduodenal vein as well as the ant superior vein revealed a vein of the hepatoduodenal ligament between the head of the pancreas and the hilum of the liver, probably draining a cranial part of the head directly to the portal vein branches of the left lobe of the liver (Fig. 8).

Very small islet cell tumours and islet cell hyperplasia cannot be located by angiography. In these cases, selective catheterization of the pancreatic veins was necessary for localization of the lesions, as the hormone concentrations in the splenic vein at the level of inflow of the draining vein were not elevated as compared to other samples.

The accuracy of both angiography and triple catheterization was in the present series higher than of one method alone. If possible, both angiography and triple catheterization should be performed for preoperative localization of endocrine pancreatic

tumours. The rate of angiographic false positive diagnoses of 60 reported investigations for suggested insulinomas was 11 per cent (KOROBKIN et coll 1971). In one case of the present material an accessory spleen was demonstrated at angiography. An angiographic differentiation between an accessory spleen and an islet cell tumour is sometimes impossible.

In patients with hyperinsulinism or glucagonoma syndrome with positive angiographic findings however only in one of six cases unexpected high insulin concentrations were found at another location than the angiographically demonstrated tumour. The number of patients is small and it is possible that multiple endocrine disturbances in the same pancreas are more common.

If blood sampling for hormone assay is performed the examination should include selective catheterization of the pancreatic veins especially if angiography did not locate a tumour. Islet cell hyperplasia and even adenomas can be missed if only sampling at different levels in the main tributaries of the portal vein is performed (Table).

Furthermore there was no evidence of increased complications if selective examinations of the pancreatic veins were performed. The complication risk was obviously correlated to the percutaneous puncture of the portal vein not to selective catheterization of the veins.

Phlebography of the pancreatic veins was necessary for proper documentation of the places of blood sampling. Knowledge of the individual venous anatomy was important for evaluating hormone concentration differences. By dissection of the veins during operation (Fig. 9) according to the phlebographic anatomy and the hormone concentrations of the sampled blood an occult adenoma and islet cell hyperplasias were found.

Selective catheterization of the pancreatic veins in an extensive manner as aimed at in blood sampling for hormone assay seems only possible using the percutaneous transhepatic approach to the portal vein. The transumbilical approach implies a course with several curves and angles which makes selective catheterization of veins of the body and tail hazardous and difficult.

SUMMARY

Based on 45 examinations the technique of selective catheterization of the pancreatic veins for blood sampling

using the percutaneous transhepatic approach to the portal vein is described. The results are compared with the angiographic findings in 16 patients with islet cell tumours or islet cell hyperplasia.

ACKNOWLEDGEMENTS

Immunocytochemistry was performed by Dr L. Larsson, Institute of Medical Biochemistry, University of Aarhus, Aarhus, Denmark. Insulin determinations were performed by Dr C. Kuhl, Department of Internal Medicine, Bispebjerg Hospital, Copenhagen, Denmark. Glucagon determinations were performed by Dr J. Holst, Department of Clinical Chemistry, Bispebjerg Hospital, Copenhagen, Denmark. Gastrin determinations were performed by Dr F. Stadil, Department of Surgery, Herlev Hospital, Copenhagen, Denmark.

REFERENCES

- BOISEN E. and SAMUELSSON L. Angiographic diagnosis of tumours arising from the pancreatic islets. *Acta radiol. Diagnosis* 10 (1970) 161.
- BONFELS S., BERNIER I., MIGNON M., LAMBERT R., BERNADES P., L'HIRONDEL C., ACCARY J. P. and KLOETI G. Metiamide treatment in five patients with Zollinger-Ellison syndrome. *Digestion* 15 (1977) 41.
- BOOKSTEIN J. J. and OBERMAN H. A. Appraisal of selective angiography in localizing islet cell tumors of the pancreas. *Radiology* 86 (1966) 682.
- FRICKE M., ZICK R. and MITZKATH J. Das Insulinom: Computer Tomogramm. *Radiologe* 18 (1978) 793.
- FUJII K., YAMAGATA S., SASAKI R., OHNEDA A., SHIOHARA and SUZUKI J. Arteriography in insulinoma. *Amer. Roentgenol.* 120 (1974) 634.
- GÖTHLIN J., LUNDEQUIST A. and TYLÉN U. Selective phlebography of the pancreas. *Acta radiol. Diagnosis* 15 (1974) 474.
- GRAY R. K., ROSCH J. and GROLI MAN J. H. Arteriography in the diagnosis of islet cell tumors. *Radiology* 97 (1970) 39.
- HOFVELS J., LUNDEQUIST A. and TYLÉN U. Percutaneous transhepatic portography. *Acta radiol. Diagnosis* 19 (1978) 643.
- INGEMANSSON S. Pancreatic and intestinal vein catheterization with hormone assay. *Bull. No. 13* Dept. of Surgery, University Hospital, S-22185 Lund, Sweden, 1977.
- HOLST J., LARSSON L. I. and LUNDEQUIST A. (a) Localization of glucagonomas by catheterization of the pancreatic veins and with glucagon assay. *Surg. Gynec. Obstet.* 145 (1977) 509.
- KUHLC LARSSON L. I., LUNDEQUIST A. and TYLÉN U. (b) Islet cell hyperplasia localized by pancreatic vein catheterization and insulin radioimmunoassay. *Amer. J. Surg.* 133 (1977) 643.
- — — and LUNDEQUIST A. Localization of insulinomas and islet cell hyperplasia by pancreatic vein catheterization and insulin assay. *Surg. Gynec. Obstet.* 146 (1978) 725.

- LARSSON L I LUNDERQUIST A and STADIL F Pancreatic vein catheterization with gastrin assay in normal patients and in patients with the Zollinger-Ellison syndrome *Amer J Surg* 134 (1977) 558
- OROBKIN M T PALUBINSKAS A J and GLICKMAN M G Pitfalls in arteriography of islet cell tumors of the pancreas *Radiology* 100 (1971) 319
- LUNDERQUIST A and TYLÉN U Phlebography of the pancreatic veins *Radiologe* 15 (1975) 198
- EICHARDT W and CAMERON R Anatomy of the pancreatic veins A post mortem and clinical phlebographic investigation *Acta radiol Diagnosis* 21 (1980) 33
- ERICSSON M HOLST J INGEMANSSON S and LUNDERQUIST A Glukagon produzierende endokrine Pankreastumoren Symptome Diagnostik Lokalisation Therapie und Verlaufskontrolle To be published in *Chirurg* (1979)
- SKJOLDBORG H and MADSEN B Selective angiography in surgical management of pancreatic insulinomas *Acta chir scand* 137 (1971) 169
- STAGE J G RUNE S J STADIL F and WÖRNING H Treatment of Zollinger-Ellison patients with Cimetidine² In *Proceedings of second international symposium on histamin H receptor antagonists* p 306 Excerpta Medica Amsterdam 1976
- STEFANINI P CARBOUJ M PATRASSI N and BASOLI A Beta islet cell tumors of the pancreas Results of a study on 1067 cases *Surgery* 75 (1974) 597
- WIECHEL K L Tekniken vid perkutan transhepatisk portpunktion (PTP) (In Swedish) *Nord Med* 86 (1971) 912

OM THE DEPARTMENTS OF RADIOLOGY LAZZAROTTO'S HOSPITAL PORTO ALEGRE HOSPITAL SIRIO
BANES SAO PAULO BRAZIL RIKSHOSPITALET OSLO NORWAY HOSPITAL SANTA ISABEL BLUMENAU
BRAZIL AND COOPER MEDICAL CENTER CAMDEN U S A

ANGIOGRAPHY IN CYSTADENOMA AND CYSTADENOCARCINOMA OF THE PANCREAS

R UFLACKER N M AMARAL S LIMA T AAKHUS
E PEREIRA and K KURODA

Primary cystic neoplasms arising from the pancreatic acinar epithelium may be benign (cystadenoma) or malignant (cystadenocarcinoma). They are usually single and often produce no symptoms. Their clinical presentation is similar and the differential diagnosis between the two forms is difficult. Histologic typing is a further difficulty in these cases.

The angiographic findings in 2 cases of pancreatic cystadenomas have been described as early as 1957 (PYRAH & COWIE) although specific angiographic features have not been described until later (SWANOV 1963 PRESSMAN et coll 1973). These tumours are rare and few reports on their angiographic appearances are available. Therefore cases from several institutions were collected to obtain a larger sample for analysis.

Material and Methods

The material consisted of 9 females 16 to 57 years of age with surgically proved cystic neoplasms of the pancreas which had been previously examined with angiography. Five of the tumours were classified as benign cystadenomas and the other 4 as malignant cystadenocarcinomas.

Three of the cystadenomas arose from the tail of the pancreas and one from the head of the pancreas. In 3 cases an upper abdominal mass was palpable. Pain was present in all patients but one. No calcifications were demonstrated within the

growths. The tumours were large ranging from 4 to 10 cm.

Two of the cystadenocarcinomas were located in the head of the pancreas and the other 2 in the tail. Their size varied between 10 and 18 cm and an abdominal mass was palpable in all patients. Jaundice was present in 2. No calcifications were found within the tumours.

Selective catheterization of the celiac splenic superior mesenteric and inferior mesenteric arteries was performed after percutaneous puncture of the femoral artery. Superselective catheterization was occasionally carried out and inferior cavography performed in one case.

Results

Cystadenoma Four of the 5 cystadenomas were demonstrated at selective angiography. Small capillary vessels and pathologic vessels were present in all cases. Three masses were highly vascularized, well delineated and smooth and with arteriovenous shunting and early venous filling (Figs 1-2). One tumour was poorly vascularized with tiny irregular vessels and faint contrast accumulation. In the case without pain no tumour was demonstrated at angiography but a splenic artery aneurysm was present. This tumour was found at operation.



a



b

Fig. 1. Large pancreatic cystadenoma in the tail displacing the splenic artery and vein. Rich vascularization of the tumour (a) as well as accumulation of contrast medium (b).



a



b

Fig. 2. Richly vascularized cystadenoma causing partial occlusion of the splenic vein (→) with venous collateral.

All cystadenomas but one were supplied by branches of the splenic artery and were clearly demonstrated as being of pancreatic origin at angiography. One cystadenoma was mainly supplied by branches of the superior mesenteric artery (middle colic artery and transverse pancreatic artery) and only tiny vessels came from the splenic artery. Colateral venous circulation existed in one of the cystadenomas

probably secondary to compression of the splenic vein which was only partially flattened (Fig. 2).

Microscopically small cysts lined by typical flat cuboidal epithelium containing serous or mucous fluid were demonstrated but no papillary projections.

Cystadenocarcinoma. All four cystadenocarcinomas

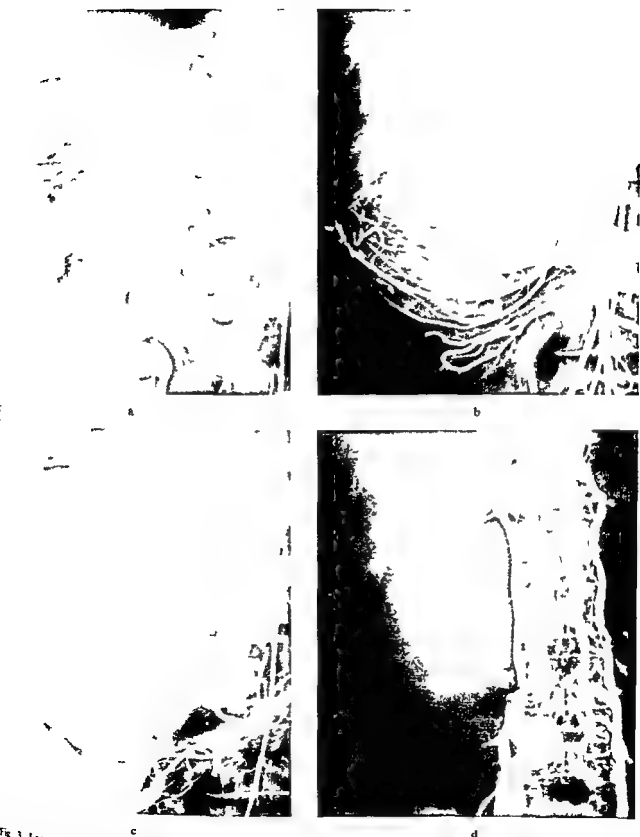


Fig 3 Large cystadenocarcinoma of the pancreatic head. a) Stenosis of the hepatic artery and displacement of the vessels. b) Tumour is partially supplied from arteries arising from the

superior mesenteric artery. c) The capillary phase is followed by arteriovenous shunting. d) Total occlusion of inferior vena cava



a



b



c

Fig 4 Pancreatic tail cystadenocarcinoma. a) Rich vascularization and tumour vessels. Splenic artery aneurysm (==) b) Infiltration of the left colic artery (==) c) Occlusion of the inferior mesenteric vein (→)

omas were demonstrated at angiography. The largest tumour was hypovascular and the other 3 were richly vascularized. Neoplastic vessels were present in all and contrast accumulation within the masses was evident. A large cavity within one of the neoplasms produced a filling defect in the parenchymatous phase.

The tumours located in the head of the pancreas produced encroachment and infiltration of the arteries of the liver and were supplied mainly by the gastroduodenal artery. Displacement of vessels and arteriovenous shunting with early filling of veins and the portal system were observed in these cases. One of the tumours was also supplied by branches of the superior mesenteric artery (inferior pancreaticoduodenal artery) and inferior cavography demonstrated total occlusion of the inferior vena cava and wide collaterals through the vertebral venous system (Fig. 3).

The neoplasms located in the tail of the pancreas produced displacement of the splenic artery and were supplied mainly by branches of this artery (Fig. 4) which was infiltrated in one case. Arteriovenous shunting was evident with early venous filling and multiple collaterals with obstruction of the splenic vein in another case. One of these cases had a splenic artery aneurysm. The tumour was supplied also by the inferior mesenteric artery because of encroachment and invasion of the left colic branch (Fig. 4) and the inferior mesenteric vein was infiltrated.

High cellularity and several mitoses were observed at microscopy. Most of the tumours contained only small cysts. In 2 cases the tumours had multiple cysts and papillary formations.

Discussion

The true incidence of cystadenomas and cystadenocarcinomas is not well known (HAUKOHL & MELANED 1950). Little is understood about their histogenesis but they are accepted as being cystic neoplasms arising from the pancreatic acinar epithelium (PIPER et coll 1962). Evidence exists that cystadenocarcinomas can develop from cystadenomas (BECKER et coll 1965, HAUKOHL & MELANED, PIPER et coll, PROBSTEN & BLUMENFELD 1960). Both tumours have the same gross aspect (SCALVINI 1960) and the definite diagnosis is established only at the microscopic examination. It is not unusual to have areas of cystadenoma mixed with carcinomatous degeneration. Gross papillary

projections may be present in both tumours but are more likely to appear in cystadenocarcinomas. Barium examination is of almost no value in the preoperative evaluation. Angiography has proved to be of highest accuracy in their diagnosis and localization.

Cystadenoma. According to BECKER et coll MOZAN in 1951 reported the first large review of cystadenomas and since then more than 250 cases have been reported (LEWIS & DORMANDY 1971). The tumours are known to be related to an increased risk of diabetes mellitus and SOLOWAY (1965) described their association with numerous metabolic and endocrinologic abnormalities. Cystadenomas almost exclusively occur in females with a predominance in a ratio 9:1 (BECKER et coll, CULLEN et coll 1963, HAUKOHL & MELANED, PIPER et coll). In the present series all the patients were females. The majority of pancreatic cystadenomas occur before 50 years of age and even in youth (PRESSMAN et coll) which also was the case in the present series (ages between 16 and 57 years). A variety of sizes is described for cystadenomas from very small to huge masses but most of the tumours are between 6 and 10 cm in diameter (BECKER et coll). The size of the tumours in the present 5 cases was between this range. The tail of the pancreas is predominantly involved in about two thirds of the cases (GALLART ESQUERDO 1953, PIPER et coll, BECKER et coll). In the present series 3 tumours were located in the tail and one in the body and head of the pancreas respectively. Few tumours have been described to contain calcifications (HAUKOHL & MELANED) in the present series no case had calcific deposits.

Several angiographic findings have been described (PYRAH & COWIE, BIEBER & ALBO 1963, SWANSON, GLENN et coll 1964, BANG 1965, RANINGER & SILDINO 1966, ABRAMS et coll 1967, PRESSMAN et coll, REUTER & REDMAN 1977) including displacement of major vessels, presence of large feeding arteries, accumulation of contrast medium within the tumour associated with pooling of contrast medium and numerous pathologic vessels. However few hypovascular tumours with large dimensions, sparse neovascularity and wide displacement of vessels have been described (ABRAMS et coll, PRESSMAN et coll). Displacement and occlusion of splenic and portal veins with presence of collaterals is also frequently found but in spite of the high incidence of collaterals only one report of

bleeding gastric varices was found in the literature (LEWIS & DORMANDY)

The differential diagnosis between cystadenoma and non functioning islet cell adenoma may be difficult (REUTER & REDMAN). However hypervascular cystadenomas are more likely to have severe arteriovenous shunting, higher flow and increased venous return. Other pancreatic lesions should not present such difficulty in differential diagnosis with hypervascular cystadenomas.

In the present series 3 cystadenomas were easily diagnosed at angiography. They were richly vascularized tumours with neovascularity, contrast accumulation and arteriovenous shunting with early venous filling. One mass was not detected at angiography but the films were of poor quality. Another tumour was hypovascular but neovascularity was present and a faint contrast accumulation occurred (Fig. 4). As in ordinary pancreatic adenocarcinoma the pancreatic origin of the growths could be determined in all cases.

Cystadenocarcinoma According to CULLEN et coll. KAUFMANN (1911) reported the first case of cystadenocarcinoma. These tumours are more rare and no more than 70 cases have appeared in the literature (BECKER et coll., CORNES & AZZOPARDI 1959, CULLEN et coll.). Pancreatic cystadenocarcinomas usually affect young females and are said to be half as common as benign cystadenomas. Frequently they grow slowly with a tendency to remain localized even when attaining a large size (SCALVINI, BECKER et coll.). The features of the present 4 cases agree with the literature except in their distribution: only 2 cases were located in the tail.

Few reports on the angiographic appearances in these tumours are available (ABRAMS et coll., RÖSCH & BRET 1965, SUZUKI et coll. 1971). They are usually described as large masses with wide displacement of arteries and hypervascularity with irregular and truncated vessels and infiltration of feeding arteries. Recently computer tomography and gray scale ultrasound of pancreatic cystadenocarcinoma has been reported (CARROL & SAMPLE 1978). The appearances are not specific though compatible with those of cystic tumours.

At angiography all the present tumours except one were hypervascularized masses with dense accumulation of contrast medium and marked neovascularity. Infiltration of feeding arteries associated with venous occlusion or marked compression of large branches were frequently found (Figs

3-4). Arteriovenous communications existed. Only one large cystic cavity was observed indicating that cystic cavities are usually small and not demonstrated at angiography. In 2 cases an atheromatous aneurysm of the splenic artery was demonstrated. Such a combination has been previously reported only once (SUZUKI et coll.).

Conclusions

Angiography not only plays a decisive role in demonstration of the origin of the tumour and its vascularity but may also permit the differentiation of a benign from a malignant lesion. Rich vascularity and arteriovenous shunts occur in benign as well as in malignant tumours but the presence of arterial and venous infiltration and encroachment indicates malignancy. Cystadenocarcinomas invade adjacent structures and simulate hepatic and gastrointestinal neoplasms. Large cystic cavities seem to be rare. A tendency exists for malignant tumours to be larger than benign ones. A chance for association of splenic artery aneurysm with these neoplasms may be present.

SUMMARY

The angiographic findings in 9 surgically proved primary cystic neoplasms of the pancreas are reported. Angiography demonstrates the extent and origin of the tumour and permits in many cases a differential diagnosis between benign and malignant lesions.

Request for reprints: Dr Renan Uflacker, Dept of Radiology, Lazzarotto's Hospital, Assis Brasil, Porto Alegre 90000, Brazil.

REFERENCES

- ABRAMS R M, BERENBAUM E R, BERENBAUM S, NGO N L. Angiographic studies of benign and malignant cystadenoma of pancreas. *Radiology* 89: 1028.
- BANG I. Ein angiographisch diagnostizierter Cystadenoma pancreatis. *Radiologie* 5 (1965).
- BECKER W F, WELSH R A and PRATT H S. Adenoma and cystadenocarcinoma of pancreas. *Surg* 161 (1965): 845.
- BIEBER W P and ALBO E J. Cystadenoma of pancreas. Angiographic diagnosis. *Radiology* 80 (1963): 7.
- CARROL B and SAMPLE W F. Pancreatic cystadenocarcinoma. CT body scan and gray scale ultrasound appearance. *Amer J Roentgenol* 131 (1978): 339.
- CORNES J S and AZZOPARDI J G. Papillary adenocarcinoma of the pancreas with resection. *Brit J Surg* 47 (1959): 139.

- CULLEN P K REMINE W H and DAHLIN D P
Clinicopathological study of cystadenocarcinoma of
pancreas Surg Gynec Obstet 117 (1963) 189
- ALLART ESQUERDO A Les cystadenomas du pancreas
Acta gastro-ent belg 16 (1953) 85
- LENN E EVANS J A HALPERN M and THORBJARNAR
SON B Selective celiac and superior mesenteric ar
tenography Surg Gynec Obstet 118 (1964) 93
- ALAOHL R H and MELAMED A Cystadenoma of the
pancreas Amer J Roentgenol 63 (1950) 234
- AUFMANN E Quoted by Cullen et coll
- EWIS A and DORMANDY J Cystadenoma of pancreas
Report of two cases Brit J Surg 58 (1971) 420
- LOZANA A Quoted by Becker et coll
- IPER C E REMINE W H and PRIESTLEY J T Pan
creatic cystadenoma Report of 20 cases J Amer
med Ass 180 (1962) 648
- RESSMAN B D ASCH T and CASARELLA W J Cyst
adenoma of the pancreas A reappraisal of angio
graphic findings Amer J Roentgenol 119 (1973) 115
- ROBSTEIN J G and BLUMENTHAL H T Progressive
malignant degeneration of a cystadenoma of the pan
creas Arch Surg 81 (1960) 683
- PYRAH L N and COWIE J W Two unusual aortocutaneas
J Fac Radiol 9 (1957) 416
- RANNINGER K and BALDINO R M Arteriographic diag
nosis of pancreatic lesions Radiology 26 (1966) 470
- REUTER S R and REDMAN H C Cystadenoma In
Gastrointestinal radiography Second edition p 174
W H Saunders Philadelphia 1977
- ROSCH J and BRET J Arteriography of pancreas Amer
J Roentgenol 94 (1965) 182
- SCALVINI L Un tumore raro del pancreas Il cisto car
cinoma (In Italian) Minerva chir 15 (1960) 1207
- SOLOWAY H H Constitutional abnormalities associated
with pancreatic cystadenomas Cancer 18 (1965) 1297
- SUZUKI T KAWABE K KAKAYASU A TAKEDA H
KOBAYASHI K KUBOTA N and HONJO I Selective
arteriography in cancer of the pancreas at a resectable
stage Amer J Surg 122 (1971) 402
- SWANSON G E Case of cystadenoma of pancreas studied
by selective angiography Radiology 91 (1963) 692

FROM THE DEPARTMENT OF DIAGNOSTIC RADIOLOGY UNIVERSITY OF CALIFORNIA DAVIS MEDICAL CENTER
ACRAMENTO CALIFORNIA 95817 AND THE DEPARTMENT OF BIOLOGY BOSTON UNIVERSITY BOSTON
MASSACHUSETTS 02118 USA

NONINVASIVE MEASUREMENT OF FETAL AND NEONATAL BLOOD FLOW

M H REID R S MACKAY and B M T LANTZ

Doppler ultrasound is widely used to assess flow in major extremity and carotid arteries but quantitative data are difficult to obtain unless the vessel lumen diameter orientation of the vessel with respect to the ultrasound beam and the fluid velocity profile are uniquely known This report discusses observations of fetal and newborn blood flows using a doppler instrument which overcomes many of the problems mentioned

Materials and Methods

A new technique employing continuous wave doppler ultrasound with doppler frequency discrimination has been reported to give excellent correlation with dye dilution and thermodilution measurements of cardiac output in animals and adult humans (correlation coefficient in dogs 0.92 MACKAY & HECHTMAN 1975 REID et coll 1980) The advantage of this particular instrument is its ability to discriminate between advancing and receding flow and selectively measure that velocity of blood in the aortic arch which is parallel to the ultrasound beam Descriptions of the instrument and results obtained in adults are reported elsewhere (MACKAY 1972 REID et coll) As part of a larger evaluation program this doppler instrument was used to measure the aortic arch flow in 6 fetuses in normal pregnancies and 2 normal newborns and the umbilical flow in 7 fetuses

For clarity a brief description of the doppler instrument is given A continuous wave 2.0 MHz doppler signal is generated and the return signal is shifted up in frequency for flow advancing toward the transducer or shifted down in frequency for flow receding away from the transducer Each of these possibilities is electronically separated by appropriate bandpass crystal filters centered above and below the center frequency of 2.0 MHz Thus advancing and receding flow can be differentiated Next the doppler return signal is mixed with the 2.0 MHz standard and an audio signal ranging from 300 to 3300 Hz is produced This is passed through a set of ten bandpass filters and an electronic switching network which results in an output voltage proportional to the instantaneous maximum doppler frequency shift at each moment of time The result is that the output signal recorded on a chart recorder represents the instantaneous maximum flow velocity within the 2.0 cm diameter doppler ultrasound beam This is the key to the success of this instrument because the measured flow obtained by ensnaring a tortuous artery is therefore measured at a position where the artery is most nearly parallel to the doppler beam Therefore the usual problem of aligning the vessel ultrasound beam is not critical For example a 25% error in alignment of the ultrasound beam and measured vessel results in only a 10% per cent under-estimate of flow

Conventional B scan ultrasound was employed to image the aortic arch and descending arch of the fetuses during routine obstetric ultrasound examination. Care was taken to assess the position and orientation of the fetus and fetal aortic arch. Only those fetuses which could be scanned from a fetal lateral approach were examined because of the necessity of directing the doppler ultrasound beam in a near axial direction to the transverse portion of the thoracic aortic arch (Fig 1). After obtaining an adequate B scan image of the thoracic arch for measurement and localization of the doppler ultrasound probe (2.0 cm diameter 0.5 cm thick disc) was placed between the B scanner transducer and the maternal abdomen and proper doppler probe positioning obtained by reference to the B scanner stored image. This is easily done by generating calibration scale dots on the B scanner and noting their position with respect to the stored image of the fetal arch. The B scan transducer was then removed and a doppler measurement made.

Visual (chart recorder) and audible observations of the doppler signal simplified the ensonification of the fetal aortic arch. Heart wall and cardiac valve velocity sounds were significantly unique to allow easy differentiation from that of flow velocity in the fetal arch. Heart movement was characteristically lower in frequency (i.e. low velocity motion) than arch blood flow. Cardiac valves had a recognizable crisp snap to their audible character. This simplified the fine adjustment of the doppler transducer and the measurement of fetal aortic flow could be obtained quite rapidly in a few minutes. Gestational ages ranged from 30.5 weeks to term.

Umbilical cord artery flow was easily obtained by ensonifying a region of the cord where at least some of the cord was parallel to the doppler ultrasound beam. This is an easy requirement to satisfy because the umbilical cord is quite tortuous in its course. A B scan image of the umbilical cord will often give a measurement of one of the umbilical artery diameters. If this is not possible a measurement of the umbilical cord diameter can be used to estimate the umbilical artery size by reference to known umbilical anatomic measurements (Fig 2 REYNOLDS 1952).

A similar technique of aortic arch measurement was employed in two healthy newborn infants (female age 48 h weight 3.86 kg male age 72 h weight 3.96 kg). B scan images of the aortic arch were obtained by scanning directly through the thin,

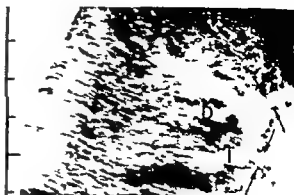
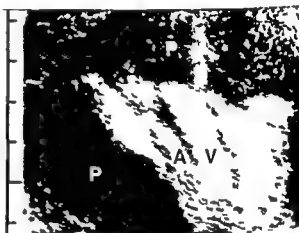


Fig 1 Aortic arch in a fetus. Calibration marks spacing 10 cm. Brachiocephalic artery (+) Left subclavian artery (-) I = ductus arteriosus I = aortic isthmus



a



b

Fig 2 Umbilical cord in a fetus. Calibration marks spacing 10 cm. A = artery P = placenta V = vein

cartilagenous sternum (Fig 3). The doppler probe appropriately placed near the suprasternal area receding flow in the aortic arch.

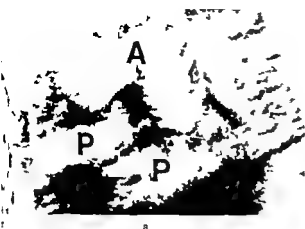


Fig 3 Aortic arch in a newborn a) Transverse scan parallel to aortic arch b) Longitudinal scan perpendicular to aortic arch

Calibration marks spacing 1.0 cm A=aorta P=pulmonary artery S=left subclavian artery

Results

The predicted and measured blood flows in the fetal transverse aortic arch, aortic isthmus and umbilical cord are summarized in the Table. The position of the doppler measurement in the aorta was largely a function of fetal position within the maternal abdomen. Fig 1 is a representative B scan image of a fetal aortic arch demonstrating the aortic isthmus and transverse arch. The aortic arch lumen diameter is obtained from these images. Fetal weights were estimated from published biparietal

diameter-gestational age and weight charts so that the data of the Table could be presented in a standardized form (ml/min/kg WIENER et coll 1977). Except for Winsberg's estimates of fetal left ventricular stroke volume, the comparison data from previous reports (Table) are derived from measurements in fetal lambs. No comparable data in undisturbed third trimester human fetuses are available. A few measurements have been reported for previable fetuses taken at hysterotomy in early pregnancy (ASSALI et coll 1960).

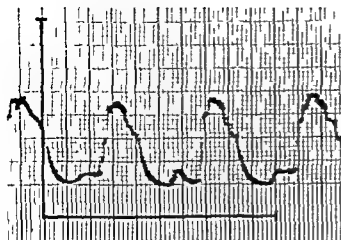
Table
Fetal blood flow (ml/min/kg)

	Transverse aortic arch	Isthmus aortic arch	Umbilical cord
WALSH & LIND (1978)	-105		
DAWES (1968)	120-159	1.0	180
MAHON et coll (1966)	-167		
ASSALI et coll (1960-1965)	-97		110
RUDOLPH (1974)	43-135	45	200
WINSBERG (1972)	-163		
Doppler			
Case 1	126		
Case 2	92		128
Case 3	112		
Case 4	115		183
Case 5		60	
Case 6		45	

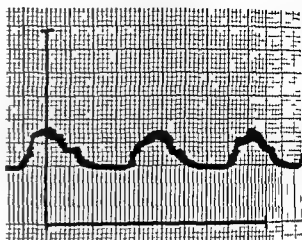
Assumes 15 ml/min/kg coronary flow. Range shown from ascending aortic arch to isthmus.

Previable human fetuses: 360 ml/min/kg combined left and right ventricular output estimate 170 ml/min/kg left ventricular output.

Comparison data from end gestation fetal sheep.



a



b



c

Fig 4 Blood velocity recordings. Calibration, abscissa—1 s ordinate—100 cm/s doppler flow velocity a) Fetus Transverse aortic arch b) Umbilical cord artery c) Newborn Descending aortic arch

Fig 2 illustrates the typical B scan appearance of the umbilical cord. Umbilical artery lumen diameter can be measured from the image or an estimate of the arterial size can be made from the umbilical cord diameter and reference to published anatomic measurements of umbilical cord (REYNOLDS)

Similar flow measurements were obtained in two healthy newborn infants with descending aortic arch lumen diameters of 7 mm. The calculated descending aortic arch blood flow was 160 ml/min/kg for the 48 hour-old female infant and 180 ml/min/kg for the 72 hour old male infant. Allowing for 25 per cent of left ventricular output to the coronary and brachiocephalic vessels previously published values for neonatal cardiac output would indicate that descending aortic blood flow should be 150 ml/min/kg (RUDOLPH 1974) 120 to 190 ml/min/kg (WALSH & LIND 1978) 200 ml/min/kg (EMMANOULIDES et al 1970). Fig 4 illustrates representative doppler blood velocity recordings from

fetal aortic arch, umbilical cord and a newborn descending aortic arch.

Discussion

The problem of ascertaining exactly the position of flow velocity measurement in the fetal aortic arch when the ductus arteriosus is functional is appreciated. Reference to the expected anatomic vascular orientations of the fetal arch and the restricted active area of the ultrasound beam indicate that the flow within the ductus arteriosus should not interfere with arch velocity measurements using this particular doppler device. Correlation with predicted results from examinations of fetal lambs is given in the Table and indicates close agreement with the doppler measurement data mentioned.

Umbilical cord flow is obtained from doubling the flow values calculated for one umbilical artery. It is not possible to measure each artery separately and

us flow calculation is thus a compromise and subject to many assumptions concerning umbilical artery sizes and flow distribution. Even with these advantages, the measured values in the Table correlate well with expected umbilical blood flow.

Neonatal aortic blood flow was measured with the Doppler ultrasound beam directed caudally from the suprasternal notch. Setting the instrument for receding flow and directing the beam toward the descending aortic arch will reject flow in the ascending arch, pulmonary artery and brachiocephalic vessels and perpendicularly oriented ductus arteriosus will not contribute to the flow measurement with this particular instrument. The measured aortic flow should then be near the junction of the ductus arteriosus with the aorta. The ductus arteriosus would be expected to be functionally closed within the first day of life (DAWES 1968).

The major error of this method of flow determination is related to uncertainties in measuring vessel lumen size at the site of the Doppler observation. Flow is proportional to the Doppler measured blood velocity and the cross sectional area of the vessel and therefore the square of the vessel lumen diameter. Ultrasonic fetal aortic measurements on the order of 7 mm are subject to at least a ± 1 mm measurement error or approximately a ± 30 per cent flow error. This error can be minimized by multiple B scans of the same area but it is unlikely that precision would improve much more than ± 0.5 mm in fetal or neonatal aortic size determination.

Another issue of some concern is the assumed velocity profile across the aorta. Good experimental evidence exists to indicate that the velocity distribution is essentially constant across the aorta except immediately adjacent to the aortic valve (McDONALD 1974, FALSETTI et al 1972, LING et al 1968, ROCKWELL et al 1974). Thus the Doppler measured velocity can be multiplied by the vessel cross sectional area to give the flow. Qualitative observations of flow using a range gated pulsed Doppler system have been described (TAYLOR et al 1979). The advantage of the continuous wave Doppler device described in this report is the Doppler shift frequency analysis which automatically selects that velocity most parallel to the ultrasound beam. This is particularly useful for example in observations of umbilical cord flow where the vessels are quite tortuous and all that is necessary is to ensnare a cluster of the cord. Variations in the assumed velocity profile secondary to vessel bends have not

been included in this analysis as it did not seem justified for the level of precision obtained. A parabolic velocity profile was assumed in the umbilical artery.

It should be noted that often the most clinically useful information is related to changes in blood flow over some hours or days. For this case the precision of the vessel diameter is immaterial provided the vessel size does not change during the course of the Doppler observations. Thus changes in blood flow in a specified vessel may be noted with accuracy.

Conclusions

Doppler ultrasound blood flow observations in undisturbed human fetuses in the last trimester of pregnancy have been described. Comparison with expected values from examinations of fetal lambs implies reasonable accuracy. The clinical efficacy of these measurements in fetal distress, labor, congenital anomalies, etc., may be speculated upon and these and other applications are currently under investigation.

SUMMARY

A newly developed Doppler ultrasound flow measuring instrument was applied to determination of aortic arch blood flow in near term fetuses and 2 neonates and to umbilical cord flow in 2 fetuses. The method and results are presented and indicate good agreement between this noninvasive technique and expected values for aortic arch flow in human fetuses and neonates.

Request for reprints: Dr M. H. Reid, Department of Diagnostic Radiology, University of California, Davis Medical Center, 4301 X Street, Sacramento, California 95817, USA.

REFERENCES

- ASSALI, N. S., MORRIS, J. A. and BECK, H. Cardiovascular haemodynamics in the fetal lamb before and after lung expansion. *Amer J Physiol* 208 (1965) 122.
- , RAURAMO, L. and PELTONEN, T. Measurement of uterine blood flow and uterine metabolism. *Amer J Obstet Gynec* 79 (1960) 86.
- DAWES, G. S. Fetal and neonatal physiology, pp. 92-96. Year Book Medical Publishers, Chicago, 1968.
- ENIMANOU, I. D., G. C. MOSS, A. J. MONSEY, CHOUCHARD, M., MARCANO, B. A. and RZESNIC, H.

- Cardiac output in newborn infants *Biol Neonat* 15 (1970) 186
- FALSETTI H L KISER K M and FRANCIS G P Sequential velocity development in the ascending and descending aorta of the dog *Circulat Res* 31 (1972) 328
- LING S C ATABEK H B FRY D L PATEL J and JANICKI J S Application of heated film velocity and shear probes to hemodynamic studies *Circulat Res* 23 (1968) 789
- MCDONALD D A Blood flow in arteries. Second edition pp 114 116 137 Camelot Press Southampton 1974
- MACKAY R S Noninvasive cardiac output measurement *Microvasc Res* 4 (1972) 438
- and HECHTMAN H B Continuous cardiac output measurement. Aspects of doppler frequency analysis *IEEE Trans Biomed Eng* 22 (1975) 346
- MAHON W A GOODWIN J W and PAUL W M Measurement of individual ventricular outputs in the fetal lamb by an indicator dilution technique *Circulat Res* 19 (1966) 191
- REID M H MACKAY R S and LANTZ B M T Non invasive blood flow measurements by doppler ultrasound with application to renal artery flow determination. To be published in *Invest Radiol* (1980)
- REYNOLDS E R M The proportion of Wharton's jelly in the umbilical cord in relation to distension of the fetal arteries and vein with observations on the fetus of Hoboken *Anat Rec* 113 (1952) 365
- ROCKWELL R L ANLIKER M and ELSNER J M Studies of the pressure and flow pulses in a viscoelastic arterial conduit *J Franklin Inst* 297 (1974) 405
- RUDOLPH A M Congenital diseases of the heart *Year Book Medical Publishers* Chicago 1974
- TAYLOR K J W ATKINSON P DE GRAFF C DEMBNER A G and ROSENFELD A T Clinical evaluation of pulse doppler device linked to gravimetric scan equipment *Radiology* 129 (1979) 745
- WALSH S Z and LIND J The fetal circulation and its alteration at birth *In Perinatal physiology* pp 156 159 Edited by U Stave Plenum Medical Co New York 1978
- WIENER S N FLYNN M J KENNEDY A W and BLOOM F A composite curve of ultrasonic biplanar meters for estimating gestational age *Radiology* (1977) 781
- WINSBERG F Echocardiography of the fetal and neonatal heart *Invest Radiol* 7 (1972) 152

EFFECT OF INTERPOSED SKIN AT DOPPLER FLOW ESTIMATION AT 5 AND 10 MHz

With a description of a calibration device

L. FORSBERG and T. OLIN

The Doppler effect was first described in the middle of the nineteenth century by Doppler & Ballot. They showed that the sound waves emitted from a moving source of sound have a higher frequency when the source is approaching the listener and a lower frequency when the sound emitter is leaving. This effect has been used for medical purposes since 1959 when SATOMURA began recording flow velocity. Sound waves reflected from moving particles are influenced in a similar mode. When a sound beam is reflected from particles moving towards the emitter the reflected frequency is higher than the emitted one, when it is reflected from particles moving away from the emitter the frequency is lower. This change in frequency is proportional to the flow velocity and is called the Doppler shift or the Doppler frequency. Quantitative flow measurements using Doppler technique have been carried out with fairly simple equipment by, for instance, STEGALL et al. (1966), BERNSTEIN et al. (1970) and LO GERFO & CORSON (1976) all reporting very promising results.

The equipment used was a continuous wave directional Doppler (Parks 806) with calibration facilities. The sound is emitted and received from piezo-electric crystals 2 mm x 5 mm each on top of a pencil probe. The frequency of the ultrasound emitted from the probe was 10 MHz (9.5 MHz). For measurements with 5 MHz a Parks 906 was used. This apparatus has no calibration facility installed, why calibration had to be made before starting this investigation.

The Doppler equipments mostly employed in flow examinations are using ultrasound in the frequency

of 5 to 10 MHz. The change in frequency is proportional to the velocity of flow in the structure examined and it is also proportional to the emitted frequency. This means that a higher Doppler frequency is obtained when examining a vessel with high flow velocity using a high frequency. The resolution of measurements is higher using a high ultrasound frequency increasing proportionally. On the other hand the attenuation of ultrasound in tissues increases with the frequency. This means that only superficial vessels can be examined with a 10 MHz probe.

The Doppler equation used for quantitative flow velocity measurements is as follows:

$$\Delta F = F_e - F_r = F_e - F_e \times \frac{c - v \cos \alpha_1}{c + v \cos \alpha}$$

where

ΔF = Doppler frequency (kHz)

F_e = emitted frequency (kHz)

F_r = received frequency (kHz)

c = velocity of ultrasound in blood 1.56×10^3 cm/s

v = velocity of flow cm/s

α_1 and α = angles between emitted and received sound beam and blood vessel

α = angle between pencil probe and blood vessel

Due to the construction of the pencil probe

$$\alpha = \frac{\alpha_1 + \alpha_2}{2}$$

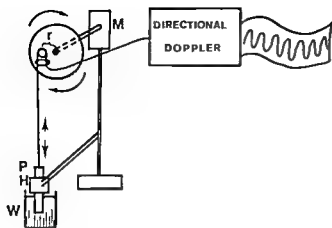


Fig 1

Fig 1 Calibrator designed for the experiments with 5 MHz Doppler equipment M = motor r = distance from peg to centre of the rotating wheel P = pencil probe H = holder W = glass of water

Fig 2 Plastic holder with a metallic screw to fasten the probe in the slide

Fig 3 Experimental design A = plastic bag containing human blood B = latex tubing C = jar for collections D = measuring glass E = Doppler probe F-G = Doppler apparatus and polygraph H = stop-watch J = clamp K = calibrator L = contact gel

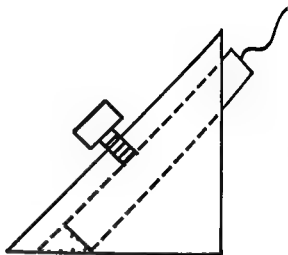


Fig 2

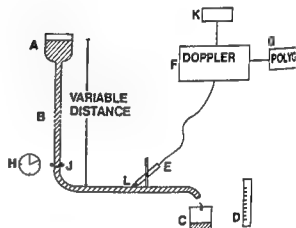


Fig 3

When $v \ll c$ this equation may be approximated by

$$F = \frac{2 F_e v \cos \alpha}{c}$$

which can also be written

$$v = \frac{\Delta F \times c}{2 F_e \cos \alpha}$$

The 5 MHz equipment Parks 906 had no calibrator which is necessary for quantitative measurements. Therefore an apparatus (Fig 1) was designed for calibration. It was constructed of a synchronized motor making a rotating wheel move a full circle per second. On this wheel the cable of the probe could be attached at different distances from the centre of the wheel. The probe was then guided by a slide allowing it to move perpendicularly to create

idealized to and fro movements. The probe was placed with the transducer in a glass of water. The apparatus gave peculiar recordings until the bottom of the glass was covered with a soft non reflecting material. The movements of the probe in the water were thus standardized and calibration procedures could start. The maximum velocity of the probe is the same as the velocity of the peg around the centre of the wheel $v = 2\pi \times$ the distance in cm between the peg and the centre of the wheel per second. First the 10 MHz probe was used. This Doppler apparatus was known to give correct information at examination of low velocities why the apparatus was used giving maximum velocities of 8 to 11 cm/s. The polygraph was calibrated with the 1000 Hz generator and then fixed in one position to give comparable readings. Velocity measurements were then performed with both 10 and 5 MHz (9.5 and 5.3 MHz). This procedure gave a calibration constant that could be used at all examinations after having

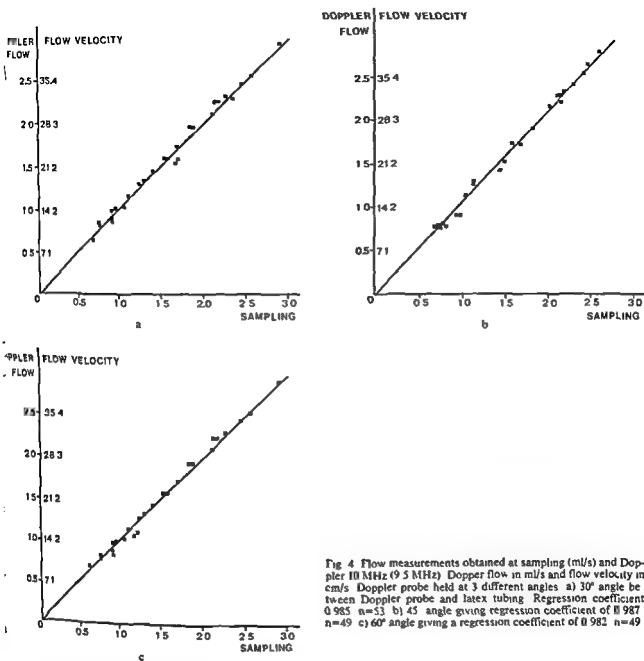


Fig 4 Flow measurements obtained at sampling (ml/s) and Doppler 10 MHz (9.5 MHz) Doppler flow in ml/s and flow velocity in cm/s. Doppler probe held at 3 different angles a) 30° angle between Doppler probe and latex tubing. Regression coefficient 0.985 n=53 b) 45° angle giving regression coefficient of 0.987 n=49 c) 60° angle giving a regression coefficient of 0.982 n=49

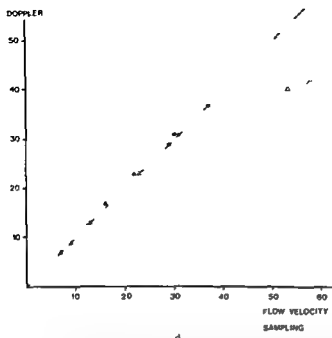
the polygraph calibrated against the 1000 Hz generator or directly against the calibrator.

The influence on the flow measurement obtained by holding the 9.5 MHz Doppler probe at different angles (30°, 45° and 60°) to the vessel (latex tubing) was examined as were the effects of interposed skin between the probe of 10 MHz and 5 MHz and the vessel. A plastic holder was designed in order to obtain reproducible and exact angles (Fig 2).

The probe used in these experiments was a penicil shaped probe with the crystals placed at its end. The experimental design is illustrated in Fig 3. A

continuous flow of blood was obtained using a plastic bag (A) connected to a latex tubing with a diameter of 3 mm (B) where the bag could be fixed at different levels above the table creating flows of varying velocities. The flow was started by opening a clamp (J). Tuned collections were performed simultaneously with the Doppler measurement. (L) represents the transmission medium (E) the Doppler probe (K) stands for the oscillator used for calibration of the apparatus (G) is the polygraph (Mingograf 800 Siemens Elema). The Doppler apparatus (F) used in the experiments was a Parks 806

FLOW VELOCITY



FLOW VELOCITY

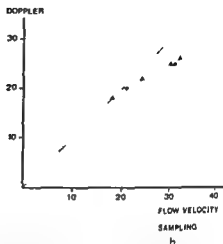


Fig. 5 Flow measurements at sampling and Doppler 10 MHz (9.5 MHz) with interposed skin. Flow velocity in cm/s. a) Direct coupling with gel (●). Interposed skin of rabbit (Δ). A 20 per cent loss in the area of 30 cm/s or more. b) Very stretched (▲) and

moderately stretched (●) human skin interposed. Extremely stretched human skin (Δ). Also here a 20 per cent loss at about 30 cm/s or more.

Directional Doppler Before every examination it was calibrated by connecting an oscillator with a known frequency (1 kHz) to the towards and away output stage.

The blood used was discarded from the blood bank. It was heparinized and mixed gently before the experiments started. At this time blood haematocrit was measured and found to be 41 and 44 per cent respectively. The temperature of the blood was 10° to 15°C during the examinations, which were performed in a room holding a temperature of 22 to 25°C. True blood flow was measured by collecting the blood for a period of 30 to 60 seconds. The cross sectional area of the latex tubing was 0.071 cm². Multiplication of this area by the values of linear flow velocity registered by the Doppler apparatus gave Doppler determinations of volumetric flow rate for comparison with the flow rate measured directly.

The influence of different tubing materials was also analysed. Polyethylene catheters were tried but could not be used since only irrelevant noise was registered, probably due to absorption and reflection of the ultrasound waves. The tubing used in the rest of the experiments was made of latex rubber with very few disturbing noises. The influence of the angle between probe and vessel was also examined

before proceeding with interposed skin. The angle between the probe and the vessel was made constant by triangular plastic holders for the probe (Fig. 7).

Comparison between measurements of flow with milk instead of blood showed no difference in information obtained with Doppler, which also was found by STEGALL *et al.* When analysing the effect of interposed skin holding 25°C (simple attenuation of ultrasound increases at lower temperatures) blood was used in the experiments where human skin was used and milk where skin from rats was used. Skin from rats turned out to have the same qualities as human skin when shaved and placed over the latex tubing with the hairy side on the tubing after covering it with gel.

Results

The effect of the angle between the 10 MHz probe and the vessel was correctly adjusted for by the formula for Doppler measurement of flow velocity (Fig. 4). The flow estimations were very close to the expected ones obtained by sampling. Measurements of flow were carried out up to velocities just over 30 cm/s. The examinations concerning the effect of interposed skin were with 10 MHz carried out up to expected flow velocities over 60 cm/s with the probe

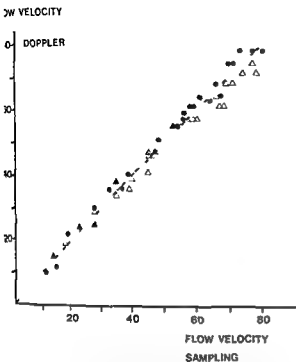


Fig. 6 Flow measurements at Doppler 5 MHz (5.3 MHz) and at sampling flow velocity in cm/s. Direct coupling between probe and skin (●). Interposed skin (Δ).

fixed in a 45° angle to the vessel. Fig. 5 shows that the Doppler technique gives about 20 per cent too low values with interposed skin when flow velocity is higher than about 30 to 35 cm/s. It also shows that Doppler signals obtained with direct contact between probe and tubing are tending to be too low when examining flow velocities of more than about 40 cm/s. Thus skin exerts a definite influence on the Doppler signal obtained with a 10 MHz probe especially when higher flow velocities are measured. The results obtained with 5 MHz appear in Fig. 6 where a good correlation is found up to velocities of at least 80 cm/s. The interposed skin had a minimum damping effect on measurements at high flow velocities.

Discussion

The experiments show that the angle between the probe and the vessel is correctly adjusted for by the formula which was theoretically to be expected. It also shows that Doppler estimations using 10 MHz were accurate up to flow velocities of at least 40 cm/s with direct coupling with gel between probe and latex tubing. What is more interesting is the effect of skin between the 9.5 MHz probe and the

vessel as well as the too low signal obtained measuring higher flow velocities ranging from about 40 cm/s and higher. The results correspond well with those of BERNSTEIN et al. and LO GERFO & CORSON who obtained accurate estimations of flow with a 10 MHz Doppler equipment corresponding to flow velocities of 30 to 35 cm/s compared with electromagnetic flowmeters.

Some kind of limitations in the 10 MHz Doppler apparatus itself seem to exist. In the present experiments interposed skin resulted in too low flow estimations from 25 to 30 cm/s and higher. The skin used was only about 1 mm thick. Thicker skin or lax skin distorted the signal progressively more. This phenomenon might be due to attenuation of higher frequencies in the interposed structures as pointed out by SEIPEL et al. It is known that the Doppler signal from a continuous wave apparatus is built up from multiple frequencies representing a mean flow velocity of the vessel examined. The transverse cross section of the vessel must be totally insonated by the sound beam to give correct readings. Attenuation of the higher frequencies might lead to a signal built up by proportionally more lower frequencies representing a flow of lower velocity than expected. The conclusion of the findings must be that measurements performed with a 10 MHz probe are somewhat underestimated when examining high flow velocities or when trying to quantify flow percutaneously at places where interposed tissue is thick.

These findings initiated experiments with 5 MHz Doppler equipment. After getting a calibrator constructed it was possible to use also this apparatus at quantitative flow measurements.

Using a 5 instead of a 10 MHz probe is supposed theoretically to give a somewhat less distinct Doppler signal due to the lower Doppler frequency received at identical flow velocities. However it seems to be of less importance compared with the better penetration abilities. The apparatus itself (Parks 906) is giving a more correct signal at higher flow velocities than did the 10 MHz apparatus (Parks 806). The effect of the interposed skin seems to be near to negligible. This means that percutaneous quantitative Doppler measurements of flow ought to be carried out with 5 MHz equipment in order to get best possible measurements especially when examining deeper lying vessels. When having a calibrator that can be used on any Doppler apparatus it is possible to use a fairly simple and not too

expensive Doppler equipment for non invasive quantitative measurements

SUMMARY

Flow measurements with high ultrasound frequencies (Doppler technique) can be used at quantitative estimations of flow. A calibrator for Doppler equipments is presented. The effect of skin as interposed material with 10 MHz and 5 MHz is discussed as are limitations in the apparatus itself especially when using 10 MHz ultrasound.

REFERENCES

- BERNSTEIN E F, MURPHY JR A E, SHEA M A and HOUSMAN L B. Experimental and clinical experience with transcutaneous Doppler ultrasonic flowmeters. *Arch Surg* 101 (1970) 21.

- LO GERFO F W and CORSON J H. Quantitative transonic blood flow measurement in Dacron grafts. *Surgery* 79 (1976) 569.
- SATOMURA S. Study of the flow patterns in peripheral arteries by ultrasonics. *Acoustical Soc of Jap J E* (1959) 151.
- SFIEPEL L, SCHMIEL F K and GLEICHMANN U. Probe me bei der Messung intravasaler Blutströmung mit Ultraschall Doppler Technik. *Med Tech* 7 (1973) 4.
- STEGALL H F, RUSHMER R F and BAKER D W. A transcutaneous ultrasonic blood velocity meter. *J appl Physiol* 21 (1966) 707.

DIAGNOSIS OF ABDOMINAL AORTIC ANEURYSMS BY AORTOGRAPHY COMPUTER TOMOGRAPHY AND ULTRASOUND

I ERIKSSON A HEMMINGSSON and P G LINDGREN

Clinical examination and aortography have been used for many decades in the diagnosis of abdominal aortic aneurysms. However the reliability of diagnosis by palpation has been claimed to vary considerably according to the experience of the clinician. Recently clinical examination was reported to give exact diagnosis in 90 per cent and aortography in 93 per cent (GORDON SMITH et coll 1978). The development of modern ultrasound has resulted in an increasing rate of diagnostic reliability (SEGAL et coll 1966 NUSBAUM et coll 1971 WINSBERG et coll 1974) which has been reported to be as high as 98 per cent (GOMES et coll 1978). Recent experiences with CT have shown that abdominal aortic aneurysms and intra aneurysmal thrombi can be diagnosed very accurately by this method in particular after contrast enhancement (GOMES 1977).

Exact preoperative determination of the upper limit of the aneurysm and its relationship to the renal arteries is of the utmost importance in planning the surgical procedure. Information about the renal arteries obtained by ultrasound has been uncertain in many cases (HAAGA & REICH 1978). On the other hand aortography has clear disadvantages in being an invasive method afflicted with some adverse effects. Therefore it was considered of value to compare the reliability of aortography and the non invasive methods ultrasound and CT in the diagnosis of abdominal aortic aneurysm and the determination of

the relation between the aneurysm and the renal arteries.

Material and Methods

Seventy-one consecutive patients were admitted for examination of a pulsating abdominal mass. In patients with only slight indication of aneurysm ultrasound was first performed. If nothing abnormal was found aortography was not carried out. A total of 71 patients were examined by ultrasound and 20 each by CT and aortography (Table I).

For aortography the catheter was introduced via the femoral or axillary arteries and films in antero posterior, oblique and lateral projections were exposed. Ultrasound was performed with a Sono Diagnost grey scale apparatus (Philips) and CT with an Ohio Nuclear Delta 50 FS apparatus (Scanning time 18 s) before and after intravenous injection of contrast medium (100 ml Conray Meglumin 280 mg I/ml).

The occurrence of an aortic aneurysm, its upper limit and relation to the renal arteries and its lower limits were evaluated with each method. In addition possible intraaneurysmal thrombus or retroperitoneal bleeding was recorded. The number of renal arteries for each kidney was noted from the films.



Fig 1 Aortography a) AP b) lateral projection. Contrast enhancement of the lumbar arteries and inferior mesenteric artery but straight left contour of the aorta below the renal arteries indicates a possible aneurysm c) CT after contrast enhancement shows a wide aneurysmal aorta with intraluminal thrombus

Most patients with a diagnosis of abdominal aortic aneurysm were treated surgically and the operative findings were correlated to the observations at the preoperative examinations

Results

In 39 patients with slight indication of aortic aneurysm no abnormality was found at ultrasound (Table I). The clinical course in these patients revealed that the abdominal discomfort was due to

Table I
Number of examinations

	Aortography	Computer tomography	Ultrasound
Normal	6	11	39
Aneurysm	13	13	8
Tumor	1	1	4
Unsuccessful			
Total	20	20	71

Table 2

Number of patients with a correct and incorrect evaluation concerning the presence of an abdominal aortic aneurysm at extension and presence of an intraaneurysmal thrombus

	Aortography (20 cases)		Computer tomography (20 cases)		Ultrasound (71 cases)	
	Correct	Incorrect	Correct	Incorrect	Correct	Incorrect
Diagnosis	18	2	19	1	67	4
Cranial extension in relation to renal arteries	8	{ 4 1	10	3	4	{ 10 14
Caudal extension	10	3	11	2	28	
Intraaneurysmal thrombus	9	4	13		15	

Calcified tumor or aneurysm not examined

unsuccessful because of intestinal gas not evaluable



Fig 2a



Fig 2b



Fig 3a



Fig 3b

Fig 2 a) Longitudinal scan through the aorta. The plane of transverse scan (b) is marked with vertical arrow. b) Transverse scan. A=aneurysm B=blood-containing part T=intra-aneurysmal thrombus VB=vertebral body VC=vena cava RK=right kidney

Fig 3 a) Aortography in a p projection. Aorta appears normal. b) CT after contrast enhancement. The partly calcified soft tissue mass cannot be distinguished from the aorta.

other causes. At clinical re examination no indication of aortic aneurysm remained and these patients were considered to have a normal abdominal aorta.

A correct diagnosis was made in 18 patients at aortography (Table 2). In the remaining 2 patients with aneurysms the angiographic diagnosis was uncertain. The inferior mesenteric artery and all lum-

bar arteries were contrast filled and no calcifications of the aneurysmal wall were present in either patient. In these 2 patients the diagnosis was established at both ultrasound and CT (Figs 1-5). At operation these aneurysms were found to contain large organized thrombi on the inner aspect of the anterior wall below the level of the inferior mesenteric artery.



Fig 4 a) Aortography a p. projection CT at b) the center of the aneurysm c) the level of the left and d) of the right renal artery. Leakage of contrast medium into the aneurysmal sac (a, b). The aneurysm does not seem to involve the renal arteries (c). CT reveals that the aneurysm involves the aorta at the origin of both renal arteries (c, d).

Ultrasound examination of the aorta was unsuccessful in 4 patients because of an abundance of intestinal gas which concealed the image and made evaluation impossible. In the remaining 67 patients a correct diagnosis was obtained in all 28 with aneurysm (Table 2, Fig. 2) and in the 39 without aneurysm i.e. 94 per cent correct diagnosis. In 19 of 20 patients CT gave a correct diagnosis. In the remaining patient a differentiation between an an-

eurysm and a calcified soft tissue tumor close to the aorta could not be made. CT was performed only after intravenous contrast enhancement in this case. Angiography revealed a normal aorta (Fig. 3) and at operation a calcified tumor.

An intraaneurysmal thrombus was found in all cases with aneurysm examined by CT (Table 2) and in 15 (Fig. 2) of the 28 cases with aneurysm examined by ultrasound. The remaining 13 patients



a



b



c



d

Fig 5 a) Aortography a p projection. Catheter cannot be passed enough to give contrast filling of the renal arteries. Lumbar arteries visible. CT b) Intraluminal thrombus outside the

contrast filled lumen of the aorta. c) Renal arteries arise from a normal part of the aorta and d) can be distinguished from the renal vein. Renal cysts on both sides.

and localized ectasias of the aorta. In 4 cases in aneurysmal thrombi were suggested at aortography but not confirmed. A diagnosis of aneurysm had appeared probable on account of a straight aortic contour and no visible lumbar arteries. In one patient a blood-conducting channel from the aortic lumen through the organized thrombus and into the space between the thrombus and the aortic wall was observed both at aortography and at CT (Fig 4).

The extension of the aneurysms in the cranial direction was demonstrated most correctly by CT (Table 7). By this method the upper limit of the aneurysm and its relation to the renal arteries could be ascertained in all patients examined for that purpose. In 4 patients aortography did not disclose this relationship (Figs 4 and 5). In 10 patients the origins of these vessels were not examined by ultrasound.

In the remaining 18 patients with aneurysm the renal arteries and their distances from the upper limit of the aneurysm was demonstrated in 4 patients at ultrasound. Extension of the aneurysm into the pelvic arteries was correctly revealed by all three methods in all patients in whom this was present.

A retroperitoneal hematoma due to a ruptured aortic aneurysm was diagnosed in one patient at CT. This was the only case of aneurysm rupture. This patient was not examined by the other methods.

Discussion

The results have demonstrated the value of ultrasound and computer tomography for diagnosis of abdominal aortic aneurysms. The reliability of both these methods seems to be at least as good as that of

aortography Concealment of the image by intestinal gas is the most important obstacle to an ultrasound diagnosis while rare diseases close to the aorta may cause difficulties in CT

The upper limit of the aneurysm and its relation to the renal arteries was most correctly revealed by CT which in this respect was more reliable than aortography The origins of the renal arteries were visible in only a few cases at ultrasound but a refinement of the equipment especially with addition of a modern real time apparatus will probably improve this result

CT was also superior to aortography in demonstrating intraaneurysmal thrombi These were also observed with ultrasonography contrary to what has been reported previously (KARP & EKLÖF 1978)

Ultrasound and CT are non invasive methods without any risks which makes the examination comfortable and safe for the patient An additional advantage of ultrasound is its freedom from ionizing radiation Ultrasound should thus be the primary method of choice in patients with possible abdominal aortic aneurysm This is in accordance with the recommendations of KARP & EKLÖF If the diagnosis is not clearly established by this method or the extension of the aneurysm not clear CT is indicated It is evident that most cases of abdominal aortic aneurysm can be treated safely without preoperative aortography

SUMMARY

Aortography computer tomography and ultrasound were compared with respect to the diagnosis and evaluation of abdominal aortic aneurysms The results show that ultrasound should be the method of choice for diagnosis and that the extension of the aneurysm towards the renal arteries is best evaluated by computer tomography Aortography can thus be omitted in most cases

REFERENCES

- GOMES M N Acta scanning in the diagnosis of abdominal aortic aneurysms *Computer Tomogr* 1 (1977) 41
- HAAKAL H G and SCHELLINGER B Ultrasonography and CT scanning A comparative study of abdominal aortic aneurysms *Computer Tomogr* 2 (1978) 10
- GORDON SMITH I C TAYLOR E W NICOLAIDES A V GOLDSMAN L KENYON J R and EASTCOTT H H G Management of abdominal aortic aneurysm *Br J Surg* 65 (1978) 834
- HAAGA J and REICH N ■ Computed tomography of abdominal abnormalities C V Mosby Saint Louis 1978
- KARP W and EKLÖF B Ultrasonography and aortography in the diagnosis of abdominal aortic aneurysms *Acta radiol Diagnosis* 19 (1978) 955
- NUSBAUM J W FREIMANIS A K and THOMFORD N R Echography in diagnosis of abdominal aortic aneurysm *Arch Surg* 102 (1971) 385
- SEGAL B L LIKOFF W ASPERGER Z and KINGSLEY B Ultrasonic diagnosis of abdominal aortic aneurysms *Amer J Cardiol* 17 (1966) 101
- WINSBERG F COLE BEUGLET C and MULDER D S Continuous ultrasound B scanning of abdominal aortic aneurysms *Amer J Roentgenol* 121 (1974) 64

TRANSCATHETER EMBOLIZATION OF THE RENAL ARTERY WITH BUCRYLATE IN RENAL CARCINOMA

ARNULF SKJENNALD BJORN KLEVMARK and JAN TRYGVE STENWIG

Surgical treatment of renal carcinoma is usually refrained from even if the tumour is infiltrating surrounding tissues or distant metastases are present.

Even without such infiltration the removal of the tumours can be technically difficult and complicated with heavy bleeding.

Embolic occlusion of the renal artery in cases of carcinoma results in infarction of the tumour and the kidney. The surgical procedure is then technically easier mainly due to less bleeding which also permits an early admittance to the renal vein for ligation to avoid discharge of tumour cells.

Several agents have been used to obtain intra-arterial occlusion. As results have not been entirely satisfactory the search for new and more suitable agents has continued. The results using Bucrylate as an embolus inducing agent are now reported.

Material and Method

The material consisted of 5 patients: 3 men and 2 women, the youngest being 51, the oldest 73 years, mean 63.6. The carcinoma was left sided in 3 and right sided in 2 cases. The largest tumour measured 9 cm x 16 cm on the films, the smallest 10 cm x 7 cm. One patient had metastases in the liver and the lungs, another in the liver and the retroperitoneal space. The latter metastases were supplied mainly from the gastro-duodenal artery. No metastases or extrarenal infiltration of the tumour were apparent in the other 3 patients.

The renal arteries were catheterized from the right femoral artery using a Surgimed mat No 8 Cat No 160 catheter. With a coaxial stop-cock a thin

ner catheter was introduced through this catheter. Bucrylate (Isobutyl 2 cyano-acrylate monomer) was injected through the inner catheter and the outer catheter continuously perfused with isotonic glucose. The effects of the Bucrylate injections were controlled by abdominal aortography in all patients 15 min after the embolization (Fig. 1).

The age and sex of the patients, size of the tumour, diameter of the renal arteries and the amount of Bucrylate injected appear in the Table.

Results

In 4 patients occlusion of the renal artery was obtained with 3.5 (Fig. 2), 2.5, 1.5 and 1 ml of Bucrylate respectively (Table). In one patient, a female aged 73, occlusion of the renal artery was incomplete following injection of 1.5 ml. However, as the patient complained of intense pain, additional agent was not injected.

Four patients were operated upon 14, 22, 30 and 38 days respectively after the intra-arterial injections. The kidneys were technically easy to remove because of only insignificant bleeding which made blood transfusions unnecessary. The arteries were hard and gritty. Coagulation necrosis of the infarcted areas, including the renal carcinomas, was present on microscopy. The arteries were thrombosed to a varying extent (Fig. 3a). Tumour tissue outside the renal capsule, including the renal vein, was visible (Fig. 3b). The 73-year-old female with incomplete occlusion of the artery was not treated surgically.

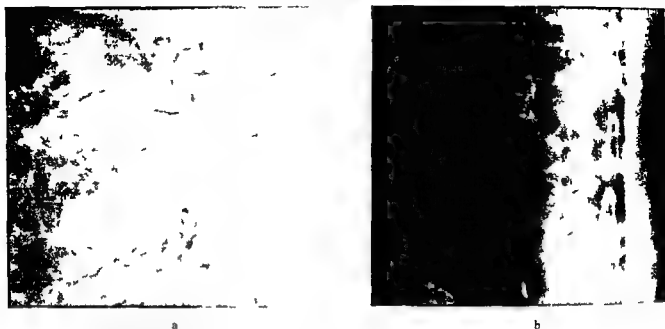


Fig 1 a) Selective injection into right renal artery. Large carcinoma. b) Abdominal aortography 15 min after injection of 1.5 ml Bucrylate. The artery is occluded.

Adverse effects were pain for one to three days and fever. Three patients had severe pain after the occlusion; the other 2 patients complained of little or no pain. In 2 of the patients fever of moderate to high degree occurred, lasting from 5 to 9 days. Pulmonary embolism was diagnosed in one patient 23 days after the embolization.

Discussion

Arterial injection of autologous clots (CARMIGNA *et al* 1978) and other autologous material (ALM GÅRD *et al* 1973, GOLD & GRACE 1975, TADAVARTHY *et al* 1975, HIGGINS *et al* 1977, BOOKSTEIN *et al* 1978, CHANG *et al* 1978) has resulted in initial occlusion of the vessel, but recanalization often occurs. BARTH *et al* (1977) reported

on long term follow up results of transcatheter embolization with autologous clots, oxycel and gelfoam in domestic swine. At 4 months recanalization was present in all cases. Thus, long lasting occlusion is probably difficult to achieve with these agents. LUNDERQUIST *et al* (1977) using gelfoam on the coronary gastric vein also recorded a high percentage of recanalization, while VIANONTE *et al* (1977) did not observe recanalization in 10 similar patients also embolized with gelfoam. The most commonly used agent for embolizing is gelfoam. In the renal artery this agent is distributed even to the more peripheral branches of the vessel.

Bucrylate rapidly undergoes polymerization and solidifies in a few seconds when mixed with blood. It has been the most successful agent used to obtain embolization of the gastric coronary vein in patients

Table

Review of the material

Age (years)	Sex	Size of tumour (cm)	Diam of renal artery (mm)	Amount of bucrylate (ml)	Pain	Occlusion
51	M	19×16	12	3.5	Strong	Yes
70	M	16×16	10	1.5	No	Yes
73	F	10×17	5	1.5	Strong	No
73	F	11×9	6	1.0	No	Yes
51	M	10×7	10	2.5	Strong	Yes



a

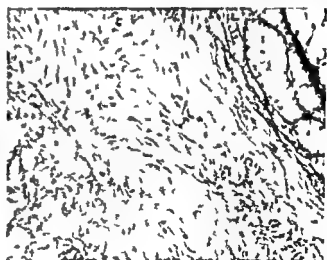


b

Fig. 2 a) Large carcinoma in left kidney b) Aortography. Complete occlusion of the renal artery after embolization with 3.5 ml Bucrylate



a



b

Fig. 3 a) Bucrylate with thrombotic material in renal arteries H & E $\times 30$ b) Lower left area. Necrotic tumour after artificial

thrombosis. Upper right area. Viable tumour tissue outside the renal capsule H & E $\times 72$

bleeding from esophageal varices due to portal hypertension (LUNDERQUIST et coll 1978) Bucrylate has also been used for control of other massive gastro-intestinal bleeding (GOLDMAN et coll 1978) CARMIGNANI et coll (1978) injected Bucrylate into the renal artery in 2 patients with renal carcinoma and obtained complete occlusion DOTTER et coll

(1975) used Bucrylate in a patient with a heavy protein losing glomerulonephritis. After the embolization the patient became anuric and the protein loss stopped. No recanalization occurred after embolization of the renal arteries in rats (CARMIGNANI et coll 1978). In contrast to gelfoam Bucrylate polymerizes and solidifies more centrally in the

artery and the effect is therefore more similar to that of a surgical ligation. Embolic reflux is a possible complication. Theoretically, due to quick solidification this effect should be easier to avoid using Bucrylate. However, reflux would probably best be prevented by using a balloon catheter (GREENFIELD et coll 1978).

In the present series intraarterial injection of Bucrylate in 4 patients resulted in complete occlusion of the artery, present also at the time of operation 14 to 38 days later. In the fifth case with incomplete occlusion surgery was not performed.

Postoperative examination of the removed kidneys showed the renal arteries totally filled with a plastic like material. It seems reasonable that these arteries should be considered permanently occluded. Large areas of necrosis and infarcted tumour tissue indicate that the tumours had effectively lost their arterial supply.

Transcatheter embolization of the renal artery is not without complications. In one of the present patients pulmonary embolism occurred. It was diagnosed 23 days after the embolization, but clinical signs indicated an earlier occurrence. It is reasonable to suggest a connection between the pulmonary embolism and the occlusion procedure. Because Bucrylate solidifies immediately after the injection, there is little reason to believe that Bucrylate particles would have passed through the tumour. A more obvious explanation is that sudden interruption of the arterial circulation decreased the flow in the renal vein, with subsequent formation of clots. This concept is supported by the delayed manifestation of the embolism.

Occluding agents acting differently may cause pulmonary embolism because the injected particles can pass through the tumour. CARMIGNANI et coll (1978) have shown that barium particles were able to pass the capillaries in rat kidneys and therefore could result in pulmonary embolism. They found that gelfoam and Bucrylate did not pass the capillaries. However, theoretically all other embolizing agents than Bucrylate might pass through arteriovenous shunts in the tumour.

Three patients experienced immediate strong ischemic flank pain, which required the administration of potent analgetics. The pain subsided over 1 to 3 days. In one case intense pain led to interruption of the injection after a small volume (1.5 ml) when complete occlusion had not yet been obtained. Two patients also had a rise in body temperature

lasting from 5 to 9 days. Flank pain and a rise in temperature have also been reported after embolization with gelfoam (GOLDSTEIN et coll 1979). This appearance seems to be independent of the agent used.

The present series is small. However, in 4 patients the intraarterial injection of Bucrylate gave convincing results, both regarding immediate complete occlusion of the artery and its duration. Bleeding at surgery was insignificant; the operations were easy to perform and the renal vein could be isolated at an early stage. The pathologic examination confirmed the radiologic and operative findings.

Intraarterial embolization should not be used routinely in cases of renal carcinoma, because inherent potential complications cannot be ignored. The main indication for the procedure appears to be the very large, highly vascularized carcinoma, especially when located in the upper part of the kidney.

SUMMARY

In 5 patients with large renal carcinomas Bucrylate was injected into the renal artery. One to 3.5 ml Bucrylate were required to obtain occlusion of the arteries. At operation 14 to 38 days later the arteries were still occluded. One patient developed pulmonary embolism; other complications were of less importance. The main indication for the procedure is very large, highly vascularized carcinomas in the upper part of the kidney. Bucrylate seems to be a suitable embolus inducing agent.

REFERENCES

- ALMGÅRD L, E. FERNSTRÖM I, HÄVERLING M and LJUNGVIST A. Treatment of renal adenocarcinoma by embolic occlusion of the renal circulation. *Brit J Urol* 45 (1973) 474.
- BARTH K, E. STRANDBERG J, D. and WHITE R. I. Long term follow up of transcatheter embolization of autologous clot, oxycel and gelfoam in domestic swine. *Invest Radiol* 12 (1977) 273.
- BOOKSTEIN J, J. NADERI M, J. and WALTER J. F. Transcatheter embolization for lower gastrointestinal bleeding. *Radiology* 127 (1978) 345.
- CARMIGNANI G, BELGRANO P, PUPPO P. and GILLANI L. Cyanocrylates in transcatheter renal embolization. *Acta radiol. Diagnosis* 19 (1978) 49.
- , MARTORANA G. and PUPPO P. Clots and gelfoam, barium and cyanocrylates in transcatheter embolization of rat kidney. *Invest Urol* 16 (1978) 9.
- CHANG J, KATZEN B. and SULLIVAN K. P. Transcatheter gelfoam embolization of posttraumatic bleeding pseudoaneurysms. *Amer J Roentgenol* 131 (1978) 649.

- BITTER C, GOLDMAN M L and RÖSCH J. Instant selective arterial occlusion with Isobutyl 2 cyanoacrylate. *Radiology* 114 (1975) 227.
- OLD R E and GRACE M D. Gelfoam embolization of the left gastric artery for bleeding ulcer. *Radiology* 116 (1975) 575.
- OLDMAN M L, LAND JR W C, BRADLEY E L and ANDERSON J. Transcatheter therapeutic embolization in the management of massive upper gastrointestinal bleeding. *Radiology* 120 (1976) 513.
- FRENEY F C, TALLMAN J M, GALAMBOS J T, BRADLEY E L, SALAM A, KHEE TIANG OEN, GORDON I J and MENNEMEYER R. Transcatheter vascular occlusion therapy with Isobutyl 2 cyanoacrylate (Bucrylate) for control of massive upper gastrointestinal bleeding. *Radiology* 129 (1978) 41.
- OLDSTEIN H M, MEDELLIN H, TALAL BEYDOUN M, WALLACE S, BEN MENACHEM Y, BRACKEN R B and JOHNSON B E. Transcatheter embolization of renal cell carcinoma. *Amer J Roentgenol* 123 (1975) 557.
- GREENFIELD A J, ATHANASOULIS C A, WALTMAN A C and LEMOURE E R. Transcatheter embolization. Prevention of embolic reflux using balloon catheters. *Amer J Roentgenol* 131 (1978) 651.
- HIGGINS C B, BOOKSTEIN J J, DAVIS G B, GALLOWAY II C and BARR J W. Therapeutic embolization for intractable chronic bleeding. *Radiology* 122 (1977) 473.
- LUNDERQUIST A, BJÖRJESEN P, ÖWMAN T and BENG-MARK S. Isobutyl 2 cyanoacrylate (Bucrylate) in obliteration of gastric coronary vein and esophageal varices. *Amer J Roentgenol* 130 (1978) 1.
- , SIMERT G, TYLÉN U and VANG J. Follow up of patients with portal hypertension and esophageal varices treated with percutaneous obliteration of gastric coronary vein. *Radiology* 122 (1977) 59.
- TADAVARTHY S M, MÖLLER J H and AMPLATZ K. Polyvinyl alcohol (Ivalon)—A new embolic material. *Amer J Roentgenol* 125 (1975) 609.
- VIAMONTE M, PEREIRAS M, RUSSELL E, LE PAGE J and HUTSON D. Transhepatic obliteration of gastro-esophageal varices. Results in acute and nonacute bleeders. *Amer J Roentgenol* 129 (1977) 237.

RADIOGRAPHIC APPEARANCES IN CROHN'S DISEASE

IV The new distal ileum after surgery

J HILDELL, C LINDSTRÖM and A WENCKERT

Postoperative recurrence of Crohn's disease has attracted considerable interest in the clinical literature and has been analysed from several clinical and pathologic viewpoints (VAN PATTTER et coll 1954, COLOCOCK & VANSANT 1960, STAHLGREN & FERGUSON 1961, BARBER et coll 1962, ATWELL et coll 1965, SCHOFIELD 1965, LENNARD-JONES & STALLER 1967, BRILL et coll 1969, WALLENSTEN 1971, WENCKERT 1971, NUGENT et coll 1973, MARSHALL 1975). On the other hand, in the radiologic literature reports discussing particularly recurrent disease are scanty (CHÉRIGIÉ et coll 1973, HILDELL et coll 1980, Part III). Recurrence has usually been considered parenthetically in conjunction with descriptions of the original disease.

The radiographic features of non-operated patients with Crohn's disease were considered previously and the postoperative radiographic appearance of the colon was analysed and discussed (Parts I, II, III, HILDELL et coll 1979, 1980). The present communication reports the postoperative radiographic appearance of the new distal ileum and correlates the findings with the preoperative distribution of the lesion, the operative procedures employed and the postoperative appearance of the colon.

Material and Methods

The material was derived from films and records of 195 consecutive patients operated upon during a 15-year period (1959–1973). Detailed information on the series is given in previous reports (Parts I, II, III).

The preoperative distribution of the lesions was assessed by a review of preoperative films, operative reports and pathologic reports (Part II).

For the present review, use was made of the postoperative films of all patients in whom the disease preoperatively was located in the distal ileum, the colon or in both and who, after resectional procedures, had an ileo-ileal or ileocolic anastomosis or an ileostomy. Thus, the material consisted of 370 small and 233 large intestine postoperative examinations performed in 150 patients in 1959 to 1976.

Most patients were radiographically examined within two years after operation, but in the beginning of the series the controls were not as regular and frequent. Thus, a few patients were not examined until 7 or 8 years postoperatively. (More detailed information concerning the radiologic follow-up is given in Table 2.) The postoperative appearance of the new distal ileum and the colon was recorded and correlated with the preoperative distribution of the lesion and the operative procedures employed (Fig. 1).

The period between 1959 and 1973 was divided into two parts: one early period, 1959 to 1968, during which 70 patients were operated upon, and one late period, 1969 to 1973, with 80 patients.

This subdivision is somewhat arbitrary; it is based on the fact that attempts at earlier surgical intervention were made during the last 4 to 5 years, and at operation it was aimed at resecting macroscopically involved intestine and also diseased lymph nodes.




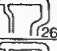



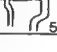





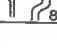
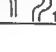

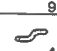

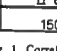
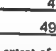
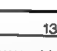
Extent at time of operation	Radiographic appearance of the new distal ileum and the colon after operation for Crohn's disease			
	No radiographic recurrence	Abnormalities characteristic of recurrence		
		Distal ileum	Distal ileum and colon	Colon
A				
B				
C				
D				
E				
F				
G				
	150	87	49	13

Fig 1 Correlation between extent of disease at time of operation, operative procedures employed and radiographic appearance of the new distal ileum and the remaining colon

Consequently the resections were more extensive during this period.

A control material was used for the evaluation of the appearance of the new distal ileum oral to an ileocolic anastomosis. This material consisted of films of 100 patients operated upon with resection of the distal ileum and right hemicolectomy for other diseases than Crohn's disease, mainly malignant lesions. None of these patients had any evidence of inflammatory disease of the intestine, neither pre nor postoperatively. A review was made of two small or large intestine examinations in each patient performed with an interval of at least six months. The length of the resected ileal segment in these patients varied between 5 and 40 cm (mean 13 cm).

Results

Control material Irregularities in the region of the anastomosis were found in some patients; they were

considered to be sequential to the operation. Otherwise the mucosal folds were regular without radiographic evidence of edema or ulceration (Fig 1).

Crohn's disease The new distal ileum was considered to be normal when the radiographic appearance was the same as in the control material.

Lesions observed at radiography consisted of abnormalities due to edema, ulceration and fibrosis. The lesions were always located in direct contact with an ileocecal valve, an ileocolic anastomosis or an ileostomy.

Four groups could be distinguished at the end of the observation period:

(1) Normal appearance and no clinical evidence of recurrent disease (78 patients, Fig 3).

(2) Edema, but no ulcers and no progression of the lesions. No clinical evidence of recurrence. This group is called edema (10 patients, Fig 4).

(3) Radiographic recurrence. Abnormalities as edema, ulceration, fibrosis and local progression. No clinical evidence of recurrence (70 patients). This group is called radiographic recurrence (Fig 5).

(4) Radiographic and clinical evidence of recurrent disease (42 patients). This group is called recurrence (Fig 6).

Groups 3 and 4 are referred to as postoperative ileitis.

The patients were distributed within these four groups in relation to the preoperative distribution of the lesions as shown in Table 1.

Normal appearance of the new distal ileum was recorded in 78 of 150 patients (52%). The frequency of normal appearance was the same in the early as in the late period.

Edema was recorded in 10 of 150 patients (7%) and was only observed oral to an ileocolic anastomosis.

Radiographic recurrence was noted in 20 of 150 patients (13%) and was observed only oral to an ileocolic anastomosis. Three of 70 patients (4%) had radiographic recurrence during the early period and 17 patients of 80 (21%) during the late period. The difference is significant ($p < 0.01$).

Recurrence was recorded in 42 of 150 patients (28%). In 22 patients the ileal recurrence was located oral to an ileocolic anastomosis, in 13 patients oral to an ileostomy and in 7 patients oral to the ileocecal valve. Twenty-eight of 70 patients (40%) had recurrence during the early period and 14 of 80 patients (18%) during the late one. This difference is significant ($p < 0.01$).



Fig 2



Fig 3



Fig 4

Fig 2 New distal ileum in a patient operated upon with resection of the distal ileum and right hemicolon because of a carcinoid in the distal ileum. No edema or ulceration.

Fig 3 Normal appearance of the new distal ileum in a patient operated upon for Crohn's disease with resection of the distal ileum and right hemicolon. The contour of the intestine is regular, the mucosal folds are thin and straight without ulcers.

Fig 4 Edema in the new distal ileum oral to an ileocolic anastomosis. The mucosal folds are broad but without ulcers.



Fig. 5 Radiograph: recurrence oral to an ileocolic anastomosis. The examination was performed 13 years after the primary operation. Fibrosis and a sinus tract. The surviving mucosal island protrudes like a polyp into the lumen of the intestine.



Fig. 6 Recurrence in the new distal ileum oral to an ileocolic anastomosis. Marked edema with broad, irregular mucosal lesions and several ulcers in the most aboral part.

Repeat radiography of the small intestine. Various aspects are summarized in Table 2. In 63 of the 78 patients with normal appearance of the new distal ileum, repeated postoperative examinations were performed; all remained normal at the following examinations.

Edema which was evident at the first postoperative examination was stationary while radiographic recurrence progressed locally.

Recurrence was evident at the first postoperative examination in 39 of 42 patients, and in 3 patients whose first examination could not be evaluated at the second.

In the majority of patients the first repeat radiography was performed within 3 years after the primary operation, in most of them before one year. Five patients were examined 3 to 5 years and 3 patients 5 to 8 years after the operation.

In 7 patients of the 42 with recurrence the radiographic lesions were demonstrable 3 to 9 years be-

fore they had given any clinical evidence of recurrent disease. Consequently these patients during part of the observation period were cases belonging to the control group: radiographic recurrence. The difference between patients who passed from normal to recurrence (0 of 78, i.e. 0%) and patients who passed from radiographic recurrence to recurrence (7 of 11, i.e. 26%) is significant ($p < 0.001$).

Comparison between lesions in the new distal ileum and postoperative appearance of the colon. Postoperative lesions in the colon were of 3 types (Part III): submucosal edema, superficial fluctuant colitis, and clinical and radiographic recurrence. The two latter types are referred to as postoperative colitis. The postoperative appearance of the colon in patients with lesions in the new distal ileum appears in Table 3.

Postoperative colitis was recorded only in patients with recurrence in the distal ileum (13 of 29 patients, Table 3) while in patients with radiographic recurrence

Table 1

Relationship between the postoperative appearance of the new distal ileum and the preoperative distribution of the lesions. Figures in parentheses indicate the number of patients operated upon during the early and later periods: 1959-1968/1969-1973

Preoperative localization of lesions	Postoperative appearance of new distal ileum				Total No. of patients
	Normal	Edema	Radiographic recurrence	Recurrence	
Distal ileum/cecum	44	10	16	18	88
Distal ileum + right hemicolon	6		4	3	13
Distal ileum + colon	26			17	43
Colon	7			4	11
Total	78 (36/42)	10 (3/7)	20 (3/17)	42 (8/14)	150 (70/80)

Eight patients operated upon with resection of the distal ileum and the right hemicolon

Table 2

Radiologic follow up by small intestine examination

Postoperative appearance of new distal ileum	No. of patients	No. of examinations	First postoperative examination (mean No. of years)	No. of patients with multiple examinations	Radiologic follow up (mean No. of years)
Normal	78	169	1.3 (0.5-8)	63	6.7 (3-15)
Edema	10	36	1.1 (0.5-7)	8	6.6 (3-15)
Radiographic recurrence	20	87	1.2 (0.5-3)	18	5.4 (3-16)
Recurrence	42	84	1.8 (0.5-7)	34	2.9 (0.5-10)
Total	150	370			

ence or edema the postoperative colon was normal or had submucosal edema.

The operative procedures employed and the extent of disease at the time of operation must be considered in order to evaluate the figures in Table 3.

In 11 of 150 patients the entire or a great part of the colon was left behind at operation (Fig 1 A-E). Seven of these patients were operated upon with segmental resection of the ileum (A + D) and the remaining 104 with resection of the distal ileum and the right hemicolon (B + C + E).

Considering the presence or absence of postoperative ileitis and postoperative colitis in these 111 patients 4 groups could be distinguished:

(1) No evidence of postoperative ileitis or colitis (61 patients B + C + E). The distal ileum and right hemicolon had been resected.

(2) Postoperative colitis but no evidence of postoperative ileitis (1 patient E). The distal ileum and right hemicolon resected.

(3) Postoperative ileitis but no evidence of postoperative colitis (36 patients A-C). Segmental resection of the ileum (A) was performed in 5 patients (A), resection of the distal ileum and right hemicolon in 31 (B + C).

(4) Postoperative ileitis and postoperative colitis (13 patients B + D + E). Segmental resection of the ileum was performed in 2 patients (D), resection of the distal ileum and right hemicolon in 11 (B + E).

Thus all 7 patients operated upon with segmental resection of the ileum (A + D) had postoperative ileitis and 2 of them (D) also postoperative colitis. Both ileal and colonic lesions existed preoperatively. The patients were operated upon because of symptoms of small intestine obstruction and at op-

Table 3

Postoperative appearance of the colon related to postoperative lesions in the new distal ileum

New distal ileum	No of patients	Postoperative appearance of the colon			
		Normal	Submucosal edema	Postoperative colitis	
				Superficial colitis	Recurrence
Edema	10	7	3		
Postoperative ileitis					
Radiographic recurrence	20	17	3		
Recurrence	29	12	4	6	7
Total	59	36	10	6	7

eration only a stenotic segment of the aboral ileum was resected

Of 104 patients operated upon with resection of the distal ileum and the right hemicolon 42 had postoperative ileitis (B + C + E) and 11 of them also postoperative colitis (B + E). None of these 42 patients had any evidence of disease in the ileal segments left behind at operation while it was substantially proved (Part III) that the colonic lesions existed preoperatively in 10 of 11 patients. Moreover only one patient had postoperative colitis without postoperative ileitis (in group 2).

Thus in 12 patients a normal ileal segment was operatively connected with a colonic segment affected by colitis. In 11 of these patients (92%) evidently a linear extension of the lesions had developed over the anastomosis to the new distal ileum.

On the contrary 31 patients had a postoperative ileitis in segments that were anastomosed to a preoperatively normal colonic segment. None of these 31 patients had any evidence of postoperative colitis. Thus linear extension across an ileocolic anastomosis was significantly ($p < 0.001$) more frequent in oral than in aboral direction.

Postoperative appearance of the new distal ileum oral to an ileostomy. Colectomy proctocolectomy and ileostomy were performed in 39 of 150 patients. In 26 of these (67%) the new distal ileum had a normal radiographic appearance postoperatively while 13 patients (33%) had a recurrence.

In 10 of the 39 patients the length of the resected segment was shorter than 20 cm. Nine of these patients (90%) had recurrence which should be compared with 4 recurrences in 29 patients (14%) with resections longer than 20 cm. The difference is significant ($p < 0.001$).

Discussion

No generally accepted definition of recurrence of Crohn's disease has appeared. Most authors have used definitions similar to the one suggested by LENNARD-JONES & STALDER. Symptomatic relapse with evidence of recurrent disease at radiographic clinical examination or both. If this definition is accepted symptomatic relapse is required for the diagnosis, which cannot be made on radiographic findings only. However several authors have commented parenthetically on the existence of radiographic lesions compatible with recurrent disease in the new distal ileum of patients without symptoms of recurrence (ATWELL et coll. BRILL et coll. KRAUSE et coll. 1971).

Asymptomatic lesions in the new distal ileum. Lesions in the new distal ileum occurred in 10 asymptomatic patients: edema in 10 and radiographic recurrence in 20.

These lesions were probably not caused by the operative procedure per se as no abnormalities of these types were observed in the control group. However the resection was more extensive in patients with Crohn's disease than in the control material. The existence and appearance of these lesions may be explained in various ways.

They could be secondary to the resection of large segments of the distal ileum. If this is true the radiographic abnormalities should be regarded as representative of a chronic lymphedema caused by the operative procedure and particularly by the extensive dissection of the lymph nodes. The persistence of these lesions in the late period may speak in favour of this theory. During this period the surgical approach became more intensive and larger segments were resected than in the early period.

Another explanation could be that the disease was more widespread than could be diagnosed on operation and minor lesions were left behind. If this is true the question arises why the patients did not have any symptoms. One possible explanation is that patients with edema and radiographic recurrence represent cases of healed disease. The disease might have been brought under immunologic control after the surgical removal of the most severely involved segments.

However, most probably radiographic recurrence may be explained on the basis of individual variations in time between the appearance of radiographic lesions and symptoms. Considering the original disease this is well known. This explanation is further supported by the fact that 7 patients who initially were cases of radiographic recurrence during the observation period developed symptoms and consequently were transferred to the recurrence group. Moreover, a significant difference in frequency was found between the early and the late period considering both patients with radiographic recurrence and patients with recurrence. It is therefore most probable that some, if not all, of the patients who at the end of the observation period were considered to have radiographic recurrence in course of time will also develop symptoms. The numerical difference between radiographic recurrence and recurrence in the early and late period will then be equalized. This is in agreement with the observations of BRILL *et coll.* who found that all patients with radiographic evidence of recurrent disease finally also had clinical evidence.

In summary, it is most likely that radiographic lesions referred to as radiographic recurrence are manifestations of Crohn's disease. Edema should probably be looked upon as sequential to more extensive resections.

Radiographic and clinical recurrent disease. Most authors agree that in the majority of patients recurrence of the disease is clinically evident within 3 years postoperatively (BRILL *et coll.* FAHRLANDER & BAERLOCHER 1971 GREENSTEIN *et coll.* 1975). However, DE DOMBAL *et coll.* (1971) have suggested that there are two types of recurrent disease—one early and one late. This opinion is shared by other authors (MARSHAK) and is true also in the present series concerning clinical recurrence of the disease. However, the results indicate that morphologic abnormalities characteristic of recurrent disease are present shortly after operation, although some pa-

tients remain asymptomatic for several years. Radiographic lesions could be demonstrated at the first postoperative examination of the small intestine in all patients with recurrence during the observation period. Moreover, no patient with an initially normal postoperative small intestine examination had subsequent recurrence of the disease and these patients were followed for 3 to 16 years (mean 6.7 years). Thus, from a radiologic point of view, no late recurrences occurred in the present series. The vast majority of recurrences was early and all recurrences could be demonstrated at the first postoperative radiographic examination. These observations suggest that in the small intestine also recurrent disease is representative of persistent disease. The late recurrences described by DE DOMBAL *et coll.* are probably representatives of the same variations of development of postoperative lesions as are radiographic recurrences in the present series.

An early diagnosis of recurrent disease can evidently be made on radiographic findings only and will then include recurrence as well as radiographic recurrence, i.e. both late and early recurrences. Consequently, there should be no need for follow-up periods of 10 years or longer to evaluate the results of the surgical management. However, during the first postoperative years, it may be difficult to differentiate between edema and radiographic recurrence and to make a diagnosis of slight inflammatory lesions. This means that a period of about 3 years is probably required to obtain an adequate diagnostic accuracy.

Localization of the lesions. It is obvious that linear extension of the disease over an ileocolic anastomosis occurred only in oral direction (11 of 12 patients) but not in aboral direction. In 31 patients with postoperative ileitis the lesions were confined to the ileal side of the anastomosis. Reports on postoperative spread of disease from the ileum to the colon can probably be explained by colonic lesions being overlooked preoperatively and left behind on operation. At microscopic examination of resected specimens of those of the 31 patients who were operated upon for recurrent disease a sharp border line was found between the diseased and the non-diseased colon. This has also been noted by other authors and has not yet been explained. One possible explanation might be obtained from the theory of lymphatic spread and non-spread that was postulated in previous reports (Parts II, III).

It is also obvious that patients in whom less than

20 cm of the distal ileum were resected in conjunction with colectomy ran a significantly higher risk of developing recurrence than patients in whom the resected ileal segment was longer than 20 cm. In a previous report the possible inter relationship between the lymphatic drainage of the colon and the small intestine and the distribution of the disease was discussed. It was pointed out that especially in the ileocecal region an abundance of anatomic variants appears but that the most aboral 15 to 20 cm of the ileum often have a lymphatic drainage in common with the cecum and part of the ascending colon. Thus it is possible that recurrence in these patients was due to exacerbation of lesions left behind on operation or to retrograde spread of the disease from diseased lymph nodes. After operation for recurrence only one patient had a second recurrence.

In 7 patients resection of a short stenotic segment of the ileum was performed and all developed recurrence. At operation most probably the stenosis in itself and changes secondary to it made a proper evaluation of the surrounding parts difficult. Microscopic examination of the resected specimens revealed that the resections were not radical and postoperative radiologic examination within two months postoperatively showed profound inflammatory lesions. If isolated ileal strictures are located in the aboral segment of the ileum they should be regarded as part of a disease of the distal ileum until otherwise proved.

Prognostic considerations. Different statistical methods have been applied to the assessment of the surgical management. Expected recurrence rates of about 90 per cent have been reported using the actuarial method (GREENSTEIN *et coll.*)

However the validity of conclusions derived from any method is strongly dependent on the data basis. In most reports recurrence is dealt with as an entity and the preoperative extent of disease and the surgical radicalness have not been considered.

It is obvious from the results in the present and previous reports (Parts I, II, III) that proper calculations cannot be made without an intimate knowledge of the preoperative distribution of the lesions. When resections were performed on the basis of an erroneous diagnosis of the macroscopic extent of disease the result almost invariably was recurrence of the disease. In the colon it was proved that recurrence was due to exacerbation of the disease in segments left behind on operation. Most probably this is true also for recurrence in the new distal

ileum although for reasons discussed (Part I, II) it cannot be demonstrated with the same evidence as in the colon.

It is obvious that in 27 of the 42 patients in the present series who had recurrence the operation was not adequate. 5 patients with disease of the distal ileum and 2 patients with ileocolic disease were operated upon with segmental resection of the ileum. In 11 patients with disease of the ileum and the entire colon the distal ileum and the right hemicolon were resected and 9 patients with ileocolic or colic diseases were operated upon with colectomy and a resection of the distal ileum that was shorter than 20 cm.

The results in the present and a previous report (Part III) indicate that the risk for these 27 patients to develop recurrence would have been far less if a more adequate type of operation had been carried out.

It should also be mentioned that in several of the remaining 15 of 42 patients with recurrence microscopic examination revealed inflammatory lesions on the surface of resection (this will be accounted for in detail in a separate report).

Statistical methods have not yet been applied to the results of the present series for calculation of recurrence rates. This will be done when the clinical review of the patients is completed. However without using statistics the results indicate that of the 150 patients (Fig. 1) 87 with no radiographic evidence of recurrent disease run a low risk of developing recurrence. Moreover several of the patients who were reoperated upon for recurrence have had no radiographic evidence of a second recurrence.

The results in this series of reports should not be understood as a recommendation for unetical use of resectional procedures. However as long as medical treatment is as disappointing as it is today and most patients sooner or later appear for surgical management continued evaluation of surgical methods is essential. It is obvious that some patients preferably should be conservatively managed and surgical intervention be reserved for complications of the disease.

In most patients however resectional procedures may be used with good results provided a careful preoperative and operative evaluation of the disease has been performed.

SUMMARY

Postoperative films of 150 patients operated upon for Crohn's disease were reviewed with regard to postopera-

abnormalities in the new distal ileum. The lesions are always located in the most aboral part of the ileum. Patients with persistent colonic disease: the ileal lesions are apparently the result of a spread of colonic lesions. Many of the remaining patients there was strong evidence that recurrent disease was representative of persistent disease.

REFERENCES

- THIEL J D, DUTHIE H L and GOLIGHER J C. The outcome of Crohn's disease. *Brit J Surg* 52 (1965) 966.
- BARBER JR K W, WAUGH J M, BEAHR O H and SAUER W G. Indications for and the results of surgical treatment of regional enteritis. *Ann Surg* 156 (1962) 479.
- KILL C H, KLEIN S F and KARK A E. Regional enteritis and enterocolitis. A study of 74 patients over 15 years. *Ann Surg* 170 (1969) 766.
- HÉRICIE E, MONNIER J P et DONELLI G. Les aspects radiologiques de récurrences de l'ileo-colite granulomateuse. *Ann Radiol* 16 (1973) 433.
- OLCOCK B P and VANSANT J H. Surgical treatment of regional enteritis. *New Engl J Med* 262 (1960) 435.
- DE DOUBAL F T, BURTON I and GOLIGHER J C. Recurrence of Crohn's disease after primary excisional surgery. *Gut* 12 (1971) 519.
- ÅHLANDER H and BAERLOCHER CH. Clinical features and epidemiological data in the Basle area. In: *Regional enteritis (Crohn's disease)*. Skandia International Symposia p 131. Edited by A. Engel and T. Larsson. Nordiska Bokhandels Forlag, Stockholm 1971.
- GREENSTEIN A J, SACKARD B, PASTERNAK B S and JANOWITZ H D. Reoperation and recurrence in Crohn's colitis and ileo colitis. Crude and cumulative rates. *New Engl J Med* 293 (1975) 685.
- HILDELL J, LINDSTROM C and WENCKERT A. Radiographic appearances in Crohn's disease. I. Accuracy of radiographic methods. *Acta radiol. Diagnosis* 20 (1979) 609.
- — — Radiographic appearances in Crohn's disease. II. The course as reflected in repeat radiography. *Acta radiol. Diagnosis* 20 (1979) 933.
- — — Radiographic appearances in Crohn's disease. III. Colonic lesions following surgery. *Acta radiol. Diagnosis* 21 (1980) 71.
- KRAUSE U, BERGMAN K and NORLÉN B. Crohn's disease: a clinical study based on 186 patients. *Scand J Gastroent* 6 (1971) 97.
- LENNARD-JONES J F and STALDER G A. Prognosis after resection of chronic regional ileitis. *Gut* 8 (1967) 332.
- MARSHAK R H. Granulomatous disease of the intestinal tract (Crohn's disease). *Radiology* 114 (1975) 3.
- NUGENT F W, VEIDENHEIMER M C, MEISSNER W A and HAGGITT R C. Prognosis after colonic resection for Crohn's disease of the colon. *Gastroenterology* 65 (1973) 398.
- SCHOFIELD P F. The natural history and treatment of Crohn's disease. *Ann roy Coll Surg Engl* 36 (1965) 258.
- STAHLGREN L H and FERGUSON L K. The results of surgical treatment of chronic regional enteritis. *J Amer med Ass* 175 (1961) 986.
- VAN PATTEN W N, BARGEN J A, DOCKERTY M B, FELDMAN W H, MAYO C W and WAUGH J M. Regional enteritis. *Gastroenterology* 26 (1954) 347.
- WALLÉN S. Results of surgical treatment in Sweden. In: *Regional enteritis (Crohn's disease)*. Skandia International Symposia p 177. Edited by A. Engel and T. Larsson. Nordiska Bokhandels Forlag, Stockholm 1971.
- WENCKERT A. In discussion with Goligher, Oberhelman and Wallén. In: *Regional enteritis (Crohn's disease)*. Skandia International Symposia p 208. Nordiska Bokhandels Forlag, Stockholm 1971.

ARTHROGRAPHIC DIAGNOSIS OF RUPTURED CALCANEOFIBULAR LIGAMENT

II Clinical evaluation of a new method

M VUUST and B NIEDERMANN

Supination trauma of the ankle joint may cause various lesions. A slight trauma may cause injury to the soft tissue alone. In cases of more severe distortions rupture of the capsule of the antero-lateral aspect of the tibiotalar joint may occur as well as rupture of the lateral ligaments. The anterior talofibular ligament ruptures first. If the supination movement continues also the calcaneofibular ligament ruptures. Isolated rupture of the latter ligament is extremely rare (PRINS 1979). Finally in severe cases rupture of the posterior talofibular ligament occurs in addition.

Surgical treatment of the more severe cases of ankle joint distortions has been increasingly used in the past which makes an accurate diagnostic method necessary. It seems difficult to compare the results in previous reports partly because of different diagnostic methods and partly because of the inaccuracy of these methods. PRINS regarded the combined rupture of the anterior talofibular and the calcaneofibular ligament as a major lesion whereas the isolated rupture of the anterior talofibular ligament was regarded as a minor lesion with no need for surgery. Therefore the exact diagnosis of these two ligament ruptures is important.

In the previous report by VUUST (Part I) the use of an oblique axial projection in arthrography of the ankle has been introduced. Criteria were proposed for distinction between ruptures of the anterior talofibular ligament and rupture of both lateral ligaments and these criteria were confirmed on experimental post mortem lesions. The present report

evaluates these criteria in a clinical series comparing their validity to those of other arthrographic criteria.

Material and Method

During a four month period 19 patients (12 men, 7 women) aged between 16 and 54 years (average 31) with ankle distortions were operated upon for ruptured lateral ligaments of the talocrural joint. All patients with sprained ankles admitted to the hospital in this period were clinically evaluated. If rupture of the lateral ligaments was suggested an arthrography was performed within 24 hours after the trauma. If the arthrography revealed a leakage of contrast medium on the antero-lateral aspect of the talocrural joint an oblique axial film was included.

Surgery was performed in cases of suggested rupture of both lateral ligaments. A uniform evaluation of the lesions was secured as only cases operated upon by the same surgeons are included in the material. This selection is random and thus the material may be regarded as consecutive.

Arthrography was performed by injection of 6 ml meglumine iohalamate (Conray meglumin 282) and 2 ml of 2 per cent Leostesin antero-medially in the talocrural joint followed by passive movements of the ankle.

The projections used were antero-posterior, later



Fig. 1. Partial rupture of the calcaneofibular ligament. Percy type II with contrast medium mainly situated anterior to the lateral malleolus. On the a.p. film (a) the contrast filled peroneal sheath

(→) is visible. Contrast medium in the malleolar fossa and around the tip of the fibula (++) on the oblique axial film (c) indicating rupture of the calcaneofibular ligament.

al and antero posterior with the foot rotated 20° laterally and medially. Furthermore, an oblique axial exposure was used as described in Part I. It should be emphasized that an exact projection is necessary for the accurate diagnosis. In order to demonstrate the reproducibility of this projection in the daily routine, the radiologic author did not perform any of the arthrographies included in the present series.

Diagnostic criteria. Two different types of criteria were used to indicate a rupture of the calcaneofibular ligament. Either a type III arthrographic finding according to PERCY et coll. (1969) or a contrast leakage on the oblique axial film using the criteria defined in Part I.

Filling of the peroneal sheath was not used in this series as an indicator of rupture of the calcaneofibular ligament preoperatively. However, in a retro-

spective evaluation, it was compared with the other criteria mentioned (Table).

Operation. At the operation a J shaped incision was made anterior to and beneath the lateral malleolus. The peroneal sheath was opened in order to obtain a precise estimation of the extension of the lateral ligament lesion. The posterior talofibular ligament was not inspected.

Results

A rupture of the calcaneofibular ligament was diagnosed correctly in all 19 cases.

At operation, rupture of both the anterior talofibular ligament and the calcaneofibular ligament was found in all 19 patients. In 13 patients both ligaments were totally ruptured, while in 6 patients the rupture of the calcaneofibular ligament was partial and combined with a total rupture of the anterior talofibular ligament. The antero posterior and lateral films were evaluated using the criteria of PERCY et coll. without knowledge of the results from the oblique axial film. The diagnostic results using the oblique axial exposures are significantly better than the two other criteria (χ^2 test $p < 0.01$, Table).

All cases without filling of the peroneal sheath had a rupture of the sheath at operation.

Discussion

The oblique axial projection is more difficult to perform than the standard projections. Nevertheless, in the present series it was possible to use this

Table

Relationship between arthrographic criteria and findings at operation

	Isolated rupture of the anterior talofibular ligament	Rupture of both lateral ligaments
Criteria of Percy	9	10
Contrast filling of the peroneal sheath	5	14
Oblique axial film	0	19
Ruptures found at operation	0	19



Fig 2 Partial rupture of the calcaneofibular ligament Percy type III with contrast medium mainly situated lateral to the malleolus no filling of the peroneal sheath Two tongues of contrast

medium the medial one indicating ruptured calcaneofibular ligament on the oblique axial film (c) Position of the ligament between arrows



Fig 3 Total rupture of the calcaneofibular ligament No filling of the peroneal sheath Ruptured calcaneofibular ligament on the

oblique axial film (c) Nearly identical appearance of contrast medium as in Fig 2c

Projection in the daily routine without special experience and with a high diagnostic accuracy.

No patients were operated upon if only an isolated rupture of the talofibular ligament was suggested. No direct conclusions can therefore be drawn as to the possibility of a false normal calcaneofibular ligament (i.e. a ruptured ligament not indicated at arthrography). However, since the diagnostic accuracy of the criteria of PERCY et coll

in the present series equals that of the series of LINDHOLMER et coll (1978) where all cases with possible lateral ligament ruptures were operated upon, it can indirectly be concluded that an erroneously normal ligament based on the oblique axial film does not play a major role.

However, after this series had been concluded one erroneous diagnosis occurred. In a patient with a total rupture of the anterior talofibular and the

calcaneofibular ligament the arthrographic finding was that of a Percy type III. On the oblique axial exposure a leakage was observed lateral to the malleolus but the contrast medium in the malleolar fossa had a well defined straight border at the position of the calcaneofibular ligament which consequently was assumed to be intact. The reason for this finding is not known but it might be caused by too few passive movements after the injection of the contrast medium.

The appearance of the leakage described in Part I (VUUST) corresponded to what occurred in the clinical series (Figs 1, 2, 3). It is possible to distinguish the contrast medium that extends around the lateral aspect of the malleolus from that situated beneath and medial to the tip of the fibula in the malleolar fossa. Only the latter indicates a rupture of the calcaneofibular ligament.

Filling of the peroneal sheath was a better criterion on rupture of the lateral ligaments than the extension of the contrast medium on the antero-posterior and lateral films: the correct diagnosis was 74 per cent. This figure is not absolute since peroneal filling was not used preoperatively as an indicator of the calcaneofibular ligament rupture. The result is in agreement with that of SPIEGEL et coll (1975), STAPLES (1975), LINDHOLMER et coll and PRINS. However, BROSTRÖM et coll (1965) found that such a filling was a reliable criterion for the calcaneofibular ligament rupture. In the present series no filling

of the peroneal sheath occurred in 5 cases despite rupture of the sheath found at operation.

SUMMARY

The validity of a new criterion for the arthrographic diagnosis of rupture of the calcaneofibular ligament is compared to that of other arthrographic criteria in a clinical series. The new criterion is found to be more reliable than those previously used.

REFERENCES

- BROSTRÖM L, LILJEDAHN S-O and LINDVALL N (1965) Sprained ankles. II. Arthrographic diagnosis of recent ligament ruptures. *Acta chir scand* 179 (1965) 485.
- LINDHOLMER E, FOGED N and JENSEN J TH (1975) Arthrography of the ankle. Value in diagnosis of rupture of the lateral ligaments. *Acta radiol Diagnosis* 19 (1975) 585.
- PERCY E C, HILL R O and CALLAGHAN J E (1969) The sprained ankle. *J Trauma* 9 (1969) 972.
- PRINS J G (1979) Diagnosis and treatment of injury to the lateral ligament of the ankle. A comparative clinical study. *Acta chir scand* (1979) Suppl. No. 486.
- SPIEGEL P K and STAPLES O S (1975) Arthrography of the ankle joint. Problems in diagnosis of acute lateral ligament injuries. *Radiology* 114 (1975) 587.
- STAPLES O S (1975) Ruptures of the fibular collateral ligaments of the ankle. *J Bone Jt Surg* 57 A (1975) 101.
- VUUST M (1980) Arthrographic diagnosis of ruptured calcaneofibular ligament. I. A new projection tested in experimental injury post mortem. *Acta radiol Diagnosis* 21 (1980) 123.

NUMERICAL ASSESSMENT OF ASYMMETRY AT SCINTIGRAPHY OF NORMAL JOINT PAIRS WITH $^{99}\text{Tc}^m$ POLYPHOSPHATE

M NØRBJERG J HEERFORDT I DISSING M JENSEN
J MØLLER and O SNEPPEN

The normal $^{99}\text{Tc}^m$ polyphosphate scintigram is usually described as being symmetric (CHARKES et coll 1973 CITRIN 1977). Only in a few reports has attention been paid to non pathologic asymmetry in articular accumulation of tracer. THRALL et coll (1974) noted asymmetry in the shoulder region in 19 of 150 patients. In 17 of these 19 cases the uptake was higher in the right shoulder. Similar but less marked differences have been found in the hips and knees. GENOE & MOELLER (1974) observed a few cases of asymmetric accumulation in otherwise normal shoulders and MERRICK (1975) found that the shoulder of the dominant side often has a higher uptake. SEBES et coll (1976) found right sided preponderance in the shoulders of 30 of 100 right sided patients and left sided preponderance in only 5 of the same group.

All these reports have been based solely upon visual evaluation of the scintigrams. As numerical assessment enables a more exact graduation such an analysis of the symmetry in some non pathologic joints was considered to be of interest. It was performed in retrospect.

Method

Scintigraphy using a 5 inch (12.5 cm) dual probe whole body rectilinear scanner with video-display processor (Elscent) was carried out 2 to 2½ hours after the administration of 444 MBq (12 mCi) $^{99}\text{Tc}^m$ polyphosphate. Particular care was taken in cor-

rect positioning of the patients in order to avoid position dependent asymmetries. The images were stored on magnetic tape for later numerical analysis on the video-display unit. Each joint was framed and the total number of counts within the frame was read on a numerical display. For each pair of joints a ratio was calculated if the number of counts was higher in the right joint the ratio was defined as pointing to the right and vice versa.

Statistically the number of counts within each frame was assumed to follow a Poisson distribution. The standard deviation (SD) of the ratio (R) is

$$SD = R \times \sqrt{\frac{1}{x} + \frac{1}{y}}$$

where x is the number of counts in the frame of one side and y the number of counts in the other frame. The ratio is said to point significantly to the right or left if $R - SD > 1$.

Material

The material comprised all recorded cases of $^{99}\text{Tc}^m$ polyphosphate bone scintigraphy in patients from this orthopaedic department during the period 1973 through 1977 excluding (1) images not technically suitable for numerical analysis (2) images with asymmetric positioning of the patients and (3) images from patients with systemic diseases such as rheumatoid arthritis osteoporosis etc.

Table
Right/left variation in joint regions

Joint pair	Ratio pointing significantly to right		Ratio pointing significantly to left		Ratio not significantly deviating from 1		Total	
	No	Per cent	No	Per cent	No	Per cent	No	Per cent
Shoulder	137	51	46	18	82	31	260	100
Sacroiliac	132	32	77	19	205	49	414	100
Knee	99	40	67	27	83	33	249	100
Ankle	65	30	51	24	98	46	214	100
Tarsus	67	32	43	20	101	48	211	100
Total	495	37	284	21	569	42	1348	100

A total of 534 images remained for analysis: some of these included only a few or a single pair of joints.

It is well known that a focal osseous lesion may entail increased tracer accumulation not only locally but also diffusely in the affected bone and possibly also in the adjacent joints (THRALL *et coll.* 1974, 1975, BESSLER 1975, GOLDMAN & BRAUNSTEIN 1976, PFANNENSTIEL & SFIMMLER 1977). Therefore from these 534 bone images the joint regions in the vicinity of a focal bone lesion were excluded. Thus a focal lesion of one tibia excluded the knee and ankle regions etc. Hip joints were excluded as by the method used it was impossible to avoid superimposition of the pelvis. Elbow and wrists were also excluded as the relatively low count rate in these regions induced larger errors in the calculation of the ratio.

After this further selection the 534 images include 1348 joint pairs suitable for evaluation of non-pathologic asymmetry (Table).

Results

In the material as a whole a significant right-sided dominance was evident in 37 per cent, a significant left-sided dominance in 21 per cent and an apparently symmetric accumulation in 42 per cent (Table). In shoulder and knee images asymmetric distribution was relatively frequent (about 70%) as compared with that in the sacroiliac, ankle and tarsal joints (about 50%).

The frequency of a significantly right-pointing ratio was highest in the shoulder joints (51%), somewhat lower in the knees (40%) and still lower in

the remaining joints. The distribution of the cases by the size of the ratio is presented in the Figure which demonstrates not only a majority with a right-pointing ratio but also among these cases a relatively large number with a marked deviation of the ratio.

Discussion

The most common source of asymmetric scintigraphic delineation of corresponding joint regions in normal individuals is no doubt an asymmetric positioning of the patient by exclusion of images from asymmetrically positioned patients. The asymmetries in the present series are assumed to reflect actual right/left variations in tracer distribution.

On the whole the asymmetries were rather small, the mean value of significant ratios being around 1.10 to 1.25 and in a large number of cases not convincingly assessable visually. This may be the explanation for the higher frequency of asymmetry in the present series as compared with previous reports (THRALL *et coll.* 1974, SEBES *et coll.*). The former authors encountered asymmetry more often in the shoulders than in the knees. This agrees with the present results: the most common asymmetric distribution occurring in shoulder joints, the next most common in knee joints and the least common in the sacroiliac, ankle and tarsal joints.

Unrecognized wear and tear phenomena have previously been suggested as a predominant cause of increased accumulation of tracer in non-pathologic joints (SEBES *et coll.*). In the knee joint in particular this is a conceivable cause of asymmetry. Otherwise the reason for the asymmetry

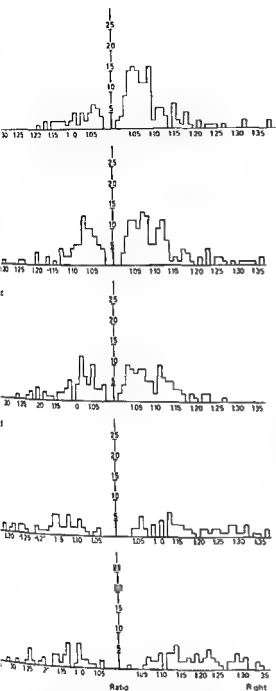


Figure 1. Distribution of asymmetry according to the ratio. Only ratios significantly deviating from 1 are included. a) Shoulder b) sacroiliac c) knee d) ankle and e) tarsal joints

especially for the increased accumulation in the right sided joints has mainly been attributed to side dominance (MERRICK JAJIĆ et coll 1978 SEBES et coll). A generally less marked increase in right sided accumulation in the joints of the lower limbs (FRALL et coll 1974) might then be ascribed to the stress being more uniform in the lower than in the upper limbs.

The lower frequency of asymmetry in the ankle and tarsal joints in the present series may be ascribed to the relatively greater measurement error in these ratios due to fewer counts in these regions. The similarly lower frequency of asymmetry in the sacroiliac joints must be viewed in the light of superimposition of a considerable soft tissue layer on the osseous tissue tending to mask a possible side difference in osseous distribution.

Conclusion In visual assessment of bone scintigraphy images slightly asymmetric distribution can hardly lead to erroneous evaluation but if the accumulation is to be evaluated more objectively numerical analysis is necessary (BAUER 1975 SNEP PEN et coll 1978). For diagnostic application of such numerical assessment normal ranges of physiologic asymmetry must be defined based upon anatomic regions and possible side dependent variations.

SUMMARY

Numerical analysis of ^{99m}Tc polyphosphate distribution in 1348 selected non pathologic joint pairs revealed a significantly higher right sided accumulation in 37 per cent a left sided dominance in 21 per cent and no significant side difference in the remaining 42 per cent. The most common level of asymmetry was the shoulder joint.

ACKNOWLEDGEMENTS

This investigation was supported by the King Christian X's the S. Andersen's the E. Celinder's the P. C. Petersen's and the J. Weimann's Foundations and by the Danish Medical Research Council project No. 512 3293.

Request for reprints: Dr Inger Dissing, Tirsbækvej 6, DK 2720 Vanløse, Denmark.

REFERENCES

- BAUER G. Progress in the use of radionuclides in orthopaedics. *Acta orthop scand* 46 (1975) 315.
- BESSLER W. Die Skelettszintigraphie Ihre diagnostischen Möglichkeiten und Indikationen im Vergleich zur Röntgenuntersuchung. *Schweiz med Wschr* 105 (1975) 175.
- CHARKES N. D. VALENTINE G. and CRAVITZ B. Interpretation of the normal ^{99m}Tc polyphosphate rectilinear bone scan. *Radiology* 107 (1973) 563.
- CITRIN D. L. Problems and limitations of bone scanning with the ^{99m}Tc phosphates. *Clin Radiol* 28 (1977) 97.
- GENOE G. A. and MOELLER J. A. Normal shoulder variations in the technetium 99m polyphosphate bone scan. *Sth med J* 6 (1974) 659.
- GOLDMAN A. B. and BRAUNSTEIN P. Augmented radioac-

- tivity on bone scans of limbs bearing osteosarcomas *J nucl Med* 16 (1976) 423
- JAJIĆ I LELČIĆ I and SCHWARZWALD M Detection of preosteoarthritic condition of the knee joint in professional drivers with ^{99m}Tc polyphosphate *Scand J Rheum* (1978) Suppl No 8 p 16
- MERRICK M V Review article Bone scanning *Brit J Radiol* 48 (1975) 327
- PFANNENSTIEL P und SEMMLER U Stellenwert der Gelenk- und Knochenszintigraphie bei benignen Skeletterkrankungen *Med Welt* 28 (1977) 73
- SEBES J I VASINRAPEE P and FRIEDMAN B I The relationship between radiographic findings and asymmetrical radioactivity in the shoulder *Radiology* 127 (1976) 139
- SNEPPEN O HEERFORDT J DISSING I JENSEN M MØLLER J and NØRBJERG M Numerical assessment of bone scintigraphy in primary bone tumors *J Bone Jt Surg* 60-A (1978) 966
- THRALL J H GESLIEN G E CORCORAN R J and JOHNSON M C Abnormal radionuclide deposition patterns adjacent to focal skeletal lesions *Radiology* 115 (1975) 659
- GHAEDELN GESLIEN G E PINSKY S M and JOHNSON M C Pitfalls in Tc^{99m} polyphosphate skeletal imaging *Amer J Roentgenol* 121 (1974) 739

CONTRAST MEDIA FOR COMPUTER TOMOGRAPHY OF THE LIVER

O. H. WEGENER, W. MUTZEL and R. SOUCHON

Computer tomography has not rendered contrast media redundant. Two well proven groups of substances are available for the intravenous injection of ionic contrast media: urographic and cholegraphic. The rational use of these media in abdominal computer tomography is now reported based on experiences from a clinical series, animal and phantom experiments.

Material and Method

An EMI CT 5005/12 general purpose scanner with scanning time of 20 seconds was used. With an image matrix of 320×320 the SD of a standardized water phantom was 1.6 per cent, i.e. ± 8 EU (EMI units). $1 \text{ EU} = 2$ Hounsfield units (HU). The animals were scanned at 120 kV and the patients at 140 kV.

Phantom experiment. A plexiglass phantom (Fig. 1) with a diameter of 18 cm with cylindric boreholes of varying diameters was scanned using a field size of 25 cm. The image of the boreholes with a scanning field size of 32.0 cm diameter would correspond to an object diameter of 1.28 to 60 mm. By variation of the photomultiplier tension the SD of the individual dots of the image was varied from the optimum of 1.5 to 63 EU. For one measurement series a potassium iodide solution was introduced at varying concentrations. An additional homogeneity correction for plexiglass was performed (wedge correction) in order to reduce shading within the phantom.

Clinical series. Volunteers without any clinically known liver disease were selected. The level of the section was determined before the injection of the

contrast medium in order to avoid motion artefacts roughly at the level of the phrenico-costal sinus. The contrast medium was injected as a bolus within one minute. This layer of the liver was scanned at preselected intervals up to 120 min after the injection. During the scan, blood samples were taken in order to determine the iodine plasma level. The doses were 0.4, 0.6 and 0.9 g I/kg body weight as meglumine diatrizoate.

Evaluation. An area of at least 2000 volume elements was selected and the mean value (with SD) determined for the entire series. The central cylinder representing the aorta was exactly fixed using a special program and the attenuation measured. The iodine content of the blood samples was determined according to Sandell-Kolthoff by means of the Technicon Autoanalyser.

Animal experiments were performed in the dog (beagle). Intubation was carried out under phenobarbital sodium anaesthesia and relaxation obtained with succinylcholine chloride. The anaesthesia was continued with nitrous oxide. During the 20-second scan, breathing was suspended on expiration.

Dosage: cholegraphic medium. meglumine iotroxinate (Biliscopin) 70 mg/kg body weight intravenously; urographic media: (1) meglumine diatrizoate (Angiografín), (2) meglumine ioglycinate (Rayvist), (3) SH H 340 AB (non ionic), (4) CT 345 and (5) CT 346 (the last development preparations of Schering AG, Berlin, Bergkamen) for bolus technique 360 mg I/kg body weight was used and for infusion 50 mg I/min/kg body weight intravenously.

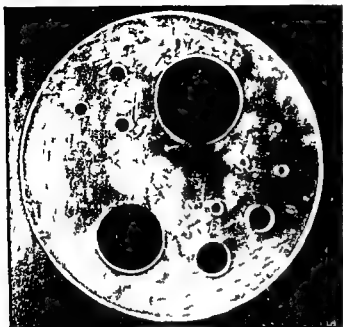


Fig 1



Fig 2a

Fig 1 Plexiglass phantom with cylindrical boreholes of various sizes

Fig 2 CT section through dog liver: a) Before and b) after injection of contrast medium. The evaluation field appears in (b)

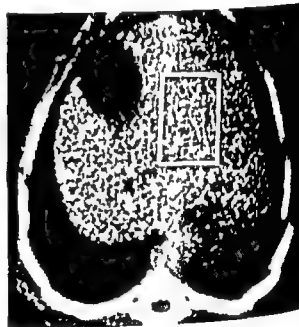


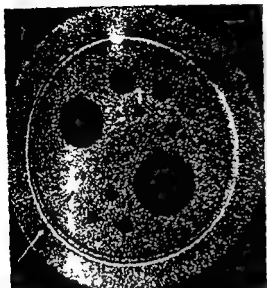
Fig 2b

The same section of the liver as in the clinical series was scanned at preselected intervals and the attenuation measured over the same area for the entire series (at least 1 000 volume elements: Fig 2)

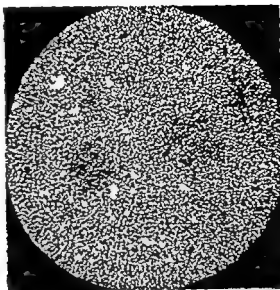
Basic considerations

A high attenuation resolving power of the computer tomography and enhancement of the differences in tissue attenuation by means of contrast media are prerequisites for diagnosing small lesions or those with a similar attenuation to that of the surrounding tissue. It is the high attenuation resolving power of computer tomography that gives it an advantage over conventional radiography. It is described by

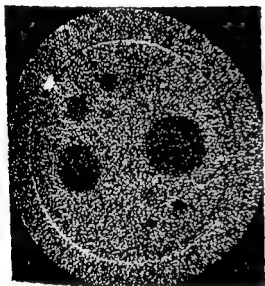
Fig 3 Computer tomography of the plexiglass phantom at various standard deviations (noise) of the image elements. Boreholes filled with water. Even the smallest borehole (1.25 mm in diameter) is detectable (→). A detail with a diameter of 10 mm (←) SD ± 3 EU. b-f) Contrast 19 EU. As the SD falls the smaller boreholes also become visible. b) SD ± 63 EU. c) SD ± 41 EU. d) SD ± 13 EU. e) SD ± 7 EU. f) SD ± 3 EU.



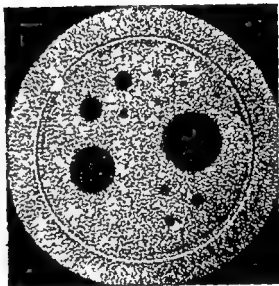
a



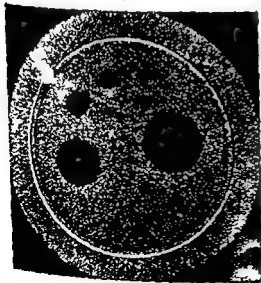
b



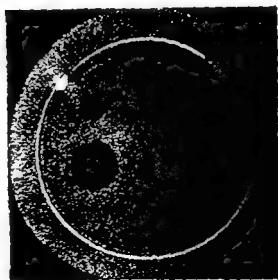
c



d



e



f

Fig 3 (For legend see opposite page)

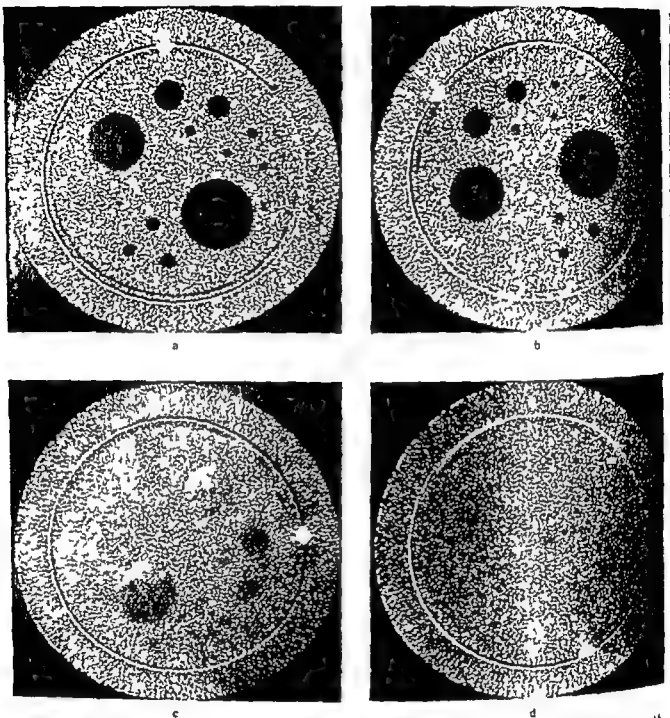
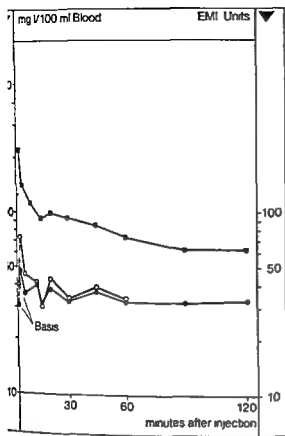


Fig. 4. Computer tomography of the plexiglass phantom at different contrasts. SD at ± 13 EU corresponds to in vivo values over the human liver. Not until the contrast is 19 EU (1.5 times SD) are

details down to 6 mm in diameter easily visible. Contrast in EU: a) 19 EU, b) 19 EU, c) 9 EU, d) 1 EU.

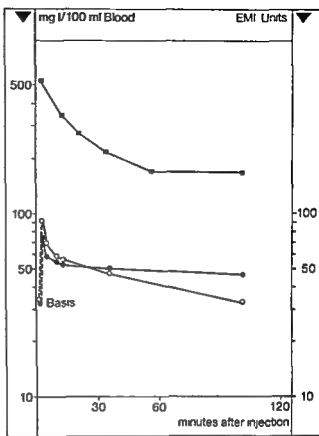
the SD of the individual dot in the image around a mean value, the attenuation value of a homogeneous material. These fluctuations appear on the image as noise and are caused by variation of the photon flux and the signal processing. Fig. 3 shows how increasing noise is accompanied by an obvious reduction in the visibility of small zones of lesser attenuation. In order to improve visibility the noise must be reduced

or the radiation dose increased. Due to the smaller radiation volume and the usually higher radiation dose, the SD of the individual dots of the image of a cranial scan is considerably smaller (about 5 times) than in the whole body field (Fig. 3c-f). However, limits to increase the radiation dose obviously exist. For this reason, the attenuation differences are enhanced using contrast media. This raises the ques-



a

5 Blood level and enhancement of liver and aorta after intravenous injection of a) 0.4 g/kg bw ($t_{1/2}$ 112 min) and b) 0.9 g/kg bw as meglumine diatrizoate ■ Blood ○ Aorta ● Liver



b

of how much such an enhancement is desirable is reasonable

The phantom experiments show that even in the presence of considerable noise larger areas are still demonstrable when small ones have already disappeared. Higher contrast alone can demonstrate small zones of lesser attenuation down to a diameter less than 1 cm. Thus for computer tomography in general radiology detail contrast diagrams can be produced. The question of the enhancement detected is at the same time a question of the size of the lesion to be detected. The competing procedures—ultrasound and scintigraphy—set the criterion if computer tomography is to be better than these it would be able to demonstrate lesions with a diameter less than 1 cm.

Under routine conditions (20 s scanning time, image matrix 320×320) an SD of 12 ± 2 EU is obtained in the area of the liver. Areas less than 1.0 cm in diameter can hardly be detected (Fig. 4c) and those of 1.2 to 1.6 cm in diameter are only just detectable if the attenuation difference to the surrounding area

is somewhat less than 1 SD (9 EU). Only a contrast of 1.5 SD (19 EU) can reliably demonstrate the areas of lesser attenuation down to a diameter of 6 mm.

This phantom experiment can only serve as a basis for estimation since it is not unconditionally transferrable to the demonstration of the liver in vivo. The reasons for this are as follows.

A background of optimum homogeneity can be obtained which is impossible in the liver having morphologic structures such as the vena porta system. Moreover, even small artefacts can influence the detectability in the borderline area.

The holes in the phantom are punched out with sharp edges giving optimum contrast. The lesions in the liver are not sharply defined and have irregular outline. A metastasis can approximately be compared with a small sphere.

The cylindric form of the holes furthermore prevents the partial volume effect which may arise in the liver in all lesions smaller than twice the width of the layer.

Since the conditions for obtaining an image in vivo

Table

Dose dependent enhancement over the base values of aorta and liver in EU after bolus injection of meglumine diatrizoate

Dose (g l/kg b.w.)	Aorta			Liver		
	7 min	9 min	20 min	2 min	9 min	20 min
0.4	49	72	15	16	13	8
0.4	32	3	3	16	11	6
0.6	35	23	19	19	18	15
0.6	51	18	20	26	22	17
0.6	38	20	16	72	13	11
0.9	78	32	31	41	20	20
0.9	57	25	(17)	43	21	16

are less favourable a contrast of at least 2 SD between pathologic and normal tissue is obviously necessary. Thus an enhancement necessary to make a lesion with a diameter of 1 cm visible against the surrounding tissue of similar attenuation must amount to at least twice the SD. Admittedly parenchymal lesions of large areas in theory require smaller quantities of contrast medium in order to be detected in practice, however superimpositions of artefacts actually call for higher enhancement.

Results

Clinical series

A chronologic representation of two typical developments of the attenuation values over the liver and aorta (blood) after bolus injection of 0.4 and 0.9 g l/kg meglumine diatrizoate appears in Fig. 5.

Immediately after the injection the values over aorta and liver fall more steeply than later on. Higher dosages show most clearly the different rates of fall in the enhancement of liver tissue and blood (aorta). The aortic values, which are at first higher than those of the liver, fall below the latter after about 15 min (Fig. 5b). The uneven course of the attenuation curves in Fig. 5a is due to artefacts and hardly shows the intersection of the two curves.

The Table gives the position for three time intervals (2, 9 and 20 min) for the three dosages selected (0.4, 0.6 and 0.9 g l/kg body weight); the following common features can be deduced:

Higher dosages produce higher initial and higher long term enhancement. A higher dosage has the strongest effect on both liver and aorta during the

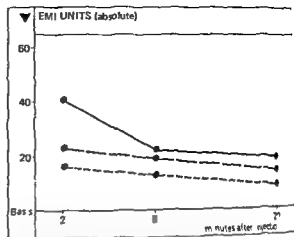


Fig. 6 Enhancement of the liver at 2, 9 and 20 min after bolus injection of meglumine diatrizoate dependent upon the administered dose applied: 0.4 — 0.6 and — 0.9 g l/kg b.w.

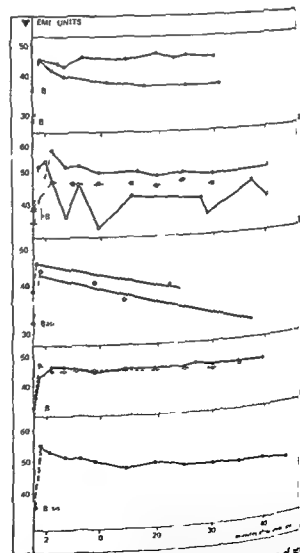


Fig. 7 Enhancement of dog liver after bolus injection of a) meglumine diatrizoate, b) meglumine iopizolate, c) contrast medium SH 340 AB 11, 65 and 89 min; d) CT 346.

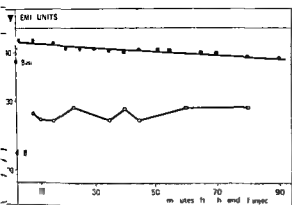


Fig. 8 Enhancement of dog liver after intravenous injection of meglumine iotroxinate t_1 about 10 h

first minutes after injection 40 EU at 0.9 g I/kg body weight compared with 16 EU at 0.4 g I/kg body weight. After 9 min the enhancements of the different dosages approach each other, lying between 11 and 22 EU (Fig. 6).

The iodine plasma level has decreased to half the initial one at 92 min (± 29) and corresponds then to that of the attenuation values over the aorta at 120 min (± 70). The enhancement over the liver lasts 2 to 3 times as long.

The results of the phantom experiments may be concluded as follows for practical use.

According to dosage the enhancement is below the value of twice the SD of the individual dot in the image, i.e. 25 EU, between 2 and 9 min after the bolus injection.

Animal experiments

Bolus injection of urographic media. The decrease in enhancement for various contrast media appears in Fig. 7. The curves allow the following conclusions:

At 5 to 15 EU the enhancement with all urographic media is of the same order of magnitude.

Due to the differences between the curves caused by artefacts neither the half life of meglumine diatrizoate nor that of meglumine ioglycinate can be determined with certainty, but it is at any rate less than 700 min.

The half life of the non ionic contrast medium SH H 340 AB at 65 min and 89 min is definitely shorter than that of the ionic contrast media.

The CT 345 and CT 346 contrast media at present under development have a very slow decrease in enhancement. Of the two the diiodized form (CT

346) produces a somewhat higher (initial) enhancement.

Bolus injection of a cholegraphic medium (meglumine iotroxinate). At the normal human dose of 0.07 g I/kg body weight a maximum enhancement of 8 EU was obtained (Fig. 8).

Bolus injection of cholegraphic plus urographic medium. The sequential application of meglumine iotroxinate and meglumine diatrizoate (same dosages as before) leads for a short period to a maximum enhancement of 18 EU (Fig. 9). The two components work on the whole additively. The mixing of meglumine iotroxinate and meglumine ioglycinate resulted in a slightly lower contrast of the liver tissue, 10 EU. The half life was comparable to that of a cholegraphic medium (Fig. 9b).

Infusion of urographic media. Higher enhancement is only attainable with an infusion technique (Fig. 10). For both meglumine diatrizoate and CT 345 an enhancement of 45 EU is obtained after 60 min (end of the infusion). A shorter infusion period leads to lower contrast (Fig. 10).

Discussion

In the phantom experiments the limitations occurring in conditions in vivo were stated. It is a question of relative contrast between lesion and surrounding tissue. Only if the pathologic process is enhanced slightly or not at all is the required 25 EU enhancement of the surrounding tissue sufficient. In most avascular and hypovascular lesions of the liver (metastases) this condition is probably as a rule fulfilled. On the other hand if the pathologic process is enhanced, higher enhancement of the surrounding tissue is necessary. Finally the administration of a contrast medium may conceal more highly vascularized lesions (hypernephroma metastases, STANLEY et al. 1976, 1977). This is also the reason why it is not feasible to give overall valid directions for the application of contrast media in abdominal computer tomography.

The cholegraphic media are taken up selectively and excreted by the intact liver cell. However, the limited cellular transport maximum must be considered. Thus despite the organ specificity limits to the enhancement of the hepatic parenchyma exist. Therefore even in infusion cholegraphy with a large amount of contrast medium a higher enhancement cannot be expected than with a bolus injection. However, the enhancement obtainable after a bolus

injection (~8 EU) is hardly sufficient considering that in the present experiments the normal generally tolerable dose was administered. Only in vascularized lesions of the liver could cholegraphic media perhaps be used supportively as the results in the clinical series suggested.

The groups of media were investigated that have hitherto been commonly used and whose properties are widely known. The iodized oil emulsions at present under development that have been reported by LAVAL JEANTET *et coll* (1976) and VERMESS *et coll* (1976) did attain a greater enhancement (30–50 HU) in an analogous animal experiment (ALFIDI & LAVAL JEANTET 1976) but the hepatocellular reaction may give cause for concern. The infusion technique gives higher enhancement (90 HU) but still offers the advantage of greater controllability. Although the experiments were carried out in a state of suspended respiration in several of the animals artefacts could not be completely eliminated. The curves of Figs 7b and 8 show the effect of these interference factors which did not allow an exact determination of the half lives. However the average image quality was quite satisfactory and almost free from artefacts.

Conclusions

- (1) With urographic media it is possible to obtain higher enhancement of the liver than with cholegraphic media.
- (2) Bolus injection of urographic media requires a higher dosage of contrast medium and a rapid scanning process.
- (3) In examination of the liver the infusion of urographic media is clearly superior to the bolus technique.
- (4) Even in cases of moderate vascularization of small hepatic lesions the lesions can be rendered visible by the infusion of urographic media.

SUMMARY

A simple phantom experiment indicates that the enhancement of abdominal organs should be twice the SD of noise in a CT image. The enhancement of liver tissue by urographic and biligratic contrast media is analysed in clinical series and animal experiments. Various substances applied alone and in combination were investigated. At present only the infusion technique of urographic media provides a sufficient enhancement of liver tissue.

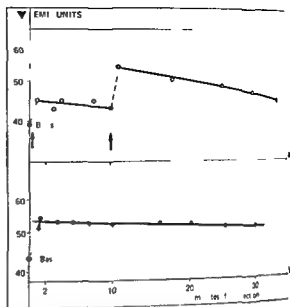


Fig. 9 Enhancement of dog liver after intravenous injection of combinations of urographic and cholegraphic media. a) First injection of meglumine iotroinate (Biliscopin 4.4 ml t_1 about 2 min) and second injection of meglumine diatrizoate (Ampipac 12 ml t_2 about 100 min) b) Mixture of meglumine iotroinate and meglumine ioglycinate (t_1 about 6 h)

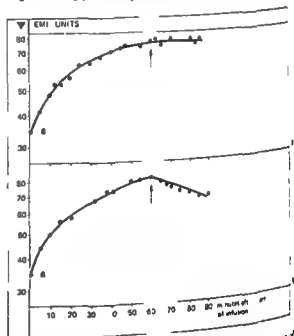


Fig. 10 Enhancement of dog liver after intravenous infusion of urographic media. a) Diatrizoate sodium b) CT 145 End of infusion indicated by arrows

ACKNOWLEDGEMENTS

The authors wish to thank Mrs G. Weiskopf, Mr K. Rodewald and Mr K. Redepenning for their very active support in the animal experiments and also Dr S. L. for placing the plexiglass phantom at their disposal. Presented at Symposium on Helikroppsdokumentation och Kontrastmedel Karolinska Sjukhuset Stockholm Sweden April 1978.

REFERENCES

- ALFIDI R J and LAVAL JEANTET M AG 60 99 A promising contrast agent for computed tomography of the liver and spleen Radiology 121 (1976) 491
- HAAGA J ■ HAVARILLA T ■ PEPE R G and COOK S A Computed tomography of the liver Amer J Roentgenol 127 (1976) 69
- LAVAL JEANTET M LANIARQUE J L DREUX P LAVAL JEANTET A M and LAUNAY J Hepatosplenography by intravenous injection of a new iodized oily emulsion Acta radiol Diagnosis 17 (1976) 49
- SHEEDY P E STEPHENS D ■ HATTERY R R MUHM J R and HARTMANN G W Computed tomography of the body Initial clinical trial with the EMI prototype Amer J Roentgenol 127 (1976) 23
- STANLEY R S SAGEL S S and LEVITT R G Computed tomography of the body Early trends in application and accuracy of the method Amer J Roentgenol 127 (1976) 53
- — — Computed tomography of the liver Radiol Clin N Amer 15 (1977) 331
- VERMESS M ADAMSON R H DOPPMAN J L and GIRTON M Intravenous hepatosplenography Experimental evaluation of a new contrast material Radiology 119 (1976) 31

PREVENTION OF EXPERIMENTAL VENOUS THROMBOSIS INDUCED
BY CONTRAST MEDIUM IN THE RAT

F H A MAFFEI H A ROLLO and V F FABRIS

Deep venous thrombosis is the most feared complication of phlebography. Although its real incidence is unknown, values as high as 24 to 33 per cent of possible thrombosis after phlebography have been published (BETTMANN & PAULIN 1977, ALBRECHTSSON & OLSSON 1976, 1979). Infusion of fluids with or without heparin to wash out the veins after the contrast medium injection has been largely used in order to reduce this complication (KAKKAR 1977, KALAF 1973, ATHANASOULIS 1975, BETTMANN & PAULIN 1977, THOMAS & MACDONALD 1978, STAMATAKIS *et coll.* 1978). The clinical experience at this hospital in Botucatu with infusion of physiologic saline containing heparin during and after phlebography seems to confirm the preventive action of heparin. The effect of various wash-out procedures on thrombosis induced by contrast medium was assessed experimentally in the rat for an evaluation of the usefulness of this method.

Material and Methods

Sixty albino rats of the Wistar strain weighing from 700 to 700 g were used. The left jugular vein was carefully dissected free under ether anesthesia and a segment about one cm long was isolated between two vascular clips. The blood within this segment was withdrawn through a 3 gauge needle and a small volume of sodium diatrizoate (Hypaque 94%, Wythrop) sufficient to fill the segment was injected. After 10 min the clips were removed and blood was allowed to recirculate in the vein. Details of this method have been described previously (MAFFEI *et coll.* 1977). The animals were then in-

cluded by randomization in one of the following groups:

Group I Control. No treatment after induction of thrombosis.

Group II Infusion of 2.5 ml of physiologic saline during 5 min through a 3 gauge needle placed cephalad to the site of the first puncture in the left jugular vein.

Group III Infusion of 25 U of sodium heparin in 2.5 ml of saline as in group II.

Group IV Infusion of 25 U of sodium heparin in 2.5 ml of saline during 5 min in the right jugular vein.

The incision was then sutured and the animal allowed to recover. After 48 hours the incision was reopened under ether anesthesia, the vein inspected and opened to see whether bleeding occurred. The whole segment was then resected, fixed in formalin 10% and embedded in paraffin. The tissues were stained with hematoxylin-eosin, elastic van Gieson and toluidine blue and examined microscopically.

In another group of 5 rats the effect on coagulation of the given amount of heparin was assessed. Under light ether anesthesia the tip of the rat's tail was cut off and 0.5 ml of blood was allowed to drop into a clean glass tube. This was immediately placed in a water bath at 37°C and the clotting time was measured. Twenty-five units of heparin in 2.5 ml of saline were then injected into the vein of the penis and the clotting time measured after 30, 60, 240 and 270 min.

Results of the four treatment groups were statis-

tically analysed by applying the test for contrast among multinomial populations (GOODMAN 1964) and the test on simultaneous confidence intervals for multinomial proportions (GOODMAN 1965) for an α of 0.05

Results

The incidence of thrombosis in the various groups appears in the Table. Occlusive thrombus was significantly more frequent in Group I (control group) and in Group II (saline infusion only) than in the groups given heparin. No difference was observed in the incidence of mural thrombosis for the different groups. Absence of thrombus was significantly more frequent in the two groups given heparin without any difference between these two groups being apparent.

When comparing the frequency of the various types of thrombus within the four groups the control and saline treated groups behaved similarly on application of the test for simultaneous confidence intervals for multinomial proportions for both groups occlusive thrombi were significantly more frequent than mural thrombi and absence of thrombi. The heparin treated groups behaved differently: no significant difference in the frequency of occlusive or mural thrombi or absence of thrombi was found in the systemic heparin group in contrast to the group with local wash out with heparin. In this latter group occlusive and mural thrombi were significantly less frequent than absence of thrombus.

Most veins without thrombosis appeared normal when examined *in situ* on section of the vein profuse bleeding occurred. However some veins were contracted and pale and little bleeding occurred when they were sectioned. Microscopic examination revealed an acute slight adventitial inflammatory reaction. The endothelium was preserved in most of the sections and looked normal except in one case in which it was swollen with degenerative lesions.

The veins with thrombosis were distended and had a dark brown colour. On section no bleeding occurred and the thrombus had a uniform dark red appearance. Microscopically the thrombi were of three types. Red formed mainly by red blood cells sometimes with small aggregates of platelets in a framework of fibrin. Fibrinous when fibrin was the main element of the thrombus and mixed when fibrin, red cells and other blood cells were observed.

Table

Incidence of thrombosis induced by contrast medium in the jugular vein of rats. Effect of different types of treatment. Percentage given in parentheses

Result	Treatment			
	Control	Wash out physiologic saline	Wash-out saline+heparin	Systemic saline heparin
Occlusive thrombus	14 (93)	14 (93)	1 (7)	4 (7)
Mural thrombus	1 (7)	1 (7)	3 (20)	3 (7)
Absence of thrombus	0 (0)	0 (0)	11 (73)	8 (17)
Total	15 (100)	15 (100)	15 (100)	15 (100)

The endothelium was absent in all the thrombosed veins. As for veins without thrombosis an inflammatory reaction around the vein was observed.

The mean clotting time in the 5 normal rats before administration of heparin was 15 ± 0.49 min. It was prolonged about 30 times 30 min after intravenous injection of heparin in all animals (mean 47 ± 5.2 min) returning to initial values after 740 min.

Discussion

It was possible to induce thrombosis in the jugular vein of rats with sodium diatrizoate as it had been previously with sclerosing substances (MAFFEI et al. coll. 1972). However although contrast medium produces endothelial injury (RITCHIE et al. coll. 1972) it was not the only cause of the development of a thrombus. The endothelial trauma caused by the clips and puncture and the stasis leading to ischemia were also important factors. The significance of these factors has previously been demonstrated in a series of 15 rats and 15 guinea pigs thrombosis occurred in 50 to 60 per cent after saline infusion only (unpublished data).

The local wash out of the vein with physiologic saline was not effective in preventing the formation of a thrombus in the present experimental model. On the other hand when heparin was added to the infusion fluid the incidence of thrombosis was significantly reduced. Systemic heparin also prevented thrombus formation although it seemed less effective.

The heparin was given only once and in a relatively low dose similar to the one used at phlebography in man. As the clotting time in rats with the used dosage of heparin was normal after 4 hours suggesting low or no action of heparin after this time it appears that the initial period was vital for the development of thrombosis. In rats and in guinea pigs subcutaneous injections of low dose heparin did not prevent thrombosis induced by sclerosing substances even when given every 12 hours (MAFFEI et coll 1972 1977). Therefore a high blood level of heparin established immediately after intravenous injection is probably an important factor in preventing the development of a thrombus.

The mechanism of heparin in preventing thrombosis in the experimental model is complex. The absence of endothelial cells in some of the sections of veins without thrombus would favour the hypothesis that heparin inhibits the initial aggregation of platelets or fibrin deposition on the exposed collagenous tissue. However the sustained absence of thrombi 48 hours after heparin injection with endothelial lesion still present is difficult to explain in view of the normal clotting time of the blood at four hours. Another possibility is that heparin acts on a not completely injured endothelium inhibiting a transitory release or activation of substances or impeding an alteration of electric potentials as suggested by SAWYER et coll (1973) all factors which would enhance platelet aggregation or fibrin formation. This second hypothesis means that the complete destruction of endothelial cells observed in all sections of thrombosed veins must have occurred secondarily to the thrombus formation.

Although both groups given heparin were significantly different from the control and saline groups the local wash out with heparin had a better effect than systemic heparin.

The concentration of heparin in the endothelium is up to 7400 times higher than in the blood after intravenous heparin injection in rats (HIEBERT & JACQUES 1976). Thus it may be assumed that large amounts of heparin entered the endothelium at the site of the injection due to a higher local blood concentration of heparin which accounted for the better results in the local wash-out group.

Although experimental data cannot be transferred directly to human beings the results may explain the low incidence of deep venous thrombosis following phlebography when heparin is used to wash out veins during and after the examination.

SUMMARY

In order to assess experimentally the usefulness of some procedures employed in man to prevent venous thrombosis following phlebography thrombosis was induced in rats using sodium diatrizoate in a temporarily isolated segment of a jugular vein. The prevention of thrombosis was attempted by washing out the vein with physiologic saline or saline plus heparin or by injecting saline plus heparin in the opposite jugular vein. Thrombosis occurred in all animals in the control group and in the group treated with saline alone. Both treatment schemes with heparin significantly reduced the incidence of thrombosis the wash out with heparin being more effective than systemic heparin.

ACKNOWLEDGEMENTS

The authors are grateful to Dr P. Cury for the statistical analyses and to Mr A. dos Santos and Mr L. Serafim for technical assistance.

REFERENCES

- ALBRECHTSSON U and OLSSON C G. Thrombotic side effects of lower limb phlebography. *Lancet* I (1976) 723.
- — Thrombosis following phlebography with ionic and non ionic contrast media. *Acta radiol. Diagnosis* 20 (1979) 46.
- ATHANASOULIS C A. Phlebography for the diagnosis of deep leg vein thrombosis. In: *Prophylactic therapy of deep vein thrombosis* p. 62. Edited by J. Frattantonio and S. Wessler. DHEW Publication No. (NIH) 76-866. Bethesda 1975.
- BETTMANN M A and PAULIN S. Leg phlebography: the incidence, nature and modification of undesirable side effects. *Radiology* 122 (1977) 101.
- GOODMAN L A. Simultaneous confidence intervals for contrast among multinomial populations. *Ann. Math. Statist.* 35 (1964) 716.
- — On simultaneous confidence intervals for multinomial proportions. *Technometrics* 7 (1965) 247.
- HIEBERT L M and JACQUES L B. The observation of heparin on endothelium after injection. *Thromb. Res.* 8 (1976) 195.
- KAKKAR V V. The 125 I labelled fibrinogen test and phlebography in the diagnosis of deep vein thrombosis. *Milbank mem. Fd. Quart.* 50 (1972) Suppl. No. 2 p. 206.
- KALAF J M. Flebografia do membro inferior. (In Portuguese.) *Rev. paul. Med.* 81 (1973) 333.
- LEA THOMAS M and MACDONALD L M. Complications of ascending phlebography of the leg. *Brit. med. J.* 2 (1978) 317.
- MAFFEI F H A, LORENZI L C, NOGUEIRA PINTO A M, LASTORIA S and FABRIS V E. Produção e prevenção da trombose letal química experimental no rato. (In Portuguese.) *Anais II Jornada Científica. FCMBB* p. 230. Botucatu, Brazil 1972.

- NOGUEIRA PINTO A M; FABRIS V E LASTORIA E
 ROLLO H A Trombose venosa experimental na
 cobaia. Efeito da heparina e de drogas que alteram a
 função plaquetária (In Portuguese) Rev bras Pesq
 med biol 10 (1977) 369
- RITCHIE W G M LYNCH P R and STEWART G J
 The effect of contrast media on normal and inflamed
 canine veins Invest Radiol 9 (1974) 444
- SAWYER P N STANCZEWSKI B POMERANCE A LUCAS
 T STONER G and SRINIVASAN S Utility of
 coagulant drugs in vascular thrombosis Electron mi-
 croscopic and biophysical study Surgery 74 (1977)
 263
- STAMATANIS J D KAKKAR V V LAWRENCE D and
 BENTLEY P G The origin of thrombi in the deep veins
 of the lower limb a venographic study Brit J Sur
 65 (1978) 499

MODIFICATION OF GREY SCALE IN COMPUTER TOMOGRAPHIC IMAGES

A. HEMMINGSSON and B. JUNG

Several authors (KIRKPATRICK et coll 1978 STEPHENS et coll 1977 BRYAN et coll 1977) claim that CT images often should be displayed with a narrow window setting (50–100 old Hounsfield units Hn). Parts of the image outside the selected band then appear completely black or white. This might detract from the evaluation of the image and essential information could be overlooked. Other grey scales than the conventional linear one might therefore be of interest, especially for hard copies of the image. At the display console the operator has access to successive window settings for analysing the whole image.

Two modified grey scales are presented. For one (Grey 1) the objective was to leave the selected band unaffected but to compress the grey scale for the rest of the image so that with a small increase in width of the selected window the remaining parts of the image are also displayed, albeit in a compressed grey scale. For the other one (Grey 2) the number of pixels per grey scale interval was kept constant. Extended regions of similar attenuation in the original image (e.g. the liver Figure) are then expanded and displayed in a grey scale with an increased number of levels, whereas boundary zones covering a small fraction of the attenuation level distribution in the image will be compressed. Thus it is displayed with a reduced number of grey scale levels. Another modification of the grey scale with a somewhat different purpose has been described by BORLAZA et coll (1978).

Material

The equipment consisted of an Ohio Nuclear Delta 50 FS with a 256×256 reconstruction matrix.

PDP 11 computers were available for program development and computations. Off-line the scanner equipment. The programs were written in Fortran with a special I/O system (TICS Task I/O Control System supplied by Uppsala Data Centre HOGSTROM 1978). The new programs were run under operating system RT 11, whereas the scanner programs were run under DOS (both supplied by Digital Equipment).

Methods

Grey 1 The operator decides the lower (Min) and upper (Max) Hounsfield numbers of the window from viewing the original image and settles a compression factor (Fact). The original image matrix is then read line by line by the program and a processed image created. Pixels within the window (Min to Max) are transferred without change and pixels with a content (Cont) less than Min are replaced by $\text{Min} - (\text{Min} - \text{Cont}) / \text{Fact}$, where Fact is restricted to 2, 4, 8, 16, 32 or 64 to allow integer arithmetics. Analogously, pixels with a content above Max are replaced by $\text{Max} + (\text{Cont} - \text{Max}) / \text{Fact}$.

Grey 2 The operator, after deciding a lower (Min) and an upper (Max) limit for the pixels to be processed, starts the program to sort these pixels in a histogram with 1000 consecutive classes of equal width. New class boundaries are then selected so that each new class contains 1/256 of the number of pixels within the window. Next the original image is searched a second time and the pixels assigned new values on the 256 class scale.



a



b



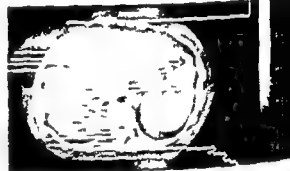
c



d



e



f

Original tomograms at window widths of a) 1002 and b) 171 Hn. c) Image processed with Grey 1 (Min 24, Max 74 Hn, Fact 8). d)

Image processed with Grey 2 (Min -170, Max +670 Hn). e) Histogram of the original image. f) Histogram of the Grey 2 image.

Results

The original image from a patient with a liver tumour is displayed in the Figure. With a window of 1002 Hn (Figure a) the contours of the body and the bony and soft tissue structures are visible, but not the tumour. At a window of 171 Hn (Figure b) the tumour is visible as a darker region in the posterior part of the right liver lobe, while the bony structures and the rest of the liver appear white. The contour of the body is not visible. When the image is processed with Grey 1, the unaffected window region in the liver with the tumour is visible, and outside this the contour of the body in the compressed grey scale at the same window level as in Figure b (171 Hn) (Figure c). At a window level of +49 Hn and a width of

50 Hn (range +24 to +74) the tumour is displayed with high contrast.

With Grey 2 a window setting of 1002 Hn displays simultaneously the contour of the body and the liver tumour (Figure d). The extension of the scale in Grey 2 is illustrated by the histograms of the original (Figure e) and processed (Figure f) images.

Discussion

A disadvantage of Grey 2 is that the attenuation of the object cannot be evaluated from the processed image. With Grey 1 this applies only for pixels outside the selected window. Such measurements then require reference to the original tomogram.

The two methods of grey scale modification demonstrate that alternatives to the conventional linear play may be found that might be better suited for artistic work. They may also be of value in demonstrating images to an audience as the contours of the body as well as the lesion in an internal organ are displayed in the same image. Also for hard copy documentation the modified CT images are of interest as they convey more information than the conventional ones displayed either with extended or narrow windows.

SUMMARY

Optimum perception of minute but relevant attenuation differences in CT images often requires display window settings so narrow that a considerable fraction of the image appears completely black or white and consequently without structure. In order to improve the display characteristics two principles of grey scale modification are presented. In one method the pixel contents are displayed unchanged within a selectable attenuation band but moved towards the limits of the band for pixels that are outside it. In the other the grey scale is arranged to a constant number of pixels per grey scale interval.

ACKNOWLEDGEMENT

The investigation was supported by grants from the Swedish Cancer Society.

REFERENCES

- BORLAZ G S, SIEGEL M, FISCHER B and KUHN L R. Double exposure technique for demonstration of osseous and pulmonary structures on a single CT film. *Amer J Roentgenol* 130 (1978) 375.
- BRYAN P J, DINN W M, GROSSMAN Z D, WISTOW B W, MCAFEE J G and KIEFFER S A. Correlation of computed tomography, gray scale ultrasonography, and radionuclide imaging of the liver in detecting space occupying processes. *Radiology* 124 (1977) 387.
- HÖGSTRÖM B. Design of interactive systems. Tics and I/O control system. In: *Proceedings of the Digital Equipment Computer Users Society*, Vol 5, p 19. Copenhagen 1978.
- KIRKPATRICK R H, WITTENBERG J, SCHAFER D L, BLACK E B, HALL D A, BRAITMAN B S and FERUCCI JR J T. Scanning techniques in computed body tomography. *Amer J Roentgenol* 130 (1978) 1069.
- STEPHENS D H, SHEEDY P F, HATTERY R R and MAC CARTY R L. Computed tomography of the liver. *Amer J Roentgenol* 128 (1977) 579.

COMPLICATIONS OF ANGIOGRAPHY IN CHILDREN
AND MEANS OF PREVENTION

B JACOBSSON H CURTIN A RUBENSON and S E SORESENSEN

The frequency of local thrombotic and distal thromboembolic phenomena occurring during percutaneous angiography has been widely evaluated depending on the method of evaluation the frequency varies from 0 to more than 50 per cent but clinically significant occlusions are usually reported to occur in 0.2 to 3.0 per cent of cases. Children have been considered to be in a high risk group especially young infants (for review see MORFESSON et coll 1976). This as well as the difficulty of performing percutaneous arterial puncture has caused some centers to limit the use of angiography in small children. This report is a prospective evaluation of 267 consecutive angiographies performed at this hospital over an eight year period. Oscillography was used to detect any pulse decrease reflecting either spasm or thrombosis. As more information about the etiology of thrombosis in connection with catheterization has become available the technique was modified with a subsequent drop in complications. As multiple factors were changed at different times no statistical analysis can be made as to which specific change was mainly responsible for the decrease in the complication rate. The modifications are described together with the reasons for their introduction.

Materials and Methods

The series consisted of 267 consecutive trans femoral angiographic examinations performed between 1970 and 1977 the majority being abdominal and the remainder including examinations of extremities skull and heart. During the interval between 1970 and 1974 angiography was performed in 14 infants (under 2 years of age) via surgical expo-

sure either because of expected difficulties in percutaneous puncture in a small child or failure with the percutaneous technique. Since 1974 the percutaneous technique has been used exclusively and in only one instance was it impossible to catheterize the vessel. The ages of the infants and children examined by the percutaneous technique were between newborn and 16 years. 26 were less than one year 58 between one and 5 years 68 between 5 and 10 years and 101 were 10 years or older. The number of examinations per year has increased particularly in the group under 5 years of age (Fig. 1). Selective catheterizations have also increased. Local anesthesia was usually used during 1970 to 1973 thereafter general anesthesia in most patients. Radiologists with varying experience performed the examinations. The puncture site was compressed for approximately 10 min following the procedure care being taken to maintain the distal pulse during compression.

Oscillography was carried out with a Gessenius Keller oscillograph before the examination and repeated following the procedure as soon as hemostasis was achieved for detecting obstructive vascular complications. If the maximum excursion differed in the two legs by more than 3 mm it was considered significant. When the maximum excursion on either side was less than 5 mm and the value on the catheterized side was less than half that of the uncatheterized side circulation was also considered impaired (JACOBSSON et coll 1973). The oscillo-

graphy was repeated during the next 4 hours if the circulation was abnormal immediately after the examination. Persistence of an abnormal value for 4 hours was used as the criterion for vascular obstruction and appropriate measures were taken. A return to normal within 4 hours indicated a transient decrease in pulse and no treatment was required.

In an effort to improve the safety of the catheterization several technical changes have been made aimed mainly at limiting the formation of thrombus on the catheter surface. Several different types of catheter were used until four years ago. Since then only the Radicath set for angiography in children (Becton & Dickinson U.S.A.) has been used. These catheters are extremely thin walled giving a maximum inner diameter while minimizing the outer diameter. This set includes a puncture needle and guide wire adapted to the catheters.

Systemic heparinization was included in the procedure during early 1976 (75 units/kg body weight). Heparinization of the catheter itself was however considered preferable and when such catheters became available in 1976 they were used instead of systemic heparinization. The catheters were heparinized by the process described by ERIKSSON *et al.* (1967). During the last three years thrombectomy has been performed with a modification of the method described by JEFFERY (1972). By this method blood is aspirated at the very moment when the tip of the catheter is leaving the lumen of the artery during simultaneous compression just distal to the puncture track and blood is allowed to spurt out for a moment. Thrombi if any around the puncture site may then either be aspirated into the catheter or washed out.

Results

Complications due to the formation of thrombus occurred in 14 cases. 8 of them (57%) in 14 exposed arteries and 6 in the 253 percutaneous approaches (2.4%, Fig. 2). In all cases in which surgery was performed (9) and in the one case that underwent repeat angiography the diagnosis of thrombus formation and occlusion could be confirmed. In the percutaneous group (Fig. 3) 3 complications occurred in the 75 patients under 5 years of age (4%), none of these in the 26 patients under one year of age. Two complications occurred in the 5 to 10-year group (3.3%) and one complication in the group 10 years and older (1%). No complications

Number of patients

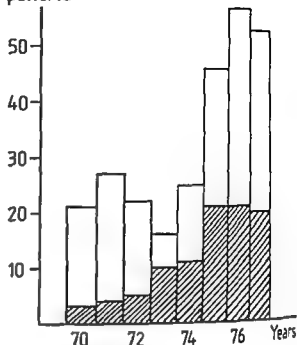


Fig. 1 Number of examinations between 1970 and 1976. The number of children under 5 years is indicated with striped bar.

have been encountered in the last 3 1/2 years. In the last 153 examinations there have been without significant morbidity. The decreasing complication rate is significant ($p < 0.02$). No significant change in the frequency of transient decrease in pulse was found when the group examined before 1974 was compared with the group after 1974. Whether general or local anesthesia was used did not influence the frequency of a transient decrease but did increase with decreasing age of the child (Fig. 4).

The thromboembolic complication rate was not related to any specific catheter or type of examination. No complication has occurred since the institution of systemic heparinization of the patient in the procedure or with use of heparinized catheters. Prolonged bleeding after withdrawal of heparinized catheters has previously been observed (FLOTH & JACOBSSON 1974) but this caused no difficulty in the present series. Of the cases with complications in the percutaneous group 5 underwent routine leg artery thrombectomy within 10 hours. Thrombosis at the puncture site was found in all 5. In the youngest patient the oscillography was abnormal in the lower leg but not in the thigh following the examination. At repeat angiography the same day an embolus in the popliteal artery was demonstrated and the catheter was treated with heparin. The treatment of com-

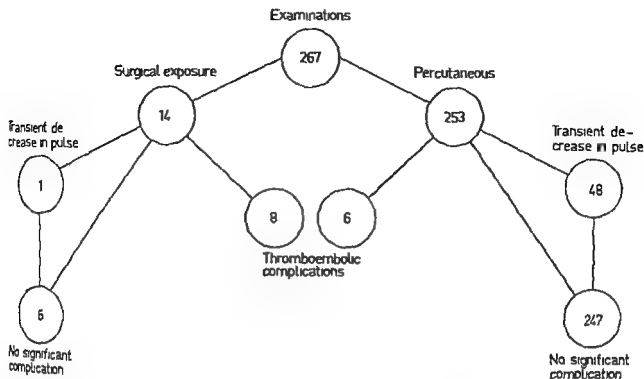


Fig. 2 Number of femoral artery catheterizations for angiography between 1970 and 1977 and complications from the procedure

ations and their long term results have been described in another report (RUBENSON et coll 1979)

Discussion

The frequency of complications associated with the surgical exposure was found to be much higher

than with the percutaneous approach and was considered to be unacceptable. This technique was therefore abandoned. With increasing experience with the percutaneous approach the femoral artery was catheterized in all children during the past 3 1/2 years with one exception.

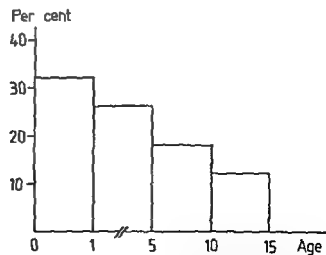
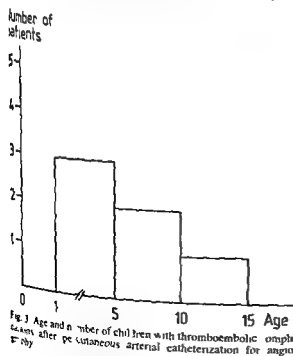


Fig. 4 Frequency of children with transient decrease of pulse after percutaneous femoral artery catheterization for angiography

The variation in the reported frequency of complications is partly due to variation in the method of detecting these complications. Methods of detection include clinical signs of decreased blood supply and pulse evaluation which rely on subjective estimations. The more objective methods include oscillography (REAL et coll 1966, WHITE et coll 1968, HOHN et coll 1969, JACOBSSON & SCHLOSSMAN 1969), plethysmography (MORTENSSON et coll 1975), Doppler evaluation (BARNES et coll 1977), routine Fogarty thrombectomy (BAKER et coll 1968) and pull out angiography (SIEGELMAN et coll 1968, FORMANEK et coll 1970). Using this last mentioned method small amounts of thrombus on the catheter are detected which may or may not result in a significant occlusion. The oscillographic method used objectively evaluates the pulses in the lower leg but cannot detect smaller thromboemboli in the more distal arteries of the foot. Although wide variance in complication rates have been reported the frequency in adults most often lies between 0.2 and 3.0 per cent. Younger patients are considered to be at greater risk. In the present series the overall rate is 2.4 per cent in children with a tendency to a slightly higher risk in the age group under 5 years (4%) but no special predilection for infants under one year. However the results also show the possibility of significantly reducing the complications thus the last 153 examinations were uneventful.

The decreased complication rate during recent years appears to be attributable to technical changes in response to growing evidence that the major factor in local thrombotic and distal thromboembolic complications is the formation of the thrombus on the catheter surface with subsequent stripping off of this thrombus as the catheter is pulled back through the wall of the artery (NEJAD et coll 1968, JACOBSSON 1969). The number of thrombi can be minimized first by using thin walled catheters resulting in a decreased surface area available for formation of thrombus. Secondly heparin inhibits the formation of thrombus. Systemic heparinization has been shown to decrease the rate of thrombotic complications (WALLACE et coll 1972, ANDERSON et coll 1974, KAPLAN et coll 1975) but this carries with it the inherent risks of anticoagulation. Localized high concentration of heparin at the blood catheter interface can be accomplished by coating the catheter with heparin obviating the necessity for systemic heparin with its potential problems (ERIKSSON et coll 1976, JACOBSSON &

SCHLOSSMAN 1973, ELDH & JACOBSSON). Stability of the heparin coating has been a problem with thrombogenicity increasing during the course of the examination (WHIFFEN & BEECKLER 1966). The heparinization method of ERIKSSON et coll provides a coating shown to be stable for many hours and even days in contact with blood (HEIDEMAN et coll 1976, OLSSON et coll 1977).

The thrombectomy is described by JEFFERY as an attempt to flush out any thrombus which may have been stripped from the catheter and remains at the site of puncture.

No other changes have been made which would account for this recent decrease in complications. The number of selective examinations and catheter exchanges has increased as has the number of smaller children. The recent examinations have been performed by radiologists with varying experience including some doing their training in pediatric radiography.

Transient changes in pulse are thought to represent spasm as rapid collateral reconstitution would presumably not result in immediate return of equal pulse bilaterally. The frequency of this spasm has not decreased during these years indicating that the local trauma at the site of puncture has not diminished. This would support the contention that the present decrease in complication rate is a result of the decreased thrombus formation on the catheter itself rather than local factors at the site of puncture.

It seems reasonable to conclude that angiography can be performed in infants and children via the percutaneous approach with a high success rate and if proper measures are taken with a low complication rate.

SUMMARY

In 267 consecutive angiographic examinations in children 14 thromboembolic complications occurred following surgical exposure, 8 complications in 14 cases and 6 complications in 253 percutaneous angiographies. The origin of thrombus during angiography has recently been clarified. Technical advances such as thin walled catheters, systemic heparinization and lately heparinized catheters decreased the complication rate significantly. No complication occurred among the last 153 examinations.

This investigation was carried out while one of the authors (H. C.) was on leave from the Department of Radiology, Presbyterian University Hospital, Philadelphia 19123, U.S.A.

REFERENCES

- BERSON J H, GIANTURCO C, WALLACE S, DODD G D and DEJONGH D. Anticoagulation technique for angiography. *Radiology* 111 (1974) 573
- GER L D, LESHIN S J, MATHUR V H and MESSER J V. Routine Fogarty thrombectomy in arterial catheterization. *New Engl J Med* 279 (1968) 1203
- KNES R W, SLAYMAKER E E and HAHN F H. Thromboembolic complications of angiography for peripheral artery disease. Prospective assessment by doppler ultrasound. *Radiology* 122 (1977) 459
- OH H and JACOBSSON B. Heparinized vascular catheters. A clinical trial. *Radiology* 111 (1974) 289
- IKSSON J C, GILLBERG G and LAGERGREN H. A new method for preparing nonthrombogenic plastic surfaces. *J Biomed Mat Res* 1 (1967) 301
- KHANEN G, FRECH R S and ANPLATZ K. Arterial thrombus formation during clinical percutaneous catheterization. *Circulation* 41 (1970) 833
- IDEAN M, JACOBSSON B and LARSSON R. Thromboresistance and stability of a heparinized polymer. *Acta radiol. Diagnosis* 17 (1976) 877
- HYA CRAENEN J J and LAMBERT E. Arterial pulses following percutaneous catheterization in children. *Pediatrics* 43 (1969) 617
- JACOBSSON B. Thromboembolism in vascular catheterization. Diagnosis, cause and prevention. Thesis. Gothenburg 1969
- and SCHLOSSMAN D. Thromboembolism of the leg following percutaneous catheterization of femoral artery for angiography. *Acta radiol. Diagnosis* 8 (1969) 97
- Thrombogenic properties of heparinized vascular catheters. *Acta radiol. Diagnosis* 14 (1973) 569
- CARLGRÉN L E, HEDVALL G and SIVERTSSON R. A review of children after arterial catheterization of the leg. *Pediatr Radiol* 1 (1973) 96
- FEFFER R F. A simple method of removing intraarterial clots formed during catheterization. *Radiology* 103 (1972) 573
- KAPLAN M A, HARRIS C N and PARKER D P. Heparinization in coronary arteriography. *Circulation* 52 (1975) 517
- MORTENSSON W, HALLBOOK T and LUNDSTROM N R. Strain gauge plethysmography for blood flow measurements in the legs of children. *Pediatr Radiol* 3 (1975) 29
- Percutaneous catheterization of the femoral vessels in children. *Pediatr Radiol* 4 (1976) 1
- NEJAD M S, KLAPPER M A, STEGGERDA E R and GIANTURCO C. Clotting on the outer surfaces of vascular catheters. *Radiology* 91 (1968) 248
- OLSSON P, LAGERGREN H, LARSSON R and RADFGRAN H R. Prevention of platelet adhesion and aggregation by a glutaraldehyde stabilized heparin surface. *Thrombosis et Hemostas* 37 (1977) 274
- REAL F J P, SCARPELLI E M, RUTTNER N and RUDOLPH A M. Arteriotomy and local circulation in children. The value of oscillometry. *J Pediatr* 69 (1966) 372
- RUBENSON A, JACOBSSON B and SORINSEN S E. Treatment and sequelae of angiographic complications in children. *J Pediatr Surg* 14 (1979) 154
- SIEGELMAN S, CAPLAN L and ANNES G. Complications of catheter angiography. Study with oscillometry and pull-out angiograms. *Radiology* 91 (1968) 251
- WALLACE S, MEDELLIN H, DEJONGH D and GIANTURCO C. Systemic heparinization for angiography. *Amer J Roentgenol* 116 (1972) 204
- WHIFFEN M and BEECKLER D. The fate of the surface heparin of GBG coated plastics after exposure to the bloodstream. *J thorac. cardiovasc Surg* 52 (1966) 121
- WHITE J J, TALLBERT J D and HALLER J A. Peripheral arterial injuries in infants and children. *Ann Surg* 167 (1968) 357

METRIZAMIDE AND METRIZOATE FOR CARDIOANGIOGRAPHY IN INFANTS

Comparison of heart rate and arrhythmia

M. HELLSTRÖM, B. JACOBSSON, S. E. SØRENSEN and B. O. ERIKSSON

Although new and non invasive methods for examination of children with congenital heart disease have been introduced such as scintigraphy and ultrasound cardiography still has to be included in the preoperative examination of these children in most cases.

Serious side effects of cardiac catheterization and angiographic procedures appear to be unavoidable at present. The hazards are particularly great in neonates and infants, especially in children with complex cardiac malformations (HO *et coll.* 1972, KROVETZ *et coll.* 1968, MCINTOSH 1968). Mortality rates as high as 12.8 per cent in infants less than one month of age have been reported by HO *et coll.* while the overall mortality in children up to 15 years of age in the same series was 1.5 per cent.

Complications are mainly considered to be due to manipulation of the catheter (GRAINGER 1965, HO *et coll.*, KROVETZ *et coll.*) and to a lesser extent to the contrast medium (GRAINGER, SWAN 1968). However, the mortality rate has been shown to be influenced by the choice of contrast medium (HO *et coll.*).

Experiments have indicated that the non ionic contrast medium metrizamide is less cardiotoxic than other contrast media in common use for cardioangiography. Thus ALMEN (1973) demonstrated that metrizamide caused less fall in blood pressure and less bradycardia when injected in the aortic bulb in cats compared with diatrizoate (Anipaque) and metrizoate (Isopaque Cerebral). In animal experiments ALMEN & ASPELIN (1975) found

that metrizamide caused less reduction in ventricular contractile force and heart rate, less rise in pulmonary artery pressure and also less injury to the aortic endothelium than various ionic contrast media.

TRAGÅRDH *et coll.* (1975) and HIGGINS & SCHMIDT (1978) demonstrated in coronary angiographies in the dog that metrizamide produces less alteration in cardiac functions than other commonly used contrast media. Following injection of metrizamide, diatrizoate and metrizoate into the right coronary artery of dogs TRAGÅRDH & LYNCH (1978) found a lower incidence of ventricular fibrillation after the injection of metrizamide compared with diatrizoate.

Metrizamide has also been used clinically for coronary angiography by ENGE *et coll.* (1977) who reported less decrease in diastolic blood pressure compared with metrizoate (Isopaque Coronar).

Therefore it seemed to be of value to find out whether the findings mentioned are also valid in the high risk group of neonates and small infants subjected to cardioangiography.

Material and Methods

The material consisted of 52 infants examined by cardiac catheterization and cardioangiography. The infants were investigated at the Children's Hospital in Gothenburg during 1976 to 1978 because of con-

Table 1

Comparison between the two groups of patients injected with either Isopaque Coronar or Amipaque LA=left atrium LV=left ventricle
RV=right ventricle

	No of patients	Mean weight (kg)	No of injections	Injection site			Contrast medium	
				LA	LV	RV	Mean dose (ml/kg/inj)	Mean flow rate (ml/s)
Isopaque Coronar	28	3.8	37	5	15	17	1.9	6.5
Amipaque	24	3.3	37	5	15	17	2.1	5.9

genital heart disease which were usually complex in nature. The ages ranged from less than one day to eight months and 62 per cent of the infants were neonates. Most of the children had serious cardiac symptoms.

The patients were not randomized but represented consecutive examinations including only children with a weight of less than 5 kg. The contrast media used were Isopaque Coronar (metrizoate 370 mg I/ml) and Amipaque (metrizamide 370 mg I/ml). The age, weight and general condition of the children did not influence the choice of contrast medium. The same contrast medium was always used for repeated injections.

The Cisl II injector used did not allow the flow rate to be preset. Catheters of slightly varying length and diameter were used. Amipaque has a higher viscosity than Isopaque Coronar and this may result in somewhat varying injection rates. Only consecutive Isopaque Coronar examinations with flow rates as close as possible to those in the Amipaque group were selected for evaluation in order to make the two groups as equal as possible.

Premedication was given to 10 children who received either a combination of pentazocine and diazepam or a combination of pethidine, promethazine and chlorpromazine. All patients were examined by cardiac catheterization and angiography in the same session. The catheters were inserted through the femoral vein after local anesthesia with lidocaine 0.5 per cent without epinephrine. Cardiac catheterization was performed with heparinized Cook's catheter No. 5 or 6 using a catheter with an occluded tip for angiography. Heparin (50–100 IU/kg body weight) was injected through the catheter immediately after its insertion in all except 6 cases.

Twenty-eight children were examined with Isopaque Coronar with a total number of 37 contrast medium injections. 24 patients with Amipaque also

with a total number of 37 injections. Five injections were made in the left atrium, 15 in the left ventricle and 17 in the right ventricle respectively (Table 1).

The mean weight of the children who received Isopaque Coronar was 3.8 kg (range 2.7–5.0 kg). The mean amount of contrast medium injected each time was 1.9 ml/kg body weight (range 1.5–2.6 ml/kg). The average flow rate of medium was 6.5 ml/s (range 5.0–8.9 ml/s) (Table 1).

The mean weight of the children who received Amipaque injections was 3.3 kg (range 2.0–5.0 kg). The mean amount of medium injected each time was 2.1 ml/kg body weight (range 1.4–2.8 ml/kg). The average flow rate was 5.9 ml/s (range 3.5–10.0 ml/s) (Table 1).

The injection time was automatically recorded by the Cisl II injector. ECG standard lead II as well as the contrast injections were recorded on an 8 channel Mingograf during the examinations. The recordings were continued for at least 10 seconds after the start of the contrast injections.

The occurrence, type and timing of immediate extrasystoles as well as change in heart frequency were recorded for each injection.

A change in frequency exceeding the variation during an observation period of 3 seconds before the injection was regarded as tachycardia or bradycardia. The maximum change of frequency and its timing in relation to the start of contrast injection were estimated. Heart frequency was measured on 3 consecutive cardiac cycles using R-R intervals.

Statistical evaluation. Proportions were compared by use of Fisher's exact test. The general permutation test of Fisher (ODF & WEDEL 1954) was used to compare the change of cardiac frequency between the Isopaque Coronar group and the Amipaque group. All p-values concern two-sided tests.

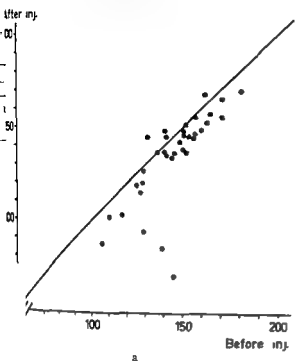
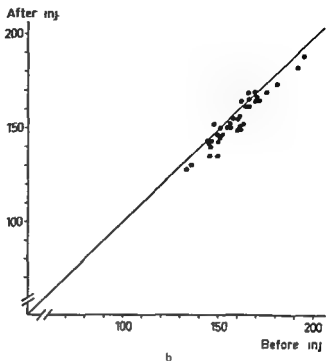


Figure 1. Change in heart rate within 10 s after injection of a) Isopaque Coronar (170 mg I/ml) and b) Amipaque (370 mg I/ml)



Results

The image quality was similar in the examinations performed with the two contrast media but no systematic evaluation was done in this respect. Most patients showed signs of discomfort and jerked during injection of Isopaque Coronar. This was rarely observed when Amipaque was employed.

Cardiac frequency A decrease in frequency after injection of Isopaque Coronar as well as after Amipaque was usually observed but no change occurred after 6 injections of Isopaque Coronar and after 8 Amipaque injections. Bradycardia was registered in 14 of 37 injections of Isopaque Coronar (22 of 28 patients) and in 26 of 37 injections of Amipaque (18 of 28 patients) (Figure). The decrease in heart rate was significantly greater ($p < 0.01$) following injection of Isopaque Coronar (14.6 beats/min) than after injection of Amipaque (6.1 beats/min) (Table 2). The maximum fall in heart rate was 70 beats/min (from 140 to 70 beats/min) after Isopaque Coronar and 14 beats/min after Amipaque. The maximum decrease in heart rate occurred at approximately the same time, 6 and 5.6 s respectively after the start of injection. A very moderate increase in heart rate was observed in 7 examinations, 4 following the injection of Isopaque Coronar and 3 following the injection of Amipaque.

Cardiac rhythm Extrasystoles during or in immediate connection to the contrast injection were recorded in 21 of 37 (57%) examinations (19 of 28 patients) using Isopaque Coronar and in 9 of 37 (24%) examinations (9 of 24 patients) using Amipaque. This difference is significant ($p < 0.01$, Table 3). A series of two or more extrasystoles (coupling) occurred after 13 injections (35%) of Isopaque Coronar and after 3 injections (8%) of Amipaque ($p < 0.01$, Table 3). The majority of extrasystoles were of ventricular origin but in 4 instances of supra-ventricular origin. The extrasystoles occurred after a mean time of 0.7 s using Isopaque Coronar and after 0.9 s using Amipaque. The extrasystoles occurred at the same time in relation to the injection irrespective of the injection site, 0.8 s after the start of injection in the right ventricle and 0.7 s after the start of injection in the left ventricle. No significant difference in arrhythmia production between right and left ventricular injections could be demonstrated. No difference in mean flow rate was found between injections giving rise to extrasystoles compared with injections not causing extrasystoles, 6.3 ml/s and 6.2 ml/s respectively. There was no correlation between the dose of contrast medium and the occurrence of extrasystoles. However, variation in dose was very moderate.

Table 2

Magnitude of bradycardia within 10 seconds after injection of contrast medium

	Heart rate (beats/min)			Time (s) after start of injection
	Before	After	Difference	
Isopaque Coronar	145.1	130.5	14.6	6.2
Ampaque	159.1	153.0	6.1	5.6

The difference between Ispaque Coronar group and Ampaque group is significant ($p < 0.01$)

Table 3

Incidence and occurrence of extrasystoles during, and immediately after injection of contrast medium

	No. of injections	Extrasystoles	Time (s) after start of injection	Coupling
Isopaque Coronar	37	21/37 (57%)	0.7	3/37 (8%)
Ampaque	37	9/37 (24%) ^a	0.9	1/37 (3%)

Discussion

The two groups of patients were well comparable regarding diagnosis, age, weight, premedication, injection site, dose and flow rate.

Bradycardia is well known to occur in cardioangiography and can be mediated via several mechanisms. One of these is due to the effect of the contrast medium on the coronary circulation either by direct depression of sinus node activity (ECKBERG *et coll.* 1974, HIGGINS 1977) or by activation of coronary baroreflexes or chemoreflexes (ECKBERG *et coll.* 1974). In animals, receptors in the heart have been found giving rise to bradycardia through vagally mediated reflexes when stimulated (ROMERO *et coll.* 1977). A similar mechanism has been suggested by FRANK *et coll.* (1975) to be partly responsible for the bradycardia observed during coronary angiography in man. Bradycardia may also be mediated by the influence of contrast medium on the brain (LUNDERVOLD & ENGFELT 1967).

In the present series bradycardia was regularly registered, more marked after Ispaque Coronar (14.6 beats/min) than after Ampaque (6.1 beats/min). The most serious bradycardia occurred after injection of Ispaque Coronar with a fall in heart rate from 140 to 70 beats/min. The most marked decrease in heart rate after injection of Ampaque was from 149 to 135 beats/min. Previously it has been demonstrated in experimental animals that

metrizamide causes less inhibition of sinoatrial automaticity (HIGGINS) and less bradycardia (ALMEIDA) than other commonly used contrast media. The present clinical findings correspond with these experiments.

Arrhythmias during or in close relation to contrast medium injections were frequently registered in the present series. Extrasystoles occurred more than twice as often after injection of Ispaque Coronar as after injection of Ampaque, and series of extrasystoles occurred more than four times as often after Ispaque Coronar. It seems reasonable to assume that series of extrasystoles are potentially more dangerous than single ones. Arrhythmias during cardioangiography may be caused by the influence of the contrast medium in the coronary circulation, either by inhibition of the conducting system or by a direct effect on the myocardial cells (HIGGINS, TRAGÄRDH & LYNCH, TRAGÄRDH *et coll.* 1974). In the present series the extrasystoles occurred within one second after the start of injection regardless of whether this was performed in the right or left ventricle. In most cases this reasonably excludes a triggering by the coronary circulation. Thus, most of the extrasystoles can be assumed to be caused by a direct local effect on the endo-myocardium, either of mechanical or chemical origin. It is well known that manipulation of the catheter in the heart can mechanically induce extrasystoles (McINTOSH).

VENABLES & HILLER 1963) During injection the catheter recoil as well as the contrast jet (KROVETZ coll 1967) may also mechanically trigger extrasystoles. Amipaque is more viscous than Isoaque Coronar. When fluids of different viscosity are injected at similar flow rates the catheter recoil effect will be the same but the difference in viscosity may cause varying jet effects. However this difference is probably of minor practical importance. Thus the less frequent occurrence of extrasystoles in the Amipaque group does not seem to be explained by mechanical factors. This suggests that at least some of the extrasystoles are caused by physical/chemical influence of the contrast medium locally on the endo-myocardium. Similar findings were reported by REFSUM & PASSWAL (1978) who observed an arrhythmogenic effect of contrast media in direct contact with isolated rat atria. In those experiments metrizamide caused less arrhythmia than metrizoate and diatrizoate.

The results of the present clinical investigation agree with previous experimental and clinical reports indicating that Amipaque is less cardiotoxic than other commonly employed contrast media for radioangiography. It seems reasonable to assume that the differences between Amipaque and Isoaque Coronar are of clinical importance especially in the examination of neonates and small infants in a bad general condition and with complicated congenital cardiac disorders.

SUMMARY

The cardiotoxic effect of Isoaque Coronar (metrizoate 370 mg I/ml) and Amipaque (metrizamide 370 mg I/ml) was analysed in 57 infants weighing less than 5 kg. In each group of patients 37 injections of contrast medium were performed and the immediate side effects, extrasystoles, change in heart frequency were recorded. Amipaque caused significantly less bradycardia and significantly fewer immediate extrasystoles than Isoaque Coronar. The results indicate a lower cardiotoxicity of Amipaque in radioangiography in infants.

REFERENCES

VENABLES T Cardiovascular effects of injection of metrizamide and other contrast media into the aortic bulb of cats Acta radiol (1973) Suppl No 335 p 209
— and ASPELIN P Cardiovascular effects of ionic monomeric ionic dimeric and non ionic contrast media Invest Radiol 10 (1975) 557
ECLAIRAC D L WHITE C W KIOSCHOS J M and ABRAHAM D F Mechanisms mediating bradycardia during coronary arteriography J Clin Invest 54 (1974) 1455

ENGE I NITTER HALG S ANDREW E and LEVORSTAD K Amipaque A new contrast medium in coronary angiography Radiology 125 (1977) 317
FRANK R J MERRICK II and LOWE H M Mechanism of the brady cardia during coronary angiography Amer J Cardiol 35 (1975) 17
GRANGER R G Complications of cardiovascular radiological investigations Brit J Radiol 38 (1965) 201
HIGGINS C II Effects of contrast media on the conducting system of the heart Radiology 124 (1977) 599
— and SCHMIDT W Direct and reflex myocardial effects of intracoronary administered contrast materials in the anesthetized and conscious dog Comparison of standard and newer contrast materials Invest Radiol 13 (1978) 205
HO C S KROVETZ J L and ROWE R B Major complications of cardiac catheterization and angiocardiology in infants and children Johns Hopk Med J 131 (1972) 247
KROVETZ J J BENSON R W and NELMASTER T Hemodynamic effects of isotonic solutions rapidly injected into the heart and great vessels Amer Heart J 73 (1967) 525
— SHANKLIN D R and SCHIEBLER G L Serious and fatal complications of catheterization and angiocardiology in infants and children Amer Heart J 76 (1968) 39
LUNDERVOLD A and ENGESET A Polygraphic recordings of EEG ECG and blood pressure during cerebral angiography with Isoaque II Acta radiol (1967) Suppl No 270 p 87
MCINTOSH II D Arrhythmias Circulation 37-38 (1968) Suppl No 3 p 27
ODEN A and WEDEL H Arguments for Fisher's permutation test Ann Statistics 3 (1975) 518
REFSUM II and PASSWAL M Arrhythmogenic and cardiodepressive effects of contrast media on isolated rat atria Invest Radiol 13 (1978) 444
ROMERO T E HIGGINS C II KIRKPATRICK S and FRIEDMAN W F Effects of contrast material on dimensions and hemodynamics of the newborn heart A study in conscious newborn lambs Invest Radiol 12 (1977) 510
SWAN H J C Complications associated with angiocardiology Circulation 37-38 (1968) Suppl No 3 p 81
TRAGARDH II and LYNCH P R ECG changes and arrhythmias induced by ionic and non ionic contrast media during coronary arteriography in dogs Invest Radiol 13 (1978) 233
— BOYE A A and LYNCH P R Cardiac conduction abnormalities during coronary arteriography in dogs Reduced effects of a new contrast medium Invest Radiol 9 (1974) 340
— LYNCH P R and VINCIGUERRA T Effects of metrizamide a new nonionic contrast medium on cardiac function during coronary angiography in the dog Radiology 115 (1975) 59
VENABLES A W and HILLER H G Complications of cardiac investigation Brit Heart J 25 (1963) 334

VARIATIONS IN VESICoureTERAL REFLUX

Influence on diagnostic validity

E. LAURIN and W. MORTENSSON

In children with vesicoureteral reflux repeat micturition cystourethrography is usually performed. Therefore every possible measure to reduce radiation dose should be seriously considered. One method is to reduce the number of films at each examination. However the inconstant nature of reflux may cause the diagnostic information to be distorted or incomplete.

The aim of the present investigation was to evaluate the risk of missing or underrating a vesicoureteral reflux at micturition cystourethrography when the number of exposures was reduced.

Material and Methods

The analysis was based on 465 micturition cystourethrograms performed in an equivalent number of infants and children aged 0 to 12 years between 4 and 6 years. Seven duplex kidneys had complete ureteral duplication, thus the competence of the ureteral orifices was evaluated in a total of 937 instances. All patients were examined because of urinary tract infection. Patients with neurogenic bladder diseases or urethral obstruction were excluded.

At micturition cystourethrography the bladder was slowly filled with contrast medium (Isopaque, Cysto Nyegaard, Norway) by means of drip infusion till the patient needed to void. One film covering the whole urinary tract was exposed before micturition. The catheter was then withdrawn and two or more films were exposed during forceful micturition. In the individual case it was considered how many films would be necessary in order to obtain

adequate information. The general intention was to keep the number of exposures low. Finally one film was exposed immediately after completed micturition to demonstrate a possible end micturition reflux. In order to obtain an opinion of irregularity of the pre micturition reflux, three films were exposed instead of one while filling the bladder in 162 of the patients with together 327 ureters. One film was exposed when the bladder was filled to one third and two thirds respectively of the calculated capacity estimated with regard to the age of the patient. The third film was exposed when the bladder was filled to tolerance. Fluoroscopy was not used.

The refluxes were classified as Grade 1 when contrast medium ascended into the ureter only, as Grade 2 when the contrast medium reached the renal pelvis, and as Grade 3 when in addition the pelvis became distended as compared with its size at urography performed with compression of the ureters. Variations of the reflux within these classes were left without notice.

The maximum reflux demonstrated in a ureter was considered to represent the true degree of reflux for that ureter, irrespective of the examination phase in which it appeared. Any deviation from this degree of reflux on any of the other films thus constituted a risk of erroneous diagnosis, the magnitude of this risk was calculated from the frequency of films demonstrating such deviations.

The probability of missing or underrating reflux of a certain degree was calculated in relation to the

Table 1

Frequency of vesicoureteral reflux in 937 ureters

	No. of ureters	Per cent of all ureters	Per cent of all reflux ureters
Isolated pre micturition reflux	10	1.1	5.9
Micturition reflux	156	16.7	92.9
Isolated end micturition		0.2	1.2
Total	166	18.0	100.0

Preceded by pre micturition reflux in approximately 80 per cent of cases

Table 2

Number of films showing micturition in 9 children with isolated pre micturition reflux in 10 ureters

Pre micturition	No. of exposures during micturition	
	2	3
Grade 1	2	4
Grade 2	1	3
Total	3	7

actual number of ureters with this particular degree of reflux. Such calculations were not influenced by the relative frequency of refluxing ureters in the total material.

The probability of missing or underestimating a reflux was calculated for the following hypothetical alternatives: (1) only one film exposed and this during micturition; (2) one film exposed after the bladder was filled and another during micturition; (3) as in (2) plus a third film exposed immediately after micturition was completed; and (4) as in (3) but two films exposed during micturition.

Results

Vesicoureteral reflux occurred in 166 of the 937 ureters examined (18%; Table 1).

Micturition reflux was the most common type but it was usually preceded by pre micturition reflux. In patients with reflux before as well as during voiding, the pre micturition reflux did not exceed the micturition reflux in any instance.

Table 3

Degree and constancy of vesicoureteral reflux during micturition related to number of films exposed during micturition

	No of exposures during micturition				Total No of ureters
	2	3	4	5-6	
Constant grade of reflux					
Grade 0	217	471	89	4	781
Grade 1	1	1	0	0	2
Grade 2	55	30	7	1	93
Grade 3	11	16	5	1	33
Total	284	518	96	7	905
Varying grade of reflux					
Grade 0 to 1	4	5	0	0	9
Grade 0 to 2	7	7	5	0	19
Grade 0 to 3	0	0	0	0	0
Grade 1 to 2	7	1	0	0	8
Grade 1 to 3	0	0	0	0	0
Grade 2 to 3	1	0	0	0	1
Total	14	13	5	0	32
Per cent with micturition reflux					
	27	11	17	43	
Per cent with varying micturition reflux					
	5	7	5	0	

Isolated pre micturition reflux appeared in 10 ureters (9 children). The grade of the refluxes and the number of films exposed during the subsequent micturition are given in Table 2. The frequency of isolated pre micturition reflux had no relation to the number of films exposed during the subsequent micturition (χ^2 test).

Isolated end micturition reflux appeared in 2 ureters (2 children), grades 2 and 3 respectively. A film had been exposed during the forceful micturition phase in both cases.

The frequency and severity of the micturition reflux varied in the films exposed during forceful micturition in every fifth ureter with micturition reflux (Table 3). Such variations did not become more frequent by increasing the number of films (χ^2 test).

In the minor group of 324 children examined with particular regard to the irregularity of the pre micturition reflux, the 3 pre voiding films showed uniform conditions in 287 ureters. In 30 ureters the reflux occurred first or was at a maximum on the third film. In the remaining 10 ureters maximum reflux occurred on the first or second film (Table 3).

Table 4

maximum degree of reflux on the first 2 films and on the third film noted during filling of bladder in cases with varying pre micturition reflux

Maximum reflux on first films	No of ureters	Reflux on third film	No of ureters
Grade 1	7	Grade 0	7
Grade 2	1	Grade 0	1
Grade 3	1	Grade 1	1
		Grade 2	1

Table 5

probability that a vesicoureteral reflux of a certain degree will be missed or underrated at micturition cystourethrography performed according to the 4 alternatives

Reflux	Alt 1	Alt 2	Alt 3	Alt 4
Fixed				
Grade 1	0.61	0.16	0.16	0.04
Grade 2	0.13	0.08	0.04	0.01
Grade 3	0.03	0.03	0.00	0.00
Total	0.77	0.27	0.20	0.05
Not fixed				
Grade 2 judged as Grade 1	0.07	0.07	0.014	0.007
Grade 3 judged as Grade 1	0.014	0.014	0.014	0.000

These 10 instances constituted a measure of the error of the present investigation in assessing the frequency and degree of pre micturition reflux as the last of the 3 films was taken consistently and used to represent the whole pre micturition

The probability of missing or underrating a vesicoureteral reflux when the number of films was reduced according to the different examination alternatives appears in Table 5

Discussion

The presence of vesicoureteral reflux substantially increases the unfavourable effect of urinary tract infection on the renal parenchyma. This effect is inversely related to the time of appearance and in particular to the degree of the reflux (KJELLBERG et al 1957; ATTIMER et coll 1963; MORTENSSON &

HELIN 1974; APERIA et coll 1976; MANLEY et coll 1976; RANSLEY 1976; VLATKOVIC et coll 1976). Micturition cystourethrography should be designed to be a guide to treatment and prognosis with reasonable accuracy. Theoretically 3 films should suffice: one exposed before, one during and one immediately after completed micturition. However the irregularity of the reflux renders it uncertain that the films actually represent the maximum possible reflux during each phase. Fluoroscopic monitoring, videotape recording or cinefluorography of the entire examination procedure has been recommended in order to exclude the risk of missing a transient reflux (GROSS & SANDERSON 1961; MELICK et coll 1962; SHOPFNER 1965; GOULD & PETERSON 1966). However it attempts to increase diagnostic reliability must be weighed against the hazards of irradiation and the consequences of an incorrect diagnosis.

The vesicoureteral reflux occurred mainly during micturition. For some reason reflux may sometimes occur only before voiding or at the end of voiding. Major refluxes were likely to occur during all the phases of micturition cystography (RUDHE 1962) and also to have a fairly constant severity.

It cannot be ruled out that the examination technique may play a role and in some cases induce at least a slight transient false reflux. However in the present investigation all observed refluxes were considered to be true.

A basis for the conclusions was the assumption that all potential refluxing ureters had actually been diagnosed. This assumption was no doubt reasonable considering the fact that no increase occurred in the frequency of clinically significant refluxes during micturition through increasing the number of exposures: neither increased the frequency of ureters with varying degrees of micturition reflux. As only one film was exposed before initiation of micturition, irregularity of pre micturition reflux was the cause of 2 per cent of ureters with transient Grade 1 reflux escaping diagnosis. These circumstances may be left without consideration as such slight refluxes apparently do not cause injury to the renal parenchyma. However an additional risk existed that Grade 2 refluxes may be missed. This risk was so small ($=0.003$) as to be considered negligible.

Variations in the degree of reflux occurred during micturition in 21 per cent of the ureters with micturition reflux. In one third of the cases it was a question of transient Grade 1 refluxes (Table 3).

Isolated reflux appearing first at end micturition was rare. It has also been reported that vesicoureteral reflux may not appear until hours after micturition, which must apparently have been incomplete (STEWART 1953, GROSS & SANDERSON). The frequency of this phenomenon cannot be determined. Such a reflux may be looked upon as a form of pre micturition reflux.

The present results show that a very high reliability may be achieved in demonstrating clinically significant vesicoureteral refluxes even when only 3 or 4 films are exposed, only 4 and one per cent, respectively, of the Grade 2 refluxes and no Grade 3 reflux would be missed. However, a slight risk of underrating Grade 3 refluxes (Table 5) was apparent.

Only the probability that a reflux would be missed or underrated when various examinations were used has been discussed. However, in discussing the benefit to cost ratio from the point of view of radiation exposure all of the non refluxing ureters must also be considered. Such a calculation will be influenced by the composition of the material, the greater the number of cases with non refluxing ureters, the less the risk of missing or underrating a reflux. In the present series no reflux occurred in 83 per cent of the ureters, this frequency corresponds fairly well with that usually mentioned in the literature. It means, for example, that the risk of missing a Grade 2 reflux, calculated in relation to the total number of ureters examined, would be approximately 0.005 when examination alternative 3 is used.

The results suggest that the element of irregularity in the nature of the vesicoureteral reflux should not lead to an unnecessarily large number of films. This is in agreement with the findings of SMITH (1966). In a group of children examined with both cineradiography and full size spot films, the frequency of reflux was only a few per cent higher at cineradiography than at examination with spot films. In the latter case 2 films were exposed, one before and one during micturition. Unfortunately the degree of the irregular refluxes was not reported.

The ordinary examination technique using full size films has several advantages: the photographic quality is high, an adequate survey of the entire urinary tract is obtained, and the antero-posterior beam direction utilizes the radiation protection the filled bladder offers to the gonads in girls (GUSTAFSSON & MORTENSSON, unpublished data).

Isotope cystography allows for continuous imaging of the entire examination without additional in-

crease in the radiation dose to the patient. The dose is on the whole very low (CONWAY in coll. 1971). Using a small number of full size spot films as alternatives 3 or 4, in combination with modern rare earth screens, the doses can also be kept very low. The measured gonad dose in girls, who constitute the majority of the patients, was insignificantly higher than the estimated dose from isotope cystography (GUSTAFSSON & MORTENSSON). However, radiography affords more detailed information regarding the evaluation of reflux, more exact.

SUMMARY

Micturition cystourethrography was performed with varying numbers of films exposed and the probability of missing a vesicoureteral reflux or underrating its severity was calculated for each series. It was concluded that a small number of exposures can give sufficiently accurate diagnosis.

REFERENCES

- APERIA A, BROBERGER O, ERICSSON N O and WIKSTRÖM I. Effect of vesicoureteral reflux on renal function in children with recurrent urinary tract infections. *Acta Intern* 9 (1976) 418.
- CONWAY J, KING L, BELMAN B and THORSON TR. Detection of vesicoureteral reflux with radionuclide cystography. *Amer J Roentgenol* 115 (1971) 70.
- GOULD H and PETERSON C. Voiding cystourethrography in children. The use of a rapid film changer. *Amer J Roentgenol* 99 (1966) 192.
- GROSS K and SANDERSON S. Cineurethrography and voiding cinecystography with special attention to vesico-ureteral reflux. *Radiology* 77 (1961) 573.
- KJELLBERG S, ERICSSON N O and RILDH U. The urinary tract in childhood. Some correlated clinical and roentgenologic observations. p. 191. Almqvist & Wiksell, Stockholm 1957.
- LATTIMER J, APERFERSON J, GEFSSON D, BAKER D A and FLEMING S. The pressure at which reflux occurs: an important indicator of prognosis and treatment. *J Urol* 89 (1963) 395.
- MANLEY C, NEUMAN N and MCALISTER W. Program for resolution of moderate primary reflux in girls. *J Urol* 115 (1976) 307.
- MELICK W, BRODEUR A and KARELIDIS D. A suggested classification of ureteral reflux and suggested treatment based on cineradiographic findings and simultaneous pressure recordings by means of the strain gauge. *J Urol* 88 (1962) 35.
- MORTENSSON W and HELLIN I. Vesico-ureteral reflux in children. *Z. Kinderchir* 15 (1974) 444.
- RANSLEY P. Opacification of the renal parenchyma in obstruction and reflux. *Pediatr Radiol* 4 (1964) 6.
- RUDHIL U. Miktionsurethrocytografi hos barn. (in Swedish.) *Sv. Lakartidningen* 11 (1966) 145.

HOFFNER CH. Cystourethrography. An evaluation of
methods. Amer J Roentgenol 95 (1965) 468
WITH A. Comparison of standard and cine cystography
for detecting vesicoureteral reflux. J Urol 96 (1966)
49

STEWART CH. Delayed cystograms. J Urol 70 (1953)
588
VLATKOVIĆ G. SCHUSTER E. and VOTAVA SPREM A.
Clinical and radiologic aspects of vesicoureteral reflux
in children. Europ J Pediat 122 (1976) 281

SIZE OF THE UNAFFECTED KIDNEY IN CHILDREN WITH UNILATERAL HYDRONEPHROSIS

M. MILER and W. MORTENSSON

Urography plays a primary role in detecting and controlling hydronephrosis. It demonstrates the renal morphology of the kidney, the collecting system and the amount of parenchyma, and the concentration of contrast medium provides approximate information on the renal function. In unilateral nephropathy, the decrease in function may also be disclosed from the degree of compensatory enlargement of the healthy kidney (MCCREIGHT & SULKIN 1967, GOSS 1964, APERIA *et al.* 1976, WIKSTAD *et al.* 1979, animal experiments KAUFMAN *et al.* 1974).

The present investigation was performed on children with unilateral hydronephrosis in order to find out whether enlargement of the unaffected kidney could reveal decreased function of the hydronephrotic kidney before this was detectable from decreased excretion of contrast medium at urography.

Material and Methods

The series comprised 32 infants and children (21 boys and 11 girls) with unilateral hydronephrosis due to pelvi-ureteric obstruction. The right kidney was affected in 9 cases and the left in 23. The age of the patients ranged from 10 days to 13 years, the median being 6 years. The presenting symptoms were palpable abdominal tumour (2 cases), proteinuria (1 case), urinary tract infection (9 cases) and abdominal pains (20 cases). The series included no patient with a duplex kidney.

The material was classified into 3 age groups because of the age-related variations in the renal size index in the reference group.

At urography 2 to 4 ml of Isopaque Cerebral (Nvegaard, Norway) were given per kg body weight to the infants and small children and 1 to 2 ml per kg body weight to the older children. Immediately following the injection, one film was exposed over the kidneys. Ureteral compression was then applied and 10 to 12 min later 2 films in different projections were exposed over the kidneys and finally a survey film of the whole urinary tract was exposed after the ureteral compression was relieved.

Renal function was assessed by the capability of excreting contrast medium at urography. Only patients in whom the function of the hydronephrotic kidney was estimated as normal ($n=23$) or possibly slightly reduced ($n=9$) were included in the series. The extra- and intrarenal parts of the pelvis including pelvic stems and calyces were moderately to markedly dilated in all cases but one; the latter case had a moderate dilatation of the pelvic confluence only. The function and the morphology of the contralateral non-hydronephrotic kidney were normal in all cases. Vesico-ureteral reflux was not present in any patient.

Renal size index was calculated as the ratio of the longest axis of the kidney to the distance from the upper border of the first lumbar vertebra to the lower border of the fourth, multiplied by 100.

The reference group was made up of infants and children without symptoms of renal disease, had normal routine laboratory tests (density and protein content of the urine, urinary sediment) and normal urography.

Table

Renal size index for the non hydronephrotic kidneys in 32 children with unilateral hydronephrosis and for a reference group. Excretion of contrast medium in the hydronephrotic kidneys as estimated as normal ($n=77$) or possibly slightly reduced ($n=9$) n =number of kidneys

Age (years)	Examination group			Reference group			
	Mean	1 SD	n	Mean	1 SD	n	
0	118	7.9	3	112	8.5	33	NS
1-6	114	7.2	4	101	5.7	28	$p<0.005$
7-13	102	5.8	25	93	5.4	119	$p<0.001$

The significance tests were made according to Student's *t* test for unpaired observations

Results

No consistent difference in the renal size index of the healthy kidney was found between children with normal or possibly slightly reduced excretion of contrast medium in the hydronephrotic kidney (Fig.)

The renal size index of the non hydronephrotic kidney was above the average in all cases but 3 in 10 cases the index was increased by more than 2 SD (Fig.)

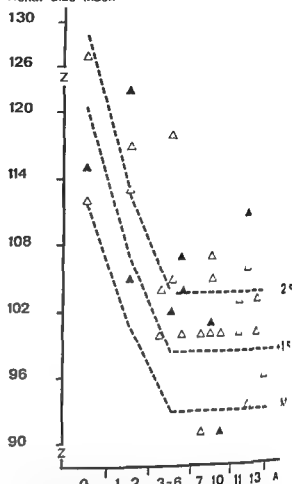
In each age group the mean value for the renal size index of the non hydronephrotic kidneys was higher than for the kidneys in the reference group (Table)

Discussion

The compensatory enlargement of the mate kidney in children with unilateral nephrectomy or nephropathy showed a high correlation between size and function: the former being expressed as parenchymal area and the latter expressed in terms of glomerular filtration rate and some tests on tubular reabsorption capacity (APERIA *et coll* 1977, 1978; WIKSTAD *et coll* 1979). However, for the sake of simplicity the length of the kidney was used instead of the area as a parameter of the renal size and function. This was also indicated by the findings of JORLLEF *et coll* (1978) that the correlation between the height of L1-L3 and the renal parenchymal area and the renal length respectively was almost identical.

The contrast medium used for urography is eliminated by glomerular filtration and concentrated by

Renal size index



Renal size index for the healthy kidney in 37 children with unilateral hydronephrosis. The function of the hydronephrotic kidney was normal in 23 cases (Δ) and possibly slightly decreased in 9 cases (▲) as estimated from urography. The broken lines indicate mean value plus 1 and 2 SD for a reference group. Age in years

the tubular water reabsorption (SAXTON 1969). The attenuation of the medium within the renal pelvis is dependent also on other factors, i.e. the dose of the medium administered, size of diuresis, dilution by retained urine in the obstructed pelvis, and the size of the pelvis. Previously it has been demonstrated that renal function may be decreased although the excretion of contrast medium into a pelvis of regular size was apparently normal (HAMB *et coll* 1973; WILKINNEYER & BOYCE 1972).

The mechanism initiating compensatory renal hypertrophy is not clearly understood for discussion of this phenomenon the reader is referred to ALLEN (1974) and EHRMANN *et coll* (1977). Increased blood flow to the healthy kidney and increased work load, especially due to the selective reabsorption in the tubuli, seem to be the main factors in eliciting renal hypertrophy while the

increasing age and renal diseases impede the compensatory response. The hypertrophy involves mainly the renal cortex and both tubular and glomerular function will increase (APERIA et coll. 1977).

The enlargement of the unaffected kidney in the present series indicated that reduced function of the hydronephrotic kidney was common although not disclosed by reduced concentration of the excreted contrast medium in the pelvis. The size of the healthy kidney thus provided complementary information on the condition of the diseased kidney. The relation between the degree of functional decrease of the hydronephrotic kidney and the degree of the compensatory enlargement of the mate kidney was not analysed. In 2 infants with no visible excretion of contrast medium on the side of the hydronephrotic kidney and therefore not included in the series the renal size index was around 140. Corrected for the different measuring techniques used this corresponded to the maximum increase in parenchymal area of the healthy kidney which was observed in children operated upon with unilateral nephrectomy during infancy (APERIA et coll. 1977). Previously it has been pointed out by HODSON & CRAVEN (1966) that the unaffected kidney may be larger than the diseased kidney in adults with unilateral hydronephrosis.

SUMMARY

Children with unilateral hydronephrosis but without evidently decreased excretion of urographic contrast medium generally had enlargement of the unaffected mate kidney indicating reduced function of the hydronephrotic kidney.

REFERENCES

- ALLEN T. Compensatory renal hypertrophy. In: Reviews of pediatric radiology, p. 411. Edited by J. Johnston and W. Goodwin. Excerpta Medica, Amsterdam, 1974.
- APERIA A, BROBERGER O, ENFENGREN K and WIKSTAD I. The relationship between renal area and renal function in different well defined childhood nephropathies. *Acta radiol. Diagnosis* 19 (1978) 186.
- — ERIKSSON N and WIKSTAD I. Effect of vesicoureteral reflux on renal function in children with recurrent urinary tract infection. *Kidney intern* 9 (1976) 418.
- — WIKSTAD I and WILTON P. Renal growth and function in patients nephrectomized in childhood. *Acta paediat. scand* 66 (1977) 185.
- EFFMANN L, ABLOW R and SIEGEL N. Renal growth. *Radiol. Clin. N. Amer.* 15 (1977) 3.
- GOSS R. Adaptive growth, p. 121. Logos Academic Press, London, 1964.
- HAMBY W, MILLER E and KAPLAN E. Renograms compared with urograms, arteriograms and function studies. *J. nucl. Med.* 10 (1969) 603.
- HODSON C and CRAVEN J. The radiology of obstructive atrophy of the kidney. *Clin. Radiol.* 17 (1966) 105.
- JORLFF H, NORDMARK J and JONSSON A. Kidney size in infants and children assessed by area measurement. *Acta radiol. Diagnosis* 19 (1978) 154.
- KAUFMAN J, DIMFOLA H, SIEGEL N, LYTTON B, KASHGARIAN M and HAYSLETT J. Compensatory adaptation of structure and function following progressive renal ablation. *Kidney intern.* 11 (1974) 10.
- MCCREIGHT CH and SULLIVAN N. Compensatory renal hyperplasia following experimental surgical deletions of the kidney complement. *Amer. J. Anat.* 110 (1967) 199.
- SAXTON H. Urography. *Brit. J. Radiol.* 42 (1969) 321.
- WIKSTAD I, APERIA A, BROBERGER O and ENFENGREN K. Vesicoureteric reflux and pyelonephritis. Long time effect on area of renal parenchyma. *Acta radiol. Diagnosis* 20 (1979) 252.
- WILKEMEYER R and BOYCE W. Validity of the intra-venous pyelogram in assessment of renal function. *Surg. Gynec. Obstet.* 135 (1972) 896.

ARTHROGRAPHY OF THE HIP IN CHILDREN

Technique, normal anatomy and findings in unstable hip joints

T. LÖNNERHOLM

Clinical signs of a congenital or acquired abnormality in one or both joints in a child generally leads to radiographic examination of the pelvis and hips. The most common indication for this examination is seen during the first year of life, is probably congenital idiopathic hip instability. ANDRÉN & VON SEYDEN (1958) have described how the radiographic examination should most suitably be performed for diagnosing this condition in the first days of life.

Conventional films of the hip in children, especially young infants, give limited information on the anatomy of the joint, as they only allow evaluation of the mineralized parts. The relation of the femoral head to the acetabulum may be difficult to assess, especially when the femoral head is not mineralized at all. The difficulties encountered in the radiographic diagnosis of hip disorders are reflected by a large number of different methods that have been described for measurement of distances and angles on the films. The main purpose of these methods is to establish the relative position of the femoral head with greater certainty. The difficulties seldom lead to poorly founded diagnoses, which may result in an unnecessarily large number of further radiographic examinations and may also have a negative influence on the choice of treatment. When information on the non mineralized components of the joint is required, arthrography must be resorted to.

As early as in the 1920s arthrography of the hip was performed on a smaller number of children with the use of iodipin, an oily contrast medium (SEEVERS 1977) or air (BRONNER 1927), but it was not until the aqueous iodine contrast media were

introduced in the 1930s that hip arthrography gained more general application. On the basis of arthrographies performed post mortem on children with normal hips, FABER (1938) and SEVERIN (1941) established criteria for the normal appearance, which still seem to be generally accepted (e.g. LAURENT 1953, GRECH 1977). An early diagnosis of congenital idiopathic hip instability was at that time uncommon, and their clinical material therefore mainly comprised children who had already begun to walk. The same is also true for a large Finnish series (LAURENT). The investigations of coxa plana (Perthes' disease) by JONSSATER (1953) included arthrography of the hip.

A small number of arthrographies on newborn infants with hip instability have been reported by PALMEIN (1961) and FELLANDER *et al.* (1970). Otherwise no Scandinavian series of arthrography appear to have been published in the last 25 years. One reason for this is the diminished need for this examination, mainly due to the present possibility of diagnosing congenital idiopathic hip instability at a very early stage. The number of arthrographies performed today is small, even in large departments of diagnostic radiology, and it therefore seemed justified to report the experiences in this department in Uppsala. Since 1972, in collaboration with the Department of Orthopaedic Surgery, arthrography has been carried out after the neonatal period in children with suggestion of hip joint instability and also in a small number of children with coxa plana.

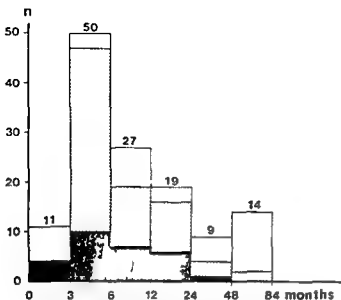


Fig. 1. Age distribution and reason for referral for the initial arthrography in 130 children. Black areas: Congenital idiopathic instability of the hip diagnosed in the neonatal period. Cross hatched areas: Congenital instability diagnosed after the neonatal period. Unfilled area: Other reasons for referral (cf. Table I).

A partly new technique for bilateral hip arthrography is described in the present report and the possibilities and limitations of the method for diagnosing abnormalities of the hip are discussed with special reference to the stereographic technique.

Definitions

Congenital idiopathic instability of the hip joint is the term used in the following to cover all grades of congenital hip instability of unknown aetiology from slight subluxation to dislocation and is considered more adequate than the generally used term congenital dislocation of the hip.

Unstable hip joint: A hip joint in which the femoral head is or can be displaced from the acetabulum partially or completely.

Acetabular dysplasia: Abnormal ossification of the iliac bone (roof of acetabulum) observed on conventional films of the hip. The chondral part of the acetabulum may appear normal or abnormal in shape at arthrography.

Neonatal period: The first month of life.

Material

Hip arthrography was performed on 130 children (91 girls, 39 boys) at this department during the period from January 1972 to December 1978. The children were examined on 185 occasions; 42 of them (34 girls, 8 boys) were examined more than once. Up to April 1973 only the affected hip was

Table I

The clinical diagnoses before the initial arthrography in 130 children

Diagnosis	No. of cases
Congenital idiopathic hip instability	99
Coxa plana	7
Snapping hip	1
Hip joint instability associated with	
Myelomeningocele	5
Cerebral palsy syndrome	4
Other neuromuscular diseases	6
Septic arthritis of the hip	5
Arthrogryposis	1
Down's syndrome	1
Total	130

examined (12 children). Subsequently the initial arthrography was always bilateral (118 children) and usually also any further arthrography after the commencement of treatment (35 of 42 children). Thus a total of 351 hip arthrographies were performed.

The ages of the patients at the first arthrography varied between 4 weeks and 6½ years (Fig. 1). Previously conventional radiography of the hips had been performed in all children as well as clinical examinations by an orthopaedic surgeon at the hospital.

The clinical diagnoses which constituted the reason for the initial arthrography are given in Table I. In the majority of cases this diagnosis was congenital idiopathic instability. Twenty consecutive cases diagnosed after the neonatal period included 11 children with such lesion have been reported in detail elsewhere (ALMBY & LÖNNERHOLM 1981). A detailed report has also been made on 9 other children from the present series in whom treatment initiated in the neonatal period was unsuccessful (ALMBY et al. 1979).

A radiographic examination of the acetabulum was also performed post mortem in a child with normal hips who died in the neonatal period.

Methods

As a rule children in whom the hip abduction was restricted by more than about 20° had been treated

by traction for varying lengths of time (up to 4 weeks) before the arthrography. In a small number of cases the traction had been combined with subcutaneous adductor tenotomy.

All children were examined under general anaesthesia. This was carried out with a nitrous oxide/oxygen mixture (2:1) and halothane (Fluothane ICI). The patients breathed spontaneously through an ordinary mask. The child was placed supine on an examination couch. Before the joint was punctured a clinical examination of the hips was performed usually by an orthopaedic surgeon but otherwise by the radiologist. Before arthrography an x-ray view of the pelvis and hips was exposed.

Radiologic equipment consisted of Mimer I (Elema Schonander) connected to an image intensification system and television unit. A focal spot of $0.6 \text{ mm} \times 0.6 \text{ mm}$ was used.

Contrast medium. In the majority (335) of the arthrograms sodium meglumine diatrizoate (Urografin 770 Schering) was used. The contrast medium employed in the other patients was iozomic acid (Rayodol Pharmacia) with an iodine content (209 mg/ml) specially adapted for arthrography. This medium has been stated to have a long absorption time (BJÖRK *et al.* 1970) but was only manufactured for a relatively short period. No detailed comparison between the contrast media was made.

Puncture technique. For the puncture a short bevel needle with OD 0.7 to 1.0 mm was used. The needle was connected to a 30 cm long polyethylene connecting tube which was attached by a 2-way stopcock to an infusion aggregate suspended about one metre above the examination couch. Before the joint was punctured the system was filled with contrast medium. In children with a unilateral hip abnormality the affected hip was always punctured first. The thigh was abducted about 20° and externally rotated. The femoral artery was palpated just distal to the inguinal fold and the position was fixed with a finger. The tip of the needle was placed on the skin surface about 1 cm medial to the arterial pulsation and the needle was then inserted in the direction of the distal part of the joint. When the needle was felt to be in the correct position in the joint the 2-way stopcock was opened and a small amount of contrast medium was infused. The needle was then left in situ with the connecting tube and the 2-way stopcock still attached while similar equipment was attached to the infusion aggregate and the other hip joint was punctured and filled with con-

trast medium to the desired extent. Thereafter the first punctured hip joint was immediately filled with a suitable amount of contrast medium. By rotating the thighs the contrast medium was distributed in the joints. In order to prevent leakage of contrast medium through the puncture track the needle (with the connecting tube and 2-way stopcock) was left in situ throughout the examination except in the first 15 arthrograms. After the examination the 2-way stopcock was opened and the contrast medium was allowed to run out before the needle was removed.

Only at one examination was the amount of injected contrast medium measured. In this case a 5-month-old girl with a normal hip joint it was 0.7 ml. The degree of filling was assessed fluoroscopically at all examinations.

Ninety per cent of the examinations were performed by the author and the remainder by another radiologist experienced in joint punctures in children.

Exposure technique. At the beginning intensifying screens of calcium tungstate were used but after 1976 rare earth screens (Lanex Regular Kodak) in combination with RP films were employed in all cases.

Two techniques were tried.

(1) Exposures with the use of a focused mobile metal grid (ratio 8/30). The film-focus distance was the longest possible i.e. 80 cm. The exposure factors were 55 to 70 kV and 30 to 60 mAs.

(2) Exposure without a grid the cassette with rare earth screens being placed directly under the patient whereby the film-focus distance was reduced to 75 cm. The exposure factors were 55 to 70 kV and 2 to 6 mAs.

A gonad shield was used in boys but not in girls. In 30 children the absorbed radiation dose was measured in the rectum and on the abdominal skin by means of thermoluminescent dosimeters. The rectal dose was one third to one fifth of the skin dose. After 8 exposures and about 3 min of fluoroscopy in children weighing 4 to 10 kg the skin dose was 8 to 14 mGy when the grid was used for all exposures and 3 to 6 mGy when it was used for only 2 of the 8 exposures (for stereoradiography). Details about the measurements of the radiation dose in different techniques of hip arthrography will be given in a forthcoming report.

Projections. Well defined projections were used. In the beginning of the series the two hips were ex-

Table 2

The position of the legs in the six standard projections

Position No	Hips				Knees flexion	Remarks
	Abduction	Flexion	Rotation	Provocation		
1	0°	10-20°	Inward 10-20°	Pull in distal direction	10-20°	
2	0°	10-20°	Inward 10-20°	Push in proximal direction	10-20°	
3	45°	0-10°	Maximally inward	-	10-20°	
4	45°	10-20°	0°	-	10-20°	2 exposures at stereo examination
5	45°	10-20°	Maximally outward	-	10-20°	
6	Maximum	90°	0°	-	90°	

posed separately (17% of all examinations) but later both hips were included in the same exposure. The legs were placed symmetrically and fixed over the knee joints. Six a.p. films of the pelvis with the legs in different positions were invariably exposed at the initial arthrography (Table 2).

In 80 per cent of the examinations in leg position 4 (Table 2) 2 films were exposed for stereoscopic analysis of the hip joints. Between the exposures the tube was moved transversally exactly 70 mm while the central ray was directed 35 mm to the right and to the left respectively of the longitudinal midline of the patient at the 2 exposures. At these examinations a plexiglass frame was placed around the pelvis and screwed into the examination table. The frame was supplied with small built in metal indicators which were projected on to the films.

Oblique or lateral views of the pelvis were seldom obtained. A larger number of a.p. views of the pelvis than those mentioned were necessary in some cases.

Evaluation of the films. The films were evaluated immediately so that a decision could be made about treatment and as to whether this could be initiated under the same anaesthesia.

The stereo film pair was inspected in a stereo roentgen comparator (SiR 3 Zeiss) at a magnification of 3X. The exposure of the metal indicators on the films allowed correct orientation of the images in the stereo comparator. In assessing the stereo pair special attention was paid to the following. The distribution of the contrast medium in the joint especially in the antero-posterior direction, the position of the femoral head in relation to the acetabulum especially in the antero-posterior direction and

the position of the head and neck of the femur in relation to the proximal femoral shaft, the mineralization of the acetabulum especially of the acetabular roof.

Depending upon the findings the hip joints were classified as follows: (1) Unstable hips (2) Stable hips (a) normal hips (b) hips in which the shape of the femoral head and acetabulum was abnormal (c) hips with retarded mineralization of the acetabular roof (acetabular dysplasia) but with no other abnormalities (3) Hips not evaluable because of technical errors.

The few hip joints which were assigned to group 2b at the initial arthrography (7 hips in 7 children with coxa plana) are not discussed in the following. For details of such cases the reader is referred to the publication of JOHNSATER. The 31 hip joints in group 2c are also excluded because most of these hips had been treated previously for congenital hip pathic instability.

The normal hip joints (group 2a) included a group which had also been found normal at all previous clinical and radiographic examinations. With certain exceptions these films were used for establishing criteria for a normal arthrographic appearance of the hip. The exceptions were hips in children whose contralateral hip had been treated by immobilization and those in children with skeletal or neuromuscular disease (e.g. myelomeningocele).

The criteria for a normal arthrography laid down by FABER and SEVERIN are as follows:

- (1) The acetabulum must enclose slightly more than half of the femoral head.
- (2) The proximal part of the edge (outer margin

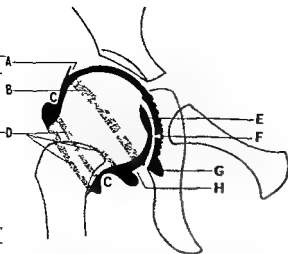


Fig. 2. Distribution of contrast medium (black areas) in a normal hip joint in infancy. A p view schematic. A Proximal part of the proximal and distally directed edge (outer margin) of the acetabular labrum. B Layer of contrast medium dorsal to the femoral head indicating the approximate position of the dorsal part of the edge of the acetabular labrum. C Orbicular zone strong circular fibres in the capsule surrounding the femoral neck preventing the joint capsule from bulging outwards. D Contrast medium around the femoral neck. E Fovea capitis femoris. F Ligamentum capitis femoris. G Contrast medium medial to the transverse ligament in the acetabular fossa. H Distal part of the edge of the acetabular labrum attached to the transverse ligament causing a broad indentation. The outline of the acetabular fossa is not quite smooth and the width of the layer of contrast medium between the femoral head and the fossa is greater than in the proximal part of the joint.

of the acetabular labrum must be pointed like a ploughshare (SEVERIN) or a rose thorn (GRECH 1977) and directed distally (Fig 2). Further it must be located in the close vicinity of a constructed transverse line (Figs 3 4) which is tangential to the distal skeletal border of the ilium on both sides (the so-called Y line).

(1) The articular surface of the femoral head must appear spherical to the naked eye.

(2) The femoral head and acetabulum must be separated by only a narrow layer of contrast medium (FAUER). Slight incongruence may be apparent in some positions of the femoral head causing accumulation of contrast medium in certain places between the articular surfaces but no wide layer of contrast medium must be present between the two surfaces (SEVERIN).

The precision of the measurements of the distances presented in the following was 0.5 mm. Consideration was paid to the magnification. The measured distances were reduced by a factor of 0.8 at exposure technique 1 and by 0.9 at technique 2.

Results

Initial arthrography. Instability was demonstrated in 111 joints. The normal hips included 62 which fulfilled the conditions mentioned and which could thus be used for establishing the criteria for a normal arthrographic appearance. Of these hips 45 were in children 2 to 12 months old, 11 were in children 13 to 24 months old and 9 were in children 25 to 72 months old.

Femoral head. In normal hip joints the size and shape of the femoral head could be easily evaluated. The fovea (Fig 2) was visible on the medial aspect in leg positions 1 and 2 and appeared as 1.4 to 8 mm (depending upon age) long flattened or even concave part on the otherwise evenly curved contour (Figs 3a b 4 left hip and Fig 5 right hip). In the stereo films the position of the femoral head and neck in relation to that of the proximal femoral shaft was evaluated. In no case was extreme anteversion or retroversion of the head or neck observed.

In the unstable hips deformity of the femoral head was common ranging from slight flattening of the proximal part of the medial contour (Fig 3 right hip) to an ovoid shape. An extremely small femoral head with a bizarre shape was found as a sequela to septic arthritis (Fig 5 left hip). In children with subluxation of the hip it was not always possible to determine the exact shape of the femoral head as accumulations of contrast medium between the femoral head and the acetabulum concealed parts of the dorsal outline (Fig 3c right hip). In the stereo films definite abnormalities of the position of the femoral head and neck in relation to the proximal femoral shaft were only observed in hips with irreducible dislocation of various origins and following septic arthritis. In these cases the femoral head and neck were extremely anteverted. These findings were confirmed at open reduction (ALMBY et al.).

Acetabulum. In the different leg positions the inclination of the pelvis varied due to the influence of the position of the lumbar spine. In leg position 3 in particular the lumbar lordosis was accentuated and in position 6 lumbar kyphosis was sometimes marked. This meant that different parts of the acetabular labrum were visible on the proximal and distal contours in a series of films. Fig 6 illustrates how the whole edge of the labrum was projected at a post mortem examination at 4 different pelvic inclinations.

In the normal hip joints the distance between the

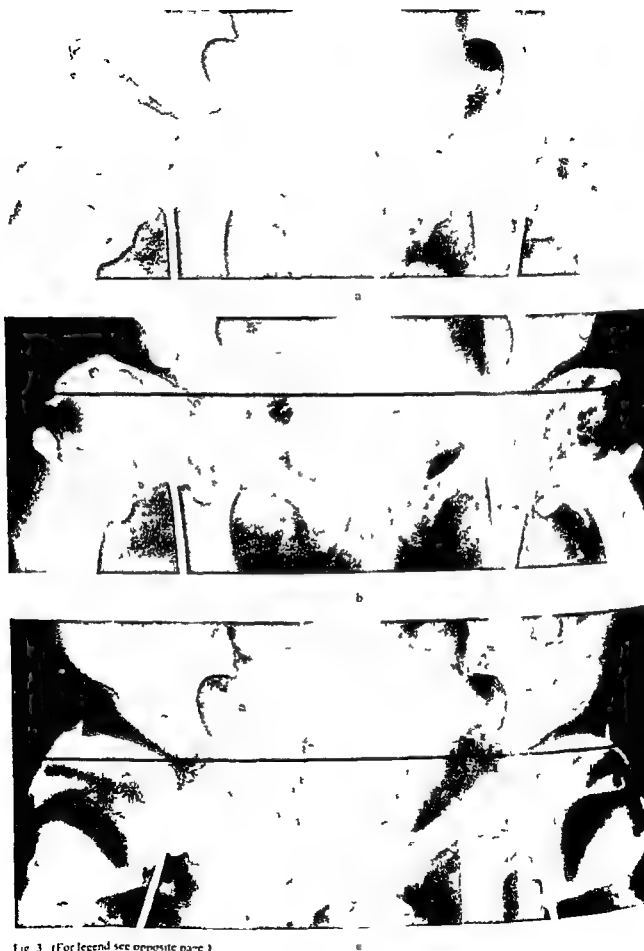


Fig. 3 (For legend see opposite page.)



4 Same boy as in Fig. 3 9 months old after 4 months treatment in a plaster spica. Clinical examination revealed nothing abnormal. The film exposed in leg position 2. On the right the layer of contrast medium between the femoral head and the acetabulum still abnormally wide. The shape of the femoral head normal. Proximal part of the edge of the acetabular labrum still but displaced 0.5 mm proximally and directed laterally.

The skeletal development of the acetabular roof only slightly retarded. Left hip still appears normal. Fovea capitis femoris and parts of the dorsal part of the acetabular labrum are marked by the 1 to 3 mm wide oblique layer of contrast medium projected over the femoral head (cf. Fig. 1). Plastic tube in the rectum for dosimetry.

but proximal part of the edge of the acetabular labrum and the Y line varied by only 1 mm or less different films from the same patient (Fig. 3 left hip). On the other hand distinct inter-individual differences depending upon age were found. Thus in children aged 2 to 12 months the edge reached a maximum of 2 mm proximal to the Y line in 21 of 43 hips (Fig. 3 left hip). In only 6 hips did it reach the level of the Y line or lie distal to this line. In children aged 13 to 24 months the edge was located between 1 mm proximal and 3 mm distal to the Y line. Among children aged 25 to 72 months it lay the level of the Y line in one case and 2 to 5 mm distal to the Y line in the others.

The edge was always pointed in shape in leg positions 1 and 2 and pointed or slightly rounded in posi-

tions 3 to 6. The part of the acetabulum forming the contour was always evenly curved except at the position of the acetabular fossa (Fig. 2, Fig. 3 left hip). The stereographic examinations yielded the following additional information:

(1) The contrast medium was largely collected in the dorsal (declivous) parts of the joints and the ventral part of the acetabular labrum was only covered in places by the contrast medium. As a rule the contrast medium accumulated to form a 3 to 4 mm wide layer in the dorsal part of the joint (Fig. 2, Fig. 5 right hip). It was not possible to decide with certainty whether this was situated between the joint capsule and the acetabular labrum. The exact position of the edge of the dorsal part of the acetabular labrum could not therefore be determined.

(2) The entire articular surface of the acetabulum was not reproduced due to the distribution of the contrast medium.

(3) Of the two skeletal contours that are invariably seen in the acetabular roof (on the a.p. view) the distal one was always located ventrally in the ilium while the proximal one was always located far dorsally. They seemed to approach one another medially but their lateral parts appeared to be essentially parallel (Fig. 7 right hip).

3 3-month-old boy with right-sided congenital idiopathic hip dysplasia diagnosed 4 weeks earlier. a) Leg position 1 b) leg position 2 c) leg position 3. Round metal indicators projected on the films. Right hip. High degree of instability. The femoral head is deformed and can be displaced in different directions. The edge of the acetabular labrum rounded in its proximal part and located 4 to 6 mm proximal to the Y line. Its shape varies according to the position of the femoral head. Outline of the acetabular fossa wavy and variable. The ligamentum capitis femoris partly visible in (b). Retarded skeletal development of the acetabular roof. Left hip: Normal.



Fig. 4. 9 month old girl (leg position 7). At the age of 6 months instability of unknown aetiology of the left hip. Cassette placed directly under the patient without grid. Left side: Femoral head dislocated proximally, lateral and dorsal to the acetabulum. It is small and has a bizarre shape, indicating that the dislocation is secondary to septic arthritis. Borderline between acetabular la-

brum and joint capsule cannot be distinguished; they are exposed between femoral head and acetabulum. The contrast medium has collected in the dechisous (dorsal) parts of the joint preventing detailed evaluation of acetabulum. Skeletal development of the ilium retarded. Right hip: Normal. Plastic tube in the rectum for dosimetry.

In *unstable* joints the appearance of the proximal edge of the acetabular labrum varied considerably. In patients with subluxation the edge was clearly rounded and displaced proximally. This edge of the labrum was abnormally mobile (Fig. 3, right hip). In irreducibly dislocated hips the borderline between the edge and the joint capsule could not be demarcated and the two formed a fold which was interposed between the femoral head and the acetabulum (Fig. 5, left hip).

At the site of the acetabular fossa the outline appeared wavy and displayed considerable variation. This was due to bulging of tissue into the joint cavity (Fig. 3, right hip). On optimum reduction this tissue became compressed into the acetabular fossa whereby the acetabular contour became normal. In irreducibly dislocated hips on the other hand the acetabular surface could not be evaluated satisfactorily (Fig. 5, left hip).

The stereographic examinations yielded the following additional information: the extent of mineralization of the acetabular roof; the mineralization deviated from the normal and was most marked dorsally. The latter was evident from the fact that the lateral part of the two contours mentioned were not parallel; the proximal (dorsal) contour diverging more or less distinctly in the proximo-dorsal direction (Fig. 7, left hip).

Relation between the articular surfaces. In normal hip joints the femoral head was always situated

centrally in the acetabulum in all leg positions; the contrast medium accumulated in different places between the articular surfaces depending on the position of the femoral head (Fig. 3, left hip; Fig. 4, right hip). When the leg was abducted 45° in internal rotation (position 5) the layer of contrast medium was generally widest (Fig. 3c, left hip). It could have a maximal width of 4 mm between the femoral head and acetabular fossa and of 2 mm between the head and the cartilaginous part of the acetabulum.

In *unstable* joints the layer of contrast medium between the articular surfaces was always wider than about 2 mm, but varied in the different leg positions. In children with only slight instability this was most clearly observed with provocation manoeuvres (leg positions 1 and 2) or at 45° abduction and maximum external rotation of the leg (Fig. 3, right hip). In patients in whom reduction was possible the optimum position of the femoral head was obtained in leg position 6 and occasionally in position 3.

The stereo films demonstrated that the femoral head was displaced to varying extents dorsally in the acetabulum in hips with marked instability. In milder degrees of instability no such displacement was observed. Only in one child who had previously had septic arthritis was the femoral head displaced ventrally.

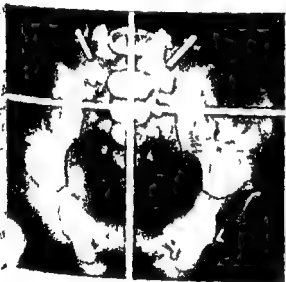
Ligamentum capitis femoris. In normal joints the ligament was visible in leg positions 1 to 5 but



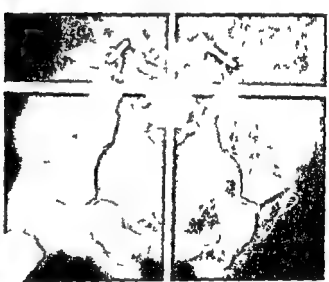
a



b



c



d

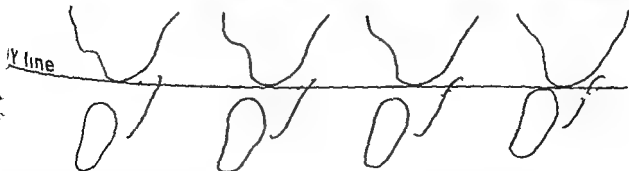


Fig. 5 Four different a.p. views of the pelvis obtained at post mortem examination of a child with normal hips. The child was born at term and died in the neonatal period. On left side the acetabular labrum has been removed and the edge of the acetabular labrum has been marked with contrast medium (Ward, Glaxo). The central ray directed on the midline at the level of the hip joints formed an angle of 30° proximally (a), 10°

proximally (b), 0° (c) and 10° distally (d) with the vertical plane. Needles and metal rods used to fix the specimen projected on the films. e) Left acetabulum from films a-d schematic. The edge of the acetabular labrum marked with a solid line in the dorsal part and with a dotted line in the ventral part. Position of the edge of the acetabular labrum in relation to a constructed line Y shown.



Fig. 7 Newly diagnosed congenital idiopathic instability of the left hip in an 14-month-old girl. Right hip. Skeletal development of the ilium normal. The proximal skeletal contour (→) was observed at stereoradiography to be located dorsally and the

distal contour ventrally in the ilium. Left hip. Acetabular dysplasia. The upper part of the proximal contour (→) came from the distal contour. The dysplasia thus most marked with dorsal part of the ilium.

could seldom be observed in its entire length. It formed an elongated 1 to 2 mm wide defect in the contrast medium from the transverse ligament to the proximal part of the fovea capitis femoris (Fig. 2 Figs 3a, b, 4 left hip).

In the unstable joints it was usually obscured by contrast medium. Occasionally the ligament appeared broad (Fig. 3b right hip).

The stereographic films were exposed in leg position 4 which was unfavourable for evaluating the ligament and in this respect the stereo films were of limited value.

Secondary arthrography. Most of these examinations were performed within one month after completion of a period in plaster of Paris. Slight instability which was not perceived at simultaneous clinical examination was often demonstrated. In such cases the femoral head could be displaced laterally in leg positions 2 and 5 whereupon the layer of contrast medium between the articular surfaces became wider than normally. A typical case of this kind is illustrated in Fig. 4. In a few patients it was also possible to displace the proximal edge of the acetabular labrum a few mm in the proximal direction. A constant finding was that the femoral head had either regained its normal shape or was considerably less deformed than at the pre-treatment arthrography. The skeletal development of the acetabular roof had always been affected favourably (Fig. 4 right hip) but had not yet become normal in more than one of 42 cases.

Technical errors. In 4 (1%) of the 351 punctured

joints no contrast medium could be injected. In some of these cases the puncture needle was probably not lying in the joint when the injection was attempted. Both examinations were among the first in the series and the failures could probably be explained by inexperience. In the other 7 hips, 3 of which had been treated previously by open reduction, the contrast medium spread extracapsularly even though the needle was considered to have been situated in the joint.

In the first 15 examinations it was found that a considerable amount of contrast medium could leak through the puncture track when the needle was removed immediately after the injection. In the subsequent examinations the needle was always left in situ until they were completed but nevertheless some leakage was usually unavoidable. However, most often it was negligible. When the needle was considered to be situated in the joint but no contrast medium flowed into it this was due to occlusion of the needle tip by a piece of tissue. In such cases repuncture with a new needle was performed.

Complications. No infections or local vascular complications occurred. In one patient a very transient general erythema, possibly caused by the contrast medium (Urografin 220), developed a few hours after the examination. Apart from brief attacks of bronchospasm in 2 patients, probably due to the anaesthetic agent (Fluothane), no other complications occurred.

Exposure technique. When the exposure was made with the cassette directly under the patient,

poorer quality were obtained than when the films used. However the quality was considered acceptable (Fig. 5) and at present all films except those for stereoscopic analysis (which require that the patient is not moved between exposures) are taken with the patient lying directly on the cassette.

Discussion

Arthrography in children is not frequently used as the number of children with hip dislocation diagnosed after the neonatal period in Sweden is very small. During the period of the present study 10 to 30 hip arthrographies were carried out in a region with a population of about 1.2 million.

Idiopathic instability of the hip was the frequent indication (76%) for the arthrography. In the present series girls were in the majority (70%) in all reported series of this condition. Most reports report no complications at all, but a few have observed isolated cases of septic arthritis (BRENNAN, GRECH). The risk of side effects was considered to be small on condition that the patients without any signs of current infection were examined and that demands for sterility equal to those at surgery could be fulfilled. Both hips were always examined even in children with unilateral symptoms, except in the early part of the disease. SEVERIN also seems to have applied this principle and this is also the general procedure in joint examinations in children. The complications are few and not serious.

In the present series it was often only after comparison between the affected and the unaffected hip that certain factors could be evaluated—in particular the position of the femoral head, the relation between the femoral head and the acetabulum, anteversion of the femoral neck and the position of the proximal femoral epiphysis and the position of the proximal femoral epiphysis in relation to the edge of the acetabular labrum in relation to the Y line.

In bilateral arthrography it is recommended that both hips be filled with contrast medium before the first exposure. Fewer exposures are then needed the exposure time will be shorter and the hips easier to compare on the films than when the two sides are examined separately. The exposures must be taken within about 10 min after the injection of the contrast medium. If a longer time elapses the medium has time to become absorbed and diluted to

such an extent that the diagnosis will be rendered difficult or impossible (BJORK, et al.). Using the technique described the interval between the injection of contrast medium on the right and left side was about one min. and the exposures were completed about 5 min later, which meant that contrast blurring was never observed. The main reasons why the arthrographies could be carried out quickly and with few failures (1%) were that the technique was simple and that only two radiologists with considerable experience in joint punctures performed the examinations. A new puncture technique was used and the method of injection of contrast medium employed by SAHLSTEDT (1976) for ankle arthrography in children was successfully applied.

The joint punctures were performed at a safe distance from the femoral artery and femoral nerve—at least 1 cm medial to the arterial pulsation. Regardless of the position of the femoral head the joints were punctured slightly lateral to the transverse ligament, where the joint capsule bulges outward to some extent (Figs 2, 3c). In cases with hip instability the needle can easily be inserted far into the acetabulum (Fig. 4, right hip) without contact with the articular surfaces and its tip can be moved sideways. Therefore it is possible even at the puncture stage to get an idea of whether or not the hip is unstable. Several other puncture techniques have been described and are summarized by GRECH.

Evaluation of the articular surfaces is rendered more difficult with much contrast medium in the joint, which also increases the risk of concealment of joint structures by extraarticular leakage. By leaving the needle in the joint during the examination the amount of contrast medium can easily be adjusted to the size of the joint, decreasing the risk of leakage.

Lateral films of the pelvis were exposed only on few occasions and were found to be of limited diagnostic value. In other descriptions of arthrographic techniques lateral views of the pelvis are not recommended.

Hip arthrography is a good example of the usefulness of stereoradiography to replace lateral exposures. At an early date SIEVERS and BRONNFELDER mentioned the value of stereoradiography but like FABER they did not describe the examination technique. LAURENT always used stereoradiography in children with congenital idiopathic instability before and after attempts at reduction.

At the exposures of the stereo films the geometry

was the same throughout. The film-focus distance and the distance which the tube was moved laterally between the two exposures were also carefully defined. The technical prerequisites for performing measurements on the films and calculating space coordinates for points in the object by means of a stereo roentgen comparator were therefore satisfied. However, there is a lack of reproducible measurement points in the hip joint at arthrography due to the uneven distribution of the contrast medium and this possibility could not therefore be utilized. However, from the subjective assessment of the stereo films, valuable additional information was obtained. In a simple way, the position of the femoral head in the antero-posterior direction, the distribution of the contrast medium in the joint and the skeletal development of the acetabulum could be determined. The stereo films revealed that severe congenital idiopathic instability in children invariably led to displacement of the femoral head dorsal to the acetabulum and that the skeletal development of the acetabular roof was most retarded in the dorsal part.

Both for arthrography and for conventional radiography in children up to at least 4 to 5 years of age the use of cassettes with rare earth screens is recommended. The cassette can be placed beneath the patient. A metal grid need not be used.

It is nowadays unusual in Sweden for congenital instability to remain undiagnosed as late as after the neonatal period and rare for the diagnosis to be made after the age of 6 months (PALMÉN 1978).

In cases diagnosed neonatally usually no radiographic examination is needed at the initial stage of treatment but routine conventional radiography at the age of a few months is generally applied (ÅLMBY & REHNBERG 1977). That conventional radiography has not always been a satisfactory diagnostic tool for the treatment is evident from the necessity for arthrography in some of these children (Fig. 1, black areas).

After the neonatal period, particularly at the ages of 1 to 6 months, hip instability is often impossible to demonstrate by clinical examination alone (ÅLMBY & LÖNNERHOLM). Primarily conventional radiography should be used. Displacement of the femur and retarded skeletal development of the acetabular roof are useful criteria for hip instability. The purpose of the arthrography is to provide a guideline for the treatment and since 1972 arthrography has been used consistently in all newly detected cases.

Several children with congenital instability were subjected to arthrography before the age of 6 months (Table 1), i.e. before they had started to bear weight on the hips. Most of these cases had more or less marked subluxation (seldom dislocation) of the femoral head and a deformity of the femoral head and acetabulum (Fig. 3). It is clear that even in a joint that has not borne weight deformity may occur. This is probably a result of fixation of the femoral head in an abnormal position consequent upon muscular imbalance, for example contractures of the hip adductors.

Traction constituted the initial part of the treatment in children with restricted abduction (more than 20°) of the hip joint. By the fact that this was applied before the arthrography in most cases with reducible instability exact reduction could be achieved at the arthrography without stretching of the hip adductors and the definitive treatment (usually immobilization in a hip spica) could be initiated under the same anaesthesia. Facilities were available for supplementing unsatisfactory traction therapy with subcutaneous adductor tenotomy in the radiologic department but only in a few cases was this necessary. Despite these measures before the reduction, femoral head necrosis in the previously unstable hip was later found in 10 per cent of a group of 20 children with congenital instability diagnosed after the neonatal period (ÅLMBY & LÖNNERHOLM).

Since arthrography was performed before the immobilization, the treatment has been individualized to a greater extent than previously. The duration of treatment is determined not only by the age of the child at diagnosis but also to a great extent by the degree of instability observed at arthrography. Arthrography has also been found in certain respects to be a more valuable method than clinical examination for assessing the result of the primary treatment (Fig. 4). In the present series some residual lengthening of the joint capsule and slight instability on provocation manoeuvres were often found despite the absence of abnormal findings at clinical examination. That these really were cases of residual conditions and not general laxity of the joints was evident by the fact that in unilateral cases the contralateral hip joint was found to be fully stable on corresponding provocation (Fig. 4).

It was also demonstrated that the cartilage components of the joint became favourably reshaped during the treatment. This has also been

and previously in older children (SEVERIN and others). However, it was not certain that the femoral ad had completely regained its normal shape after reduction treatment even in children under one year (ALMBY & LONNERHOLM). Therefore, it would be of interest to follow up such children for a longer period than has been possible hitherto.

The criteria for normal arthrographic appearance recommended by FABER and SEVERIN are based on findings at post mortem examinations (mostly newborn infants) and clinical arthrographies in children under one year of age. From the present series, criteria for a normal arthrography in infants aged 2 to 12 months may be suggested on a more valid basis than has been possible previously.

(1) The proximal part of the edge (outer margin) of the acetabular labrum is stable even when weight is borne on the femur. The margin is pointed or slightly rounded and is directed latero-distally. In all views of the pelvis the edge shall not lie at a distance of more than 2 mm on the proximal side of the Y line.

(2) The acetabulum encloses a little more than half of the femoral head. This is only an estimation as it cannot be expected that the entire edge of the acetabular labrum will be visible.

(3) The femoral head appears spherical to the naked eye except at the site of the fovea.

(4) The ligamentum capitis femoris forms a 1 to 2 mm wide defect in the contrast medium between the articular surfaces.

(5) The width of the layer of contrast medium between the articular surfaces varies depending on the position of the femoral head. The layer should be no wider than about 4 mm between the femoral head and the acetabular fossa and 2 mm between the remaining parts of the head and acetabulum to be regarded as normal.

Conclusions

(1) Hip arthrography can be performed in infants and children with a high degree of success and a very low risk of complications.

(2) It is of advantage to perform the examination under general anaesthesia at least in children under about 7 years of age.

(3) Arthrography yields detailed information about the size, shape and position of the femoral head and of the configuration of the joint cavity. Information though not detailed is also obtained on

the anatomy of the acetabulum and the ligamentum capitis femoris. Stereoradiography will give further information on the hip joint.

(4) An orthopaedic surgeon should be present at the arthrography. His task should be to perform a clinical examination of the hips before the joint is punctured and to be prepared to initiate the most suitable form of treatment, e.g. immobilization with a hip spica after closed reduction under the same anaesthesia.

SUMMARY

A method by which bilateral hip arthrography was performed under general anaesthesia in 130 infants and children 1 month to 7 years of age is described. Significant contractures of the adductor muscles had been corrected before the examination. Most of the children were girls with unilateral congenital idiopathic hip instability detected before the age of one year. From films exposed in standardized projections valuable information was obtained about the configuration of the joint cavity and the size and shape of the femoral head. Criteria for normal appearance in infants of ages 2 to 12 months are presented. More reliable details on the relation between the articular surfaces, the radiographic anatomy of the acetabulum and the distribution of the contrast medium were yielded by stereoradiography. Closed reduction was usually accomplished successfully during the arthrography which made beginning of definitive treatment under the same anaesthesia possible.

REFERENCES

- ALMBY B and RENBERG L. Neonatal hip instability. Incidence, diagnosis and treatment at the University Hospital Uppsala 1960-1964 and 1970-1974. *Acta orthop scand* 48 (1977) 642.
- and LONNERHOLM T. Hip joint instability after the neonatal period. Diagnosis and treatment of 20 consecutive cases. *Acta orthop scand* 49 (1978) 371.
- and HJELMSTEDT Å. Neonatal hip instability. Reason for failure of early abduction treatment. *Acta orthop scand* 50 (1979) 315.
- ANDRESEN L and VON ROSEN S. The diagnosis of dislocation of the hip in newborns and the primary results of immediate treatment. *Acta radiol* 49 (1958) 89.
- BJÖRK L, ERIKSSON U and INGELMAN II. A new type of contrast medium in arthrography. *Amer J Roentgenol* 109 (1970) 606.
- BRONNER H. Der diagnostische Wert der Luftfüllung des Gelenkraums bei der angeborenen Hüftverrenkung. *Zbl Chir* 54 (1927) 237.
- FABER A. Untersuchungen über die Ätiologie und Pathogenese der angeborenen Hüftverrenkung. Georg Thieme Verlag, Leipzig 1938.

- FELLANDER M, GLADNIKOFF H and JACOBSSON E In stability of the hip in the newborn Acta orthop scand (1970) Suppl No 130 p 36
- GRECH P Hip arthrography Chapman and Hall London 1977
- JONSSATER S Coxa plana A histopathologic and arthrographic study Acta orthop scand (1953) Suppl No 12
- LAURENT L E Congenital dislocation of the hip Acta chir scand (1953) Suppl No 179
- PALMEN K Preluxation of the hip joint Acta paediat 50 (1961) Suppl No 129
- Personal communication 1978
- SAHLSTEDT B Simultaneous arthrography of the talar and talonavicular joints in children I Technique Acta radiol Diagnosis 17 (1976) 545
- SEVERIN E Contribution to the knowledge of congenital dislocation of the hip joint Acta chir scand (1947) Suppl No 63
- SIEVERS R Röntgenographie der Gelenke mit Jodipon Fortschr Röntgenstr 35 (1927) 16

AVULSION FRACTURE OF THE PROXIMAL TIBIAL METAPHYSIS

Report of a case

L. DANIELSSON and G. THEANDER

traumatic injury to the knee in childhood may be various types of fractures involving the proximal metaphysis of the tibia. Most of these are common and well known but avulsion of a proximal fragment has apparently not been described previously. The present report concerns the clinical diagnosis of such avulsion and an analysis of factors responsible for this exceptional type of fracture.

Case report

A 12-year-old girl was vaulting the buck horse during physical education classes at school. Missing a jump she hit the proximal surface of her left knee against the top of the horse's back. The injury was first believed to be trivial but after a few days she sought medical advice because of increasing difficulty in walking. Physical examination revealed that when walking the girl's left leg was slightly swollen but the skin was normal in colour although its temperature appeared somewhat elevated. Pain and tenderness were localized not to the actual site of the blow but to the proximal aspect of the medial tibial condyle. There was a 10° extension deficit of the joint. This was accompanied by a flexion of the hip. ESR was 38 mm in one hour. Radiographs of the left knee were reported to show osteolytic and sclerotic abnormalities of the tibial metaphysis and a periosteal reaction. Biopsies were considered suggestive of osteosarcoma or tumour and biopsy was scheduled at a later date for the diagnosis and treatment of bone tumours. The patient was sent in advance but were lost. Therefore

a radiograph was repeated 15 days after the accident. The tibial metaphysis was again found to be irregular in structure but the previous diagnosis proved to be incorrect: the trabecular disarrangement was caused by a fracture with incipient callus. This fracture which was confirmed by tomography extended from the epiphyseal plate 4 cm distally separating a posteromedial fragment of the metaphysis. The fragment was wedge shaped tapering distally and consisted of trabecular as well as cortical bone. Slight tilting of the fragment had resulted in a diastasis which also tapered distally (Figure).

Close inquiry into the history revealed the following circumstances of the accident. When approaching the vaulting horse the girl noticed that the springboard deviated to the left. During takeoff the board slipped and the jump got askew. The girl tried to adjust the vault by maximum abduction of her left leg but could not avoid hitting the horse with the left knee which was extended whereas the hip was abducted and rotated outwards. The collision forcefully flexed the hip and simultaneously pain was experienced not only at the site of the blow which was anterior but also on the posteromedial aspect of the knee.

After the fracture had been recognized the request for biopsy was cancelled and the knee was immobilized in plaster which was removed 10 days later. By then the knee was no longer painful and joint motion had become normal but the circumference of the left thigh had decreased by 2 cm. Periparticular demineralization had occurred but the radiographic findings were otherwise unaltered. No further treatment was given. After another month healing of the fracture was complete the muscular atrophy and the demineralization had disappeared and also the ESR was normal. Nine months after the accident she had resumed physical training and was in an excellent condition.



Left knee 15 days after accident: a) A.p. view b) tomography c) oblique view. Fracture (→) d) Lateral view tomography. Posteromedial fragment of metaphysis slightly displaced.

Discussion

It is evident that the fracture sustained in the present case was not directly caused by the impact of the knee against the horse. The dorsal position of the

fragment and the diastasis clearly indicate avulsion fracture. This is a common type of sport injury in childhood and adolescence, but the usual sites of avulsion are the epiphyses and various apophyses and ossification centers. A truly metaphyseal avulsion

have never before been observed in any site of metaphyseal avulsion in this case: consideration of some special anatomic of the knee joint

the posterior and medial surfaces of the tibial epiphysis are covered by the synovial membrane which extends to the cartilaginous epiphyseal plate the adjacent part of the metaphysis: of attachment of the fibrous joint capsule (WACHSMUTH 1972) The medial wall of the intercondylar notch intervenes with the broad medial collateral ligament and its posterior wall is similarly supported mainly by the semimembranosus tendon. In the knee joint this flat tendon divides into 3 bundles of fibres which partly blend with the

The middle bundle extends distally into the tibial fascia as well as to the tibial metaphysis. The lateral bundle turning proximally forms the oblique ligament of the capsule and the tibial collateral ligament which runs a more transverse course in the tibia beneath the medial collateral ligament (WACHSMUTH 1940)

The tendons of the semimembranosus and semitendinosus muscles form the medial hamstring whereas the lateral hamstring consists of the semitendinosus tendon. The semitendinosus tendon inserts into the tibia but this attachment close to the tibial tuberosity is mediated by the pes anserinus which is composed of other tendons. The biceps femoris is attached mainly to the fibula. Since the long head of the biceps muscle and both of the medial hamstring muscles originate at the ischial tuberosity these muscles are extensors and adductors of the hip as well as flexors of the knee. The semimembranosus and semitendinosus muscles also act as medial rotators of the leg (APPLETON et coll

in the knee is extended the tension of the hamstring muscles will restrict flexion of the hip. If the knee is abducted, forceful flexion of the hip may cause an avulsion fracture at the ischial tuberosity where all of the strong hamstring muscles originate. Such avulsion may occur on the side of the leading leg of a hurdler and is frequently found after other strenuous activities such as acrobatics, dancing, football, sprinting and skiing (MILCH & SCHLONSKY & OLIX 1972; LEHNHARDT & SCHLONSKY 1974; ENLÖF et coll 1979). However if the hip is in a similar position but also rotated outwards the biceps muscle will be relatively lax and will not participate in the traction acting on the ischial

tuberosity. Under these special conditions the tension of the medial group of hamstring muscles might avulse their tibial rather than their ischial attachment.

Vaulting the horse requires a combination of abduction and outward rotation of the hips and extension of the knees but since the rules stipulate vertical posture of the body when passing the horse the hips at this moment should not normally be in a position of flexion. But if the legs hit the horse their sudden arrest will tilt the body forward. The resultant flexion of the hips might be expected to cause an avulsion fracture either at the ischial tuberosity or less likely at the tibial insertion of the hamstring tendons yet even the ischial site of avulsion seems to be rare in this sport. Since collision with the horse can obviously not be uncommon the tibial fracture observed in the present case strongly suggests some extraordinary kind of strain on the medial hamstring of the left leg.

It is therefore noteworthy that the accident was claimed to have been caused by skewness and slipping of the springboard and that the manoeuvre made to overcome these difficulties implied exaggerated abduction of the left leg. When hitting the horse the leg was thus in an unusual position which is known to favour avulsion and which also explains the remarkable site of fracture.

The initial erroneous evaluation of the injury may have been due partly to the abnormal ESR which seems to have been merely coincidental but the extreme rarity of metaphyseal avulsion is probably the main explanation why recognition of the fracture was delayed. Awareness of the fact that this type of avulsion can occur and knowledge of its radiologic appearance should help to prevent future confusion with other lesions.

SUMMARY

The radiologic appearance of avulsion fracture of the proximal tibial metaphysis is described and the conditions under which this rare type of injury may occur are analysed.

REFERENCES

- APPLETON A B, HAMILTON W J and TCHAPEROFF I C
C Surface and radiologic anatomy 4th edition W
Heffer & Sons Ltd Cambridge 1958
ENLÖF O, HILGOSSEN C and LINDHAM B Normal varia-

- tions and posttraumatic appearances of the tuberosity of ischium in adolescence. *Ann Radiol* 22 (1979) 77
- KOISSCH F. *Rauber Kopsch Lehrbuch und Atlas der Anatomie des Menschen*. Band I. 16. e Auflage. Georg Thieme Verlag, Leipzig 1940
- LANG J und WACHSMUTH W. *Praktische Anatomie*. Band I. Teil 4. Bein und Statik. 2. e Auflage. Springer Verlag, Berlin Heidelberg New York 1972
- LEHNHARDT K und DIFISCH C. Abrissstrukturen der Beckenapophysen. *Z Orthop* 112 (1974) 193
- MILCH H. Ischiolapophysiolysis. A new syndrome. *Ch Orthop* 2 (1953) 184
- SCHLONSKY J and OLIN M L. Functional disability following avulsion fracture of the ischial epiphysis. *J Bone Jt Surg* 54-A (1972) 641

EFFECTS OF PERCUTANEOUS FEMORAL ARTERY CATHETERIZATION ON LEG GROWTH IN INFANTS AND CHILDREN

W. MORTENSSON

Several reports have pointed out the risk that catheterization of the femoral artery causes retardation of leg growth. This complication has been mentioned in casuistics: the observed differences in length between the two legs ranged between 5 and 35 mm (RUDOLPH 1968, WHITE et coll. 1968, NEBEL et coll. 1969, TAKAHASHI & KAWANAMI 1970, JACOBSSON et coll. 1973, BLOOM et coll. 1974).

The phenomenon has also been systematically investigated. BASSETT et coll. (1968) found shortening of the leg on the catheterized side in 24 of 28 children aged 0 to 14 years who had been subjected to femoral artery catheterization after surgical exposure. The difference in length between the legs varied from 3 to 18 mm, the tibia being primarily affected.

The risk of growth retardation after percutaneous catheterization has also been investigated. ROSENTHAL et coll. (1972) found the distance from the anterior superior iliac spine to the lateral malleolus of the ankle joint to be at least 8 mm shorter on the catheterized side than on the other leg in almost 3 per cent of the children. The authors also commented upon the inexactness of the external measuring technique. HAWKER et coll. (1973) probably using external measurement found that the length of the legs agreed within ± 5 per cent; the findings were not further commented upon but seem to include children with a considerable leg length inequality. GAUTHIER et coll. (1973) were unable to prove any risk of inducing growth retardation by percutaneous catheterization. However, they found that usually the two legs varied in length.

With the exception of one third of the patients of GAUTHIER et coll. assessment of the leg length was made before catheterization.

BASSETT et coll. found that the degree of growth retardation in the catheterized leg paralleled the decrease in ipsilateral peripheral arterial pulses as estimated by oscillometry or by palpation. They therefore considered thrombotic complications to be the cause of impaired growth. Thrombosis of the femoral artery was in fact demonstrated by angiography in a few cases (WHITE et coll., JACOBSSON et coll., BLOOM et coll.) in most instances following catheterization after surgical exposure of the artery.

Further experiences are necessary to elucidate the relationship between growth disturbance and percutaneous catheterization of the femoral artery: prevention and treatment of the complication depends on knowledge of its causes and the natural history and clinical significance of the subsequent inequality in leg length.

Material and Methods

The material comprised 78 infants and children in whom percutaneous catheterization via the femoral artery had been performed. Approximately 80 per cent of the patients had been subjected to heart catheterization and the remainder to catheterization of the coeliac, superior mesenteric or renal arteries.

The material was divided into two main groups. Group I consisted of 42 patients who had undergone previous heart catheterization by means of catheter insertion through one of the femoral arteries and were submitted for another similar examination. All children admitted during a given period and fulfilling these criteria were included, irrespective of whether or not possible thromboembolic complica-

Table 1

Age (years) at catheterization and length (years) of follow up in 78 infants and children exposed to percutaneous catheterization of the femoral artery

	No of cases	Age at catheterization				Length of follow up		
		Range	Median	Mean	SD	Median	Mean	SD
Group 1 A	9	0-9	2.1	2.8	3.4	6.3	5.5	7.7
Group 1 B	4	0-12	4.5	4.2	5.0	3.0	3.1	1.9
Group 1 C	6	0-9	7.4	3.2	3.3	4.7	4.4	7.9
Group 1 D	23	0-14	6.0	6.3	4.2	3.0	3.3	1.5
Group 2	36	0-14	6.4	7.1	3.7	1.5	2.0	1.3

tion existed in fact such a complication was suggested in one case only. In conjunction with repeat cardioangiography, angiography of the iliac arteries and the previously catheterized femoral artery was also performed (MORTENSSON 1976). The length of the legs was measured at the same time. The angiographic findings guided the further classification of the patients into 4 subgroups: 1 A with total occlusion and 1 B with partial occlusion of the previously catheterized femoral artery; 1 C with minor thrombotic lesions in the artery; and 1 D with a normal artery.

Group 2 consisted of 36 patients. The lengths of their legs were assessed immediately before the primary catheterization and again at the follow up. Since there was no clinical suggestion of thrombotic complication, angiography was not performed.

The age of the patients at catheterization and the length of the follow up period, i.e. the time lapse between the catheterization and the follow up, are given in Table 1. This period was in no case shorter than one year.

The pre-catheterization measurements of the legs of 122 infants and children, including the patients in group 2, were used as reference values.

The length of the femur and the tibia was recorded separately by means of orthodiaphorography. With the leg resting directly on a long cassette, 3 exposures were made in sequence on the same film, using FFD 150 cm and slit collimator with the central beam focused precisely on the hip, knee and ankle joint respectively (Fig. 1). The leg and the film were kept stationary during the procedure. The length of the bones was then measured directly on the film. Two complete sets of films and measurements were made of each bone, the average being used.

The reliability of the measurements was analyzed by the variance of the results from the two measurements of the same bone and expressed by standard deviation. Whether the length of the femur or the tibia was assessed, the standard deviation was approximately 0.5 mm and was nearly the same at all ages. Any difference in length between the two legs of less than 2 mm may thus be explained by the measuring error.

The absorbed dose was 0.2 mJ weighted mean active bone marrow dose 30 μ Gy and gonadal dose 30 μ Gy to a 6 year-old boy (the median age in the material).

Results

The reference group. The difference in length between right and left femur, right and left tibia or right and left leg (=femur plus tibia) respectively appears in Table 2.

Difference in length between male bones occurred with equal frequency in all ages and was of practically the same magnitude. In 60 per cent of the cases the length difference between the two legs was within 1 mm; in 2 cases it was more than 10 mm (Fig. 2c). No predominance in bone length on either side was found.

Table 2

Difference (mm) in length between the femur and the tibia or between the femur plus tibia (i.e. the leg) of the 122 infants and children, constituting a reference group

	Range	Mean	SD	SD
Femur	0-11	1.4	1.5	0.1
Tibia	0-7	1.4	1.6	0.14
Total leg	0-7	1.4	1.5	



Fig 1 At orthodiagram radiography 3 different exposures were made on the same film with the central beam focused on the hip, knee and ankle joint respectively. The length of femur and tibia was measured separately on the film.

Group 1 The results of the length measurements are given in Fig 2 and Table 3. Leg length inequality was not encountered among the patients with uncomplicated catheterization (subgroup 1 D).

Patients with thrombosis following catheterization of the femoral artery frequently had shortening of the ipsilateral leg. The degree of growth retardation roughly paralleled the severity of the thrombotic lesion. The femora were primarily affected and in the subgroups with total or partial occlusion of the femoral artery (subgroups 1 A and 1 B) the length inequality between the catheterized and non-catheterized side was statistically significant ($p < 0.001$).

The tibia was also shorter on the catheterized side in several cases; however, the mean value of length discrepancy did not differ significantly from that of the reference group.

Group 2 The difference in growth between the bones on the catheterized and the non-catheterized side during the follow-up period appears in Fig 3. No general difference in the growth rate of the bones on the two sides existed. In one child a slight decrease was found in growth rate of the leg on the catheterized side as compared with that of the other leg and in 7 instances the growth of the catheterized leg exceeded that of the other leg.

Discussion

A good conformity in length existed between the right and left leg in most of the individuals of the reference group. A discrepancy in length of less than 5 mm must be accepted as normal (Table 2). Even a greater length difference may occur without causing complaints (SHARRARD 1971). Eight mm was therefore somewhat arbitrarily chosen as the smallest limb inequality which possibly may cause symptoms; this would give a margin of confidence and make comparison possible with previous reports on growth retardation following arterial catheterization.

Leg inequality of 8 mm or more occurred in 5 of the 78 catheterized patients. All 5 belonged to group 1 and thus there was no information on a possible length discrepancy present already before the primary arterial catheterization. In 3 cases the catheterized leg was the shorter one and the differences in length were therefore intuitively classified as resulting from complications. This would then give approximately the same frequency of growth retardation as found by ROSENTHAL et al. In two of the cases with marked length inequality the shorter leg was on the non-catheterized side and angiography showed normal arteries. This emphasized, as did the 2 cases in the reference group with marked differences in leg length, the risk of erroneously ascribing a shorter leg on the catheterized side to catheterization complication. Nevertheless the close relation between thrombosis in the catheterized femoral artery and growth retardation of the ipsilateral leg and the reverse situation, i.e. no growth retardation when the artery was normal, strongly supported the hypothesis that arterial thrombosis was the cause of growth retardation. The probability that the results demonstrated in Fig 2c would occur at a random

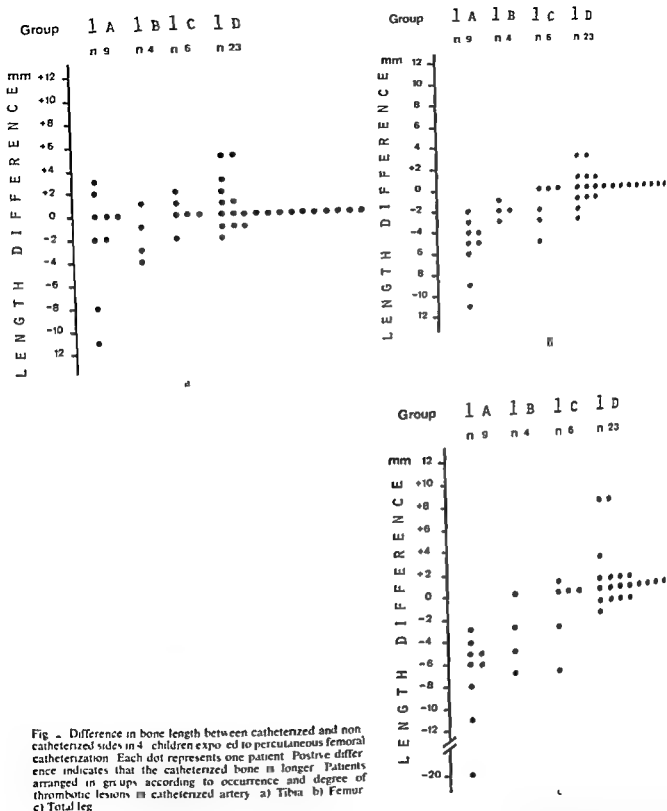


Fig. 1. Difference in bone length between catheterized and non-catheterized sides in 4 children exposed to percutaneous femoral catheterization. Each dot represents one patient. Positive difference indicates that the catheterized bone is longer. Patients arranged in groups according to occurrence and degree of thrombotic lesions in catheterized artery: a) Tibia, b) Femur, c) Total leg.

distribution was less than 0.01. Premature closure of the physis did not occur in any case.

The ultimate degree of leg shortening in patients with thrombosis varied and was possibly related to the age of the patients at the time of catheterization—the younger the patients, the greater the growth

retardation. The phenomenon could not be further evaluated, however, because of the small number of patients with confirmed thrombotic complications, and because most of them belonged to the same group. Any growth retardation factor will cause greater leg length inequality if it occurs during

Table 3

Group 1 Length difference (mm) between femur tibia and femur plus tibia (total leg) of the catheterized and non-catheterized side in 47 children previously exposed to percutaneous catheterization of the femoral artery. The patients are arranged according to the condition of the previously catheterized artery as assessed at angiography.

Group 1	No of cases	Length difference					
		Femur		Tibia		Total leg	
		Mean	SD	Mean	SD	Mean	SD
A Total occlusion	9	-5.6	7.7	-0.0	1.6	-9.9	
B Partial occlusion	4	-7.0	0.8	-1.8	1.5	-8.8	0
C Discrete thrombosis	11	-1.7	1.1	+0.1	1.3	-1.1	3.0
D Normal artery	23	+0.1	1.4	+0.5	1.8	+0.0	

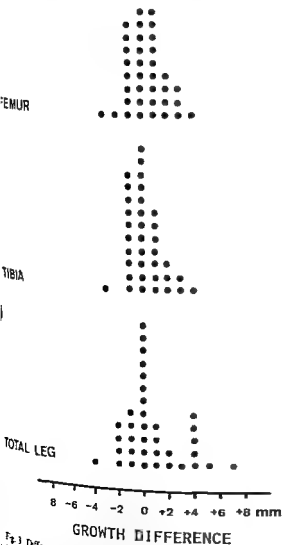


Fig. 3 Difference in growth of bones between catheterized and non-catheterized sides during follow-up period in 46 children exposed to percutaneous femoral catheterization. Positive value indicates that growth was greater on catheterized than on non-catheterized side.

period of otherwise rapid growth as in infancy and early childhood (ANDERSON et al 1964).

The duration of the growth impeding action is also related to the ultimate length inequality of the legs. However, no relation could be proved between the degree of leg length difference and the length of the follow-up period. The longer follow-up period present in children with thrombosis following catheterization is ascribed to the fact that most of the thrombotic complications occurred during the early period of the series. In this context it should be mentioned that preliminary results of an investigation in progress suggest that the growth retardation effect following thrombosis of the femoral artery seems to operate a definite limited period only. The growth rate of the mite bones is then re-equalized.

If the difference in length between the two legs amounts to 10 mm, the leg inequality may give rise to low back pain and gonarthrosis in adults (DIXON & CAMPBELL SMITH 1969; CLARKE 1972; WALSH 1973). Therefore, it may seem advisable to take corrective measures to prevent such complaints. However, according to SHARRARD, leg length discrepancy in children will rarely be considered for correction unless it is at least 25 mm. In the present series, leg length discrepancy of at least 10 mm was observed after catheterization in 2 children. The frequency identical to that of the reference group. The length differences were 11 and 20 mm, respectively, and the only symptoms were lumping and the need of operative correction was thus questionable according to SHARRARD's criteria. The risk of causing clinical significant leg length inequality at arterial catheterization is therefore considered to be

More marked differences in leg length have been reported and it is apparently not completely clear what troubles even moderate leg inequality may cause later on in life (CLARKE). Measuring the leg length after catheterization seems therefore to be advisable. Careful exterior measurements should be sufficient as a screening test.

The present results strongly suggest that thrombosis of the femoral artery was the sole cause of growth retardation. The primary step in preventing growth disturbance is therefore to make an adequate assessment of the blood flow to the catheterized leg after completed catheterization and if thrombosis has occurred to perform thrombectomy without delay. If growth disturbance has been established the ultimate degree of length difference can probably be determined after 18 to 24 months.

SUMMARY

The risk and the mechanism of inducing leg growth retardation at catheterization of femoral artery was investigated in infants and children. The ultimate degree of leg inequality and the possible clinical significance of the complication were discussed.

REFERENCES

- ANDERSSON M, MESSNER M and GREEN W. Distribution of lengths of the normal femur and tibia in children from one to eighteen years of age. *J Bone Jt Surg* 46 A (1964) 1197.
- BASSETT F, LINCOLN C, KING T and CANENT R. Inequality in size of the lower extremity following cardiac catheterization. *South med J* 61 (1968) 1013.
- BLOOM J, MOZERSKY D, BUCKLEY C and HAGGOD C. Defective limb growth as a complication of catheterization of the femoral artery. *Surg Gynec Obstet* 118 (1974) 524.
- CLARKE G R. Unequal leg length: an accurate method of detection and some clinical results. *Rheum phys Med* 11 (1972) 385.
- DIXON A and CAMPBELL SMITH S. Long leg arthropathy. *Ann rheum Dis* 28 (1969) 359.
- GAUTHIER N, HASSAN M and LABRUNE M. Is femoral artery puncture associated with disturbances of growth of the lower limbs? *Ann Radiol* 16 (1973) 197.
- HAWKER R, PALMER J, BURY J, BOWDLER J and CHITT MAJER J. Late results of percutaneous retrograde femoral arterial catheterization in children. *Brit Heart J* 35 (1973) 447.
- JACOBSSON B, CARLGREN L, HEDVALI G and SIVERTSON R. A review of children after arterial catheterization of the leg. *Pediat Radiol* 1 (1973) 96.
- MORTENSSON W. Angiography of the femoral artery following percutaneous catheterization in infants and children. *Acta radiol. Diagnosis* 17 (1976) 581.
- NEBESAR R, FLEISCH D, POLLARD J and GRISCOM T. Arteriography in infants and children. *Amer J Roentgenol* 106 (1969) 81.
- ROSENTHAL A, ANDERSSON M, THOMSON S, PAPPAS and FYLER D. Superficial femoral artery catheterization. Effect on extremity length. *Amer J Dis Child* 124 (1972) 240.
- RUDOLPH A. Complications occurring in infants and children. In: Cooperative study on cardiac catheterization. *Amer Heart Ass Monography* No. 0. New York 1968.
- SHARRARD W. Paediatric orthopaedics and fracture. p. 415. Blackwell, Oxford and Edinburgh 1971.
- TAKAHASHI M and KAWANAMI H. Femoral catheter techniques in cerebral angiography. *Brit J Radiol* 43 (1970) 771.
- WALSH M. Limb length following femoral shaft fracture in children. *J Irish med Ass* 66 (1973) 447.
- WHITE J, TALBERT J and HULLER J. Peripheral arterial injuries in infants and children. *Ann Surg* 167 (1968) 757.

VOLUNTARY HABITUAL DISLOCATION OF THE HIP IN CHILDREN

H. PETTERSSON, G. THEANDER and L. DANIELSSON

Recurrent dislocation of the hip may be a sequela of traumatic injury (GLASS & POWELL 1961; HENSELEY & SCHOFIELD 1969; DALL et coll 1970; GAUL 1973). It may also be due to skeletal dysplasia or to laxity caused by malformation or by disease of the connective tissue (HASS & HASS 1958; PACKER et coll 1977; HADDAD & DREZ 1974). Voluntary habitual dislocation of the hip in childhood is a condition in which none of these explanations seems to be valid. The present report concerns the clinical and radiologic features of this unusual disorder.

Case report

The patient is a boy with no family history of musculoskeletal disease. He was born at term of a normal pregnancy and routine examination in the maternal ward during palpation of the hip joints revealed nothing abnormal. He learned to walk at 12 months of age. At 2½ years he was admitted because of nocturnal leg pain. His mother could give the child relief by massaging his legs and during such massage she had heard clicking of his hips. Clinical examination still revealed nothing abnormal and no treatment was given. One year later the boy had developed the habit of producing a loud click by combined flexion-adduction and rotation of the left thigh. He had no pain and he stopped practising the habit in bed, which disturbed his sleep. Clinical re-examination revealed slight hyperextensibility of the first metacarpophalangeal joints. The movements of the hips appeared normal. Radiographs of the pelvis in the supine position at rest revealed nothing abnormal (Fig. 1). On request the boy proved capable of dislocating the left femoral head posteriorly. Radiography demonstrated that the dislocation was brief, the maximum dislocation lasting less than 10 s.

second. At the moment of dislocation a click was heard and gas appeared in the joint.

No treatment was given. The patient came in again to persuade the boy to stop his habit. As a result the boy had not produced any click for more than a year and had almost forgotten how to do it. The clinical and radiologic findings were normal. However, after instruction the boy was able to repeat his old trick and cine radiography again confirmed brief posterior dislocation of the left femoral head, though less marked than previously. Intraarticular gas occurred instantaneously on the dislocation as before, but no clicking was heard.

Survey of previous cases. A search of the literature revealed 6 previous cases in which voluntary recurrent dislocation of one or both hips has been radiologically demonstrated in childhood (HILGENREINER 1932; HEIDSIECK 1939; HEIKKINEN & SULA-MAA 1971; BROUDY & SCOTT 1975). The main findings in these cases are briefly summarized in the Table, which also gives the sex of the children, the age at which symptoms of the dislocation had first been noticed, and the age at confirmation. It appears that 5 of these 6 children were girls with dislocation of the right hip, whereas the boy had bilateral dislocation. That the diagnosis was established at 2 years of age in one case and at about 5 years in the others, that the dislocation was invariably accompanied by a clicking sound and by the occurrence of intraarticular gas, and that it was painful in only one case.

The clicking sound was invariably heard on dislocation and in one case also on reduction (Case 1).



Fig 1a



Fig 1b



Fig 2

Fig 1 Normal AP view of the hips at 3 1/2 years

Fig 2 Cineradiography at flexion, adduction and inward rotation of left thigh. Intraarticular gas in posteriorly dislocated left hip

Intraarticular gas was stated to occur on the dislocation in Cases 2 and 6 and can also be observed in the illustrations in Case 1. Although in the last mentioned case HILGENRFINER seems not to have realized that gas was present in the joint, he observed that when the femoral head was displaced the ligamentum teres became radiologically visible.

The dislocation was described as posterior in 5 cases and seems to have been so also in the remaining one (Case 1). In all the cases it was provoked by flexion, adduction and inward rotation of the thigh. No laxity of other joints was found except in Case 4 in which the fingers, wrists and knees were hyper-

flexible and hyperextensible, and in Case 6 in which the shoulder joints later proved unstable.

Case 4 is exceptional also in other respects. The mother of this girl had had recurrent dislocation of both shoulders and one of her knees. After the birth the hip of the daughter had begun to click. It occasionally became locked in the faulty position and had to be reduced by traction. The hip was sometimes painful and she began to limp. Despite this history the hip proved only slightly unstable when first examined at 3 years of age, and radiography as well as arthrography at that time revealed no abnormality except slight widening of the joint space. Two years later

Table

Previous reports of habitual voluntary dislocation of the hip in children

Reference	Sex	Age (years) at onset of symptoms	Age (years) at confir- mation	Side	Pain	Clicking		Intra- articular grains	Treatment
						On dis- location	On re- duction		
HILGENREINER	F	2	2	R	-	+	-		1 year
HEDGECOCK	F	<4	5	R	-	+	-		3 months
HEIKKINEN & SILLANMÄ	M	11	5	R L	-	+	-		3 years
HEIKKINEN & SILLANMÄ	F	<2	5	R	+	+	-		1 year
BRADY & SCOTT	F	4½	4½	R	-	+	-		
BRADY & SCOTT	F	Unknown	5	R	-	+	-		

dislocation was radiologically confirmed the symptoms had progressed and the muscles of the thigh had become atrophic. The hip was therefore treated surgically and immobilized for 3 months operatively. At operation the joint capsule was found to be wide enough to permit intracapsular relocation of the femoral head but was otherwise normal. The ligamentum teres was missing but the labrum labrum glenoidale and femoral head were normal. After overlapping and plication of the capsule posteriorly the dislocation could no longer be provoked on the operation table. At repeat examination one year later dislocation had allegedly not recurred. The hip movements and the radiologic findings were then normal.

One child was treated with immobilization of the hip for 9 months (Case 2). She was then symptom free for a year after which habitual dislocation recurred. In another case immobilization with an abduction splint was tried (Case 3) but dislocation recurred even in the splint which was therefore discarded. This child still had habitual dislocation at 16 years of age but when re-examined at 16 years the hips had become stable and were clinically and radiologically normal.

Follow up was included also in the reports of 2 children who received no treatment. One of these was still a year later able to dislocate the hip but had abandoned the habit (Case 5). The other one was re-examined after 7 years (Case 6). She no longer dislocated the hip which appeared clinically and radiologically normal but in the meantime she had developed the ability to provoke posterior subluxation of both shoulder joints.

DISCUSSION

The present case of bilateral habitual dislocation of the hip and the previous cases on unilateral dislocation several strikingly similar features viz. the history prompting examination the early onset of symptoms the posterior dislocation of the femoral head the manoeuvre provoking the dislocation and the clinical and radiologic findings. The children had neither a history of trauma nor any congenital or acquired dysplasia and nothing indicated a previous disease. One girl had pain in the affected hip atrophy of the thigh and a limping gait (Case 4) but since these slight disabilities gradually developed after dislocation had become habitual they were probably exceptional complications of the habit rather than manifestations of any predisposing abnormality. Pain is not known to have occurred in the other cases except the present one in which it was only transient.

Further features common to most of the children include female sex (5 cases) unilateral affection (6 cases) right sidedness of dislocation (6 cases) and stability of all joints other than the hips (all cases except one in which the ability to subluxate the humeral heads later developed). Hypermobility of some joints e.g. in the hands was noticed in 2 cases but since this finding is not uncommon in childhood its significance is doubtful. The follow up available in 6 cases shows no tendency of the dislocation to become permanent or to cause severe injury. Although limited experience suggests that the habit of dislocation may be abandoned even without treatment.

Since most of the features mentioned differ from those of other dislocations of the hip it appears justified to conclude that the unusual ability to dislocate the hip voluntarily constitutes a specific pediatric entity. It seems to involve preferentially the right hip of otherwise normal young girls for a limited period of time. In the diagnosis of this entity the typical history is of obvious importance but also the findings at clinical and radiologic examination appear significant. The occurrence of a clicking sound and of intraarticular gas deserves particular interest.

Although the sound in Case 1 was claimed to occur both on dislocation and on reduction in all other cases it was heard only on dislocation. It thus differs from the slight clicking sometimes found in newborn infants with congenital dislocation of the hip. On palpation the neonatal clicking is elicited at the moment when the femoral head is felt to slip back to a normal position (the so called Ortolani click). The sound heard on voluntary habitual dislocation appears to have invariably been rather loud resembling that produced in many normal subjects when traction is suddenly applied to a joint e.g. in a digit.

As early as in 1897 it was radiologically demonstrated that the sound elicited in a finger joint by traction is due to momentary loss of contact between the joint surfaces and that at the same moment gas occurs in the joint space (FICK 1910). Since then gas has been found under various circumstances in many other joints including the hips (for references see MAGNUSSEN 1937, RAVELLI 1955). Such an accumulation of gas has often been referred to as a vacuum phenomenon because it is explained by reduction of the intraarticular pressure liberating gas from the tissues. THOMAS & WILLIAMS (1945) who examined the knees of healthy subjects in a decompression chamber showed that gas invariably appeared in these joints on simulated rapid ascent to 35 000 feet (about 10 670 m) altitude. They aspirated the gas for analysis and found it to consist of nitrogen, oxygen and carbon dioxide in approximate equilibrium with the normal blood gases.

Even at ordinary altitudes gas may occur without traction in some joints particularly when the limbs are held in certain positions. This was first noticed in the shoulder by MAGNUSSEN who found that gas sometimes occurred in the joint if in the recumbent position the arm was extended along the head and that it disappeared on flexion. In the hip gas may be seen in a lateral view obtained in the recumbent

position (the so called frog or Cleaves position of the hip also called Lauenstein's position) but it does not appear at change of posture (SEYSS 1959). These events which quite frequently may be observed in children with normal joints suggest that in the hip and shoulder the intracapsular space varies in volume with the position of the limbs.

It might be thought that gas would accumulate even more readily in a joint when dislocation occurs but in most dislocations this seems to be prevented by abnormalities not allowing sufficient reduction of the intraarticular pressure. In dislocation caused by malformation or trauma the capsule may be incomplete or have been ruptured and in neurogenic dislocation various other types of dislocation the normal support of the surrounding tissues is absent. It is known from post mortem experiments with human joints that if the soft tissues outside the intact capsule have been removed traction separating the joint surfaces will cause the capsule to bulge into the joint space which is thereby reduced or even eliminated (FICK 1910). HEIDSIECK found at radiography of a case with habitual dislocation of the hip caused by progressive muscular dystrophy no gas to occur in the joint when the femoral head was being dislocated. It is assumed that in this disease a similar absence of capsular support *in vivo* prevents gas from accumulating in the joint.

Radiologic observations made at the moment when dislocation occurs or immediately afterwards have been rare except in infants with congenital dislocation of the hip. In this hospital the dislocation in such infants is radiologically demonstrated in the first week of life. The examination is made at dislocation has been detected on palpation and films are exposed while the femoral head is manually displaced. The films invariably include a picture of both hips obtained in the frog position with or without traction of the thighs. In a recent report the radiologic findings the films in 124 newborn infants with dislocation of one or both hips were viewed (PETERSSON & THANDER 1961). Despite the traction gas was never observed in the hip joints whether dislocated or not.

In congenital dislocation of the hip a transitory abnormal laxity of the soft tissues of the pelvis and hips is a precondition for the displacement of the femoral head (ANDERSSON 1962). The observed fact of dislocation and traction to provoke accumulation of gas in the hip joints in newborn infants with this disease is therefore not surprising but the obser-

on is noteworthy in the present context because it
tror h suggests that neither dislocation nor trac
on will cause gas to accumulate in a joint unless the
apsule is eff ctively supported by surrounding tis
u s

It might consequently be assumed that in habitual
— voluntary dislocation of the hip the gas invariably
ound to occur in the joint reflects not only com
— el teness of the capsule but also proper stability of
— ts surroundings. The findings made at operation in
— use 4 and the course of the condition in the cases
ollowed up are consistent with this assumption
Th demonstration of gas in the joint thus appears to
— be valuable both as a clue in the differential dia
gnosis between the various kinds of habitual disloca
— tion and as an indication of a favourable prognosis

SUMMARY

The clinical and radiologic findings in a child with
habitual voluntary dislocation of the hip are reported
Observations made in this case and in 6 others on record
suggest that this rare condition is a specific pediatric entity
with a good prognosis

REFERENCES

- ANDREU L. Pelvic instability in newborns. *Acta radiol*
(1967) Suppl No 212
BLODY A S and SCOTT R D. Voluntary posterior hip
dislocation in children. *J Bone Jt Surg* 57 A (1975)
116
DALL D, MACNAB I and GROSS A. Recurrent anterior
dislocation of the hip. *J Bone Jt Surg* 52 A (1970) 774

- FICK E. Allgemeine Gelenk- und Muskelmechanik. In:
Handbuch der Anatomie und Mechanik der Gelenke
Band 2 Abt 1 Teil 2 Herausgegeben von K. von
Bardeleben. Verlag von Gustav Fischer, Jena 1910
GALL E W. Recurrent traumatic dislocation of the hip in
children. *Clin Orthop* 90 (1973) 107
GLASS A and POWELL H D W. Traumatic dislocation of
the hip in children. *J Bone Jt Surg* 43 B (1961) 29
HADDAD R J and DREZ III. Voluntary recurrent anterior
dislocation of the hip. *J Bone Jt Surg* 56-A (1974) 419
HASS J and HASS R. Arthroclasis multiplex congenita.
J Bone Jt Surg 40-A (1958) 665
HEIDISIECK E. Gasbildung im frisch luxierten Gelenk. *Zbl
Chir* 66 (19 9) 2344
HEIKKINEN E S and SILLANPAA M. Recurrent dislocation
of the hip. *Acta orthop scand* 42 (1971) 55
HENSLEY C D and SCHOFIELD G W. Recurrent disloca
tion of the hip. *J Bone Jt Surg* 51 A (1969) 57
HILGENRIVER H. Ein Fall von willkürlicher Luxation
der Hüfte beim Kleinkinde. *Z orthop Chir* 56 (19 2)
259
MAGNUSSEN W. Über die Bedingungen des Hervortretens
der wirklichen Gelenkspalte auf dem Röntgenbilde.
Acta radiol 18 (1957) 7
PACKER J W, LEFKOWITZ L A and RYDER C T.
Habitual dislocation of the hip treated by innominate
osteotomy. *Clin Orthop* 83 (1972) 184
PETTERSSON H and THEANDER G. Ossification of femoral
head in infancy. II. Ossification in infants treated for
congenital dislocation. *Acta radiol Diagnosis* 20
(1979) 180
RAVELLI A. Das Vakuum Phänomen (R. Ficksches
Zeichen). *Fortschr Röntgenstr* 83 (1955) 236
SEYSS R. Das Vakuumphänomen im Bereich des Hüft
gelenkes. *Fortschr Röntgenstr* 90 (1959) 140
THOMAS S F and WILLIAMS O L. High altitude joint
pains (bends): their roentgenographic aspects. *Radio
logy* 44 (1945) 259

CONGENITAL DEFORMITIES OF SKULL CAUSED BY FETAL LIMBS

G THEANDER and J THUNANDER

Moulding of the head of the fetus is a physiologic event during delivery but this change in shape is sometimes abnormal in degree, site or duration and moulding may occur also before birth. Skewness of the face, for example, with malocclusion of the bite may develop in utero if the fetus habitually keeps its head turned to one side, the lower jaw being pressed against the shoulder. This origin of facial moulding was detected by PARMALEE (1931) and independently by BROWNE (1936).

Prenatal moulding of a calvarial bone has occasionally been shown to result from maternal abnormalities such as a uterine fibroid (BARR 1952) but may be caused also by the fetal limbs. When examining a newborn baby with congenital bilateral impression of the forehead and slight malformation of the feet, BROWNE noticed that on extension of the legs and flexion in the hip joints, each foot thus brought into contact with the forehead fitted into the ipsilateral concavity of the skull. He concluded that both types of deformities had been provoked by mutual pressure exerted by this position of the legs. In the 2 cases now reported congenital deformities of the skull are explained by the position of the fetal arms.

Case reports

Case 1 was a girl born in a head presentation. The pregnancy had been uneventful but intrauterine asphyxia in the final stage of labour prompted assistance of delivery with vacuum extraction. The observed amount of amniotic fluid appeared normal. The forehead of the baby was found to be deformed on the right side by a broad furrow running parasagittally with a lateral slope toward the temple. A much shallower but otherwise similar concavity was observed at the corresponding site on the left side.

The Apgar score at one min was 7. The baby appeared irritable and was rather pale.

Radiographic examination of the skull one hour after birth failed to demonstrate the slight deformity on the left side but clearly showed a right-sided impression of the frontal squama and traumatic lesions of the soft tissues. Several views were obtained to evaluate the degree and extent of the impression. These excluded fragmentation of the bone and showed that the concavity was limited by the coronal suture and the midline (Fig. 1). A swelling and a surrounding circular groove extending across the posterior part of the sagittal suture had obviously been shaped by the suction of the vacuum cup and the pressure by its brim. Another swelling, first situated outside the right parietal bone, resembled a cephalhematoma but on re-examination a few hours later it proved to be a subgaleal hematoma. It had in the meantime moved to the left side of the skull and extended into the neck, displacing the left auricle laterad. Despite these swellings the soft tissues in the concavity of the bone were on both occasions normal in thickness (Fig. 2).

The limbs of the baby were normal and the shape of the feet did not correspond to that of the forehead, but when the right wrist was placed against the skull its dorso-radial surface proved to fit exactly into the right frontal impression (Fig. 3). The other wrist similarly matched the slight deformity on the left side.

The subgaleal bleeding caused no trouble except transient anemia. Neurologic examination revealed nothing abnormal and the skull deformity decreased without treatment. A minor concavity on the right side was still visible after 9 months but one year later only slight flattening persisted. General growth and development were unremarkable.

Case 2 was a boy born in a foot presentation and had a parietal deformity on the left side. At the end of delivery 3½ hours after onset of labour his arms had been brought down from a position along the head. The observed amount of amniotic fluid was normal. The Apgar score was 5 at one min but improved to 9 in 2 min.



a

Fig. 1 Case 1. Right-sided concentric impression of frontal squama.

Radiographic examination of the skull immediately after birth showed a deep impression of the posterior part of the left parietal bone. The concavity was about 5 cm in diameter and was limited by the lambdoid and sagittal sutures. The bone was not fragmented and no swelling of the soft tissues existed (Fig. 4a).

The general condition of the baby appeared excellent and no treatment was given. When re-examined 22 hours later the deformity had already regressed (Fig. 4b) but the external concavity was still visible and proved to correspond perfectly with the dorsal surface of the left wrist (Fig. 4c). The deformity disappeared in a couple of weeks. Subsequent development has been unremarkable.

Discussion

Impression of part of a calvarial bone is a relatively uncommon variety of the skull deformities encountered in newborns. When found at birth it is usually attributed to fracture sustained during delivery. Such birth fractures may be caused either by obstetrical instruments or by the bony portions of the birth canal, e.g. the normal promontory or pubic bones, an exostosis of the spine or some prominence due to deformity of the pelvis. On the other hand, similar impressions may be the residues of prenatal fractures caused by abdominal trauma to the mother during the pregnancy (AYTON & LEVY 1965; ALFANDI & DAVIS 1969).



b

The impression fractures of the skull in utero like those occurring early in infancy usually lack macroscopic fragmentation of the bone and callus production. This type of injury, widely referred to as a ping-pong ball fracture, thus causes osseous abnormalities similar to those which may result from moulding of the skull in utero. Deformities of either origin have exceptionally been found prenatally at Caesarean section (BARR) vaginal palpation (GLHA RAJ 1976) or radiographic examination (RAWL 1957; ALEXANDER & DAVIS) but calvarial impression by the fetal limbs seems never to have been observed before birth. Conclusive evidence of such an impression can be obtained after birth only if the site and shape of the deformity are characteristic enough to disclose the causative former position of the limb.

The possibility that the feet may cause impression of the skull was illustrated by CAFFEY (1949) by a drawing based on the observations made by BROWNE. Since that drawing has been reproduced by CAFFEY in all subsequent editions of his text book and by various other authors as well, it has long been wellknown, but surprisingly few original observations are on record. A search of the literature revealed only 2 further cases in which the calvarial bones were cluded or suggested to have been deformed in utero by the fetal feet (BERNHART

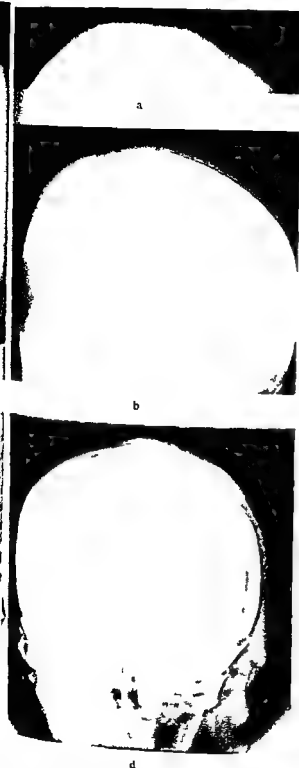


Fig 7 Case 1 Calvarial soft tissues a-c 1 hour after birth d) a few hours later Posterior parietal swelling shaped by extractor (a) Hematoma moving from right side (b) to left and extending into neck (d) No swelling outside osseous impression (c)

coll 1966 WAGNER et coll 1968) In a case reported by KYLE & JENKINSON (1973) a frontal impression detected after delivery was claimed to have been produced by the humerus of an arm found in the second stage of labour to prolapse in front of the head. The delivery had occurred spontaneously

before treatment could be given and a clinical diagnosis of fracture seems to have been taken for granted. Although radiologic findings were considered to lend support to this diagnosis the evidence given seems equally consistent with prenatal moulding by the arm.

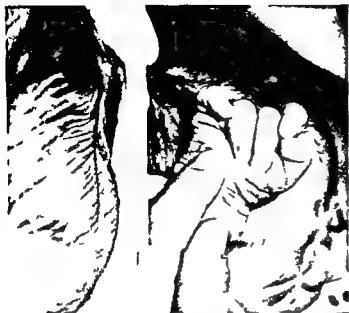


Fig. 3a

Fig. 3b



Fig. 4a

Fig. 4b

Fig. 3 (Case 1) a) External shape of deformity b) Position of arm fitted into deformity

Fig. 4 (Case 2) a) Immediately after birth. Impression of left parietal bone. No swelling of overlying soft tissues b) 22 hours later. Regression of deformity c) Position of arm fitted into deformity



Fig. 4c

In view of the difficulties in recognizing the origin of a congenital calvarial impression, the few deformities on record attributed to moulding by the fetal limbs are unlikely to reflect the true incidence of such deformation. Both the present cases were found in the course of one year. They thus suggest that prenatal impression of the skull by the fetal limbs is not an extreme rarity, and they confirm that the limb involved can be an arm as well as a leg. Although the position of the arm responsible for the deformity was observed during delivery in only one of the cases, the diagnosis was established

in both by demonstrating that a causative position could be reproduced after birth. This diagnostic manoeuvre was prompted by the radiologic findings.

The main purpose of the radiography was to exclude a bone fragment that might have injured the brain, but also the appearance of the soft tissue proved informative. The absence of a hemispheric concavity of the deformed bone in both cases did not support the initial assumption of a fetal fracture. It cannot be excluded with certainty that the instantaneous impression without fragments is characterizing a ping-pong ball fracture, may be

usually not be accompanied by bleeding. However, in this case this was considered unlikely because in the present cases of undisputable fracture of this type sustained after birth a local hematoma has invariably been demonstrable.

According to CAFFEY, cranial depression present at birth and not associated with edema or hemorrhage of the overlying soft tissues are usually due to long standing faulty fetal position rather than to recent birth injury. In the available original reports attributing calvarial moulding to the fetal limbs the soft tissues were not specifically mentioned and radiographic examination was carried out only in the case reported by WAGNER et al. Their findings were illustrated by an x-ray view of the skull showing biparietal impressions resembling ping pong ball fractures, but the soft tissues are not visible and the differential diagnosis was not discussed. The observations made in the present cases are consistent with the opinion expressed by CAFFEY and strongly suggest that radiologic evaluation of the soft tissues may afford a valuable clue to the diagnosis. Although experience is still insufficient to assess the validity of this statement, the finding of normal soft tissues outside a congenital impression of the skull should prompt an attempt to reproduce an explanatory position of the limbs.

It appears likely that a limb responsible for perinatal moulding has been kept in the causative position for some time if not habitually before birth. It is known that improper position of the fetus may reflect insufficiency of intrauterine space due, for example, to oligohydramnios or some major malformation or tumor. Since no such abnormality

existed in the present cases, it is not possible to explain why the arms of these fetuses were pressed against the skull in utero.

SUMMARY

Two cases are reported in which congenital impressions of the skull were explained by the position of the arms in utero.

REFERENCES

- ALEXANDER JR E and DAVIS JR C H. Intra uterine fracture of the infant's skull. *J Neurosurg* 30 (1969) 446.
- ANTON J H M and LEVY L F. Congenital moulding, depressions of the skull. *Brit med J* 1 (1965) 1644.
- BARR S J. Unusual pressure effect of a fibroid. *J Obstet Gynec Brit Emp* 59 (1952) 529.
- BERNSTEIN M, FRANCOIS E and FREDERICH A. Depressions osseuses congénitales secondaires à un vice de position fœtale. *Pédiatrie* 11 (19 6) 604.
- BROWNE D. Congenital deformities of mechanical origin. *Proc roy Soc Med* 79 (1936) 1409.
- CAFFEY J. *Pediatric X-ray diagnosis*. Second edition. Year Book Medical Publ., Chicago 19 0.
- GLASSER D H. Intrauterine spontaneous depression of fetal skull. A case report and review of literature. *J reprod Med* 16 (1976) 321.
- KYLE J W and JENNISON D. Depressed fracture in the newborn. *Brit med J* III (1973) 698.
- PARNIAEE A H. Moulding due to intra uterine posture, facial paralysis probably due to such moulding. *Amer J Dis Child* 47 (1931) 1155.
- RAWI A E. Depressed skull fracture in utero: a case report and review of the literature. *J S C med Ass* 53 (1957) 44.
- WAGNER M L, RUDOLPH A J and SINGLETON E B. Neonatal defects associated with abnormalities of the amnion and amniotic fluid. *Radiol Clin N Amer* 6 (1968) 279.

FROM THE DEPARTMENTS OF NEURORADIOLOGY, PEDIATRIC RADIOLOGY AND CLINICAL NEUROPHYSIOLOGY, KAROLINSKA Sjukhuset S 16401 STOCKHOLM AND THE DEPARTMENT OF PEDIATRIC RADIOLOGY, SÄCHSSKA BARNSjukhuset S 11669 STOCKHOLM, SWEDEN

ACCURACY OF ECHOVENTRICULOGRAPHY AS COMPARED WITH COMPUTER TOMOGRAPHY IN CHILDREN

U. ERASMIE J. HANSON and H. RINGERTZ

Computer tomography (CT) is in many respects the ideal method for examination of the cerebral ventricles. The method is non-invasive without risk of serious complications. It is comfortable for the patient and gives a clear conception of the size and form of the cerebral ventricles as well as of the brain and subarachnoid space. However, a CT examination is rather expensive and time-consuming and involves a radiation dose to the patient. Furthermore, in children sedation is often required and occasionally general anesthesia (ERASMIE & BERGSTRÖM 1979).

A mode echo-ventriculography (echo-VG) is an alternative examination method for the cerebral ventricles (SJOEGREN 1967). It does not provide the same detailed information as CT but gives a conception of the size of the ventricles and is much less time-consuming and expensive. It involves no radiation hazard. These properties seem to make echo-VG suitable as a screening method. Most previous evaluations of echo-VG in comparison with echo-encephalography (SJOEGREN et coll 1968, HANSON et coll 1975, KRUGSMAN 1977) and with CT (HANSON et coll, SKOLNICK et coll 1979) have indicated a good correlation between the different methods at least regarding the size of the lateral ventricles although less favourable results have also been reported (SYNEN et coll 1976). The purpose of the present investigation was to further evaluate the accuracy of echo-VG in children as compared with

CT. An attempt was also made to find out if some disorders were more likely than others to give less accurate results and if so to analyse the reasons as well as their clinical consequences.

Material and Methods

In a series of 144 children, 70 girls and 74 boys (0 to 15.2 years, median age 2.2 years), echo-VG and CT examination were as a rule performed the same day. The interval between the examinations did not exceed one week in any of the cases. A Mark I EMI scanner with a 160×160 matrix at 120 kV was used for the CT examinations. The slice thickness was 10 mm for children over one year and 5 mm for children below one year. On the CT examination the anterior horn index and the body index were determined—the anterior horn index = the distance between the lateral walls of the anterior horns of the lateral ventricles divided by the largest internal skull diameter (LINDGREN 1971) and the body index = the width of the lateral ventricles at the body divided by the internal diameter of the skull at the same site (HANSON et coll).

The echo-VG was performed with a Siemens Echo-encephalograph T Kraukrämer system type USIP 11 E using a piezoelectric crystal of 2 MHz. The distance between the lateral walls of the lateral

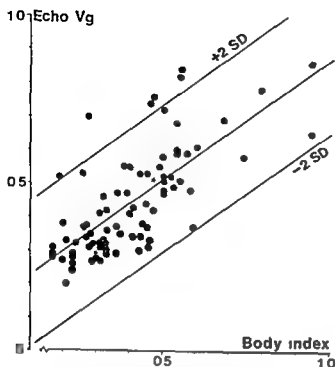


Fig. 1. Distribution of echo VG findings and CT body index in the 117 cases in which both were observable. ● = one case, ○ = two cases. Regression line with ± 2 SD is given ($r=0.725$).

ventricles a few centimeters above the external auditory meatus was determined. The lateral ventricular index (Sjogren's index) was calculated by dividing this distance with the external diameter of the head (including bone and skin) at the same site (Sjogren et al., 1964; HANSON et al., 1971). The examinations were usually carried out by one of three experienced technicians.

Computerized statistical calculations were performed with standard formulae and computer programs.

Results

The number of cases in which it had been possible to calculate the different indices, the minimum and maximum value for each index, average value

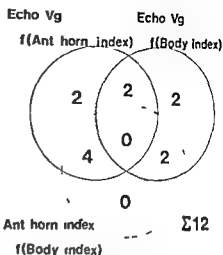


Fig. 2. Venn diagram. Distribution of the 17 cases that deviate more than 2 SD in the regression between the ventricular indices.

standard deviation (SD) and median value are given in Table 1.

The material divided in groups depending on the distribution of observable indices with average age, SD and distribution of children over and under the median age for each group appears in Table 2.

The echo VG was successful in 86 per cent of all cases, in 97 per cent for patients below 2.2 years and in 75 per cent for patients over 2.2 years. On CT the anterior horn index was measurable in 9 per cent, in 96 per cent for children below 2.2 years and in 83 per cent for children over 2.2 years. The body index was obtainable in 67 per cent, in 83 per cent for children below 2.2 years and in 51 per cent for children over 2.2 years.

The distribution in Table 2 of age relative to observable indices deviates with high significance from random ($p < 0.001$). The smaller the child the greater the probability to register all indices with both methods.

Besides dilatation of the ventricles additional findings were recorded in 18 cases. Collapsed ventricles on CT were observed in 9 cases, aged 8.3 ± 3.9 years.

Table 1

Number of patients in which the different indices were observable and statistical findings for each index

Index	Number	Minimum	Maximum	Mean	SD	Median
Ant. horn	13	0.10	0.93	0.38	0.14	0.34
Body	97	0.16	1.00	0.40	0.17	0.36
Echo-VG	14	0.0	0.86	0.41	0.15	0.35

Table 2

Distribution of observable indices in 144 patients in relation to the median age, 2.2 years. For each combination of observable indices is given average age and SD of the patients

Ant horn index	Body index	Echo VG index	Number		Age	
			<2.2 years	>2.2 years	Mean	(SD)
x	x	x	57	31	3.1	(4.1)
x	-	x	11	15	4.6	(4.3)
-	-	x	7	8	6.0	(4.1)
x	x	-	7	6	8.3	(5.6)
x	-	-	0	8	10.6	(4.2)
-	-	-	0	4	7.1	(5.0)

x = Observable index

- = Not observable index

Only asymmetry in 2 cases: asymmetry with cyst or hygroma in 2 cases; cyst or hygroma in 2 additional cases without asymmetry; midline deviation on echo-VG in 2 cases (3 and 6 mm) and finally missing CT sections in one case. The age of the last 9 cases was 1.9 ± 4.7 years, which represents a significant deviation from the group with collapsed ventricles ($p < 0.05$). The 88 patients in which all 3 indices could be calculated had higher average indices than the rest of the patients. Their anterior horn index 4.7 ± 0.13 and echo VG index 0.44 ± 0.16 deviated highly significantly ($p < 0.001$) from the corresponding values 0.30 ± 0.12 and 0.33 ± 0.10 respectively of the remaining patients.

The overall correlation coefficients between the 3 indices as well as corresponding coefficients for patients under and above the median age and girls and boys are given in Table 3.

No difference in any respect could be demonstrated between patients with echo VG and CT examination the same day and those with one to ten days between the examinations.

The equations for the linear regression between the 3 indices and corresponding residual deviations are listed in Table 4. Twelve patients with a deviation more than 2 SD from the regression lines between CT and echo VG indices in Table 4 are shown in the Venn diagram in Fig. 2. All of them had abnormal lateral ventricles. Six of them deviated more than 2 SD from the regression lines between body index and echo VG index (Fig. 1).

Discussion

The brain and the cerebral ventricles surrounded by the skull bones is no ideal object for ultrasound examination. The skull bones may be too thick and absorb too much energy to permit recording of echoes from the ventricles. In children, especially in newborns and infants, the conditions are more favourable as the cranium is thinner and recording of the ventricular echoes is consequently easier and more precise. It is quite possible to perform B mode echo VG in children (ADAPOV et al., 1965; SKOL

Table 3

Correlation coefficients (r) between CT and echo-VG indices. Number of patients within parentheses

		Echo-VG/ ant horn index	Echo-VG/ body index	Ant horn index/ body index
All		0.617 (113)	0.75 (89)	0.779 (96)
Under	years	0.609 (67)	0.774 (58)	0.815 (59)
Above	years	0.604 (46)	0.673 (31)	0.66 (37)
Girls		0.595 (46)	0.731 (47)	0.643 (49)
Boys		0.686 (57)	0.746 (41)	0.884 (47)

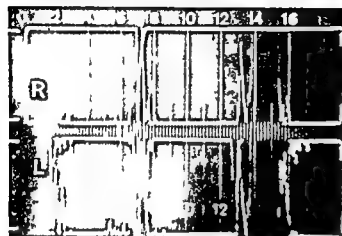


Fig. 3. CT and echo-VG from a 4-month-old girl with dilatation of posterior horn (anterior horn index 0.9, body index 0.78 and echo-VG 0.0).

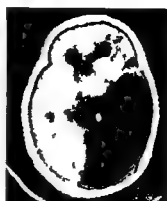


Fig. 4. CT and echo-VG from a 4-month-old girl with a cystic malformation in her right hemisphere (anterior horn index 0.4, body index not measurable and echo-VG 0.69).

(NICK et coll.) which gives more detailed information than A scan but inferior quality as compared with CT. In our experience B scan is much more difficult to handle than A scan, requiring a cooperative or sedated patient. Therefore CT has been preferred for detailed examinations and A mode echo VG for screening and follow up examinations. In the present series the echo VG was successful in 97 per cent of the patients below 2.2 years but only in 75 per cent of the patients over 2.2 years. In the younger age group the mean ventricular size was somewhat larger than in the older age group—a fact that may be a contributing cause for the better result in the younger age group. On CT it was often difficult to discern the body and occasionally the anterior horns of slender lateral ventricles. In a few cases movement artefacts complicated the evaluation. Thus it was possible to calculate the body index only in 67 per cent of the cases and the anterior horn index in 90 per cent. The result was better for children below than over 2.2 years. The better result in the younger age group is probably

due to the fact that the mean ventricular size was larger in this group and thus the ventricles were easier to delineate. Even in the not measurable cases on CT it was possible to evaluate the size and shape of the ventricular system and to demonstrate or exclude hydrocephalus. This was evidently not the case in echo VG.

Previous reports have indicated good accuracy of echo VG in children (SJOGRÉN et coll.) and in a mixture of children and adults (HANSON et coll.) while SYNEK et coll. reported less favourable results.

Table 4

Equations for the linear regressions between CT and echo-VG indices and their respective standard deviations

Equation	Residual deviation
Echo-VG = 0.691 × ant. horn index + 0.144	0.17
Echo-VG = 0.71 × body index + 0.151	0.10
Ant. horn index = 0.650 × body index + 0.164	0.08



Fig. 5 CT and echo-VG from a 3-month-old boy with dilatation mainly of anterior and posterior horns (anterior horn index 0.43 and echo-VG 0.30)

in adults. This seems to indicate better accuracy in younger patients. It is well known that echoes are more easily obtained the younger the patient is. The recording is also facilitated by large ventricles. SJÖGREN et coll recorded echoes at a more frontal site than HANSON et coll and KRUGSMAN et coll. It seems that the ventricular wall in the body region reflects the ultrasound better which was also the conclusion made by KRUGSMAN. Because CT is a more suitable method for comparing the accuracy of echo-VG than encephalography as the air might distort the ventricles (LINDGREN, JIRAT 1966, OBERSON et coll 1969, ØIGAARD 1971, LARSEN et coll 1972, PROBST 1973, MOSELEY et coll 1977). In the present series no difference existed in the correlation between echo-VG and the anterior horn index in the different age groups. The correlation between echo-VG and the body index was only slightly higher in the younger than in the older age group. The difference was not statistically significant and did not exceed the difference between the two series where no difference could be expected. SJÖGREN & REUBEN (1976) used a planimetric

method in a single suitable CT section in order to assess the size of the ventricles on CT. However, planimetry is an elaborate method and it remains doubtful whether any advantages could be achieved compared with linear measurements. Therefore the latter approach was preferred. Comparing the two CT indices with the echo-VG index it must be borne in mind that the different indices are measured in different ways and represent different parts of the lateral ventricles. In the anterior horn index the width of the anterior horns is compared with the largest internal skull diameter. The index will consequently fall below 1.0 even if there is no brain parenchyma at all at the site of the anterior horns. In echo-VG the width of the lateral ventricles was compared with the skull diameter including skin and bone while in the body index it was compared with the internal skull diameter. The echo-VG index is less clearly defined as the position of the transducer was changed until the best possible ventricular echoes were found. Nevertheless the echo-VG index and the body index were measured in the same region, thus it is natural that the correlation between them should be better than between echo-VG and anterior horn index.

An analysis of 12 cases with a deviation of more than 2 SD from the regression lines between Sjögren's index, anterior horn index and body index showed that all of them had abnormal lateral ventricles (Fig. 2). In 7 cases with a localized dilatation of the posterior horns the anterior horn index and the body index were low while Sjögren's index was high (0.29, 0.28 and 0.70 respectively in the case shown in Fig. 3) because the transducer had to be placed in a more posterior position than usual in order to receive distinct echoes. The 5 cases with a deviation more than 2 SD between the regression lines between body index and echo-VG index are all of this type (Fig. 1). This explains why all 6 deviating cases have higher echo-VG index than body index as in the figure. Thus no case was underestimated more than 2 SD with echo-VG. In 3 cases both the anterior and posterior horns were dilated but a near normal width of the body of the lateral ventricles (Fig. 5). The anterior horn index is high (0.68) while the body index is only slightly elevated (0.43) and Sjögren's index normal (0.40). In one case with a localized dilatation of the anterior horns the anterior horn index was high (0.76) but not the body index (0.31) or Sjögren's index (0.35). In one case (Fig. 4) a cystic malformation in the right hemisphere caused a high

Sjogren's index (0.69) in comparison with the anterior horn index (0.43). The body index was not measurable. The asymmetry and lack of midline structure was observed in echo VG and a malformation was suggested. Thus in all these 12 cases the discrepancy between echo VG and CT was ostensible and explained by the anatomic shape of the lateral ventricles and different sites of measurement. The anatomic information obtained from the CT examination facilitates the evaluation of the echo VG examination. An initial CT examination is therefore very valuable in follow up examinations with echo VG.

Conclusions

- (1) The accuracy of echo VG as compared with CT is fairly good in children.
- (2) For an accurate anatomic examination of the cerebral ventricles CT is the method of choice.
- (3) Discrepancy between echo VG and CT indices is often explained by the anatomic shape of the lateral ventricles and different sites of measurements.
- (4) Echo VG is useful as a screening method and for follow up examinations in children.

SUMMARY

The accuracy of echoventriculography (echo VG) using CT findings as a reference has been examined in 144 children. Lateral ventricular index on echo VG was compared with anterior horn and body indices on CT. The correlation coefficient was 0.617 and 0.725 respectively. Twelve cases with a deviation exceeding 2 SD in the regression between the indices were analysed. The conclusion is that echo-VG is fairly accurate and useful as a screening method and for follow up examinations in children.

REFERENCES

- ADAMS B D, CHASE N E, KRICEFF I I and BATTIST A A F. Cerebral ultrasonic tomography. *Radiology* 84 (1965) 115.

- ERASMIE U and BERGSTROM M. Computer tomography of the head in children. Technical aspects. *Acta radiol* Diagnosis 20 (1979) 282.
- HANSON J, LEVANDER B and LILIELOST B. Size of the intracerebral ventricles as measured with computer tomography, encephalography and echoventriculography. *Acta radiol* (1975) Suppl No 346 p 98.
- JIROUT J. Changes in the size of the subarachnoid space after the insufflation of air. *Acta radiol* 46 (1966) 81.
- KRUGSMAN J B. Echo encephalographic measurement (A scan) of the lateral ventricles in children: reliability. *Clin Neurol Neurosurg* 80 (1977) 1.
- LIN S T, POTTS D G and DECK M D F. Changes in the ventricular size during fractional pneumoencephalography. *Radiology* 104 (1972) 585.
- LINDGREN E. Encephalography in cerebral atrophy. *Acta radiol* 35 (1951) 277.
- MOSELEY I F, LOH L and DU BOLLAY H. Effects of general anaesthesia on size of cerebrospinal fluid spaces during and after pneumoencephalography. *J Neurol Neurosurg Psychiatr* 40 (1977) 1033.
- OBERSON R, CANDARIUS G and RAAD N. Height of fourth ventricle. Normal variability during pneumoencephalography. *Acta radiol* Diagnosis 9 (1969) 193.
- SIGAARD A. Changes in ventricular size during pneumoencephalography. *Neuroradiology* 3 (1971) 8.
- PROBST F P. Gas distension of the lateral ventricles at encephalography. *Acta radiol* Diagnosis 14 (1974) 1.
- SJÖGREN I. Echoencephalography in paediatric practice with special regard to measurement of the ventricular size. *Acta paediat Scand* (1967) Suppl No 14.
- , BERGSTROM K and LODIN H. Echoencephalography in infants and children. Comparison with cerebral pneumography in measuring ventricular size. *Acta radiol* (1968) Suppl No 278.
- SKOLNICK M L, ROSENBAUM A E, MATZLA T, GUTHKELCH A N and HEINZ E R. Detection of dilated cerebral ventricles in infants. A correlation study between ultrasound and computed tomography. *Radiology* 131 (1979) 447.
- SYNEK V and REUBEN J B. The ventricular brain size using planimetric measurement of EMI scans. *Brit J Radiol* 49 (1976) 233.
- , MATOUSEK M and SVENDSEN P. Ultrasonic measurement of the lateral ventricular system in adults: a comparative study of A mode echoventriculography and pneumoencephalographic investigation in 40 selected patients. *Opusculum med* 21 (1976) 147.

COMPUTER TOMOGRAPHY IN SUPERIOR SAGITTAL
SINUS THROMBOSIS

JAN BRISNAR

Thrombosis of the cerebral veins and venous sinuses is a comparatively rare condition which may develop either secondary to an infectious lesion in the vicinity of the venous structures (septic thrombosis) or without such a connection (primary or aseptic thrombosis). Aseptic thrombosis has been reported as a complication to pregnancy in various inflammatory or tumorous conditions as well as in moribund states but may also occur without any demonstrable etiologic factor. A detailed review of the literature is given in a monograph by KALBAG & WOOLF (1967). The aim of the present report is to discuss the diagnostic problems on the basis of 4 cases examined by computer tomography (CT). 3 of them also by cerebral angiography.

Methods Standard serial cerebral angiographic techniques were employed. CT was performed using an EMI 1010 head scanner with 160×160 matrix and 10 mm nominal section thickness. For contrast enhancement 100 ml Isopaque Cerebral (280 mg I/ml) was given in slow intravenous injection directly followed by scanning.

The case histories as well as the clinical and radiologic findings are presented in the Table.

Discussion

As evident from the present cases as well as from the literature (LEMMI & LITTLE 1960; KALBAG & WOOLF; GABRIELSEN & HEINZ 1969) the symptoms and signs associated with a superior sagittal sinus thrombosis may vary considerably. The mortality rate has been estimated to be 30 per cent (KENDALL

1948). The real mortality is probably considerably lower as the clinical diagnosis especially in less severe cases is difficult while the autopsy diagnosis is easy. The clinical course and the prognosis are determined by the development of collateral venous channels. In this context the location and extent of the thrombosis, anatomic variations as well as the rate of evolution of the condition will be of crucial importance (KALBAG & WOOLF).

Headache is the most common single symptom and often precedes the other symptoms by hours, days or even months (KALBAG & WOOLF). In the present series 2 patients had headache and vomiting for a month before onset of other symptoms. The headache may be associated with facial neuralgia as in case 3. Following the acute episode of cerebral venous thrombosis, headache may remain as an isolated symptom for years (HUHN 1961). In case 2, headache persisted 4 months after disappearance of other symptoms.

Convulsions, either generalized or Jacksonian seizures, are common. Focal seizures in these cases have a tendency to spread (BIEMOND 1935) as demonstrated by the only patient in the present series exhibiting seizures (case 2).

Disturbance of the motor function is frequently encountered; it occurred in 2 of the present patients (cases 1 and 2). Ascending hemiplegia due to successive spread of the thrombosis has been pointed

From the Department of Diagnostic Radiology, University Hospital S-185 Lund, Sweden. Submitted for publication 16 May 1979.

Table

Summary of case histories clinical and neurologic findings in 3 patients with angiographically confirmed and one patient with possible thrombosis of the superior sagittal sinus

Case No	Sex age pre vious diseases	History on admission	Clinical signs	Ophthalmoneuro logic findings	Brain scintigraphy	Computer tomography
1	F 43 previously healthy	4 w headache vertigo vomiting Day of admission paresthesia left side weakness	Left hemiparesis deviation conjugate to right left central facial palsy	Normal	—	Extensive bilateral intracerebral hem- orrhages with sur- rounding low at- tenuating regions
2	F 46 Crohn's disease and healed pul- monary tu- berculosis	4 w headache fever vomiting followed by epileptic seizures (After admission tran- sient loss of muscular strength in right hand)	Normal neurologic findings	Normal	Normal 1 w before admission 3 w later positive at site of CT lesion	Small right frontal hemorrhage with surrounding ede- ma. In 1 st d re- sorption of hem- orrhage (Fig 3a) Probably normal
3	M 62 previously healthy	5 d severe head- ache round right eye and cheek 2 d high fever	Normal neurologic dental and ENT findings	Normal on admis- sion 4 w later bilateral papille dema (2 D) with hemorrhages de- teriorating following month	—	
4	F 68 diabetes mellitus	3 w confusion ab- dominal pains vomit- ing minor seizures sudden deterioration with persistent loss of consciousness	Normal neurologic findings before loss of con- sciousness	—	1 w before loss of consciousness findings consistent with right frontal tumour	After loss of con- sciousness right frontal malignant tumour. Extensive left sided hem- orrhage with sur- rounding edema (Fig 4)

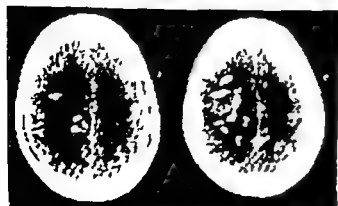
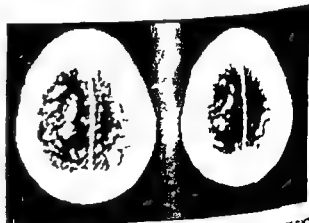


Fig 1 Case 1 Sudden onset of left sided hemiparesis CT on admission Bilateral multiple intracerebral hemorrhages surrounded by low attenuation regions (left) with moderate en-



hancement (right) At angiography occlusion of the superior sagittal sinus

Table (cont.)

Angiography	Further course
Bilateral frontoparietal masses occul- sion of frontoparietal part of superior sagittal sinus	Progressive deterioration death 2 d after admission in cerebral herniation Autopsy confirmed diagnosis
1 w after admission Partial thrombosis of posterior third of superior sagittal sinus (Fig. 2b)	Gradual improvement but some remaining headache
4 w later Thrombo- sis of posterior 1/3 of superior sagittal sinus (Fig. 3)	Almost complete disappearance of pains and papilledema in 6 m

Death 3 d after admission
No autopsy

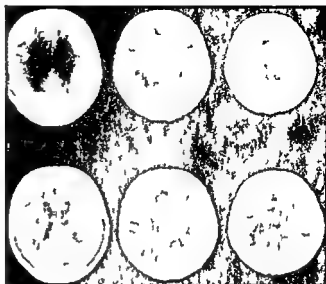


Fig. 2a

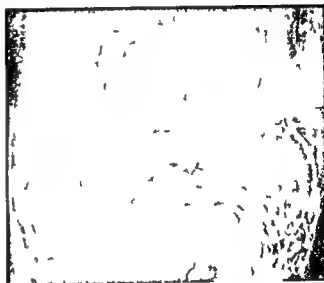


Fig. 2b

Fig. 1 Case 1. Epileptic seizures following one month's history of headache. a) CT (upper row) rightsided hemorrhage surrounded by region of low attenuation. Two weeks later a second CT (lower row) demonstrates resorption of the hemorrhage. At the same time abnormal at brain scintigraphy with ^{99m}Tc per technetate. b) Oblique a.p. view. Carotid angiography another 4 w later. Defective filling of posterior part of the superior sagittal sinus and irregular tortuous cortical veins.

Fig. 3 Case 3. One month after onset of severe facial pains and progressive papillary edema normal CT examination. Five months later left-sided carotid angiography. Occlusion of posterior part of superior sagittal sinus with collateral circulation through tortuous cortical veins.



Fig. 3



Fig. 4 Case 4 One week's symptomatology consistent with a brain tumour. Right sided frontal lesion found at ^{99}Tc brain scintigraphy. CT one week later: upper row before, lower row following i.v. contrast medium. In addition to findings consistent

with a malignant frontal right sided tumour with a rim enhancement, also a large left sided low attenuation region with multiple hemorrhages.

out to be a typical form of paralysis among these patients (BONNET & GAILLARD 1942). The paralyzes may vary in extent and intensity: may change from hemiplegia to monoplegia or the reverse or from side to side (DUBOIS 1956). Case 1 had a progressive paralysis; case 2 a brief period with loss of muscular strength in the right hand as well as a rightsided facial palsy. It has been suggested that convulsory manifestations indicate that the thrombosis is no longer limited to the superior sagittal sinus but has spread into the cortical veins (KALBAG & WOOLF).

Cranial nerve symptoms or signs are normally not observed in cases with a thrombosis limited to the superior sagittal sinus and indicate thrombotic involvement of the cavernous sinus (N III-V-VI) or the jugular bulb (N IX-XI) also.

In some cases, as in case 1, early signs of raised intracranial pressure rapidly progress into lethargy and coma.

Papilledema, the most evident sign in case 3, was present in 10 of 18 patients in the material of KALBAG & WOOLF.

The variable symptomatology in cases with a

thrombosis of the superior sagittal sinus makes the clinical diagnosis difficult, especially in the absence of known predisposing factors such as a puerperal state or oral contraceptives (BUCHANAN & BRAZINSKY 1970). Thus in none of the present cases was the diagnosis of thrombosis clinically contemplated before angiography or (case 1) CT. *In vivo* thrombosis can be conclusively diagnosed only by means of angiography demonstrating a partial (case 2, Fig. 2b) or complete (case 1, case 3, Fig. 3) occlusion of the sinus as well as tortuous irregular cortical veins. In recent years CT has in many centers replaced angiography as the primary radiologic procedure in the evaluation of neurological conditions with a symptomatology like the one encountered in cases with a thrombosis of the superior sagittal sinus. Therefore it is of interest to establish whether the CT findings in such patients are characteristic so as to suggest a sinovenous occlusion indicating angiography.

A few reports concerning the CT appearance of intracranial sinovenous thrombosis have appeared (BUONANNO *et al.* 1978; KINGSLEY *et al.* 1977; WENDLING 1978). WENDLING described one case

13 month old child with a thrombosis of the great sinus of Galen and the straight sinus who at CT exhibited increased attenuation in the region of the occluded vessels

BLOMANN *et coll* reported on 11 patients with intracranial sinovenous occlusion 6 of them with a non infectious venous thrombosis and an acute clinical onset. In 5 patients the thrombosis involved the superior sagittal sinus in the 6th patient both middle cerebral veins were thrombotized. Of these 6 cases presented at CT with distinct radiologic findings in one case multiple bilateral intracerebral hemorrhages in one a solitary intracerebral hematoma and in the third a low attenuation region exhibiting contrast enhancement. 3 of the 6 patients the ventricles were small in 1 contrast enhancement was observed and in 2 an empty sella. In a non enhanced region at the site of the superior sinus in sections perpendicular to the sinus anteriorly. If occurring on different levels this latter abnormality was considered pathognomonic. Conversely the presence of an iso attenuating clot in the sinus. In only one of these patients was the CT examination considered normal.

KINGSLEY *et coll* presented 5 patients with angiographically confirmed primary aseptic thrombosis of the superior sagittal sinus. All 4 patients died within the first week after ictus had either small ventricles on the initial scan or ventricular enlargement on subsequent scans. One patient had slight swelling of one hemisphere and one had bilateral low attenuation areas with hemorrhage.

It is a well known fact that multiple intracranial hemorrhagic infarcts are often found at autopsy in cases with extensive sinovenous thrombosis (KALBAL & WOOLF). It is therefore not surprising that CT in some cases with a thrombosis of the superior sagittal sinus demonstrates bilateral multiple hemorrhages surrounded by low attenuation regions. This was the case in case 1 (Fig 1). In case 4 a thrombosis would explain the otherwise confusing CT findings (Fig 4) as well as the rapid impairment of the condition of the patient. The finding of multiple or even bilateral intracranial hemorrhages in a traumatic patient is strongly indicative of the presence of thrombosis of the superior sagittal sinus. In cases with a single intracerebral hematoma surrounded by a low attenuation region as in case 2 (Fig 2a) the probability of an underlying thrombosis is much less. However it should be borne in mind that the possibility exists

Whether the ventricles are slightly compressed is often difficult to determine from a single CT examination. In case 1 the extensive hemorrhages compressed the ventricular system (Fig 1). Cases 2 and 3 had normal ventricular size at the initial scan as well as at subsequent examinations. However the serial CT examinations reported by KINGSLEY *et coll* indicated that a sagittal sinus thrombosis often causes a compression of the ventricles. The finding of a small ventricular system though highly unspecific should therefore call attention to the possibility of a thrombosis of the superior sagittal sinus.

No gyral enhancement increased attenuation along the occluded venous channels or a non enhanced region was found in the present series.

It is debatable whether the diagnosis of sinovenous occlusion has any major therapeutic implications. The frequent association between sinovenous occlusions and hemorrhagic infarcts has led to a reluctance to use anticoagulants. GUTTEFINGER & KOKMEN (1977) reported 3 patients treated with anticoagulants for a sinus thrombosis. 2 died from hemorrhagic intracerebral complications. It was concluded that the risk of untoward complications was great enough that one should rely on more conservative therapy with antiedematous agents and anticonvulsants.

SUMMARY

Three angiographically confirmed cases and one possible case of aseptic superior sagittal sinus thrombosis had CT findings ranging from apparently normal to single or even bilateral multiple intracerebral hemorrhages surrounded by low attenuation regions. The latter finding in particular suggests a possible superior sagittal sinus thrombosis.

REFERENCES

- BIFORD A. Clinical symptoms of so-called spontaneous thrombosis of superior longitudinal sinus. *Ned T Geneesk* 79 (1935) 5422
- BONNET P *et GAILLARD E*. Thrombo phlébite latente du sinus latéral droit. *Lyon med* 168 (1942) 97
- BUCHANAN D S and BRAZINSKI J H. Dural sinus and cerebral venous thrombosis. Incidence in young women receiving oral contraceptives. *Arch Neurol* 22 (1970) 440
- BLOMANN F S, MOODY D M, BALL M R and LASTER D W. Computed cranial tomographic findings in cerebral sinovenous occlusion. *J Comp Ass Tomogr* 2 (1978) 281

- DUBOIS J Les thrombo phlebitis cerebrales du post partum Gynec et Obstet 55 (1956) 472
- GETTLEFINGER D M and KOKMEN E Superior sagittal sinus thrombosis Arch Neurol 34 (1977) 2
- GABRIELSEN T O and HEINZ E R Spontaneous aseptic thrombosis of the superior sagittal sinus and cerebral veins Amer J Roentgenol 107 (1969) 579
- HUHN A Die Differentialdiagnose der Hirnvenen - und Sinusthrombose Acta neurochir (Wien) (1961) Suppl No 7 p 355
- KALBAG M and WOOLF A L Cerebral venous thrombosis with special reference to primary aseptic thrombosis Oxford University Press London 1967
- KENDALL D Thrombosis of intracranial veins Brain (1948) 386
- KINGSLEY P E KENDALL B E and MURPHY J F Superior sagittal sinus thrombosis an evaluation of the changes demonstrated on computed tomography J Neurol Neurosurg Psychiat 41 (1978) 1065
- LEMAN H and LITTLE S C Occlusion of intracranial venous structures Arch Neurol 3 (1960) 159
- WENDLING L R Intracranial venous sinus thrombosis diagnosis suggested by computed tomography Amer J Roentgenol 130 (1978) 978

COMPUTER TOMOGRAPHY IN THE EVALUATION OF SUBARACHNOID HEMORRHAGE

B. LILIEQUIST and M. LINDQVIST

The introduction of computer tomography (CT) in 1973 has changed most aspects of conventional neuroradiology. The impact of the new method has been great and the indication for most if not all conventional neuroradiologic procedures has been modified or even considerably changed. Thus encephalography has almost entirely been replaced by CT. Cerebral angiography still is indispensable for the examination of patients with subarachnoid hemorrhage as the size and shape of an arterial aneurysm cannot be assessed in detail by CT scanning. Angiography on the other hand seldom gives any detailed information about the volume and extension of a possible intracerebral hematoma following rupture of an aneurysm nor does it reveal cerebral blood or a penetration of blood into the cerebral ventricles.

A single angiography of the relevant vessel has been favoured over a complete angiographic examination as the initial procedure (KENDALL et coll 1976) on the argument that a new bleeding is seldom due to a rupture of a second aneurysm when multiple aneurysms are present. The initial angiography can be limited to the vessel harbouring the aneurysm when a definite location of the aneurysm is indicated clinically or if in other cases the site of the aneurysm could be more adequately determined. This would be of advantage if the modern trend to operate saccular intracranial aneurysms at an early stage after a subarachnoid bleeding will be the dominating surgical policy.

In order to evaluate CT in subarachnoid hemorrhage a review of 68 consecutive patients has been performed as an extension of a previous report (LILIEQUIST et coll 1977). Some of the patients are included in both reports. Special interest has been focused upon the time relationship between the initial bleeding and the persisting appearance of blood in the cisterns and also upon the possibility offered by the new method to reveal infarctions.

Material

The material consisted of 68 consecutive patients whose sex and age distribution does not diverge from what is commonly found in a population of patients with subarachnoid hemorrhage (Table 1).

All patients were referred on clinical suggestion of subarachnoid bleeding; all had blood in the CSF at lumbar puncture. In all patients CT scanning was the first diagnostic procedure followed by cerebral angiography in all but 3 patients. In one of these 3 patients CT demonstrated a cerebellar hemorrhage which was evacuated; in another the intracranial circulation abolished at the time of angiography due to a huge intracerebral hematoma; the third patient died before angiography could be performed. In these 3 cases the hematoma could subsequently be shown not to have been caused by a ruptured aneurysm.

Table 1

Sex and age distribution of 68 patients with clinical signs of subarachnoid hemorrhage examined with CT and cerebral angiography

Age (years)	Women	Men	Total
<20	1	1	2
20-29	-	2	2
30-39	4	4	8
40-49	9	8	17
50-59	10	11	21
60-69	11	2	13
70+	5	3	8
Total	37	31	68

One vessel angiography was carried out in 5 patients, two vessel angiography in 15 and three vessel angiography in 32 patients.

In 10 patients no aneurysm could be found at angiography or autopsy. In 8 of these three vessel angiography was carried out, in one two vessel examination and in one a carotid angiography only.

In 55 of the 68 patients at least one intracranial arterial saccular aneurysm was demonstrated. One patient was excluded from the series since gross artifacts at CT scanning prohibited a detailed analysis. In 2 patients an intracerebral hematoma was evident on CT, not caused by the aneurysm, documented at angiography. For a further analysis 52 patients with subarachnoid hemorrhage caused by confirmed aneurysm rupture remain (Tables 2-3).

Results

The time relationship between the initial bleeding and CT evidence of blood in the CSF spaces in the 52 patients is illustrated in Fig. 1.

Table 2

Number of aneurysms in 52 patients with subarachnoid hemorrhage caused by rupture of aneurysm

No. of cases	No. of aneurysms
41	1
8	2
3	3
Total	66

Table 3

Site and number of aneurysms in 52 patients with subarachnoid hemorrhage caused by rupture of aneurysm

Site	Number
Middle cerebral artery	19
Anterior communicating artery	13
Posterior communicating artery	7
Pericallosal artery	4
Basilar artery	2
Posterior inferior cerebellar artery	6
Anterior inferior cerebellar artery	1
Ascending frontal artery	1
Total	66

In the 32 patients who were examined within 7 days after the bleeding episode, blood could be identified in the cisterns in 27. In another 11 patients 17 examinations were carried out within 3 to 5 days. 6 of these patients had blood in the cisterns. Among the remaining 9 patients examined after the elapse of 5 days, blood in the cisterns was apparent in only one patient. Altogether 22 repeat examinations were performed after the elapse of 5 days. Blood was demonstrated on one examination only, in a patient with an aneurysm on the posterior inferior cerebellar artery with clinical indication of repeat bleeding.

In 31 patients with one or several aneurysms and blood in the cisterns at CT scanning, the ruptured aneurysm was identified. In search for a diagnostic feature related to the site of the aneurysm, the distribution of the blood in the cisterns was analysed in those patients (Table 4).

In 7 of 8 cases with middle cerebral artery aneurysms, blood was found in one or both Sylvian fissures (Fig. 2) and all cases with anterior communicating artery aneurysm had blood in the interhemispheric fissures and suprasellar cisterns (Fig. 3). In posterior communicating artery aneurysm 7 of 8 had blood in the suprasellar cisterns and 6 of 8 also in the ambient cistern. Both pericallosal artery aneurysms had blood in the interhemispheric fissure and the pericallosal cistern. Aneurysms located within the posterior cranial fossa as well as one aneurysm on the posterior communicating artery had blood in the pontine and posterior cerebellar cisterns.

Among the 52 patients with aneurysms 18 had an intracerebral hematoma. Hematomas in the frontal lobe were caused by rupture of an anterior com-

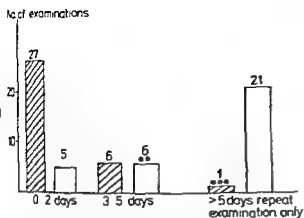


Fig. 1 Blood in subarachnoid cisterns demonstrated at CT after subarachnoid bleed. Hatched Blood in cisterns. Unhatched Blood in cisterns. Location of the aneurysm: 1 anterior communicating artery, 2 posterior communicating artery, 3 pericallosal artery, 4 posterior inferior cerebellar artery, 5 middle cerebral artery, 6 posterior communicating artery, 7 posterior inferior cerebellar artery, 8 repeat bleed.



Fig. 2

Fig. 3

Fig. 2 Aneurysm of middle cerebral artery. Blood in both Sylvian fissures predominantly on the side of the aneurysm.

Fig. 3 Aneurysm of anterior communicating artery. Blood in the interhemispheric fissure and suprasellar cisterns as well as a small midline hematoma.

communicating artery aneurysm or (in one case) a pericallosal artery aneurysm. Hematomas in the temporal lobe in the Sylvian fissure or in the basal ganglia were found with aneurysms on the middle cerebral artery. A small hematoma in the midline, presumably in the cisterna lamina terminalis, was a characteristic finding in anterior communicating artery aneurysms as was a hematoma in the pericallosal cistern with pericallosal artery aneurysms.

Repeat CT examinations were performed in 22 patients and cerebral angiography in 20 of them on the same day as the repeat CT scanning. Vascular spasm was present at 16 angiographic examinations. In 10 of these patients no clinical indication of brain ischemia existed and CT scanning did not disclose infarction. In the remaining 6 patients a deterioration of the clinical condition was recorded and in 5 of

them the CT scan had changed to abnormal either indicating infarction (3 cases) or newly formed hematomas (2 cases). In 3 patients without spasm at angiography or a deterioration of the clinical condition the CT scan was without abnormality. One patient had no spasm at angiography but clinical signs of brain ischemia. CT scanning revealed a newly formed hematoma. No repeat angiography was performed in 2 patients in both the clinical condition deteriorated and in both CT findings indicated edema or infarction.

Discussion

In 33 of 44 patients (75%) examined by CT within 5 days of the bleeding episode, blood could be recorded in the subarachnoid cisterns. The number of

Table 4

Distribution of cisternal blood in 31 patients with either a single aneurysm or identified multiple aneurysms

	Interhemispheric fissure	Sylvian fissure bilat	Sylvian fissure unilat	Suprasellar cistern	Ambient cistern	Pontine cistern	Pontocerebellar cistern	Pericallosal cistern
Middle cerebral artery	4/8	6/8	1/8	4/8	3/8	-	-	1/8
Anterior communicating artery	10/10	1/10	3/10	4/10	3/10	-	-	-
Posterior communicating artery	3/8	1/8	5/8	7/8	6/8	1/8	1/8	-
Pericallosal artery	2/2	-	1/1	1/1	-	-	-	2/2
Posterior inferior cerebellar artery	-	-	-	1/1	1/1	1/1	-	-
Anterior inferior cerebellar artery	-	-	-	1/1	1/1	-	1/1	-

patients with altered attenuation values in the cisterns was certainly higher as only those cases where the attenuation values were distinctly above the values of the brain tissue were defined as blood in the cisterns. If the CT scanning was performed within 2 days 27/32 patients (81%) had blood in the cisterns. No blood was found in 5 patients with the following location of the aneurysm: one on anterior communicating, one on posterior communicating artery, one on posterior inferior cerebellar and 2 on pericallosal artery. In 6 further patients examined within 5 days without blood in the cisterns the aneurysm location was: one on middle cerebral, 3 on posterior communicating and 2 on posterior inferior cerebellar artery.

These results are in accordance with those reported by KENDALL *et al.* and confirm the high accuracy of CT scanning in the detection of subarachnoid hemorrhage.

The lowering of the cisternal attenuation values after the elapse of 5 days is probably due to the disintegration of the hemoglobin molecule, it coincides in time with the appearance of vascular spasm.

No strict correlation was found between the distribution of blood in the cisterns and the site of the ruptured aneurysms although some features are discernible. In rupture of an anterior communicating aneurysm blood is commonly found in the suprasellar cisterns, both Sylvian fissures as well as in the interhemispheric fissure with a small localized hematoma in the cisterna lamina terminalis (Fig. 3). A flat hematoma in the pericallosal cistern may be found with rupture of a pericallosal artery aneurysm. Presence of blood in one Sylvian fissure or a preponderance of one side sometimes with a localized small or large hematoma in the Sylvian fissure occurred with middle cerebral artery aneurysms. Blood in the pontine or ponto cerebellar cisterns only occurred with a posterior fossa localization indicating vertebral angiography as the first angiographic procedure. The distribution of blood in the ventricle has not been analysed in detail. Apparently blood can be present in the fourth ventricle without being detectable in the lateral ventricles in rupture of a supratentorial aneurysm, probably because of a retrograde circulation of the cerebrospinal fluid. The distribution of blood is not only depending upon the localization and direction of the aneurysm but probably also upon the position of the head during the bleeding episode (HAYAKAWA & WATZ 1978).

An analysis of these appearances together with the existence of a hematoma will usually be sufficient to decide the vessel to approach primarily in angiography. Large hematomas in the basal ganglia with or without blood in the Sylvian fissure can be found with middle cerebral artery aneurysm and in such cases an angiography is necessary for exclusion of such an aneurysm when there is no evidence of blood in the cisterns.

The unique potential of CT to detect pathological alteration of the brain substance makes it possible to record not only intracerebral hematomas but also regions with edema or necrotic brain tissue. The vascular spasm occurring as a secondary phenomenon in subarachnoid hemorrhage 3 days or later after the bleeding episode is still of questionable significance as it may be angiographically evident without any clinical signs of brain ischemia. On the other hand a high degree of vascular spasm is a regular accompanying phenomenon to ischemia of the brain or a manifest infarction. During the period of angiographically demonstrated vascular spasm only those patients with clinical signs of ischemia had CT findings indicating an infarction or (in one case) a new intracerebral hematoma.

Conclusions

CT scanning is a useful and reliable method to identify a subarachnoid bleeding provided the examination is performed within 2 days of the bleeding. The distribution of cisternal blood can be identified which in combination with the localization of a possible intracerebral hematoma yields a rather good predictability as to the site of the ruptured aneurysm even when multiple aneurysms are present. Thus the subsequent angiography can be directed to the relevant vessel in most cases, simplifying the identification of the ruptured aneurysm.

Repeat examination demonstrates a good correlation between CT findings and the existence of a clinically important ischemic lesion due to arterial spasm. Angiographic spasm seems to be of no significance if not associated with clinical signs. On CT a repeat bleeding can be differentiated from an infarction.

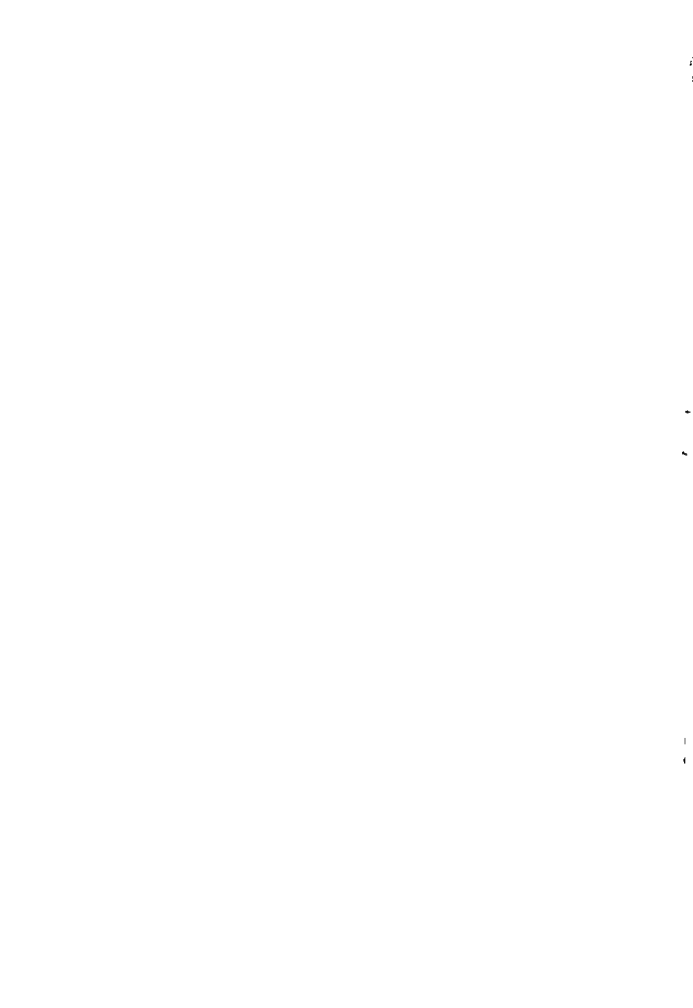
CT should be the first diagnostic procedure followed by angiography. Repeat angiography can be replaced by repeat CT for examination of patients with deterioration of the clinical condition.

SUMMARY

Repeat CT scanning and cerebral angiography has been performed in 33 consecutive patients with subarachnoid hemorrhage. Blood in the subarachnoid cisterns could be discerned in 27 of 32 patients provided the examination was performed within 2 days of the bleeding. The distribution of cisternal blood can be identified which in combination with the localization of a possible intracerebral hematoma yields a rather good predictability as to the site of the ruptured aneurysm. The subsequent angiography can thus be directed to the relevant vessel in most cases. Repeat CT scanning can replace angiography in the evaluation of patients with deterioration of the clinical condition.

REFERENCES

- HAYAKAWA T and WALTZ G. Influence of head position on the prognosis of experimental subarachnoid hemorrhage. *Arch Neurol* 35 (1978) 206.
- KENDALL B E, LEE B C P and CIAVERIA E. Computerized tomography and angiography in subarachnoid hemorrhage. *Brit J Radiol* 49 (1976) 483.
- LILLIEQUIST H, LINDQVIST M and VALDIMARSSON E. Computed tomography and subarachnoid hemorrhage. *Neuroradiology* 14 (1977) 21.



FROM THE DEPARTMENT OF RADIOLOGY HARVARD MEDICAL SCHOOL, PETER BENT BRIGHAM HOSPITAL, BETH ISRAEL HOSPITAL, BOSTON, MASSACHUSETTS 02115 AND MTERLING WINTHROP RESEARCH INSTITUTE, RENSSELAER, NEW YORK 12114, USA

EPIDUROGRAPHY WITH METRIZAMIDE IN RHESUS MONKEYS

D. K. KIDO, R. A. BAKER, A. SAUBERMANN, J. SALEM,
W. C. SCHOENE and P. FOURNIER

Epidurography, a procedure that can demonstrate protruded intervertebral discs concealed within the epidural space, has not been widely accepted because ionic water soluble contrast media are toxic in the subarachnoid space where they are capable of causing hypotension, convulsions and even death (VOZRAK 1964, LUYENDIJK & VAN VOORTHUISEN 1966, NAGAMINE 1970). However, epidurography with metrizamide (Amipaque, Nyegaard, Oslo, Norway), a non ionic water soluble contrast medium, appears to be safe since it is relatively non toxic in the subarachnoid space (GONSETTE 1973, SKALPE et coll. 1973, HAUGHTON et coll. 1977).

Materials and Methods

The series consisted of 12 adult Rhesus monkeys (*Macaca mulatta*) equally divided into 3 groups. In each group of 4 monkeys, epidurography with metrizamide was performed in 3 monkeys and an epidural injection of physiologic saline was performed on the fourth monkey, who acted as a control. Before the injection of contrast medium, the monkeys were anesthetized with intramuscular ketamine hydrochloride (10 mg/kg) and booster doses were given every 20 to 30 min. The lumbar and sacral regions were shaved and cleaned.

In Group I, one epidurography was performed in each monkey with a No. 17 gauge needle (1.50 mm), fluoroscopically directed through the sacral hiatus with the monkey in the prone position. Advancement of the needle to the S1-S2 interspace was performed after the monkey had been turned laterally. 3

to 5 ml of metrizamide was injected into the epidural space at concentrations of 200 or 280 mg I/ml and in the control monkey 5 ml of saline. CT scans of the lumbosacral region were performed on one monkey following epidurography.

In Group II, 2 epidurographies were performed in each monkey, the first in a manner similar to the one in Group I, in the second a catheter was used. The catheter was advanced through the needle to the L7-S1 interspace after the needle had been introduced through the sacral hiatus. Three to 5 ml of metrizamide (280 mg I/ml) was injected and in the control monkey 5 ml of saline. CT scans of the lumbosacral region were performed on 2 monkeys.

In Group III, a lumbar myelography was performed immediately followed by epidurography. The myelography was carried out by fluoroscopically advancing a No. 22 gauge needle (0.72 mm) between the L7-S1 spinous processes and injecting 1 to 2 ml of metrizamide (200 or 280 mg I/ml) into the subarachnoid space. The epidurography was performed immediately after the myelography by either advancing the needle into the anterior epidural space or repositioning it laterally where an additional 3 ml was injected. In the control monkey 3 ml of saline was injected into the subarachnoid and epidural spaces. CT scans of the lumbosacral region were performed on one monkey.

In all groups, the position and extension of the contrast medium was recorded by radiography. All

Table
Review of the epidurographies performed with metrizamide

Injection technique	Concentration (mg/ml)	Volume (ml)	No of examinations	Difficulty during puncture	Quality of examination	Interval between last epidurography and killing (days)	Mortality
Epidurography							
Group I Needle	700	5	1	+	Good	30	Normal
	280	3	1	+	Good	3	Infection
	780	5	1	0	Good	7	Normal
	Saline	5	1	0	-	3	Normal
Group II Catheter	280	-	2	+	Good	70	Degeneration
	280	3-5	2	+	Good	40	Normal
	780	5-5	2	+	Good	11	Normal
	Saline	5-5	2	0	-	70	Normal
Myelography and epidurography							
Group III	200	3/3	1	0	Poor	77	Normal
	280	1/3	1	0	Good	4	Normal
	780	2/3	1	0	Good	45	Normal
	Saline	3/3	1	+	-	0	Normal

monkeys were periodically examined for any change in behavior or physical activity. The weights of the animals were recorded at the beginning and end of the investigation period. The monkeys were killed at approximately 3, 21 and 42 days after the last epidurography. The lumbar and sacral vertebrae and accompanying femoral nerves were removed en bloc and fixed in a 15 per cent physiologically buffered formalin solution for approximately two weeks before the spinal cords with meninges and epidural tissues were removed. Representative sections were made of the lumbar and sacral spinal cord and femoral nerves. Specimens were embedded in paraffin and stained with hematoxylin-eosin.

Results

Puncture of the sacral hiatus in Groups I and II was frequently difficult (5/12) because of the relatively large needle when compared with the size of the sacral hiatus. During difficult punctures the monkeys were often repositioned because needle depths could not be determined fluoroscopically with the monkeys prone and centering of the needles was equally difficult with the monkeys on their sides. Subsequent needle advancement to the S1-S2 level frequently resulted in the needle tip hitting the bone.

It was then withdrawn slightly and redirected. In 7 of these monkeys bleeding occurred but cerebrospinal fluid was never detected in the needle. Advancement of the catheter in the epidural space to the S1-S2 level was more time-consuming because optimum catheter positioning required manipulation with guide wires.

A total of 9 metrizamide epidurographies were performed in Group I and II (Table). The epidural space was well outlined with contrast medium regardless of the concentration of metrizamide. The anterior portion of the epidural space was demonstrated on lateral films while the lateral portion was outlined on postero-anterior and oblique films (Fig. 1). Nerve root sleeves were occasionally outlined beyond the intervertebral foramina (Fig. 1). Because of a partial injection of contrast medium into the subarachnoid space nerve roots were demonstrated in one monkey. Three ml of metrizamide usually filled the epidural space to the upper thoracic region while 5 ml usually filled the entire epidural space from the sacrum to the cervico-capital junction. Films exposed approximately 10-15 min following injection showed a decrease in concentration of the medium, the margins between the contrast medium and nerve roots being less well defined. Films exposed at the conclusion of the

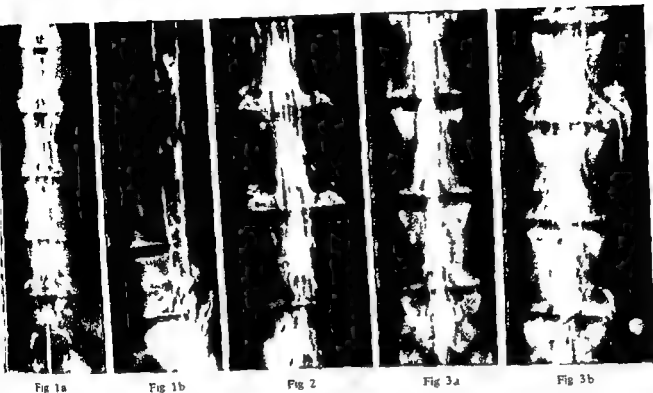


Fig 1a

Fig 1b

Fig 2

Fig 3a

Fig 3b

Fig 1 Metrizamide epidurography a) A p. projection. Lateral epidural space and the nerve root sleeves demonstrated b) Lateral projection. Ventral epidural space outlined

Fig 2 Lateral recesses demonstrated. Contrast medium extends through several intervertebral foramina partially outlining peripheral nerves. Medium has also inadvertently entered the subarachnoid space

Fig 3 a) Myelography. Subarachnoid space and nerve roots demonstrated b) Epidurography. Spinal needle moved from the subarachnoid space to right lateral epidural space. Contrast medium in the epidural space difficult to observe except where it has extended through the intervertebral foramina

umination occasionally showed contrast medium the pelvicalyceal system

Three monkeys from Groups I and II were scanned following epidurography. The scans showed that metrizamide clearly outlined the dura at the borders with the bony canal were difficult to fine even with manipulation of the window width level because of their similar attenuation (Fig 1). It was not possible to evaluate metrizamide and its relationship to nerve roots in either the intervertebral foramen or paravertebral soft tissue.

No change in behavior or physical activity occurred in the monkeys in Group I and II. However, significant microscopic abnormalities were observed in 3 monkeys in which the sacral punctures had been difficult. The first monkey killed 3 days after the epidurography had an acute inflammatory reaction involving the sacral dura and its adjacent epidural space. This inflammation was present in the epidural space but did not involve the epidural nerve or ganglia. Occasional inflammatory cells were seen in the subarachnoid space. The wall of one blood vessel within one sacral spinal root showed acute inflammation. Cul-

tures of the epidural space were not taken because gross abnormalities were not present. In the second monkey killed 3 weeks after the last epidurography the advancement of the needle had been difficult resulting in bleeding through the needle. Microscopically degeneration of at least one dorsal spinal root and at least one peripheral nerve fascicle was found (Fig 4). Both axons and myelin sheaths were degenerated and associated with some macrophages. These abnormalities suggested that this process was at least weeks but not months old. No abnormality was found in the 2 control monkeys.

The myelography in Group III did not require the monkey to be repositioned and was successful as long as the needle was maintained in the midline. The epidurography was more easily performed by repositioning the needle into the lateral epidural space than by advancing it into the anterior portion of the epidural space.

The myelography outlined the subarachnoid space (Fig 3a). The epidurography which followed outlined the epidural space but the contrast medium in the subarachnoid space distracted

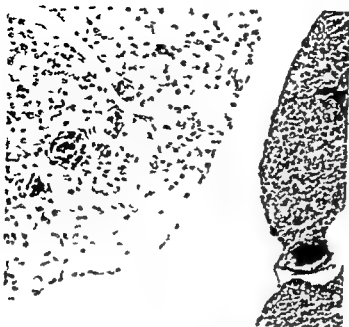


Fig 4

Fig 4 Degenerating nerve fascicle in the cauda equina. Hema-toxylin stain.

Fig 5 CT scan through a lumbar vertebra. Width and position of epidural space. The outer border is poorly defined (→).

Fig 6 CT scan through a lumbar vertebra. In the center of the spinal canal is a homogeneous high attenuating area representing subarachnoid metrizamide. Epidural contrast medium surrounds the subarachnoid space. Some medium extends into the paravertebral soft tissues (→).

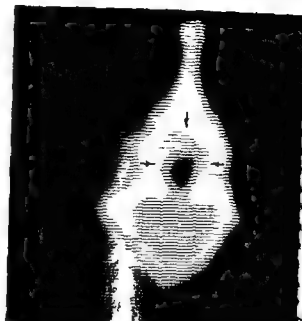


Fig 5

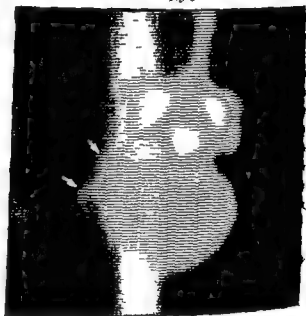


Fig 6

tion of the epidural space (Fig 3b). CT scans were also difficult to evaluate because of contrast medium in both the subarachnoid and epidural space (Fig 6). No clinical or microscopic abnormalities were found in the monkeys in Group II.

Discussion

Epidurography using ionic water soluble contrast media has proven effective in diagnosing herniated intervertebral discs. The reported diagnostic accuracy in epidurography (90%) appears to be higher than that in subarachnoid myelography (YAMAMURA 1967). The reasons for this high accuracy are

twofold: (1) disk protrusions and herniations deform the epidural space before they deform the subarachnoid space; thus contrast examination of the epidural space allows earlier and more accurate diagnosis of these lesions; and (2) correlation between the patient's original symptoms and complaints of pain during the injection of contrast medium has been helpful in diagnosing herniated discs (LUYENDIJK & VAN VOORTHUISSEN 1966).

Metrizamide, a non-ionic water soluble contrast medium, demonstrates the epidural space as well as ionic water soluble media but has the advantage of being relatively non-neurotoxic in the subarachnoid

space. The necessity of having a safe water soluble subarachnoid contrast medium was evident in one monkey where medium was inadvertently injected into both the epidural and subarachnoid space. Epidurography by either ionic or non ionic contrast media causes less morbidity than myelography as long as the subarachnoid space is not violated. In fact the morbidity has been sufficiently low to allow some authors to suggest that this procedure can be performed on an out patient basis (KETTUNEN & SALENIUS 1963; BROMAGE *et coll.* 1978).

Metrizamide epidurography in dogs resulted in no adverse clinical reactions or injury to tissues around the epidural space which could be attributed to metrizamide (KIDO *et coll.* 1978) and the same results were achieved in the present series of monkeys. The acute inflammatory infiltrate found in the epidural space, dura and around one blood vessel in one of the spinal root fascicles is probably secondary to an infection which occurred during a break in sterile technique. The degeneration of the dorsal spinal root in another monkey is consistent with Wallerian degeneration of approximately 3 weeks duration. It is reasonable to attribute this to trauma possibly tearing a nerve root which occurred during a difficult needle advancement during which bleeding occurred through the needle. It seems reasonable to suggest the use of metrizamide for epidurography in humans since the procedure can detect concealed discs and is safe if care is taken to maintain sterile conditions and the patient is monitored during the needle manipulation.

SUMMARY

Epidurography with metrizamide was performed on 9 Rhesus monkeys; physiologic saline was substituted for

metrizamide in 3 control monkeys. Metrizamide successfully outlined the epidural space without causing any adverse clinical effects or direct tissue injury.

ACKNOWLEDGEMENT

Supported in part by Sterling Winthrop Research Institute.

REFERENCES

- BROMAGE P R, BRANWELL E S B, CATCHLOVE R F, HIL BELANGER G and PEARCE C G A. Pendurography with metrizamide. Animal and human studies. *Radiology* 128 (1978) 123.
- GONSETTE R E. Metrizamide as contrast medium for myelography and ventriculography. *Acta radiol* (1973) Suppl No 335 p 346.
- HOSHINO T. Diagnosis of intervertebral disc hernia with pendurography. *Orthop Surg* 17 (1966) 464.
- HAUGHTON V M, HO K C and LARSON S J. Experimental production of arachnoiditis with water soluble myelographic media. *Radiology* 123 (1977) 681.
- KETTUNEN K and SALENIUS P. Pendurography in the lumbar region for the diagnosis of protruded intervertebral discs. *Ann Chir Gynaec Fenn* 52 (1963) 709.
- KIDO D K, SCHOENE W C, BAKER R A and RUBIN BAUGH C. Metrizamide epidurography in dogs. *Radiology* 128 (1978) 119.
- LUYENDIJK W and VAN VOORTHUISEN A E. Contrast examination of the spinal epidural space. *Acta radiol* 5 (1966) 1051.
- NAGAMINE K. Clinical and biochemical study of accidents in pendurography. *Nagoya J med Sci* 32 (1970) 429.
- NOZAKI K. Experience in side effect of pendurography. *Diagn Treatm (Tokyo)* 4 (1964) 156.
- SJALPE I O, TOBERGSEN T, AMUNDSEN P and PRESTHUS J. Lumbar myelography with metrizamide. *Acta radiol* (1973) Suppl No 335 p 367.
- YAMAMURA T. Studies on the pendurographic examination for lumbar disc herniation. *J Jap Orthop Ass* 41 (1967) 991.

FROM THE DEPARTMENT OF NEURORADIOLOGY (DIRECTOR B LILIEQUIST) UNIVERSITY HOSPITAL ■ 90185
LMA AND THE DEPARTMENT OF NEURORADIOLOGY (DIRECTOR T GREITZ) KAROLINSKA SJUKHUSET
S 10401 STOCKHOLM SWEDEN

CISTERNAL ABNORMALITIES PRODUCED BY CLINICAL TUMOURS IN THE POSTERIOR CRANIAL FOSSA

III Tumours of the brain stem and pontine angle

M LINDQVIST

Previously cisternal distortions produced by experimental tumours in the posterior fossa (LINDQVIST & MÖLLER 1978 LINDQVIST 1978) and pneumographic cisternal distortions in a clinical series of cerebellar tumours (LINDQVIST 1980a) and fourth ventricle tumours (LINDQVIST 1980b) have been reported. In the present report the cisternal alterations associated with tumours in the brain stem and the pontine angle are described.

DAVIDOFF & EPSTEIN (1950) reported 2 cases of pontine angle tumours examined with encephalography. LINDGREN (1950) emphasized the advantages of encephalography over ventriculography for the examination of the posterior fossa. Encephalography permitting a more comprehensive analysis of the subarachnoid cisterns both in the diagnosis of pontine angle tumours and for distinguishing tumours of the brain stem from extraaxial tumours such as chordomas of the clivus. LINDGREN & DI CHIRO (1953) reported characteristics of the aqueduct and quadrigeminal cistern with different tumour locations and ROBERTSON (1957) briefly described some cisternal distortions in brain stem tumours. LINDQVIST published a detailed analysis of the normal anatomy of the subarachnoid cisterns (1959a) as well as the pneumographic findings in tumours in the pontine angle (1959b). He also briefly reported some cisternal abnormalities occurring in tumours of the pons (LILIEQUIST 1963). ISHERWOOD (1972) presented a pneumographic technique for demonstration of very small tumours in the pontine angle.

Definitions The orientation of the structures of the posterior fossa is that given by CORRALES & GREITZ (1972) i.e. supero inferiorly parallel to the clivus antero posteriorly at right angles. The definitions used in the present report are the same as those used previously (LINDQVIST & MÖLLER LINDQVIST 1978 1980a b). For nomenclature and a schematic survey of the normal anatomy of the cisterns see LINDQVIST (1980a Fig 1).

Material and Methods

The material consisted of patients with tumours of the brain stem or the pontine angle examined with encephalography during the period 1969 to 1975 belonging to the same clinical material as the cerebellar and fourth ventricle tumours previously reported by LINDQVIST (1980a b). Patients previously operated upon in the posterior fossa were excluded. Cases with brain stem tumours of the quadrigeminal plate and adjacent structures were also excluded partly because the pneumographic findings in these types of tumours have been reported in detail by GREITZ (1972) and partly because information on the exact position and type of these tumours is often not available.

The examination technique was the same as in the previous reports on cerebellar tumours (LINDQVIST 1980a) and intraventricular tumours of the fourth ventricle (LINDQVIST 1980b).

In many cases with brain stem tumours surgical and microscopic confirmation was not available since patients with this tumour location are as a rule given radiation therapy without surgical intervention. Tumours in the pons and medulla oblongata were therefore included even if no surgical confirmation existed provided that the size and position of the tumour were clearly demonstrated at the neuroradiologic examinations. In a total of 21 cases were excluded: 2 cases because the size and position of the tumour could not be definitely established one because the encephalography failed for technical reasons and one because the films had been lost. The remaining 17 cases form the basis for the present analysis of tumours of the brain stem.

Of a total of 70 cases with tumours in the pontine angle only those were included in which the type and position of the tumour was established at surgery or autopsy within 6 months from the time of the pneumography. The following cases were therefore excluded: 12 patients with small pontine angle tumours because they were treated with closed stereotactic radiation surgery (LEKSELL 1971) instead of open surgery; 12 not operated upon for other reasons (usually old age or complicating disease) and outside the settled time interval between pneumography and surgery or autopsy. The remaining 40 cases form the basis for the analysis of the pontine angle tumours.

The sex and age distribution of the material appears in Figs 1 and 2 and the tumour type in Table 1.

The brain stem tumours were divided into (Table 2): (a) tumours growing mainly in the medulla oblongata (or to the same extent in the medulla oblongata and the pons) and (b) tumours growing mainly in the pons.

The pontine angle tumours were divided into (Table 2): (i) tumours limited to the pontocerebellar cistern; (b) tumours mainly indenting the cerebellar hemisphere; (c) tumours indenting both the cerebellar hemisphere and the brain stem; and (d) tumours mainly indenting the brain stem.

The position of each tumour was established by two experienced neuroradiologists who had access to all neuroradiologic examinations, surgical and autopsy reports.

The pneumographic films were reviewed analysed and recorded in the same way as in previous reports on tumours of the cerebellum and the fourth ventricle (LINDQVIST 1980a, b). Thus all lateral tumours were treated as if situated on the

No of cases

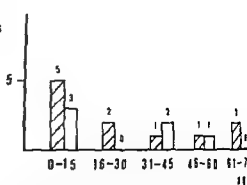


Fig. 1 Sex and age distribution of 17 cases of brain stem tumours. ■ males □ females

No of cases

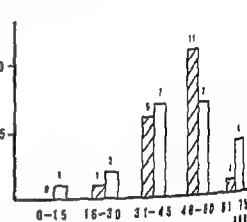


Fig. 2 Sex and age distribution of 40 cases of pontine angle tumours. ■ males □ females

right side and all midline tumours with a tendency to lateralization were treated as if the predominant side was right sided.

Results and Discussion

In Tables 3, 4 and 5 the air filling and the characteristic distortion of the most important cisternal structures are presented. Some cisternal features which it may be used to distinguish different subgroups of brain stem and pontine angle tumours appear in Tables 6 and 7. Only cisternal structures that were filled in at least 20 per cent of the cases and regarded as valuable for locating the tumours or distinguishing them from other types of tumour in the posterior fossa were included.

Cisterna magna

Tonsillar herniation was present in 29 per cent of the brain stem tumours and in 45 per cent of the pontine angle tumours (Table 3). In the former tonsillar herniation occurred only in tumours of the pons but not in medulla oblongata tumours. In the latter

Table 1

Classification of brain stem and pontine angle tumours in children and adults

Type of tumour	Children (0-15 years)	Adults (16 years or more)	Total	
	No of cases	No of cases	No of cases	Per cent
Tumours of the brain stem				
Brain stem glioma	8	9	17	29.8
Tumours of the pontine angle				
Neurinoma	1	35	36	63.2
Meningioma	0	2	2	3.5
Cholesteatoma	0	1	1	1.8
Chordoma	0	1	1	1.8
Total	9	48	57	

Microscopic confirmation not available in 11 of the cases

Table 2

Brain stem and pontine angle tumour Subgroups according to position

			No of cases
Brain stem tumours	a Tumour mainly in the medulla oblongata (or equally in the medulla oblongata and the pons)	5	17
	b Tumour mainly in the pons	12	
	Total		
Pontine angle tumours	a Tumour limited to the cistern	4	40
	b Tumour mainly indenting the cerebellar hemisphere	17	
	c Tumour indenting both the cerebellar hemisphere and the brain stem	15	
	d Tumour mainly indenting the brain stem	4	
	Total		

Table 3

Filling and distortion of the cisterna magna in tumours of the brain stem and the pontine angle. All lateral tumours treated as if situated on the right side. Symbols and abbreviations: a=anterior, p=posterior, s=superior, i=inferior, R=right, L=left, 0=no change, (+)=minimal change or increase, ++=moderate change or increase, ---=marked change or increase, (-)=minimal decrease, --=moderate decrease, ---=marked decrease, open spaces=structure not possible to evaluate.

Tumour position	Brain stem		Pontine angle	
	Fill ing (%)	Distor tion	Fill ing (%)	Distor tion
Cisterna magna				
1 Extracranial part				
lat proj	100		95	
tonsillar herniation		(+)		(+)
a p displacement of cervical medulla		p+		p(+)
2 Interhemispheric part				
lat proj	100		100	
s i diameter		-		-
3 Foramen of Magendie				
lat proj	82		72	
a p displacement		p++		p(+)
4 Valleculla axial proj	71		87	
width		+		(-)
lateral displacement		0		L+
5 Retrotonsillar spaces				
lat proj	23		30	
a p displacement		p++		p(+)
s i displacement		i++		i+
6 Cerebellomedullary fissures				
a right side axial proj	41		60	
a p displacement		p+		p(+)
lateral displacement		R(+)		L+
b left side axial proj	41		60	
a p displacement		p+		0
lateral displacement		L(+)		L+
7 Paravermian sulci axial proj	47		35	
width of inferior vermis		+		0
lateral displacement of inferior vermis		0		L+

tonsillar herniation was more common (50%) and more marked when the ventricular system was widened (Fig. 7) than when not widened but a slight tonsillar herniation was also relatively common (32%) with normal ventricular size.

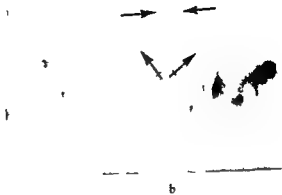
The absence of tonsillar herniation in cases with tumours in the medulla oblongata is explained by the

fact that the tumour displaces the tonsils posteriorly and separates them to such an extent that they can not herniate through the foramen magnum (Fig. 3).

The slight degree of tonsillar herniation which is common in connection with pontine angle tumours without hydrocephalus or other signs of increased intracranial pressure may probably be explained by



a



b



c

Fig. 3. Tumour of the medulla oblongata. a) Axial view. The vallecula widened (\rightarrow); the retrotonsillar spaces (\leftrightarrow) between the tonsils and the inferior vermis opened up. The lateral recesses (\rightarrow) of the fourth ventricle surround the expanded medulla oblongata. b) Axial tomography through the vallecula (\rightarrow). The cerebellomedullary fissures (\leftrightarrow) separated and slightly displaced posteriorly by the expanded medulla oblongata. c) Lateral midline tomography. The foramen of Magendie (\rightarrow) markedly displaced posteriorly by the expanded medulla oblongata. Cervical medulla (\rightarrow) displaced posteriorly below the foramen magnum.

cause the tumour directly displaces the ipsilateral tonsil posteriorly and inferiorly.

Posterior displacement of the cervical medulla below the foramen magnum was often present in the brain stem tumours, especially in cases with a tumour in the medulla oblongata (Fig. 3c). In the case of pontine angle tumours such a distortion occurred only when the tumour was indenting the brain stem.

A moderate compression of the interhemispheric part of the cisterna magna against the occipital crest was observed both in brain stem and pontine angle tumours.

The foramen of Magendie was markedly dis-

placed posteriorly in cases with tumour of the brain stem. In tumours of the medulla oblongata the degree of posterior displacement was as a rule the same superiorly as inferiorly (Fig. 3c), while in tumours of the pons the displacement was more marked superiorly (Fig. 4c, Table 6). In tumours of the pontine angle posterior displacement of the foramen of Magendie occurred when the tumour was indenting the brain stem but not when it was mainly indenting the cerebellar hemisphere (Table 7).

The vallecula was markedly widened in cases with tumour of the medulla oblongata (Fig. 3a, b) but was of normal or only slightly increased width in pontine

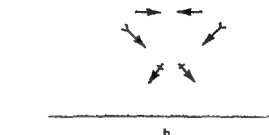


Fig. 4. Brain stem tumour with its main component in the pons. a) Axial view. The vallicula (→) not widened and situated in the midline. b) Axial tomography through the vallicula (→). Only slight compression of the lateral recesses (←) of the medullary cistern. Cerebellomedullary fissures (↗↘) not displaced. c) Lateral tomography. The foramen of Magendie (→) displaced posteriorly particularly in its superior part. The inferior vermis (↖) displaced posteriorly and slightly inferiorly. The posterior part of the superior surface of the pons (↗) tilted superiorly in the interpeduncular cistern.

tumours (Fig. 4a, b, Table 6). Slight lateral displacement of the vallicula occurred in some asymmetric brain stem tumours.

With tumours of the pontine angle the width of the vallicula was as a rule normal or slightly decreased when the tumour was indenting the cerebellar hemisphere but slightly increased when it was indenting the brain stem (Table 7). In most cases of pontine angle tumour the vallicula was displaced laterally which was more marked when the tumour was indenting the brain stem than when it indented the cerebellar hemisphere (Table 7).

A widening of the vallicula occurring with tumours of the medulla oblongata but not with

tumours of the pons has previously been pointed out by CORRALES (1972). The vallicula was often filled in pontine angle tumours as pointed out by LILIEQUIST (1959b). He also mentioned that the posterior part of the vallicula was often more displaced than the anterior part giving it a characteristic oblique position in the axial projection. This appearance was, however, not a constant finding in the present material, being present only in 4 cases (Fig. 5c).

The intertruncular spaces were more often filled in pontine than in medullary oblongata tumours. They were as a rule markedly displaced posteriorly and inferiorly in both kinds of brain stem tumour (Fig.

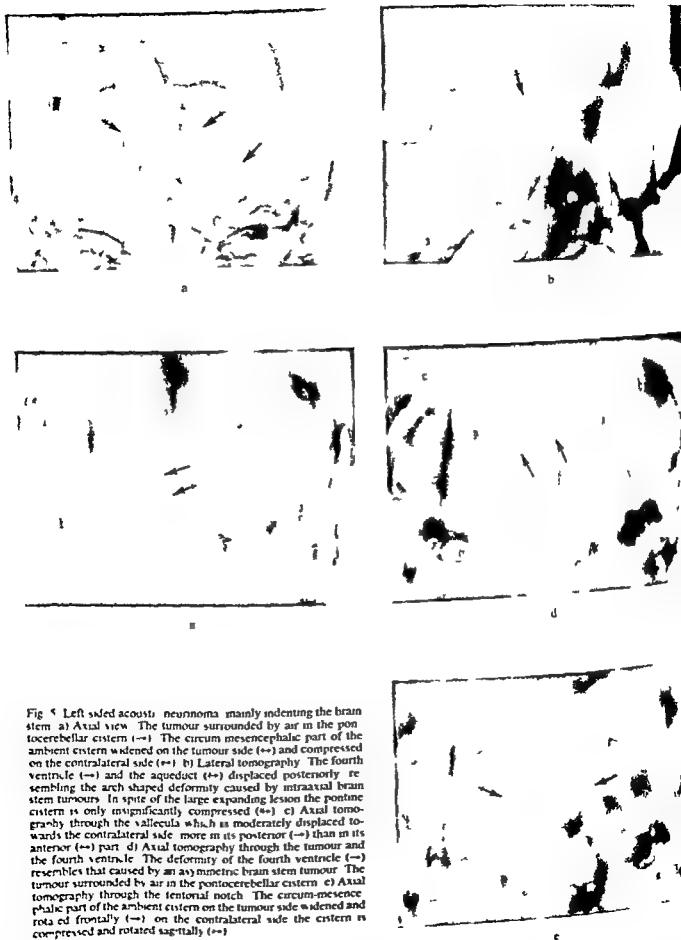


Fig 5 Left sided acoustic neuroma, mainly indenting the brain stem. a) Axial view. The tumour surrounded by air in the pontocerebellar cistern (\rightarrow). The circum mesencephalic part of the ambient cistern widened on the tumour side (\leftrightarrow) and compressed on the contralateral side (\rightarrow). b) Lateral tomography. The fourth ventricle (\rightarrow) and the aqueduct (\leftrightarrow) displaced posteriorly, resembling the arch shaped deformity caused by intraaxial brain stem tumours. In spite of the large expanding lesion the pontine cistern is only insignificantly compressed (\leftrightarrow). c) Axial tomography through the vallicula which is moderately displaced towards the contralateral side (\rightarrow) more in its posterior (\leftrightarrow) than in its anterior (\leftrightarrow) part. d) Axial tomography through the tumour and the fourth ventricle. The deformity of the fourth ventricle (\rightarrow) resembles that caused by an asymmetric brain stem tumour. The tumour surrounded by air in the pontocerebellar cistern. e) Axial tomography through the tentorial notch. The circum-mesencephalic part of the ambient cistern on the tumour side widened and rotated frontally (\rightarrow). On the contralateral side the cistern is compressed and rotated sagittally (\leftrightarrow).



a



b



c

Fig 6 Brain stem glioma in the pons and medulla oblongata a) Encephalography lateral tomography The retrotonsillar space (\leftrightarrow) markedly displaced posteriorly and inferiorly The prepyramidal fissure (\leftrightarrow) markedly displaced posteriorly Large amount of air in the cisterna cerebelli superior which is not compressed The quadrigeminal cistern (\leftrightarrow) and the precentral fissure (\leftrightarrow) displaced posteriorly b) Encephalography axial tomography at the level of the pontocerebellar cisterns The lateral part (\rightarrow) of the pontocerebellar cisterns less compressed than the medial part (\leftarrow) c) Ventriculography lateral tomography Typical deformity of the aqueduct and the fourth ventricle

a) In cases of pontine angle tumour a moderate inferior displacement of the retrotonsillar spaces was noted but only slight posterior displacement

The cerebellomedullary fissures were separated and displaced posteriorly in the medulla oblongata tumours (Fig 3b) while in cases with pure pontine tumours they appeared normal With pontine angle tumours the cerebellomedullary fissure on both sides was displaced towards the contralateral side The cerebellomedullary fissure on the side of the tumour was in addition somewhat displaced posteriorly if the tumour indented the brain stem but not if it indented only the cerebellar hemisphere

The paravermian sulci indicate the width of the inferior vermis A slight widening of the vermis was

present in brain stem tumours as well as in pontine angle tumours indenting the brain stem In most cases of pontine angle tumour a lateral shift of the inferior vermis towards the contralateral side was also noted

The cerebellomedullary fissures indicate the border between the medulla oblongata and the tonsils An expanding lesion in the medulla oblongata will cause separation and posterior displacement of these structures The displacement of the retrotonsillar spaces in brain stem tumours is due to the fact that the tumour displaces the tonsils and the inferior vermis posteriorly and inferiorly The inferior vermis thus becomes compressed resulting in an increased width

Table 4

Filling and distortion of the medullary cistern, pontine cistern and the pontocerebellar cisterns in tumours of the brain stem and the pontine angle. Tumour positions, symbols and abbreviations as in Table 3. Additional abbreviations: Ra=right side rotated anteriorly, Rp=right side rotated posteriorly.

Tumour position	Brain stem		Pontine angle	
	Fill- ing (%)	Distor- tion	Fill- ing (%)	Distor- tion
Medullary cistern				
1. Premedullary part				
lat. proj.	53		60	
a.p. diameter		--		-
Lateral recesses				
right side axial proj.	84		92	
a.p. diameter		-		+
lateral extension		-		++
2. left side axial proj.	88		90	
a.p. diameter				-
lateral extension				-
3. Diameter of medulla oblongata				
a.p. diameter lat. proj.		++		(+)
transverse diam.				
axial proj.		--		(-)
4. Lateral displacement of medulla oblongata axial proj.		0		L+
5. Rotation of medulla oblongata relative to axis parallel to axis		0		Rp+
Pontine cistern				
lat. proj.	100		97	
a.p. diameter		--		-
tendency of superior part of pons to recede from incisura		(+)		(+)
Pontocerebellar cisterns				
1. Right side axial proj.	8		87	
wid. h. of lateral part		-		++
wid. h. of medial part		--		++
2. Left side axial proj.	76		85	
wid. h. of lateral part		-		-
wid. h. of medial part		--		-

Medullary cistern

The premedullary part of the medullary cistern was compressed against the clivus in the cases with brain stem tumour (Table 4) as a rule more in medulla oblongata tumours than in pontine tumours (Table 6). A similar compression occurred in the pontine angle tumours, most marked in tumours indenting the cerebellum (Fig. 7) least in those indenting the brain stem (Fig. 5b).



Fig. 7. Pontine angle tumour indenting the cerebellar hemisphere. Hydrocephalus. Encephalography, lateral projection. Tonsillar herniation (→), marked compression of the pontine cistern (→) and of the premedullary part of the medullary cistern. Widening of the pericallosal cistern (→).

In the brain stem tumours both lateral recesses of the medullary cistern were compressed in both directions, the compression being more marked in the medulla oblongata tumours than in those in the pons.

With pontine angle tumours the lateral recess was widened on the side of the tumour and compressed on the contralateral side (Fig. 8).

The medulla oblongata was markedly expanded in cases with tumour of the medulla oblongata. In cases with pontine angle tumour it often appeared compressed on the tumour side in the axial projection, particularly when the tumour indented the cerebellar hemisphere. In the lateral projection the medulla as a rule was of normal size, but cases with an apparent expansion of the brain stem in this projection were also encountered when the tumour was indenting the brain stem. In pontine angle tumours the medulla oblongata was often rotated posteriorly on the tumour side in the axial projection and in addition displaced towards the contralateral side.

Thus, brain stem tumours situated in the pons produce relatively small distortions of the medullary cistern, while tumours in the medulla oblongata compress all parts of this cistern. This is especially evident in view of the intimate relation of the cistern to the medulla oblongata.

Pontine angle tumours displace the medulla

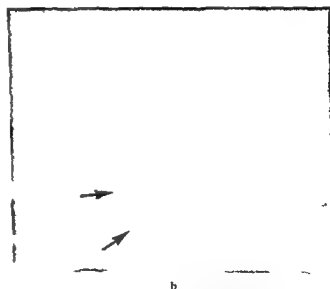


Fig 8 Right sided acoustic neuroma mainly indenting the cerebellar hemisphere. a) Axial view b) Axial tomography through the medullary cistern. On the tumour side the lateral

recess of the medullary cistern widened (\longleftrightarrow) and the medulla oblongata rotated posteriorly (\rightarrow)



Fig 9 Right sided acoustic neuroma mainly indenting the cerebellar hemisphere. a) Axial view b) Axial tomography at the



level of the pontocerebellar cisterns. The brain stem (\rightarrow) deformed and rotated posteriorly on the tumour side

longata towards the contralateral side and also cause posterior rotation of the medulla on the side of the tumour. This causes widening of the lateral recess of the medullary cistern on the tumour side inferior to the tumour, a characteristic appearance that has been described by LILIEQUIST (1959b).

Pontine cistern

The pontine cistern was markedly compressed in the a.p. direction in cases with brain stem tumours (Table 4). With pontine angle tumours the compression was moderate and usually more marked when the tumour indented the cerebellar hemisphere (Fig



Fig. 10 Tumour of the medulla oblongata. a) Axial tomography through the pontocerebellar cisterns. The lateral parts of the pontocerebellar cisterns (→) slightly compressed while the medial parts are totally compressed. b) Lateral tomography. The interpeduncular cistern (→) is normal. Foramen of Magendie displaced posteriorly to the same extent in its superior (→) as in its inferior (↘) part. The inferior vermis (↘) displaced posteriorly.

) than when it indented the brain stem (Fig. 5b Table 7).

In the pontine angle tumours deformation of the pons on the tumour side was often observed in the axial projection and at the same time the pons was somewhat rotated posteriorly on that side in some cases also slightly displaced laterally towards the contralateral side (Fig. 9).

The local deformity of the pons on the side of the tumour was described by LILJEQVIST (1959b) in the

Table 5

Filling and distortion of the interpeduncular cistern, ambient cistern and quadrigeminal cistern in tumours of the brain stem and the pontine angle. Tumour position symbols and abbreviations as in Tables 3 and 4. Additional abbreviations: fr=frontal, sag=sagittally, ia=inferior end rotated anteriorly, ip=inferior end rotated posteriorly.

Tumour position	Brain stem		Pontine angle	
	Fill- ing (%)	Distor- tion	Fill- ing (%)	Distor- tion
Interpeduncular cistern				
Lat. proj.	100		97	
a.p. diameter		II		0
s.s. diameter		-		(-)
s.s. displacement of pons	s+			s(+)
s.s. inclination of the pos- terior part of the superior surface of the pons	s+			0
Ambient cistern				
Circum mesencephalic part				
axial proj.				
a. width of posterior part				
right side	71	0	75	+
left side	71	0	70	0
b. width of anterior infra- tentorial part				
right side	35	0	71	+
left side	35	II	49	0
c. width of anterior supra- tentorial part				
right side	35	-	77	+
left side	47	-	67	0
d. rotation around sagittal axis perpendicular to chiasm				
right side		sag(+)		fr+
left side		sag(+)		sag(+)
Quadrigeminal cistern				
1. Body of cistern lat. proj.	76		87	
a.p. displacement		p++		fr(+)
inking of quadrigeminal plate		0		0
rotation of inferior end of quadrigeminal plate		ip++		fr(+)
2. "Precentral fissure				
lat. proj.	76		79	
a.p. displacement		fr++		fr(+)

following way. In the postero-anterior view it appears as a layer of air running along the surface of the deformed pons. Behind this air layer the tumour may however penetrate more deeply into the pons. The medial border of the pontine angle tumour can



a

Fig 11 Brain stem tumour with its main component in the pons. Lateral tomography a) Encephalography b) Ventriculography. The peripontine cistern (→) markedly compressed in the superior-inferior direction. Marked posterior displacement of the



b

quadrangular cistern (←→) and precentral fissure (←→). The superior cerebellar cistern (→) markedly compressed and the superior vermis deformed as in expanding lesion in the anterior compartment. The tonsils herniated (←→) below the foramen magnum.



a

Fig 12 A right-sided pontine angle tumour indenting the cerebellar hemisphere and the brain stem. a) Asial tomography at the level of the auditory canals. The ambient cistern widened (←→) superior to the tumour. The contralateral pontocerebellar cistern (←→)



b

moderately compressed both laterally and medially. b) Lateral tomography. The widened ambient cistern superior to the tumour well demonstrated (←→). The interpeduncular cistern (←→) and the quadrangular cistern (←→) are normal.

is often not be established at encephalography. At ventriculography or at computer tomography these tumours often reach surprisingly far in the medial direction.

Pontocerebellar cisterns

Both in medulla oblongata and pons tumours the lateral part of the pontine angle cisterns was sym-

metrically compressed (Table 4). The compression reached further laterally in cases with tumours of the pons (Fig 6b) than in those with the tumour limited to the medulla oblongata (Fig 10a).

With pontine angle tumours the cistern of the tumour side was markedly dilated but at the same time partly occupied by the tumour. Sometimes air filling of the cistern occurred also lateral to the

Table 6

Brain stem tumours. Cisternal distortions useful for differentiation of tumours in the pons from those in the medulla oblongata. Symbols and abbreviations as in Tables 3-5

Tumour position	Medulla oblongata	Pons
Cisterna magna		
1 Extracranial part lateral projection		
a tonsillar herniation	0	+
b a.p. displacement of the cervical medulla	p+	p(+)
2 Foramen of Magendie lateral projection		
a a.p. displacement of upper part	p++	p++
b a.p. displacement of inferior part	p++	p+
3 Vilecula axial projection		
a width	++	+
4 Cerebellomedullary fissure axial projection		
a a.p. displacement	p++	0
b lateral displacement	+	0
Medullary cistern		
1 Premedullary part lateral projection	--	-
2 Lateral recess axial projection		
a a.p. diameter	--	-
b lateral extension	--	-
Pontocerebellar cisterns axial projection		
a width of medial part	--	--
b width of lateral part	(-)	--
Interpeduncular cistern lateral projection		
a inclination of the posterior part of the superior surface of the pons	II	+++
Quadrigeminal cistern lateral projection		
a a.p. displacement	0	p++
b a.p. rotation of inferior end	p+	p++

tumour. This was most common with small tumours but was also encountered in some cases with large tumours (Fig. 5a-d). The contralateral pontine angle cistern was in a rule moderately compressed in cases with pontine angle tumours.

The difference in width between the medial and the lateral part of the pontine angle cistern is to some extent characteristic for brain stem tumours a feature that has not been reported previously. RUGGIERO (1957) is a rule found no distortions of the pontine angle cistern in cases of brain stem tumour. On the other hand the typical distortions of these cisterns in pontine angle tumours are well known and LINDQVIST (1959b) also described the compression of the contralateral pontine angle cistern

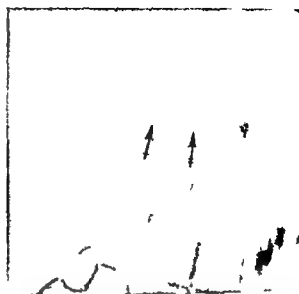


Fig. 13. Tumour of the pons and the mesencephalon. Lateral tomography. Marked local widening of the quadrigeminal cistern. Marked posterior displacement of the quadrigeminal plate and the precentral fissure (==).

Interpeduncular cistern

Neither in brain stem nor in pontine angle tumours was the a.p. diameter of the cistern reduced (Table 5). On the other hand the supero-inferior diameter was reduced in brain stem tumours, usually more tumours of the pons (Fig. 11a) than in tumours of the medulla oblongata (Fig. 10b). The compression of the cistern in this direction was also more marked in cases with widening of the ventricular system. Moderate supero-inferior compression of the cistern was also encountered in cases with pontine angle tumours with widening of the ventricular system.

With tumours in the pons the posterior part of the upper surface of the pons was tilted superiorly (Fig. 4c) while such a distortion was not demonstrated in tumours of the medulla oblongata (Fig. 10b) or the pontine angle (Fig. 12b). A moderate upward displacement of the pons occurred in both groups of brain stem tumours. On the other hand in pontine angle tumours only a slight upward displacement was found.

The distortion of the interpeduncular cistern thus to be explained only partly by hydrocephalus with widening of the anterior part of the third ventricle (LINDQVIST 1980a). Some of the abnormalities, i.e. the superior displacement of the pons in brain stem tumours and the superior tilt of the posterior part of the upper surface of the pons in pontine tumours are probably due to direct influence on the cistern by the tumour itself.

Table 7

Pontine angle tumours. Cisternal distortions useful for differentiating pontine angle tumours. Symbols and abbreviations as in Tables 3-6

Tumour position	Tumour, mainly indenting		
	Cerebellum	Cerebellum and brain stem	Brain stem
Cisterna magna			
1 Foramen of Magendie lateral projection a p displacement	0	p(+)	p+
2 Valleculla axial projection a width	(-)	(-)	+
b lateral displacement	+	+	++
Medullary cistern lateral projection			
width of premedullary part	--	-	
Pontine cistern lateral projection			
width	-	(-)	0
Quadrangular cistern lateral projection			
a a p displacement	p(+)	p(+)	p+
b a p rotation of inferior end	p(-)	p(+)	p+

Ambient cistern

The circum mesencephalic part of the ambient cistern was only slightly deformed in cases with brain stem tumours (Table 5). With pontine tumours a tendency towards compression of the anterior supratentorial part of the cistern and towards sagittal rotation of the cistern on both sides was noted.

In the case of pontine angle tumours the width of the cistern was as a rule increased on the side of the tumour and normal on the contralateral side. An obvious rotation frontally on the tumour side and the rotation sagittally on the contralateral side was also noted (Fig. 5a-e for a detailed description of these complex rotation movements cf. LINDQVIST 1978 p. 572). The widened ambient cistern on the tumour side was sometimes also demonstrated in the lateral projection (Fig. 12).

The widening of the ambient cistern on the tumour side in cases of pontine angle tumour was described by LILIEQUIST (1959b) as a common and typical finding in this type of tumour.

Quadrangular cistern

In the case of tumour in the medulla oblongata the distortion of the quadrangular cistern was slight

and often consisted only of a small posterior rotation of the inferior part of the quadrangular plate and posterior displacement of the precentral fissure (Table 6). On the other hand pontine tumours caused marked posterior displacement of both the quadrangular plate and the precentral fissure (Fig. 11 Table 6).

Pontine angle tumours indenting the brain stem altered the quadrangular cistern as with brain stem tumours (Table 7). Other types of pontine angle tumour caused only slight distortion of the quadrangular cistern.

In 2 cases with pons tumours a marked local widening of the quadrangular cistern was observed (Fig. 13).

The typical deformity of the aqueduct and the quadrangular cistern associated with brain stem tumours was described by LINDGREN & DI CHIRO and by LILIEQUIST (1963).

Remainder cisterns

The crural cisterns delineate the anterior lateral part of the cerebral peduncles. In 4 cases of pontine tumour the peduncles were expanded indicating extension of the tumour to the mesencephalon.

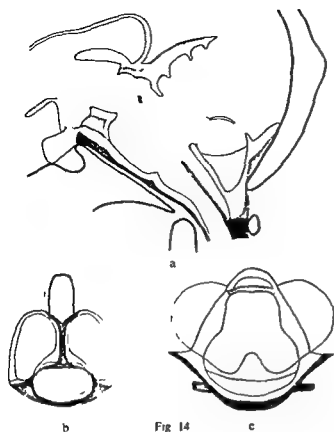


Fig 14

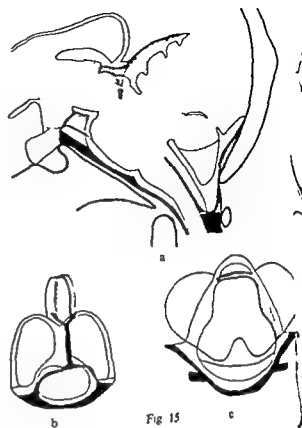


Fig 15

Fig 14 Drawings of some important cisternal deformities in tumours of the vermis. a) Lateral view. b) Axial view of the cisterns inferior to the fourth ventricle. c) Axial view of the cisterns adjacent to the tentorial notch. The normal appearance of the cisterns indicated by means of continuous lines. Cisternal structures possible to evaluate in tumour cases indicated with shaded areas. (From Lindqvist 1980a, Fig 16.)

Fig 15 Drawings of some important cisternal deformities in tumours of the right cerebellar hemisphere (cf Fig 14). (From Lindqvist 1980a, Fig 17.)

Fig 16 Drawings of some important cisternal deformities in tumours from the roof of the fourth ventricle (cf Fig 14). (From Lindqvist 1980b, Fig 8.)

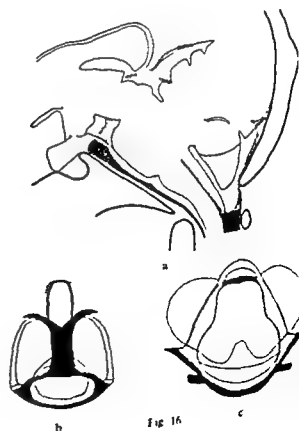


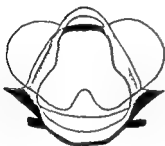
Fig 16



a

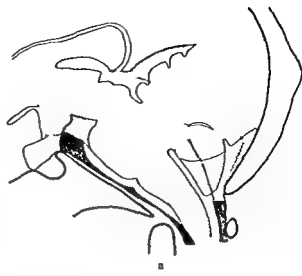


b



c

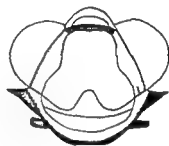
Fig 17



a



b



c

Fig 18



a



b



c

Fig 19

Fig 17 Drawing of some important cisternal deformities in tumours from the floor of the fourth ventricle (cf Fig 14) (From LANDQVIST 1960b Fig 9)

Fig 18 Drawing of some important cisternal deformities in tumours of the brain stem (cf Fig 14)

Fig 19 Drawings of some important cisternal deformities in tumours of the right pontine angle (cf Fig 14)

*Typical cisternal features of brain stem tumours
and pontine angle tumours*

Lateral projection

Tumours of the brain stem	Tumours of the pontine angle
Tonsillar herniation with tumours of the pons but not of the medulla oblongata	Tonsillar herniation in many cases particularly in those with widening of the ventricular system
Compression of the interhemispheric part of the cisterna magna against the occipital crest	Compression of the interhemispheric part of the cisterna magna against the occipital crest
Posterior displacement of the foramen of Magendie	Some posterior displacement of the foramen of Magendie in cases with tumours indenting the brain stem
Marked posterior and inferior displacement of the retrotonsillar spaces	Moderate posterior and slight inferior displacement of the retrotonsillar spaces
Marked compression of the medullary and pontine cisterns	Moderate compression of the medullary and pontine cisterns more marked in tumours indenting the cerebellar hemisphere than in tumours indenting the brain stem
Moderate supero-inferior compression of the interpeduncular cistern moderate upward displacement of the pons In pontine tumour superior tilting of the posterior part of the upper surface of the pons but not in medulla oblongata tumours	Only slight supero-inferior compression of the interpeduncular cistern and slight upward displacement of the pons
In cases with pontine tumours marked posterior displacement of the quadrigeminal plate and the precentral fissure as well as posterior rotation of the inferior part of the quadrigeminal plate In tumours of the medulla oblongata slight posterior rotation of the inferior part of the quadrigeminal plate and marked posterior displacement of the precentral fissure	No or very slight distortion of the quadrigeminal cistern In tumours indenting the brain stem slight posterior rotation of the inferior part of the quadrigeminal plate and some posterior displacement of the precentral fissure may occur

Axial projection

Tumours of the brain stem	Tumours of the pontine angle
Slight widening of the inferior vermis	Contralateral displacement of the inferior vermis and slight widening of the vermis particularly in cases with tumours indenting the brain stem
Width of the vallecula markedly increased in tumours in the medulla oblongata normal in pontine tumours	Normal width of the vallecula which is often displaced towards the contralateral side
Cerebellomedullary fissures separated and displaced posteriorly in medulla oblongata tumours unchanged in pontine tumours	Cerebellomedullary fissures both sides displaced contralaterally on the tumour side also posteriorly
Compression of the lateral recesses of the medullary cistern most marked in medulla oblongata tumours	The lateral recess of the medullary cistern where the tumour side comes on the contralateral side Medulla oblongata rotates posteriorly on the tumour side and displaced toward the contralateral side
Both pontocerebellar cisterns uniformly compressed with tumours of the pons In medulla oblongata tumours the medial part of the cisterns more compressed than the lateral part	The pontocerebellar cistern on the tumour side markedly widened and totally or partially occupied by the tumour Moderate compression of contralateral pontocerebellar cistern
Very slight distortion of the circum mesencephalic parts of the ambient cistern	The circum-mesencephalic part of the ambient cistern widened on the tumour side and rotated frontally The cistern on the contralateral side rotated sagittally

In most cases of pontine angle tumour with filling of the crural cisterns no abnormality was noted but in some cases the peduncle on the tumour side was displaced posteriorly or medially. This should indicate extension of the tumour into the tentorial notch which was also confirmed by the surgical report in the majority of these cases.

The superior cerebellar cistern was possible to evaluate in the lateral projection in approximately half of the cases. In all cases of brain stem tumour with filling of this structure the superior vermis was compressed similar to the findings in expanding lesions in the anterior compartment of the posterior fossa (Fig. 11).

In cases of pontine angle tumour the shape of the superior vermis was usually normal but in some cases, particularly in those with the tumour indenting the brain stem, the vermis was slightly compressed as in expanding lesions in the anterior compartment.

The chiasmatic cistern was filled in nearly all cases. As in cases with other tumour positions in the posterior fossa (LINDQVIST 1980a, b) this cistern was often compressed when hydrocephalus was present but was otherwise without distortion.

The cistern of the lamina terminalis was filled in a little less than one third of the cases and was without abnormality.

The pericallosal cisterns were filled in the axial projection on one or both sides in approximately 20 per cent of cases with brain stem tumours and in approximately 35 per cent of those with pontine angle tumours. The wings of the ambient cistern were filled in approximately 30 per cent with brain stem tumour and in 60 per cent with pontine angle tumour. The cisterna veli interpositi was filled in approximately 10 per cent in brain stem tumour and in 20 per cent in pontine angle tumour. All these cisterns were often widened in cases with supratentorial ventricular dilatation (Fig. 7) but otherwise without distortion. In cases with unilateral filling no correlation was found between the filled side and the tumour side, which is in agreement with the finding in cases with other tumour positions in the posterior cranial fossa (LINDQVIST 1980a, b).

The cisternal distortions for different tumour locations in the posterior fossa based on the results reported in Parts I, II and III are summarized in Figs 14 to 19. Figs 14 and 15 demonstrate the cisternal distortions in tumours of the vermis and the right cerebellar hemisphere respectively (LINDQVIST

1980a). Figs 16 and 17 those in tumours originating from the roof and floor of the fourth ventricle (LINDQVIST 1980b) and Figs 18 and 19 those in cases with tumours of the brain stem and pontine angle respectively. Typical cisternal distortions associated with tumours of the brain stem and pontine angle are listed on page 354.

Within the groups the cisternal features vary somewhat between different cases due to the size and position of the tumour, the absence or presence of hydrocephalus etc., nevertheless the cisternal distortions are usually so characteristic that the different tumour groups can be distinguished from each other.

SUMMARY

The pneumographic appearances of the subarachnoid cisterns have been analysed in detail in a clinical series of 17 patients with brain stem tumours and in 40 with pontine angle tumours. The cisternal distortions may be used to distinguish tumours in the pons from tumours in the medulla oblongata and also to distinguish tumours of the pontine angle with different modes of growth, e.g. tumours mainly indenting the cerebellar hemisphere from those mainly indenting the brain stem. The results should be applicable also for an analysis of cisternal pathology by other methods such as computer tomography and cisternography with positive contrast media.

ACKNOWLEDGEMENTS

The investigation was supported by grants from the Swedish Cancer Society and the Medical Faculty, University of Umeå.

REFERENCES

- CORRALES M.: Fourth ventricle. III. Intra- and extra-axial tumours. *Acta radiol. Diagnosis* 12 (1972) 370.
- and GREITZ T.: Fourth ventricle. II. Tumours of the cerebellum. *Acta radiol. Diagnosis* 12 (1972) 241.
- DAVIDOFF L. M. and EPSTEIN M. S.: The abnormal pneumoencephalogram. Lea & Febiger, Philadelphia, 1950.
- GREITZ T.: Tumours of the quadrigeminal plate and adjacent structures. *Acta radiol. Diagnosis* 12 (1972) 513.
- ISHERWOOD J.: Air meatography. *Clin. Radiol.* 23 (1972) 65.
- LEASELL I.: A note on the treatment of acoustic tumours. *Acta chir. scand.* 137 (1971) 763.
- LILJFELT B. (a): The subarachnoid cisterns. An anatomic and roentgenologic study. *Acta radiol.* (1949) Suppl. No. 185.
- (b): Pontine angle tumour. Encephalographic appearances. *Acta radiol.* (1959) Suppl. No. 188.
- Lumbar encephalography in pontine and intracerebellar tumours. *Acta radiol. Diagnosis* 1 (1967) 593.

- LINDGREN E. Encephalographic examination of tumours in the posterior fossa. *Acta radiol* 34 (1950) 331
- and DI CHIRO G. The roentgenologic appearance of the aqueduct of Sylvius. *Acta radiol* 39 (1953) 117
- LINDQVIST M. Cisternal changes produced by experimental balloon tumours in the posterior cranial fossa. A post mortem investigation. *Acta radiol. Diagnosis* 19 (1978) 561
- (a) Cisternal abnormalities produced by clinical tumours in the posterior cranial fossa. I Cerebellar tumours. *Acta radiol. Diagnosis* 21 (1980) 85
- (b) Cisternal abnormalities produced by clinical tumours in the posterior cranial fossa. II Fourth ventricle tumours. *Acta radiol. Diagnosis* 21 (1980) 129
- and MÖLLER A. Postmortem radiography of the subarachnoid cisterns. *Acta radiol. Diagnosis* 19 (1978) 1
- ROBERTSON H G. *Pneumoencephalography*. Blackwell Scientific Publications, Oxford 1957
- RUGGIERO G. *L'encephalographie fractionee*. Masson, Paris 1957

IDIOPATHIC HYPERTROPHIC SUBAORTIC STENOSIS

III Analysis of the myocardial fibre shortening of the free left ventricular wall
by means of geometric models

G KVAM

The unique shape of the hypertrophic muscular interventricular septum in idiopathic hypertrophic subaortic stenosis (IHSS) convex longitudinally and concave transversely towards the left ventricle (HUTCHINS & BULKLEY 1978) results in an isometric mode of contraction of the septum (Part I B KVAM 1980). Some degree of contraction of the wall around the septal attachment most probably causes the thickness of the attachment to be reduced; therefore the more axial parts of the septum increase in thickness contributing to a straightening out of the transverse concavity during the contraction. The outer wall at the septal attachment also increases in thickness in systole. Consequently this increase in wall thickness effects a squeezing of the septum from the sides and the apical end. Therefore it increases slightly in thickness contributing to the decrease in left ventricular volume.

The systolic septal shortening is markedly reduced (Part I A KVAM 1980) and the septum does not bend towards the right ventricle during the systolic contraction. It therefore acts as a suspender for the rest of the wall. For the sake of simplicity it is here regarded as a stiff flat structure with the free wall attached around its sides and one end the free wall encroaching upon the septum during contraction. The diastolic transverse section of the left ventricular cavity in IHSS may then be regarded as a half circle the diameter representing the septal wall (Part I B).

When the free (non septal) wall contracts its increase in thickness consequently causes some expulsion of the ventricular volume. Therefore a thick wall does not have to shorten to the same extent as a thin wall in order to effect the expulsion of a certain amount of blood.

The change in relative oblongity of the cavity during contraction also influences the effect on the ventricular volume produced by a certain degree of myocardial fibre shortening.

CATE *et coll* (1977) proposed that the systolic function of the left ventricle can be maintained by three different compensatory mechanisms (1) increase in dimension (Starling mechanism) (2) increase in systolic thickening and (3) increase in systolic contraction velocity.

In this report other mechanisms secondary to the specific geometry as described are discussed and evaluated. These mechanisms cannot be regarded as compensatory in the ordinary sense of the word. They represent geometric properties of the heart itself and determine which compensatory mechanisms are possible in a given heart. The compensatory mechanisms which then occur should be dependent upon the tension distribution in the ventricular wall, the state of the heart muscle, the function of the valvar apparatus, the blood pressure and other physiologic variables.

IHSS is characterized by a high ejection fraction (EF) and an early ejection of a large fraction of the stroke volume (SV) (HERNANDEZ et coll 1964 GOTSMA & LEWIS 1974). The specific geometric shape and mode of contraction of the left ventricle in IHSS may explain these facts. The maximum velocity of the free wall myocardial fibre shortening in IHSS may be normal and the degree of the systolic fibre shortening is probably subnormal.

A model has been designed for calculating the myocardial fibre shortening of the free wall in IHSS during systolic contraction. Another model was designed for calculating the fibre shortening of the normally shaped left ventricular wall from cardioangiographic parameters. Both models were designed with a certain degree of similarity in an attempt to keep systematic errors similar. They were built up from geometrically simple structures in order to keep the arithmetic simple.

The myocardial fibre shortening of the free left ventricular wall in IHSS is compared with the fibre shortening of the left ventricular wall in control patients. The two models are evaluated with respect to the effect of alteration of the different input values.

Materials and Methods

The material consisted of the same 4 IHSS patients as in Parts I and II (KVAM 1980). They were males, age range 24 to 64 years, with subaortic chambers and subaortic pressure gradients from 35 to 130 mmHg and with elevation of the left ventricular end diastolic pressures. Three had a slight mitral regurgitation, negligible relative to the stroke volume. The heart frequency had a mean value of 83 beats per minute (range 64-95). One of these patients was later operated upon and had the diagnosis confirmed.

The 10 patients in whom biplane cineangiography had been performed (Part I B) were used as controls. They were aged 23 to 60 years and examined because of anginal pain but with normal coronary angiography and with normal cine left ventricular examinations. The heart frequency had a mean value of 66 beats per minute (range 55-80, SD 8.6).

The cineangiography was performed as described in Part II and the enlargement factors were determined according to the catheter grid technique.

In both groups of patients an end diastolic and a subsequent end systolic frame were identified as

the one with the largest and smallest ventricular area respectively before any contraction or dilatation could be observed.

The end diastolic volume (EDV) was estimated from the biplane cine films. A reduction method was applied for the area of the IHSS left ventricular cavities in the 60° right posterior oblique (RPO) view to compensate for the septal bulge as described (Part II). The end diastolic areas A_{RAO} and A_{RPO} were planimetrically determined and the longest ventricular axes L_{RAO} and L_{RPO} measured. The width W_d was then calculated from the 30° right anterior oblique (RAO) view and the depth D_d from the 60° RPO view according to the ellipse formula $x=4A/\pi L$.

The 60° RPO length is considerably shortened. Therefore the 30° RAO length is used for the calculation of EDV which was calculated according to the ellipsoid formula as

$$\frac{\pi}{6} LWD$$

L equals the length, W the width and D the depth after correcting for magnification.

The 30° RAO frames every third frame during systole including the end-diastolic and the end systolic frames were analysed. The areas A were planimetrically determined and the lengths L from the apex to the center of the aortic rings measured. With a constant relationship k_1 between the width and the depth of the cavity during systole and with an enlargement factor k the ventricular volume according to the ellipsoid formula is

$$\frac{1}{k_1} \left(\frac{1}{k} \right)^3 \frac{\pi}{6} L \frac{4A}{\pi L} = k \frac{A^2}{L}$$

The relative volume kV were accordingly calculated as A/L . From these relative volumes and from the known EDV the ventricular volumes were calculated for every frame analysed.

The width according to the ellipse formula is $4A/\pi L$. The relationship between the length and the width of the cavity L/W was calculated as $\pi/4A$ from the end-diastolic frame in the IHSS group and from all the frames in the control group.

The end-diastolic thickness t_{ed} of the free left ventricular wall was measured in the 60° RPO projection. This projection was used because the outer contour of the left ventricle could not be adequately identified on the end-diastolic 30° RAO cine frames.

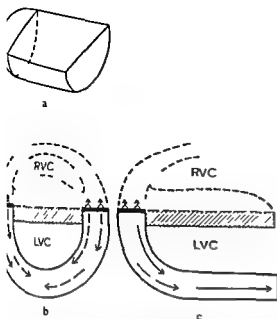


Fig. 1 IHSS left ventricular model in diastole. a) Perspective drawing of the model cavity. A semicylinder ending in a quarter sphere representing the apical part. b) Transverse section of the model showing the semicylindrical part. The model ends along the upper half line. c) Longitudinal section of the model. LVC Left ventricular cavity. RVC Right ventricular cavity. The solid arrows indicate lines of contraction of the free left ventricular wall. Small arrows indicate counterforce from the right side of the heart which is not included in the model calculation. Hatched parts indicate septum.

of the patients with IHSS. The wall thickness was measured along a line at right angles to the ventricular contour from a point on the outer wall 2 cm from the intersection between the septum and the outer ventricular contour (2 cm distance after multiplying with the enlargement factor). The measured wall thickness was then multiplied by the enlargement factor to obtain t_{ma} . The model was designed to avoid measuring the apical wall as it has a thinner wall than the rest of the cavity.

For each calculation of fibre shortening in the model group the following parameters were used: (1) the end-diastolic volume, (2) the intermediate or end systolic volume, (3) the end-diastolic myocardial wall thickness t_{ma} , (4) the end-diastolic length width relationship L_0/W , and (5) the intermediate or end systolic length width relationship L_s/W .

Four parameters were used as input values in the IHSS model. The design of this model is such that the relationship between the long and the transverse axis of the model cavity is automatically determined directly dependent upon the other input parameters during the simulated systolic contraction.

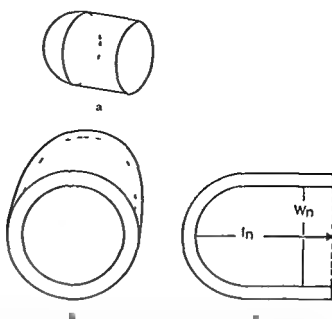


Fig. 2 Normal left ventricular model. a) Perspective drawing of the model cavity with its semispherical apical end and continuing as a cylinder with the other end open corresponding to the outflow tract. b) Transverse section of the cylindrical part of the model with a circular outline and even wall thickness. The half crescent part indicates the right ventricle which is not part of the model. c) Longitudinal section of normal left ventricular model. L_n is the length and W_n the width of the model cavity.

Therefore the fifth input parameter listed the intermediate or end systolic length width relationship was excluded.

The model representing the end-diastolic IHSS left ventricular cavity appears in Fig. 1 a. The transverse section of this diastolic model cavity is a half circle. It is formed as a semicylinder with one end open the other end continuing into a quarter sphere representing the ventricular apex. The middle part of the left ventricular cavity is shallower than the rest because of the septal bulge. The septal surface is represented in the model by a flat plane. The main error in using an even height of the semicylindrical part of the model cavity is therefore primarily an error in the configuration of the model septum.

The normal left ventricular cavity resembles more a full circle on transverse sections of anatomic specimens (MCALPINE 1975). The model representing a normal left ventricular cavity is illustrated in Fig. 2 a. At transverse section it appears as a circle. The ventricle is formed as a cylinder with one end open representing the ventricular outflow tract. The other end is closed by a hemisphere representing the model apex.

The length of the diastolic cavities in the IHSS

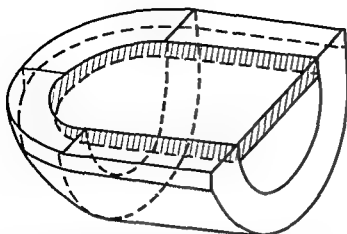


Fig. 3 Perspective drawing of the IHSS left ventricular model in diastole. The upper flat surface corresponds to the heavy line and its continuation in the interventricular septum in Fig. 1 b and c. The model septum indicated along its borders by oblique lines was given half the thickness of the rest of the ventricular wall which has a thickness equal to the measured free wall in the patient. The outer shape and size of the upper plane are kept constant during the systolic contraction of the model.

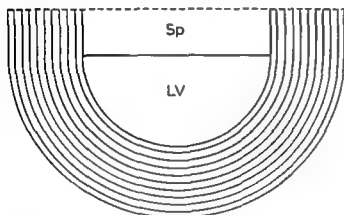


Fig. 4 Transverse section of the diastolic IHSS model. Sp, Interventricular septum of the model; LV, Left ventricular cavity of the model. The contracting wall of the model is divided into 10 concentric elements of even and identical thickness for the calculation of the diastolic volume weighted mean myocardial area A_d .

and in the control model is equal to the length of the semicylinder/full cylinder plus the radius of the quarter sphere/half sphere respectively. The width of the IHSS and the control model cavities is equal to twice the radius of the semicylinder/full cylinder respectively. The radius of the quarter sphere/half sphere obviously is equal to the radius of the semicylinder/full cylinder respectively. Designating this common radius r_d , the length of the semicylinder/full cylinder may be expressed as $k \cdot r_d$.

In each analysis of fibre shortening a value of k was used which made the relationship between the length and the width of the model cavity equal to the

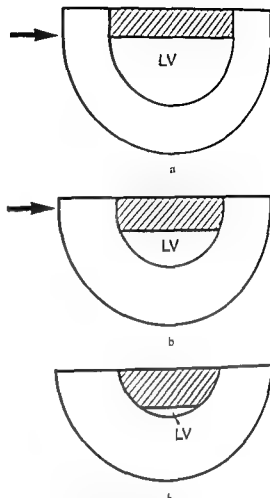


Fig. 5 Transverse sections of the IHSS left ventricular model. a) Diastolic situation (corresponds to Fig. 4). The arrows mark the transition between the outer semicylindrical part and the straight part which borders the septum. This straight part has identical thickness to the free wall of the model. b) Upon contraction the straight part above the arrows is first reduced the septal thickness increases when the free wall thickness increases. c) Further contraction when the straight part is reduced to zero the model forms an outer and an inner circular segment. The ventricular cavity narrows increasingly because of fibre shortening of the wall and because of increasing septal thickness. LV, Left ventricular cavity of the model.

diastolic length-width relationship L_d/W_d of particular patient, i.e.

$$\frac{(1+k)r_d}{2r_d} = \left(\frac{L_d}{W_d} \right) \cdot k = \left(2 \frac{L_d}{W_d} - 1 \right)$$

IHSS model calculations. The diastolic IHSS model cavity has an inner radius r_d . The length-width relationship k_d of the model cavity is given by the value L_d/W_d of the patient's left ventricle. The volume V_d of the diastolic model cavity equals

$$\frac{\pi}{3} r_d^3 + \frac{\pi}{2} r_d^3 (2k_d - 1)$$

in V_d get the EDV value of the patient then

$$\frac{\pi r_d^3}{6} (7 + 3(2k_d - 1)) = \text{EDV and } r_d = \sqrt[3]{\frac{6\text{EDV}}{\pi(6k_d - 1)}}$$

as accordingly calculated

The diastolic IHSS model was given an even non uniform wall thickness t_{md} of the particular patient wall curves around the semicylinder and the quarter sphere and continues up on the sides and at the end of the septum of the model. Both the diastolic septum and the model wall stops abruptly in a plane parallel to the plane representing the septal left ventricular wall (Fig. 1 b, c). The thickness of the diastolic septum is $k_{id} t_{md}$ and this is obviously the thickness of the horseshoe shaped part of the wall surrounding the septal attachment (Fig. 3). k_{id} was given the value 0.5.

Knowing the inner radius r_d , the wall thickness t_{md} and thus also the outer radius ($r_d + t_{md}$), the volume of the semicylinder $k_d r_d$ and the septal thickness $k_{id} t_{md}$, the outer diastolic volume of the model was calculated. Then the septal volume was calculated hereafter the volume of the wall myocardium = outer volume minus the volumes of the model and the cavity.

The free wall including the part corresponding to the septal attachment was divided into 10 concentric elements with equal and even thickness (Fig. 4). For each element the inner and outer surfaces and the arithmetic mean between them was calculated. The mean surface was then multiplied by the thickness of the particular element. The sum of the surface volume products of each element was divided by the sum of the volumes of the elements (the volume of the model outer wall). In this way the volume weighted mean myocardial area in the diastolic model was calculated.

30 cine angiography does not show any outward movement of the left anterolateral heart border during systole. This is reflected by letting the outer plane of the model (Fig. 3 uppermost) remain constant in shape and dimension during the simulation of the systolic contraction. The average increase in the overall IHSS septal thickness during systolic contraction has been reported from 8.5 per cent to 22.5 per cent (ROSSEN et al. 1974, COHEN et al. 1975, CATE et al. 1974). The compression of the septum is rather modest when interposed as it is between the right and left ventricular walls and thus also the increase in thickness of the myocardial wall around the septal attachment.

This is depicted in the model by making the septum rather thin but letting the outer wall around the septal attachment have the same thickness and mode of contraction as the rest of the free wall.

The catenoid like IHSS left ventricular septal surface convex longitudinally and concave transversely is characterized by an overall similar pressure on either side (HUTCHINS & BULKLEY). Very small additional pressure is needed to move the wall. Therefore it is reasonable to suppose that a major part of the systolic increase in septal thickness contributes to the narrowing of the left ventricle.

These two aspects were reflected in the model by letting the whole increase in the septum encroach on the left ventricle but letting the septum only have half the thickness of the free wall ($0.5 t_{md}$). The muscular interventricular septum of the IHSS heart has more than 1.3 times the thickness of the free wall.

Fig. 5 a is a transverse section of the cylindrical part of the IHSS model in diastole. The outer height of the model is the greatest distance from the uppermost septal plane to the outer non septal wall measured along a line at right angles to the uppermost septal plane. The systolic contraction is initiated by reducing the outer height. This is first performed by keeping the outer shape and size of the semicylinder and quarter sphere but reducing the height of the straight part (above the arrows in Fig. 5 a, b). Upon further contraction the straight part is reduced to zero.

Thereafter the semicylinder and quarter sphere are changed into a cylindrical segment and a semi-spherical cap respectively in order to simulate a contraction beyond this (Fig. 5 c).

The free wall of the model bordering the cavity and the septum increases in thickness during the simulation of the systolic contraction but the thickness of the wall remains even.

The outer volume of the whole diastolic model is now known. The difference between the outer diastolic volume and the outer systolic volume is equal to the difference between the volumes of the model cavity $V_d - V_s$, V_d and V_s being the end-diastolic and the systolic model cavity volumes respectively.

The volume V_s of the septum plus the wall bordering the septum in diastole corresponding to the straight part above the arrows in Fig. 5 a was calculated.

If $V_d - V_s = V$ then the systolic model keeps an outer shape of a semicylinder plus a quarter sphere plus a straight part with a height of zero or

If $V_d - V_s > V_{str}$, the systolic model obtains an outer shape of a cylindrical segment plus half a spherical cap

The further calculation depends upon this comparison of the volumes. If $V_d - V_s < V_{str}$ then the following relationships prevail. The volume of the straight part is reduced by a volume equal to $V_d - V_s$. The new systolic straight part therefore obtains a volume equal to $V_{str} - (V_d - V_s)$ which is the volume above the arrows in Fig 5 b. This volume is divided by the area of the outer limiting plane of the model (corresponding to the uppermost plane in Fig 3). The thickness of the systolic new straight part above the arrows in Fig 5 b was thereby calculated.

The volume inside the contractile wall i.e. the septal volume S plus the systolic cavity volume V_s has a form similar to the outer volume: an inner semicylinder plus a quarter sphere both with an inner radius r and in addition the straight part which is a flat structure with a new known thickness. This flat structure is formed as a semicircle with radius r_s plus a rectangle with the same length as the semicylinder kr_d and the width $2r_s$. K and r_d are known values. This volume is expressed as a function of r : $f(r) = S + V_s$. The inner radius r_s is calculated by solving $|f(r) - (S + V_s)| < 0.01 \text{ ml}$ using the principle of bisection (FORSYTHE et coll 1974).

In the model the ventricular surface of the septum is flat parallel to the outer septal plane during systolic contraction. The systolic model cavity thereby becomes a semispherical cap continuing as a cylindrical segment. Both of them have the radius r_s of the associated sphere/associated circle respectively. The length of the cylindrical segment is kr_d . These values are now known. Therefore the volume of the systolic model cavity can be expressed as a function of the cavity height (equal to the height of the circular segment depicted on the transverse section in Fig 5 b): $V_s = g(h)$.

The height of the cavity was calculated by solving $|g(h) - V_s| < 0.01 \text{ ml}$.

The outer systolic radius obviously equals the outer diastolic radius equal to $r_d + t_{md}$. The inner systolic radius r_s of the contractile wall known, the systolic wall thickness equals $(r_d + t_{md}) - r_s$. The form and thickness of the free wall of the model is now known in systole. As for the diastolic IHSS model (Fig 4) the free systolic wall was divided into 10 concentric elements and the volume weighted systolic mean area A was calculated.

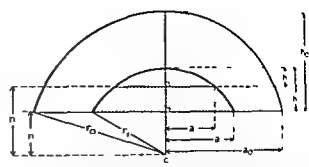


Fig 6 Transverse section of the IHSS systolic model semi-spherical cap/semicylindrical segment variant. The same as Fig 5 c but turned upside down. c: Center of the associated sphere. r: Radius of the outer segment. a: Half the chord of the outer segment. h: Half the chord of the cavity segment. h1: Height of the inner segment. n: Distance from the circular center to the outer septal plane. e: Distance from the circular center to the inner septal plane. r0: Radius of the outer segment. r1: Radius of the inner segment.

If $V_d - V_s > V_{str}$, the outer volume of the systolic model is smaller than the original outer semicylindrical/quarter spherical parts of the diastolic model. The outer septal plane is constant in shape and dimension from the diastolic to the systolic model. The outer systolic model is formed in this instance as a semispherical cap plus a cylindrical segment (Fig 5 c transverse section).

This transverse section is redrawn in Fig 6 upside down with the septal plane below. The center of the associated circles of the outer and inner circular segments c is also drawn. The outer and inner heights h and h_1 and also the height of the cavity h are shown. The corresponding half chords a_0 , r_1 and n are also shown as well as the radii r_0 and r_1 of the associated circles of the outer and inner circular segments.

The outer volume of the systolic model V_m is equal to the muscle wall volume V_m plus the septal volume S plus the systolic cavity volume V_s . V_m is known (equal to the outer diastolic radius i.e. $r_d + t_{md}$) and the length kr_d of the cylindrical segment is also known. The outer volume was now expressed by means of the formulas for the semispherical cap and cylindrical segment (Table 1) by means of h : $V(h) = V_m + S + V_s$. h was calculated by solving $|V(h) - (V_m + S + V_s)| < 0.01 \text{ ml}$.

The distance n from the circular center to the outer septal plane appears in Fig 6. According to Pythagoras $a_0^2 + n^2 = r^2$. Obviously $h + n = r$.

Accordingly $a_0 + n^2 = (h + n)^2$ and $n = (a_0^2 - h^2)/2h$. h_1 and a_0 known n was calculated. The whole inner segment in Fig 6 has a radius r_1 and a half chord r_1 . The distance n from the center

Table 1

The formulas applied in the HISS model calculations. r The radius of the wall layer being calculated. R_d The radius of the inner ventricular cavity in diastole. h_d The length of the diastolic model cavity divided by its width. h The height of the circular segment and semispherical cap being calculated. t_s The thickness of the straight part (above the arrows in Fig. 5 a and b). The horseshoe shaped band is the area of active muscle bordering the septum above the arrows in Fig. 5 a and b corresponding to the upper straight parts on transverse section in Fig. 3.

Volumes	
The quarter sphere	$\frac{\pi}{3}r^3$
The semicylinder	$\frac{\pi}{2}r^2(2h_d-1)r_d$
The base plate	$\left[\frac{\pi}{2}r^2 + (r^2h_d-1)r_d\right]t_s$
The semispherical cap	$\frac{\pi}{6}h(3r-h)$
The cylindrical segment	$\left[r^2 \cos\left(\frac{r-h}{r}\right) - (r-h)\left(\frac{r-h}{r}\right)\right](r^2h_d-1)r_d$
Areas	
The quarter sphere curved part	πr^2
The semicylinder curved part	$\pi r(h_d-1)r_d$
The horseshoe shaped band of straight part	$[r^2 + (h_d-1)r_d]t_s$
The semispherical cap curved part	πrh
The cylindrical segment curved part	$r^2 \cos\left(\frac{r-h}{r}\right) + h_d-1)r_d$
Outer septal plane	$\frac{\pi}{2}r^2 + (h_d-1)r_d r$

ular center to the common chord is obviously identical for the inner and the outer segment. According to Pythagoras $a+n=r$. The height of the inner segment is h_1 . Obviously $h_1+n=r_1$.

Therefore $a^2+n^2=(h_1+n)^2$ i.e. $n=h+2h_1$ and $a=\sqrt{h^2+2h_1n}$. n is known and a is expressed as a function of h_1 . The volume of the model inside the wall representing the active myocardium was now expressed by means of the volume formulas for the half spherical cap and the cylindrical segment (Table 1) with h_1 as the only variable: $V(h_1)=V+S$ and it obviously is equal to the cavity plus the septal volumes. h_1 was calculated by solving $|V(h_1)-(V_s+S)| < 0.01$ ml.

The model cavity is a circular segment on transverse section the cavity segment. It has a common arc and thus a common center c and radius r_1 with the inner segment. The distance from the cavity

segment to the circular center c is $n-h$ as well as n are now known. $h_1+n=r_1$.

The height h of the cavity segment plus the distance n also equals r . Therefore $h+n=h+n$ i.e. $n=(h+n-h)$. a is half the chord of the cavity segment. According to Pythagoras $n+a=r-(n+h)$ i.e. $a=(n+h)-n$.

Substituting the expression above for n in this last equation $a=(n+h)-(h+n-h)$ and $a=\sqrt{(n+h)^2-(h_1+n-h)^2}$ are obtained.

In this manner both n and a were expressed as variables of the cavity height h . Again using the volume formulas for the semispherical cap and the cylindrical segment the systolic cavity volume was now expressed as an equation with only h as variable: $V(h)=V_s$. The cavity height h was calculated by solving $|V(h)-V_s| < 0.01$ ml.

In this systolic model the thickness of the wall

representing the contractile myocardium obviously is the difference between the outer and inner heights $t_m = h_o - h_i$. t_m was calculated

The shape and thickness of this wall is now known. As for the diastolic IHSS model (Fig. 4) the wall was also in this case divided into 10 concentric even and equally thick walled elements. Using the surface and volume formulas for the semi-spherical cap and the cylindrical segment the volume weighted mean systolic myocardial area A_s was calculated in principle as described for the calculation of the diastolic mean area. The formulas applied appear in Table 1 (BRONSTEIN & SEMENDYAYEV 1973).

Normal model calculations. In the normal model the calculations are simpler. If r_d is the internal radius of the normal model cavity in diastole and K_d the diastolic length-width relationship then (Table 2)

$$\frac{2}{3}\pi r_d^3 + \pi r_d(2K_d - 1)r_d = EDV \quad r_d = \sqrt[3]{\frac{3EDV}{\pi(6K_d - 1)}}$$

r_d was accordingly calculated. The length of the cylindrical part is $(2K_d - 1)r_d$. The model was given an even wall thickness equal to the diastolic wall thickness t_{md} of the patient analysed (Fig. 2 b, c). The outer diastolic radius is thus $r_d + t_{md}$. Using the formulas for the hemisphere and the cylinder the outer model volume was calculated. Subtracting the cavity volume V_d from this outer volume the myocardial wall volume of the model V_m was calculated.

The wall of the diastolic normal model was divided into 10 concentric elements with even and equal wall thickness (Fig. 4). The volume weighted mean myocardial area in diastole A_d was then calculated as described for the IHSS model but using the appropriate formulas (Table 2).

The normal model in systole is much simpler than the IHSS systolic model. The normal heart contracts more concentrically. The model cavity was designed with the same shape as the diastolic model cavity: a hemisphere continuing in a cylinder with one end open corresponding to the outflow tract (Fig. 2). The relationship between the length and the width of the model cavity was given a value identical with the measured length-width relationship of the patient's left ventricle in the particular systolic phase being analysed. The inner cavity radius in

Table 2

The formula is applied in the normal model calculations. r The radius of the wall layer being calculated. R The radius of the inner ventricular cavity. L The length of the model cavity divided by its width.

Volumes	
The hemisphere	$\frac{2}{3}\pi r^3$
The cylinder	$\pi r^2(L-1)r$
Areas	
The hemisphere	πr^2
The cylinder	$\pi r L$

systole is r_s . The cylindrical part in systole was accordingly given a length

$$r \left(2 \frac{L_s}{W_s} - 1 \right)$$

L_s and W_s are the length and the width of the patient's left ventricle in the actual systolic phase. This is exactly parallel to the normal diastolic model.

V_s is the volume of the systolic model cavity and $L_s/W_s = K$. Then

$$r = \sqrt[3]{\frac{3V_s}{\pi(6K_s - 1)}}$$

r_s the internal radius of the systolic model cavity was accordingly calculated.

The systolic wall thickness t_m of the model is even. The outer radius of the systolic model accordingly equals $r + t_m$. The outer volume equals V_s plus the muscle volume V_m which is known from the diastolic model. The outer volume was expressed with the outer systolic radius as the only variable: $f(r_o) = V_s + V_m$. r_o was calculated by solving $f(r_o) - (V_s + V_m) < 0.01$ ml.

The systolic wall thickness t_m was then calculated as the difference between the outer and the inner radius.

Thereafter as described for the diastolic model the wall was divided into 10 concentric elements (Fig. 4) and the volume weighted mean systolic area A_s was calculated.

Irrespective of whether a heart from the control group was analysed by means of the normal model or a heart with IHSS was analysed by means of the IHSS heart model the left ventricular shortening was calculated according to the same formula. A_d is the volume weighted mean area of the

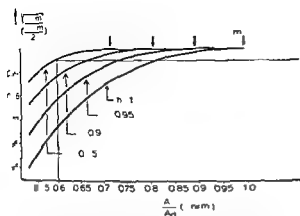


Fig. 7 Graphical drawing of calculations showing the error of m as the square root of the product of the systolic average length and width expressed as fraction of the corresponding diastolic values instead of the arithmetic mean value of the systolic length and width expressed in the same manner in the calculation of average systolic fibre length A . Volume weighted mean myocardial area of the model in systole A_s Volume weighted mean myocardial area of the model in diastole A_d Average systolic length expressed as a fraction of corresponding diastolic length m Average systolic width expressed as a fraction of corresponding diastolic width n . The expression \sqrt{nm} exactly substitutes the expression $(n+m)/2$ in the calculation of average systolic fibre length and thus in the calculation of systolic fibre shortening only when $n=m$ (upper arrow).

wall representing the actively contracting myocardium in diastole A is the corresponding volume weighted mean area in the particular phase of the systole being analysed. The myocardial fibre shortening (in per cent) was calculated according to the formula

$$\left(1 - \sqrt{\frac{A_s}{A_d}}\right) 100$$

According to anatomic drawings the myocardial wall is layered and the fibres are oriented in definite directions depending on layer and location (SOBOTTA & BECHER 1957; KATZ 1977). However it is very difficult to recognize these different layers in macroscopic sections of the heart (MCALPINE 1975). No functional difference exists between the different parts of the contractile left ventricular wall as it behaves quite as a single muscle.

The area reduction and the consequent increase in wall thickness are both reflected in the systolic reduction of the mean area of the myocardial wall. It is the area reduction which effects the reduction of the cavity volume. The mean area reduction could be used directly as an estimate of the systolic contraction.

In a geometric sense the mean fibre shortening

may be defined by relating it directly to the lengthwise and crosswise shortening of the mean area.

The mean diastolic area A_d may be reduced to a rectangle with the same area and with the length a and the width b . The mean systolic area may correspondingly be reduced to a rectangle with the area A_s with the length na and the width mb .

The average lengthwise shortening of the myocardial wall is less marked than the average transverse shortening and therefore $m < n$. The wall shortens both lengthwise and crosswise therefore both n and m are smaller than unity.

The length of any fibre which runs obliquely will during myocardial contraction shorten in an oblique direction. This shortening may be described by vector principles as occurring partly lengthwise partly crosswise. It may be regarded as contributing both to the overall lengthwise shortening and the overall crosswise shortening and the overall shortening in these two directions is described by the factors n and m .

The systolic fibre shortening in the longitudinal direction expressed as fraction of the corresponding diastolic fibre length equals $na/a = n$. The systolic fibre length in the transverse direction expressed as fraction of the corresponding diastolic fibre length equals $mb/b = m$.

The overall fibre shortening may be defined as the arithmetic mean of the lengthwise and the crosswise shortening. The fibre shortening expressed as a fraction of the diastolic fibre length thus equals

$$\frac{(1-n) + (1-m)}{2} = \left(1 - \frac{n+m}{2}\right)$$

Expressed in per cent of the diastolic fibre length this equals

$$\left(1 - \frac{n+m}{2}\right) 100$$

The expression actually used to calculate the fibre shortening was

$$\left(1 - \sqrt{\frac{A_s}{A_d}}\right) 100 \text{ per cent}$$

According to the statements mentioned $A = namb$ and $A_d = ab$. Therefore

$$\sqrt{\frac{A_s}{A_d}} = \sqrt{\frac{namb}{ab}} = \sqrt{nm}$$

In Fig 7 $\sqrt{nm}/(n+m)/2$ is shown for the different values of n at different values of As/Ad . The actual values for the systolic areas were from 0.57A_d and upwards in the control group and from 0.79A_d upwards in the IHSS group.

In the model calculation the systolic length of the long axis in a wall layer approximately corresponding to the mean area expressed as a fraction of the corresponding diastolic length had a smaller value than 0.9 in the end of systole in the control group. In the IHSS group this value was larger than in the control group.

Fig 7 shows that the effect of using the term $\sqrt{nm} (= \sqrt{As/Ad})$ instead of $(n+m)/2$ gives an underestimation of the systolic fibre length as a fraction of the diastolic fibre shortening. By the end of systole the calculated fibre shortening in the control group had an average value of 19.1 per cent and the overestimation in terms of fibre shortening was less than 1.25 per cent.

In the IHSS group the calculated fibre shortening by the end of systole had an average value of 9.8 per cent and the overestimation in this group was then less than 0.6 per cent in terms of fibre shortening.

In the early half of systole the overestimation for both groups is smaller than this but actually a little higher in the IHSS group than in the control group. This is because in this phase of systole the calculated area reduction is similar in the two groups but n has a higher value in the IHSS group.

\sqrt{nm} equals $(n+m)/2$ only when $n=m$ i.e. when the lengthwise and the crosswise shortening expressed as fractions of the diastolic values are equal. However the overestimation caused by using the one term for the other does not interfere with the general arguments presented in the following.

The calculations were performed on a Texas Instruments programmable pocket calculator TI 59 equipped with a thermic writer PC 100B.

Results

The cardiographic data which were used as input variables in the model evaluation of the fibre shortening for the two groups of patients appear in Table 3 as mean values, ranges and standard deviations. According to the description of the models only the diastolic length width relationship was used as input value in the IHSS model. In the normal model the specific length width relationship of the

Table 3

Left ventricular cardiographic data from the IHSS and control groups of patients presented as mean values, ranges and standard deviation. (Rather many decimals indicate that the values are intermediate results)

Left ventricular parameters	IHSS group	Control group
End-diastolic volume	116.0 ml	157.9 ml
Range	103-130	87-149
SD	11.1	29.6
Mid systolic volume	43.7 ml	101.4 ml
Range	42-49	61-122
SD	3.7	0.7
End systolic volume	17.3 ml	46.7 ml
Range	14-23	4-64
SD	4.0	13.7
Systolic ejection fraction	0.85	0.01
Range	0.82-0.88	0.63-0.99
SD	0.04	0.04
Ventricular length/ width relationship (L/W)		
End diastole	2.74	1.60
Range	1.94-4	1.42-0.9
SD	0.77	0.17
Mid systole		1.86
Range		1.47-2.1
SD		0.3
End systole		2.1
Range		1.6-6
Diastolic muscle thickness	2.06 cm	0.91 cm
Range	1.79-2.37	0.64-1.11
SD	0.24	0.16

particular systolic situation being analysed was always used as input value. For this reason there is an empty space in Table 3 for the IHSS group.

The average end-diastolic volumes are smaller in the IHSS group (the chance that the diastolic volumes come from the same population is less than 5 per cent assuming normal distribution i.e. $p < 0.05$). The mid systolic volume is clearly smaller in the IHSS patient group ($p < 0.005$). The end systolic volume is also smaller in the IHSS group ($p < 0.01$). The ejection fraction is clearly larger in the IHSS group ($p < 0.001$). The end-diastolic length width relationship is definitely larger in the IHSS group ($p < 0.0005$) and the diastolic free wall is thicker ($p < 0.0005$).

In Fig 8 the average length width relationship through the systolic period is shown for the

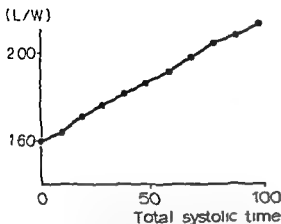


Fig 8 Left ventricular length divided by the calculated width (L/W) for the control group. Average values interpolated at every 10 per cent systolic time interval.

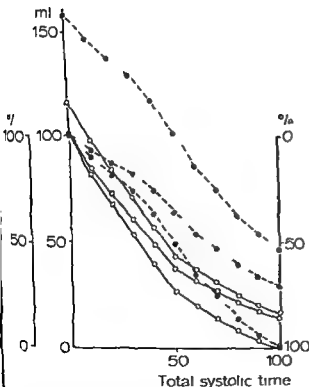


Fig 9 Left ventricular volumes interpolated at every 10 per cent systolic time interval, presented in 3 different ways for the two groups of patients. IHSS group (O). Control group (●). Upper curve in each group. Left ventricular volume in ml (inner left hand scale). Middle curve in each group. Left ventricular volume as per cent of EDV (outer left hand scale). Lower curve in each group. Percentage of stroke volume which has been ejected (right hand scale).

control group at every 10 per cent systolic interval. The width decreases relatively more than the length.

In Fig 9 the average ventricular volumes at every 10 per cent systolic interval are given in three different ways for the two groups of patients. In each group the upper curve represents the ventricular volume in ml (inner left hand scale), the middle curve the left ventricular volume in percentage of LDV (outer left hand scale), the lower curve the percentage of the stroke volume ejected (right hand scale). The figure illustrates lower ventricular volumes, higher EF and faster ejection of the stroke volume in the IHSS group.

The left ventricular data from the IHSS and the control group (Table 1) were used as input parameters in the model calculation of fibre shortening.

At mid systole the calculated fibre shortening among the IHSS patients had an average value of 7.1 per cent (range 5.7–8.5, SD 1.2), in the control group 8.1 per cent (range 4.7–11.5, SD 1.9). This difference is not significant.

At the end of systole the calculated average shortening among the IHSS patients had an average value of 9.8 per cent (range 8.8–11.4, SD 1.1), in the control group 19.1 per cent (range 15.7–24.7, SD 3.0). This difference is highly significant ($p < 0.0005$).

The mean patient values for every 10 per cent systolic time interval were used as input parameters in the models. In Fig 10 the fibre shortening is plotted together with the fraction of the stroke volume ejected at every systolic time interval for both groups. The calculated fibre shortening is similar for the two groups during the first half of systole; thereafter the fibre shortening lags more and more behind in the IHSS group. A certain degree of fibre shortening causes the ejection of a larger fraction of the stroke volume in the IHSS group than among the controls.

The height of the IHSS model cavity averaged 1.60 cm at half systolic time and 0.77 cm at the end of systole. The height of the normal model cavity (the diameter) averaged 4.23 cm at half systolic time and 3.13 cm at the end of systole. From the model analysis using the mean patient values as input, the cavity heights of the two models at every ten per cent systolic time interval appear in Fig 11. The rapidly decreasing height of the IHSS model cavity illustrates the slit-like form of the cavity towards the end of systole.

The influence on the calculated fibre shortening of the different input parameters was examined. They

Fibre shortening Stroke volume ejected

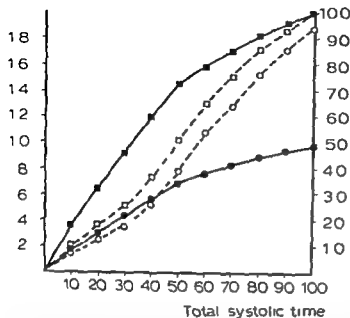


Fig. 10 Per cent fibre shortening (left hand scale) and percentage of the stroke volume ejected (right hand scale) for the 2 groups of patients using mean values as input values in the model calculations. Systolic period expressed as percentage of the full systolic period elapsed along the abscissa. Average fibre shortening is similar for the 2 groups of patients during the first half of the systole. From then on fibre shortening lags more and more behind in the IHSS group. Fibre shortening in the IHSS group (●) and the control group (○). Stroke volume ejection in the IHSS group (■) and in the control group (□).

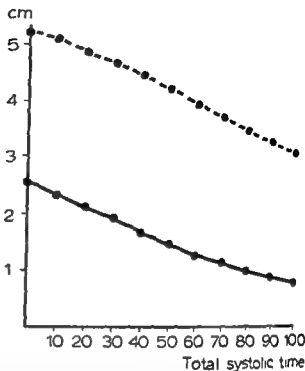


Fig. 11 Calculated height of the IHSS model cavity (—) and calculated diameter of the control model cavity (---) along the systolic period. Average patient values from each group were used as input parameters.

were varied one at a time keeping the others constant at average patient values. V_d and V_s were also varied in parallel keeping the same relationship between them as between the average EDV and ESV.

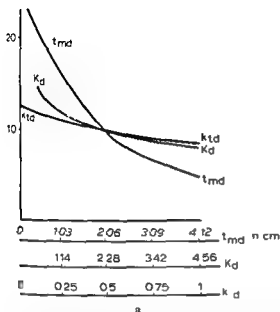
In the control model the diastolic and systolic length-width relationships were also varied in parallel. The relative magnitude of the two was then for each calculation kept constant as between the average end-diastolic and end systolic length-width relationship.

The influence of the different input parameters on the IHSS model calculation of fibre shortening appears in Fig. 12. Increasing the muscle thickness, increasing the length-width relationship of the diastolic left ventricular cavity, or increasing the left ventricular part of the septum relative to the free wall thickness, all decreased the calculated mean fibre shortening which was necessary to perform the average volume reduction from end-diastole to end systole in the IHSS group (Fig. 12). Obviously, to reduce the end systolic volume the contractile wall must contract more and to effect volume

reduction from a large end-diastolic volume to a fixed end systolic volume the wall must also contract more. Increasing the end systolic and the end-diastolic volume together, the systolic ejection fraction staying constant, also demands more mean fibre shortening, but not to the same degree as when only the end-diastolic volume is larger (Fig. 12b).

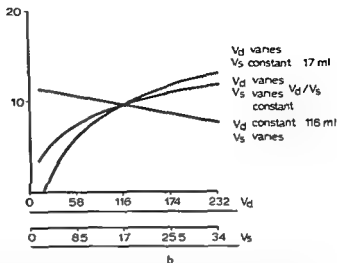
The corresponding influence of the input parameters in the normal model estimates of the fibre shortening is shown in Fig. 13. When the end diastolic volume increases or the end systolic volume decreases the estimation of fibre shortening as expected increases. When both the end-diastolic and the end systolic volume increases, but V_d/V_s remains constant, actually meaning that the ejection fraction remains constant, the estimate of fibre shortening changes very little, only increasing from 19 to 20.5 per cent when the diastolic volume increases from 100 to 300 ml (Fig. 13). With increasing myocardial thickness the necessary fibre shortening to perform the cavity volume reduction from the standard V_d to the standard V_s is reduced. The opposite is also true. With decreasing myo-

Percent mean fibre shortening



1) Input parameters in the IHSS model varied systematically. Average patient values are used for all parameters not shown (end systolic values are used). Effect on calculated fibre shortening shown. a) Effect of varying diastolic free wall thickness t_{md} and relative thickness k_d of the model septum (actual

Percent mean fibre shortening



diastolic thickness of the model septum k_d). Influence of varying the diastolic length width relationship k_d of the model cavity also shown. b) Effect of varying end diastolic volume V_d alone and together with end systolic volume V_s relationship between them kept constant. Effect of varying V_s alone also shown.

dial thickness the mean fibre shortening necessary to effect this volume reduction is increased (Fig. 13 b).

If a normal ventricle with diastolic volume of 179 ml and with average length width relationship of 1.5 dilates to a new end-diastolic volume of 300 ml keeping its length width relationship then according to the model the end-diastolic myocardial wall thickness is reduced from 0.91 cm to 0.65 cm. This heart must perform 18.9 per cent less left ventricular fibre shortening to obtain an ejection fraction of 0.704 when the end-diastolic volume is 157.9 ml but 22.9 per cent mean fibre shortening to reach the same systolic ejection fraction when the end-diastolic volume is 300 ml.

The curves in Figs 12 and 13 are extended into probable regions of the values for the different input parameters. Within reasonable limits of these parameters the calculated and systolic fibre shortening of the IHSS model is always much less than the fibre shortening of the normal model at the end of systole.

Discussion

The smaller EDV in the IHSS group has been discussed in Part II.

As long as the ejection fraction and therefore the relationship between V_d and V_s of the model is constant the estimation of fibre shortening is not much dependent upon a very exact measurement of the EDV used as input V_d of the model. This is apparent from Figs 12 b and 13 a. The relationship between V_d and V_s used as input variables is independent of the exact value of V_d because V_s was calculated from the measured V_d by using the relative volumes through the systolic period.

The measured wall thickness in the control group is somewhat smaller on the average than reported by DODGE (1971) for normal patients measured on the lateral wall. The wall thickness in the control group was also measured by a planimetric method (RACKLEY et coll. 1964) from the 30° RAO view and corrected for magnification. The average value was then 0.985 cm (range 0.80–1.23, SD 0.16) in the control group. These values were also used as input instead of the muscle thickness as measured in the 60° RPO view. At 50 per cent systolic time the calculated shortening had a mean value of 7.8 per cent (range 4.9–9.9, SD 1.3) and at the end of systole the calculated shortening was 18.5 per cent (range 16.1–20.9, SD 1.5). The latter mean values do not differ significantly from the mean values calculated

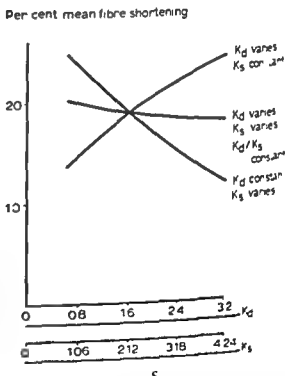
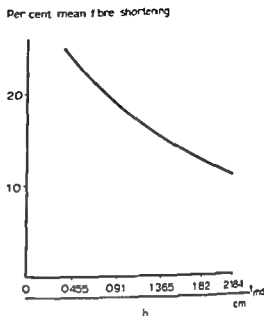
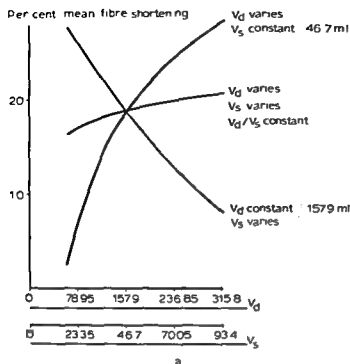


Fig. 13 Input parameters in the control model varied systematically. Average patient input values are used for all parameters not varied (end systolic values are used). Effect on calculated fibre shortening shown: a) End-diastolic volume and end systolic volume varied alone and together. In the latter case the relationship between them and thus the ejection fraction kept constant; b) Diastolic wall thickness varied; c) Diastolic length-width relationship K_d varied alone and together with the corresponding end systolic value K_s . Relationship between the 2 (K_d/K_s) kept constant, K_s also varied alone.

when the myocardial wall thickness as measured on the 60° RPO film was used (8.1 and 19.1 per cent respectively).

The pulse frequency was different in the two groups ($p < 0.01$). The relationship which has been shown between cavity form, fibre shortening and expulsion of the stroke volume is present nevertheless. The calculations of the fibre shortening are

strictly geometric and not influenced by the heart rate. The relationships shown are present but other interrelated relationships are present as well as between heart rate, stroke volume and cardiac output and between heart rate, EDV, ESV and the inotropy of the heart. A most complex relationship (H. F. K. et al. 1978).

The applied geometric models are simplifications

both for the normal left ventricle and for the IHSS left ventricle but they serve to illustrate essential differences between the two

The flat diastolic left ventricular wall of the septum in the IHSS model is a geometric simplification of the catenoid like surface, convex longitudinally and concave transversely. Longitudinal sections of the IHSS septum show that the longitudinal concavity causes a larger bulging towards the cavity than the transverse concavity curves away from the cavity (FARRER BROWN 1977 HUTCHINS & BLACKLEY). The IHSS left ventricular cavity is long relative to the width and the longitudinal curvature does not seem less marked than the transverse per length unit. The design of the model septal surface as a flat plane seems an acceptable approximation of the overall bulging towards the left ventricular cavity when the transverse section is designed as half a circle

The increase in thickness of the model septum averaged about 40 per cent in the IHSS group during full systolic contraction. However the model septum was only half as thick as the model free wall in diastole. In the actual heart with IHSS the interventricular septum is at least 1.3 times as thick as the free wall (EPSTEIN et coll 1974 MARON et coll 1977 REDWOOD et coll 1974). The effect of the catenoid surface which has no net pressure across its wall is most probably that the greater part of the total septal thickening occurs towards the left ventricular cavity. If at least 10/13 of the septal thickening occurs in this direction then a layer of the septum at least as thick as the free wall participates in the narrowing of the left ventricular cavity ($1.3 \times 10/13 = 1$).

The increase in thickness of a septal layer at least as thick as the free wall towards the left ventricular cavity is represented in the model by a more than twice as large systolic increase in septal thickness of the septum less than half as thick. The 40 per cent systolic increase in thickness of the model septum represents an overall increase in thickness of the patient interventricular septum of 20 per cent or less. This is in agreement with echographic measurements (COHEN et coll).

The angiographically observed increase in thickness are avoided by only measuring the diastolic thickness. This is considerably more marked than according to the calculations of the model. This may in part be explained by encroachment of the papillary muscle and the trabeculae during late systole. These

possible mistakes in the systolic increase in thickness are avoided by only measuring the diastolic thickness and thereafter calculating the systolic thickness according to the principles of even wall thickness and constant myocardial volume (HUGEN HOLTZ et coll 1969).

The myocardial wall seems to have a somewhat uneven thickness (MCALPINE). The actual systolic increase in wall thickness may be unevenly distributed. The left ventricular myocardial mass in the control group was according to the model 162 g on the average (range 103–213 SD 35 myocardial density 1.05 BARDEEN 1918). These estimates of the myocardial mass in the control group lie within an acceptable range (BLACKLEY et coll) even though the heart has an uneven wall thickness.

The calculated average end systolic fibre shortening in the control group was 19.1 per cent. In vitro stimulation of cat papillary muscle with an isometric myograph showed increasing tension from 70 to 100 per cent of an optimum length whereafter the tension decreased (the optimum muscle length had a resting sarcomere length of 2.18 measured after glutaraldehyde fixation SONNENBLICK & SKELTON 1974). The calculated estimates of fibre shortening are thus within an acceptable physiologic range even though the actual systolic increase in thickness of the heart wall may be unevenly distributed.

During systole the posterolateral wall narrows the ventricular cavity making it more and more slit like. As shown the free wall fibre shortening is very effective in expelling the stroke volume. The work per unit fibre shortening is increased. The consequence is work hypertrophy of the free wall.

The narrowing of the ventricular cavity during the late part of systole is marked in the apical and middle parts of the cavity. The posterior and septal walls actually meet except along an axial small part of the cavity. This open part is caused by the transverse concavity. In the other parts in which septal and posterior walls meet significant further shortening of the posterior wall is impossible. Therefore the apical and middle parts of the posterior wall perform essentially isometric contraction during the latter part of systole with hypertrophy as a consequence.

The basal part of the ventricular cavity near the valvar apparatus is deeper than the middle and apical parts. The posterior wall therefore runs obliquely from the valvar apparatus to the more shallow middle part relative to the septal plane. During con-

traction the basal part contracts more concentrically because the contractile part of the circumference is larger in this part of the cavity. Thus the basal part of the posterior wall does not move actively in the anterior direction to the same degree as the middle and apical parts. Consequently it does not perform late systolic isometric contraction: this stimulus to work hypertrophy is thus absent.

Towards the middle third of the cavity the most basal part of the posterior wall is transitional in this respect. It encroaches upon the septum definitely more than the part attached to the valvar apparatus. The most basal part of the posterior wall also moves anteriorly towards the membranous part of the septum, reflected in a late systolic oval shape of the mitral ring. But it does not move anteriorly as fast as the middle part because of a larger circumference with a more concentric contraction. The effect of this is that during the first half of systole the posterior wall is increasingly tilted relative to the septal plane. During the latter part of systole, as the most basal part continues its contraction, this tilting is reduced.

The overall systolic fibre shortening of the most basal part therefore lies more within a normal range. The tilting causes the speed of the systolic contraction to appear increased at echography during the first part of the systole, and the reduction of the tilting during the latter part produces the echographic impression of the systolic thickness reaching a plateau, as described by COHEN *et coll.* They found a total systolic thickening within the normal range. However, the measured echographic velocity of this thickening was increased during the first half of systole, then a plateau was reached. No conflict therefore exists between their observations and the present ones, but the evaluation of their data is different.

IHSS also exists in a non-obstructive form (EPSTEIN *et coll.*). The basal part of the left ventricular posterior wall does not have the obstructive stimulus to work hypertrophy either in this variant of the disease. This explains why the posterior wall hypertrophy in these cases is uneven: the most basal part not being hypertrophic. ROBERTS (EPSTEIN *et coll.*) states that an unusual type of distribution of myocardial thickness, however, is found in patients with the nonobstructive form of the disease. In these patients, the portion of the left ventricular free wall directly behind the posterior mitral leaflet always is of normal thickness (confirming the echo-

cardiographic findings) even when major portions of the remainder of the left ventricular free wall may be thickened.

The microstructural abnormalities of the hypertrophic interventricular septum are not specific, but occur also in the free left ventricular wall in IHSS as well as in other conditions with isometric myocardial contraction (BULKLEY *et coll.* 1977; HUTCHINS & BULKLEY 1978; WIGLE & SILVER 1978).

In the free wall of the IHSS left ventricle myocardial anatomic abnormalities characteristic of isometric contraction are observed in non-obstructive cases of the disease: in cases with obstruction the myocardium is more normal (MARON *et coll.* 1974). The reason is probably that when subaortic obstruction occurs, the isometric contraction of the free wall is slowed down considerably in the latter part of systole. The obstruction acts like a buffer, damping the abrupt isometric contraction which would otherwise occur, and which actually occurs when the free wall encroaches upon the septum in non-obstructive cases.

According to the calculations and the previous argumentation, the free left ventricular wall in IHSS has a normal velocity of the myocardial fibre shortening during the first part of systole relative to the systolic time span. During the latter part of the systolic period, however, the free wall performs an essentially isometric contraction, except for its most basal part. A certain degree of fibre shortening causes the expulsion of a larger part of the stroke volume than normally. Work hypertrophy of the free wall ensues, both for this reason and because of isometric contraction and subaortic stenosis.

The fact that a smaller degree of free wall fibre shortening causes the expulsion of a larger fraction of the stroke volume than normally is based on the ejection fraction is larger than normally, is based on both functional and anatomic abnormalities which may be summarized as follows: (1) a non-bending septum with no persisting concavity away from the ventricular cavity, and with a markedly reduced shortening, acting as a suspender for the rest of the wall; (2) some increase in the septal thickness, reducing the ventricular cavity; (3) myocardial hypertrophy of the non-septal wall; (4) a long ventricular cavity relative to the width; (5) a shallow left ventricular cavity; and (6) a somewhat smaller EDV than in normal patients.

Conclusion. During the first part of the systolic period, the myocardial fibres of the free left ventricular

cular wall in IHSS shorten with the same speed as normal left ventricular fibres relative to the systolic time span. The myocardial contraction causes however the expulsion of a larger fraction of the stroke volume per unit fibre shortening even with the high ejection fraction of IHSS. The reasons for this are attributed to the geometric geometry of the left ventricle in IHSS.

During the latter part of the systolic period the IHSS left ventricular free wall except the part close to the valvar apparatus performs essentially an isometric contraction.

SUMMARY

Left ventricular cineangiographic data from 4 patients with idiopathic hypertrophic subaortic stenosis (IHSS) and 10 control patients have been analysed by means of geometric models. The myocardial fibre shortening of the free left ventricular wall in IHSS has been compared with the fibre shortening of the left ventricular wall in the control group. During the first half of systole the fibre shortening occurs equally fast in the two groups but during the second half it lags clearly behind in the IHSS group. The stroke volume is ejected much faster in the IHSS group and the ejection fraction is much higher. This is caused by several factors related to both functional and anatomic derangements of the left ventricle and the interventricular septum: (1) A hypertrophic septum contracting isometrically with no persisting concavity away from the left ventricular cavity acting as a suspender and the posterior wall encroaching upon the septum in a kit like manner. (2) Some increase in septal thickness narrowing the ventricular cavity. (3) A hypertrophic non-septal ventricular wall. (4) A long ventricular cavity relative to the width. (5) A shallow left ventricular cavity. (6) A somewhat smaller EDV than normal.

ACKNOWLEDGEMENTS

Professor Jan Gothlin gave valuable assistance both during discussions and in the preparation of the manuscript. Associate Professor Jon Lekven, Dig Rangesnes, consultant mathematician, Richard Enstgate, physicist, and Lars Høiem and Carl Mørth, consultant radiologists, all contributed in various ways during the course of the work towards the final production of the manuscript. Materials for the investigation were supplied by the Dept. of Clinical Physiology, Haukeland University Hospital. Mrs G. E. Johansen and other members of the photographic department of the University of Bergen, Haukeland Hospital, section, placed their technical skill at the author's disposal.

REFERENCES

- BARDEEN C. R. Determination of the size of the heart by means of the x rays. *Amer J Anat* 23 (1918) 432.
- BRONSHTEIN I. N. and SEMENDYAYEV K. A.: *Geometry. In A guide book to mathematics* p. 195. Verlag Harri Deutsch, Zurich 1973.
- BULKLEY B. H., WEISFELD M. L. and HUTCHINS G. M.: Isometric cardiac contraction. A possible cause of the disorganized myocardial pattern of idiopathic hypertrophic subaortic stenosis. *New Engl J Med* 296 (1977) 135.
- CATE T. F. J., HUGENHOLTZ P. G. and ROELANDT J.: Ultrasound study of dynamic behaviour of left ventricle in genetic asymmetric septal hypertrophy. *Brit Heart J* 39 (1977) 627.
- COHEN M. V., COOPERMAN L. B. and ROSENBLUM R.: Regional myocardial function in idiopathic hypertrophic subaortic stenosis. An echocardiographic study. *Circulation* 52 (1975) 842.
- DODGE H. T.: Determination of left ventricular volume and mass. *Radiol Clin N Amer* 9 (1971) 459.
- EPSTEIN S. E., HENRY W. L., CLARK C. E., ROBERTS W. C., MARON B. J., FERRANS V. J., REDWOOD D. R. and MORROW A. G.: Asymmetric septal hypertrophy. NIH conference. *Ann Intern Med* 81 (1974) 640.
- FORSYTHE A. I., KEENAN T. A., ORGANICK E. I. and STENBERG W.: *Numerical applications in Computer science. A first course* p. 617. John Wiley & Sons, New York 1974.
- FARRER BROWN G.: Primary cardiomyopathies. In: A colour atlas of cardiac pathology p. 91. Wolfe Medical Publications, London 1977.
- GOTSMAN M. S. and LEWIS M. S.: Left ventricular volumes and compliance in hypertrophic cardiomyopathy. *Chest* 66 (1974) 498.
- HERVANDEZ M. E., GREENFIELD JR J. C. and McCALL M. W.: Pressure flow studies in hypertrophic subaortic stenosis. *J Clin Invest* 43 (1964) 401.
- HUGENHOLTZ P. G., KAPLAN E. and HULL E.: Determination of left ventricular wall thickness by angiography. *Amer Heart J* 78 (1969) 513.
- HUTCHINS G. M. and BULKLEY M. H.: Catenoid shape of the interventricular septum. Possible cause of idiopathic hypertrophic subaortic stenosis. *Circulation* 58 (1978) 39.
- ILJEBEEK A., LEKVEN J. and KILL G.: Cardiac performance: independence of adrenergic ionotropic and chronotropic effects. *Amer J Physiol* 234 (1978) 525.
- KATZ A. M.: Structure and function of cardiac muscle. In: *Physiology of the heart* p. 1. Raven Press, New York 1977.
- KYAM G.: Idiopathic hypertrophic subaortic stenosis I. Interventricular septum during the systolic contraction. A. The shortening of the muscular interventricular septum. B. Analysis of the protruding non-bulging muscular interventricular septum. *Acta radiol Diagn* 1 (1980) 53.
- Idiopathic hypertrophic subaortic stenosis II. T.

- shallow left ventricular cavity. *Acta radiol. Diagnosis* 21 (1980) 165
- MARON B J, FERRANS V J, HENRY W L, CLARK C E, REDWOOD D R, ROBERTS W C, MORROW A G and EPSTEIN S E. Difference in distribution of myocardial abnormalities in patients with obstructive and nonobstructive asymmetric septal hypertrophy (ASH). Light and electron microscopic findings. *Circulation* 50 (1974) 436
- HENRY W L, ROBERTS W C and EPSTEIN S E. Comparison of echocardiographic and necropsy measurements of ventricular wall thickness in patients with and without disproportionate septal thickening. *Circulation* 55 (1977) 341
- MCALPINE W A. The normal heart. In: *Heart and coronary arteries. An anatomical atlas for clinical diagnosis: radiological investigation and surgical treatment* p 9. Springer Verlag, Berlin Heidelberg New York 1975
- RACKLEY C E, DODGE H T, COBLE Y D and HAY R E. A method for determining left ventricular mass in man. *Circulation* 29 (1964) 666
- REDWOOD D R, SCHERER J L and EPSTEIN S F. Bi-ventricular cineangiography in the evaluation of patients with asymmetric septal hypertrophy. *Circulation* 49 (1974) 116
- ROSSIGN R M, GOODMAN D J, INCHAM R F and POIR R L. Ventricular systolic septal thickening and excursion in idiopathic hypertrophic subaortic stenosis. *New Engl J Med* 291 (1974) 1317
- SHAH P M. Echocardiography in the diagnosis of hypertrophic obstructive cardiomyopathy. *Amer J Med* 62 (1977) 830
- SOROTTA J and BECHER H. Herzmuskulatur. In: *Atlas der deskriptiven Anatomie des Menschen* 7 Teil p 202. Urban & Schwarzenberg, München, Berlin 1957
- SONNENBLICK E H and SKILLTON C L. Reconsideration of the ultrastructural basis of cardiac length-tension relations. *Circulat Res* 35 (1974) 517
- WOLFE E D and SILVER M D. Myocardial fiber diameter and ventricular septal hypertrophy in asymmetrical hypertrophy of the heart. *Circulation* 58 (1978) 378

ULTRASOUND EXAMINATION OF LESIONS IN THE THORAX

L. FORSBERG and U. TYLÉN

Various echogenic qualities make possible a differentiation between cystic and solid lesions by ultrasound. In the thorax the normally aerated lung parenchyma reflects ultrasound preventing examination of intrapulmonary lesions whereas lesions in contact with the thoracic wall are within reach. Therefore ultrasound may be used to differentiate lesions possible to drain from organized effusions and solid tumor.

Material and Methods

Thirty five patients were examined once or several times during one year. A grey scale B scan unit with 3.5 and 5 MHz transducers was used. The patients were examined in supine and sitting positions. First a longitudinal scan of the liver was made with the patient supine in order to get a proper setting of the ultrasound apparatus. The subphrenic area was then examined. When the gallbladder and the intrahepatic vessels were demonstrated without internal echoes with good penetration of the liver the patient was moved to a rotatable chair where longitudinal scans were taken at 2 cm intervals of the dorsal and lateral parts of the hemithorax of interest. Ventrally located lesions were more often examined with transverse scans. When the diaphragm could be demonstrated its movements were measured with a longitudinal scan in maximum inspiration and expiration over the mid-dorsal area with the patient in sitting position. The two scans were exposed on the same film to facilitate the measurement (Fig. 1). The margins of an effusion were marked on the skin of the patient its depth measured (Fig. 2) and the deepest spot indicated.

Results

Because of failure to drain fluid at repeat thoracocentesis 28 patients were referred for examination. On films exposed in the lateral decubitus position no free fluid had been demonstrated. Echo free encapsulated effusion was diagnosed in 25 of these cases (Fig. 2) while in 3 multiple echoes within the lesion indicated organization of the effusion. Successful puncture confirmed the findings in those patients with lesions without internal echoes. In another 2 patients pus had been obtained at previous punctures and ultrasound demonstrated organized exudate (Fig. 3). In one patient no aeration of the right hemithorax was found on chest films. At the ultrasound examination a large amount of fluid was found. After thoracocentesis a small cell carcinoma was revealed. A malignant lesion was also confirmed in a patient with pericardial effusion (Fig. 4). Three patients were referred due to a suggestion of a pericardial cyst which was confirmed in 2 (Fig. 5). In the third case a necrotic tumor was demonstrated.

Discussion

Ultrasound examination of the thorax during the 1960s and the beginning of the 1970s was performed with A mode equipment measuring pleural effusion and pleural thickening (VIKKERI 1970, GORDON 1973, GRZYMSKI *et coll.* 1976). When B mode and grey scale were available the examinations became more morphologic giving better detail (TAYLOR *et coll.* 1973). However the use of the method is still limited due to the reflexion in the aerated lung.

Ultrasound examination of the thorax may be per-



Fig 1 Longitudinal scan of the dorsal part of the right hemithorax of a patient with pleural effusion in maximum inspiration and expiration showing diaphragmatic movements



Fig 2 Encapsulated pleural effusion with em marking Pleur effusion (E) and rib (R)



Fig 3 Organized empyema containing multiple echoes



Fig 4 Areas of organization within effusion. Pun ture yielded only small amounts of hemorrhagic fluid. Cytologic exam revealed pericardial carcinoma. Heart (H) pericardial effusion (E)

formed in various ways. BOUTIN *et coll* (1976) and HIRSCH *et coll* (1978) used only transverse scans while DOUST *et coll* (1975), RAVIN (1977) and LAING & FILLY (1978) used only longitudinal scans. POIRIER *et coll* (1975), LANDAY & HARLESS (1977) and CUNNINGHAM (1978) took advantage of both transverse and longitudinal scans. Transverse scans seem to be of less value in lesions located dorsally and laterally than in ventrally located lesions due to enhanced rib artefacts. It is recommended that both modalities be used to obtain optimum information.

The very sensitive modern B scanners are sometimes hard to adjust to avoid creation of false echoes or erasure of the true ones. LAING & FILLY used

the kidney for adjusting the setting while at this department the liver was used. This was considered practical as examination of the liver and the subphrenic area is necessary to avoid missing lesions which may be connected with pleural disease. Abscesses, intrahepatic or subphrenic, are difficult to diagnose by other means. Computer tomography has to some extent improved the possibilities for diagnosing such lesions but ultrasound is a faster and also less expensive method. It is a well known fact that gas in the stomach often prevents examination of the left subphrenic area and diaphragm. The thorax on the left side must be examined from the back. The normally aerated lung covers the diaphragm



a

Fig 5 Rounded tumor in the heart II or ante on chest radio-
graphy. Ultrasound examination showed a cystic lesion con-



b

firming the diagnosis pericardial cyst (C) a) Longitudinal scan
b) Transverse scan of the lesion

completely and only artefacts are seen on the screen. When the diaphragm can be demonstrated from the dorsal aspect of the thorax, a pathologic condition must exist. COSGROVE *et coll.* (1978) have pointed out the interesting phenomenon that 'ghost lesions' may be observed in the lung region due to changes in the liver because of the reflecting ability of the right hemidiaphragm when covered with normal lung tissue. Such lesions do not appear when the abnormalities are present on the thoracic side of the diaphragm.

Ultrasound is of great value in the treatment of patients with encapsulated fluid. The method has been particularly valuable in those patients in whom multiple unsuccessful attempts at puncture of a possibly fluid-filled cavity have been made. The method of drawing the margins of the lesion with an extra sign at the deepest place often seems to be of more value than just marking the best spot for puncture (HIRSCH *et coll.*).

Relatively new intrathoracic hematomas may have the same appearance as encapsulated fluid (LAING & FILLY) but no traumatic lesions were encountered in the present material.

The differentiation between a solid tumor and a cystic lesion may be facilitated by ultrasound in some cases. The demonstration of a pericardial cyst is easy and accurate and puncture may therefore be omitted. Moreover, the method may be used as a guide in fine needle biopsy of solid lesions adherent to the thoracic wall.

SUMMARY

Thirty-five patients with intrathoracic lesions were examined once or several times during one year with B-scan grey scale ultrasound. The difference between encapsulated fluid, organized exudate or empyema and solid tumor is discussed, as is the procedure of the examination and the possibility of using ultrasound for diagnostic punctures.

REFERENCES

- BOUTIN B, FARISSE P, AIMINO R, ROSELLOR E, PIETRI H. Interet de l'echotomographie en pathologie pleuropulmonaire. *Poumon* 32 (1976) 9.
- COSGROVE D O, GARBUIT P and HILL C H. Echoes across the diaphragm. *Ultrasound in Med Biol* 3 (1978) 385.
- CLANNINGHAM J J. Gray scale echography of the lung and pleural space. *Cancer* 41 (1978) 1329.
- DOLST B D, BAUM J K, MAKALADIN F and DOUST V L. Ultrasonic evaluation of pleural opacities. *Radiology* 114 (1975) 135.
- GORDON D J. Ultrasonic diagnosis of disease of the lungs and pleura. *Proceedings of the British Medical Ultrasonics Group*. *Brit J Radiol* 46 (1973) 567.
- GRYNSKI J, KRAKOWKA P and LYPACEWICZ G. The diagnosis of pleural effusion by ultrasonic and radiologic techniques. *Chest* 70 (1976) 33.
- HIRSCH J H, CARTER S J, CHIKOS P M and COLACURCIO C. Ultrasonic evaluation of radiographic opacities of the chest. *Amer J Roentgenol* 130 (1978) 1153.
- LAING F C and FILLY M A. Problems in the application of ultrasonography for the evaluation of pleural opacities. *Radiology* 126 (1978) 211.
- LANDAY M and HARTLESS W. Ultrasonic differentiation of right pleural effusion from subphrenic fluid on lon-

- itudinal scans of the right upper quadrant. Importance of recognizing the diaphragm. *Radiology* 123 (1977) 155.
- POIRIER R, ROSELLO R, KLEISBAUER J P et LAVAL P. Interet diagnostique de l'echotomographie dans les affections thoraciques peripheriques. *Rev franç Mal resp* 3 (1975) 263.
- RAVIN C E. Thoracocentesis of loculated pleural effusions using grey scale ultrasonic guidance. *Chest* 71 (1977) 666.
- TAYLOR K J W, CARPENTER B A and MCCREADY V R. Grey scale echography in the diagnosis of intrathoracic disease. *J clin Ultrasound* 1 (1973) 84.
- VIIKARI M. Ultrasound examination of pleural plaques. Experimental, pathological and clinical studies. *Acta radiol* (1970) Suppl No 301.

FROM THE DEPARTMENTS OF DIAGNOSTIC RADIOLOGY (DIRECTOR PROF P EDHOLM) OTOLARYNGOLOGY
 DIRECTOR PROF G ASCHAN) AND PATHOLOGY I (DIRECTOR PROF O GRÖNTÖFT) UNIVERSITY HOSPITAL
 REGIONSJUKHUSET S 58185 LINKÖPING SWEDEN

ANGIOGRAPHY IN LARYNGEAL CARCINOMA

H SÖKJER and J OLOFSSON

The usual examinations of patients with laryngeal carcinoma are mirror laryngoscopy, palpation, otolaryngoscopy and radiography including conventional films, tomography and laryngography. These examinations can usually be relied upon to give adequate information on the superficial extension of the tumour (OLOFSSON & SÖKJER 1977, 1979). Vocal cord fixation and radiologic evidence of cartilage involvement are indicative of deep tumour invasion. However, these abnormalities do not give precise information on the depth of invasion which is vital to know for the correct selection of patients for partial surgery with preservation of laryngeal function. Thus, other diagnostic methods are needed.

The arterial anatomy in normal and carcinoma laryngeal specimens was investigated (SÖKJER & OLOFSSON 1979) in order to elucidate whether delineation of laryngeal carcinoma could be improved by the application of angiography. The normal arterial anatomy of the larynx was found to be fairly constant. Arterial abnormalities in the carcinoma specimens corresponded to microscopic evidence of tumour invasion of the pre epiglottic space, lateral spread to the thyroid cartilage and spread of the tumour outside the larynx by penetrating the cricothyroid membrane. Information concerning spread to these regions is important for decision on the surgical management.

Angiography has now been applied in a clinical series in order to assess whether this examination could be of clinical value. No such report appears to have been published previously.

The larynx is supplied from the superior and inferior laryngeal arteries (RAUBER & KOPSCH 1955)

the superior laryngeal artery which is the main laryngeal artery usually originates from the superior thyroid artery although it may originate directly from the external carotid. This has been found to be the case in 13.4 per cent of Europeans and in 4.2 per cent of Japanese (ADACHI 1928). The cricothyroid artery, another branch of the superior thyroid artery, anastomoses with the superior laryngeal artery lateral to or through the cricothyroid membrane. The inferior laryngeal artery, a branch of the inferior thyroid artery, accompanies the recurrent laryngeal nerve to enter the lower posterior part of the larynx.

The superior laryngeal artery usually enters the larynx through the thyrohyoid membrane above the posterior half of the thyroid cartilage (ADACHI) but it may enter through the thyroid foramen in the upper posterior part of the thyroid cartilage. This occurred in about 4 per cent of a French material (TERRACOL & GUERRIER 1951) and in about 20 per cent of two Japanese series (ADACHI OKI 1958).

Within the larynx the superior laryngeal artery runs immediately medial to the thyroid cartilage and gives origin to 5 main branches (SÖKJER & OLOFSSON Fig 1). An ascending branch supplies the epiglottis and the vallecula and also gives off branches to the pre epiglottic space; one of these vessels often originates directly from the superior laryngeal artery. A dorsal branch runs beneath the mucosa of the anterior part of the piriform sinus to anastomose with the medial division of the inferior laryngeal artery in the postcricoid region. A ventral branch runs deep to the false vocal cord and larynx

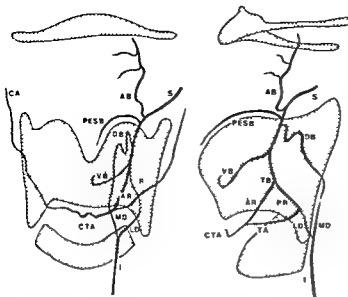


Fig 1 Normal arterial anatomy of the larynx a) A p view b) Lateral view AB=ascending branch AR=anterior ramus CA=cricothyroid artery CTA=anterior cricothyroid arcade DB=dorsal branch I=inferior laryngeal artery LD=lateral division MD=medial division PESB=proximal branch to the pre-epiglottic space PR=posterior ramus S=superior laryngeal artery TA=transverse arcade TB=terminal bifurcation VB=ventral branch

geal ventricle in an anterior direction to terminate above the anterior commissure. The superior laryngeal artery ends in a terminal bifurcation where it divides into an anterior and a posterior ramus. The level of the terminal bifurcation varies from about 5 mm above the superior surface of the vocal cord to about 5 mm below. The anterior ramus runs lateral to the thyroarytenoid muscle in an antero-caudal direction towards the anterior part of the cricothyroid space. It leaves the larynx lateral to the cricothyroid membrane to anastomose with the cricothyroid artery and with the arteries of the opposite side via the anterior cricothyroid arcade. The posterior ramus runs lateral to the lateral cricothyroid muscle to anastomose with the lateral division of the inferior laryngeal artery. The anterior and posterior rami may be linked by a transverse arcade.

Material and Methods

Over a two-year period (1976 to 1978) laryngectomy was performed in 11 male patients with laryngeal carcinoma (It was contemplated in one other but not actually carried out). Angiography was performed in 8 of these patients and these constituted

the present series. The other 3 patients were elderly men with recurrent carcinoma whose treatment would probably not have been influenced by the outcome of angiography.

Five cases had primary glottic, one case transglottic carcinoma—probably arising in the supra-glottic region—and 2 cases primary epiglottic carcinoma. In 2 cases angiography was performed after radiation therapy on detection of a recurrence whereas in the other 6 cases angiography was carried out before any kind of treatment had been given. In one case the angiography was performed 2 years before laryngectomy whereas in the other 7 patients it was performed immediately before operation or preoperative irradiation.

The following methods of examination were used: mirror laryngoscopy, palpation and radiography comprising conventional films, tomography and laryngography. After the radiologic examination direct laryngoscopy was carried out, the operating microscope and 90° optical instruments were used (OLFSSON & SÖKJER).

Angiography was performed on the side that was the more extensively involved by the tumour. The common carotid artery was punctured, a Hanase catheter with OD 1.57 mm was inserted so that it entered the superior thyroid artery. The tip of the catheter had been shaped as a semicircle about 2 cm in diameter. In the first five magnified lateral views were obtained using 0.3 mm focus. The injection of contrast medium elicited swallowing with movement of the larynx even when metrazamide was used. This necessitated general anaesthesia which was used only in the three last patients. The procedure applied in these patients which was considered to be superior was as follows. To enable good subtraction to be obtained the films were exposed during apnoea. Propofol Cerebral was used as contrast medium and 3 to 9 ml was injected at a rate of 3 ml/s. Three series of films were exposed: an ordinary r.p. a lateral stereographic projection using a 1.0 mm focus and a 12.1 grid with a FFD of 90 cm in lateral view using a 0.1 mm focus and 2.1 magnification. The exposure rates were 2 per s for 4 s and then 1 per s for 4 seconds. Kodak G film and X-omatic screens were used.

Angiography was performed in 5 of the 8 laryngectomy specimens.

All the laryngectomy specimens were who were organ serial sectioned and the angiographic and microscopic findings were compared.



a



b



c



d

Fig. 1. Glottic carcinoma with sub- and supraglottic extension on the right side. fixation of the vocal cord and a metastatic submandibular node. Preoperative radiation therapy was followed by wide field laryngectomy in which the right lobe of the thyroid gland was removed and a right neck dissection. a) Conventional film lateral view. Destruction of the anterior part of the thyroid cartilage. b) Laryngography p.p. view. Tumour of the right

hemilarynx. c) Angiography of the right superior thyroid artery lateral and a.p. views (subtraction). Superior laryngeal artery (→). Anterior ramus occluded at the terminal bifurcation (→→). Ventral branch not demonstrated. Anterior cricothyroid arcade (---). d) placed anteriorly. Pooling in a node with metastasis.



Fig 3 Same case as Fig 2. Coronal sections a) through the midpart of the vocal cord and b) the anterior commissure. Arrows indicate the ulcerated tumour of the right hemilarynx invading the thyroarytenoid muscle (a) and the anterior part of the thyroid cartilage with spread outside the larynx through the cricothyroid membrane (b). c) A p. angiography of the laryngeal ectomy specimen. Both superior laryngeal arteries demonstrated

Results

In one case the tumour was superficial and the angiographic appearances were normal.

In another case the angiographic appearance was considered normal and no cartilage invasion was observed on the conventional films. Originally combined treatment was planned but because the tumour regressed rapidly during irradiation and neither the routine examinations nor the angiography indicated deep tumour invasion it was decided to give a full course (66 Gy). When two years later recurrence was observed a lateral low voltage conventional film showed destruction of the anterior thyroid cartilage. The patient's general condition was too poor to allow a total laryngectomy. No angiography was performed. Partial vertical laryngectomy using an anterior commissure technique was carried out (SOM & SILVER 1968). At microscopy invasion of the cartilage was found but no spread beyond the larynx.

In 4 cases microscopic evidence of deep lateral invasion existed. Corresponding angiographic abnormalities were present in 3 of these (Figs 2-5) and possibly also in the fourth. In one of these cases the angiography was also indicative of tumour penetration of the cricothyroid membrane and also of a metastasis in a lymph node. In another case (Fig 5) the angiographic changes were subtle but definitely pathologic. In one case the films were suggestive of

by injection into the right one. Branches distal to the origin of the dorsal branch (→) on the right side not demonstrated. C=cricoid cartilage. E=epiglottis. T=thyroid cartilage.

Comment: Two metastatic nodes were found in the neck specimen. One normal parathyroid gland was present at the lower pole of the thyroid lobe.

occlusion of the anterior ramus which however could be a normal variant—the anterior ramus being replaced by the transverse arcade (SÖNJER & OLOFSSON Fig 1).

In 2 cases with epiglottic carcinoma the extensive invasion of the pre epiglottic space detected at microscopy was not demonstrated at the preoperative angiography in one of these neither at the angiography of the laryngectomy specimen.

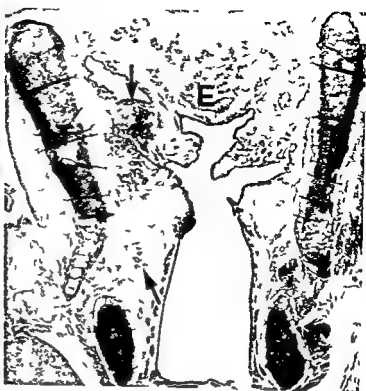
Both the normal and the pathologic soft tissues of the larynx displayed more or less marked accumulation of contrast medium in the capillary phase. In one case a defect probably represented the tumour (Fig 4). Otherwise the accumulation of contrast medium did not afford conclusive evidence of deep tumour infiltration. Slight neovascularity and early venous draining were found in one case.

No complications ascribable to the angiography were encountered.

Fig 4 Transglottic, probably primary supraglottic carcinoma on the right side of the larynx. Vocal cord fixed. No evidence of cartilage invasion on the conventional films. a) Laryngography p.a. view. Arrows indicate tumour. b) Coronal section through the anterior third of the vocal cords. Arrows indicate the tumour which has a transglottic distribution in along the thyroarytenoid muscle. No invasion of cartilage. c) d) Angiography of the right superior thyroid artery. Lateral (c) and coronal (d) views. The ventral branch is almost occluded (c) and the anterior ramus (→) is partly filled via the cricothyroid artery (c). Defect in the capillary pool (→ in d). C=cricoid cartilage. E=epiglottis. T=thyroid cartilage.



a



b



c



d

Fig 4 (For legend see opposite page)

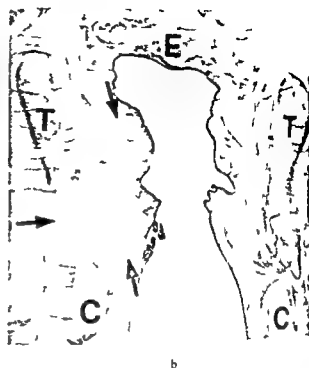


Fig 5 Glottic sub- and supraglottic carcinoma on the right side with fixation of vocal cord and cartilage invasion on conventional films. a) Angiography of right superior thyroid artery lateral view (subtraction). Anterior ramus is irregular (↔) Ventral branch normal (→) b) Coronal section through mid-portion of vocal cords. Tumour (arrows) invades lower part of right thyroid ala. C=cricoid cartilage. E=epiglottis. T=thyroid cartilage.

Discussion

From the previous investigation of the arterial anatomy in laryngeal specimens (SÖKJER & OLOFSSON) it was concluded that angiography might prove a useful aid in determining whether the tumour is approaching the thyroid ala invading the pre-epiglottic space or the piriform sinus or spreading outside the larynx through the cricothyroid membrane.

Catheterization of the superior thyroid artery was easy to carry out but attempts to catheterize the superior laryngeal artery were unsuccessful and elicited arterial spasm. Selective injection into the superior laryngeal artery should be possible when this vessel originates directly from the external carotid artery.

Most of the angiographic information was provided by the lateral views. Stereoscopic radiography is necessary to distinguish the laryngeal vessels from the superimposed branches of the superior thyroid artery. Information obtained from these films was useful in analysing details in the magnification series.

Because the injection of contrast medium into the superior thyroid artery elicited a swallowing with movement of the larynx and hypopharynx—even when metrizamide was used as contrast medium—general anaesthesia was needed (FACFRBERG 1977).

Arterial displacement indicated tumour spread anteriorly through the cricothyroid membrane in one case. Lateral spread was not suggested by such displacement but vascular occlusions were found in 2 cases and possibly also in another case. In 2 of these cases the tumour spread into the thyroid cartilage. Because of the location of the vessels just medial to the thyroid cartilage, arterial occlusion indicates that the tumour is only approaching and not necessarily invading the cartilage. Changes in caliber of the arteries suggestive of tumour encasement were present in one case. Tumour neovascularity and early venous draining were not prominent features. A defect within the accumulation of contrast medium visible in the AP view in one case (Fig. 4) corresponded to the extension of the tumour in the whole-organ sections. In one case no

conclusions could be drawn concerning the reliability of angiography for delineating the laryngeal carcinoma as it was performed two years before the partial laryngectomy.

Thus it is evident that the laryngeal arteries can be demonstrated by angiography. Moreover with this technique it is possible to detect abnormal features providing information concerning the deeply invading tumour that is not supplied by generally applied methods of examination. However in 2 cases with epiglottic carcinomas and major invasion of the pre epiglottic space the angiographic appearances were considered to be normal indicating that invasion of the pre epiglottic space may not be possible to assess by angiography. In this region computer tomography may provide supplementary information (MANCUSO et al 1978). In glottic carcinoma angiography may be useful in assessing the lateral and anterior spread. However the number of patients is too small for any definite conclusions to be drawn.

SUMMARY

Angiography was performed in 8 patients with laryngeal carcinoma. The findings suggest that angiography can provide useful information on deep tumour invasion but further experiences are needed before any definite conclusions can be drawn.

REFERENCES

- ADACHI B. Anatomie der Japaner. Vol. I. Das Arterien system der Japaner. Band I. S. 66. Verlag der Kaiserlich Japanischen Universität. Kyoto 1928.
- FAGERBERG G. Angiographic localization of parathyroid adenomas. Acta radiol. Diagnosis 19 (1978) 7.
- MANCUSO A. A. CALCATERRA T. C. and HANAFFEW N. Computed tomography of the larynx. Radiol. Clin. N. Amer. 16 (1978) 195.
- OKI T. The distribution of blood vessels in the larynx (In Japanese with extensive English summary). J. Otorhinolaryng. Soc. Japan 61 (1968) 1827.
- OLOFSSON J. and SÖKJER H. Radiology and laryngoscopy for the diagnosis of laryngeal carcinoma. Acta radiol. Diagnosis 18 (1977) 449.
- and SÖKJER H. Radiologic assessment of laryngeal carcinoma. A clinico pathologic comparison based on whole organ serial sections. Acta radiol. Diagnosis 20 (1979) 789.
- RAUBER A. A. und KOPSCH F. Lehrbuch und Atlas der Anatomie des Menschen. 19. Aufl. Durchgesehen und verbessert von F. Kopsch. Band I. S. 546-564. Georg Thieme Verlag. Stuttgart 1955.
- SÖKJER H. and OLOFSSON J. Arterial anatomy in the normal larynx and in laryngeal carcinoma. Radiography of specimens. Acta radiol. Diagnosis 20 (1979) 917.
- SOM M. L. and SILVER C. E. The anterior commissure technique of partial laryngectomy. Arch. Otolaryng. 87 (1968) 139.
- TERRACOL J. et GUERRIER Y. Le système artériel du larynx. Etude anatomique. Montpellier med. 39/40 (1951) 341.

FROM THE DEPARTMENT OF DIAGNOSTIC RADIOLOGY (DIRECTOR PROF ■ BOJSEN) UNIVERSITY HOSPITAL
S-113 LUND SWEDEN AND THE DEPARTMENT OF PHYSIOLOGY (DIRECTOR PROF L GARBY) ODENSE
UNIVERSITY DK 8000 ODENSE DENMARK

ADRENERGIC AND CHOLINERGIC RESPONSES IN THE UTEROPLACENTAL VASCULAR BED OF THE GUINEA PIG

N EGUND and A M CARTER

The pregnant uterus of the guinea pig is supplied with blood by radial arteries arising from an arterial loop formed by anastomosis of the ovarian and uterine arteries (EGUND & CARTER 1974 CHAICHAREON et coll 1976). Techniques for the selective catheterization of these two arteries have been developed (EGUND & CARTER) to enable pharmacangiographic investigations of the utero-placental circulation in an animal with ■ discoid haemochorial placenta similar to that of man (EN DERS 1965). The basic adrenergic and cholinergic responses of the uterine and maternal placental vas-
culature in guinea pigs are now reported

Material and Methods

The material consisted of 76 guinea pigs (*Cavia porcellus*) of mixed breed. They were given pelleted fodder (Astra Ewos Sweden) hay and water ad libitum. Tocopherol and selenium (Eselen N vet Ferring Sweden) was added to the drinking water. Experience has shown that pregnant guinea pigs on a standard diet without this supplement may exhibit hypotension, impaired placental circulation and placental infarction, also some dead fetuses are found (INGELMAN SUNDBERG 1949). At examination the guinea pigs weighed between 730 and 1460 g (mean 1036 g). The stage of gestation, estimated from the mean weight of the fetuses in each litter (DRAPER 1920) ranged from 44 to 66 days (mean 60 days).

General anaesthesia was obtained by the intramuscular injection of sodium pentobarbitone (Mebumal vet ACO Sweden) in an initial dose of 20 mg/kg body weight. Rectal temperature recorded with an electrothermometer was maintained at a constant level with the aid of an infrared lamp (Osram Siccatherma 250 W Sweden). Arterial blood pressure was recorded electromanometrically from a catheter in an axillary artery. Selective catheterization of the ovarian or uterine artery was performed during magnification fluoroscopy as previously described (EGUND & CARTER). A fine polyethylene catheter (OD/ID=0.6/0.3 mm Surgimed Denmark) was used for the ovarian artery. The intra-arterial part of the uterine catheter had ■ similar dimension but was prepared by drawing out the last 3 cm of a catheter (OD/ID=1.0/0.6 mm) that provided less resistance to the flow of contrast medium. The uterine catheter was advanced from the ipsilateral superficial or deep femoral artery and the ovarian catheter from the right carotid artery.

Serial angiography with geometric magnification (EGUND & CARTER) was performed before and at various times after the injection of drugs. Each series comprised 7 films exposed at intervals of 1 s followed by a further 5 films at intervals of 2 s. The contrast medium used was meglumine metrizoate (Isopaque Cerebral Nyegard Norway). The volume injected was 0.6 ml for the ovarian artery and

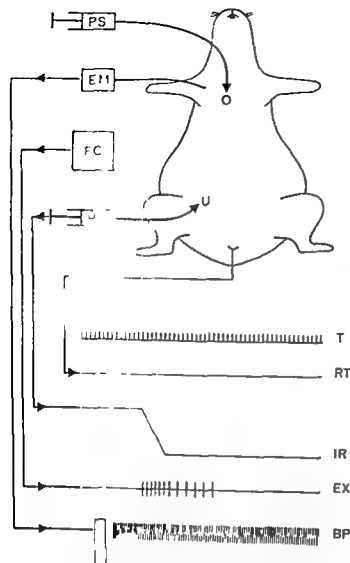


Fig. 1 Schematic drawing of the experimental arrangement. An ovarian artery (O) is catheterized from the right carotid artery or a uterine artery (U) from the right femoral artery. The catheter is connected to a high pressure syringe (PS) for contrast medium injection. Blood pressure in the right axillary artery is recorded with an electromanometer (EM) and rectal temperature with an electrothermometer (RT). An automatic film changer (FC) is placed beneath the animal. The lower half of the diagram represents a typical tracing from the potentiometer writer, which registers the following variables: Time in seconds (T), rectal temperature (RT), contrast medium injection rate (IR), film exposures (EX) and arterial blood pressure (BP).

0.8 ml for the uterine artery. The contrast medium was injected using a high pressure syringe and its course was registered on a direct writing polygraph so that the exact rate of injection could be determined (Fig. 1).

The effect of the following substances was evaluated: noradrenaline bitartrate (Apoteksbolaget, Sweden), phenoxylbenzamine hydrochloride (Dibenzyl, Smith Kline & French, England), acetylcholine chloride (Hoffmann-La Roche, Switzerland) and atropine sulphate (ACO, Sweden). Drugs



Fig. 2 Application of spillover flowmeter technique to a vessel. Uterine blood flow. Contrast medium is injected at a known rate through a catheter with its tip in the mouth of the uterine artery. U = uterine artery, I = iliac artery. a) Rate of blood flow equal to rate of contrast medium injection: uterine artery completely filled. b) Rate of blood flow less than rate of injection: resulting in spillback of contrast medium into iliac artery. c) Rate of blood flow exceeds injection rate and contrast medium is diluted with blood, resulting in unsatisfactory filling of uterine artery.

were injected intra-arterially through the angiography catheter. Each dose was dissolved in 1 ml isotonic saline solution; the molar concentration being adjusted to allow for the dead space of 0.1 to 0.2 ml between the syringe and the catheter tip. If a drug was found to alter uteroplacental circulation, an attempt was made to establish the smallest dose that could elicit a clearly identifiable response. This involved a comprehensive series of preliminary experiments. The definitive experiments reported are summarized in the Table.

The rate of uterine blood flow was estimated by the spillover flowmeter technique (OLIN & REDMAN 1966; CARTER *et al.* 1971; Fig. 2). The rate of injection of the contrast medium is known and if it is the same as the rate of blood flow in the uterine artery, this vessel will be filled completely (Fig. 2a). If the rate of injection is too fast, a spillback of contrast medium into the iliac artery occurs (Fig. 2b).

Table

Number of experiments with selective injection of drugs into the uterine and/or ovarian arteries (pregnant guinea pigs)

Drug	Uterine artery	Ovarian artery
Noradrenaline	5	5
Phenoxylbenzamine	6	4
Phenoxylbenzamine followed by noradrenaline	6	5
Acetylcholine	4	1
Atropine	4	1
Atropine followed by acetylcholine	7	1



a



b



c



d

Fig 3 Serial angiography of the right ovarian artery in a pregnant guinea pig about 48 days post coitum. Two film series are shown exposed 25 s (a, c) and 65 s (b, d). (a) Start of contrast medium injection. Corpora lutea in the (b) and ovarian vein (V). Other symbols as in Fig 4. (c) Arterial phase with contrast medium in a placental artery. The injection rate (10.7 ml/min) exceeds the blood flow as evidenced by spillback into the aorta. (b) Late placental arterial phase. (d) Phenylephrine.

examination 10 s after selective injection of 25 nmol phenylephrine. (c) Calibre of the ovarian artery has increased and the arterial phase is somewhat more advanced than the corresponding control film. The injection rate (13.6 ml/min) is in equilibrium with the blood flow demonstrated by the absence of spillback into the control examination. (d) The selective injection of phenylephrine indicates a faster circulation. The placenta is more distally situated.



Fig. 4 (For legend see opposite page.)

2b) If the rate of injection is too slow the contrast medium will be diluted with blood and the filling of the uterine artery will be unsatisfactory (Fig. 2c). The same principle can be used to evaluate ovarian blood flow if it is borne in mind that a minor amount

of contrast medium split into the aorta may not be diluted and therefore not be visible. Arterial blood pressure was measured to ensure that observed changes in blood flow were the result of altered vascular resistance rather than of changes in



e

Fig. 4 Serial angiography of the right ovarian artery in a pregnant guinea pig about 59 days post coitum. Two films from each series are shown: exposed 4 s (a, c, e) and 10 s (b, d, f) after start of contrast medium injection. Letters indicate the catheter in the abdominal aorta (C), the kidneys (K), the utero-ovarian arterial loop (L), the ovarian artery (O), placental arteries (P) and radial arteries (R). Control: a) Arterial phase. The contrast medium has not yet reached the placenta but the dilated radial arteries which supply it are well demonstrated. b) Early capillary phase. Repeat examination after selective injection of 0.5 nmol noradrenaline.



f

c) Arterial vasoconstriction is apparent. d) Circulation is markedly delayed compared with the corresponding control film and even in later films less contrast medium in the placental blood vessels indicating impairment of the placental circulation. Repeat examination after 25 nmol phenoxybenzamine followed by 0.5 nmol noradrenaline. e) No vasoconstriction is evident as after noradrenaline alone; instead slight dilatation of the ovarian artery. Filling of the placental arteries indicates a more rapid circulation than at control examination. f) Later capillary phase than in corresponding control film confirming that the circulation is faster.

perfusion pressure. In the guinea pig the ovarian and uterine arteries anastomose forming an arterial loop that supplies the ovary and the pregnant uterus. The calibre of the arterial loop was assessed at three separate points on each film.

Additional information was obtained by measuring the following circulation times. From the start of the injection until the point at which contrast medium appeared in placental arteries; from this point until the placental capillary phase; and from the end of the injection until the point at which contrast medium had disappeared from the radial arteries (arterial washout time cf. LINGARDH & LUNDSTRÖM 1974). Note was also made of possible changes in the filling of the placenta and of the utero-ovarian vein.

Some vasoactive drugs are able to evoke uterine contractions of an intensity sufficient to affect the placental blood supply (CARTER & OLIN 1973). In order to avoid uterine trauma the intra uterine pres-

sure was not recorded in connection with the angiography. However, if a drug was found to reduce the placental blood supply its effect on the myometrium was checked in separate experiments where the drug was injected selectively into the uterine or ovarian artery during registration of the intra uterine pressure through a sponge tipped catheter (BENGTSSON 1968).

Results

The guinea pigs had a mean arterial blood pressure of 9.3 ± 1.0 kPa (69.8 ± 7.6 mmHg). Selective injection of drugs in the uterine or ovarian artery in doses sufficient to affect uteroplacental circulation resulted in no alteration of systemic blood pressure.

Noradrenaline 0.5 nmol/kg evoked a decrease in both uterine blood flow and ovarian blood flow associated with arterial vasoconstriction. Severe impairment of the placental blood supply also oc-



a



b



c



d

Fig. 5 (For legend see opposite page.)



Fig. 5 Serial angiography of the left uterine artery in a pregnant guinea pig about 54 days post coitum. Two films from each series are shown: exposed 3 s (a) and 6 s (b) after start of contrast medium injection. Letters indicate the catheter in the external iliac artery (C), a thermistor probe (T) and radial arteries (R). Control: a) Arterial phase in which contrast medium has just reached a placental artery (\rightarrow). Spillover of contrast medium into iliac arteries and their branches reveals that the rate of uterine blood flow is smaller than the injection rate (6.8 ml/min). b) Early placental capillary phase. Repeat examination 17 s after selective injection of 0.5 nmol acetylcholine. c) Contrast medium is diluted with blood: filling of uterine artery and its branches unsatisfactory since the rate of blood flow exceeds the

rate of injection (7.5 ml/min). Contrast medium has advanced further in the placental arteries (\rightarrow) than in the corresponding control film. d) Late capillary and venous phase in the placenta which should be compared with the early capillary phase of the corresponding control film. Repeat examination after another injection of 0.5 nmol acetylcholine. e) Injection rate increased more than twofold (17.5 ml/min) and is in equilibrium with rate of blood flow, resulting in good filling of uterine and placental arteries (\rightarrow). Calibre of uterine artery larger than in the control film. f) Early capillary phase 6 s after start of injection almost comparable with control film after 12 s. Evidently a significant increase in rate of uteroplacental circulation.

currer considerably less contrast medium reached the placenta than at control angiography and the circulation was sluggish (Fig. 4). Lower doses (0.01–0.25 nmol/kg) had no effect except in one experiment where 0.25 nmol/kg noradrenaline caused a slight decrease in the calibre of the uterine artery. Intra uterine pressure was unaffected by the selective injection of 1 nmol/kg noradrenaline.

The effect of phenoxybenzamine at injection into the uterine artery was variable. Thus 25 nmol/kg phenoxybenzamine had no effect in two guinea pigs and caused slight vasodilatation in two others whilst in two experiments vasodilatation an in

crease in blood flow and a reduction of circulation times occurred. The effect at injection into the ovarian artery was more consistent. 25 nmol/kg phenoxybenzamine evoked a strong vasodilatation and increased the rate at which contrast medium traversed the placenta (Fig. 3).

Noradrenaline 1 nmol/kg had no effect on utero placental circulation when injected into either the ovarian or the uterine artery subsequent to the injection of 25 nmol/kg phenoxybenzamine.

The primary effect of acetylcholine was vasodilatation and an increase in ovarian and uterine blood flow (Fig. 5). However the calibre of the main ste

of the ovarian artery changed only little compared with the dilatation that occurred in more peripheral arteries. This effect was invariably obtained with 5 nmol/kg and was usually produced by as little as 0.5 nmol/kg acetylcholine. When the dose was increased to 50 nmol/kg vasodilatation was maintained or accentuated but less contrast medium reached the placenta. The motility of the uterus was also affected by this dose of acetylcholine causing a visible shift in position of the blood vessels with a single sequence of films. However, the magnitude of the myometrial response to acetylcholine varied considerably as determined from intra-uterine pressure recordings.

No change in blood flow or circulation time was observed either 30 s or 10 min after the injection of atropine into the ovarian or uterine artery. Transient dilatation of the uterine artery was sometimes seen after atropine but vessel calibres otherwise remained unchanged.

All the effects of acetylcholine were effectively blocked by 10 nmol/kg atropine.

When vascular resistance decreased following the injection of acetylcholine or phenoxybenzamine a greater number of placental vessels were often filled (Fig. 3) suggesting a shift in the partition of placental blood flow between the ipsilateral uterine and ovarian arteries.

Discussion

The effect of adrenergic and cholinergic drugs on the extrinsic arterial supply of the uterus of the guinea pig has been examined in a perfusion preparation by BILL (1968). Although the findings were used in support of a theory concerning the control of uterine vascularity in pregnancy (BILL 1974) they have not been corroborated in guinea pigs with intact uteroplacental circulation. Some experiments have been performed with adrenaline (GIRARD *et al.* 1971) and atropine (BILL & BROWN 1971) but in neither case was the drug injected selectively into the uterine artery. Furthermore although the ovarian artery provides an important part of the uteroplacental blood supply in the guinea pig (ELCROD & CARTER) no attempt has been made to evaluate the response of this vessel to vasoactive substances.

Noradrenaline increases the resistance to flow in perfused uterine arteries; a weak response is obtained with 0.03 nmol and 0.3 nmol produces a clear effect (BILL 1968). The sensitivity of the uterine

artery is evidently similar *in vivo* as vasoconstriction and a reduction of uterine blood flow were observed after the injection of 0.52 nmol noradrenaline *in line* (0.5 nmol/kg body weight). A similar response was obtained when the corresponding dose was injected in the ovarian artery. These effects of noradrenaline are evidently mediated by α adrenergic receptors as they are inhibited by phentolamine *in vitro* (BILL 1968) and phenoxybenzamine *in vivo*.

The association of adrenergic nerves with the uterine vessels of the guinea pig has been demonstrated histochemically and their transmitter content apparently decreases during pregnancy (SJOBERG 1968). Nevertheless when isolated uterine arteries from pregnant guinea pigs are stimulated electrically they are able to release noradrenaline (BILL & VOGT 1971). Further evidence for an adrenergic innervation of the uterus during pregnancy was obtained by giving selective injections of phenoxybenzamine in a dose known to inhibit the response to exogenous noradrenaline. When the drug was given in the uterine artery it evoked vasodilatation in four guinea pigs and a gradation in response occurred suggestive of varied sympathetic tonus. It should be emphasized that these animals were under light anaesthesia and a normal body temperature and had an adequate arterial blood pressure that was unaffected by the phenoxybenzamine. A vasodilator response to phenoxybenzamine has previously been demonstrated in the uterine vascularity of the rabbit (CARTER & OLIN 1972).

Isolated uterine arteries are in a condition of minimum tonus and do not respond to acetylcholine (BILL 1968). If tonus is raised by adding noradrenaline to the surrounding bath intra-arterial injection of acetylcholine elicits vasodilatation. The effect is almost maximum in the dose range 0.44 to 4.4 nmol and a decrease in perfusion pressure is elicited by as little as 55 fmol (BILL 1968). The present results indicate that the uterine artery of the guinea pig is considerably less sensitive to acetylcholine when in a state of physiologic tonus. The smallest dose found to evoke vasodilatation or an increase in uterine blood flow was 0.53 nmol (0.9 nmol/kg body weight). This suggests that if a cholinergic vasodilator mechanism exists in the uterus of guinea pigs and other species including man (BILL 1967, 1971) its importance may have been overemphasized. It is interesting to note that although human uterine arteries appear to receive adrenergic innervation perfused vessels do not respond

acetylcholine even when their tonus has been raised by noradrenaline (BELL 1969)

An interesting difference was found in sensitivity of acetylcholine between the main stem of the ovarian artery and the remainder of the utero-ovarian arterial loop. It exhibited little change in calibre on injection of the drug even when the rate of ovarian blood flow increased. The rise in blood flow was clearly associated with increased conductance in the uteroplacental vascular bed but it was not possible to assess whether the ovarian vasculature was affected.

If a large dose of acetylcholine 50 nmol/kg is injected into the uterine or ovarian artery its immediate effect is to reduce the blood supply to the placenta. The increased resistance to flow is evidently presented by the intra uterine part of the vasculature since the extrinsic uterine arteries remain dilated. It is probably ascribable to compression of the blood vessels due to myometrial contraction rather than to vasoconstriction.

The response of the uteroplacental vasculature to acetylcholine was abolished by the previous injection of 10 nmol/kg atropine confirming that acetylcholine is acting through muscarinic receptors (BELL 1968). BELL & BROWN assigned an important physiologic role to these receptors as they observed a decrease in the calibre of the uterine arteries following the injection of large doses of atropine 144 to 1440 nmol/kg into the aorta. It was attempted to confirm their results by selective injection into the uterine and ovarian arteries of 10 nmol/kg atropine. A dose that is sufficient to inhibit the response to exogenous acetylcholine. No diminution of vessel calibre occurred suggesting that cholinergic innervation is of minor importance as a determinant of uterine blood flow under physiologic conditions. This does not preclude the possibility that the uteroplacental circulation is protected by cholinergically mediated vasodilatation during for instance a rise in sympathetic tonus in response to stress (BELL 1968) has clearly documented the extreme sensitivity to acetylcholine of perfused uterine arteries in the presence of noradrenaline.

SUMMARY

The effects on uterine and maternal placental circulation of adrenergic and cholinergic drugs injected selectively in the ovarian and uterine arteries of guinea pigs were analysed by serial angiography. Noradrenaline 0.5

nmol/kg was found to cause a reduction in both ovarian and uterine blood flow associated with arterial vasoconstriction and impairment of the placental circulation. This response could be prevented by α -adrenergic blockade with 25 nmol/kg phenoxybenzamine. At injection into the ovarian artery phenoxybenzamine alone increased ovarian blood flow and elicited arterial vasodilatation. At injection into the uterine artery the response was more variable but vasodilatation was observed in four animals of six. Acetylcholine 0.5 to 5.0 nmol/kg evoked an increase in both ovarian and uterine blood flow and arterial vasodilatation. When the dose was increased to 50 nmol/kg dilatation of the extrinsic uterine arteries was maintained but the placental circulation was reduced due to concomitant contraction of the myometrium. All the effects of acetylcholine could be blocked by prior administration of 10 nmol/kg atropine. This dose of atropine did not affect uterine or placental circulation when given alone.

ACKNOWLEDGEMENT

The investigation was supported by a grant from the Swedish Medical Research Council (Project No B77 14X 605 11).

REFERENCES

- BELL C. Dual vasoconstrictor and vasodilator innervation of the uterine arterial supply in the guinea pig. *Circulat Res* 23 (1968) 279.
- Evidence for dual innervation of the human extrinsic uterine arteries. *J Obstet Gynaec Brit Cwlth* 76 (1969) 1123.
- Distribution of cholinergic vasomotor nerves to the parametrial arteries of some laboratory and domestic animals. *J Reprod Fertil* 27 (1971) 53.
- Control of uterine blood flow in pregnancy. *Med Biol* 52 (1974) 219.
- and BROWN M. J. Arteriographic evidence for a cholinergic dilator mechanism in uterine hyperaemia of pregnancy in the guinea pig. *J Reprod Fertil* 27 (1971) 59.
- and VOGT M. Release of endogenous noradrenaline from an isolated muscular artery. *J Physiol (Lond)* 215 (1971) 509.
- BENGTSSON L. P. The sponge tipped catheter. A modification of the open end catheter for recording of myometrical activity in vivo. *J Reprod Fertil* 16 (1968) 115.
- CARTER A. M. and OLIN T. Effect of adrenergic stimulation and blockade on the uteroplacental circulation and uterine activity in the rabbit. *J Reprod Fertil* 9 (1972) 251.
- Variation in the effect of acetylcholine on myometrial activity and maternal placental blood flow in the rabbit. *J Reprod Fertil* 35 (1973) 73.
- GOTHLIN J. and OLIN T. An angiographic study of the structure and function of the uterine and maternal placental circulation.

- central vasculature in the rabbit *J. Reprod. Fertil.* 25 (1971) 201
- CHAICHAUFON D. P., RANKIN J. H. and GINTHER O. J. Factors which affect the relative contributions of ovarian and uterine arteries to the blood supply of reproductive organs in guinea pigs *Biol. Reprod.* 15 (1976) 281
- DRAIER R. L. The prenatal growth of the guinea pig *Anat. Rec.* 18 (1920) 369
- EGUND N. and CARTER A. M. Uterine and placental circulation in the guinea pig. An angiographic study *J. Reprod. Fertil.* 40 (1974) 401
- ENDERS A. C. A comparative study of the fine structures of the trophoblast in several hemochorial placentas *Amer. J. Anat.* 116 (1965) 29
- GIRARD H., BRUN J. L. and MUFFAT JOLY M. An angiographic study of the sensitivity to epinephrine of the uterine arteries of the guinea pig. A comparison with angiotensin *Amer. J. Obstet. Gynec.* 111 (1971) 687
- INGELMAN SUNDBERG A. Abruptio placentae in vitamin deficient guinea pigs *Acta endocrinol.* 7 (1949) 335
- LINGÅRDH G. and LUNDSTRÖM B. Renal blood flow determined by angiography *Acta radiol. Diagnosis* 1 (1974) 529
- OLIN T. and REDMAN H. Spillover flowmeter. A preliminary report *Acta radiol. Diagnosis* 4 (1966) 317
- SJÖBERG N. O. Considerations on the cause of disappearance of the adrenergic transmitter in the uterine nerve during pregnancy *Acta physiol. scand.* 79 (1968) 516

FROM THE RESEARCH LABORATORIES DEPARTMENTS OF DIAGNOSTIC RADIOLOGY AND CLINICAL CHEMISTRY MALMÖ ALLMÄNNNA SJUKHUS S-214 01 MALMÖ SWEDEN AND THE RESEARCH DEPARTMENT NYE GAARD & CO OSLO NORWAY

PROTEINURIA FOLLOWING NEPHROANGIOGRAPHY

V Influence of calcium and magnesium ions in non ionic contrast media

S HOLTÅS T ALMÉN K GOLMAN and L TEJLER

The introduction of the tri iodinated contrast media in common use has lowered the risk of renal injury induced by contrast medium but decreased renal function following urography and various angiographic procedures has been relatively frequently reported (STARK & COBURN 1966 SIDD & DECTER 1967 MCEVOY et coll 1970 PORT et coll 1974 ANSARI & BALDWIN 1976 OLDER et coll 1976 TEJLER et coll 1977b MILMAN & GOTTLIEB 1977 HARKONEN & KJELLSTRAND 1977 KRUMLOVSKY et coll 1978).

The decrease in renal function has been measured and quantitated using different techniques and parameters (LASSER 1967 ALMÉN 1971). Proteinuria is one sign of injury to the kidney and it has recently been demonstrated that it regularly occurs after nephroangiography both in man (TEJLER et coll 1977a) and in dog (HOLTÅS et coll 1978a). Proteinuria following angiography was found both when ionic (metrizoate diatrizoate) and non ionic (metrizamide C 29) contrast media were used. In attempts to reduce the proteinuria in dogs it was shown that the chemical structure of the contrast medium was of greater importance in causing proteinuria than the high osmolality of the contrast medium solution (HOLTÅS et coll 1978b). The experimental substance C 29 induced significantly less proteinuria than the other contrast media tested (HOLTÅS & TEJLER 1979). Analyses of the molecular sizes of the excreted proteins disclosed that the contrast media increased the glomerular permeability (TEJLER et coll 1977a).

The stability of cell junctions in membranes is strongly dependent on the presence of calcium ions

(SÖGREN 1967 ROSE et coll 1977). Addition of calcium and magnesium ions to metrizoate and calcium or calcium and magnesium ions to C 29 have previously (SALVESEN et coll 1967 GOLMAN 1979) been shown to decrease blood brain barrier permeability following selective cerebral angiography. Whether addition of these ions to contrast media would also decrease the glomerular leakage of proteins induced by nephroangiography has been investigated and the results are now reported.

Material and Methods

Dogs The experiments were performed on mongrel dogs weighing on the average 21 kg (range 12–38 kg) anesthetized with pentobarbitone and breathing spontaneously through an endotracheal tube. Arterial and urinary bladder catheterizations were performed as previously described (HOLTÅS et coll 1978a).

The dogs were divided into 3 groups. The concentration of urinary albumin was recorded following injection into one renal artery of the non ionic contrast medium C 29 (group I) C₂₉+CaCl₂ (group II) or C₂₉+CaCl₂+MgCl₂ (group III). The number of dogs in the groups, the dose and composition of the contrast medium solutions are given in the Table.

Urine samples were obtained via the transurethral catheter before and 15, 30 and 60 min after the injection.

Rats Wistar rats weighing 240 to 350 g were an-

Table

Relative increase of urinary albumin (max. postinj. conc./preinj. conc.) in the different experimental groups (Dogs I-III, Rats A-E). The concentration of all contrast media solutions was 1.0 mmol/l (370 mg/l/ml)

Group	No. of animals	Injected material	Dose (ml/kg)	Electrolytes (mmol/l)		Relative increase of urinary albumin (median and range)
				CaCl ₂	MgCl ₂	
I	9	C 29	0.5	—	—	49 (1.6-17000)
II	12	C 29	0.5	10	—	375 (8-7300)
III	21	C 29	0.5	5	2.5	150 (1.7-4800)
A	10	Metrizamide	1.0	—	—	76 (0.7-70)
B	10	Metrizamide	1.0	7.5	—	14 (4-77)
C	10	Metrizamide	1.0	25	—	54 (18-95)
D	10	C 29	1.0	—	—	2.3 (1.1-6.3)
E	10	0.9% NaCl	1.0	—	—	1.5 (0.6-3.7)

Statistical evaluation of differences in relative increase of urinary albumin between the groups: I-II $p < 0.05$, I-III and II-III no significant differences, I-D $p < 0.005$, A-B no significant difference, A-C $p < 0.05$, A-D $p < 0.01$, D-E $p < 0.05$.

esthetized with pentobarbitone and placed supine. Laparotomy was followed by an incision into the urinary bladder and a polyethylene tube (Intramedic PE 60 Clay Adams) for urine sampling was introduced and sutured in place. Another polyethylene tube for contrast medium injection was placed retrogradely in the aorta and sutured in such a position that the tip of the tube was just below the origin of the left renal artery. The superior mesenteric artery was ligated in order to avoid the escape of contrast medium via this route. The solution to be examined was then injected with a speed of 10 ml/min. At this speed the solution was forced to a level 2 to 3 mm above the origin of the right renal artery and flowed through both renal arteries as confirmed on a film exposed one second before the end of the injection.

The rats were divided into 5 groups. The concentration of urinary albumin was recorded following injection into the aorta of the non ionic contrast medium metrizamide (group A), metrizamide with addition of different doses of CaCl₂ (groups B and C), C 29 (group D) and 0.9% (w/v) NaCl (group E). The number of rats in the groups, the dose and composition of the contrast media solutions are given in the Table.

Urine was collected before and after the injections during 30 minute periods.

Albumin assays. The concentration of albumin and creatinine in the urine was determined as previously described (HOLTÅS et al. 1978). For the albumin assay in rats goat anti-rat albumin anti-

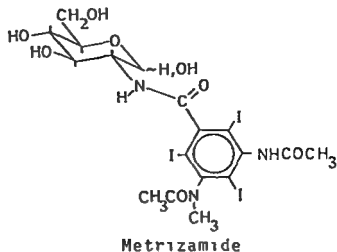
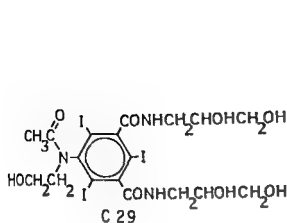
serum (Cappel Inc. USA) was used. Concentrations of urinary albumin were expressed per gram creatinine thereby relating albumin excretion to glomerular filtration rate. Pooled canine and rat plasma was used as standards in the albumin assays. They were assigned a concentration value of 100 arbitrary units of albumin per liter.

The ratio between the maximum postinjection concentration of urinary albumin and the preinjection value was calculated for each animal. For this ratio the term relative increase of urinary albumin is used. Differences were considered significant when p values ≤ 0.05 were obtained by the Mann-Whitney rank sum test or Wilcoxon's test for paired observations.

The structural formulae of the contrast media metrizamide (Ampiquin) and C 29 which have been used in the experiments are given in the Figure.

Results

Dogs. Following unilateral nephroangiography with C 29 significant increases ($p < 0.005$) in the concentration of urinary albumin were observed in all groups (Table). Addition of CaCl₂ and MgCl₂ to a final concentration of 5 mmol/l and 2.5 mmol/l respectively to C 29 did not influence the relative increases of urinary albumin but when CaCl₂ was added to a concentration of 10 mmol/l significantly higher relative increases ($p < 0.05$) occurred compared with those found following nephroangiography with C 29 alone (Table).



Chemical structure of C 29 and metrizamide

The median preinjection concentration of urinary albumin in the dogs was 0.51 (range 0.069–3.6) arbitrary units/g creatinine.

Rats Following bilateral nephroangiography with metrizamide or C 29 significant ($p < 0.05$) increases in the concentration of urinary albumin were observed in all groups whereas injection of 0.9% (v/v) NaCl did not cause such increases (Table). The relative increases of urinary albumin were lower ($p < 0.01$) following injection of C 29 than after any of the metrizamide formulations. Addition of CaCl_2 to a final concentration of 7.5 mmol/l to metrizamide did not influence the relative increases of urinary albumin following nephroangiography but when CaCl_2 was added to a concentration of 25 mmol/l significantly higher ($p < 0.05$) relative increases were observed (Table).

The injection of C 29 in rats resulted in significantly lower ($p < 0.005$) relative increases of urinary albumin than injection of C 29 in dogs. The median preinjection concentration of urinary albumin in the rats was 6.4 (range 2.7–11) arbitrary units/g creatinine.

Discussion

Following nephroangiography massive albuminuria occurs in man (TEJLER et coll 1977a) and in dog (HOLTÁS et coll 1978a). The present results show that the non ionic contrast media metrizamide and C 29 also induce albuminuria in rats.

The preinjection concentrations of urinary albumin in the rats were about 10 times higher than in the dogs. This might be the reason why significantly lower ($p < 0.005$) relative increases of urinary albumin

following injection of C 29 occurred in rats than in dogs.

C 29 induces significantly less albuminuria following angiography in dogs than metrizamide (HOLTÁS & TEJLER). In the present experiments injection of C 29 induced significantly lower ($p < 0.01$) albuminuria than metrizamide also in rats. This indicates that the chemical structure of the contrast medium is more important as a factor causing albuminuria than the osmolality since solutions of C 29 and metrizamide have about the same osmolality at equal iodine content.

Contrast media increase the permeability of the blood brain barrier during cerebral angiography (JEPPSSON & OLIN 1975; RAPOPORT 1976) and a protective effect has been observed when calcium and magnesium ions were added to the ionic contrast medium metrizoate (SALVESEN et coll.) and the non ionic C 29 (GOLMAN). In the present investigation no such beneficial effect on the glomerular membrane was found since addition of calcium and magnesium ions to C 29 in dogs and calcium ions to metrizamide in rats did not reduce the albuminuria following angiography. When calcium ions were added to C 29 in higher concentration (10 mmol/l) in dogs and to metrizamide (25 mmol/l) in rats the albuminuria increased significantly.

Calcium ions are important components of the desmosome structure which is involved in the cell to cell adhesion and depletion of calcium ions by chelating agents causes separation of cell junctions in some membranes (SØGNET, ROSE et coll.). This might be the mechanism responsible for the beneficial effect of calcium ions on the permeability of the blood brain barrier during cerebral angiography.

The present results indicate that other mechanisms are involved in the increased glomerular permeability following nephroangiography since no beneficial effect was observed after addition of calcium ions. The increased permeability of the glomerular membrane when high concentrations of calcium ions were added to the contrast media cannot be explained at present.

SUMMARY

The influence on albuminuria following nephroangiography was investigated after addition of Ca^{2+} to the non ionic contrast medium metrizamide (Amipaque) in the rat and after addition of Ca^{2+} or Ca^{2+} and Mg^{2+} to the experimental non ionic contrast medium C 29 in the dog. When Ca^{2+} or Ca^{2+} and Mg^{2+} were added to metrizamide or C 29 in concentrations two to three times the plasma level no influence occurred. Higher concentrations of Ca^{2+} (10–25 mmol/l) in the metrizamide or C 29 solutions resulted in increased albuminuria.

ACKNOWLEDGEMENTS

This investigation was supported by grants from the Medical Faculty, University of Lund, the Swedish Medical Research Council (Project No. 3483) and the Segerfalk foundation. The authors wish to thank and read Olvind Grimmer for advice on the rat albumin analyses and Anita Burnett, Eckert Holtz and Gull Åkerman for expert technical assistance.

REFERENCES

- ALMÉN, T. Toxicity of radiocontrast agents. In: *Radio contrast agents*, p. 443. Edited by P. K. Knoefel. Pergamon Press, London, 1971.
- ASSARI, Z. and BALDWIN, D. S. Acute renal failure due to radiocontrast agents. *Nephron* 17 (1976) 28.
- GOI MAN, K. The blood brain barrier: Effects of nonionic contrast media with or without addition of Ca^{2+} and Mg^{2+} . *Invest Radiol* 14 (1979) 305.
- HARKÖNEN, S. and HILLSTRAND, C. Exacerbation of diabetic renal failure following intravenous pyelography. *Amer J Med* 63 (1977) 939.
- HOLTÅS, S. and TEJLER, L. Proteinuria following nephroangiography. IV. Comparison in dogs between ionic and non ionic contrast media. *Acta radiol Diagn* 20 (1979) 13.
- ALMÉN, T. and TEJLER, L. (a) Proteinuria following nephroangiography. II. Influence of contrast medium and catheterization in dogs. *Acta radiol Diagn* 18 (1978) 33.
- — (b) Proteinuria following nephroangiography. III. Role of osmolality and concentration of contrast medium in renal arteries in dogs. *Acta radiol Diagn* 19 (1978) 401.
- JEPSSON, P. G. and OLIN, T. Cerebral distribution of contrast medium and paradoxical location of the blood brain barrier in the rabbit. *Acta radiol Diagn* 18 (1975) 577.
- KRUMLOVSKY, F., SIMON, N., SANTHANAM, S., DE GREGIO, F., ROXE, D. and POMARANCE, M. Acute renal failure. Association with administration of radiographic contrast material. *J Amer med Ass* (1978) 125.
- LYSSER, E. C. The urinary system. In: *Dynamic factors in roentgen diagnosis*, p. 40. Edited by E. C. Lysser, Williams & Wilkins, Baltimore, 1967.
- MCEVOY, J., MCGOWAN, M. G. and KUMAR, R. Renal failure after radiological contrast media. *Brit med J* 4 (1970) 717.
- MILMAN, N. and GOTTHEB, P. Renal function after high dose urography in patients with chronic renal insufficiency. *Clin Nephrol* 7 (1977) 250.
- OLDER, H., MILLER, J., JACKSON, D., JOHNSON, J. and THOMPSON, W. Angiographically induced renal failure and its radiographic detection. *Amer J Roentgenol* 126 (1976) 1039.
- PORT, F. K., WAGONER, R. D. and FULTON, R. E. Acute renal failure after angiography. *Amer J Roentgenol* 121 (1974) 344.
- RAPOPORT, S. I. *Blood brain barrier in physiology and medicine*, p. 164. Raven Press, New York, 1966.
- ROSE, B., SIMPSON, I. and LOEWENSTEIN, W. R. Calcium ion produces graded changes in permeability of membrane channels in cell junctions. *Nature* 267 (1977) 625.
- SALVENDY, S., NILÉN, P. I. and HÖLTERMAN, H. Ameliorating effects of calcium and magnesium ions on the toxicity of isotonic sodium. *Acta radiol* (1961) Suppl. No. 270, p. 17.
- SININ, J. and DICHTER, A. Unilateral renal damage due to massive contrast dye injection with recovery. *J Urol* 97 (1967) 30.
- SÖCKEN, E. A method for the preparation of suspension of intestinal mucosal cells by means of calcium chelators. *Acta vet scand* 8 (1967) 76.
- STARK, F. and COBLER, J. Renal failure following methyl glucamine diatrizoate (Renografin) angiography. Report of a case with unilateral renal artery stenosis. *J Urol* 96 (1966) 848.
- TEJLER, L., ALMÉN, T. and HOLTÅS, S. (a) Proteinuria following nephroangiography. I. Clinical experiences. *Acta radiol Diagn* 18 (1977) 634.
- FRIBERG, M., ALMÉN, T. and HOLTÅS, S. (b) Proteinuria following renal arteriography. Report of two cases. *Acta med scand* 202 (1977) 131.

PROTEINURIA AFTER SELECTIVE NEPHROANGIOGRAPHY IN MAN

Comparison of three contrast media

J. KRÅKENES, B. ELSAYED, J. GOTHLIN and M. FARSTAD

Proteinuria following angiography as an indication of possible kidney injury has only lately been noticed in man (TEJLER *et al.* 1977). They reported massive proteinuria after intraarterial injection into the kidney of meglumine metrizoate in 25 of 28 patients. In dogs HOLTÅS & TEJLER (1979) demonstrated proteinuria not only after use of meglumine metrizoate but also after meglumine diatrizoate and metrizamide. The present investigation deals with the possible occurrence of proteinuria following aortography and selective nephroangiography in a clinical series of patients. Three different contrast media were used.

Material and Methods

The material consisted of 45 males and 15 females referred for routine nephroangiography. Premedication: 0.6 mg of atropine and 10 mg of diazepam was given. Lumbar aortography using 40 ml of contrast medium preceded the selective examination at which 10 to 30 ml of medium was injected into the renal artery uni- or bilaterally. The contrast media used were Isopaque Cerebral (meglumine metrizoate 590 mg/ml and Ca metrizoate 11 mg/ml with an iodine content of 280 mg I/ml), Lurografin 60 (Na amidotrizoate 80 mg/ml meglumine amidotrizoate 520 mg/ml with an iodine content of 292 mg I/ml) and Ampaque (metrizamide 280 mg I/ml).

The procedure was the same in all patients. The

contrast medium to be used was taken from a predetermined random table. No differentiation between angiographically normal and abnormal kidneys has been made. In 4 patients phlebography of the inferior vena cava (120 ml of contrast medium in each patient) was performed but otherwise no additional angiographic procedure. The mean total amount of contrast medium used in each patient was 115 ml (range 45 to 350 ml). The sampling and analysis of urine was performed immediately before 2 hours, 24 hours and when possible 2 or 3 days after the procedure. All samples were kept frozen at -20°C until analysed. At that time the type of contrast medium used was not known.

The following analyses were carried out on the collected material:

Total protein (BRADFORD 1976). Coomassie brilliant blue G method was applied utilizing a set of reagents manufactured by Bio Rad Laboratories, California, USA. The influence of the contrast media on the absorbance (A_{595}) of the dye-protein complex was of no significance.

Creatinine was quantitated by the standard Technicon SMA 12/60 method.

Albumin (mol wt 65000), **Immunoglobulin G** (IgG) (mol wt 150000–160000) and **α -macroglobulin** (mol wt 725000). These were assayed using the Mancini single radial immunodiffusion (SRID)

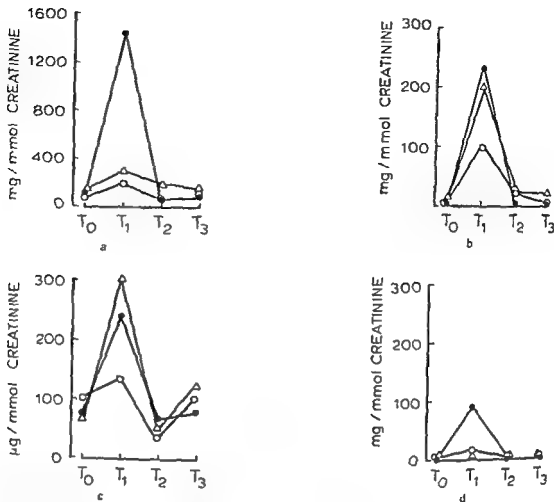


Fig 1 Median values of a) total protein b) albumin c) β_2 microglobulin and d) IgG in urine from patients examined by selective nephroangiography before (T_0) 2 h (T_1) 24 h (T_2) and 2 to 3 days

(T_3) after injection of contrast media: ● Iopaque Cerebral Amipaque △ Urografin 60°.

technique (MANCINI *et al.* 1965). The LC (low concentration) immunodiffusion Partigen plates (Behring AG) were applied for the analyses.

β_2 -microglobulin (mol wt 12000) (PETERSON & BERGGÅRD 1971). β microglobulin was estimated by the radio-immuno assay Phadebas test (Pharmacia Sweden).

Protein concentrations were calculated as mg protein/mmol creatinine for total protein, albumin and IgG globulin and as μ g/mmol creatinine for β microglobulin.

None of the contrast media interfered with the determinations of proteins when added to urine up to a concentration of 50 per cent.

Results

Most patients had slightly elevated values of total protein in urine before angiography. As the aim of the investigation was to evaluate the effect of injection into the renal artery, no attempt was made to

evaluate whether the proteinuria was pathological or physiologic.

Wide variations in total protein values were observed both before and 2 hours after injection of contrast medium with a range of 0 to 400 mg/mmol. The high correlation between total protein, IgG and albumin appears in Table 1.

Patients with albuminuria also excreted IgG and β microglobulin.

Table 1

Correlations between different proteins in urine from 40 patients before injection of contrast medium. $n=40$. The correlations were calculated from log transformed values (Spearman's correlation coefficients).

	Albumin	β_2 microglob	IgG
Total protein	0.70	0.01	0.44
Albumin		0.15	0.14
β_2 microglobulin			
$p < 0.0001$			

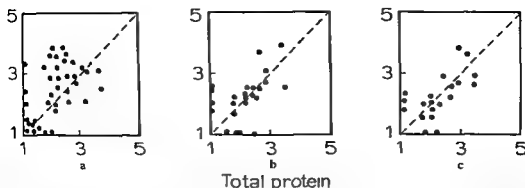


Fig. 1 Scatter diagram of the correlations of the values of total protein in urine in patients examined by selective nephroangiography before (abscissa) and after (ordinate) injection of contrast media a) Values after 7 h (n=50 r=0.47 p=0.001) b) After 7-14 h

(n=36 r=0.56 p=0.0001) c) After 2 to 3 days (n=21 r=0.59 p=0.001) All values given as log transformed values (mg/mmol creatinine)

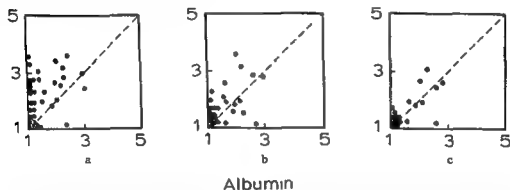


Fig. 3 Scatter diagram of all albumin values before (T) and after 7 h (T₇) 7-14 h (T₇₋₁₄) and 2 to 3 days (T₂₋₃) All values given as log transformed values (mg/mmol creatinine) Abscissa corre-

sponds to T values The ordinate corresponds to T₇ T₇₋₁₄ and T₂₋₃ values respectively a) n=48 r=0.22 p=0.071 b) n=37 r=0.67 p=0.00001 c) n=2 r=0.75 p=0.00003

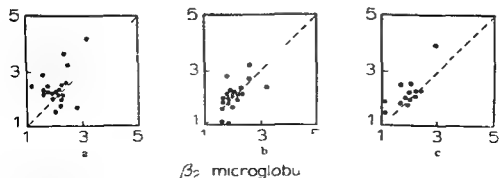


Fig. 4 Scatter diagram of β_2 microglobulin values at T (abscissa) and T₇ T₇₋₁₄ and T₂₋₃ (ordinate) All values are log transformed

($\mu\text{g}/\text{mmol}$ creatinine) a) n=46 r=0.44 p=0.0009 b) n=35 r=0.54 p=0.0004 c) n=4 r=0.6 p=0.0006

Table 2

Effects of individual contrast media on the changes in protein excretion 2 hours after selective nephroangiography and aortography (between T_0 and T_1) β -microglobulin is given as $\mu\text{g}/\text{mmol}$ creatinine other proteins as mg/mmol creatinine

Protein	Contrast medium	Number of patients with			Increase (median)	95% confidence interval of changes of proteinuria
		Decrease	No change	Increase		
Total protein	Isopaque	1	0	16	1770	131-2430
	Ampaque	5	0	11	133	-10-100
	Urografin	4	3	11	80	0-100
Albumin	Isopaque	2	4	10	109	0-1690
	Ampaque	3	0	12	70	7-100
	Urografin	5	2	10	71	-10-240
β_2 microglobulin	Isopaque	3	0	13	17	7-704
	Ampaque	5	0	9	18	-77-477
	Urografin	1	0	15	110	35-1211
IgG	Isopaque	1	6	10	90	0-100
	Ampaque	2	5	8	4	0-30
	Urografin	2	8	7		0-50

$p < 0.01$ (Wilcoxon one sample test)

$p < 0.001$

microglobulin and other proteins were not correlated possibly due to the fact that the concentration of β microglobulin was 3 orders of magnitude less than albumin (Fig. 1). Two hours after angiography the median values of total protein, albumin and β microglobulin increased significantly (Fig. 1). Median values of total protein after Isopaque was significantly higher than after the other contrast media (Fig. 1a). However, no significant differences were found in the increase of albumin, IgG and β microglobulin after angiography within the patient groups receiving any particular contrast medium. All protein levels returned to preangiographic values within 24 hours and remained so at the 2nd or 3rd day control. The slight increase (Fig. 1) in β microglobulin 2 to 3 days after angiography was not statistically significant. Fig. 2 demonstrates a significant correlation between the preangiographic and the 2 h, 24 h and the 2 or 3 day values of total protein. A considerable albumin excretion occurred in many patients 2 h after angiography (Fig. 3). At this time no significant correlation between T_0 and T_1 values for albumin was found but it became significant after 24 h (T_1) and remained so at day 2 and 3.

Two h after angiography β microglobulin had increased moderately (Fig. 4) but the values were significantly correlated with the preangiographic values and remained so at 24 h and day 2 and 3. The

increase in IgG was small and no meaningful correlation was obtained.

α macroglobulin was not found in urine from any patient at any time.

The results indicate a selective increase in glomerular permeability shortly after injection of contrast medium into the renal artery. This increase was in the present material completely reversible in almost all patients.

The calculated changes in urinary protein excretion 2 h after angiography for each contrast medium are given in Table 2. The increase in total protein was highly significant after Isopaque but of no significance after either Urografin or Ampaque.

A small but significant ($p < 0.01$) increase in albumin excretion was found after Isopaque whereas the increase after Urografin and Ampaque was not statistically significant.

β microglobulin increased significantly ($p < 0.01$) after Urografin and Ampaque. A similar increase in IgG excretion was found exclusively after Isopaque ($p < 0.01$). No persistent proteinuria was observed after any contrast medium (Figs 1-4).

Discussion

The results indicate that selective nephroangiography using Isopaque, Urografin or Ampaque

ed by a transient increase in glomerular permeability and moderate decrease in tubular reabsorption in the kidney. The changes are somewhat marked after Isopaque. The transient nature of changes indicates that no persistent lesions are present. Using iodopyracet and metrizoate IDBOHRN (1954) IDBOHRN (1956) BERG *et coll* (1957), KIRKLAND (1959) KIRKLAND & HASLOCK (1961) reported albuminuria after nephroangiography but TEJLER *et coll* reported the phenomenon only after metrizoate in man and HOLTÅS & TEJLER (1967) after diatrizoate, metrizoate and metrizamide also in dogs. Possible side effects of nephroangiography in both man and animal have been discussed by BERG *et coll* (1963) GRAZI *et coll* (1967) TALNER *et coll* (1972). TEJLER *et coll* offer two explanations for the fact that proteinuria has not been reported before their report.

The proteinuria induced reaches its maximum within few hours after angiography and is of limited duration. Immunologic assay not influenced by the high concentration of contrast medium is needed for the recognition of the proteinuria.

Proteinuria caused by nephroangiography is mainly due to an increase in glomerular permeability as demonstrated by the protein assay data. In addition, the degree of albuminuria observed cannot be explained by impairment of merely the tubular reabsorption (HARDWICKE *et coll* 1970). An increase in glomerular permeability is further demonstrated by the presence of IgG in urine (mol wt 150 000) normally retained by the glomerular barrier (STROMBERG & WALDMANN 1974). The glomeruli exhibit some sort of selectivity in the protein filtration as demonstrated by the differences in clearance of IgG and albumin (RENNIE 1971, HARDWICKE *et coll*). Furthermore, as α macroglobulin (mol wt 725 000) was not present in any urine sample, gross vascular injury in the kidneys is unlikely.

In normal patients β microglobulin (mol wt 22 000) passes through the glomerular filter before it is catabolized by the renal tubular cell (RAYNSKOV 1973). The samples containing high concentration of β microglobulin had similarly high concentrations of albumin. The increase in β microglobulin may be explained by a probable overload of tubular reabsorptive capacity due to elevated glomerular protein leakage (HARDWICKE *et coll*, RENNIE) and does not necessarily mean an actual lesion of tubular cells. The decrease of β microglobulin has parallelly fol-

lowed that of albumin further supporting the conclusion drawn.

BROMAN & OLSSON (1948) and ZINNER & GOTTLÖB (1959) have demonstrated that intravascular injection of contrast medium can change the epithelial morphology and vascular permeability. Similar effects are likely to occur in glomerular capillaries. BERG *et coll* demonstrated injury to the tubular epithelium in the rabbit after intraarterial injection of acetrizoate, iodopyracet and diatrizoate but no changes occurred after diatrizoate. EVENSEN & SKALPE (1971) using metrizoate in rabbits observed a moderate increase in the mitotic activity of tubular cells indicating healing after tubular lesions. Extensive investigations on the molecular and cellular levels are needed to reveal the mechanisms of the proteinuria following angiography.

SUMMARY

The proteinuria following aortography and selective nephroangiography in 60 patients using Isopaque, Cerebral Urografin 60% and Ampaque was investigated. The results indicate an increase in glomerular permeability and possibly an overload of tubular reabsorptive capacity after angiography. The changes are transient. No permanent injury to the kidney appears to occur.

ACKNOWLEDGEMENT

The authors wish to thank Mrs Bent Johannesen and Mrs Grethe Monsen for their excellent technical assistance. All calculations and significance tests were performed by Cand. real Dag Vaula, EDB section of the Medical Faculty, University of Bergen Medical School.

REFERENCES

- BERG N O, IDBOHRN H and WENDEBERG B. Investigation of the tolerance of the rabbit's kidney to newer contrast media in renal angiography. *Acta radiol* 50 (1958) 285.
- BRADFORD M. A rapid and sensitive method for the quantitation of microgram quantities of proteins utilizing the principle of protein-dye binding. *Analyt Biochem* 72 (1976) 248.
- BROMAN T and OLSSON O. The tolerance of cerebral blood vessels to a contrast medium of the diodrast group. *Acta radiol* 30 (1948) 326.
- EVENSEN A and SKALPE T. Cell injury and cell regeneration in selective renal arteriography in rabbits. *Invest Radiol* 6 (1971) 99.
- CRIVELLO S, LEONETTI G, ROMANO S, BONAZZI O, LITTA R. Osservazioni sull'azione nefrotica di ripetute di mezzo di contrasto in cor e di

- teriografia renale selettiva. Atti dell'accademia dei fisiocritici in Siena (In Italian) Sezione Med fis 16 (1967) 789
- HARDWICKE J CAMERON J S HARRISON J F HUMLE II and SOOTHILL J F Proteinuria studied by clearances of individual macromolecules. In: Proteins in normal and pathological urine. Part III p 111. Edited by Y Manuel J P Revillard and H Bethel Karger Basel New York 1970
- HOLTAS S and TEILER L Proteinuria following nephroangiography. IV Comparison in dogs between ionic and non ionic contrast media. Acta radiol Diagnosis 20 (1979) 13
- INBOHRN H Tolerance to contrast media in renal arteriography. Acta radiol 45 (1956) 141
- and BERG N On the tolerance of the rabbit's kidney to contrast media in renal angiography. Acta radiol 42 (1954) 121
- KIRKLAND J Massive albuminuria following aortography. Lancet 2 (1959) 1144
- and HASLOCK M Transient proteinuria following injection of contrast media. Lancet 1 (1961) 693
- KONC T MEANY T DUSTAN H and SONES F Safety of selective renal arteriography. Amer J med Sci 246 (1963) 527
- MANCINI G CARBONARE A II and HERFMANS J F Immunochemical quantitation of antigens by single radial immunodiffusion. Immunochemistry 1 (1964) 235
- PETERSON P A and BERGGÄRD I J Isolation and properties of human retinol transporting protein. J Biol Chem 246 (1971) 25
- RAVNSKOV K On renal handling of plasma proteins. With special reference to α microglobulin β microglobulin lysozyme and albumin. Scand J Urol Nephrol (1973) Suppl No 20
- RENNIE I D Proteinuria. Med Clin N Amer 55 (1971) 213
- STROBER W and WALDMANN T A The role of the kidney in the metabolism of plasma proteins. Nephron 11 (1974) 35
- TALNER L RUSHMER H and COEL M The effect of renal artery injection of contrast material on urinary enzyme excretion. Invest Radiol 7 (1972) 311
- TEILER L ALMÉN T and HOLTAS S Proteinuria following nephroangiography. I Clinical experiences. Acta radiol Diagnosis 18 (1977) 634
- ZINNER G and GOTTLIEB R Morphologic changes in vessel endothelium caused by contrast media. Angiology 1 (1959) 207

FROM THE DEPARTMENT OF DIAGNOSTIC RADIOLOGY (DIRECTOR PROF P. VIRTAMA) UNIVERSITY
CENTRAL HOSPITAL SF-20520 TURKU FINLAND

CONTRAST ENHANCEMENT PHARMACOKINETICS IN EXPERIMENTAL PANCREATITIS, DIABETES AND SUBCUTANEOUS GRANULOMA

P. B. DEAN, L. KIVISAARI and M. KORMANO

Contrast enhancement of the pancreas in computed tomography has been of only limited aid in the clinical differential diagnosis of pancreatic lesions (KIRKPATRICK et coll 1978, GERHARDT et coll 1979). Therefore animal experiments were designed to examine the calculated contrast enhancement in experimental pancreatitis and diabetes in the rat. For comparison experimental subcutaneous granulomas were examined as well. The effect of time upon the amount of contrast medium within the pancreas and other tissues following the intravenous injection of the contrast medium was analysed. Preliminary results have been presented in part previously (KORMANO et coll 1979).

Materials and Methods

Sixty Sprague Dawley rats, 3 months old, were used, 20 each with diabetes, pancreatitis and granulomas.

In order to induce diabetes an intravenous injection of Streptozotocin (60 mg/kg) was given 30 days before the pharmacokinetic experiment. All the rats became diabetic and had permanent glucosuria.

Pancreatitis was induced after laparotomy under intraperitoneal pentobarbitone anaesthesia. A blunt needle was passed through the duodenum through the papilla of Vater into the pancreatic duct and the common bile duct was temporarily occluded with an atraumatic clamp to prevent regurgitation into the biliary ducts. Olive oil (0.1 ml) was injected in 30 seconds after which the laparotomy incision was

closed. Every animal developed pancreatitis with pancreatic oedema, peritoneal fluid and typical calcifications. Twenty hours after induction of the experimental pancreatitis, ^{131}I diatrizoate and ^{131}I albumin were injected for the pharmacokinetic experiments. Eight rats died after the injection and only 12 could be used in the experiments.

In the 20 rats used as the control series, sponges measuring $1\text{ cm} \times 1\text{ cm} \times 0.5\text{ cm}$ were implanted subcutaneously in the left anterior abdomen 10 days before the pharmacokinetic experiments in order to produce a well-matured granulomatous tissue response (DOHERTY et coll 1977). Samples were taken both from the granulomatous tissue adhering to the sponge and from the fluid within the sponge as well as from the pancreas for control.

Under intraperitoneal pentobarbitone anaesthesia a mixture of unlabelled and ^{131}I meglumine diatrizoate (Angiografin) mixed with ^{131}I human serum albumin (The Radiochemical Centre, Amersham, England) was injected into each animal in 5 seconds. The meglumine diatrizoate concentration in the mixture was 512 mg/ml, the dose per rat 1300 mg/kg (612 mg I/kg) and activity 2.03 GBq/ml (54.8 $\mu\text{Ci/ml}$). Corresponding values for the human serum albumin were 1.92 mg/ml, 4.86 mg/kg and 2.03 GBq/ml (54.8 $\mu\text{Ci/ml}$). The animals were killed either 40 seconds or 2, 5, 15 or 60 min by removal of the heart at thoracotomy. The following samples were taken: mixed blood from the thoracic cage and tissues from

Table

The calculated contrast enhancement (HU) and distribution volumes of dextran and albumin in normal diabetic and pancreatic pancreases as well as in granuloma tissue at various times after intravenous injection

Tissues		Time				
		40 s	2 min	5 min	15 min	60 min
Pancreatic tissue						
Control series	Contrast enhancement	HU \pm SEM 33.4 \pm 1.4	22.7 \pm 1.8	21.6 \pm 4.2	11.8 \pm 0	4.2 \pm 0.4
	Contrast distribution volume	$V_c \pm$ SEM 19.5 \pm 1.1	19.6 \pm 1.9	28.3 \pm 5.4	25.2 \pm 2.5	10.1 \pm 3.0
	Albumin distribution volume	$V_a \pm$ SEM 3.3 \pm 0.4	3.6 \pm 0.3	3.2 \pm 0	3.4 \pm 0.1	4.3 \pm 0.4
Diabetes series	Contrast enhancement	HU \pm SEM 24.4 \pm 0.8	20.4 \pm 2.0	14.4 \pm 0.4	11.4 \pm 0.8	7.0 \pm 3.0
	Contrast distribution volume	$V_c \pm$ SEM 15.0 \pm 1.2	18.5 \pm 1.7	22.7 \pm 0.8	23.7 \pm 1.8	20.1 \pm 4
	Albumin distribution volume	$V_a \pm$ SEM 3.4 \pm 0.5	3.8 \pm 0.5	4.8 \pm 0.4	4.5 \pm 0.4	4.8 \pm 0.6
Pancreatitis series	Contrast enhancement	HU \pm SEM 48.4 \pm 2.2		34.6 \pm		9.6 \pm 5.2
	Contrast distribution volume	$V_c \pm$ SEM 27.5 \pm 1.0		41.6 \pm 4.2		7.4 \pm 9.9
	Albumin distribution volume	$V_a \pm$ SEM 2.5 \pm 0.3		2.8 \pm 0.2		7.9 \pm 1.7
Granuloma tissue						
Control series	Contrast enhancement	HU \pm SEM 18.4 \pm 2.0	30.0 \pm 3.6	31.6 \pm 0.8	29.4 \pm 2.2	9.6 \pm 1
	Contrast distribution volume	$V_c \pm$ SEM 10.7 \pm 1.0	26.7 \pm 4	41.6 \pm 1.1	64.3 \pm 5.4	174.6 \pm 68.5
	Albumin distribution volume	$V_a \pm$ SEM 1.5 \pm 0.1	1.8 \pm 0.1	2.1 \pm 0.3	2.2 \pm 0.1	3.4 \pm 0.5

pancreas, liver, spleen, kidney (renal pelvis excised and drained), stomach, duodenum and rectus abdominis muscle. The samples were placed in pre-weighed test tubes, capped, weighed and the ^{125}I and ^{131}I activities measured as described in detail previously (DEAN *et al.* 1978). The total tissue iodine content was calculated from the activity of the tissue samples. The potential contrast enhancement in Hounsfield units at 120 kV peak was then estimated from the iodine concentration using the data of HINDMARSH (1975). Contrast distribution volume was calculated by dividing each tissue contrast concentration by the blood concentration as described previously (DEAN *et al.*).

Results

While the control animals carrying granulomas were healthy, both the diabetic and the pancreatic animals were seriously ill. The average plasma concentrations of contrast medium were similar in all groups.

Contrast medium accumulation in the pancreas (Table). The highest contrast concentration and calculated enhancement of the pancreas was observed at 40 seconds in each experimental group. No significant difference was observed between the enhancement of normal and diabetic pancreas, but in pancreatitis a markedly increased accumulation throughout the one hour observation period (Fig. 1) was found. The volume of distribution in the pancreas was likewise nearly identical in control and diabetic rats for the first 5 min, against a larger distribution volume in pancreatitis (Fig. 2). At one hour a very large pancreatic volume of distribution (about 70%) was found with a large variation in both control and pancreatic rats, but a relatively low pancreatic distribution volume (30%) in the diabetic rats. The distribution volume of albumin representing the intravascular volume was of the same magnitude in the pancreas in the three experimental groups. Thus, there was no evidence of capillary breakdown and albumin leakage in the pancreatic animals indicating that the accumulation of con-

CALCULATED CONTRAST ENHANCEMENT

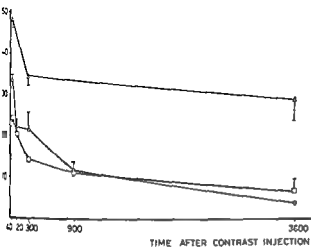


Fig 1

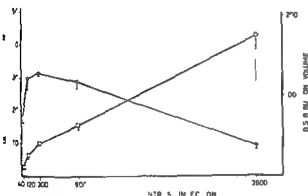


Fig 3

DISTRIBUTION VOLUME

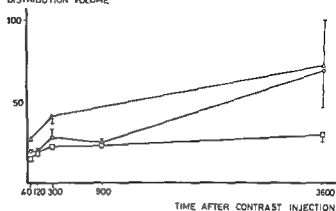


Fig 2

Fig 1 Calculated contrast enhancement ($\text{HU} \pm \text{SEM}$) of rat pancreas in relation to time (seconds) after intravenous injection of 1300 mg/kg diatrizoate Δ Pancreatitis \circ Control \square Diabetes

Fig 2 Distribution volume ($\% \pm \text{SEM}$) of diatrizoate in rat pancreatic tissue after intravenous injection (seconds) Δ Pancreatitis \circ Control \square Diabetes

Fig 3 Calculated contrast enhancement ($\text{HU} \pm \text{SEM}$) and distribution volume ($\% \pm \text{SEM}$) of diatrizoate in experimental subcutaneous granuloma of the rat after intravenous injection (seconds) \circ Contrast enhancement \square Distribution volume

last medium occurred in the oedematous extra cellular space in pancreatitis

Contrast medium accumulation in granuloma (Table Fig 3) In the granuloma tissue the accumulation was delayed and prolonged relative to the pancreas and to other tissues examined with the highest calculated contrast enhancement obtained at 5 min. The distribution volume of contrast medium rose rapidly and steady throughout the experiment. At one hour the concentration of medium in the granuloma tissue was higher than that in the blood accumulation into the granuloma exudate was the same as that in the granuloma tissue. The albumin distribution readings were low indicating relatively sparse undamaged vascularity responsible for delayed wash in and wash-out of the contrast medium into the granulomatous tissue and exudate.

Neighbouring organs of the pancreas The contrast medium kinetics in the neighbouring organs (liver spleen kidney stomach duodenum abdominal muscle) and in the plasma did not differ as

far as accumulation distribution or albumin space was concerned when the control diabetic or pancreatic animals were compared

Discussion

The kinetic behaviour of contrast medium in the control pancreatic tissue was nearly identical to that published previously in a report dealing with contrast media kinetics in normal tissues (DEAN et coll). Streptozotocin causes irreversible destruction of the beta cells (JUNOD et coll 1969) which are the principal component of the pancreatic islets. In 30 days diabetes causes no microscopic changes in the exocrine pancreas or its vascularity which comprise the main part of the pancreatic tissue mass (KIVISAARI 1979). The absence of significant change in the kinetic behaviour of the contrast medium in the pancreas following experimental diabetes is therefore no surprise providing that the general hemodynamic balance is not markedly inter-

ferred with by other consequences of diabetes KIVISAARI also suggested that vascular alterations may occur following long term diabetes especially in muscular vessels but such morphologic alterations were not reflected in the contrast enhancement of the individual tissues

Pancreatitis induced by olive oil is relatively mild. It produces a patchy inflammation with interstitial oedema and increased blood flow in the pancreas (PAPP et coll 1966 GOODHEAD 1969 KIVISAARI). The contrast enhancement either calculated or measured from clinical scans does not reflect increased blood flow unless a concomitant marked increase in the contrast containing blood volume of the organ occurs. The present results show no increase in the blood volume of the pancreas in the pancreatic rats although flow changes may have occurred. The increased contrast medium accumulation in this situation probably results from the distribution of the medium into an enlarged interstitial fluid space representing oedema.

The absence of uniformity of the pancreatitis produced in the rats is reflected in the data. However under such experimental conditions the abnormalities are likely to be much more uniform than those occurring clinically. As demonstrated by the present experiment changes occur in the tissue contrast kinetics caused by mild acute pancreatitis which theoretically could be detected by contrast enhanced CT scanning. Several limiting technical factors artefacts and inhomogeneity of the lesions interfere with their detectability in clinical CT and make kinetic contrast enhancement examination of pancreatic patients with a slow body scanner unrewarding (KIVISAARI et coll 1979).

The granuloma tissue contrast medium kinetics was completely different from that of the normal diabetic or pancreatic pancreas and the neighbouring tissues. In the stage of development of the experiment granuloma tissue was characterized by a delayed wash in and wash-out of the medium into a poorly vascularized large interstitial fluid volume. In clinical practice such a phenomenon is commonly observed in brain lesions where the absence of background enhancement makes contrast medium accumulation easily detectable (GADO et coll 1975 STEINHOFF & AVILES 1976 LEWANDER et coll 1979). Delayed and intense enhancement also occurs for example in the thickened walls of a pancreatic pseudocyst (KIRKPATRICK et coll) but rapid renal excretion of the contrast medium does not

usually allow significant uptake into the cyst fluid. Some contrast medium may enter into the glandular lumen of the exocrine pancreas itself which would account for the excessively high distribution volume readings at one hour in the present experiments. Why such phenomena did not occur in diabetic rats is not readily explainable.

The present experiments show increased contrast enhancement in the pancreas in pancreatitis. That such an increase has not been clinically appreciable may result from scanning artefacts and inability of presently available scanners to resolve or demonstrate sufficiently small differences in contrast enhancement. A general lack of appreciation of the importance of the time course of contrast enhancement and the difficulty in quantitating contrast enhancement at specific times after injection are undoubtedly also contributing factors. Improvements in scanner design particularly allowing entire organs to be scanned immediately after contrast injection (ROBB 1978) should improve the clinical application of contrast enhancement. Arterial infusion of a contrast medium during scanning (HACKFR & BECKER 1979 PRANDO et coll 1979) greatly raises the level of enhancement and improves its clinical usefulness in slow scanners. Further experimental work to define contrast enhancement in pathological conditions is needed to direct clinical attention to its potential for differential diagnosis.

SUMMARY

Contrast medium concentration in the pancreas as a function of time after intravenous bolus injection was measured in 12 rats with oil induced acute pancreatitis, 9 rats with Streptozotocin induced diabetes and 9 rats with subcutaneous granuloma induced by sponge whose pancreatic tissue was used as a control. No significant effect of diabetes was observed. Calculated distribution volume and contrast enhancement in the pancreas were increased in pancreatitis relative to diabetes and controls. The increased enhancement was due to a relatively higher accumulation into the extravascular fluid considered to represent pancreatic oedema. An even more marked and delayed enhancement was observed with the granuloma tissue and exudate apparently on a similar basis. There appears to be a possibility of differential diagnosis of some pancreatic lesions using contrast enhanced CT.

ACKNOWLEDGEMENTS

Dr Georg Zollner, Schering AG, Berlin, placed at labelled diazotrate to the authors at disposal. The technical assistance of Mrs Annelma Viitonen is gratefully acknowledged. The investigation was supported by a grant from the Signa Juselius Foundation, Helsinki.

REFERENCES

1. JÄRP B, KORMANO M and KIVISAARI L. The diagnostic potential of contrast enhancement pharmacokinetics. *Invest Radiol* 13 (1978) 533.
2. RYNN S, ANTTILA M and DEAN O B. Penetration of naproxen and salicylate into inflammatory exudates in the rat. *Ann rheum Dis* 36 (1977) 244.
3. COLEMAN H, PHELPS M E and COLFMAN R E. An intravascular component of contrast enhancement in computed tomography. Parts I and II. *Radiology* 117 (1975) 589-595.
4. LINDNER P, DURING M and KAMPHUES R. Density measurements of abdominal organs in CT. In: *Total body computerized tomography*, p 150. Edited by P Gerhardt and G van Kaick. Georg Thieme Stuttgart 1979.
5. GRINEAD B. Vascular factors in the pathogenesis of acute hemorrhagic pancreatitis. *Ann roy Coll Surg Engl* 45 (1969) 80.
6. LICKER H and BECKER H. Angio CT. In: *Total body computerized tomography*, p 256. Edited by P Gerhardt and G van Kaick. Georg Thieme Stuttgart 1979.
7. KROGH T. Elimination of water soluble contrast media from the subarachnoid space. *Acta radiol* (1975) Suppl No 346, p 45.
8. LAMB A, LAMBERT A E, STAUFFACHER W and REINOLD A. Diabetogenic action of Streptozotocin. Relationship of dose to metabolic response. *J clin Invest* 41 (1969) 179.
9. PATRICK R H, WITTENBERG J and SCHIAFFER D L. Scanning technique in computed body tomography. *Amer J Roentgenol* 130 (1978) 1969.
10. KIVISAARI L. The effect of experimental diabetes and pancreatitis on the microcirculation of the rat pancreas. *Scand J Gastroenterol* 14 (1979) 689.
11. KORMANO M and RANFACKKAO V. Contrast enhancement of the pancreas in computed tomography. *J Computer Ass Tomogr* 3 (1979) 722.
12. KORMANO M, DEAN P B and KIVISAARI L. Experimental studies on tissue identification with contrast enhancement kinetics. In: *Total body computerized tomography*, p 115. Edited by P Gerhardt and G van Kaick. Georg Thieme Stuttgart 1979.
13. LEWANDER R, BERGSTRÖM M and BERGVALL U. Contrast enhancement of cranial lesions in computed tomography. *Acta radiol Diagn* 19 (1978) 529.
14. PAPI M, MAKARA G B, HAJTMAN B and CSACI L. A quantitative study of pancreatic blood flow in experimental pancreatitis. *Gastroenterology* 51 (1966) 524.
15. PRANDO A, WALLACE S, BERNARDINO M and LINDELL M JR. Computed tomographic arteriography of the liver. *Radiology* 130 (1979) 697.
16. ROBB R. High resolution temporal cardiac tomography. Presented at the 64th scientific assembly of the Radiological Society of North America, Chicago, Illinois, 1978.
17. STEINHOFF H and AVILES C H. Contrast enhancement response of intracranial neoplasms. Its validity for the differential diagnosis of tumours in CT. In: *Cranial computed tomography*, p 151. Edited by W Lankester and H Kazner. Springer Verlag Berlin Heidelberg New York 1976.

RADIOLOGIC EVALUATION OF CHONDROMALACIA PATELLAE

F. LUND and B. E. NILSSON

Several morphometric methods for the evaluation of chondromalacia patellae at radiography have been introduced in the past (WIBERG 1941, FURBER 1952, BRATTSTRÖM 1960, FICAT & BIZOU 1972, STOUGÅRD 1975). The measurements suggested are the relationship in size and the angulation between the medial and lateral aspects of the patello-femoral joint and variables representing the size and shape of the patella itself. Normal values have also been calculated for some of these variables (FICAT & BIZOU). Subchondral sclerosis of the patella has been suggested as indicating chondromalacia (FURBER, DEPALMA 1954, FICAT et coll 1972). In addition to such morphometric measurement it was decided to include measurement of the position of the patella (patella alta, BLACKBURN & PEEL 1977). Finally, in investigations of chondromalacia patellae at this department, a shallow excavation centrally in the subchondral bone of the patella has been considered to be related to chondromalacia.

A series of morphometric variables in relation to an established diagnosis of abnormalities in the patello-femoral joint surface is now reported.

Material and Methods

The material consisted of 66 patients, 33 men and 33 women, with suggested abnormalities in the patello-femoral joints. Arthroscopy, operation or both had been performed in all cases. In conjunction with the arthroscopy or the arthrotomy, the abnormalities of the patello-femoral joints were classified according to OUTERBRIDGE (1961) as follows:

Grade I: Light brown-yellow discolouring of the articular cartilage, yields to the touch of the arthroscope or a blunt instrument, no fragmentation or fissuring.

Grade II: Fragmentation and fissuring in an area of 1-3 cm or less.

Grade III: Fragmentation and fissuring in an area of more than 1-3 cm.

Grade IV: Erosion of the articular cartilage down to the subchondral bone. This grade cannot be distinguished from patello-femoral arthrosis.

With this classification the patients were distributed as follows: Normal patello-femoral joint, 23 patients (=normal); chondromalacia patellae grade II and III, 26 patients (=chondromalacia); and chondromalacia patellae grade IV or patello-femoral arthrosis, 17 patients (=arthrosis).

Only patients in whom, before the arthroscopy or arthrotomy, radiography with a fairly good lateral and axial view of the patella had been performed were included; otherwise the radiography followed the standard procedure and no films were obtained specially for this investigation. No radiologic abnormality indicating gonarthrosis was observed on the films. After this selection, all films were mixed and evaluated blindly with regard to the diagnosis. The variables recorded appear in Fig. 1. The sclerosis was measured and classified as the extent of sclerosis divided by the patellar joint surface on the lateral film and the degree of excavation was classified as non-existent, possible or obvious.

Results

No difference was found between patients with normal patello-femoral joints, patients with chondromalacia and patients with arthrosis or grade IV chondromalacia (Table I) in any of the anthropo-

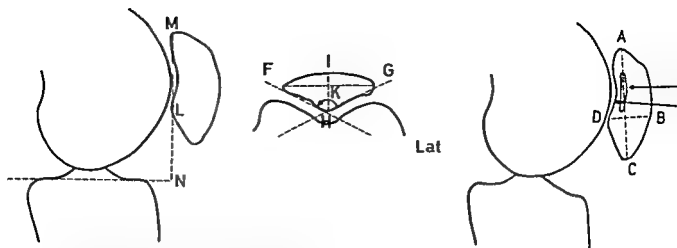


Fig 1 Morphometric variables Wiberg angle FHG Patellar depth index FG/HK Patellar shape index GH/FH Patellar relative thickness lateral BD/AC Patellar relative thickness axial

view IH/FG Patella alta variable LN/ML E Excavation Sclerosis

Table 1

Distribution of roentgen morphometric variables between sexes and diagnostic groups (average \pm SD)

Measurement	Women (n=33)	Men (n=33)	Normal (n=23)	Chondromalacia (n= 6)	Arthrosis (n=11)
Sclerosis					
Wiberg angle (degrees)	0.057 ± 0.062 122 ± 11	0.043 ± 0.030 131 ± 10	0.045 ± 0.028 124 ± 11	0.047 ± 0.008 125 ± 11	0.011 ± 0.008 131 ± 11
Patellar depth index	3.70 ± 0.81	4.03 ± 0.62	3.79 ± 0.60	3.76 ± 0.74	4.13 ± 0.86
Patellar shape index	1.46 ± 0.38	1.29 ± 0.20	1.30 ± 0.17	1.45 ± 0.36	1.30 ± 0.21
Patellar relative thickness lateral	0.43 ± 0.04	0.43 ± 0.05	0.44 ± 0.05	0.43 ± 0.04	0.4 ± 0.05
Patellar relative thickness axial view	0.47 ± 0.04	0.43 ± 0.05	0.46 ± 0.05	0.44 ± 0.05	0.46 ± 0.05
Patella alta variable	0.84 ± 0.13	0.80 ± 0.15	0.84 ± 0.16	0.84 ± 0.15	0.78 ± 0.15

metric variables except for an increased frequency of a radiologically obvious excavation of the patella in the lateral view of patients with chondromalacia. They differed significantly not only from controls ($0.01 > p > 0.001$) but also from cases with arthrosis ($0.05 > p > 0.02$, Table 2). Excavation was equally common in both sexes.

Discussion

With improved radiographic technique and with a larger number of subjects it is possible that minor and significant differences may be demonstrated between anatomically normal patello-femoral joints and joints with chondromalacia. However the data of the present series indicate that these differences could never be of such a magnitude that

the measurement could be of diagnostic value for the individual patient with patello-femoral pain. The finding of an excavation (Fig 2) seems to be more reliable. In the present series this excavation occurred in all 26 patients with chondromalacia except two. Excavation of the patellar subchondra

Table 2

Chi square representation of patellar excavation in relation to diagnosis

Excavation	Normal	Chondromalacia	Arthrosis
None	11	5	7
Possible	8	5	1
Obvious	6	19	



Fig 2 Patellar excavation and the arthrotomy finding in the same patient 19 year old man with patello-femoral symptoms since one year Two months after radiography the knee was

operated upon The lesion of the patellar cartilage was classified as chondromalacia grade III

bone was noted by HAGLUND (1926) who assumed that this abnormality was related to trauma FICAT (1970) referred to it as *l'encoche de Haglund* ØVRE (1936) and others have stated that it is too common to be of clinical importance The abnormality is frequently observed in films of patients with chondromalacia illustrated in the literature and was commented upon by SMILLIE (1974) although it has not been systematically explored previously The excavation of the patellar subchondral bone in combination with a smooth or even bulging patellar cartilage at arthroscopy suggests that the patellar cartilage may be thicker than average Since it has been demonstrated by WIBERG and others that the patellar joint surface has the thickest hyaline cartilage of all joints in the human body additional thickening may be an obstacle for the distribution and perfusion of fluid through the cartilage Therefore nutritional deficiencies which have been suggested as one cause of chondromalacia (HIRSCH 1944) may occur A causative relationship between the excavation of the subchondral bone and the chondromalacia or simply an interaction by some other unknown variable may exist Even if other diagnostic means today are available for the diagnosis of abnormalities in patello-femoral joint such as arthrography (HORNS 1977) and arthroscopy (LUND & NILSSON 1980) the radiologic abnormality described may be of interest for the evaluation of standard knee films

SUMMARY

In a series of patients in whom the patello-femoral joint had been examined by arthroscopy in conjunction with arthrography or both previously obtained films were reviewed A series of radiologic morphometric measurements with bearing on the shape of the patella and the patello-femoral joint was carried out and compared between patients who had normal patello-femoral joints patients with chondromalacia grade II or III and patients with chondromalacia grade IV or arthrosis No difference between the three groups in any of the variables was found However a shallow excavation in the subchondral bone was observed in the lateral view of the patella in most of those patients with proven chondromalacia patellae

ACKNOWLEDGEMENTS

Financial support was obtained from the Swedish Medical Research Council (project No B 77 17X 2737 09B) and the Greta and Johan Kock and Alfred Osterlund Foundations

REFERENCES

- BLACKBURN J S and PEEL T E A new method of measuring patellar height *J Bone Jt Surg* 59 B (1977) 241
- BRATTSTRÖM H Patella shape and degenerative changes in femoro-patellar joint *Acta orthop scand* 29 (1960) 153
- DEPALMA A F Diseases of the knee Lippincott Philadelphia 1954

- FICAT P. Pathologie femoro patellaire. Masson & Cie Paris 1970
- und BIZOU H. Chondromalacia patellae und femoro-patellare Arthrose. *Helv. chir. Acta* (1967) Suppl. No 11
- PHILIPPI J., CLZACO J. P., CABROL S. et BILLOSI J. Le syndrome d'hyperpression externe de la rotule (S. H. P. E.). *J. Radiol. Electrol.* 53 (1972) 845
- FURMAIER A. Über die Röntgenologie des Femoro Patellargelenkes mit besonderer Berücksichtigung der Diagnose der Chondropathia patellae. *Arch. orthop. Unfallchir.* 45 (1952) 126
- HAGLUND P. Die hintere Patellarkontusion. *Z. Chir.* 53 (1926) 1757
- HIRSCH C. A contribution to the pathogenesis of chondromalacia of the patella. A physical, histologic and chemical study. *Acta chir. scand.* (1944) Suppl. No 83
- HUNTS J. W. The diagnosis of chondromalacia by double contrast arthrography of the knee. *J. Bone Jt. Surg.* 59 A (1977) 119
- LUND F. and NILSSON B. E. Arthroscopy of the patello-femoral joint. To be published in *Acta orthop. scand.*
- OUTERBRIDGE R. E. The etiology of chondromalacia patellae. *J. Bone Jt. Surg.* 43 B (1961) 767
- OWRI A. Chondromalacia patellae. *Acta chir. scand.* (1936) Suppl. No 41
- SMILLIE I. S. Disease of the knee joint. Churchill Livingstone, Edinburgh and London 1974
- STOLCFARD J. Chondromalacia of the patella. Incidence, macroscopical and radiographical findings at autopsy. *Acta orthop. scand.* 46 (1975) 809
- WIBERG G. Roentgenographic and anatomic studies on the femoro patellar joint. With special reference to chondromalacia patellae. *Acta orthop. scand.* (1941) Suppl. No 12

SACROILIAC JOINT INVOLVEMENT IN CLASSICAL OR DEFINITE RHEUMATOID ARTHRITIS

A. DE CARVALHO and H. GRAUDAL

Few reports have appeared concerning lesions of the sacroiliac joint in connection with rheumatoid arthritis (SHARP 1957, DIXON & LIENCE 1961, SIEVING & LAINE 1963, DIXON 1964, WILKINSON & KLE 1966). The present report is part of a radiologic survey of the progression of rheumatoid arthritis in all limb joints (DE CARVALHO et coll. 1980) in the cervical spine (DE CARVALHO & GRAUDAL 1980) and in the sacroiliac joints. The purpose is to describe this progression in relation to the duration of the disease and to investigate the association of certain clinical and laboratory manifestations with the more or less severe progression of the disease.

Material and Methods

The material consisted of the same 188 patients with classical or definite rheumatoid arthritis described previously (DE CARVALHO et coll.). A total of 564 radiographic examinations of the sacroiliac joints was performed. The sacroiliac joints were exposed with the patient lying supine and the side concerned being raised by 15 to 25°. In most cases, antero-anterior films were also exposed with the beam directed cranially 5 to 10°. However, in order to reduce the radiation dose, these films were not taken if survey film of the pelvis was available. All films were evaluated by the same observer (A.C.) without knowledge of the clinical findings.

Arthritic lesions of the sacroiliac joints were classified according to 5 grades.

Grade 0: normal findings

Grade 1: slight or doubtful changes (for example osteoporosis)

Grade 2: small but definite erosive lesions with blurring of the joint surfaces

Grade 3: more severe erosive lesions of the joint surfaces, possibly with some degree of ankylosis caudally in the joint

Grade 4: definite ankylosis (Fig. 1)

The frequency of the abnormalities was mapped in relation to the time of clinical onset of the disease. As the degree of involvement of the right and the left sides was identical, both sides are considered simultaneously in the following comments. Together with the radiographic examinations, a number of clinical and laboratory parameters were recorded. For statistical purposes, the mean degree of involvement of the sacroiliac joints, which were examined in each period of duration of the disease, was calculated. For this purpose, the weight 0 was attached to the grades 0 and 1 of the degree of involvement and the weights 1 to 3 were attached to the grades 2 to 4. This was done in order to avoid grade 1, which is an uncertain or non-specific stage. The mean degree of involvement, as expressed in this manner, was found to behave almost as a linear function of the square root of the duration of the disease and thus a linear regression analysis was justified. The basic statistical method has been discussed previously (DE CARVALHO et coll.).

After dividing the patients into two groups, a group with positive findings (noduli, high ESR, etc.) and a control group (without such findings but with rheumatoid arthritis), it was possible in each case to compare the regression lines by means of a scale 0 to 4 of the degree of divergence. 0 means that no differ-

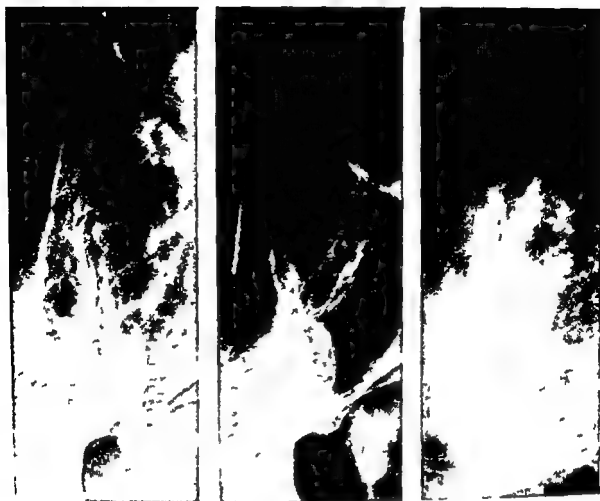


Fig. 1 Grades 2 to 4 illustrated in the same joint with increasing duration of the disease

ence was found between the two groups 1, 2 and 3 express increasing degrees of divergence between the distributions and degree 4 expresses two completely separated distributions. Equivocal results were indicated by the letter E most frequently in cases of intersecting regression lines. The figures of the 0 to 4 scale are accompanied by a sign + indicating a positive relation between the factor tested and more severe degrees of involvement of the joints. Moreover the *p*-value was calculated in each case. The parameters tested and the control groups appear in Table 2. Details concerning the laboratory parameters can be obtained from published reports (BICHEF *et coll.* 1957, FABER & FLILING 1965, FLILING *et coll.* 1967, DE CARVALHO & GRAUDAL 1980). For statistical purposes the duration of the disease was divided into periods of one year when the duration was 1 to 13 years. With longer durations the periods were 14 to 15, 16 to 17, 18 to 20 and 21 to 25 years.

Previously the average degree of involvement in 20 groups of limb joints and in each segment of the cervical spine was reported (DE CARVALHO *et coll.*). For an analysis of the relation between the degree of involvement of these joint groups and the degree of sacroiliac lesion the series was divided into a group with positive finding and a control group using lesion of the sacroiliac joint as the distinguishing feature. This was done as regards 27 joint groups (Table 3). The degree of divergence between the interest group and the control group was also classified according to the 0 to 4 scale.

Results

The distribution of the radiologic abnormalities as related to the duration of the disease appears in Table 1 and Fig. 2. The percentage of joints with grade 2 to 4 showed only a slight tendency to increase with the duration of the disease. The percent

Table 1

Percentage of sacroiliac joints with rheumatoid arthritic lesions of grade 0 to 4 as related to the duration of the disease based on 564 radiographic examinations (1128 joints)

Duration of the disease (years from onset)	No of classified joints	Severity of the affection				
		Grade 0	Grade 1	Grade 2	Grade 3	Grade 4
1-2	112	32.1	35.7	29.5	2.7	0
3-4	157	23	41.5	29.6	5.9	0
5-6	130	22.3	37.3	38.5	5.4	1.5
7-8	132	21.2	33.3	40.9	4.6	0
9-10	132	17.4	29.6	40.9	8.3	3.8
11-12	94	19.2	29.6	40.4	9.6	4.3
13-15	140	12.1	32.9	46.4	6.4	2.1
16-20	134	6	47.5	36.6	14.9	0
≥21	107	3	33.3	53.9	7.8	2

Table 2

Relationship between the course of rheumatoid arthritis in the sacroiliac joints and clinical and laboratory parameters

Group with positive findings	Controls	Degree of divergence (group with positive findings)	p <
Age at the onset ≥41 years	Remaining patients	+1	0.03
Women	Men	-1	0.1
Presence of subcutaneous nodules	No nodules	E	0.05
Elevated ESR (≥41 mm/h) at least at one time	Remaining patients	+1	0.005
Very elevated ESR (≥91 mm/h) at least at one time	Remaining patients	+1	0.005
Rheumatoid factor present. Latex test or Rose Waaler test positive at least at one time	Rheumatoid factor absent in all investigations	0	0.5
Latex test and Rose Waaler test both positive at least at one time	Remaining patients	0	0.2
High titre of the Rose Waaler test (>160) at least at one time	Remaining patient	-1	0.01
Very high titre of the Rose Waaler test (≥640) at least at one time	Remaining patients	0	0.25
Organ non specific antinuclear antibodies present (+, ++ or +++) at least at one time	Organ non specific anti nuclear antibodies absent in all investigation	0	0.06
Organ non specific antinuclear antibodies strongly positive (+++) at least at one time	Organ non specific anti nuclear antibodies absent + or ++ in all investigations	1	0.005
Granulocyte specific antinuclear antibodies present (+, ++ or +++) at least at one time	Granulocyte specific anti nuclear antibodies absent in all investigations	0	0.1
Granulocyte specific antinuclear antibodies strongly positive (+++) at least at one time	Granulocyte specific anti nuclear antibodies absent + or ++ in all investigation	1	0.3

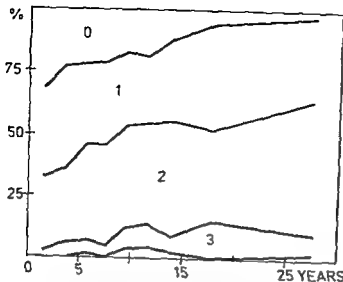


Fig. 2 Distribution of grades 0 to 4 of joint involvement as related to the duration of the disease. Areas between the curves express the relative frequency of each grade

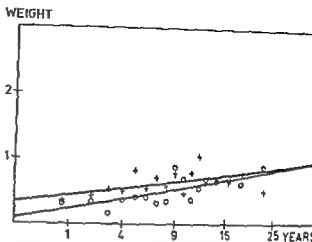


Fig. 3 Relation between the average degree of sacroiliac joint involvement and an age >40 years at the onset of the disease (+) Controls (0). Degree of divergence $+1$ ($p < 0.03$)

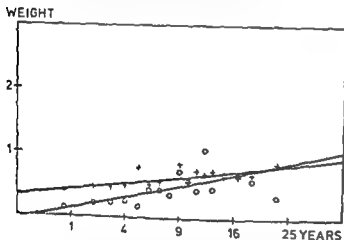


Fig. 4 Relation between the average degree of sacroiliac joint involvement and an increased ESR (>41 mm/h) at one time at least (+) Controls (0). Degree of divergence $+1$ ($p < 0.005$)

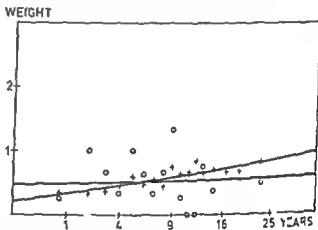


Fig. 5 Relation between the average degree of sacroiliac joint involvement and presence of rheumatoid factor (+) Controls (0). Degree of divergence 0 ($p < 0.5$)

age with ankylosis (grade 4) was low and showed no tendency to increase with the duration of the disease. Grade 3 was also relatively infrequent. Most joints involved had slight erosive abnormalities (grade 2) while the remaining joints were normal or with unspecific abnormalities (grades 0 and 1).

The relationship between clinical and laboratory parameters and the severity of the involvement of the sacroiliac joints is given in Table 2. The apparent discrepancy between slight degrees of divergence ± 1 and some significant or highly significant p -values is due to the fact that grade 3 and 4 lesions are rarely present. This means that the average degree of involvement was low despite significant divergence between the groups tested. The factors definitely related to more severe degrees of involve-

ment were an age at onset ≥ 41 years (Fig. 3) and an ESR ≥ 41 and ≥ 91 mm/h at least at one time (Fig. 4). An inverse relation was found with Rose-Waaler titre >160 .

No certain relationship was established between the degree of involvement and the following factors: sex, seropositivity for the rheumatoid factor, positivity of both the Rose-Waaler and the latex tests, very high titres (≥ 640) of the Rose-Waaler test and the presence or strong positivity of organ non-specific and granulocyte specific antinuclear antibodies.

The relationship between the degree of involvement of the sacroiliac joints and the remaining joint groups appears in Table 3.

Bothers occurred only in two men and one

Table 3

Difference in the degree of affection in joint groups when the patients are selected according to the presence or degree of sacroiliac lesion and compared with controls. The degree of divergence between the regression lines for the average degree of affection expresses this difference

Joint group	SI joint affection of grade 3-4 at least once (as compared with the remaining patients)		SI joint affection of grade 2 at least once (as compared with the patient group where no certain lesion was detected)	
	Degree of divergence	p <	Degree of divergence	p <
C1-C2 segment	+2	0.001	0	0.8
C2-C3 segment	+2	0.0005	+1	0.03
C3-C4 segment	+1	0.001	+2	0.001
C4-C5 segment	+1	0.25	+2	0.0005
C5-C6 segment	+1	0.04	+2	0.0005
C6-C7 segment	0	0.6	+	0.0005
C7-Th1 segment	+1	0.15	+2	0.0005
Shoulder	+3	0.0005	+2	0.0005
Elbow	+3	0.0005		0.6
Wrist	+3	0.0005	+1	0.01
CMC1 thumb	+4	0.0005	+2	0.005
CMC -5	+4	0.0005	+2	0.0005
MCP 1 thumb	+3	0.0005	+1	0.1
MCP 2-5	+3	0.0005	+1	0.0005
PIP fingers	+3	0.0005	+1	0.01
IP 1 thumb	+1	0.2	0	0.3
DIP fingers	+2	0.04	0	0.5
Hip	+4	0.0005	+3	0.0005
Knee	+4	0.0005	+1	0.02
Ankle	+3	0.0005	+3	0.0005
Tarsus	+3	0.0005	+3	0.0005
Metatarsal joint	+3	0.0005	+	0.0005
MTP 2-5	+2	0.001	+2	0.001
MTP 1 hallux	+	0.05	0	0.2
PIP toes	+2	0.0005	+1	0.04
IP 1 hallux	+2	0.0005	+	0.0005
DIP toes	+1	0.1	0	0.4

C Cervical segment CMC Carpometacarpal joints MCP Metacarpophalangeal joints PIP Proximal interphalangeal joints DIP Distal interphalangeal joints IP Interphalangeal joints MTP Metatarsophalangeal joints

who were seropositive no seronegative patients had psoriasis

Discussion

General agreement concerning the value of the anteroposterior projections for the sacroiliac joints exists

The use of the oblique projection was based partly on tradition partly on the desire not to change the technique in order to provide comparable results during a long period of observation. Others have preferred the postero-anterior projection (GRAINGER 1960) the antero-posterior projection (FORESTIER 1964) or tomography (WILKINSON &

MEIKLE) Although tomography was performed on several of the present patients the results have not been used for evaluation purposes in this report.

The findings confirm that severe grades of sacroiliac lesions are rare in rheumatoid arthritis even after many years of the disease but small erosions occur rather frequently. In other series of patients with rheumatoid arthritis abnormalities of the sacroiliac joints have been found in 47 per cent of 90 patients (SHARP et coll. 1954) and in 36 per cent of 120 joints in advanced stages of the disease (DIXON). Unequivocal lesion was found in 22 per cent of 81 patients (MASON et coll. 1959). Abnormalities that seem to correspond to grades 2 to 4 in the present classification have been found in 36.7 per cent of women with rheumatoid arthritis (SIEVERS & LAINE 1963) but also in 16.3 per cent of a control group. The high percentage of grade 2 involvement after 1 to 2 years from the onset and the rather flat curves in Fig. 2 suggest that at least part of the involvement may be caused by factors other than rheumatoid disease. This is in accordance with the findings of DIXON & LIENCE and SIEVERS & LAINE. On the other hand the positive relation of both grade 2 and 3 to 4 to severe involvement of practically all other joints and of grades 2 to 4 to a high ESR suggest a connection with the severity of rheumatoid arthritis. However the positive relation of sacroiliac lesion to an age at onset ≥ 41 years distinguishes this involvement from that of all limb joints except the distal interphalangeal joints of the fingers and toes. Moreover definite involvement of the sacroiliac joints was not associated with seropositivity for rheumatoid factor or with the presence of granulocyte specific antinuclear antibodies although these factors are associated with more severe degrees of involvement in most limb joints except the distal interphalangeal joints (DE CARVALHO & GRAUDAL). A positive relation to a higher age at onset and absence of relation to sex are features that differ from those of ankylosing spondylitis. Furthermore the radiologic appearance differs from that of ankylosing spondylitis: the tendency towards developing ankylosis was slight; no tendency towards reactive sclerosis was found; involvement more often occurred in the central ends of the joints; erosions were often ill-defined; pseudo-widening of the joint space was rarely found where narrowing was the rule.

The findings in the sacroiliac joints give rise to the question what the abnormalities indicate. Generally

a relation to the severity of rheumatoid arthritis rather than the immunologic condition is suggested.

SUMMARY

In 188 patients with rheumatoid arthritis 564 radiologic examinations of the sacroiliac joints were performed. Severe blurring of the joint space or ankylosis were uncommon. The involvement was related to an age > 40 years at the onset, high values of the ESR and involvement of most joint groups in the limbs and cervical spine. Sex, presence or high titres of the rheumatoid factor and antinuclear antibodies were unrelated to lesions of the sacroiliac joints. A relation to the severity of rheumatoid arthritis rather than to the immunologic condition is suggested.

ACKNOWLEDGEMENT

The authors wish to express their gratitude to Anders Holst Andersen and Bent Jørgensen, advisory statisticians, for invaluable assistance. This investigation has been supported by the Danish Medical Research Council.

REFERENCES

- BICHEL J, HOLTEF C, JENSEN K. B. and CHRISTENSEN A. S. The Rose-Walker test with special reference to cancer. *Acta med scand* 158 (1957) 351.
- CARVALHO A. DE and GRAUDAL H. Radiographic progression of rheumatoid arthritis related to some clinical and laboratory parameters. To be published in *Acta radiol. Diagnosis*.
- Cervical spine involvement in classical or definite rheumatoid arthritis. To be published in *Acta radiol. Diagnosis*.
- and JØRGENSEN B. Radiologic evaluation of the progression of rheumatoid arthritis. *Acta radiol. Diagnosis* 21 (1980) 115.
- Evaluation of the progression of rheumatoid arthritis. Significance of age at onset and sex. To be published in *Acta radiol. Diagnosis*.
- DIXON A. ST. J. The sacro-iliac joint in adult rheumatoid arthritis. In: *Proceedings of the International Symposium on the radiological aspects of rheumatoid arthritis* p. 267. Excerpta Medica, Amsterdam 1964.
- and LIENCE F. Sacro-iliac joint in adult rheumatoid arthritis and psoriatic arthropathy. *Ann rheum Dis* 20 (1961) 247.
- ELLING P., GRAUDAL H. and FABER V. Organ specific and organ non specific auto-antibodies in rheumatoid arthritis. *Acta med scand* 182 (1967) 707.
- FABER V. and ELLING P. Anti nuclear factors (ANF) as determined by the immunofluorescent antibody technique. *Acta med scand* 177 (1965) 499.
- FORSTNER J. Sacro-iliac joints. In: *Proceedings of the International Symposium on the radiological aspects of rheumatoid arthritis* p. 277. Excerpta Medica, Amsterdam 1964.
- GRANDTNER H. G. The radiology of ankylosing spondylitis. *Rheumatism* 16 (1960) 3.

- MASON R M MURRAY R S OATES J K and YOUNG A C A comparative radiological study of Reiter's disease, rheumatoid arthritis and ankylosing spondylitis. *J Bone Jt Surg* 41 (1959) 137
- ROPER M W BENNET G A COBB S JACOB R and JESSAR R A 1958 revision of diagnostic criteria for rheumatoid arthritis. *Bull rheum Dis* 9 (1958) 157
- SHARP J Differential diagnosis of ankylosing spondylitis. *Brit med J* 1 (1957) 975
- CALKINS E COHEN A S SCHUBART A F and CALABRO J J Observations of the clinical, chemical and serological manifestations of rheumatoid arthritis based on the course of 154 cases. *Medicine (Baltimore)* 43 (1954) 41
- SIEVERS K and LAINE V The sacro-iliac joint in rheumatoid arthritis in adult females. *Acta rheum scand* 9 (1963) 222
- WILKINSON M and MEINLE J A K Tomography of the sacro-iliac joints. *Ann rheum Dis* 25 (1966) 433

EXTERNAL BONY AUDITORY CANAL AND THE TYMPANIC BONE

Morphologic properties and influences on the tomographic reproduction

O. ECKERDAL and J. AHLQVIST

The external auditory canal is developed postnatally. At the time of birth the tympanic membrane is attached to the border of the tympanic ring and is situated in close relation to the surface of the skull. At an early stage the brain capsule has a fairly even surface. Several cranial superstructures, as the superorbital bone, the otic and the mastoid bone, develop postnatally and a gradual divergence between the internal and external skull surfaces occurs (WEINMANN & SICHER 1955). In the tympanic region the bone remodelling involves a development of the roof of the external auditory canal. The tympanic bone develops directly from the C-shaped ring at the middle ear. This bone forms the floor and the anterior wall of the auditory canal which is normally closed in the third year of life (WEINMANN & SICHER).

The significance of morphologic variations and their influence on the reproduction in the tomographic images may be of clinical interest (VALVASORI & PIERCE 1964, LAPAYOWNER & CLIFF 1969, ECKERDAL & AHLQVIST 1979). The morphology of the tympanic bone, an integrated part of the temporomandibular joint and the external auditory canal, varies (ECKERDAL et coll. 1978). In the closed medial part of the skeletal auditory canal small defects can persist even in the adult stage. WEINMANN & SICHER calculated the percentage to almost 20% while ECKERDAL et coll. reported 5.2 per cent in an autopsy material.

Factors influencing the tomographic reproduction may be defined in a generalized form. Such analyses are most often made on different kinds of test objects of a well-defined nature (MATTSSON 1969,

LITTLETON 1970). However, in the diagnostic situation it is of interest to learn about the special image formation in the relevant morphologic area.

In phantom experiments intended to decide the limits of reproduction of small skeletal defects in subtle bony walls of the head, VON REISNER (1970) demonstrated the multi-causal situation when reproducing true anatomic objects. Not only the angulation of a bony wall but its thickness had a direct influence on the image formation. Other factors were environmental such as adjacent high attenuating parts of the object, relations to soft tissues or gas-filled cavities, the tomographic movement and angulations. ECKERDAL (1973) made an image formation analysis of generalized as well as specialized character in an investigation of the petrous bone and the proximal part of the mandible. The conclusions as concerns image formation factors were in agreement with those of VON REISNER.

The external auditory canal falls within the image field in several types of examinations. The morphologic conditions including soft tissues and gas-filled cavities in the area of interest vary. Consistently image phenomena may exist, perhaps not even realized, which in the individual diagnostic situation may be of interest.

A morphologic radiographic investigation on an autopsy material was performed, analysing the geometry and dimensions of different parts of the closed bony auditory canal, the width of the tympanic bone separating the temporomandibular joint cavity and the auditory canal. The osseous struc-

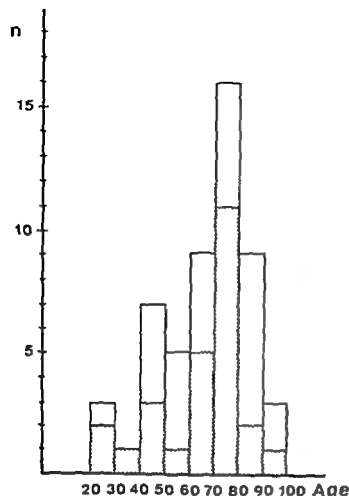


Fig. 1. Age and sex distribution. □ males, ■ females.

tures of the tympanic bone were also analysed. The morphologic base defined in this way created a basis for an analysis of the evaluation of clinical tomographic examinations and offered a possibility to analyse and describe some aspects of the nature of the tomographic hypocycloidal method *per se*.

Material and Method

Fifty-three autopsy specimens, 26 males and 27 females, consisting of the temporal bone and the proximal part of the mandible were used. Age and sex distribution appear in Fig. 1. The specimens were chosen at random during a 6-year period. No known developmental disturbances were accepted. The specimens were deep frozen, embedded in carboxymethyl-cellulose and frozen in a mixture of dry ice and hexane (ULBRICH coll. 1971). Tomography of the specimen blocks was performed and sectioning in a microtome in corresponding sagittal layers (ECKERDAL 1973). The tomograph was Philips Massiot with hypocycloidal movement, nominal focal size 0.6 mm, the exposure time was 6

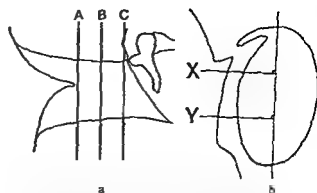


Fig. 2. a) Diagrammatic representation of the external bony auditory canal in a p. aspect. Three sagittal morphologic layers A, B, C are indicated. These layers were used in the morphometric calculation of the area of the auditory canal. b) Diagrammatic representation of a sagittal morphologic layer. The system was used to calculate the thickness of the tympanic bone separating the auditory canal from the temporomandibular joint. A line with the auditory canal approximately parallelized with a tangent to the posterior wall of the mandibular joint cavity was divided into three even parts. The thinnest part of the tympanic bone inscribed between the perpendiculars X and Y was measured.

seconds at 53 kV and 25 mA. Siemens Saphir intensifying screens and Kodak RP film were used.

Microradiography of the specimens was performed according to the technique previously described (ECKERDAL 1972). The microtome section were adhered to a cellulose tape (3M 810). The information was gained from layers of different kinds which were related to each other with the aid of the three-dimensional orientation system visible in the tomograms as well as in photos of the specimen sections. Thus the information was gained from tomograms, microradiograms and histologic preparations of 20 μ m microtome sections (ECKERDAL 1973).

The microradiograms and sometimes as supplements the histologic sections adhered to the cellulose tape were projected and enlarged in a Werth Profile projector Record 72 as described by ECKERDAL & AHLQVIST. The different measurements were taken on three sagittal sections integrated in a continuous series where the preserved individual layers were separated by 1 mm. The selected sections were taken from the totally closed part of the bony auditory canal according to the system indicated in Fig. 2a. In the schematic drawing of an auditory canal in a p. aspect the chosen morphologic layers were A) the first lateral one where a total closure of the auditory canal is to be found, B) a layer in the middle of the closed part of the canal with a length of 6.5 mm (measured) and C) the last medial layer within the complete auditory canal. When the individual closed auditory canal had an uneven millime-

Table 1

Area (mm²) of the skeletal auditory canal in three different morphologic sections

Age	Total group			Females			Males		
	x	S	Range	x	S	Range	x	S	Range
External	65.5	13.0	41.3-90.8	65.0	11.7	48.0-87.3	66.1	14.8	41.3-90.8
Central	50.7	9.7	32.5-87.8	51.6	10.6	36.0-8.8	50.0	8.8	3.5-69.8
Medial	47.5	9.8	33.8-78.8	47.9	10.4	36.3-78.8	47.1	9.3	33.8-73.3

ter length the central layer of calcification B was displaced one step medially in 45 cases and laterally in 8 cases. The latter was due to inadequate quality in the preservation of these layers. The level numbers could thus be 23, 26 or 28 mm. The thickness of the bony wall separating the auditory canal and the temporomandibular joint was recorded according to a system accounted for in Fig. 2b. A line within the auditory canal approximately parallelized with the tympanic wall was divided into three even parts. The thinnest part of the tympanic bone in between the perpendiculars X and Y was measured. Taking the measurements on the enamel paper a sliding calliper was used. The area of the closed part of the auditory canal was calculated on the tracings with an Aristo planimeter.

Because the morphologic and positional factors were decided through the histologic and radiographic approach it proved to be possible to evaluate the tomographic images with close attention to the influence of morphologic variation in succeeding layers.

Results

Morphologic considerations The external bony auditory canals proved to have continuous changes of calibre as well as of shape when analysed in succeeding sagittal layers: tomographic or histologic. The results of the calculations of the calibres of the sagittal projections of the canals are summarized in Table 1. The changes of the calibre are transformed and given in a two-dimensional and schematic drawing where the canal is given in a postero-anterior view (Table 2). On the basis of these results the canals could be divided into 3 groups: cone shaped, hour glass shaped, ovoid shaped. The difference between the areas in layers A, B, C could be considerable despite the relatively short interindividual distances which depended on




the total length of the canal. These distances were maximally 5 mm but as a mean 3 mm. In 4 cases the areas in the medial layers were 40 per cent of the lateral. The corresponding value of the whole group was 75 per cent. In one case only a remarkable widening was observed in the medial layer which was 68 per cent larger than the lateral. Even the hour glass shaped canals proved to have lateral orifices larger than the medial (Table 1).

It was not only the calibre of the bony auditory canal which varied but also the shape as observed in lateral sections. This was represented by a wide spectrum of for example: strict circular, oval, heart shaped or triangular form (Fig. 3). Different shapes could be present in the same specimen. In some cases the main character could be oval but the angulation of its long diameter changed from layer to layer to describe a screw like canal (Figs. 4, 5).

The anterior bony wall of the auditory canal had rich morphologic variation. The width of the wall is given in Table 3. The mean value of the width was similar in the lateral and central parts (A, B) whereas the medial part (C) in the vicinity of the middle ear was considerably thinner. The range of the wall dimensions was fairly wide: 0.21 to 4.10 mm for the

Table 2

Relation between the areas in the three sagittal layers of the bony auditory canal transformed to a schematic drawing. Three different types are recorded as regards alibi: o = oval shape, m = middle ear

Shape	Number	Per cent
	34	64.1
	17	3.1
	2	3.8

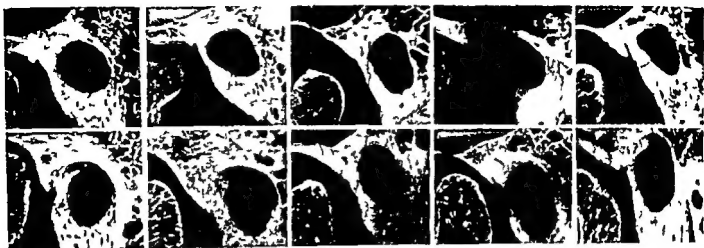


Fig. 3. The shape of the external bony auditory canal varies considerably, for example circular, oval, triangular, trapezoidal

and heart-shaped. Microradiography, 20 μ m sections from different specimens.

total group (Table 3). The values were greater regarding males but the differences between the sexes were not significant. The bony structure differed on comparing the very thin walls with the thick ones. The thin walls were composed of compact cortical bone. The thicker walls sometimes revealed a subtle structure composed of minute cavities. Some different types are illustrated in Fig. 6.

Radiographic considerations. Straight auditory canals with minor variation of the calibre were sharply delineated in the tomographic images provided that the long axis of the canal was parallel or only deviated up to 15°. When the auditory canals had considerable calibre changes within short distances or too wide angulation, partly or totally the tomographic images were characterized by marginal blurring. The character and degree of this blurring was related to the constellation of individual morphologic properties. When tomography of screwlike canals was performed it was possible in succeeding tomographic images to perceive a marginal tomo-

graphic blurring successively displaced around the periphery of the image of the canal (Figs 5, 6). Further skeletal demarcations in the tomographic images of the tympanic bone found in explanation in the existence of ultimately thin bony walls. A true reproduction of the central and medial part of the canal in these cases demanded an optimum orientation of the tympanic bone. The tolerance of deviation from a parallel relation between the skeletal surface and a perpendicular was remarkably lower than the theoretic one for these thin bone walls.

Discussion

Comments on the methods. The area is inscribed within the contours of the canals (Table 1) cannot be simply transformed to length dimensions. The change of shape of the canals interferes with the dimensions of the auditory canal as they can be perceived in, for example, postero-anterior projections. Even if the measurements of the area are

Table 3
Width of the tympanic bone in the anterior wall of the auditory canal

Layer	Width (mm)								
	Total group			Females			Males		
	\bar{x}	S	Range	\bar{x}	S	Range	\bar{x}	S	Range
Lateral	1.50	0.6	0.34-3.65	1.4	0.64	0.34-7.8	1.58	0.67	0.44-3.65
Central	1.50	0.7	0.6-4.10	1.4	0.67	0.6-4.7	1.64	0.76	0.32-4.1
Medial	1.1	0.5	0.1-5.4	1.2	0.55	0.1-5.1	1.74	0.47	0.55-5.4

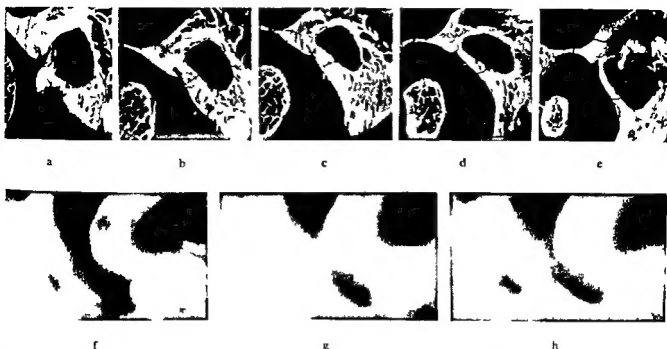


Fig 4 Different shapes of the bony auditory canal present in the same specimen. The angulation of the long diameter of the bony auditory canal is gradually changing to describe a screw like canal. The sections could be correlated according to the scheme

Sagittal levels of the images (mm)	Microradiography				
	72	5	27	29	31
	Tomography				
	25	3	7	3	29

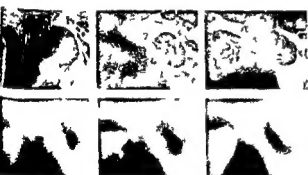


Fig 5

Fig 5 Change of the shape and angulation of the long diameter of the bony auditory canal. Correlation scheme

Sagittal levels of the images (mm)	Microradiography		
	75	77	31
	Tomography		
	6	78	30

identical in the three observed layers the canal may seem to be cone shaped (Table 2)

The sagittal layers may randomly be at right angles to the long axis of the bony auditory canal but almost always a small deviation exists from this angle which is the optimum one as concerns reproduction in the tomographic image. The angle relation can also vary within an individual canal depending on its curvature. Should actual angle deviation be great this will affect the geometry of the projected bony auditory canal i.e. the round one is reproduced with oval form. Angle deviations should be taken into account when evaluating the areal relations in Table 1.

The bony wall separating the auditory canal and the joint was measured in the thinnest part of a central third according to the system demonstrated in Fig 2b. It proved in some specimens to be difficult to decide a representative measurement distance. The reason for this may be illustrated by Fig 5a where the bony wall has an extremely thin part in the superior fusion. However this part cannot be representative for the thickness of the wall as a whole. Therefore a fixed calculation system was preferred.

Comments on the radiographic evaluation. Despite a normal skeletal and soft tissue morphology the tomographic image may demonstrate blurred

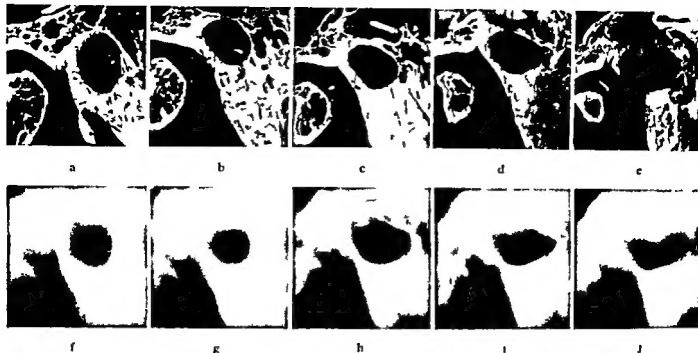


Fig 6 Marginal tomographic blur generated by the continuously changing shape diameter and angulation of the bony auditory canal Correlation scheme

Sagittal levels of
the images (mm)

Microradiography 23 6 77 8 10
Tomography 23 74 6 8 10



Fig 7

Fig 7 Clinical case with longstanding pain from the joint and ear a) Tomographic image from the initial examination revealed a possible osseous lesion b) c) Repeat tomography Changed angle relation optimized as regards the tympanic bone This was intact the faint primary demarcation was due to a very thin bone wall and too wide angulation

contours generated by a too great angle between the surface of the skeletal part and a perpendicular to the tomographic table. In the present series several morphologic explanations to a blurred depiction of skeletal contours of the auditory canal existed. Certain auditory canals revealed considerable calibre changes within short layer distances sometimes supplemented by a slight bending of the osseous canal. The demonstrated continuous change of the geometry of the canal in the lateral view was also an essential factor. A special case was the screwlike canals where the blurred sector of the auditory canal described a gradual change of position which thus had a simple morphologic explanation. A positional change at a new tomographic exposure will give a slight change in the appearances of blurred contours depending on the new tangential relations.

The thickness of the tympanic bone differed considerably which was demonstrated by the range

0.21 to 4.10 (mm). The interplay between dimensional factors and angulations in contour creating in tomographic images systematically described by VON REISNER was observed also in this investigation. An angle deviation of the thin walls was associated with strongly blurred contours or even a false image a discontinuity in the depiction of the skeletal demarcation of the auditory canal simulating a skeletal defect (ECKFRID 1973, ECKFRID & AHQVIST). This is further illustrated in Fig 7. The patient was examined because of long term obscure pain from the ear and the temporomandibular joint. The validity of the image of a skeletal defect in the primary image sequence was tested by an image in a changed angulation and by a comparison with the contralateral auditory canal. The contour of the tympanic bone was reproduced in the second sequence. The tympanic bone on the control side proved to be thicker which also was a diagnostic

problem. It is not known from the literature to what extent a skeletal asymmetry in this region must be expected. The explanations mentioned of total or partial blurring of skeletal contours have had skeletal morphologic explanations as well as positional.

An essential question is how to differentiate an image with incomplete skeletal demarcations depending on a pathologic process of the bone from those where the explanation will be morphologic or positional. In an early phase of a pathologic process perhaps only characterized by a broken cortical surface it is not always possible to make a simple and rapid differential diagnosis based on tomography. This may seem to be confusing. The ordinary opinion about the high tomographic efficiency is based on results from investigations which are concerned with the tomographic reproduction of details (VON REISNER ECKERDAL 1973). However the objects of these investigations are often well circumscribed and defined defects even located on other morphologic entities. The character of these defects often differs from that of primary cortical osseous defects of inflammatory or tumorous origin. This also explains why the capacity of detail reproduction is not an indisputable parameter in estimating the efficiency of tomography in reproducing early pathologic non penetrating processes in the tympanic bone. Differential diagnostic problems may be caused by anatomic defects (ECKERDAL et coll.) and in particular possible asymmetry between the two sides. It is of clinical interest to achieve a comparable positioning of the patient on the tomographic table in order to avoid false evaluation.

The perception of the contours of thin skeletal parts may be influenced by attenuation generated by additional soft tissues of inflammatory or tumorous origin. Already blurred contours are naturally most apt to be further extinguished. The limit of reproduction may even be exceeded. This could seem to be opposed to the findings of VON REISNER. He concluded that the reproduction in tomographic images of small skeletal defects in bony partitions was not affected by the presence or absence of soft tissue in or immediately around the actual defect. But he made some essential additional assumptions that

the bony partitions were not too thin, the defects larger than 4 mm and the reproducible conditions in other respects favourable.

SUMMARY

The external bony auditory canal is morphologically defined as concerns the shape and calibre in successive plane parallel histologic sections of the petrous bone. The sagittal dimensions and structural appearances of the tympanic bone are demonstrated. The morphologic properties defined constitute a basis for the evaluation of the tomographic image formation in this region.

Request for reprints: Docent Olof Eckerdal, The Institute for Postgraduate Dental Education, S-552 56 Jonköping, Sweden.

REFERENCES

- ECKERDAL O. A method for combined microradiographic and histological analysis of non decalcified hard tissues. *Acta odontol scand* 30 (1972) 327.
- Tomography of the temporomandibular joint. Correlation between tomographic image and histologic sections in a three-dimensional system. *Acta radiol* (1973) Suppl. No 329.
- and AHLQVIST J. Thin bony walls in the temporomandibular joint. Morphologic properties and tomographic reproduction. *Acta radiol. Diagnosis* 20 (1979) 385.
- AHLQVIST J, ALEHAGEN U and WING K. Length dimensions and morphologic variations of the external bony auditory canal. *Dento-Maxillo-Fac. Radiol* 7 (1978) 43.
- LAPAYOWKER M S and CLIFF M M. Bone changes in acoustic neuromas. *Amer J Roentgenol* 107 (1969) 652.
- LITTLETON J T. A phantom method to evaluate the clinical effectiveness of a tomographic device. *Amer J Roentgenol* 108 (1970) 847.
- MATSSON O. Control of a tomographic system. *Acta radiol. Diagnosis* 8 (1969) 433.
- VON REISNER K. Experimentelle Untersuchungen zur Detailerkennbarkeit im Röntgenschnittbild des Schädels. *Fortschr. Röntgenstr.* 113 (1970) 332.
- VALVASSORI G E and PIERCE R H. The normal internal auditory canal. *Amer J Roentgenol* 92 (1964) 1232.
- WEINMANN J P and SICHER H. Bone and bones. Fundamentals of bone biology. Second edition. C V Mosby Company, St. Louis 1955.
- ULLBERG S, HANMARSTRÖM L and APPELGREN I. E. Autoradiography in pharmacology. *International Encyclopedia in Pharmacology and Therapy* Section 78 Vol 1 (1971) 221.